FAZIA ALI TOUDERT

ENERGY PERFORMANCE OF BUILDINGS UNDER URBAN CONDITIONS

THEORY AND APPLICATION WITH FOCUS ON URBAN CLIMATE AND BUILDING CONSTRUCTION

2017 | HABILITATION

technische universität dortmund

Fakultät Architektur und Bauingenieurwesen
August-Schmidt-Str. 8 | 44227 Dortmund

TO MY PARENTS

TABLE OF CONTENTS

ACKNOWLEDGEMENTS

The methodological developments in PART I of this report were conducted during a position funded by the German foundation for Research (DFG) in the framework of the project Energy Performance of Urban Buildings EPUB. The author is highly indebted to the DFG for this valuable support at the beginning of her post-doctoral career.

The practical PART II of this research, which deals with the city of Stuttgart was carried out within the project KLISGEE conducted in the framework of the programme KLIMOPASS-Teil 1 funded by the federal Land Baden-Württemberg, to whom the author is also grateful. Further thanks go to the state capital Stuttgart for kindly providing support and some key data, to the German Weather Services (DWD) and to the LUBW for providing further climate data used in this work.

As further contributors to the work, Dipl.-Inf. Sven Böttcher worked on the implementation of TEB in TRNSYS during the EPUB project, and M. Sc. - Geogr. Limei Ji substantially helped with the KLISGEE project and assumed in particular the GIS tasks. The author wishes to thank them expressly for their efficient collaboration and for their commitment as team members in the activities of the Chair for Energy Efficient Buildings EEB. Preliminary joined publications already exist.

For their constant support, I would like to express my sincere thanks to Prof. Dr.-Ing. Habil. Wolfgang Willems (TU Dortmund), Prof. Dr. rer. nat. Bernhard Middendorf (TU Dortmund, University of Kassel), and to Prof. Dr.-Ing Helmut Müller (TU Dortmund).

The assistance of the TEB-Team, Dr. Valéry Masson, Dr. Aude Lemonsu, and Patrick le Moigne, during the working phase with TEB is also kindly acknowledged, as well as the support of Dipl.-Stat Corina Auer with the DOE experimental design plans. Further thanks go to more colleagues and friends for their support in one way or another during this research period.

Not least, I wish to express my warmest thanks and deep gratitude to my family, in particular my parents, for their invaluable support in spite of the distance and during my visits and business trips in Algeria.

FOREWORD

This work reports on the main findings of two complementary research projects (EPUB, KLISGEE) but not on all aspects addressed in these projects due to space limitations. A number of items were omitted or shortened with the intention of reporting on them later in specific publications. These include inter alia: i) The climate change issue in its relation to building energy demand prognosis; ii) the thermally relevant characterisation of a city structure, and iii) the application of the method and comparison of the results on other climate types (e.g. Mediterranean and Saharan Climates).

The author would like to draw the attention of the reader that the results presented here replace the preliminary ones reported previously in conferences (e.g. ICUC 2015, CLIMA 2010 and 2013, BAUSIM 2010 and JITH 2015) or in progress reports due to continuous improvements in the simulation scenarios and settings throughout the projects' duration time (see list of references).

The author's opinion is that working with numerical modelling must be careful as it suffers from uncertainty related to the physics of the models as well as to their handling. In this work, it has been strived to provide an accurate description of the assumptions made and to limit sources of errors, yet with no full confidence of success. Many thanks in advance for any feedback and enjoy the reading.

July, 2017

To cite this report:

Ali-Toudert, Fazia (2017): Energy performance of buildings under urban conditions – Theory and application with focus on urban climate and building construction. 333 pp. Habilitation Thesis. TU Dortmund University.

ABSTRACT

This research intends to be a contribution in fostering the interdisciplinary work on climate and energy issues with focus on buildings explicitly located in urban areas. It seeks to explore the link between urban and building physics to characterize the interdependences between outdoor and indoor climate and the impact on the resulting energy demand of buildings.

The work addresses two key issues: First, it aims to understand how urban microclimates evolve hence focuses on identifying the part of responsibility urban and building thermo-physical attributes have in modifying the urban energy balance fluxes, surface and air temperatures as well as the formation of canopy heat and cool islands. Secondly, it assesses the consequences of these modified urban energetics and thermal conditions on the energy performance of buildings subject to these boundary conditions.

The research method relies on numerical modelling for its speed and versatility, and combines four components:

i) the Town Energy Balance Model TEB for the urban microclimate prediction, with
ii) the non-stationary building energy model TRNSYS for simulating the thermal behaviour indoors and the resultant energy demands for ensuring thermal comfort,
iii) the statistical design of experiments method DOE for handling the complexity of the task by providing systematic exploration plans, and
iv) additionally the GIS techniques, applied to a spatially extended real city for the pre-processing, post-processing and mapping of urban climate and energy demand results.

The work consists of two complementary parts with different objects of study. PART I deals with theory-based urban office buildings and PART II addresses the city of Stuttgart as real case study. Both investigated objects are located at a European mid-latitude for which representative boundary climates are utilized. For the theoretical office buildings, a test reference year (TRY12, Mannheim) of the German weather services DWD is used. For Stuttgart, long-term weather recordings for 10 years (2003 - 2012) are available for use. For comparison purposes regarding the influence of the climate type, additional calculations are carried out for the Mediterranean and warm location of Algiers.

In PART I, extensive parameter studies (including sensitivity analyses) are conducted with the aim of exploring the mechanisms underlying the formation of urban microclimates. Decisive urban and building thermo-physical indicators are varied. Urban canyon-like structures with various solar orientations are simulated. Building constructive features including win-

dow ratio, thermal insulation, thermal inertia, in addition to the shortwave albedo and longwave emissivity as radiative surface properties are investigated. The effects of further settings related to the building use and operation are also checked. The target key metrics are the energy balance fluxes at the canyon facets, the surface and air temperatures within the canyon, as well as the resulting indoor energy demands for heating, cooling, lighting and ventilation.

For comparison, the building simulations are run under standard and urban climate conditions in order to isolate the role of the urban microclimate on the energy demands. The results are discussed for the building as a whole as well as for the floors and façade's orientation with reference to the view factor implied by the urban canyon vertical profile.

PART II employs the same investigation method using Stuttgart city as case study. The focus of the calculations is placed on the possibly highest spatial resolution downscaled to the single building. Using 2D and 3D city maps and further statistics about the buildings, thermally relevant indicators for buildings and city blocks are calculated by means of GIS. The peculiarity of this approach draws on the generic and abstracting modelling of the thermally relevant properties of the buildings instead of describing them using their real physical attributes. On the one hand, this procedure enables the feasibility of the task in keeping the processing time manageable. On the other hand, it allows for subsequent transferability of the results using statistically determined mathematical models.

This work confirms the importance of all investigated variables and provides a hierarchical quantification of their influence on both urban microclimate and building energy demands. In particular, the anthropogenic heat, the canyon geometry, and the thermal inertia appeared to have evident effects on the magnitudes and the time course of the warming or cooling of the canyon air. Under urban microclimate conditions, the cooling increases owing to dominating canopy heat island effects, whereas the heating demand mostly decreased for the same reason.

The building simulations in PART I show that the effect of the microclimate is highest in the case of thermally weak insulated building envelope with largely glazed façades. The massive construction also appears to be more advantageous than the lightweight construction. For the simulation settings assumed, the useful energy demand under urban microclimate conditions for heating and lighting decreases, whereas the energy demand for cooling and ventilation increases in comparison to standard climate conditions. The reduced sky view at street level affects negatively the energy demand for heating and lighting because of the diminished potentials for solar and daylight potentials, whereas the need for cooling and ventilation are reduced. In total, lower floors are disadvantaged in comparison to upper floors.

The comparison with the Mediterranean climate shows similar energetic behaviour outdoors as well as indoors regarding the relevance and effects of the investigated variables. However, the daily cycle and magnitude of the urban microclimate changes are different. Indoors, the share between heating and cooling are reversed, leading to a different pattern of the total energy demand.

The investigation of real conditions at Stuttgart city reveals a number of challenges. For time processing reasons, the extensive results about the urban microclimates must be reduced to a few climate clusters in order to be used in the subsequent building simulations. Moreover, the accurate modelling of the city structure and buildings is partly hindered by the lack of detailed row data, even though it is technically possible. Nevertheless, the comparison of the calculated energy demands against recorded consumption data for heating shows good agreement and confirm thereby the pertinence and practicality of the generic modelling applied.

Finally, this research demonstrated the suitability of combining TEB, TRNSYS, DOE and GIS in handling these interdisciplinary tasks. However, it also points out the necessity of developing an integral urban – building energy model for improving the prediction accuracy and reducing the time costs. The first milestone of such a model in form of TEB version for use within the TRNSYS environment is presented in this work. The so-called TEB – Type 201 solves numerous practical issues and improves the user friendliness and processing capabilities of the original TEB. The synchronised urban – building energy model in outlook must include the feedback loop between indoor and outdoor microclimate via the shared building envelope at each time step, thereby implementing an interdisciplinary approach, which will bring substantial knowledge from urban climatology and building science operationally together.

Keywords:
urban microclimate, canopy heat island, energy demand, generic numerical modelling, temperate climate, subtropics, TEB, TRNSYS, DOE, GIS

ZUSAMMENFASSUNG

Die Energieeffizienz Urbaner Gebäude - Theorie und Anwendung mit Fokus auf Stadtklima und Baukonstruktion

Die vorliegende Arbeit ist in erster Linie durch den Entschluss motiviert eine Verbindung zwischen Stadt- und Gebäudemaßstäbe in Bezug auf Klima und Energiefragen durch eine interdisziplinäre Vorgehensweise herzustellen. Bestehende Fachkenntnisse der Stadtbauphysik und Bauphysik werden kombiniert, um die Zusammenhänge zwischen Außen- und Innenraumklima besser verstehen und quantifizieren zu können.

Die Arbeit befasst sich mit zwei Zielsetzungen: Im ersten Schritt sollen die Prozesse hinter der Entstehung von städtischen Mikroklimata ermittelt werden. Der Schwerpunkt liegt darin, die Rolle thermo-physikalischer Attribute von Gebäuden und Stadtstrukturen bei der Veränderung der urbanen Energiebilanz, der Oberflächen- und Lufttemperaturen und somit der Mechanismen zur Bildung von urbanen Wärmeinseln bzw. Kühlinseln zu identifizieren. Im zweiten Schritt werden die Konsequenzen dieser modifizierten thermischen Situation auf das energetische Verhalten von Gebäuden untersucht, die diesen Randbedingungen unterliegen.

Die Forschungsmethode beruht auf der numerischen Modellierung, motiviert durch ihre Geschwindigkeit und Vielseitigkeit und kombiniert folgende Komponenten:

i) Das Stadtklimamodell TEB für die städtische Mikroklimaprognose mit dem
ii) dynamischen Gebäudeenergiemodell TRNSYS zur Simulation des thermischen Verhaltens im Innenraumbereich und des daraus resultierenden Energiebedarfs zur Gewährleistung des thermischen Komforts,
iii) die statistische Versuchsplanung DOE für die Handhabung der Komplexität der Aufgabe durch die Bereitstellung von systematischen Untersuchungsplänen und
iv) ergänzend die GIS-Techniken, für die Anwendung an einer räumlich ausgedehnten realen Stadt, für die Vorverarbeitung von Ausgangsdaten, Nachbearbeitung und Kartierung von Rechenergebnissen der urbanen Mikroklimata und Gebäudeenergie bedarfswerten.

Die Arbeit gliedert sich in zwei komplementäre Abschnitte (PART I und PART II) mit verschiedenen Untersuchungsobjekten. PART I beschäftigt sich mit theoriebasierten Bürogebäuden und PART II setzt sich mit der Stadt Stuttgart als reales Untersuchungsobjekt auseinander. Beide Studienobjekte liegen in einer mitteleuropäischen geographischen Breite und werden anhand repräsentativer Klimadaten untersucht. Bei den theoriebasierten Bürogebäuden

wird ein Testreferenzjahr des Deutschen Wetterdienstes (TRY12, Mannheim) angenommen. Für Stuttgart liegen langjährige meteorologische Messdaten über 10 Jahre (2003 – 2012) vor. Für Vergleichszwecke werden in PART I zusätzliche Berechnungen für die Mittelmeerlage Algiers als Warmklimaregion durchgeführt.

In PART I werden umfangreiche Parameterstudien (einschließlich Sensitivitätsanalysen) mit dem Ziel, die zugrundeliegenden Mechanismen der Bildung von urbanen Mikroklimata zu untersuchen, durchgeführt. Für die städtische Umgebung und das Gebäude werden wichtige thermophysikalisch relevante Indikatoren variiert. Straßenschluchtstrukturen mit verschiedenen Höhen-Breiten-Verhältnissen und Himmelsausrichtungen werden simuliert. Gebäudebezogen werden Fensterflächenanteil, Wärmedämmung, Bauart sowie die Reflektions- und Emissionsgrade als Oberflächenstrahlungseigenschaften untersucht.

Zielgrößen sind die an den Canyon-Oberflächen bestehenden Energie- und Wärmeflüsse, die Oberflächen- und Lufttemperaturen, sowie der Nutzenergiebedarf im Innenraum für Heizen, Kühlen, Beleuchten und Belüften. Vergleichend werden die Simulationen in TRNSYS sowohl mit als auch ohne Einfluss des städtischen Mikroklimas durchgeführt, um dessen Einfluss zu quantifizieren. Die Ergebnisse werden einerseits für das Gebäude als Ganzes erörtert, anderseits durch die Differenzierung von Geschossen und Himmelsausrichtungen genauer unterschieden.

PART II beschäftigt sich, mittels derselben Untersuchungsmethodik, mit dem großflächigen Kerngebiert der Stadt Stuttgart. Der Fokus der Berechnungen wird auf die höchstmögliche räumliche Auflösung bis hin zu den Einzelgebäuden gelegt. Anhand von 2D und 3D Stadtkarten und weiteren statistischen Gebäudedaten werden thermisch relevante Indikatoren für Einzelgebäude und für Baublöcke mit GIS-Techniken berechnet. Die Besonderheit dieses Ansatzes besteht darin auf eine abstrahierende Modellierung der Gebäude zurückzugreifen, ohne sie mit ihren tatsächlichen physikalischen Eigenschaften beschreiben zu müssen. Dies ermöglicht einerseits den Zeitaufwand für Vorbereitung, Bearbeitung und Auswertung zu minimieren und somit die Durchführbarkeit der Aufgaben zu gewährleisten und andererseits nachträglich die Ergebnisse mit Hilfe von statistisch ermittelten mathematischen Modellen zu übertragen.

Schlussfolgernd bestätigt diese Arbeit die Bedeutung aller untersuchten Variablen und stellt eine hierarchische Quantifizierung ihres Einflusses auf das städtische Mikroklima und den Energiebedarf auf Gebäudeebene dar. Insbesondere die Variablen anthropogene Wärme, das Höhe-Breite-Verhältnis einer Straße und die thermische Trägheit der Gebäudehülle - gegeben durch ihre Bauart - zeigen klare Auswirkungen auf die Erwärmung oder Abkühlung der Luft im Canyon-Volumen. Unter Berücksichtigung des urbanen Mikroklimas ergibt sich ein grö-

ßerer Nutzkältebedarf der Gebäude aufgrund der Wärmeinseleinflüsse, während der Heizwärmebedarf im Vergleich aus demselben Grund kleiner wird.

Die Gebäudesimulationen im PART I zeigen, dass der Einfluss des Mikroklimas im Falle einer schlecht gedämmten und großzügig verglasten Gebäudehülle am Größten ist. Auch die massive Bauart erweist sich vorteilhafter bezüglich des Energiebedarfes als die Leichtbauart.

Für die angenommenen Simulationseinstellungen, nimmt der Nutzenergiebedarf für Heizen und Beleuchten im Vergleich zu Standard Klimarandbedingungen ab, während der Nutzenergiebedarf für Kühlen und Belüften zunimmt,. Die teils eingeschränkte Himmelsicht auf Straßenniveau beeinflusst, aufgrund der reduzierten Sonnen- und Tageslichtpotenziale, den Nutzenergiebedarf für Heizen und Kühlen negativ, während der Nutzkälte- und Lüftungsbedarf weniger werden. Demzufolge sind insgesamt Geschosse auf Straßenniveau gegenüber den oberen Geschossen benachteiligt.

Der Vergleich mit dem Mittelmeerklima zeigt in Bezug auf die Relevanz und Auswirkungen die untersuchten Parameter ähnliche energetische Verhalten sowohl Außen- als auch Innen. Allerdings ist der Tagesverlauf und Größenordnung der Mikroklimatischen Änderungen unterschiedlich. Im Innenraum, ist der Anteil zwischen Heizen und Kühlen umgekehrt, welches zu verschiedenen Gesamtnutzenergiemuster führt.

Die Untersuchung einer realen Stadt zeigt einige Herausforderungen. Es müssen die umfangreichen Ergebnisse zum Stadtklima Stuttgart aus Rechenzeitgründen auf wenige repräsentative räumlich differenzierte Klimacluster reduziert werden, um sie zur Gebäudesimulation nutzen zu können. Ebenso ist eine genaue Modellierung der Stadtstruktur und der Gebäude, trotz technischer Möglichkeiten, aufgrund des Mangels an genaueren Rohdaten nicht vollständig realisierbar. Trotzdem erweist der Vergleich der errechneten Heizwärmebedarfswerte gegenüber den aufgezeichneten Verbrauchsdaten eine gute Übereinstimmung und bestätigt damit eindeutig die Relevanz und Anwendbarkeit der erarbeiteten generischen Methode.

Abschließend belegt diese Forschungsarbeit die Tauglichkeit der Verknüpfung zwischen TEB, TRNSYS, DOE und GIS bei der Abwicklung der definierten Aufgaben. Sie weist allerdings auch auf die Notwendigkeit hin, ein integrales städtebauliches Energiemodell zur Verbesserung der Klima- und Energieprognose im Bauwesen und zur Reduzierung des Zeitaufwandes zu entwickeln. Der erste Meilenstein eines solchen Modells wird in dieser Arbeit in Form eines eingebetteten TEB in der TRNSYS-Umgebung namens TEB-Type 201 vorgestellt, welches die Benutzerfreundlichkeit und die Verarbeitungsmöglichkeiten des ursprünglichen TEB verbessert. Noch weiterzuentwickeln ist die Rückkopplungsschleife an der Schnittstelle der Gebäudehülle, zwischen Innen- und Außenraum, um die synchrone Simula-

tion zu jedem Rechenzeitpunkt zu ermöglichen. Damit wird einen interdisziplinären Ansatz geschaffen, der die Fachkenntnisse aus der Stadtklimatologie und Bauphysik operationell verbindet.

Stichworte:
Urbanes Mikroklima, städtische Wärmeinsel, Energiebedarf, generische Modellierung, mäßiges Klima, Subtropen, TEB, TRNSYS, DOE, GIS

RÉSUMÉ

La performance énergétique des bâtiments en milieu urbain – Théorie et application centrées sur le climat urbain et la construction des bâtiments

Cette recherche est une contribution au travail interdisciplinaire sur les questions liées au climat et à l'énergie appliquées à des bâtiments explicitement situés en milieu urbain. Elle cherche à travers le lien entre la physique du bâtiment et la physique urbaine à caractériser les interdépendances entre les climats extérieur et intérieur et leur impact sur la demande d'énergie des bâtiments.

Ce travail traite deux questions clés: Premièrement, il vise à comprendre les mécanismes de formation des microclimats urbains et se concentre sur l'identification du rôle des attributs thermo-physiques de la structure urbaine et des bâtiments dans la modification des flux du bilan énergétique urbain, des températures de surface et de l'air ainsi que la formation d'îlots de chaleur ou fraicheur dans la canopée urbaine. Deuxièmement, il évalue les conséquences de ces conditions radiatives et thermiques modifiées sur la performance énergétique des bâtiments.

La méthode d'investigation repose sur la modélisation numérique, choisie pour sa vitesse et sa polyvalence et combine quatre composants:

i) le modèle Town Energy Balance TEB pour la prévision du microclimat urbain,
ii) le modèle non stationnaire d'énergétique du bâtiment TRNSYS pour simuler le comportement thermique intérieur et la demande d'énergie qui en résulte pour assurer le confort thermique,
i) la méthode statistique plan d'expérience DOE pour gérer la complexité du sujet en fournissant des plans d'exploration systématique, auxquels s'ajoute
ii) les techniques d'information géographique SIG, appliquées à une ville réelle de grande étendue spatiale pour le pré-traitement, post-traitement et la cartographie des résultats relatifs au climat urbain et à la demande d'énergie.

Ce travail se compose de deux parties complémentaires traitant des objets d'étude différents (PART I et PART II). La PART I étudie des bâtiments de bureaux théoriques et la PART II est une application sur le cas réel de la ville de Stuttgart. Les deux objets d'étude sont situés à une latitude moyenne en Europe centrale au climat tempéré et pour laquelle des données climatiques représentatives sont utilisées. Pour les bâtiments théoriques, le fichier climatique TRY12 (test reference year) des services météorologiques allemands DWD est utilisé. Pour

Stuttgart, des données météorologiques mesurées pour une période 10 ans (2003 - 2012) sont disponibles. À des fins de comparaison concernant l'influence du type de climat, des calculs supplémentaires sont effectués pour le site d'Alger situé en climat méditerranéen chaud.

Dans la PART I, des études paramétriques extensives (incluant des analyses de sensibilité) sont menées dans le but d'explorer les mécanismes sous-jacents à la formation des microclimats urbains. Des indicateurs thermiques décisifs à l'échelle urbaine et à l'échelle de la construction sont variés. Des structures de type canyon urbain pour diverses orientations solaires sont simulées. Les caractéristiques constructives étudiées incluent la proportion des ouvertures, l'isolation thermique, l'inertie thermique, auxquels s'ajoutent l'albédo et l'émissivité comme propriétés radiatives de surface. Les effets d'autres paramètres liés à l'utilisation et au fonctionnement du bâtiment sont également examinés. Les quantités cibles analysées sont les flux du bilan d'énergie du système canyon, ses températures de surface et de l'air, ainsi que les exigences énergétiques intérieures résultantes pour le chauffage, le refroidissement, l'éclairage et la ventilation.

À titre comparatif, les simulations sont conduites pour des conditions climatiques standard et urbaines afin d'isoler le rôle du microclimat urbain sur les besoins énergétiques. Les résultats sont discutés pour le bâtiment dans sa totalité ainsi que différencié par étage et par façade en référence au concept d'ouverture au ciel ou vue du ciel induites par le profil vertical du canyon urbain.

La deuxième partie PART II utilise la même méthode d'investigation sur la ville de Stuttgart tout en centrant l'attention sur la résolution spatiale la plus haute possible allant jusqu'à l'échelle du bâtiment individuel. En utilisant des cartes 2D et 3D de la ville ainsi que d'autres statistiques sur les bâtiments, les indicateurs thermiquement pertinents pour les bâtiments et les ilots urbains sont calculés au moyen des SIG. La particularité de cette approche consiste dans la modélisation générique et abstraite des propriétés thermiques des bâtiments au lieu de leur description sur la base de leurs attributs physiques réels. D'une part, cette procédure permet la faisabilité de cette recherche en garantissant un temps de calcul raisonnable. D'autre part, elle permet la transférabilité ultérieure des résultats en utilisant des modèles mathématiques déterminés statistiquement.

Ce travail confirme l'importance de toutes les variables étudiées et fournit une quantification hiérarchique de leur influence sur le microclimat urbain et sur la demande énergétique dans les bâtiments. En particulier, la chaleur anthropique, la géométrie du canyon et l'inertie thermique se révèlent avoir des effets évidents sur le réchauffement ou le refroidissement de l'air du canyon en termes de magnitude et de cycle journalier. Dans les conditions de microclimat

urbain, la demande d'énergie pour le refroidissement augmente en raison des effets dominants de l'île de chaleur dans la canopée, alors que la demande de chauffage diminue pour la même raison.

Les simulations de bâtiments dans la PART I montrent que l'effet du microclimat est le plus élevé dans le cas d'une enveloppe de bâtiment faiblement isolée thermiquement et des façades largement vitrées. La construction massive apparait comme plus avantageuse que la construction légère. Pour les conditions de simulation supposées, la demande d'énergie utile diminue pour le chauffage et pour l'éclairage, et augmente pour le refroidissement et pour la ventilation sous des conditions microclimatiques urbaines comparées à des conditions climatiques standard. La vue réduite du ciel au niveau de la rue affecte négativement la demande d'énergie pour le chauffage et l'éclairage en raison des potentiels solaires diminués, alors que les besoins de refroidissement et de ventilation sont réduits. Au total, les niveaux inférieurs sont défavorisés par rapport aux étages supérieurs.

La comparaison avec le climat méditerranéen montre un comportement énergétique similaire à l'extérieur et à l'intérieur concernant la pertinence et les effets des variables étudiées. Cependant, le cycle journalier et l'ampleur des changements du microclimat urbain sont différents. Dans les espaces intérieurs, la proportion entre le chauffage et le refroidissement est inversée, ce qui entraîne une tendance différente de la demande d'énergie totale.

L'enquête sur les conditions réelles de la ville de Stuttgart révèle un certain nombre de défis. Pour des raisons de temps de calcul, les résultats obtenus sur les microclimats urbains doivent être réduits à quelques groupes climatiques, lesquels sont utilisés dans les simulations des bâtiments ultérieures. En outre, la modélisation précise de la structure urbaine et des bâtiments se révèle en partie entravée par le manque de certaines données brutes, bien que leur prise en compte soit techniquement possible. Néanmoins, la comparaison des besoins calculés en énergie par rapport aux données de consommation enregistrées pour le chauffage montre une bonne concordance et confirme ainsi la pertinence et l'applicabilité de cette méthode de modélisation générique.

Enfin, cette recherche a démontré l'opportunité de combiner TEB, TRNSYS, DOE et SIG dans le traitement interdisciplinaire de cette problématique. Cependant, elle souligne également la nécessité de développer un modèle énergétique intégral urbain - bâtiment pour améliorer la précision du pronostic et réduire les temps de calcul. Le premier jalon d'un tel modèle est présenté dans ce travail sous la forme d'une version TEB utilisable dans l'environnement TRNSYS. Le TEB - Type 201 résout de nombreux problèmes pratiques et améliore la convivialité d'utilisation et les capacités de traitement du modèle TEB original. Le modèle syn-

chronisé à développer doit inclure la boucle de rétroaction entre microclimat intérieur et extérieur via leur interface commune, à savoir l'enveloppe de bâtiment, pour chaque pas de simulation, mettant ainsi en œuvre une approche interdisciplinaire, qui réunit les connaissances de la climatologie urbaine et de la science du bâtiment de façon opérationnelle.

Mots clés:
Microclimat urbain, îlot de chaleur, canopée urbaine, demande énergétique, modélisation générique TEB, TRNSYS, DOE, SIG,

LIST OF SYMBOLS

Abbreviations and Acronyms

Symbol	Full designation
a.g.l	above ground level
a.r.l	above roof level
ALG	Algiers
CDD	Cooling degree days
DOE	design of experiments
GF	glazed façade
H/W	building height to street width ratio
HDD	Heating degree days
HVAC	heating, cooling, ventilating and air conditioning
LARSIM	A hydrological model, source of the climate data for Stuttgart in PART II
LI	Lightweight construction
LST	local standard time
MA	massive construction
MAN	Mannheim
OU	outside usage time: nighttime (19:00 – 4:00) and week-ends
PART I	theoretical part of this research dedicated to urban office buildings
PART II	practical part of this research dedicated to the city of Stuttgart
PF	perforated façade
RF	row façade
SET I	sensitivity analysis of TEB (set of 729 runs)
SET II	parameter study for urban climate prediction in TEB (set of 81 runs)
SET III	parameter study for building energy demand prediction in TRNSYS using standard rural climate data (set of 54 runs by location)
SET IV	as SET III but using TEB calculated urban climate data (set of 54 runs by location)
SET V	sensitivity analysis in TRNSYS (set of 1458 runs)
TEB	town energy balance model
TRNSYS	transient systems simulation programme
TRY12	test reference year N°12 from the DWD climate classification of Germany, station: Mannheim
UCI	urban cool island
UHI	urban heat island
UT	usage time: (7:00 – 18:00) plus 2 hours preheating (5:00 – 7:00)
UTC	coordinated universal time

Variables used in the parameter studies in PART I

Symbol	Description
A	aspect ratio (H/W)
B	solar orientation
C	window ratio
D	thermal insulation (thermal transmittance U-value)
E	thermal inertia
F	albedo (shortwave reflectance)
G	emissivity (longwave emittance)
L	floor level
H	anthropogenic heat (traffic and industry)
P	roof plan density
S	shading devices efficiency
V	ventilation rate during usage time UT
N	ventilation rate outside usage time OU
I	internal heat gains due to lighting

Variables used in the parameter studies in PART II

Symbol	Description
A	aspect ratio (H/W)
T	building type of use
U	thermal insulation (thermal transmittance U-value)
S	shape coefficient
W	window ratio
V	heated building volume
H	average building height
B	built to ground surface for built density
F	heat release from traffic

Subscripts

symbol	Description
a	air
can	canyon
comf	comfort
F5 – F1	Difference between floor 5 and floor 1
frc	forcing height above roof level (here 2 m a.r.l.)
frm	frame
fw	facing wall
FW	anthropogenic heat flux from wall
gls	glass
h	horizontal
i	numbering of items (e.g. floor height, material layer, etc.)
in	indoor
IND	industry
LW	longwave
mrt	mean radiant temperature
op	operative
ou	outdoor
s	surface
scan	surface of canyon facets incl. weighted walls and road
sroad	surface of road

sroof	surface of roof
stn	standard = rural
SW	shortwave
swall	surface of wall
TRF	traffic
urb	urban
v	vertical
wdw	window

Roman letters

Symbol	Quantity	SI Units
A	surface area (see subscripts: wall, wdw)	m^2
A_i	view factor of facing wall at floor height i, range 0 to 1	-
B_i	view factor of street at floor height i, range 0 to 1	-
C_p	pressure coefficient	-
CS	annual cool sum	°C a^{-1}
D	shortwave diffuse solar radiation (see subscripts h, v)	W m^{-2}
DLP	daylighting potential	%
D_{eq}	equivalent thermal insulation or transmittance incl. walls and windows (= U_{eq})	W m^2 K^{-1}
E_{in}	indoor illuminance	Lux
E_{ou}	outdoor illuminance	Lux
Eshade	reflection ratio of shading device (Eshade = 1- Fc), range 0 to 1	-
Fc	transmission ratio of shading device (Fc = 1 - Eshade), range 0 to 1	-
G	shortwave global solar radiation	W m^{-2}
HS	Annual heat sum	°C a^{-1}
Q	heat flux (energy balance) or	W m^{-2} or
	specific useful energy demand of building	kWh m^{-2} a^{-1}
Q*	all-wave net radiation	W m^{-2}
Q_E	turbulent latent heat flux	W m^{-2}
Q_F	total anthropogenic heat flux from traffic and industry (sensible and latent)	W m^{-2}
Q_{FIND}	anthropogenic heat flux from industry (sensible H and latent E)	W m^{-2}
Q_{FTRF}	anthropogenic heat flux from traffic (sensible H and latent E)	W m^{-2}
Q_G	sub-surface or conductive heat flux	W m^{-2}
Q_H	turbulent sensible heat flux	W m^{-2}
Q_{FR}	anthropogenic indoor heating flux at roof	W m^{-2}
Q_{FW}	anthropogenic indoor heating flux at wall	W m^{-2}
Q_{FBLD}	heating heat flux inside building	W m^{-2}
ΔQ_S	storage heat flux	W m^{-2}
ΔQ_{SW}	storage heat flux at wall	W m^{-2}
ΔQ_A	Advection heat flux	W m^{-2}
ΔQ_{u-s}	Heat flux difference between urban and standard climate conditions ($Q_{urb} - Q_{stn}$)	W m^{-2}
$Q_{SW}^{\downarrow}$	Incoming shortwave radiation	W m^{-2}
$Q_{SW}^{\uparrow}$	reflected shortwave radiation	W m^{-2}
$Q_{LW}^{\downarrow}$	Incoming atmospheric longwave radiation	W m^{-2}
$Q_{LW}^{\uparrow}$	Outgoing terrestrial longwave radiation	W m^{-2}
Q_{heat}	Annual useful heating energy demand (using urban climate data)	kWh m^{-2} a^{-1}
Q_{cool}	annual useful cooling energy demand (using urban climate data)	kWh m^{-2} a^{-1}
Q_{light}	annual useful lighting energy demand (using urban climate data)	kWh m^{-2} a^{-1}
Q_{vent}	annual useful lighting energy demand (using urban climate data)	kWh m^{-2} a^{-1}

Q_{soltr}	annual passive solar gains	kWh m^{-2} a^{-1}
$Q_{TOT\ I}$	annual total useful lighting energy demand for heating, cooling and lighting	kWh m^{-2} a^{-1}
$Q_{TOT\ II}$	annual total useful energy demand for heating, cooling, lighting and ventilation	kWh m^{-2} a^{-1}
RH	relative humidity	%
S	shortwave direct solar radiation (see subscripts h, v)	W m^{-2}
S_{fw}	average direct solar radiation reflected from facing wall	W m^{-2}
S_g	direct solar radiation reflected from street ground	W m^{-2}
SVF	sky view factor, range from 0 to 1 for horizontal and 0 to 0.5 for vertical surface	-
T	temperature (see subscripts: a, can, comf, frc, mrt, op, ou, s)	°C, K
T_{scan}	surface temperature of canyon facets (weighted street and walls)	°C
T_{sgrd}	temperature of surroundings (incl. street ground and buildings)	°C
T_{sky}	sky temperature	°C
T_{stn}	air temperature from standard climate data	°C
T_{urb}	urban air temperature adjusted using TEB	°C
ΔT_{u-s}	air temperature difference between urban and standard climate ($T_{urb} - T_{stn}$)	K
U	thermal transmittance (see subscripts: frm, gls, roof, wall, wdw)	W m^{-2} K^{-1}
U_{eq}	equivalent thermal transmittance incl. opaque and transparent elements (=D_{eq})	W m^{-2} K^{-1}
V	wind speed	m s^{-1}
WR	window ratio (proportion of openings in a façade), range o to 1	-
HSH	frequency of warming of canyon air	hours
CSH	frequency of cooling of canyon air	hours
a	per annum, per year	a^{-1}
e_p	primary energy factor	-
q	specific humidity	g kg^{-1}
c	specific heat capacity	kJ kg^{-1} K^{-1}
g	solar heat gain coefficient, range from 0 to 1	-
frac	Fraction of surface (wall, road, roof)	-

Greek letters

Symbol	Quantity	SI Units
α	albedo (solar reflectance), range from 0 to 1	-
α	view factor angle of facing wall	degrees
β	view factor angle of facing road	degrees
ε	emissivity, range from 0 to 1	-
λ	thermal conductivity	W m^{-1} K^{-1}
ρ	volumetric mass density	kg m^{-3}
σ	sky view factor	degrees
τ	light transmission coefficient, range from 0 and 1	-
κ	heat capacity	J K^{-1}

Nota:
This list includes the symbols mentioned in the main document. Further quantities occurring in the equations given in the Appendices are described there.

I

INTRODUCTION

1. MOTIVATION, OBJECTIVES AND SCOPE

1.1. The Global Context

Climate and Energy are major challenges that are increasingly the focus of attention of the scientific community as well as policymakers and broad societies worldwide. Whether it is about climate change, urban climate, energy efficiency, renewable energy, or within inclusive sustainability discourses, the related problems and imperatives for action are complex and interlaced, so that it urgently call for comprehensive commitment and interdisciplinary work (see e.g. IPCC 2014, Edenhofer et al. 2014, Seto et al. 2014).

In support of that, international bodies and coordinating frameworks do exist, either in form of the IPCC[1] or as supported by the UNFCCC[2]. The IPCC assesses the science, impacts and future risks related to climate change, and suggests options for adaptation and mitigation. The UNFCCC[3] and its related COPs[4] go along with institutional commitments at country level, with the objective being to stabilize the greenhouse gas concentrations GHG in the atmosphere. The 2015 Paris agreement[5], being the current universal binding framework, sets the limit of global warming in this century to 2 °C compared to pre-industrial levels and encourage the pursuit of the efforts towards a lower limit of 1.5 °C. The novelty thereby is also that "nationally determined contributions" (NDCs) document country-specific tangible adaptation and mitigation plans.

At European scale, the issue was recognized earlier and specific climate and energy targets already exist (see EEA[6], EEA 2016). For 2020, the 20-20-20 target applies, meaning 20% less GHG, 20% more renewables and 20% improved energy efficiency. For 2030, this target increases to 49-27-27. Germany is at the forefront of these efforts and strongly commits to the energy transition from fossil to renewable energies via its ambitious programme *Energiewende*, which monitors the progress and regularly reports on it (see BMWi Energiewende

[1] IPCC: Intergovernmental Panel on Climate Change (since 1988) initiated by the UNEP and WMO. Website: http://www.ipcc.ch/index.htm. It provides regularly assessment reports on climate change. The current one (5th) is available at http://www.ipcc.ch/report/ar5/

[2] UNFCCC: United Nations Framework Convention on Climate Change: A treaty negotiated at the Earth Summit in Rio 1992 and in force since 1994. Website: http://newsroom.unfccc.int/

[3] UNFCCC: United Nations Framework Convention on Climate Change: A treaty negotiated at the Earth Summit in Rio 1992 and in force since 1994. Website: http://newsroom.unfccc.int/

[4] COP: Conference of Parties is an annual conference of the UNFCCC organized since 1995, from which the COP21 hold in Paris in 2015.

[5] Paris Agreement: Outcome of the COP21 (2015) succeeding to the Kyoto Protocol of 1997 (in force 2005), and currently ratified by 143 parties from 197. Website: http://unfccc.int/paris_agreement/items/9485.php

[6] EEA: European Environment Agency, Website: http://www.eea.europa.eu/

2017). Table 1 gives an overview of the achievements in 2015 and further prospects. The energy concept adopted in Germany is twofold: to promote upstream the expansion of the renewable energies (supply) and to improve steadily the energy efficiency (use) downstream. The Renewable Energy Sources Act EEG[7] (EEG 2014) primarily governs the energy supply and the national action plan on energy efficiency NAPE implements the energy efficiency goals as part of the Climate Action Programme 2020. Thereby, the *Energiewende* puts a special focus on the following drivers: electricity market, buildings, energy grids and research & innovation.

Table 1: Quantitative targets of the energy transition in Germany and status quo (2015) (BMWi Energiewende 2016)

Targets	2015	2020	2030	2040	2050	measures
Greenhouse gas emissions						
Greenhouse gas emissions (compared with 1990)	-27.2 %*	at least -40%	at least -55%	at least -70%	-80% to -95%	2020 Climate Action Programme
Renewable energy						
Share of gross final energy consumption	14.9%	18%	30%	45%	60%	Renewable Energy Sources Act, Market Incentive Programme, Renewable Energies Heat Act, greenhouse gas quota, etc.
Share of gross electricity consumption	31.6%	at least 35%	at least 50% Renewable Energy Sources Act 2025 40 to 45%	at least 65% Renewable Energy Sources Act 2035 55 to 60%	at least 80%	Renewable Energy Sources Act
Share of heat consumption	13.20%	14%				
Share in transport sector	5.20%	10%**				
Efficiency and consumption						
Primary energy consumption (compared with 2008)	-7.60%	-20%			-50%	National Action Plan on Energy Efficiency
Final energy productivity (2008–2050)	1.3%/year (2008–2015)	2.1%/year (2008–2050)				
Gross electricity consumption (compared with 2008)	-4.00%	-10%			-25%	
Primary energy consumption in buildings (compared with 2008)	-15.90%				-80%	
Heat consumption in buildings (compared with 2008)	-11.10%	-20%				National Action Plan on Energy Efficiency, Efficiency Strategy for Buildings, Climate Action Programme
Final energy consumption: transport (compared with 2005)	1.30%	-10%			-40%	2020 Climate Action Programme, Mobility and Fuel Strategy, Electric Mobility Act, Car Efficiency Labels, EU CO_2 fleet emission targets

Source: In-house figures from the Federal Ministry for Economic Affairs and Energy, December 2016

* Provisional figure for 2015 **EU goal. Target set by Directive 2009/28/EC.

[7] EEG: First release in 2000, updates in 2014 and 2016. The latter has entered into force in 01.2017as EEG 2017.

In this respect, cities are of prime importance because being locations for high concentrations of goods, activity and services; they greatly attract people with a sustained increasing trend. According to UN DESA PD (2014), the world urban population has exceeded the rural population since 2007. From 30% in 1950 (746 million), it has grown to 54% in 2014 (3.9 billion) and is expected to reach 66 % in 2050 (6.4 to 6.9 billion) making urban settlements experience a rapid spatial expansion and densification. This affects dramatically and durably their total energy consumption and global environmental quality.

According to IPCC, urban areas account for between 71% and 76% of CO_2 emissions from final global energy use (Seto et al. 2014). Greenhouse gas emissions from the buildings sector have more than doubled since 1970, accounting for 19% of global GHG emissions in 2010, including indirect emissions from electricity generation (Edenhofer et al. 2014). One major consequence at local scale is the formation of a particular climate within cities, known as *urban climate*, characterised by contrasting thermal and air quality conditions in comparison to the countryside and this jeopardizes their sustainability. The United Nations (UN DESA PD 2014) stresses the need for integrated policies towards sustainable urbanisation and set this as one of the 16 key targets of the latest resolution of the United Nations for sustainable development (see UN SD 2016).

Specifically to the building sector, the Energy Savings Act *Energieeinsparverodnung EnEV* (EnEV 2016) is the mandatory thermal regulation standard in Germany. Since its first release in 2002, successive versions biannually updated have been in use (current 2013, sometimes documented 2014 or 2016). Unceasingly, the EnEV has been forcefully sharpened following the overarching federal goal of the energy transition. The EnEV relies on three consecutive principles: Heat conservation by means of a properly designed and well- insulated building envelope, efficiency of HVAC systems and the additional use of renewable energy technologies.

1.2. Relevance of the Work

Within the global context of energy transition and towards the mitigation of and adaptation to global warming specifically applied to cities and buildings, the present work draws its relevance from the following statements and assumptions. These are thoroughly discussed in the light of the current published literature in section I - 2 (p 27) dedicated to the state of the art.

1. *An interdisciplinary contribution:*

Urban and building professionals increasingly face up to design energy-efficient buildings, which must become standard practice. This goal must take into account the distinctive climatic feature of the urban environment into which they most likely stand. This is best achieved if physically sound climate knowledge as provided by the urban climatology is anchored in building design on the one hand and if building design imperatives are better understood by climatologists. In spite of their original divergences in methods and goals, promising collaboration is emerging and it builds on the growing convergence between the two disciplines. This results from a progressive shift of interest in a top-down approach in urban climatology and a bottom-up approach in building science. The focus from both sides is then placed on the building envelope as active shared outdoor - indoor interface. The present work clearly acts in this framework and perspective by addressing both climate and building sciences interactively and at high level of detail (see section I - 2.1, p 35).

2. *Use and development of multiscale and integral investigation methods:*

In order to understand and quantify the energetic and thermal interactions between building indoors and urban outdoors, there is a need to use and further develop integral and multiscale investigation methods. In this regard, the present work demonstrates the pertinence of combining several calculation models and techniques employed on theory-based and practical objects to reach this goal. It also shows ways for the development of a new integral model for climate and energy prediction for buildings under urban conditions as increasingly discussed and advised in the current literature (see section I - 2.3, p 35 and section I - 5, p 157).

3. *The climate in cities needs to be quantified prior to building energy modelling:*

The present research relies on the assumption that using standard data from weather stations, generally located in the countryside, for describing the urban ambient boundary conditions in building simulation models is inappropriate. This approach, even though convenient and still widespread, is only valid in rural sites and not applicable in urban structures for two main reasons. Firstly, specific urban climate and microclimates take place within urban areas, which differ from the data recorded in standard weather stations. Secondly, the reduced sky

view and mutual obstructions between buildings, induced by their proximity, decrease the sunlight and daylight potentials for indoor use in the daytime and slow down the heat release in the nighttime, resulting in urban heat or cool islands. Typically, urban air temperatures are higher and may increase the energy needed for cooling in the summer and reduce the heating demand in the winter. Therefore, a non-stationary quantification of the microclimate changes within urban structures is necessary to act as boundary conditions for buildings. In the absence of systematic weather data recording within cities, it is crucial to find ways to predict the radiative and thermal changes due to the urban fabric and urban activity in order to better quantify possible interactions with the indoor climates and impacts on energy demands (see section I - 2.4, p 45).

4. *The design of energy-efficient buildings starts at urban level:*

A climate-sensitive urban design aware of energy conservation will certainly promote the implementation of energy-efficient buildings, for without a top-down working approach, the potential of success becomes strongly compromised. Typically, a weak exploitation of passive climate-sensitive design strategies and renewable energies leads to buildings with high demands for heating, cooling and artificial lighting, and hence consume more fossil energy and electrical power. This, in turn, increases the ambient urban air temperatures because of increased heat release and harmful gas emissions to outdoors and again to more energy need, and so forth. This vicious cycle can only be broken if low-energy buildings are designed (see section I - 2.4, p 45). The present work quantitatively demonstrates the effects of the building construction on outdoor climates and adds thereby to the knowledge available about their effects on indoor climate. In so doing, the work discusses not only the effects of the urban microclimate on the building thermal behaviour but also the part of responsibility of typical building design choices on the development of urban microclimates and stresses by this means their interdependence.

5. *Demonstration on a real case study at high spatial and temporal resolution:*

Following a theoretical investigation, the present work shows for the first time the ways urban climate can be considered in building energy modelling for an extensive real case study area of several square kilometres at the detail level of individual buildings and city blocks. The chosen temporal scope of 10 years and the dynamic calculation at hourly basis is also challenging. In this respect, the work provides an original and reliable method for keeping the calculation times manageable while maintaining a high level of data processing. It hence illustrates the pertinence of a new method and its usefulness in practice (see section III, p 167).

1.3. Objectives of the Work

The wide objectives of this research are dual:

1. Content-related: New knowledge gathering about the mechanisms underlying the formation of urban microclimates and the impacts of these microclimates on the thermal behaviour and energy demand of buildings and
2. Methodological: To seek the improvement of the investigation methods, which link between urban and building scales in terms of climate and energy prediction.

More specifically, the objectives of the work are as follows:

3. To quantify the microclimate changes within an urban structure (expressed as canyon-like) due to its geometrical and thermo-physical properties. The target key metrics include the urban energy balance fluxes, air and surface temperatures.
4. To investigate the effects of urban microclimates as boundary condition on the energy demand of buildings, mainly for heating and cooling. The work additionally addresses the lighting and ventilation (versus daylighting and natural ventilation).
5. To explore the differences related to the climate type in urban microclimate formation and energy demand of buildings by addressing temperate and Mediterranean climates.
6. To explore the effects of the sky view factor on the indoor energy demand, which expresses the openness to the sky of the various building floor levels in combination with the façade's solar orientation.
7. To find out the extent building construction, expressed by its thermally relevant properties: window ratio, thermal insulation and thermal inertia, influence the outdoor microclimates and indoor energy demands.
8. To quantify the modifying effects of various scenarios of building use and operation on the energy demand as further critical numerical simulation settings.
9. To establish a hierarchy of importance among all investigated variables with respect to their impact on the urban microclimate and building energy demand.

From a methodological point of view, this research also focusses on the following objectives:

10. To illustrate and demonstrate the relevance of combining several calculation models and techniques, in order to solve the complexity of the study.
11. To improve the capabilities of a building energy model to account efficiently for the urban climate. This is a key issue, which will bridge the gap between urban modelling and building modelling in relation to climate and energy.

12. To use a statistical approach in order i) to quantify the targets key metrics announced above and to identify the causal – effect systematic, and ii) as an alternative to deal with a spatially extensive study area by applying a generic characterisation of the objects instead of modelling real typologies.
13. This research addresses theoretical buildings and a real city. In the theory-based objects, all variables are systematically investigated in order to assess their possible importance. In the real case of study, the suitability of the applied method is verified, especially in relation to the available climate and city data.

1.4. Structure of the Work

The present report is organised in five chapters. The core of the work consists of two balanced parts, PART I and PART II:

[I] **The introduction** addresses i) the motivation, objectives and scope of the work, ii) broaches the state of the art on all items covered by this research and iii) explains the methodological concepts and choices.

[II] **The theoretical PART I** is a background investigation based on theoretical urban office buildings using systematic parameter studies and including sensitivity analyses. This part applies to temperate and Mediterranean climates.

[III] **The practical PART II** demonstrates the relevance of the subject, the applicability of the proposed method and its adjustment to the real conditions of Stuttgart city.

[IV] **Summary, Outlook and Conclusion**: The major findings from PART I and PART II are summarized in this chapter, together with a discussion about the limits of the work and advisable outlook.

[V] **The Appendices** are lists of information that are indispensable to fully understand the work (e.g. boundary conditions, mathematical formulations, additional results, etc.) but removed from the main document for the sake of conciseness and in order to keep the thread of the whole work clear.

Figure 1 schematizes the structure of the work, differentiated in a theoretical part (PART I, see chapter I, p 63) and an application part (PART II, see chapter III, p 167). The investigation method as delineated in Figure 1 is commented in section I - 3, p 55.

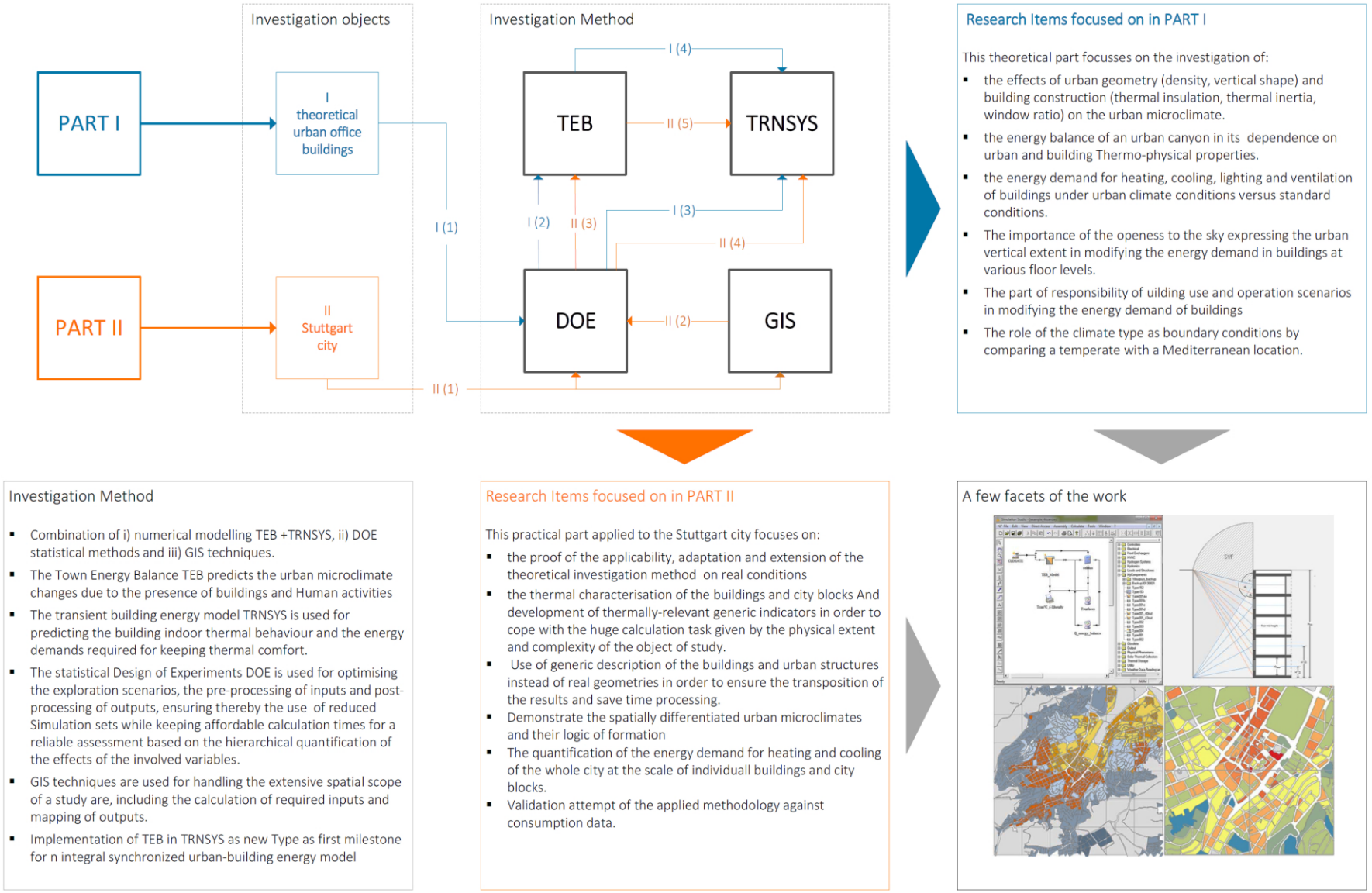

Figure 1: Objectives, method and structure of the work including the theoretical PART I (urban office buildings) and the practical PART II (City of Stuttgart)

2. STATE OF THE ART

This chapter sums up a literature review on the key items addressed in this research. It includes: i) the evolution in time and current technical content of urban climate research, ii) a review on the numerical modelling of climate and energy at urban and building scales, iii) selected findings about the energy performance of buildings explicitly located in urban context, and iv) further background items useful for understanding some choices made in the present work.

2.1. Urban Climate Research

The pioneering work of Howard (1833), followed one century later by Chandler (1965) about the climate of London, revealed that cities experience a different climate, characterised by warmer air, compared to the surrounding countryside. Reams of later studies on various sites have incessantly confirmed this statement (see e.g. Landsberg 1981, Santamouris and Kolokotroni 2016). Meanwhile, urban warming has become a cross-disciplinary well-known fact and urban climatology has emerged as a full-fledged scientific discipline (see e.g. IAUC[8]). The studies on urban climate and more specifically on urban heat island UHI have intensified substantially over the years, providing investigations from most diversified scientific perspectives. The traditional physically-based fundamental research, including phenomena understanding, development of new methods and techniques, data gathering and processing, etc., is being supplemented by applied research which focuses on adaptation and mitigation techniques, or knowledge transfer to planning and design. Societal oriented research centred on human well-being with respect to thermal comfort, air quality and health care as well as works with economical purpose that highlight aspects of energy savings and costs are further integral components in urban climate research. Moreover, multiscale approaches, typically downscaling and upscaling from urban towards building scale and vice-versa, are more frequently observed, and motivated by the will to account for spatial interconnections of climatic effects.

The profusion in urban climate research is clearly visible in the incremental number of published reviews with diversified focus points in an attempt for some sorting (e.g. Asimakopoulos et a. 2001, Arnfield 2003, Kanda 2006, Masson 2006, Oke 2006a, Souch and Grimmond 2006, Roth 2007, Martilli 2014, Santamouris 2016, etc.). These topical reviews illustrate quite

[8] IAUC: International Association on Urban Climate http://www.urban-climate.org/

well the broadening scope as well as the increasing multidisciplinary connections. Likewise, this observation can be made in the thematic overlapping and spatial shifting of the dedicated international conferences on the subject, for instance ICUC[9] from the climate science side and PLEA or IBPSA[10] from the building science side, to name just a few events. Moreover, urban climate research increasingly gains in visibility beyond its community in particular because of its strong connection to climate change and global warming issues (see e.g. Kuttler et al. 2015).

Climate research in both fields of discipline has a lengthy history of over fifty years, however, the interdisciplinary work remains limited because of their different methods, objects of study and goals (Mills et al., 2010). This makes the translation of urban climate research findings into building design poorly implemented (Grimmond et al. 2010a, Mills et al. 2010) in spite of the general claim for its necessity and urgency (e.g. Oke1988a, Arnfield 1990, Mills et al. 2010, Grimmond et al. 2010b).

Urban climatologists first concentrated on the urban heat island (UHI), as major phenomenon that describes the impact of urbanization on the climate. Progressively, they moved towards microscale as the urban geometry, surface and building attributes have been ascertained to be decisive in the formation of the UHI (see e.g. Oke 1982, Arnfield 2003, Oke, 2006a). The focus was then placed on understanding the surface-air energy exchanges between the urban canopy and the overlaying boundary layer, but less on the buildings themselves (Mills et al. 2010). On the contrary, building specialists have been interested for a long time in the effects of environmental factors on buildings, however with insufficient reference to the city as modifying context in relation to the prevailing climate. Nevertheless, rules of thumbs for climate-sensitive urban design have been early disseminated and geometric aspects have also been thematised (e.g. Knowles 1981, Golany 1996, Givoni 1997, etc.), yet these were primarily qualitative and descriptive and rarely focussing on the underlying urban physics. It is only with increasing interdisciplinary collaboration that urban design recommendations have become more argued based on technicalities (e.g. Oke 1988a, Grimmond et al. 2010a).

Technically speaking, the urban climate results from the disturbance of the physical and chemical state of the atmospheric boundary layer due to the presence of three-dimensional physical objects, such as buildings and vegetation. These increase the aerodynamic surface roughness, modify the air flow patterns, substantially alter the shortwave and longwave radia-

[9] ICUC: International Conference on Urban Climate, organised by the IAUC http://www.urban-climate.org/icuc/

[10] PLEA: Conference on Passive and Low Energy Architecture and Urban Design http://plea-arch.org/
IBPSA: International Building Performance Simulation Association http://www.ibpsa.org/

tion fluxes, the surface and air temperatures, air humidity, and bring considerable additional emissions from human-made sources such as traffic, industry, power stations, heating and cooling of buildings (i.e. CO_2, CH_4, NO, NO_2, O_3, etc.). Applied urban climatology addresses two main areas, thermal and air quality. Albeit interacting, the present work focusses on the thermal component.

Technically oriented works seek a better understanding of the physics behind the causality of the phenomena and processes underlying the formation of the urban climate. In this respect, matters of interest cover every issue known to be of influence on one or more terms of the urban energy balance (see next section), that is affecting the net all-wave radiation and the resulting fluxes for turbulent sensible and latent heat as well as storage and advection heat fluxes. The studies typically focus on:

i) the radiative, thermal and aerodynamical effects of the three dimensional urban structure (i.e. aspect ratio, sky view factor, roof plan density, urban layout, building arrangements, etc.),
ii) the thermal and energetic properties of the urban surfaces (impervious or not, shortwave reflectance, longwave emissivity),
iii) wind drag effects due to increased urban roughness given the typical vertical city extension, and urban ventilation through the urban structure,
iv) provision or lack of green and water in connection with their impacts on the ratios of sensible and latent heat fluxes, and
v) the quantification and effects of the anthropogenic heat release from diverse sources.

Obviously, the notion of spatial scale is crucial when addressing all these matters. The urban atmosphere consists vertically of several layers (see Oke 1988b). The urban canopy layer (UCL) is the layer from the ground surface to about the building roof level. In this layer, microclimates take place caused by site characteristics. The urban boundary layer (UBL), conditioned by local and mesoscale effects, takes place above the UCL and evolves up to a limit where urban effects become negligible. The urban boundary layer subdivides upwards into a roughness layer, a turbulent surface layer and a mixing layer. Temporally, the urban effects in the UCL are strongly coupled with the sun course, therefore, the urban microclimate is better understood by considering daily rhythms and time steps of an hour or less.

The most characteristic phenomenon of the urban climate is certainly the urban heat island UHI, which expresses the air temperature difference between the urban area and the rural surroundings. Meanwhile, decades of research have clarified many features of the UHI as enumerated by Oke (1982) and mostly confirmed by Arnfield (2003) as follows. The UHI is

greatest at night when the stored heat is discharged. It increases with decreasing wind (still air conditions) thereby preventing or retarding the heat released to be transported away. The UHI is higher in the warm half of the year because of more solar radiation received, absorbed and transformed. It also rises under fine weather conditions with clear sky because of a lower nocturnal cooling in contrast to the rapid cooling of the free horizon countryside. The UHI tends to increase with increasing city size and/or population due to the production of additional heat by urban activity and with increasing city density because of more heat storage.

Yet, beyond these general findings, the UHI has been reported from experimental studies to be much diversified depending on the geographical location, climate type, weather conditions, structural city attributes in terms of size, density, population, activities, etc. Santamouris (2016) with further reference to Santamouris (2007, 2014a and 2015) provides an extensive list of measured data of urban heat island from the early fifties up-to-date for cities worldwide. Typical UHI values lie around 3 to 5 K but a maximum UHI of 12 K was reported for Athens and Lodz. In spite of the generally admitted and partly confirmed causes of the urban heat island, the large scope of UHI intensities, times of occurrence and spatial distribution observed call for caution by generalisations. For instance, an approximate constant UHI value as suggested e.g. by Pültz and Hoffmann (2007) or the simplified adjustment procedure of air temperature based on city size and density as suggested in the updated TRY (DWD 2011) for use in building engineering is too rough to be helpful. Instead, timely and spatially differentiated data, as focused on in this research, are necessary for a later use at building scale.

The increasing awareness for the existence and consequences of the urban climate on resources and people are also visible in the overarching discourse about urban sustainability. Criteria-based systems for the assessment of sustainable urban development (e.g. CASBEE, LEED and DGNB) dedicate progressively more assessment criteria to urban climate and climate change. Figure 2 schematizes a handling concept by pointing out causal-effect dependences within the new system CAMSUD. In CAMSUD, the climate change and urban climate are allocated for the first time a stand-alone main category (see Ali-Toudert and Ji 2017).

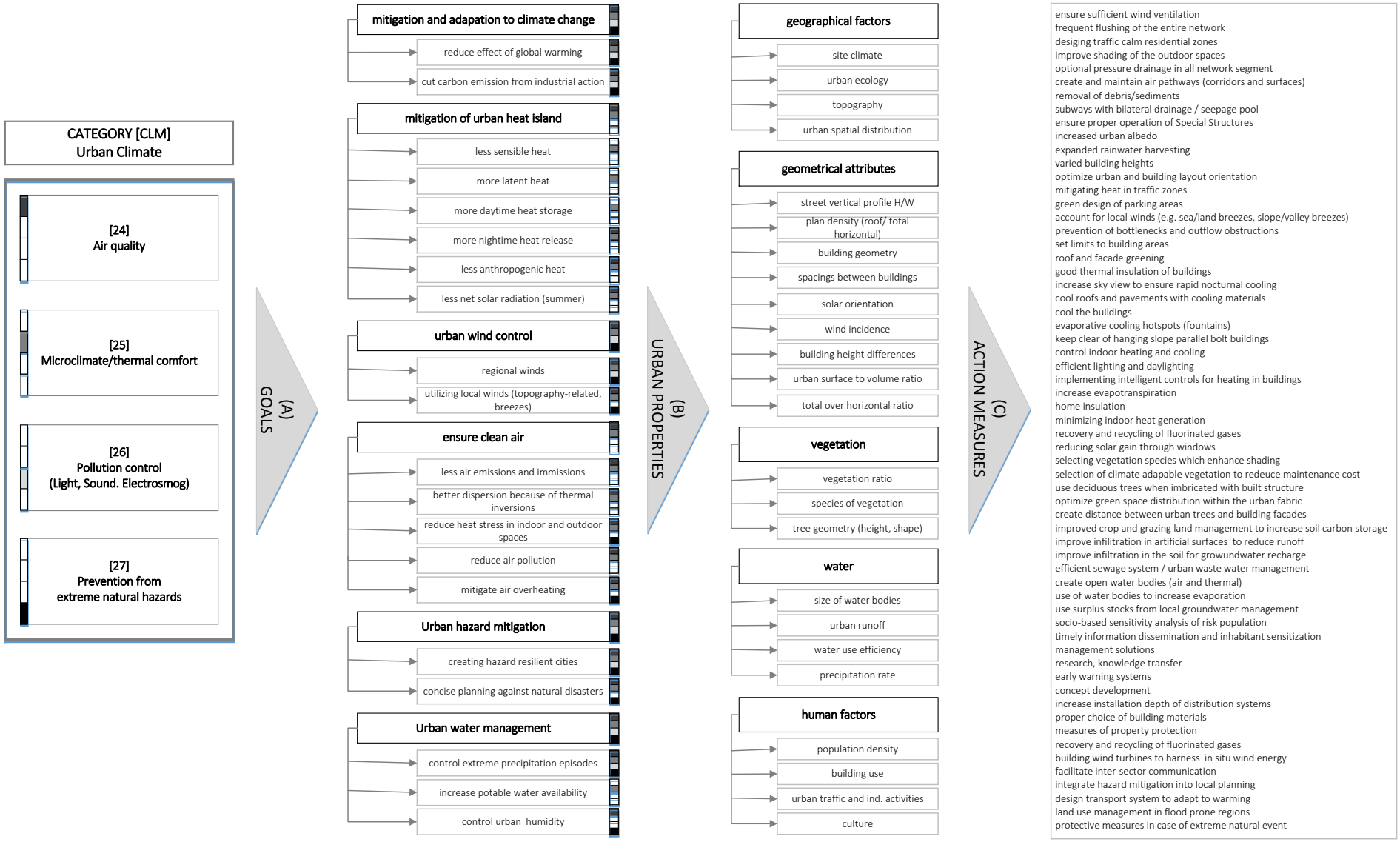

Figure 2: Handling of the urban climate issue as topical category in the urban sustainability assessment system CAMSUD

2.2. The Urban Canyon Energetics and Microclimate

The urban energy balance is the key to understand the mechanisms underlying the formation of the urban climate and microclimate. Oke (1988b) gives the equation as follows:

$$Q^* + Q_F = Q_H + Q_E + \Delta Q_S + \Delta Q_A \quad (1)$$

The all-wave net radiation Q^* and the anthropogenic heat Q_F are balanced by the turbulent sensible and latent heat fluxes Q_H and Q_E, respectively, by the heat storage in the urban fabric (ΔQ_S) and possible horizontal advection (ΔQ_A). The last term of advection is often assumed negligible for a system embedded in a homogenous environment. The net all-wave radiation Q^* writes as:

$$Q^* = Q_{SW}^{\downarrow} + Q_{SW}^{\uparrow} + Q_{LW}^{\downarrow} + Q_{LW}^{\uparrow} \quad (2)$$

Where $Q_{SW}^{\downarrow}$ is the incoming and $Q_{SW}^{\uparrow}$ the reflected shortwave solar radiation, $Q_{LW}^{\downarrow}$ and $Q_{LW}^{\uparrow}$ are the incoming atmospheric longwave and outgoing surface heat radiation, respectively. Appendix 1 gives the calculation procedure of the urban energy balance as handled by the TEB model, used in this research.

Table 2 decrypts equation (2) and gives an overview of examples on possible natural and human-made modifying factors, partly based on Oke (1982). Evidently, the urban fabric strongly affects the formation of the urban climate. Therefore, building design, urban design and planning decisions all condition the formation, temporal rhythm and spatial distribution of the urban climate and microclimates as sketched in Figure 2. With reference to the physical phenomena in Table 2, Ali-Toudert (2007c) proposed the following conceptual categories for a climate-sensitive urban design: openness to the sky (solar and sensible thermal), urban porosity (wind), directionality of urban layout (solar and wind), building envelope (solar, thermal, wind) and green and water (latent thermal).

The urban canyon, usually described as aspect ratio or height-to-width ratio (H/W) describes a 3D volume delimitated by a street flanked by a continuum of aligned buildings. The street needs to be long enough to perform as a canyon, i.e. with minimal lateral effects (see e.g. Oke 1988a). The urban canyon has been widely considered as the structural unit for describing an urban structure in a simplified manner. Therefore, most studies at the urban canopy layer UCL have extensively dealt with the energetics of the urban canyon.

Table 2: Urban energy balance terms and their dependence on natural and human-made factors

symbol | item		Urban and climate feature	modifying process and urban effect
$Q_{SW}^{\downarrow}$	incoming ↓ shortwave solar radiation	sun, cloud cover canyon geometry	The 3D geometry of the urban structure captures more solar radiation because of more receiving surfaces and more multiple reflections between the canyon facets. Deep canyons lead to more differentiated sub-spaces of shade and sun exposure depending on the sun position given by the site location, time of day and solar orientation. The cloud cover is decisive in the share between direct and diffuse solar radiation.
$Q_{SW}^{\uparrow}$	outgoing ↑ shortwave solar radiation	albedo or SW reflectance	The absorption versus reflection of the global solar radiation received at the surface depends on the albedo, which depends inter alia on the surface colour, texture and solar incidence.
$Q_{LW}^{\downarrow}$	incoming ↓ longwave radiation	pollutants sky view factor	The absorption of SW and re-emission as LW radiation increases with air pollution (gas, particles and aerosols). The sky view factor of an urban surface weights the amount of LW radiation received.
$Q_{LW}^{\uparrow}$	outgoing ↑ longwave radiation	sky view factor emissivity	The emissivity and sky view of the surfaces decide on the rate of longwave heat release. The heat available for release depends on the surface temperatures governed by their degree of sun exposure and thermal mass of the material.
Q_F	anthropogenic heat release	traffic industry buildings	Possible sources are heat waste from motor traffic, industry, power stations, HVAC systems in buildings as well as transmission heat losses through the building envelope.
Q_H	turbulent sensible flux	canyon geometry wind speed airflow sun exposure	The sensible heat flux is potentially higher due to more surfaces given the 3D urban geometry. It depends on the airflow at the surfaces. The reduced wind speed reduces the amount of convective heat released to air. The potential of available heat to be transported to the air depends on the sun exposure and on the thermal properties of the urban surfaces and materials, which affect the absorption and storage of solar radiation.
Q_E	turbulent latent flux	water vegetation paved surfaces urban activity	The absence of green and water means a lack of water evaporation and evapotranspiration and hence less latent heat. Impervious surfaces imply fast drainage of precipitation and reduce water availability as well. Additional water vapour due to urban activity may increase the latent heat.
ΔQ_S	heat storage	building materials canyon geometry	More storage in the urban fabric is fostered by the thermal mass of urban and building materials (heat capacity, mass density). The heat storage increases in urban context due to more surfaces induced by the 3D urban structure.
ΔQ_A	advection	wind thermal gradient	Lateral thermal effects leading to air displacement support advective heat flow but is prevented by the presence of obstructions to wind flow. In homogenous environment, it is generally neglected.

Based on field measurements, Nunez and Oke (1977) provide a good synopsis of the urban canyon energy balance as daily cycle and show the interdependences between the various fluxes for a unity-like north-south NS oriented canyon in Vancouver (see as well Oke 2006b). Yoshida et al (1990) report on a similar field investigation for an east-west canyon EW. These works clearly demonstrate that the solar exposure of the canyon facets is decisive on the heat fluxes observed at the surfaces and hence on the surface and air temperatures. Moreover, Nakamura and Oke (1988) show the impact of the surface radiative and heat fluxes on the air temperatures in detail at a half-meter distance and across a canyon throughout the day for a similar canyon shape oriented EW in Japan. The surface temperatures are strongly correlated to solar exposure whereas the air temperatures are comparatively less affected due to air mixing except close to the surfaces. The difference between surface and air temperature in the shade do not exceed 5 Kelvin, whereas this difference easily reaches 30 K in the sun.

The aspect ratio also decides on the resulting wind flow regime in-canyon, either isolated, interfering or skimming (see Oke 1988a). Wind incidence parallel to street axis and shallow streets better promote urban ventilation than perpendicular incidence and deep canyons. A double counter circulating vortices can take place in very deep canyons. Oblique direction improves the wind flow within the urban fabric, further supported by lateral and frontal spacing between buildings. Wind flowing at some angle with respect to street axis offers a better potential for indoor ventilation than a perpendicular or parallel wind incidence because of higher pressure differences between the opposite façades.

In a previous research, the author dealt extensively with the microclimate within an urban canyon in relation to outdoor thermal comfort using the ENVI-met numerical model (Ali-Toudert 2005, Ali-Toudert et al. 2005, Ali-Toudert and Mayer 2006, Ali-Toudert and Mayer 2007a and 2007b). The study demonstrates the dependence of the canyon air temperature on the aspect ratio, solar orientation, canyon shape and the presence of green. The optimal depth of a street canyon H/W for ensuring thermal comfort depends on the solar orientation, which emphasizes the importance of the canyon geometry. An EW street axis allows better penetration of the solar radiation in the canyon volume, whereas NS streets are mostly exposed around noon. The pertinence of a symmetrical or asymmetrical street profile depends on the sun path and so on the solar orientation as well (Ali-Toudert and Mayer 2017b). Moreover, Ali-Toudert and Mayer (2007a) recorded the shortwave and longwave irradiations coming from different directions as captured by a pedestrian within an EW canyon in Freiburg. The mean radiant temperature, which sums up this radiant environment appears to be much more influenced by the exposure and shading patterns than the air temperature, thereby affecting in

first instance the thermal sensation of comfort or discomfort (see also Ali-Toudert et al. 2005). Beside these findings about the best geometrical choices for avoiding outdoor heat stress in the summer, the work also pointed out possible seasonal conflicts between the need for solar protection in the summer outdoors, favoured by narrow streets, and solar access in the winter indoors, better reachable with wide streets. The present work is, therefore, in continuity with that study by addressing the critical issue towards finding a compromise solution.

2.3. Urban and Building Energy Modelling

As justly noticed by Arnfield (2003), numerical modelling in urban climate research is growing in popularity for its perfect suitability to dealing with the complexities and non-lineairites of urban climate systems, difficult to capture with field measurements. In principle, it is possible to differentiate between three categories of models:

i) Urban models which exclusively consider the urban atmosphere and where the buildings are considered as boundaries to the system,
ii) Models which focus on the urban energetics but explicitly include a more or less simple building model and for which the indoor energy balance is also solved,
iii) Building models which are primarily concerned with the indoor energy balance, and in which the urban surroundings are included with variable level of detail, but mostly limited to the geometric modelling of the surroundings as obstructions to solar radiation.

In each category, the modelling concepts are evolving towards more comprehensiveness and synergies are observed between them. In the following, various models at the interface between urban and building scales are introduced and compared in their concepts, capabilities and limitations.

2.3.1. Urban Surface – Atmosphere Models

Much diversified urban surface – atmosphere models do exist and they differ in complexity level, targeted applications, data and computer processing needs. When modelled, the urban surface is defined variably according to its morphology (either 2D or 3D), type of surface cover, spatial scale, additional anthropogenic sources of heat, of water, etc. The possible application range from mesoscale modelling, global climate modelling, air quality, heat island studies, upper boundary conditions, energy assessments, weather forecasting, which deal with one or more layers of the atmosphere, i.e. urban canopy, surface layer, boundary layer, etc. (e.g. Arnfield 2005, Arnfield 2006, Grimmond et al. 2009).

To gain more clarity around this issue, a research project (Grimmond et al. 2009, Grimmond

et al. 2010b and Grimmond et al. 2011) undertook an intercomparison of available urban-atmosphere exchange models, and seek to answer the following methodological questions:

- What are the main physical processes that need to be resolved for a realistic simulation of the urban energy balance exchanges?
- How complex does a model need to be and which parameter information is required in order to produce a realistic simulation of urban surface fluxes and temperatures?
- Do these models produce realistic physical simulations of urban heat exchange?
- How do the models perform in terms of cost (computer time and data requirements) and benefit (improved model prediction)?

The outlook was to identify the main priorities of the field research in order to gather the correct variables at the correct scales for model evaluation.

In the run-up to this investigation, Grimmond et al. (2009) extensively reviewed a large number of urban surface models which predict the energy balance fluxes and further useful output key metrics like temperatures and wind speed. The models cover a wide range of concepts for representing the urban environment, i.e. in increasing complexity as bulk, single-layered or multi-layered. These models either include vegetation or not, i.e. are dry or include latent heat from evapotranspiration, with the vegetation being integrated in the model as interacting with other fluxes or taken as separate tile. The urban surface might be described as a whole canyon unit or differentiated after facets (roof, walls, road), with or without specified orientation (sunlit vs. shaded). The parameters describing the built form also vary greatly between the models (geometry like H/W, surface radiative properties, materials thermal properties, etc.). The anthropogenic term is variably specified, either as fixed internal temperature and traffic counts or as input per time step. The input describing the boundary climate conditions are variable from one model to another, in particular the wind direction is ignored in some models, input to turbulence are seldom, either because they are calculated by the model or simply parameterized. The shortwave and longwave radiation are differentiated variably in direct and diffuse components, and information to soil temperature and soil humidity varies in detail.

Grimmond et al. (2010b) reports on Phase 1 of this intercomparison. It includes 33 urban surface energy balance models, which all run in offline mode to avoid additional boundary effects resulting from a coupling with upstream atmospheric models. The task was a comparison with one set of field measurements for Vancouver. The authors reported evidence that some classes of models perform better for individual fluxes but no model calculates all fluxes with the same accuracy. Statistically, the simpler models mostly perform as well as the more complex models. The best overall performance of all schemes is found generally for the net

all-wave radiation and least capability for latent heat flux. In phase 2 of that project (Grimmond et al. 2011), the intercomparison was based on increasing levels of information provided in successive four stages: 1) forcing data and site information only, 2) basic surface cover fractions, 3) urban morphology and 4) urban material characteristics.

To summarize the findings: a wide range of performance per flux is found and no model is overall better. This clearly affects the applicability of the models including vegetation or not with important impact on the latent heat flux. This study also reveals that increasing complexity does not necessarily improve performance. Simple and complex models performed better than medium-complex models. The authors conclude by advising caution in applying any urban land surface model since no model performs well across all fluxes and name an ensemble approach as a conceivable alternative.

Available urban surface models have diversified concepts and physical basis but show many similarities, and some of them are partly inspired from each other as illustrated in Figure 3 and explained below. It is worth mentioning that the TEB concept appears to have often served as a basis to new models or as part of coupled models with larger scope. Kusaka et al. (2001) proposed an urban canopy model similar to Masson's (2000) model but explicitly includes solar orientation and diurnal solar azimuth angle and with the possibility of considering several canyons with different orientations. Sunlit and shaded parts of the canyon are hence explicitly differentiated. Martilli et al. (2002) developed a scheme named urban canopy parameterization UCP (or BEP: building effects parameterization) to represent the impact of urban buildings on airflow in mesoscale atmospheric models where buildings effects are parameterised per grid-averaged variables. The model includes the building density as function of height. Kikegawa et al. (2003) and Kondo et al. (2005) combined three self-developed models to account for mesoscale MM (Kondo 1995), a 1D urban canopy CM (Kondo and Liu 1998) and a building BEM model (Kikegawa et al. 2003). Oleson et al. (2008) developed their CLMU model following TEB and coupled it with the vegetation Community Land Model CLM3 of Dickinson et al. (2006). Salamanca et al. (2010) proposed a BEM model that aims at investigating the interactions between urban climate, air pollution and energy consumption including the heat generated by buildings in the urban environment. The model is coupled upstream with the mesoscale BEP of Martilli et al. (2002). It mostly consists of an ideal building representative of all buildings within a grid cell based on the Kikegawa et al. (2003) model with some difference in the computation of the solar radiation coming into the building, the treatment of the windows and the computation of the heat gained or released for cooling and heating purposes. The model includes the natural ventilation, the heat release originating from

occupants, equipment and air conditioning. By contrast, to the 2D models mentioned above, Kanda et al. (2005a and 2005b) proposes a 3D urban canopy model, with the conventional heat transfer expressed as network of resistance as used by Masson (2000) and Kusaka et al. (2001). Marcciotto et al. (2010) also refer to TEB in developing their urban canopy model UCM, which handles the walls separately, and is further coupled with a one-dimensional vertical turbulence transport model.

Table 3 compares a number of urban canopy models in more detail and highlights their similarities and differences in their main features and the conceptualized complexity of urban climate modelling. Exemplarily Appendix 2 puts side by side two urban canopy models, ENVI-met (Bruse and Fleer 1998, Bruse 1999, ENVI-met 2017) and TEB including subsequent updates and shows their points of convergence and divergence, and their ability or not to be coupled with building scale models. Positive sign means favourable feature versus negative sign for less favourable feature. The +/- sign means the feature is partly useful. The description in Table 3 is partly taken from Grimmond et al. 2010b).

Because this research uses TEB, the successive updates are shown in Figure 3 and Table 4 and briefly recalled hereafter. Hamdi and Masson (2008) replaced the simple layer scheme in TEB by a multi-layered SBL scheme following the methodology described in Masson and Seity (2009) where a drag force scheme, inspired from vegetation models, is included according to Martilli et al. (2002). It accounts for the vertical effects of the buildings, yet considering one surface energy balance i.e. without vertical differentiation of the heat fluxes. The authors reported an improvement inter alia in the prediction of the wind speed, turbulent heat flux and air temperature. Lemonsu et al. (2012) includes in TEB the solar orientation of canyon axis (road and walls) so that the energy balance differentiates each wall. Moreover, modelling a fraction of garden inside the canyon is added using its own vegetation energy balance as alternative to its connection to ISBA in SURFEX. A new Building Energy Module (BEM) developed by Bueno et al. (2012a) replaced the former simple building. For a better modelling of the internal building energy balance, the walls are no longer opaque but include windows and their solar protections, building and floor mass are added as well as HVAC systems. The ventilation schemes can be either natural (open windows) or mechanical (HVAC). After comparing the results of this BEM against those of the dynamic building energy model EnergyPlus, Pigeon et al. (2014) improved further features.

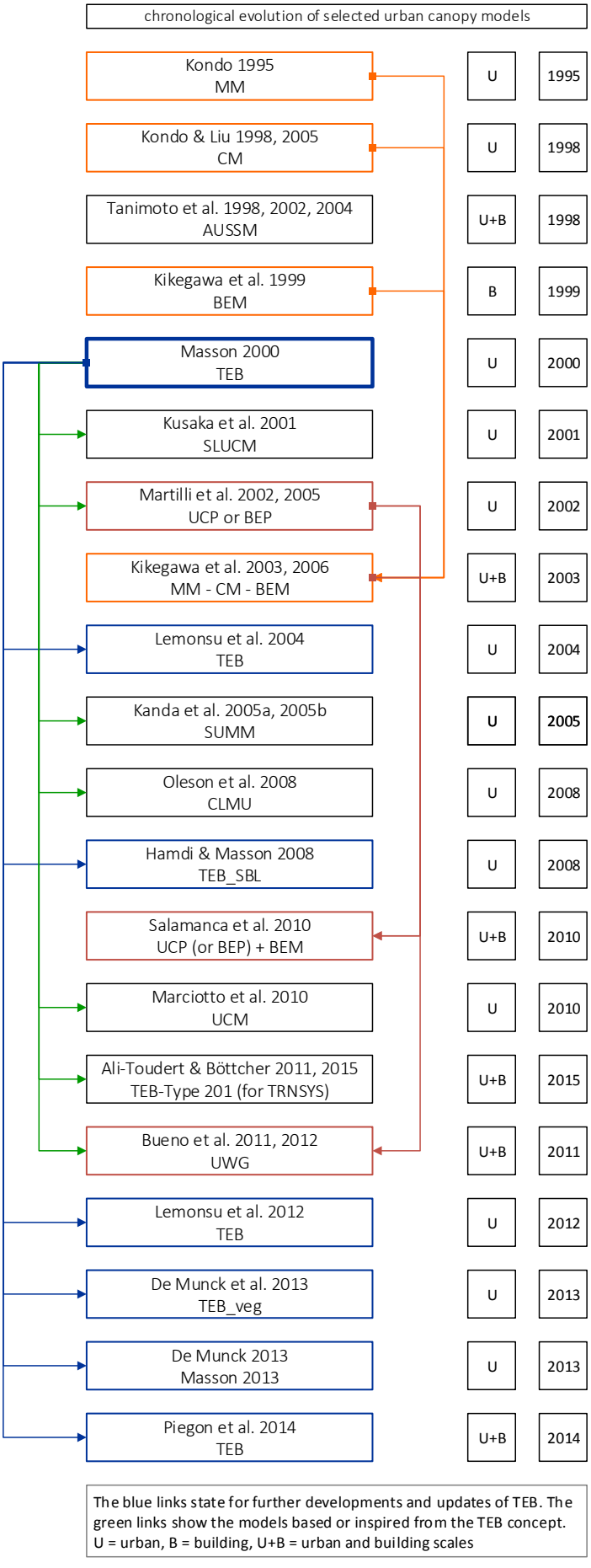

Figure 3: Similarities in the physical background of urban surface – atmosphere models

Table 3: Comparison of some key features describing a selection of urban canopy models

Scale: Mesoscale M, urban U, B Building
Dimensions: 1D, 2D, 3D
Vertical Layering: single SL, multiple ML
SW and LW Reflections: one O, multiple M, infinite I
Orientation included: yesY, no N
Turbulence included: yes Y, no N
Vegetation: not included N, as separated tile ST, integrated I
Latent heat included: yes Y, no N (water and/or snow)
anthropogenic heat: none N, fixed F, variable V
Building Height: constant C, variable V

ID	author	year	acronym	**scale** mesoscale M, canopy C, building B			**dimension** 1D, 2D or 3D			**vertical layering** single SL, multiple ML		**SW & LW reflections** one O, multiple M, infinite I			**solar orientation**		**turbulence** included as model M, simply parameterized P		**vegetation** not included N, as separated tile ST, integrated I			**Soil** included as sub-model Y, no N		**Latent heat (water)** included yes Y, not included N		**anthropgenic heat** none N, fixed F, variable V			**building height** constant C, variable V		**urban and building heat storage** included yes Y, not included N	
				M	C	B	1D	2D	3D	SL	ML	O	M	I	Y	N	M	P	N	S	I	Y	N	Y	N	N	F	V	C	V	Y	N
1	Mills	1993	-		■			■					■			■							■		■	■			■		■	
2	Kondo and Liu	1998*	CM	■	■		■		■		■		■		■				■			■		■		■		■			■	■	
3	Bruse	1999	ENVImet		■				■		■	■			■		■					■	■		■				■	■			■
4	Masson	2000	TEB		■			■		■				■		■		■				■	■		■			■	■	■		■	
5	Kusaka et al.	2001	SLUCM		■			■		■			■		■			■				■		■		■	■				■	■	
6	Martilli et al.	2002	BEP	■	■			■			■				■			■				■		■		■	■				■	■	
7	Kikegawa et al.	2003	MM-CM-BEM	■	■	■	■		■	■		■				■						■	■		■				■	■		■	
8	Chimklai et al.	2003	AUSSSM TOOL		■			■			■					■		■	■			■		■				■				■	
9	Bozonnet et al.	2005	-		■		■					■			■				■				■		■	■			■		■	
10	Kanda et al.	2005	SUMM	■	■				■	■			■		■			■			■		■		■	■			■				■
11	Hamdi and Masson	2008	TEB_SBL	■	■		■			■			■		■			■	■				■		■		■		■		■		
12	Oleson et al.	2008	CLMU		■		■	■		■			■		■			■			■	■		■			■			■	■		
13	Salamanca et al.	2010	BEP + BEM		■	■	■				■						■				■		■		■		■	■	■		■		
14	Marciotto et al.	2010	-		■		■				■		■		■		■		■				■		■	■			■		■		
15	Bueno	2010	UWG	■	■			■	■				■		■		■				■	■		■				■		■	■		
16	Bouyer et al.	2011	FLUENT + SOLENE		■	■			■	■						■	■			■		■			■	■					■		
17	Huttner	2012	ENVImet 4.0		■	■	■		■		■		■		■		■				■	■			■	■				■	■		
18	De Munck et al.	2013	TEB_veg	■	■	■			■							■	■		■				■		■			■		■			■
19	Pigeon et al.	2014	TEB	■	■	■		■	■	■	■		■		■			■	■				■		■		■			■			■
20	Ali-Toudert and Böttcher	2015	Type 201		■	■		■		■			■			■		■	■				■		■			■	■	■		■	

Nota: Only references of first publications are named. Updates and further publications are ignored here for sake of conciseness. (*) paper of 2005 used.

De Munck et al. (2013) added the modelling of green roofs as a particular form of vegetation. De Munck (2013) added the possibility of irrigation of green roofs, gardens and watering of roads as well as possible solar panels (thermal or PV). TEB model has been evaluated on numerous real sites, such as for Mexico City and Vancouver (Masson et al. 2002), for Marseille (Lemonsu et al. 2004), for Lodz (Offerle et al. 2003) and Paris (Pigeon et al. 2014). Colombert (2008) did further theoretical work for Paris.

The present research adds to these works by proposing a version of TEB for use under the TRNSYS environment, which allows the adjustments of the urban microclimate prior to building energy modelling. Section II - 5 (p 157) describes the new TEB-Type 201.

Table 4: Selected references dealing with the development, updates and application of TEB

reference	year	issue related to TEB (*)				issue addressed
		name	D	R	A	
Masson	2000	TEB (1)	✓			First release of TEB
Masson et al.	2002	TEB (2)	✓		✓	Mexico city, Vancouver
Offerle et al.	2003	TEB			✓	Lodz
Lemonsu et al.	2004	TEB (3)	✓		✓	Marseille
Hamdi and Masson	2008	TEB_SBL	✓			multilayer scheme
Colombert	2008	TEB			✓	Paris (theoretical)
Lemonsu et al.	2006	TEB			✓	Marseille
Lemonsu et al.	2010	TEB			✓	Montreal
Lemonsu et al.	2012	TEB (4)	✓			solar orientation, garden fraction
Bueno et al.	2011	TEB + EnergyPlus		✓		Coupling of TEB and EnergyPlus
Bueno et al.	2012a	BEM	✓			new BEM for TEB
Bueno et al.	2012b	UWG			✓	Based on TEB concept
Hamdi et al.	2012	TEB			✓	Brussels
De Munck et al.	2013	TEB_veg	✓			green roofs
De Munck	2013	TEB_veg	✓			irrigation and solar panels
Hamdi et al.	2014	TEB	✓		✓	Brussels
Pigeon et al.	2014	TEB	✓		✓	BEM update, Paris
Ali-Toudert and Böttcher	2015	Type 201		✓		TEB as Type 201 in TRNSYS
(*) D: development and update of TEB numbered in brackets, R: re-use in another form, A: application to real case studies.						

2.3.2. Urban – Building Energy Models

Robust calculation tools, which address the outdoor – indoor interdependences, i.e. which link between the thermally related physical processes occurring in the external urban atmosphere and those occurring in the internal spaces, are rare and still in development. This largely explains the relatively limited studies that focus on building energy modelling with explicit consideration of urban boundary effects.

However, some convergence between the two modelling scales can be currently observed: Urban climate models try to describe the building as a dynamic thermal boundary with better description of the thermo-physical properties of its envelope and by dynamic indoor temperatures instead of stationary indoor boundary conditions.

One explanation of lacking urban-building coupled models is that urban climate models as well as building energy models vary substantially depending on their i) physical basis, ii) scope, iii) temporal and spatial resolution and hence on their iv) inputs and final outputs. All of which are decisive in their ability or not to be coupled in one calculation tool. Urban canopy models are typically developed within the disciplines of urban climatology or geo-informatics, whereas building energy models are normally target object of building physics. The direct consequence is that the findings capitalized in urban climatology in understanding and modelling the energetics of the urban atmosphere mostly remains ignored in building physics' applications. Inversely, the in-depth level of detail reached in building modelling (e.g. detailed depiction of the building elements, multi-zoning, advanced HVAC settings, non-stationary modelling, large simulation periods, etc.) fails in urban canopy models. The former one considers the building envelope as boundary, mostly as one single thermal zone assumed to be in comfort range, whereas the latter considers the outdoor boundary conditions as known and corresponds to the information provided by standard weather stations or climate generating software.

Nevertheless, the issue has progressed meanwhile and some convergence between the two modelling scales can be currently observed. Because of the scale interdependences (meso, local and micro) and depending on the focus privileged, there are several ways for conceiving urban-building energy models in the literature. In this respect, Bueno (2012) interestingly provides different conceptual approaches for solving the same question of improving accuracy in predicting the urban climate effects in view of use in building science. Each concept decides on the extent of the system (e.g. urban canopy or mesoscale) and the level of detail of its parts (e.g. simple or sophisticated building model) and on the feedback loops between these parts (e.g. mesoscale and canopy, canopy and building).

A number of research initiatives can be mentioned which follow the goal of developing urban-building coupled models (coded U+B in Figure 3). For instance, there is the urban weather generator UWG using TEB including an improved building model (Bueno 2010, Bueno et al. 2012b), EnergyPlus combined with TEB (Bueno et al. 2011), the coupled BEM - Solene - Fluent model (Bouyer 2009, Bouyer et al. 2011), the BEP-BEM model (Salamanca et al. 2010), the AUSSSM model (Tanimoto et al. 1998, Chimklai et al. 2003, Tanimoto et al. 2004), The MM-CM-BEP model (Kikegawa et al. 2003), the airflow zonal model of Bozonnet et al. (2005), or the latest developments of ENVI-met 4.0 (Huttner 2012, ENVI-met 2017).

The concepts targeting this urban – building linkage can be distinguished in top-down and bottom-up concepts. Top-down concepts apply for surface energy balance models, which attempt to provide a better description of the urban areas as 3D structure to overcome the inaccuracy of a simple parametrization of a 2D urban surface. Urban canopy models try to include the building as a thermally dynamic boundary with better description of the thermo-physical properties of its envelope and by assuming dynamic indoor air temperatures instead of constant indoor thermal conditions (Kikegawa et al. 2003, Salamanca et al. 2010 and Bueno et al. 2012a). The building seeks to reproduce the main processes of its operation while keeping a rather simple description (simple geometry, multi-layered building elements, heat gain sources, HVAC, etc.). The energetic processes taking place between the buildings and the atmosphere is better included (e.g. Masson 2000, Kusaka et al. 2001, Martilli et al. 2002 and Bueno et al. 2012c). In addition, the waste heat from the buildings is dynamically included in the urban energy balance (e.g. Chimklai et al. 2003, Kikegawa et al. 2003 and Salamanca et al. 2010). In this case, the building as physical object and its operation are generally kept simple, within one single or few thermal zones.

By contrast, bottom-up approaches apply to those models focusing first on the building as complex and seeking to extend its boundaries to include the surrounding built environment and atmosphere (e.g. Bueno et al. 2011). In this case, powerful in-stationary building energy models are used in connection upstream with an urban canopy model. The present work belongs to this second category and proposes a new implementation of TEB in the building energy model TRNSYS, similarly to Bueno et al. (2011) who embedded TEB in Energy Plus (see section II - 5, p 157).

Another modelling approach on the subject is the one including computational fluid dynamics CFD methods. The review of Georgatou and Kolokotsa (2016) CFD urban climate models shows that the building is rarely included and the focus is placed on outdoor space. Yet, alt-

hough rarely used because of the high processing times, some attempts do exist. For example, ENVI-met proposes a 3D interface in its fourth version by means of which the building as thermal zone can be modelled more accurately e.g. as multilayer building elements including heat storage (Huttner 2012). However, the simulation focusses on a daily cycle and not on long periods as often requested in building energy modelling where both heating and cooling seasons have to be assessed. Bouyer et al. (2011) integrated a self-developed building thermal model as sub-model in the urban thermo-radiative model Solene, which was then coupled with the CFD Fluent. In order to save calculation time also judged high by the authors, the resolution of momentum, continuity and turbulence equations are disabled after initialisation and the velocity and turbulence fields are computed only once with the assumption of wind forced convection only. The authors report that the solar irradiance is the most influent parameter on the building energy consumption and point out the necessity of a detailed simulation of infrared radiative and convective fluxes.

Allegrini (2012) coupled CFD, radiation and building energy models for the study of the urban heat fluxes. The choice of this approach was motivated by the highly spatially resolved temperature and flow fields including turbulence and convective heat fluxes. In an application, Allegrini et al. (2015) investigated the effects of wind driven ventilation combined with various building geometries organised in six generic urban morphologies on heat fluxes in order to optimize the design of urban areas in terms of heat removal, hence as efficient way for mitigating the urban heat island. Allegrini et al. 2016 studied the impact of radiation exchange between buildings in urban street canyons on space cooling demands of buildings. The authors underlined the time costs of the CFD approach.

2.3.3. Building Energy Models

Optimising buildings in view of energy efficiency relies inevitably on numerical modelling. This practice is better established and more advanced than the simulation of urban canopy climate. There are two types of numerical energy models for buildings: the stationary and non-stationary ones. The stationary models are generally fast and easier to operate because they are less demanding in terms of expertise as these mostly rely on predefined boundary conditions, usually given by standards in force, and made ready to use in “pre-formatted” software. Accordingly, the pre and post-processing times are relatively short. In Germany, for instance, the energy saving act EnEV is the first reference framework, technically implemented by the DIN V 18599, as well. It gradually replaces the DIN 4108. Available software like Energieberater (Hottgenroth 2017) or IDF (Fraunhofer 2017) provides a user-friendly inter-

face based on these standards. The aim of such programs is to help fulfil the mandatory requirements of energy performance. Another example of a stationary calculation aid developed in Germany is the PHPP program, which is somehow different as it seeks to implement the passive house (Passivhaus) as a particular energy efficient building concept (Passivhaus 2017).

Non-stationary or the so-called dynamic methods, by contrast, are more powerful in terms of energy optimisation capabilities but at the same time more challenging because they demand for technical expertise and processing time. Dynamic programs for building energy simulation are complex because of numerous interacting considerations; they include:

1. Detailed physical and thermal attributes of the building.
2. HVAC operation scenarios, from simple to complex schemes.
3. Usage patterns and human behaviour in relation to thermal comfort preferences.

While simple tools may suffice at early design stages, ones that are more sophisticated are required at advanced stages for optimised design. Non-stationary methods are typically advisable for large-scale building projects where detailed calculations can lead to substantial energy savings in comparison to simplified procedures and for research purposes where the focus is put on understanding the physics behind the results.

Crawley et al. (2005 and 2008) mentioned a large number of available comparative studies of existing tools and provided themselves with an extensive review of twenty major building energy simulation programs. They pointed out the difficulty of the comparison because of the absence of a common language to describe what the tools could do. This applies for instance to the nuances of a capability, since this might have several levels.

2.4. Energy Performance of Urban Buildings

The performance of buildings specifically located in urban areas and accounting for modified climate boundary conditions has been partly addressed. The focus is mainly put on the effects of the urban heat island (UHI) and climate change. The discussion on the degree of validity of standard climate data in urban areas is one main issue that has grown in the last few years and the general claim is thereby a necessary adjustment of this information. These investigations are conducted from different perspectives, including:

i) the impact of the UHI on air conditioning loads and electricity consumption in buildings (e.g. Hassid et al. 2000, Santamouris et al. 2001, Papadopoulos 2001, Santamouris 2014b, Santamouris et al. 2015),
ii) the impact of the UHI on the heating or cooling degree days (e.g. Christenson et al.

2006, Kikegawa et al. 2006, Papakostas et al. 2010),

iii) the impact of the UHI on heating and/or cooling indoor energy consumptions or demands (e.g. Santamouris et al. 2001, Frank 2005, Kolokotroni et al. 2006, Ihara et al. 2008, Vidrih and Medved 2008, Papakostas et al. 2010, Kolokotroni et al. 2012),

iv) the effects of the urban density on sunlight and daylight potentials (e.g. Li et al. 2006, Li and Wong 2007; Strømann-Andersen and Sattrup 2011),

v) the variation of ambient urban air temperature according to climate change models (e.g. Belcher et al. 2005, Jentsch et al. 2008),

vi) proposals for the adjustment of the test reference years to urban climate or to climate change (e.g. Pültz and Hoffmann 2007, Vidrih and Medved 2008, Jentsch et al. 2015) and

vii) comparative analyses between urban and rural conditions based on long-term measured data (e.g. Hauser et al. 2006, Papakostas et al. 2010), etc.

Kikegawa et al. (2003) numerically investigated the effects of waste heat from air conditioning in the Otenmachi Japanese city and reported that a cut-off of the anthropogenic heat Q_F leads to about 1 K decrease in outdoor temperature and up to 6% cooling savings. Based on the same method, Ohashi et al. (2007) reported an increase for Tokyo of 1 to 2 K outdoor air temperature on weekdays in office areas due to Q_F waste heat, whereas this effect disappears during weekends. Kikegawa et al. (2006) found by means of a multi-scale urban climate simulation system that reducing anthropogenic heat caused by air conditioning in summer may lead to a decrease of up to 1.2 K of the air near ground and up to 40% less cooling load.

Hauser et al. (2006) compared the building energy demand using standard TRY climate data and measured data for Kassel. They found out that the differences are important, especially in terms of summer overheating, with the former source being less constraining and inaccurate. Pültz and Hoffmann (2007) discussed the validity of the TRY, which do not take into account the urban heat islands (especially heat waves) on one hand and the climate change (future projections until 2100) on the other hand. The key metrics investigated were the intensity and frequency of overheating hours in office buildings and their dependence on various climate data sets (standard TRY, climate change scenario, etc.). The authors also concluded that subsequent differences exist, which make standard TRY inappropriate. Vidrih and Medved (2008) investigated the effect of climate change on energy demand of buildings by "correcting" the TRY using simple mathematical models for Slovenia. They confirmed the decrease of the net heating energy demand and the increase of the net cooling energy demand. Frank (2005) for Switzerland observed the same trends. Similarly, Jentsch et al. (2008) and Jentsch

et al. (2015) proposed methods to integrate the future UK climate scenarios into the widely used climate data Typical Meteorological Year (TMY2), Test Reference Year (TRY) and design summer years (DSY) for building simulation (so-called "morphing" calculation after Belcher et al. (2005). Simulations of a case study also highlighted the potential impact of climate change on future summer overheating hours inside naturally ventilated buildings. Papakostas et al. (2010) investigated the impact of the global warming on the energy consumption for heating and cooling in Greece using two sets of measured climate data covering successive periods and reported the decline in heating degree days (HDD) and the rise in cooling degree days (CDD) as consequence of global warming. Accordingly, the indoors heating energy demand decreased whereas the cooling energy demand increased.

In a review, Santamouris (2014a) with reference to various studies (e.g. Akbari et al. 1992, Hassid et al. 2000, Cartalis et al. 2001, Santamouris et al. 2001, Akbari and Konopacki 2004, Kolokotroni et al. 2012, Hirano and Fujita 2012) reports that higher urban temperatures increase the energy consumption for cooling and raise the peak electricity demand. Santamouris et al. (2015) comparatively analysed the impact of ambient temperature increase on electricity consumption on eleven studies and reported that for each 1 K temperature increase, the increase of the peak electricity load varies between 0.45 % and 4.6%. Further analysis of fifteen studies showed that the actual increase of the electricity demand varies between 0.5 % and 8.5 % for 1 K air temperature increase. Santamouris (2014a) reviewed tens of published studies, based either on numerical or experimental methods, in order to evaluate the UHI mitigation potential of reflective and green roofs. He reported that the ambient temperature decreases in average by 0.3 K as mean value and 0.9 K as peak value per 0.1 rise of the albedo. If only roof albedo is considered, a decrease of 0.2 K can be reached. Using green roofs may lead to air temperature decrease between 0.3 and 3 K.

These comparative studies rely either on modelled or on measured data of urban air temperatures. Yet, recorded data are much less available because urban weather stations are not as widespread as standard weather stations and field data are often limited to shorter time periods when available. Moreover, these studies give no information on the obstructing effects of the surrounding built environment. Studies trying to prognosticate the future climate change face the problem of a variety of possible scenarios and hence the reliability of the prognosticated results. Therefore, the results are informative but hardly generalizable; a better description of the simulation conditions and a clear working systematics is required to reach some transferable conclusions.

Moreover, the climate issue in urban areas raises the problem of seasonal conflict between

desired solar access in the winter and solar protection in the summer. In a previous research, the author demonstrated the effects of the urban structure on outdoor thermal comfort (i.e. Ali-Toudert 2005, Ali-Toudert et al. 2005, Ali-Toudert and Mayer 2006, Ali-Toudert and Mayer 2007a, Ali-Toudert and Mayer 2007b). One important finding was that street geometry given by the aspect ratio H/W and the solar orientation play a dominant role in the thermal environment in open urban spaces. Deeper streets combined with a nearly north-south N-S street axis orientation mitigate more efficiently in duration and spatially spread the thermal stress in the summer in comparison to wide east-west E-W oriented streets. Yet, the first structure decreases and at the same time the potential of passive solar gains inside the buildings in the cold season whereas the second case is preferable in the winter.

A low urban plan density together with a privileged orientation of the buildings to the south is preferable to promote a sufficient sun exposure of the façades and street floors in the northern hemisphere. This typically results in a shaped building envelope according to the course of the sun, i.e. so-called solar envelope (Knowles 1981). However, solar access refers to winter needs for passive heating, which are often in conflict with summer needs for shading since the former implies compactness and the latter implies openness to the sky. This argues for a simultaneous assessment of urban choices on indoor and outdoor climate as a whole, on a daily, monthly and yearly basis in order to find a satisfying design compromise. There is one key difference between outdoor and indoor space when dealing with thermal comfort. Outdoors, it is mostly about summer thermal comfort and avoidance of thermal heat stress, whereas indoors it is about thermal comfort all year round, i.e. avoidance of cold stress in the winter and heat stress in the summer. Oke (1988a) argues that a “zone of compatibility” which ensures a compromise between apparently conflicting objectives in urban design can be found. This work seeks to be a contribution in this sense.

Furthermore, the evaluation of the energy performance and efficiency of a building in itself is complex, even in free locations. There are so many parameters involved, each of which has an effect. It is likely that conflicts amongst them emerge, creating complexities which are not easily resolved. For example, shallow plan buildings or largely glazed buildings promote passive solar gains and daylighting but increase overheating risks in the summer and large heat losses during the night, depending on the thermal mass, window properties and ventilation rates. On the contrary, a deep building plan is heat conservative but less optimal for passive solar and daylighting, which in turn implies more artificial lighting and hence internal heat gains and cooling need and so forth.

Consequently, the effects of all relevant building indicators need to be assessed, including the

building envelope: shape (geometry, dimensions), materials (e.g. opaque vs. transparent), thermal insulation and thermal mass and building use (e.g. residential, offices, schools, sport facilities, etc.). The energetic target metrics are solar heat gains, heating, cooling, lighting, daylighting, ventilation and hence the total energy demand.

Numerous parametric studies on building energy performance (e.g. Schlenger 2009, Alameddine 2011, etc.) illustrate this complexity quite well. By addressing the role of manifold building indicators in promoting low energy efficient office buildings, they showed the intricate underlying interrelationships between all factors and confirmed the importance of factors like building compactness, thermal insulation of the envelope, window ratio, window properties, shading devices, façade's orientation and ventilation. Yet, these studies considered offices in a free location and this complexity is obviously exacerbated under urban conditions with additional modifying factors. The question arising is therefore: How would these individual effects change within urban environments? Furthermore, these studies suffer a methodological weakness due to the failure in a systematic investigation, which would properly account for the manifold interactions between the addressed variables. Consequently, the results are hardly generalizable.

Even though the task seems overwhelming at first, the author believes that providing useful guidelines to the building designer is possible if a hierarchical relevance is established among all variables involved. The present research seeks to provide some answer in this direction and to be a contribution for outweighing the lack of interdisciplinary work in this field area.

2.5. Indoor Thermal Comfort

ANSI/ASHRAE Standard 55 (2013) defines thermal comfort as the condition of mind that expresses satisfaction with the thermal environment. In spite of this simple definition, maintaining thermal comfort for the occupants of a space is a complex issue because it combines objective and subjective factors referring to physiological (thermoregulation), psychological (perception) and behavioural (adjustment) dimensions. Two main approaches exist, which rely on one or more of these dimensions: the energy balance and the adaptive approaches. The energy balance approach relies on the physics of the heat exchange of the body with its environment, while the adaptive approach relies on the resilience of people to adapt to thermal environment via their psyche and behaviour. A full review and discussion around thermal comfort certainly outrun the scope of this research. Thermal comfort assumptions set the background condition and directly affect the resulting energy calculations for heating, cooling and ventilation in buildings. Therefore, it is important to address the following purpose: i) to

define the appropriate input setting conditions expected to be perceived as comfortable, preferably at the lowest energy costs, ii) to properly understand the consequences of these assumptions on the resulting building energy demands and iii) to privilege the use of the adaptive thermal comfort approach for free-running buildings.

Standards on thermal comfort do exist, which also set or advice the boundary conditions for building energy evaluations. The first reference to thermal comfort valid in Germany and Europe is the standard DIN EN ISO 7730. Additionally, the DIN EN 15251 sets the indoor environmental input parameters for design and assessment of energy performance of buildings with reference to thermal comfort requirements. The American ANSI/ASHRAE Standard 55 (2013) can be referred to as further as sound guideline on indoor thermal comfort.

Thermal comfort understood as satisfaction with the thermal environment is conditioned by numerous climate-related as well as subject-related factors. Figure 4 and Figure 5 show two complementary ways on how to assess, ensure, or restore thermal comfort. Both figures use the psychrometric chart, which puts into relation air temperature (dry bulb, wet-bulb, dew point temperatures) and humidity (absolute, relative) as main climatic factors. Figure 4 is well known and commonly used in architecture at early design stages for the analysis of a climate type (see e.g. Givoni 1976, Lechner 2014). The diagram shows the main climate-responsive design priorities as either passive or active according to particular ranges of air temperature and humidity. An application is given in section II - 1.6 (p 90) and in Ali-Toudert and Weidhaus (2017).

Figure 5 looks similar to Figure 4 with the difference that the former relates on the x-axis to the outdoor air temperature T_{ou} and the second to the operative temperature T_{op} indoors. Moreover, Figure 5 addresses the adaptive capability of humans by assuming larger thermal comfort zones that accounts for clothing level differentiated for the summer and the winter.

Climate factors affecting thermal comfort include air temperature (T_a), mean radiant temperature T_{mrt}, air humidity (q or RH) and wind speed (v). A person indoors perceives not only the prevailing air temperature but also the surrounding radiant environment governed by the enclosing surface temperatures T_s, usually summed up as mean radiant temperature. The operative temperature accounts for the influence of these two key metrics. If simply calculated, T_{op} is the arithmetic average between T_a and T_{mrt}. Detailed calculation of T_{mrt}, by contrast, accounts for the real geometry of the space, and uses the view factors of the surfaces from the person's perspective as the weighting factors for their radiative heat release. A good balance between air and surface temperatures help reach a comfortable operative temperature. The difference between air and surface temperatures depend on the thermal insulation quality and

thermal mass of the building components. Surface temperatures are more influenced by the outdoor air temperature in case of weak thermal insulation because of high transmission heat transfer, whereas low thermal mass leads to smaller difference between air and surface temperatures because of low heat storage capacity. This stresses the importance of building design and construction on thermal comfort. The wind speed has an additional influence on thermal comfort but is generally less decisive indoors compared to the temperatures owing the small magnitude and variation it experiences in sheltered spaces. Increased circulating air enhances thermal comfort under humid-warm conditions because it supports the body's evaporative cooling. As draught, however, it might be perceived negatively under cold conditions. In case of natural ventilation, the indoor air humidity depends on site's climate. To this respect, it can affect thermal comfort greatly especially in case of particularly humid or dry climates. The psychrometric chart illustrates this very well. Too high air humidity prevents evaporative cooling and a too low humidity provokes uncomfortable dryness e.g. of eyes and throat. Otherwise, the impact of indoor air humidity is moderate compared to temperatures. Additionally, the subject's properties in terms of clothing insulation and metabolic rate modify the thermal perception further. The DIN EN 7730 provides all information on all these aspects. A widely accepted way to assess thermal comfort is the physiologically based energy balance method, which aims at assessing the combined effects of climate and subject related factors on thermal equilibrium perceived as thermal comfort. Thermal heat stress or cold stress expresses some positive (heat gain) or negative (heat loss) deviation from this equilibrium, respectively.

The outcome of energy balance based methods is a thermal index. One of the well- known thermal indices is the predicted mean vote PMV, based on the Fanger's model and embedded in the EU standards. The PMV thermal index scale ranges from – 3 (very cold) to +3 (very hot) and where ± 0.5 expresses neutrality and comfort. Other thermal indices exist, such as the standard equivalent temperature SET implemented in the American standard, which better handles the case of high indoor air speeds.

Another way to handle thermal comfort is the adaptive approach, which adopts wider comfort ranges by assuming psychological and behavioural assets of people in adjusting to surrounding thermal conditions. This includes adaptation by means of appropriate seasonal clothing insulation but also because of different expectations correlated to prevailing weather conditions, e.g. more tolerance for heat under hot summer conditions. (see e.g. De Dear and Brager 2001, De Dear and Brager 2002, Nicol and Humphreys 2002).

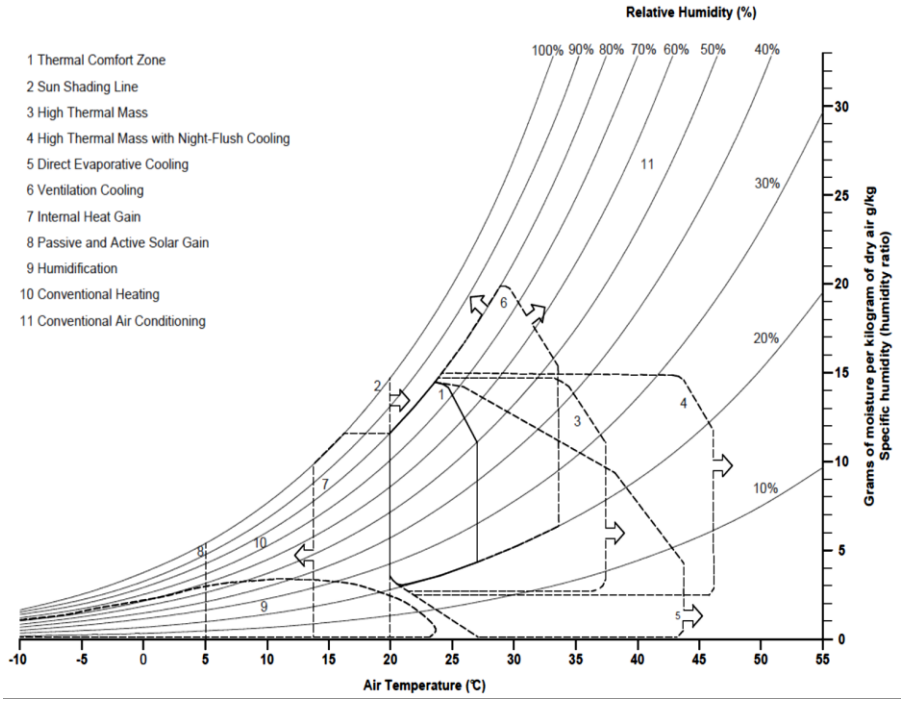

Figure 4: passive and active climate-sensitive strategies for keeping or restoring thermal comfort conditions (redrawn from Lechner 2014)

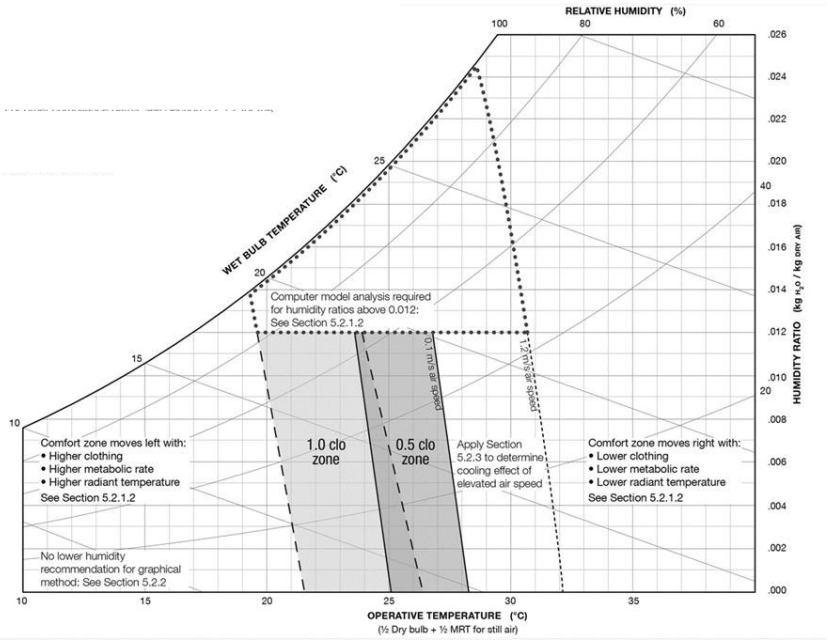

Figure 5: The psychrometric "thermal comfort" chart (source: ANSI/ASHRAE Standard 55, 2013)

Whether thermal comfort is assumed adaptive or related to heat balance, the issue deserves further discussion as it intrinsically combines objective and subjective aspects as reviewed by Halawa and van Hoof (2012). De Dear and Brager (2002) discussed the new adaptive comfort standard (ACS) adopted as revision in the American ASHRAE standard 55 which is dedicated to the thermal comfort. They analysed 160 naturally ventilated buildings. The adaptive model is of particular relevance for free-running buildings in contrast to air-conditioned ones, i.e.

naturally versus mechanically ventilated buildings. The adaptive model is meanwhile implemented in the ANSI/ASHRAE standard 55. In other terms, assessing the thermal environment in buildings in order to quantify the energy costs allows some handling latitude linked to the setting inputs for the dynamic building energy simulations. This is introduced hereafter based on the prevailing standards as theoretical background for the choices explained later in the section about the investigation plan I (section II - 1, p 67).

The standard DIN EN 15251 specifies the input parameters to be set for the indoor climate for use in the design of buildings and facilities and for the assessment of their energy performance. This Standard also specifies methods for long-term evaluation of the resulting indoor climate and energy efficiency calculations. The DIN EN 15251 specifies several different categories of indoor climate (I to IV) which correspond to different levels of comfort following similar categories given in DIN EN ISO 7730. The comfort room temperature T_{comf}, as shown in Figure 6, is calculated as function of the outdoor air temperature T_{ou} using equation (3) according to DIN EN 15251 (NA part, category II[11]) and to equation (4) according to ASHRAE.

$$T_{conf} = 18 + 0.25\,T_{ou} \tag{3}$$

or

$$T_{conf} = 17.8 + 0.31\,T_{ou} \tag{4}$$

At ambient outdoor temperatures below 16 °C and over 32 °C, T_{comf} is 22 °C and 26 °C, respectively. In-between, the tolerance range for the operative temperature is ± 2 K from that comfort room temperature. This tolerance range accounts for the ability of the user to adapt to the thermal situation by means of an appropriate insulating clothing, typically 0.5 clo in the summer and 1.0 in the winter (for details see DIN EN ISO 7730). A light activity with 1.2 met (= 70 W m^{-2}) is also assumed. An admissible deviation from the tolerance range of the operative temperature can be calculated by means of a degree-hour criterion DH (T_{op}). The category II is still considered as fulfilled if the operative temperature deviates in less than 1% of the whole period of use from the predefined range up to ±2 K. The overstepping and undercut frequencies need to be calculated separately and then summed up according to the following equation (5), where n_d is the number of hours of the day and d_y the days of the year where the space is in use.

[11] Category II in DIN EN 15251 corresponds to category B in DIN EN ISO 7730, which expresses thermal neutrality with a predicted mean vote PMV = ± 0.5 and people percentage of Dissatisfaction PPD < 10 %

$$DH\ (T_{op}) = 1/100\ (n_d\ d_y).\ 2 \qquad (\text{in Kh a}^{-1}) \qquad (5)$$

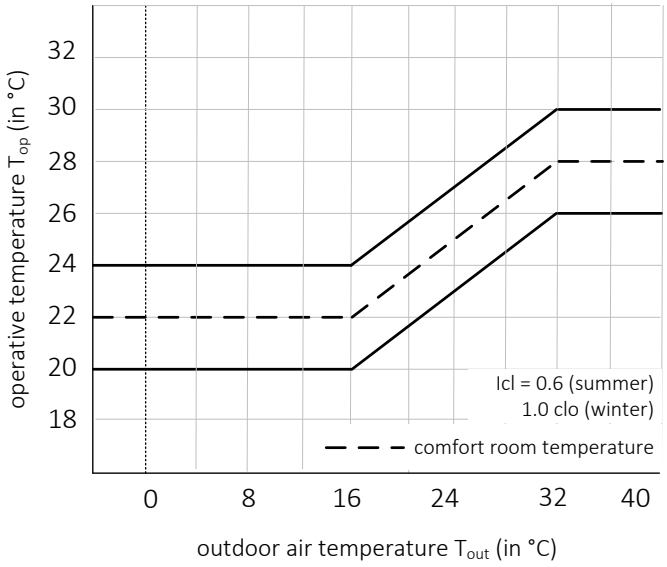

Figure 6: Comfort room temperature and permissible operative temperature range (source: DIN EN 15251)

2.6. Related Standards and Guidelines

The urban climate issue is addressed in several standards dedicated to buildings from which the DIN V 18599 (part 10) and the VDI 2078. The VDI 2078 (2015) provides a new division of climates in Germany, which is based on the updated DWD (2011) with consideration to the urban climate. City centres are assumed to count over 10^6 inhabitants and be high-density built-up areas without large green spaces. Based on the division of Germany under VDI 2078 (19969 which is based on 250 weather stations, the 15 TRY are better differentiated according to more cooling load zones so that local climate aspects like topography, vegetation or city versus countryside are better included. The national appendix of DIN EN 12831 considers cities with more than 20000 inhabitants, considering the climate zones as given in DIN 4710. In the stationary procedure, the shield effects of obstructing environments are generally considered as approximate reduction factors.

3. THE INVESTIGATION METHOD

The investigation method used in this research combines i) numerical modelling, ii) statistical methods and iii) GIS techniques. Figure 7 illustrates the investigation plan, in which the coloured links refer to the successive flow of information and use of the models and techniques. Numerical modelling is preferred for its ability to handle complex issues with acceptable processing time. This is particularly relevant for supporting the extensive parametric studies conducted in this research.

1. The urban canopy model (Town Energy Balance TEB) and the dynamic building energy model (TRNSYS) are used for the quantification of the thermal conditions in outdoor and indoor spaces, respectively, and for clarifying their energetic logic and dependence on the structural urban and building attributes. TEB and TRNSYS are used in PART I and PART II.
2. The statistical method Design of Experiments DOE is used for the pre-processing of the required inputs and post-processing of the generated outputs in TEB and TRNSYS in PART I and PART II. The advantage of DOE is to optimize the investigation scope and help generalize the findings by means of a systematic exploration plan.
3. The GIS techniques are used in PART II is dedicated to a large case study area. GIS enable a reliable and spatially differentiated pre-processing of building and urban data as well as a post-processing the results in form of maps.

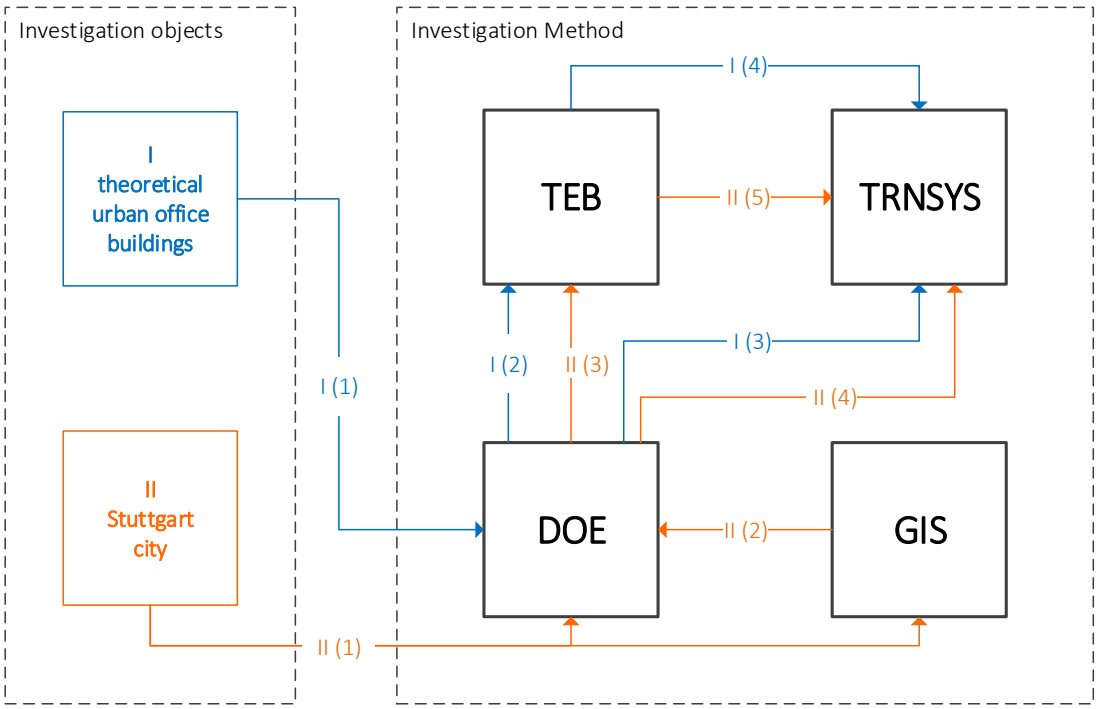

Figure 7: Scheme of the applied investigation method on theoretical and real case studies (PART I and PART II) using TEB, TRNSYS, DOE and GIS, including the information fluxes between them.

As illustrated in Figure 7, TEB, TRNSYS and DOE are used for theoretical urban office building (PART I) whereas GIS is additionally employed for the real case study of Stuttgart city for which the spatial distribution also plays a role (PART II). The numbered links show the successive information and processing flow. TEB, TRNSYS, DOE and GIS are introduced in the following. The detailed investigation plans for PART I and PART II are explained in section II - 1 (p 67) and section III - 1 (p 169), respectively.

3.1. The Town Energy Balance Model TEB

The TEB model is a bi-dimensional surface scheme, which belongs to the category of urban canopy models. The concept and physical background of TEB including its main improvements can be read in Masson (2000), Masson et al. (2002), Lemonsu et al. (2004) and Lemonsu et al. (2012). The following description concerns the version used in this research, which does not include the latest updates. TEB solves the energy balance of an urban structure by considering the urban canyon as a structural unit (see Figure 8). The urban canyon is described with three multi-layered opaque surfaces: one roof, one street and two walls of the same height and infinite length solved together. Up to nine layers of materials with individual thermal properties can be modelled given their thermal conductivity, heat capacity and volume density. Albedo and emissivity are given for each facet. The energy balance is solved for each surface separately, and the radiative exchanges between the canyon facets are included.

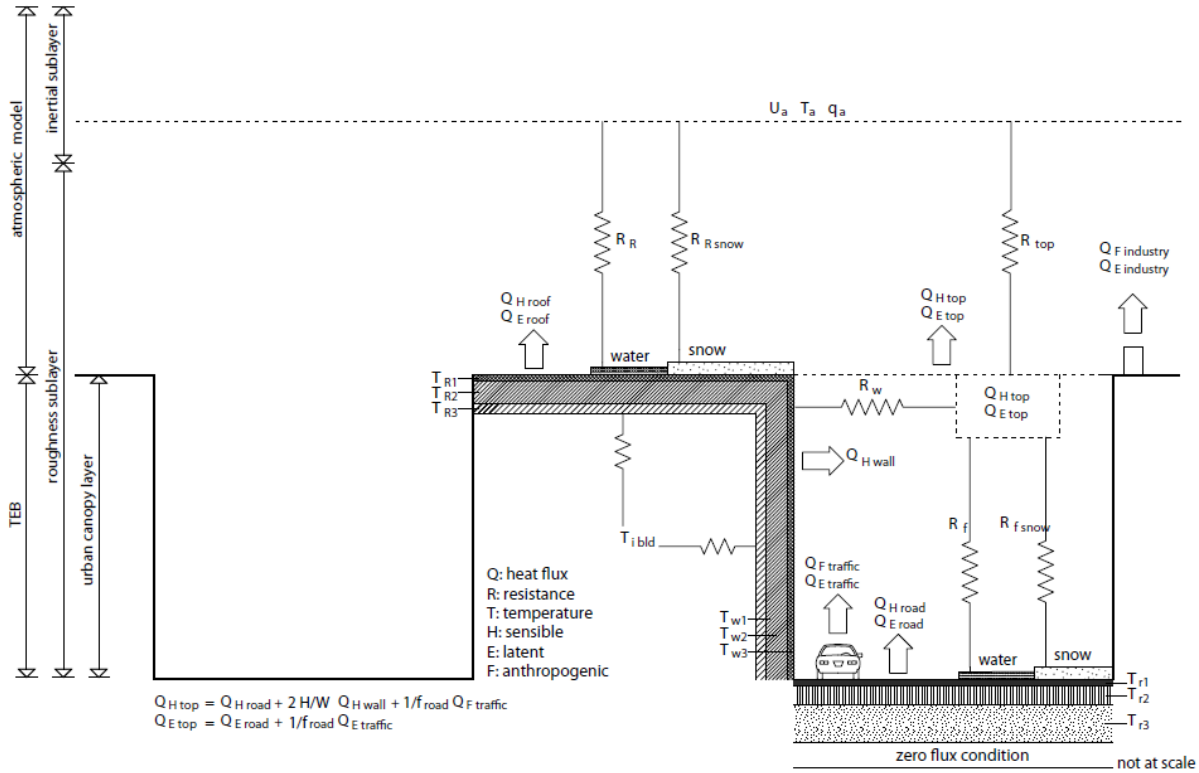

Figure 8: Schematic of the urban canyon TEB Model Concept showing the involved fluxes (redrawn from Masson 2000)

Sensible and latent anthropogenic heat fluxes are accounted for either originating from traffic or industry. The heat storage in the canyon fabric is included involving possible indoor heating. The model as used in this research is vertically single-layered and considers the canyon volume as one unit. Assumption is made for equally probable orientation, i.e. no differentiation in relation to solar orientation. Hence, the calculation of the radiation fluxes on the canyon facets as well as the shading patterns in-canyon is averaged. In this research, the model is run in offline mode (also known as forcing mode) i.e. the climate data are provided as inputs by the user at a certain boundary above roof level, instead of a coupling with an upstream atmospheric model (e.g. MESO-NH in the SURFEX). The TEB model predicts inter alia the turbulent heat fluxes, surface and air temperatures. TEB provides the air temperature inside the urban canyon as average for the whole canyon volume.

As mentioned in section I - 2.3 (p 35), TEB has inspired several other canopy models and has been successfully validated against observations. This confirms a general agreement within the scientific community on the appropriateness of its concept in spite of its simplicity.

3.2. The Transient Building Energy Model TRNSYS

For this research, it was essential to use a robust in-stationary building model which simulates at small time steps, handles complex simulation tasks including detailed building constructions and HVAC operation settings and includes the 3D urban surroundings. For instance, EnergyPlus, TAS, or TRNSYS would have been appropriate. The TRaNsient SYstem Simulation model TRNSYS (Klein et al. 2004, TRANSSOLAR 2017 and WISC 2017) has been chosen because of the author's skills to operate it and because of its combination with TEB and further related advantages (see next section). The main features of the software are summarized below, whereas a full description can be found in the references cited above. For a comparison with other models, refer to Crawley et al. (2005 and 2008).

TRNSYS is a well-established simulation environment in use since 1975 for solar systems design, building thermal performance, electric power simulation, etc. The level of detail of TRNSYS complies with many standards like ENV-12977-2 or ANSI/ASHRAE Standard 140-2001 (WISC 2017). The TRNSYS package consists of two main sub-programs: 1) TRNSYS Studio, a graphical front-end that houses all aspects of the TRNSYS simulation procedure (Figure 66) and 2) TRNBuild - a graphical interface for describing the geometry, construction and HVAC settings for multi-zone buildings. Additionally, TRNEdit is supplied for editing the TRNSYS input files, creating own parameter runs and other stand-alone TRNSYS-based applications. The TRNEXE runs the simulation.

TRNSYS supports the modelling of multi-zone buildings and solves the energy balance for each thermal zone considering one air node is located centrally. The energy balance at boundary zone elements (wall, floor, roof, window, etc.) considers several nodes within the element and one final node at the surface. Most importantly, the simulation is non-stationary so that short time steps (few minutes) are possible for long simulation periods (years). Although conceived for and focussing on indoors, TRNSYS takes into account the shading effects on the façades and openings, by either using Type 67 (up to version 16) or by using the plugin TRNSYS-3D, which is one main novelty of the release TRNSYS 17. The TRNSYS-3D add-on provides the possibility to draw the building as 3D object in SkechUp™ and to let shading and sky view matrices be calculated in TRNBuild.

The modular design system of TRNSYS makes it a versatile and upgradeable tool. Each module, known as "TYPE", is a subprogram for a specific calculation issue, having inputs and providing outputs. A component library contains a large number of TYPEs. A TRNSYS simulation project consists of a combination of several TYPEs, which are interconnected in a logical manner, so that the outputs of one TYPE serve as inputs for another one. In addition to the appropriateness of TRNSYS for the objectives of the present work, it was chosen for its compatibility of use with TEB (see next section) and author's experience in operating it.

3.3. The Combined Use of TEB and TRNSYS

The originality and challenge of this research is methodological in dealing with the thermal behaviour and energy demand of buildings (indoor climate) specifically taken under urban boundary conditions (outdoor climate). Therefore, one urban canopy and one building energy model are combined to cope with the shortage of an integral model, which would deal simultaneously with outdoor and indoor climates. This issue and the differences in the available methodological approaches, scope and resolution of urban climate models and building energy models have been discussed in section I - 2.3 (p 35). The following arguments motivated the choice for the TEB – TRNSYS combination in this research:

1. *Compatibility of inputs:* Both TEB and TRNSYS can run i) for a simulation period freely defined by the user, e.g. a typical year or longer, ii) for a time step defined by the user, e.g. one hour or a few seconds and iii) with external climate data as inputs (e.g. TRY or DWD data, EPW, TMY, etc.). This makes it possible to use the outputs of TEB as inputs for TRNSYS in a next step.
2. *Simulation duration:* Both TEB and TRNSYS models are fast computing. For instance, a simulation with TEB and TRNSYS lasts a few minutes for a simulation peri-

od of one year taken at hourly basis (8760 hours). This is a key advantage for the numerous and large parametric studies conducted in this research.

3. *Detailed description of the object of study:* Both TEB and TRNSYS allow a sufficiently detailed description of the building system's shared boundary surfaces, i.e. multilayer depiction of external walls, roofs and streets, including the thermal and radiative properties of each material and/or surface.
4. *TEB-Type for TRNSYS:* TEB has been embedded as a new component in TRNSYS for better efficacy during use. So, the TEB simulations are very conveniently undertaken under TRNSYS instead of the original less user-friendly version operating under Linux. The convenient modular assembly of TRNSYS is one decisive reason for the re-implementation of TEB as new Type within it (Ali-Toudert and Böttcher 2011a, 2015, 2017). Section II - 5 (p 157) describes this programming task in detail.

In this study, each simulation runs in two steps:

- At urban level: The urban canyon model TEB is used for simulating the urban microclimate changes due to the urban structure itself, i.e. warming or cooling of the urban canyon at street level including possible canopy heat or cool island effects. The new urban air temperature is adjusted from standard climate data and is assumed to correspond to the actual ambient temperature under which the urban building effectively performs.
- At building level: TRNSYS 17 is used for the calculation of the required energy demands to maintain thermal comfort conditions under urban climate conditions. The output urban air temperature provided by TEB serves as input ambient temperature for TRNSYS. The effects of the built surroundings in reducing the sky view, solar access as well as the additional in-canyon solar reflections are accounted for.

3.4. The Statistical Design of Experiments DOE

The Design of Experiments (DOE) is a method for planning experiments and analysing their results statistically in order to understand the functional dependence between inputs and outputs underlying the process in question (see e.g. Dean and Voss 1999, Box et al. 2005).

In case of an extensive parameter study, the choice of the factors to be varied, their number and the steps at which they are varied is crucial in order to quantify properly the dependences between inputs and outputs. On the one hand, testing all possible combinations (i.e. full-factor experimentation) can be expensive and/or time-consuming at processing stages (e.g. laboratory experimentation, numerical modelling), as well as at post-processing stages (results analysis). On the other hand, making a limited number of experiments based on non-proofed hy-

pothesis of parameter relevance may result in overlooking important impacts of inputs on outputs through the overlay of interdependence between the inputs themselves. This is typical in cases of parametric studies based on the "one-factor-at-a-time" OFAT variation procedure.
The DOE method or plan offers a way to optimize the experimentation planning and processing in order to achieve the accuracy desired while keeping acceptable time expenditure and research costs. DOE plans are increasingly used in natural and engineering sciences to cope with the difficulty of investigating a very large number of cases consisting of all possible parameter combinations. Figure 9 shows the DOE concept, which consists of a selection of combinations deduced from a full factorial plan, including main effects and double or more interactions between factors, while some overlapping of effects at further levels is ignored.

1. It gives reliable information on the importance of the variables involved (independent variables) within a clear hierarchy of the target key metrics (dependent variables) with possibly limited number of single experiments.
2. It enables the quantitative description of the functional interdependence between inputs and outputs by means of regression analysis in form of a predictive mathematical model, i.e. transferable to more values than the ones explicitly investigated.

With respect to the present research, the DOE method presents the following advantages:

3. A second order polynomial function expresses the output target metric Y as a function of all relevant inputs X_i with the DOE steps set at an equidistant, coded (-1), (0) and (+1) as shown in Figure 10. A generalizable formula in form of [$Y = a + b_1X_1 + b_2X_2 + b_3X_1^2 + b_4X_2^2 + b_5 X_1X_2 \ldots$] thereby expresses the main effects (e.g.b_1X_1) and double interactions (e.g. $b_5 X_1X_2$) being either linear (e.g. b_1X_1) or quadratic (e.g. $b_3X_1^2$).

In this study, both full and partial factorial analyses are utilized. Full factorial analyses are performed where computing-time needed for preparing and running all possible combinations remains reasonable. In this case, a full factorial matrix for p variables and n steps per variable consists of n^p experiments. In cases where the number of simulations becomes too large, part factorial analysis is carried out, which includes the main effects of each individual variable, as well as double interactions on the targeted outputs. Full factorial plans were mostly applied for the theory-based urban office buildings (e.g. [SET I] in section II - 1.4, p 85). Part factorial experiments were particularly useful in other cases, either to shorten the calculation time (e.g. [SET II] in section II - 1.4, p 85), or for both saving time costs and enable technical feasibility such as in the investigation on the city of Stuttgart (see section III - 1.3, p 175). The results were post-processed by means of the software IBM SPSS Statistics (IBM SPSS 2017).

2^{k-p} runs	k factors													
	2	3	4	5	6	7	8	9	10	11	12	13	14	15
4	F	III												
8		F	IV	III	III	III								
16			F	V	IV	IV	IV	III	III	III	III	III	III	III
32				F	VI	IV	IV	IV	IV	IV	IV	IV	IV	IV
64					F	VII	V	IV	IV	IV	IV	IV	IV	IV
128						F	VIII	VI	V	V	IV	IV	IV	IV

2^{k-p} runs	k factors							
	3 A B C	4 A B C D	5 A B C D E	6 A B C D E F	7 A B C D E F G	8 A B C D E F G H	9 A B C D E F G H I	10 A B C D E F G H I
4	2^{3-1} III C = AB							
8	2^3 FULL	2^{4-1} IV D = ABC	2^{5-2} III D = AB E = AC	2^{6-3} III D = AB E = AC F = BC	2^{7-4} III D = AB E = AC F = BC G = ABC			
16		2^4 FULL	2^{5-1} V E = ABCD	2^{6-2} IV E = ABC F = BCD	2^{7-3} IV E = ABC F = BCD G = ACD	2^{8-4} IV E = BCD F = ACD G = ABC H = ABD	2^{9-5} III E = ABC F = BCD G = ACD H = ABD I = ABCD	2^{7-4} III D = AB E = AC F = BC G = ABC
32			2^5 FULL	2^{6-1} VI F = ABCDE	2^{7-2} IV F = ABCD G = ABDE	2^{8-3} IV F = ABC G = ABD H = BCDE	2^{9-4} IV F = BCDE G = ACDE H = ABDE I = BCDE	2^{10-5} IV F = ABCD G = ABCE H = ABDE I = ACDE J = BCDE
64				2^6 FULL	2^{7-1} VII G = ABCDEF	2^{8-2} V G = ABCD H = ABEF	2^{9-3} IV G = ABCD H = ACEF I = CDEF	2^{10-4} IV G = BCDF H = ACDF I = ABDE J = ABCE

legend

- design of resolution III or lower (overlaping of main effects with 2-interactions, not recommended)
- design of resolution IV (overlapping of main effects with 3-interactions, 2- with other 2-interactions proceed cautiousely, must resolve 2-ways interactions)
- design of resolution V and better (overlaping of main effects with 4-interactions, 2- with 3-interations, good, main and 2-ways effects can be estimated clearly)
- full factorial (no overlaping between main effects and interactions)

k = number of factors
p = number of factors confounded with high order effects
The DOE plans explained here are based on 2-steps (-1) and (+1) for each factor

k = number of factor p = number of factors confounded with high order effects
design of resolution III or lower (overlaping of main effects with 2-interactions, not recommended)
design of resolution IV (overlapping of main effects with 3-interactions, 2- with other 2-interactions proceed cautiousely, must resolve 2-ways interactions)
design of resolution V and better (overlaping of main effects with 4-interactions, 2- with 3-interations, good, main and 2-ways effects can be estimated clearly)
full factorial (no overlaping between main effects and interactions)

Figure 9: Number of experiments m for factors p at 2-steps variations of n (linear) depending on the degree of completeness of mutual interactions (redrawn from Kavanaugh 2017)

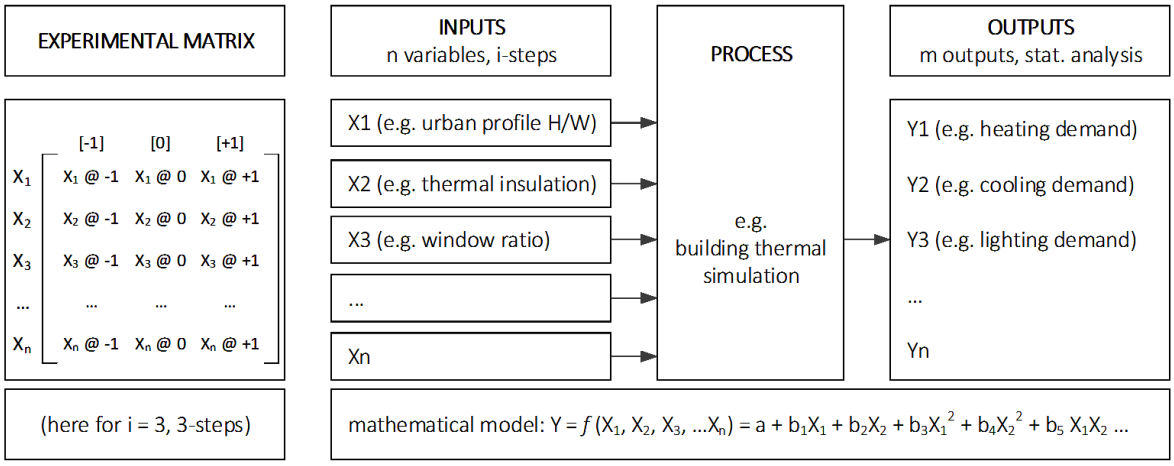

Figure 10: Schematic of the Design of Experiments concept used in this research

3.5. The Geographic Information Systems GIS

The GIS is an information system that captures, processes, manages and analyses spatial or geographical data. In this research, GIS technique using the software ArcGIS 10.1 (ESRI 2012) was used in PART II dealing with Stuttgart for the pre-processing and post-processing of data (Figure 11).

With the help of GIS, the city structure and building characteristics are parameterized spatially with focus on a multi-scale data analysis (building, city block). These include the structural, formal and thermal attributes of the urban structure and individual buildings based on 2D and 3D city maps. For the post-processing of the results generated by TEB and TRNSYS, GIS is used for mapping the mathematical models describing the urban climate changes and building energy demands.

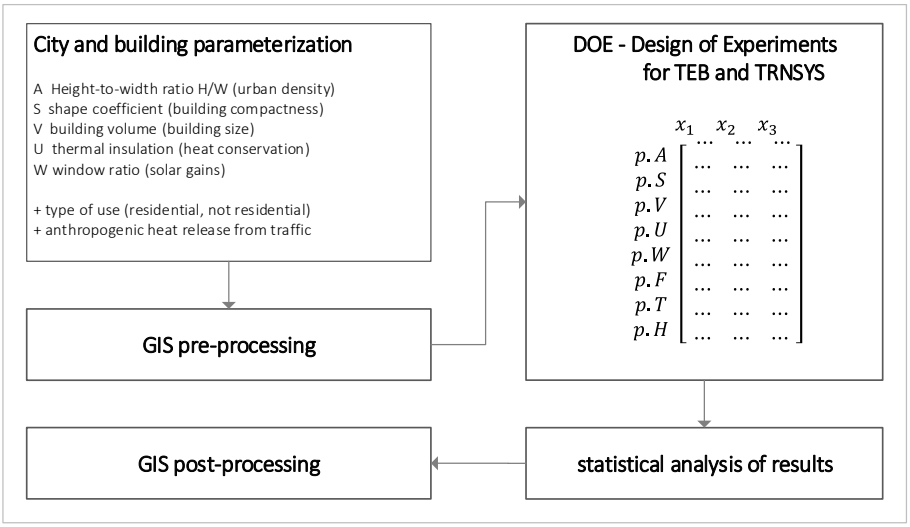

Figure 11: Combined use of GIS and DOE for data pre-processing and post-processing as used in PART II for the investigation of Stuttgart city

3.6. Objects of Investigation

This research is applied on two case studies 1) theory-based urban office buildings and 2) the city of Stuttgart as real case study. The two case studies have different focus points in their investigation, making them complementary in content.

3.6.1. Theoretical Urban Office Buildings

In order to assess the part of responsibility of urban geometry and building construction in modifying the urban microclimate, single office buildings embedded in urban environment are simulated. Consequently, the resulting indoors energy demand can be highlighted. The multi-story building simulated enables the analysis of the effects of the urban density by differentiating the results according to floor height and solar orientation. In addition to heating

and cooling, (day) lighting and ventilation are further addressed. A systematic analysis of the variables involved, complemented by a sensitivity analysis help understand the interactions of all involved factors. A comparison with the Mediterranean climate type adds to the comprehension of the role of the climate as boundary condition.

3.6.2. The City of Stuttgart

The investigation of the city of Stuttgart provides the following added value in comparison to the first case study. The methodology proposed in this research (TEB, TRNSYS and DOE) and used in the theoretical case for systematic parametric analysis is being assessed for a real case study in order to check its viability. It extends the handling of numerical modelling and assessment of urban climate and indoor energy demand to more modifying factors depending on the quantity and quality of the information available on the city. The spatial distribution of the target metrics to be prognosticated is set as focus, which calls for the use of the GIS techniques.

II

THE THEORETICAL PART I: URBAN OFFICE BUILDINGS

1. INVESTIGATION PLAN OF PART I

PART I of this research reports on the numerical simulations undertaken on a series of theoretical buildings embedded in urban structures and their thermally relevant properties were systematically varied according to a DOE investigation plan.

In the next sections, a particular focus is placed on explaining the choices made for the simulation settings because inputs are fundamental in interpreting numerically generated results. Indeed, the huge amount of variables involved are inherent to sophisticated numerical models such as those used here and the wide range of possible options make this task more difficult. A systematic effort to refer to standards and guidelines (e.g. DIN, ISO and VDI) or available literature is made with emphasis on methodological soundness or possible alternatives. In so doing, the attention of the reader is drawn to the relative character of the results from these boundary conditions. Moreover, the objects of investigation described below are partly not identically modelled in TEB and in TRNSYS because of their different concepts and requirements. A detailed description of the objects is privileged when possible, yet a number of simplifications in the inputs were necessary and this is explained subsequently.

1.1. The Office Building and Urban Surroundings

1.1.1. The Urban Structure

Figure 12 illustrates the investigated urban structures. A number of canyon-like urban structures are investigated for various street vertical profiles (height-to-width ratio H/W), solar orientations and thermally relevant building properties including thermal insulation, thermal mass and window ratio. The urban density is expressed by means of shallow, unity-like and deep shaped canyons. Three equally distant façade orientations are considered in order to cover the full 360° horizon range. Simulations run for an office building, centrally located in a stretched urban canyon structure, having two external façades facing two different solar orientations. The building develops over five floors and each office has one external wall with openings directed towards one orientation at a time (Figure 12). Because the focus is placed on the thermal exchange outdoor - indoor, the ten outlying offices are simulated but not the internal mid-zones considered as equal thermal boundary spaces.

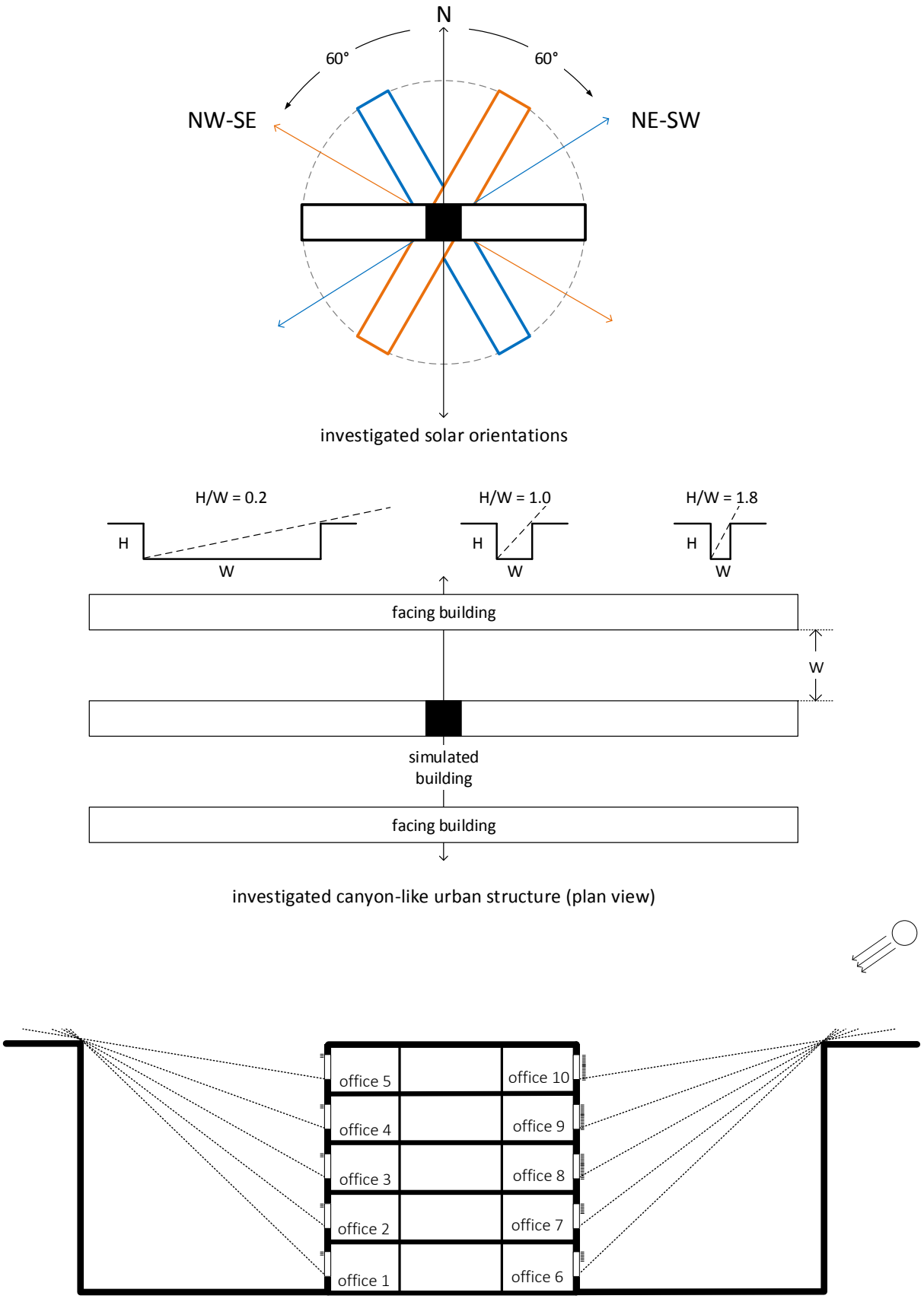

Figure 12: Schematic of the office building geometry and construction including 10 externally exposed thermal zones and embedded in a canyon structure as simulated in TRNSYS

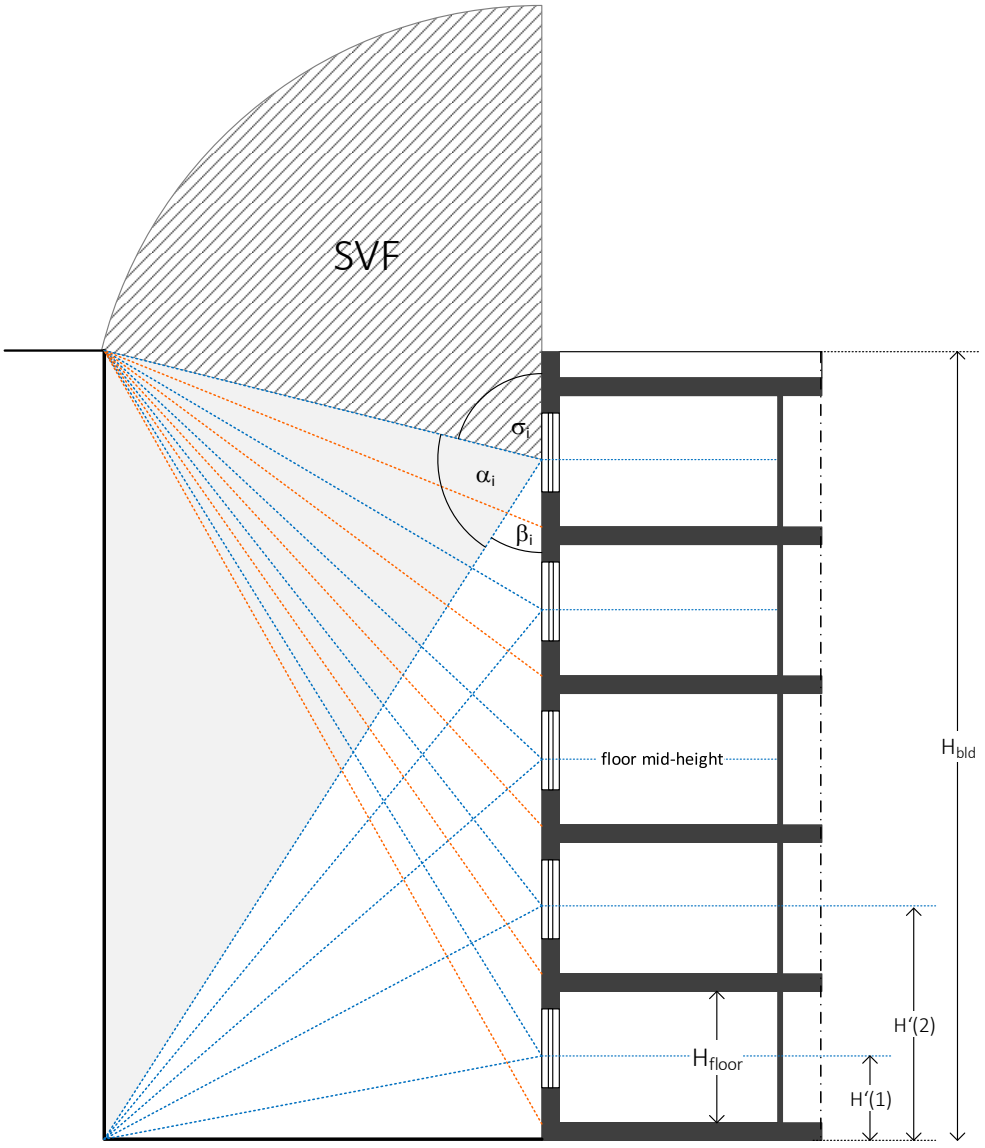

Figure 13: Urban geometry of the investigated building including the sky and surface view factors

Figure 13 shows the vertical arrangement of the offices including their view factors. The blue lines drawn at floor's mid-height refer to the reference points used for setting the view factors of the sky, facing wall and ground, necessary for calculating the diffusely reflected solar radiation and longwave emitted radiation from the surroundings for each floor. The orange lines, starting at floor level, are used for determining the potential for solar exposure of the external walls and openings, expressed as shading masks provoked by the built surroundings. Table 5 lists the dimensions assumed.

1.1.2. The Office Building

This section describes the buildings as simulated in TEB and TRNSYS. The building is simulated in TEB as one bulk entity, being the physical boundary to the canyon volume. In TRNSYS, however, part of the building slab consisting of several single offices is simulated with the assumption of its repetitiveness and representativeness for the whole. The dimensions of the office room (Figure 14, Table 6), assumed to be cellular (i.e. occupied by one person), are in accordance with typical German guidelines for office design and use (e.g. Eisele and Staniek 2005, Staniek and Staniek 2011) and it is similar to some extent to those used by Müller et al. (2005), Emembolu (2004) and Schlenger (2009). The design of the office building components is kept as simple as possible because the focus is placed on the thermal relevance rather than on constructive considerations. Table 7 and Table 8 provide a simplified modelling used in TEB. Table 9 and Figure 15 describe the multi-layer building components for the lightweight and massive construction as modelled in TRNSYS. The constructions in Table 9 and Figure 15 follow in principle the examples given in the guideline VDI 2078 with a few simplifications in order to i) enable a proper modelling of the wide variety of case studies and 2) account for constraints due to the numerous combinations given by the extensive parametric study plan. For example, the exterior wall is modelled as a double-shell wall with a thermal insulation layer in-between. The thermal insulation thickness is varied to fit the required final thermal transmittance of the element depending on each case study. The two wall layers are of same thickness in all cases (i.e. 12 cm for massive and 4 cm for lightweight construction) in order to concurrently assess the effect of the same thermal mass on the thermal environment both outdoors and indoors. The exterior wall of the lightweight construction is simulated like a sandwich element but using thin layers of lightweight concrete in order to facilitate the comparison with the massive construction. The mass density is halved and the thickness is one-third so that the heat storage capacity of the lightweight exterior wall is 1/6 of the massive construction. Usually, the effective heat storage for a building component is assumed 10 cm at most (see Appendix 4), so that 12 cm suffice to understand the effects of the thermal inertia on the thermal situation. Moreover, for comparison purposes, the internal dimensions and volume of the office rooms could be kept identical in all simulations in spite of the case-to-case small differences in the building envelope's elements (e.g. thickness of external walls and floor plates) because TRNSYS considers final useful internal room dimensions. The air space in the internal building components is modelled in TRNSYS as a massless stationary air layer with no specification of thickness. External building components with a ventilated air space layer were avoided because they are less accurate to simulate.

Table 5: Geometry and dimensions of the investigated office building and urban structures in TRNSYS

item	quantity	comments
building height	18 m	constant
street width	90 | 18 | 10 m	variable, function of target H/W
building width	18 m	constant (only variable in the sensitivity analysis)
aspect ratio H/W	0.2 | 1.0 | 1.8	shallow, unity-like and deep canyon, respectively
floor height (incl. floor plate)	3.4 m	averaged for both massive and light-construction
floor plate (+/- false ceiling)	0.4 m	averaged from 0.35 m (MA) and 0.45 m (LI)

Table 6: Dimensions of the investigated office rooms in TRNSYS

item	quantity (1)	comments
office width	2.8 m	Single use
office length	5.0 m	workplace placed next to the windows
office finished ceiling height	3.0 m	averaged for both massive and light-construction
office room volume	42 m^3	
useful surface area	14 m^2	medium workplace need per person according to (2)
façade surface area	8.4 m^2	
facade design (window ratio)	30% | 60% | 90%	perforated, row and glazed façade, respectively
window surface	2.52 | 5.04 | 7.56 m^2	related to window ratio 30%, 60% and 90%
working plane	0.8 m	according to (2)
(1) see e.g. Eisele and Staniek (2005), Staniek and Staniek (2011) (2) DIN V 18599-10; in DIN 5034-2 set at 0.85 m		

Table 7: Thermal properties of the multi-layered building elements as simulated in TEB

wall and roof elements (1) (3)		Thickness d	thermal conductivity λ	heat capacity c
		m	W m^{-1} K^{-1}	kJ m^{-3} K^{-1}
massive [MA]	dense concrete	0.12 (2 layers)	2.1	2400
mediumweight [MD] (4)	mid-dense concrete	0.08	1.3	1800
lightweight [LI]	light concrete	0.04 (2 layers)	0.619	1200
thermal insulation [TI]	mineral insulation	variable (2)	0.05	72
(1) The façade is assumed as double-skin concrete exterior wall with a thermal insulation layer in-between. (2) The thickness of the insulating layer depends on the required U-value of building element () (3) The units are given in this table as required by TEB				

Table 8: Urban geometry and building thermal properties as input variables in TEB

Variable		TEB assumptions
A	aspect ratio H/W	building fraction, wall over horizontal
B	solar orientation	ignored (assumption of equal probability for all orientations)
C	window ratio	no windows in TEB, indirectly included via a mean thermal transmittance $U = U_{wall} A_{wall} + U_{wdw} A_{wdw,}$ where A_i is the fraction of the surface.
D	thermal insulation	multi-layer construction given by heat capacity, thermal conductivity, thickness per layer
E	thermal inertia	

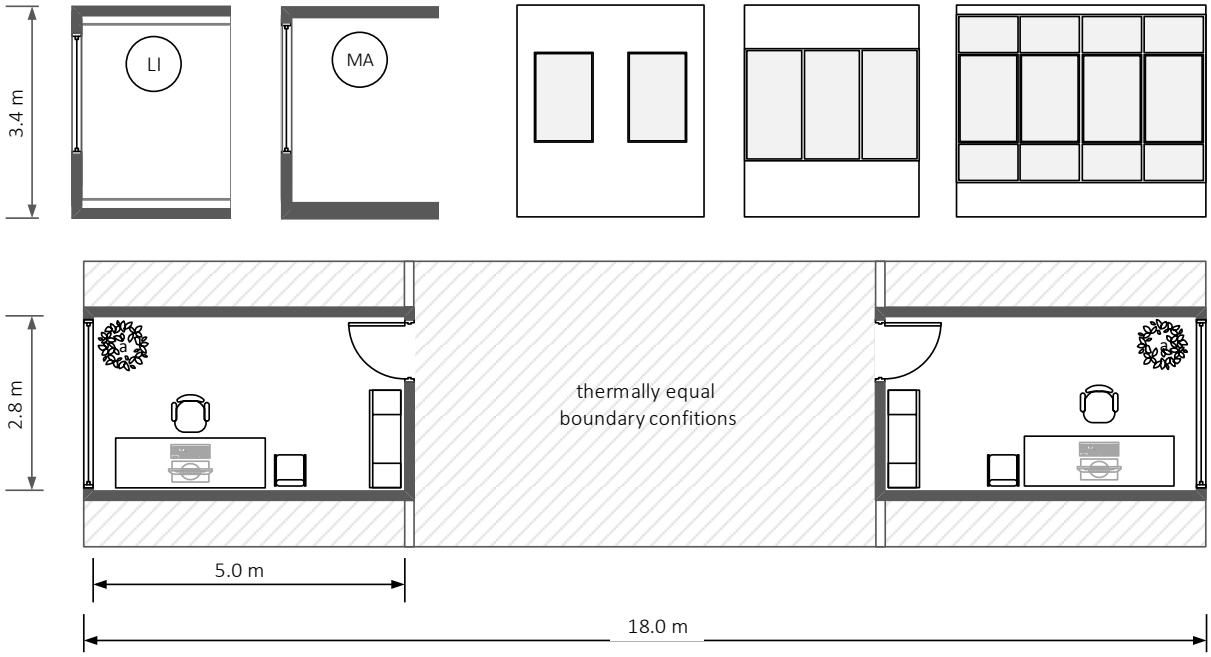

Figure 14: Simulated single office buildings embedded in thermally equal boundary conditions with massive or lightweight construction and various window ratio levels

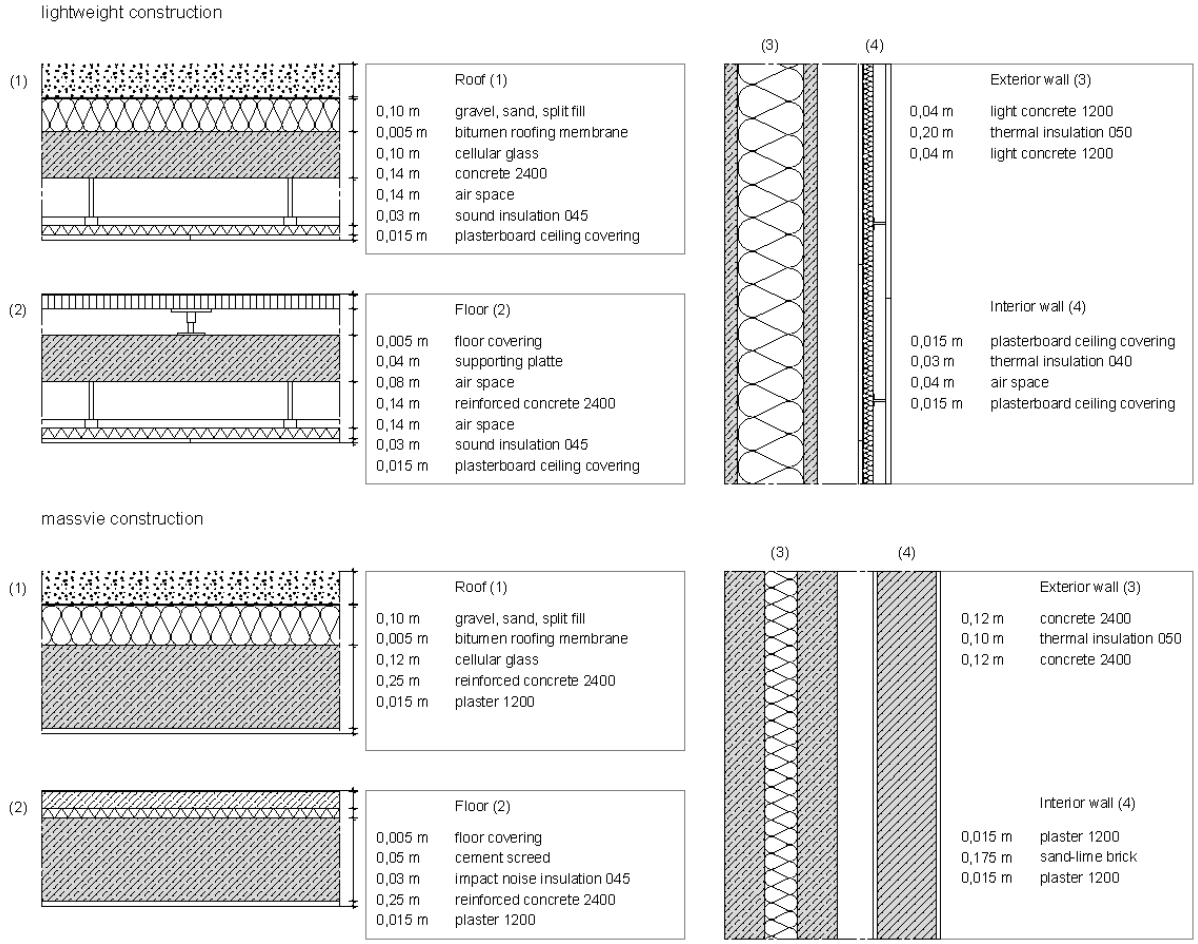

Figure 15: Boundary elements of the office rooms as simulated in TRNSYS for lightweight and massive construction

Table 9: Building elements and the thermal properties of the material layers for the lightweight construction and massive construction

lightweight construction		material layer	total thickness	d	λ	ρ	c	c ρ
				m	kJ h^{-1} m^{-1} K^{-1}	kg m^{-3}	kJ kg^{-1} K^{-1}	kJ m^{-3} K^{-1}
floor	1	floor covering	0.45	0.005	0.61	1000	1.0	1000
	2	supporting platte		0.04	0.47	700	1.0	700
	3	air space(1)		0.08	resistance = 0.047 h m^2 K kJ^{-1}			
	4	reinforced concrete 2400		0.14	7.56	2400	1.0	2400
	5	air space		0.14	resistance = 0.047 h m^2 K kJ^{-1}			
	6	sound insulation 045		0.03	0.16	100	1.8	180
	7	plasterboard ceiling covering		0.015	0.76	900	1.0	900
roof	8	plasterboard ceiling covering	variable	0.015	0.76	900	1.0	900
	9	sound insulation 045		0.03	0.16	100	1.8	180
	10	air space		0.14	resistance = 0.047 h m^2 K kJ^{-1}			
	11	concrete 2400		0.14	7.56	2400	1.0	2400
	12	cellular glass		variable(2)	0.16	100	1	100
	13	bitumen roofing membrane		0.005	0.61	1200	1	1200
	14	gravel. sand. split fill		0.1	5.04	1800	1	1800
interior walls	15	plasterboard ceiling covering	0.1	0.015	0.76	900	1.0	900
	16	thermal insulation 040		0.03	0.14	80	0.9	72
	17	air space		0.04	resistance = 0.047 h m^2 K kJ^{-1}			
	18	plasterboard ceiling covering		0.015	0.76	900	1.0	900
exterior wall (3)	19	light concrete 1200	variable(2)	0.04	2.23	1200	1	1200
	20	thermal insulation 050		variable(2)	0.18	80	0.9	72
	21	light concrete 1200		0.04	2.23	1200	1	1200

massive construction		material layer	total thickness	d	λ	ρ	c	c ρ
				m	kJ h^{-1} m^{-1} K^{-1}	kg m^{-3}	kJ kg^{-1} K^{-1}	kJ m^{-3} K^{-1}
floor	1	floor covering	0.35	0.005	0.61	1000	1	1000
	2	cement screed		0.05	5.04	2000	1	2000
	3	impact noise insulation 045		0.03	0.16	100	1.8	180
	4	reinforced concrete 2400		0.25	7.56	2400	1.0	2400
	5	plaster 1200		0.015	1.26	1200	1.0	1200
roof	6	plaster 1200	variable(2)	0.015	1.26	1200	1.0	1200
	7	reinforced concrete 2400		0.25	7.56	2400	1.0	2400
	8	cellular glass		variable(2)	0.16	100	1	100
	9	bitumen roofing membrane		0.005	0.61	1200	1	1200
	10	gravel. sand. split fill		0.1	5.04	1800	1	1800
Interior walls	11	plaster 1200	0.205	0.015	1.26	1200	1.0	1200
	13	sand-lime brick		0.175	2.02	1200	1	1200
	14	plaster 1200		0.015	1.26	1200	1.0	1200
Exterior wall(4)	16	concrete 2400	variable(2)	0.12	7.56	2400	1.0	2400
	17	thermal insulation 050		variable(2)	0.18	80	0.9	72
	18	concrete 2400		0.12	7.56	2400	1.0	2400

The thermal properties originate from the TRNSYS database.
(1) The air space is modelled in TRNSYS as massless with no specification of thickness. Here, thickness is just indicative
(2) The thickness of thermal insulation set according to the target thermal transmittance of the exterior wall
(3) The exterior wall LI is simplified as 3-layers elements for modelling practicality in TEB and TRNSYS (thermally relevant not constructive)
(4) The exterior wall MA is 6 times heavier than the LI (2 times denser and 3 times thicker)

1.2. Urban-related Additional Calculations in TRNSYS

A number of equations were manually added in the TRNSYS project in order to account for some missing calculations related to the built surroundings. This is especially important in this research where the focus is put on the effects of urban conditions on the thermal behaviour of buildings. These include the calculation of the diffusely reflected shortwave radiation, the longwave radiation originating from the surroundings and the indoor illumination (Figure 16). The geometrical principle of calculation based on the view factors and differentiated by floor level is sketched in Figure 17. In order to keep this report clearly laid out, only the background of this issue is introduced hereafter, whereas the detailed calculation procedures are compiled in Appendix 5.

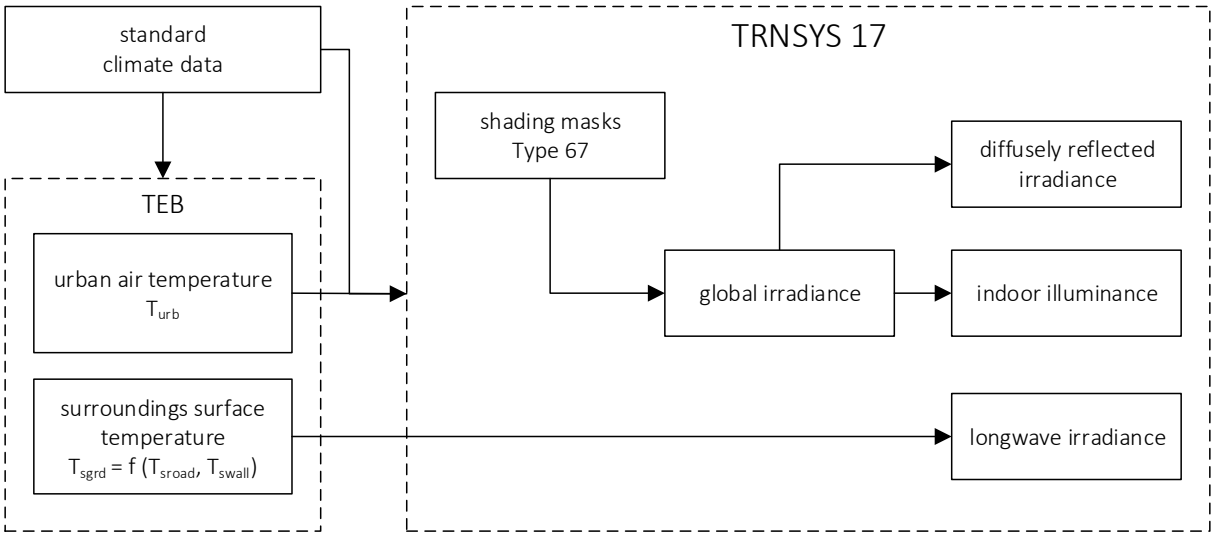

Figure 16: Additional urban related calculations as implemented in the TRNSYS projects in PART I

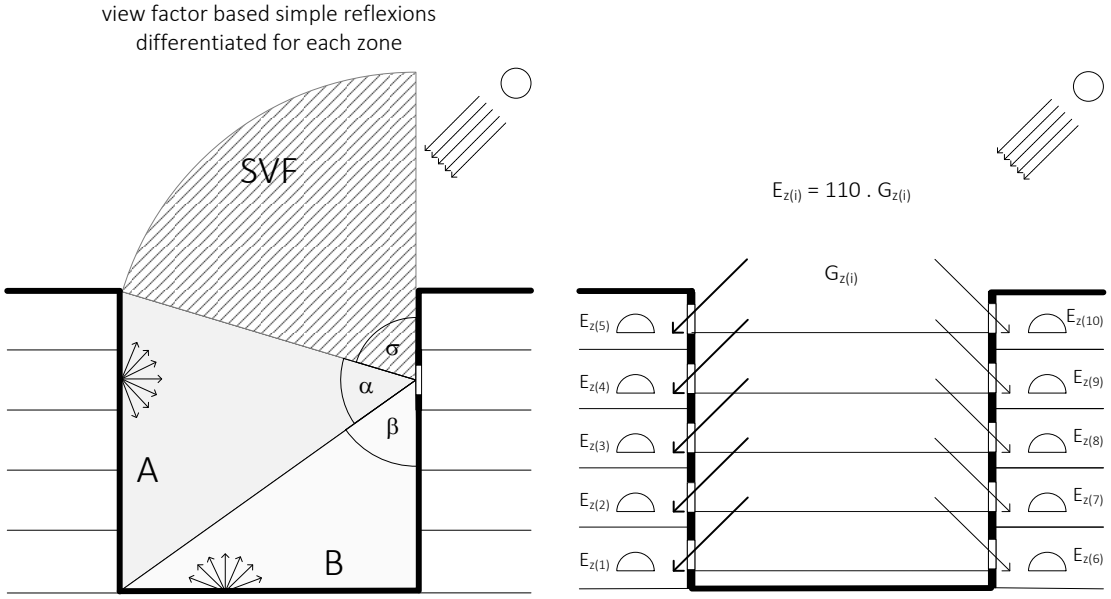

Figure 17: The calculation scheme for the diffusely reflected irradiance and indoor daylight illuminance

1. Shortwave radiation fluxes in the urban canyon

Solar radiation plays a key role in the energy balance of a surface. Within an urban canyon, shading patterns change the solar radiation availability on its facets throughout the day. Moreover, the shortwave radiation trapped in-canyon is diffusely reflected by the walls and ground and must be taken into account. The mask effects due to neighbouring buildings can be included in TRNSYS-Studio either using Type 67 or, since the release 17 of TRNSYS, by means of the add-on TRNSYS3D for SketchUp®, which generates a shading matrix of the imported geometries in TRNBuild. Both Type 67 and the imported shading matrix set i) the direct solar radiation equal to zero if the sun height is lower than the shading mask and ii) weights the diffuse radiation using the actual sky view factor. So far, the obstructions effects are taken into account. However, the diffusely reflected solar radiation inside the canyon is not included, which depends on i) the street and facing wall view factors, ii) the albedo of each canyon surface iii) the façade construction (walls vs. windows) and iv) whether the shading devices are in use or not for each time step t. Therefore, this shortage was manually solved using internal equations in TRNSYS Studio as itemised in Appendix 5.

2. Longwave radiation fluxes in the urban canyon

TRNSYS takes into account the exchange in the longwave range between the simulated building surfaces and the sky by means of the fictive sky temperature T_{sky}. The longwave radiation exchange with the built surroundings is simplified by considering an average surface temperature T_{sgrd}, usually considered to equal the outdoor ambient air temperature T_{out}. In real cases, however, a surface temperature is close or higher up to 5 K to T_a only in shaded cases, whereas irradiated surfaces experience up to 30 K higher values as T_{out}. The asymmetrical longwave irradiances inside a canyon due to different exposure patterns were measured and reported by Ali-Toudert and Mayer (2007a). In order to improve this feature, the T_{sgrd} is calculated as an average value of the canyon surface temperatures based on TEB output temperatures for road and wall surfaces, T_{sroad} and T_{swall}, respectively (see Appendix 5).

3. Indoor illuminance

Daylighting is always preferable to artificial lighting because it enhances visual comfort and supports energy savings (VDI 6011, DIN EN 12642). Therefore, artificial lighting is assumed only when daylight is not sufficient. To this end, it is crucial to quantify the natural illuminance available indoors for each office at each floor level. Illuminance depends on the solar radiation, sky conditions, the mask effects due to the built surroundings, the shading devices possibly in operation as well as on the geometrical and optical properties of the addressed indoor spaces. Appendix 5 describes the calculation procedure used in this work.

4. Urban wind

In connection with building energy modelling, the wind boundary conditions are relevant for natural ventilation settings. A ventilation rate expresses the amount of air change volume in a room per hour, which unit is h^{-1}. If natural, it depends on the opening's geometry and area, on outdoor wind velocity (speed and incidence) and on indoor-outdoor air temperature difference. The add-on TRNFlow for TRNSYS includes the wind flow engine COMIS, which enables the calculation of the wind flow between building thermal zones indoors and provides some connection with outdoors. However, the capabilities of TRNFlow in the latter case are limited. TRNFlow requires as input the wind pressure coefficients Cp on the external facades, which are limited to one height outdoors. Cóstola et al. (2009) reviewed various Cp calculation procedures as implemented in different building energy models and reported on the uncertainty of using such C_p values. Moreover, owing the fact that heat losses due to ventilation are well known to be decisive on the final energy demand for heating and cooling, it has been decided to handle the air change in this study as predefined ventilation rate in the absence of reliable information on this issue. The ventilation rate is assumed similar for all investigated urban structures and floors. Indeed, the wind velocity is only available at mid-canyon height (using TEB) and the wind pressure coefficients C_p values when calculated are mostly wall averaged (i.e. same for lower and upper floors). Furthermore, the dynamic behaviour of the user in opening and closing the windows may greatly overlap the importance of the only wind pressure on the façades due to geometry and wind exposure aspects. The external heat transfer coefficients are kept equal for all thermal zones for the same reason.

In PART I of this study, the ventilation rates refer to the minimum air change required for keeping a healthy air quality. The ventilation rates are assumed small enough to be realistic with partial opening of the windows even for the lowest floors in dense urban structures. A pivot-hung window enables 0.8 h^{-1} up to 2.5 h^{-1} air change and even with shading devices up to 1.5 h^{-1} (see e.g. Schild and Willems 2013).

For the sake of completeness, the results in terms of energy demand are also discussed in case the required ventilation is mechanical as worst-case scenario.

Solving the issue of urban wind influence on indoor ventilation is complex and would require the coupling of urban canopy and building energy models in order to address: i) the reduction of wind speed, ii) the change in wind incidence and iii) the resulting wind pressures and convective heat transfer coefficients at different heights, as well as iv) the thermally induced indoor ventilation due to temperature gradients. CFD methods are predestined for such tasks but are hardly useful because very time consuming as already discussed in the state of the art.

1.3. Urban and Building Simulation Settings

1.3.1. Main Simulation Settings in TEB and TRNSYS

The buildings investigated account for well-known thermally decisive urban and building parameters as listed in Table 10. For the climate investigation using TEB, two sets are simulated: i) a sensitivity analysis [SET I] in Table 11 and ii) an excerpt of it [SET II] in Table 12 whose outputs are later used for the energy building simulations using TRNSYS. Table 11 and Table 12 follow a typical DOE plan with a 3-steps equidistance principle coded [-1], [0] and [+1]. Setting 3-steps aims at highlighting not only the linear but also non-linear relationships (i.e. incl. quadratic terms). The values of the variables at each step have been chosen to be as large as possible within a realistic range. The variables A and B and P are urban related, the variables C, D and E refer to building properties, while F and G are surface related. The choices made are commented below. The street vertical profile expressed by the ratio between building height H and street width W, also known as aspect ratio H/W, is varied to account for the effects of urban density. Mainly, the aspect ratio has a direct effect on i) the availability versus obstruction of the solar radiation on the canyon facets and so the potential for thermal heat storage and indoor passive solar gains and ii) on the heat release, especially at night, which depends on the sky view factor SVF.

Table 10: Investigated urban and building parameters as variables in PART I including their ID coding

ID	Investigated parameter as variable	use in TEB		use in TRNSYS	
		SET I	SET II	SET III, SET IV	SET V
A	aspect ratio H/W	√	√	√	√
B	solar orientation	–	–	√	√
C	window ratio	– [(1)]	– [(1)]	√	√
D	thermal insulation	√	√	√	√
E	thermal inertia	√	√	√	√
F	albedo (shortwave reflectance)	√	– [(2)]	– [(2) (4)]	– [(2) (4)]
G	emissivity (longwave emittance)	√	– [(2)]	– [(2)]	– [(2)]
L	floor level	–	–	√	√
H	anthropogenic heat (traffic | industry)	√	– [(2)]	–	–
P	plan density (roof surf./total)	√	– [(2)]	–	–
S	shading devices efficiency	–	–	– [(3)]	√
V	ventilation rate during usage time	–	–	– [(3)]	√
N	ventilation rate outside usage time	–	–	– [(3)]	√
I	internal heat gains	–	–	– [(3)]	√

[(1)] In TEB, the window ratio C is indirectly accounted in the thermal insulation D.
[(2)] These parameters are set as constants. [(3)] These parameters follow constant scenarios.
[(4)] The shortwave reflectance of the shading devices when in use is included.

The three steps of A state for shallow, unity-like and deep canyons and express low, medium and high density, respectively. The building height remains constant (18 m) and the street width varies. The orientation of the façades B is decisive on the exposure of the indoor spaces to solar radiation and so on the potential of passive solar gains in the cold season and solar protection against overheating in the cold season. The selected orientations seek to cover the whole horizon of 360° and include the north-south orientation N-S, NW-SE and NE-SW orientation with a 60° deviation from north towards west and east, respectively (Figure 12).

The ratio of window area to external wall is decisive in relation to the amount of solar energy and daylight that is available indoors. The window ratio is varied in a wide range from a few openings with a perforated façade at 30%, to about half-glazed with a row-glazing façade at 60% and fully glazed with a glass façade at 90%. Moreover, the window usually has weaker thermal insulation than other opaque parts of the building envelope and this makes the window ratio important in this respect.

The thermal insulation for walls, roofs and windows is investigated by setting three levels corresponding to weak, medium and good thermal insulation given by the heat transmittance (U). Inspired from the reality, the steps for the thermal insulation of walls and windows were compatibly chosen, i.e. within the same insulating quality range. This implies an interdependency, which can be expressed by an equivalent thermal transmittance U_{eq} (see Appendix 4). The light transmission coefficient (τ) is also set at an equidistance to ensure a proper daylighting comparison according to the DOE plan. The solar heat gain coefficient (g) shows only minimal deviation from equidistance because realistic glazing products were chosen. The heat transmittance of window U_{wdw} is calculated by assuming 90% glazing and 10% frame in all cases for practical reasons. To account for thermal inertia, the building is assumed either lightweight, mediumweight or massive construction. In TEB simulations, these three steps were simulated, whereas in TRNSYS, only the lightweight and massive constructions were analysed. This is due to the difficulty of numerically determining three equidistant levels of thermal inertia for all internal surfaces enclosing the thermal zones (see Appendix 4). The surface solar reflectance given by the albedo (α) is varied within a range of 0 to 0.5, which corresponds to full and half absorption, as these are most likely to occur is reality and much higher albedos are less common. The long-wave emissivity is assumed to vary from full to half emissivity absorption, as these are most likely to occur is reality and much lower emissivity is less common. The object simulated in TRNSYS being a multi-story building, three floors were specifically considered in the vertical analysis: the ground (F1), mid-canyon (F3) and top floor (F5).

Table 11: Canyon geometry and construction settings for the sensitivity analysis [SET I] using TEB (729 runs)

item	ID	variable	unit	[-1]	[0]	[1]
urban context	A	aspect ratio H/W (H = 18 m)	-	0.2	1	1.8
	P	plan density (roof surf.)	m	9	18	27
human activity	H	anthropogenic heat traffic | industry	W	0 | 0	60 | 20	120 | 40
building construction	D	thermal insulation walls (1)	W m^{-2} K^{-1}	3.0	1.6	0.2
		thermal insulation roof	W m^{-2} K^{-1}	0.6	0.35	0.1
	E	thermal inertia (2)	kJ m^{-1} K^{-1}	light	medium	massive
surface properties	F	albedo	-	0	0.25	0.5
	G	emissivity	-	0.5	0.75	1
location		Mannheim: 49.52°N, 8.55°E (TRY12)				

(1) Average of opaque and transparent parts are based on window ratio of 30%, 60% and 90%.
(2) The heat capacity (c, ρ) and thickness (d) are varied at equidistance to fit the steps of E (see Table 7).

Table 12: Urban and building simulated variables and their 3-step values for the parametric study [SET II] used in TEB (81 runs) and TRNSYS (54 runs)

item	ID	variable		unit	[-1]	[0]	[1]
urban context	A	aspect ratio H/W (H = 18 m)		-	0.2	1.0	1.8
	B	solar orientation		degrees	NW-SE (N - 60°)	N-S (N = 0°)	NE-SW (N + 60°)
Building	C	window ratio		%	perforated façade, 30%	row façade, 60%	glazed façade, 90%
	D	thermal insulation	U_{wall}	W m^{-2} K^{-1}	0.65	0.4	0.15
			U_{gls} | U_{wdw}		2.1 | 3.3	1.4 | 2.1	0.7 | 1.0
			U_{roof}		0.60	0.35	0.10
	E	Thermal inertia		kJ m^{-1} K^{-1}	light	Medium (1)	massive
	L	Floor level		-	ground floor F1	mid-canyon floor F3	top floor F5
Further details							
glazing properties	light transmission τ			-	0.786	0.706	0.625
	solar heat gain coefficient g			-	0.702	0.589	0.407
	glazing layers			- mm	double 5.7/12.5/5.7	double 4/16/4	triple 4/8/4/8/4
climate and location	temperate climate			Mannheim: 49.52°N, 8.55°E (source: TRY12)			
	Mediterranean climate			Algiers: 36.75°N, 3.00°E (source: Meteonorm)			

(1) The middle step E = 0 was simulated in TEB but not in TRNSYS. See text for further explanation.
The anthropogenic heat (H) is used in TEB and set to 10 | 20 (30 from 7:00 to 19:00, otherwise 10)
The albedo (F) is set to 0.1 for roads and 0.2 for wall and roof and the emissivity (G) is set to 0.94 in TEB.
In TRNSYS, F and G are differentiated between opaque and transparent parts, accordingly.
With respect to the plan density P, the building width is set equal to 18 m in TEB.

The offices are simulated by assuming thermal neutrality with laterally adjacent offices and mid-zones. Moreover, thermal neutrality at ground floor is assumed given the usual presence of underground floor. The Mid-European climate was investigated by means of a DWD Test Reference Year (TRY12, representation station Mannheim). The choice of TRY12 is in line with PART II dedicated to the city of Stuttgart also located in the climate region N°12. Additionally, the simulation plans [SET II], [SET III] and [SET IV] are applied to the Mediterranean climate (Algiers, 36.75°N, 3.00°E) for the purpose of comparison between a temperate climate with a dominating heating season and a warm climate with long summer and more cooling need. Due to space constrains, the results about the Mediterranean Algiers are synoptically reported in section II - 4 (p 145).

The same settings considered in TRNSYS simulations are taken into account in TEB simulations upstream, with some adjustments conditioned by some differences in the input information required by the two programs. Appendix 3 exemplarily lists the inputs of a TEB simulation as used in this research, with the following assumptions:

1. Surface temperatures of walls, road, roofs, deep road temperature and building indoor temperature are start values for the first simulation time step. The deep road temperature is known to be nearly constant over the year and is assumed equal to the annual mean temperature of the assumed location. The start building's indoor air temperature is assumed to be 20 °C. Surface temperatures of roof, walls and road are assumed equal to air temperature at simulation start time. Albedo and emissivity are kept constant for all case studies (except in the sensitivity analysis).
2. Building materials: roofs and walls are input in TEB as simulated in TRNSYS, except that the heat transmittance is summed for opaque and transparent parts of the façades since TEB only assumes opaque walls. For practical reasons, walls and roofs are assumed in TEB to be of the same construction.
3. Anthropogenic heat is taken into account as an additional term in the energy balance of the urban canyon. Sensible heat for traffic Q_{FTRFH} and industry Q_{FINDH} are required. TEB assumes that heat release from traffic occurs during daytime hours from 7:00 to 19:00 and from industry the day round (24 hours). Rough estimations of anthropogenic heat are available in the literature, e.g. Sailor and Lu (2004), however cannot be considered as representative owing the wide range of possibilities depending on city size, urban density, population density, nature and intensity of urban activities, etc. (see also Ichinose 1999, Fan and Sailor 2005, Oke 2006b, Kuttler 2010). With reference to Sailor and Lu (2004), Q_{FTRF} is set equal to 20 W m^{-2} and Q_{FIND} to 10 W m^{-2},

which correspond to moderate values. Hence, the total anthropogenic heat flux assumed equals 30 W m^{-2} in the daytime hours from 7:00 to 19:00 and 10 W m^{-2} at night, which reproduces a realistic daily profile of Q_F. Yet, neither seasonal or weekday/weekend sensible heat release was considered nor was anthropogenic latent heat considered, due to the lack of reference information, although this is technically possible using the new TEB-Type 201.

4. The canyon is assumed dry for TRY12 and Algiers, i.e. no precipitation or snow is considered because this information is not available.

The number of simulation in TEB is reduced to one-third (81 instead of 243 per location), because the variable B (solar orientation) is ignored in TEB, as the model considers an urban structure with equally available orientations. In TRNSYS, the simulation sets are reduced to two-thirds (54 instead of 81 runs) because the medium-weight construction (E = 0) has been omitted.

1.3.2. Building Operation and HVAC Settings in TRNSYS

A number of local and international standards and guidelines do exist, which set recommendations or settings requirements for the numerical prediction of the thermal behaviour and energy demand of buildings. These include in particular DIN V 18599, the DIN EN 15251, DIN 4108 (2 and 6) and the VDI 2078. The building as a physical object and the HVAC simulation settings as applied in all simulation ensembles in PART I of this research refer to this literature with an effort to keep them simple and at the same time realistic.

Table 13 lists the main assumptions for heating, cooling, lighting, ventilation, internal gains and shading devices and Figure 18 summarizes them graphically.

The building usage time period (UT) or operation period spans from 7:00 to 18:00 (DIN V 18599-10). The remaining daily hours (nighttime and weekends) are named “outside usage time OU” in this report. The heating follows a schedule starting at 5:00, i.e. 2 hours earlier than the occupation time schedule in order to allow a preheating of air before work time starts (DIN V 18599-10). Heating assumes a typical set air temperature of 21 °C for non-residential buildings during operation, whereas a night sink down to 17 °C is assumed outside the operation period (DIN V 18599-10). The cooling is planned from a set indoor air temperature of 26 °C as overheating cut-off with an air humidity set to 60% for latent heat calculations. According to DIN V 18599-10 and DIN EN 15251, setting indoor temperature at 20 °C for heating and 24 °C for cooling are also possible. The choice made here is motivated by the assumption of a certain capability of the user to thermal adaptation, which enlarges the range of his ther-

mal tolerance, especially in the summer and if the building is naturally ventilated. According to DIN V 18599-10, higher room temperatures are admitted in the arrangements of cooling systems at high ambient temperatures. DIN EN 15251 also suggests dynamic comfort room temperatures depending on the prevailing outdoor air temperature. See section I - 2.5 (p 49) for a discussion about thermal and adaptive comfort.

Table 13: General settings of the building operation in TRNSYS simulations

item	schedule	description
building description	time	office use; 2 offices per floor with opposite orientations dimensions: 2.8 x 5 = 14 m^2, 3 m height, Façade 9.52 m^2, volume 42 m^3 10 thermal zones, arranged vertically in 5 floors
office occupation	UT	usage time UT from 7:00 - 18:00 on weekdays (1)
	OU	outside usage times OU between 18:00 and 5:00 and on weekends (1)
	UT	1 person for 14 m^2 (moderate occupation surface), 1 persons in one office (1)
heating	UT	set temperature T_a = 21 °C, from 5:00 to 18:00 (i.e. 2 hours preheating)
	OU	set temperature T_a = 17 °C (nighttime and weekend sink)
cooling	UT	set temperature T_a = 26 °C, air humidity for cooling = 60%
	OU	no cooling
infiltration rate	UT, OU	0.1 h^{-1} (permanent)
ventilation rate	UT	Hygienic air renewal 0.9 h^{-1} if UT; Additional ventilation: 1.0 h^{-1} if $T_{op} > 24$ °C and $T_{out} < T_{op}$ down to 22 °C
	OU	1.0 h^{-1} if $T_{op} > 24$ °C and $T_{out} < T_{op}$ down to 18 °C
internal gains	UT	From 1 person at 75 W and from 1 computer at 100 W (1) artificial lighting at 13 W m^{-2} with 40% convective if no sufficient daylight
shading devices	UT	ON if the incident global radiation at the window $G_{wdw} > 200$ W m^{-2} OFF if the incident global radiation at the window $G_{wdw} < 160$ W m^{-2} shading factor Fc = 0.25 (i.e. 75% reflected solar radiation)
artificial lighting	UT	ON if Illuminance from daylight $E_{in} < 500$ Lux OFF if Illuminance from daylight $E_{in} > 700$ Lux
UT = during usage time; OU = outside usage time (1) DIN V 18599		

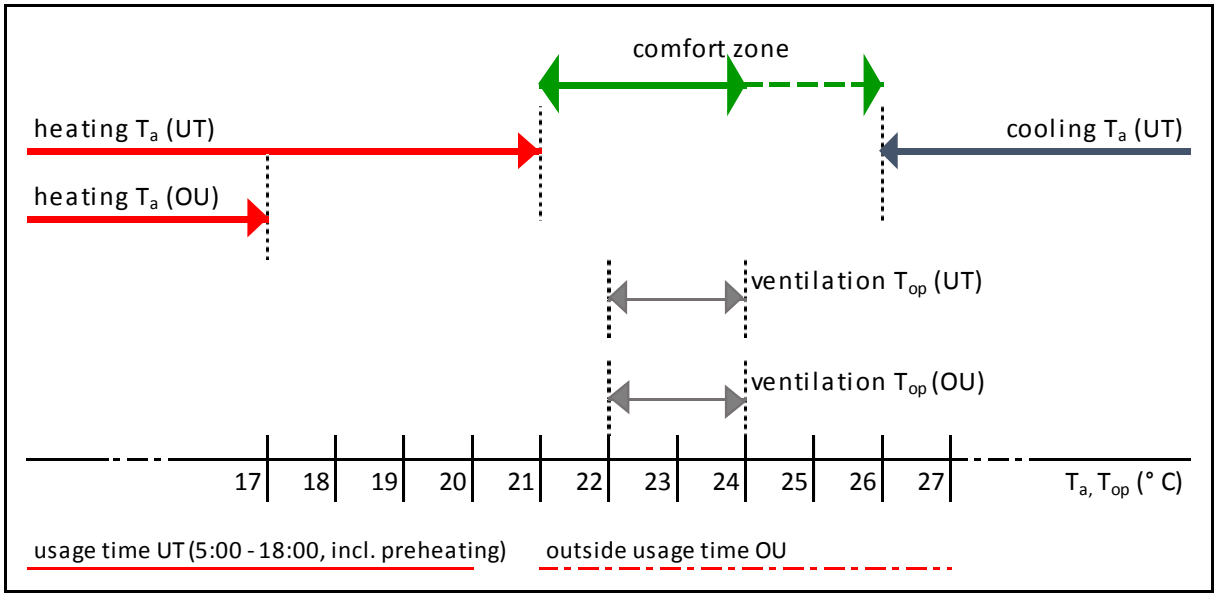

Figure 18: Schematic on the TRNSYS building operation and HVAC settings as 0/1 step functions

The total ventilation rate is threefold and consists of i) leakage infiltration, ii) air change required for hygienic reasons and iii) additional ventilation for preventing overheating (see VDI 2078). A ventilation rate of 0.9 vol. h^{-1} during UT is assumed based on the requirement of a minimum of 40 m^3 fresh air per person (DIN V 18599-10). The office room has a volume of 42 m^3 and occupied by one person. The resulting minimal air change of 0.952 is rounded up to 1.0 h^{-1}, with 0.1 h^{-1} covered by the continuous infiltration due to leakage.

Furthermore, a preventive measure for overheating is foreseen where the user would open the windows further if the operative temperature T_{op} exceeds 24 °C until a lower threshold of 22 °C (UT) is reached again (only if T_{out} is lower than T_a and T_a above 21 °C). This measure is realistic and at no charge and would reduce the need for mechanical cooling. An air change rate of 1.0 h^{-1} is assumed in this case. Outside the usage time period (nights and weekends), a similar temperature dependent ventilation is foreseen in order to decrease the need for cooling the day later with a lower threshold of 17 °C. This measure is implemented using mechanically controlled windows or via air flaps. Hence, the building is assumed to be naturally ventilated unless mechanical ventilation cannot be avoided e.g. for noise or pollution disturbance. Hence, air change is assumed to occur with air temperature and humidity identical to those prevailing outdoors. Even if assumed to be mechanical, extensive tests showed that the sum of cooling and ventilation (OU) energy demands is lower than the cooling demand alone if no ventilation (OU) is planned. For the sake of completeness, the scenario of a mechanical ventilation is also addressed in the interpretation of the results about the ventilation rates.

Temperature dependent settings (e.g. ventilation rate) consider operative temperatures T_{op}, which are more relevant in describing the human sensation of comfort or discomfort than the air temperature taken alone because T_{op} also includes the radiative surrounding environment. The operative temperature T_{op} is set as arithmetic mean value between air and surface temperatures of a thermal zone, which is a good approximation for simple geometries. For office use, an illuminance of 500 Lux is required (VDI 6011, EN 12464-1). Artificial lighting is used when the daylight potential is not sufficient. Lighting is operated if the indoor daylight is less than 500 Lux and is switched off at 700 Lux. The indoor illuminance as such being unavailable, it is approximated from the solar irradiance transmitted indoors through the windows as explained in Appendix 5. The windows are equipped with shading devices, which operate if the incident solar radiation on the façade is higher than 200 W m^{-2} and are set off for a lower threshold of 160 W m^{-2}. These thresholds were set after a series of preliminary tests. The shading devices are exterior blinds with an efficiency of 75%, i.e. they reflect 75% (Eshade = 0.75) and transmit 25% (Fc = 0.25) of the incident radiation into the room (DIN 4108-6).

Obviously, all these settings must be kept in mind when interpreting the results about energy demands. Yet, since these boundary conditions are kept identical, the relative comparison between the case studies undertaken in this research is reliable. An attempt to optimise these settings was undertaken beforehand by accounting for their predictable interdependencies, which may be either positive or negative as outlined in Figure 19. In other words, what can be attributed to urban and building design and what to the operation of the building? Indeed, the solar availability on the building façades may have contrasting effects on the energy demand for heating, cooling, lighting and ventilation and depend partly on the user defined internal settings, i.e. how the shading devices operate? More solar potential on the façades theoretically means more potential for solar gains; however, these may be suitable or not depending on the season. If solar radiation at the façade is excessive, then the shading devices are activated, which in turn means more use of artificial light to compensate the reduced daylight indoors. Artificial lighting is intrinsically a supplementary internal heat gain, which may counterbalance the less passive solar gains in the winter. The complexity of these interactions between solar availability outdoors, shading control at the façade, indoor solar gains and daylight versus artificial lighting explains 1) the difficulty of an intuitive prognosis and 2) confirms the necessity of a detailed parametric modelling as proposed in the next section (see [SET IV]).

Appendix 3 lists the input parameters for an office with one workstation as modelled here According to DIN V 18599-10. The marked items are used in this work, whereas the others are not because they are either not applicable or irrelevant. This standard assumes an annual period of use of 250 days using a stationary calculation method. This study assumes that the offices are not in use only on weekends. This corresponds to 261 days, the resulting energy demands are about 1% higher. Reduction factors for internal heat gains, or partial non-operation of the artificial lighting or cooling system due to temporary absence of the users as assumed in DIN V 18599-10 for stationary calculations are not considered here because they are less relevant in case of dynamic calculations. A reduction factor for solar and optical efficiency of windows due to possible dirt is ignored as well.

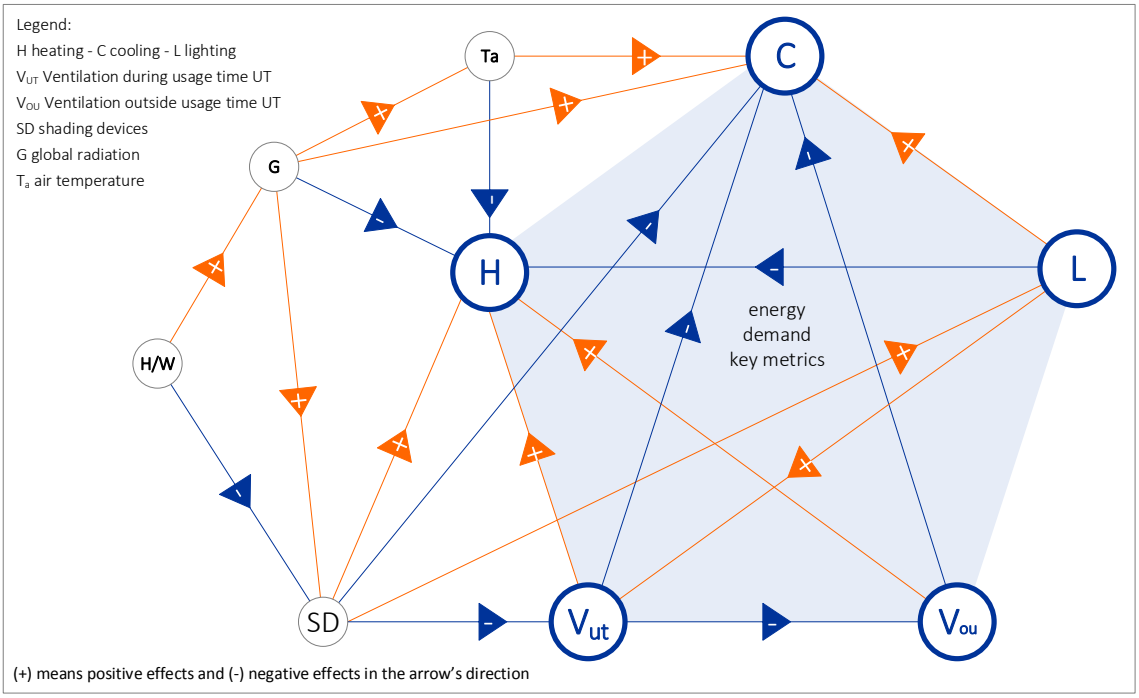

Figure 19: Interdependences between the various key metrics for energy demand in buildings including heating, cooling, lighting and ventilation

1.4. The Simulation Sets in TEB and TRNSYS

The present research consists of several series of simulations using TEB and TRNSYS, which are summarized in Table 14 and commented hereafter.

Table 14: Overview of the TEB and TRNSYS simulation sets and involved variables

sets	aim	variables	input climate	Climate type	runs	comments
SET I	TEB sensitivity analysis	A, D, E, F, G, H, P	Standard (rural)	MAN	729	B ignored, C indirectly included in D part factorial DOE plan (full factorial = 2187)
SET II	TEB urban microclimate modelling	A, D, E	Standard (rural)	MAN	81	B ignored, C indirectly included in D, F, G, H, P set to constants, full factorial DOE plan
				ALG	81	
SET III	TRNSYS Building energy modelling	A, B, C, D, E	standard (rural)	MAN	162	full factorial DOE plan (E at two steps)
				ALG		
SET IV			urban climate	MAN	162	full factorial DOE plan
				ALG		
SET V	TRNSYS sensitivity analysis	S, V, N, I	urban climate	MAN	1458	part factorial DOE plan (full factorial = 4374) SET (II) used as basis
(A) aspect ratio H/W, (B) solar orientation, (C) window ratio, (D) thermal insulation, (E) thermal inertia, (F) albedo (reflectance), (G) emissivity, (H) anthropogenic heat, (L) floor level, (P) plan density, (S) shading devices, (V) ventilation rate during usage time, (N) ventilation rate outside usage time, (I) internal heat gains due to lighting. MAN = Mannheim (TRY12), ALG = Algiers						

SET I – Sensitivity Analysis of TEB

The sensitivity analysis of the TEB model aims at exploring the dependence between the energy balance terms and the resulting microclimate in-canyon upon the physical properties of the canyon. In [SET I], the parameters A to E are varied according to Table 11 and consists of a part-factorial DOE plan of 729 simulation runs from a full-factorial plan of 2187. The reduced plan highlights the decisive effects including the main effects of the individual variables as well as their double interactions in a non-linear relationship. This systematic investigation in [SET I] helps better understand the results gathered as excerpt in [SET II]. This sensitivity analysis is also an illustration of the practicality of TEB-Type 201 in pre- and post-processing for parametric studies.

SET II – Urban Microclimate Prediction using TEB

The [SET II] serves the adjustment of the standard climate data using TEB prior to building energy simulations using TRNSYS. Therefore, it is an excerpt of [SET I] with less parameters assumed as variables, i.e. A, D and E (Table 14). [SET II] is run according to Table 12 using a full factorial matrix, which corresponds to 81 simulation runs per location and climate boundary conditions. The calculated in-canyon air temperature is then used as input in TRNSYS.

SET III and SET IV – Building Energy Demand Prediction

[SET III] and [SET IV] are TRNSYS simulations series using standard climate and urban climate respectively. The comparison between the two sets enables the understanding of the effects of the urban microclimate on the thermal behaviour and energy demand of the buildings indoors. The variables relate the physical and thermal properties of urban and buildings as listed in Table 12. These parameters depend on design choices and optimizing them is decisive in building design if passive strategies for energy efficiency are focused on. In [SET III] and [SET IV], the operation and HVAC conditions follow Table 13.

SET V – Sensitivity Analysis of Building Scenarios of Use and Operation

[SET V] extends the informative value of [SET II] in that building operation and HVAC internal settings are set as additional variables. This sensitivity analysis aims at investigating the modifying impact of user's preferences and behaviour as one further decisive issue regarding the final indoor energy demands. These includes: shading devices efficiency S, ventilation rate during usage time (V) and outside usage time (N) and Internal heat gains (I) from people, equipment and artificial lighting). In [SET V], the parameters (A) to (E) follow the same settings as [SET IV], whereas (S), (T), (N) and (I) follow Table 15 in a part factorial DOE plan counting 1458 runs. This two-step building investigation ([SET IV] and [SET V]) makes it

possible to isolate the effects of the thermo-physical properties of the built structure from the user dependent choices, in spite of their interdependency.

Such extensive scenarios for parametric studies are only feasible and suitable under three conditions: i) the calculation time is reasonable, ii) an automated processing system is provided to avoid time-consuming manual changes of settings and iii) if the time for post-processing of the results is reasonable with no loss in information or accuracy. These conditions are fulfilled (see section II - 5, p 157).

Table 15: Variables of the parametric study for the HVAC boundary conditions

ID	variables	unit	as used in [SET II]	as varied in [SET III]		
				[-1]	[0]	[+1]
S	shading device Fc	-	0.25	0.1	0.5	0.9
T	ventilation rate during UT	h^{-1}	1 + 1	1 + 0 = 1	2 + 2 = 4	3 + 4 = 7
N	ventilation rate outside UT (OU)	h^{-1}	1	0	2	4
L	internal gains (artificial lighting)	W m^{-2}	13	13 x 0.2	13 x 2.0	13 x 3.8

1.5. Post-Processing of the Simulation Outputs

Table 16 and Table 17 summarize the target key metrics for TEB and TRNSYS simulations and their post-processing. Appendix 6 lists some equations for the preparation of the outputs in the required from. For the calculation of the totals, two scenarios have been considered: the first one assumes the ventilation to be natural as operated by the user and is not included in the Total TOT I. This is realistic because incoming air for ventilation was assumed without any thermal preconditioning i.e. having outdoor air temperature. The second scenario, assumed as worst case, includes the ventilation as additional energy demand (TOT II).

1.5.1. Post-Processing of TEB Outputs

The urban air temperature T_{urb} calculated at mid- height within the canyon is the main output gathered with TEB as it corresponds to the adjusted air temperature from the standard climate as needed one step later for the TRNSYS simulations. More key metrics, which sum up the hourly results in one value per simulation and year, are calculated to allow some transversal comparison between the case studies. These are listed in Table 16 and commented below.

i) Heat island intensity (UHI) or cool island intensity (UCI) given by the difference between the predicted urban canyon air temperatures to standard input air temperature, i.e. $\Delta T_{u\text{-}s}$ ($T_{urb} - T_{stn}$) in Kelvin.

ii) Frequency of warming and cooling of canyon in comparison to standard input climate and given in hours (HSH, CSH).

iii) Magnitude of warming and cooling of canyon in comparison to standard input climate and expressed as temperature sum in Kelvin (HS, CS).

iv) Heating degree days, with base 18 °C including urban climate effects and compared to input climate (HDD, ΔHDD).

v) Cooling degree days, with base 24 °C including urban climate effects and in comparison to input climate (CDD, ΔCDD).

vi) Moreover, the energy balance terms of the urban canyon is taken as a whole system and as single facets.

1.5.2. Post-Processing of TRNSYS Outputs

The selected outputs from the TRNSYS simulations to be post-processed are listed in Table 17. These key metrics are integrated over the simulation period as annual values. Figure 20 shows the ways the single outputs were spatially cumulated, either per single zone (10 outputs), or as averages for the whole building (1 output), for each orientation (2 outputs) and by floor level .5 outputs). This enables a global assessment as well as a differentiation according to the urban relevant aspects of solar exposure and sky view.

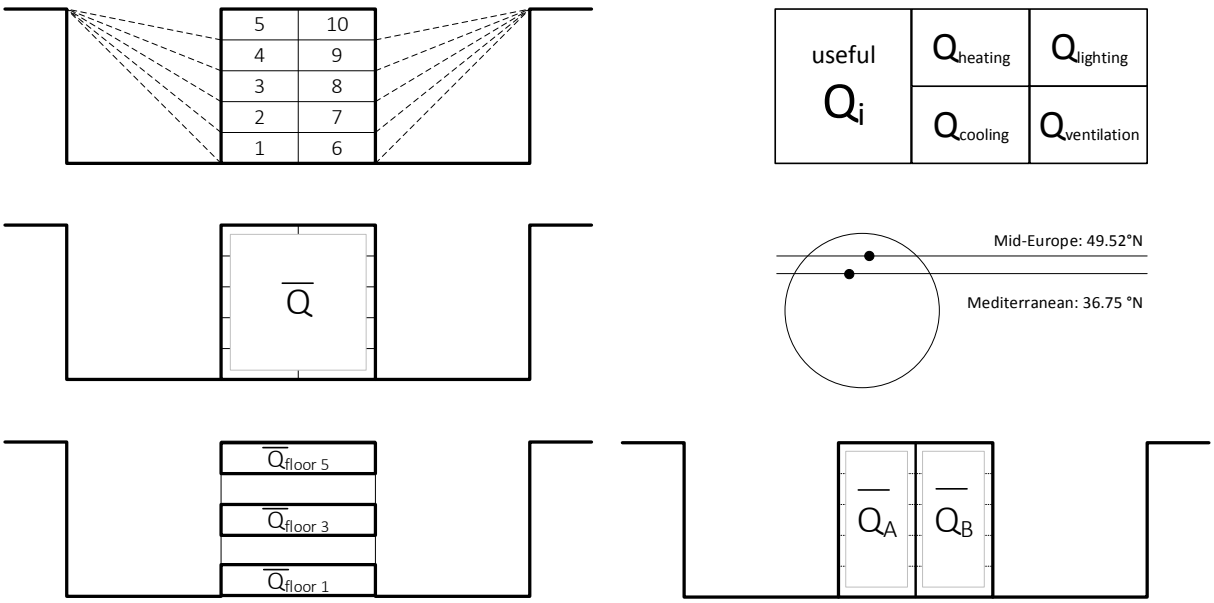

Figure 20: Post-processed outputs of TRNSYS simulations

Table 16: Post-processed outputs of TEB to canyon thermal behaviour and energy balance

	TEB outputs	Key metric	ID	unit
1	urban air temperature	$\Delta T_{u-s} = (T_{urb} - T_{stn})$	UHI, UCI	Kelvin (hourly)
2	Frequency	Warming: Σ UHI hours if $(T_{urb} - T_{stn}) > 0$	HSH	hours (of a year)
		Cooling: Σ CHI hours if $(T_{urb} - T_{stn}) < 0$	CSH	hours (of a year)
3	Intensity	Warming: Σ UHI in Kelvin if $(T_{urb} - T_{stn}) > 0$	HS	Kelvin (year sum)
		Cooling: Σ UCI in Kelvin if $(T_{urb} - T_{stn}) < 0$	CS	Kelvin (year sum)
4	effect on Building	Heating degree days: $T_{urb} < 18$ °C	HDD	degree day
		Cooling Degree Days: $T_{urb} > 24$ °C	CDD	degree day
5	Energy balance terms of the canyon and walls (**)	Net radiation Q* (SW + LW)	Q*	W m^{-2}
		Conductive heat flux	Q_G	W m^{-2}
		Heat storage in the fabric	ΔQ_S	W m^{-2}
		Turbulent sensible heat flux	Q_H	W m^{-2}
		Turbulent latent heat flux	Q_E	W m^{-2}
		Anthropogenic heat (outdoor)	Q_F	W m^{-2}
		Building heating (indoor)	Q_{FBLD}	W m^{-2}
(*) The UHI states for urban heat island when ΔT_{u-s} $(T_{urb} - T_{stn})$ is positive and UCI for urban cool island when ΔT_{u-s} $(T_{urb} - T_{stn})$ is negative. (**) refer to Appendix 1 for equations				

Table 17: Post-processed outputs of TRNSYS to building thermal behaviour and energy demand

TRNSYS outputs		Key metric	ID	SI unit
1	Thermal	heating	Q_{heat}	kWh m^{-2} a^{-1}
2		cooling	Q_{cool}	kWh m^{-2} a^{-1}
3	Lighting	artificial lighting	Q_{light}	kWh m^{-2} a^{-1}
4		daylighting potential	DLP	%
5	Ventilation	during usage time UT	$Q_{vent(ut)}$	kWh m^{-2} a^{-1}
6		outside usage time OU	$Q_{vent(ou)}$	kWh m^{-2} a^{-1}
7		V = T(UT) + V(OU)	Q_{vent}	kWh m^{-2} a^{-1}
8	Passive Solar	solar gains transmitted indoors through windows	Q_{soltr}	kWh m^{-2} a^{-1}
9	Thermal Comfort	potential for heat stress (cooling hours)	HSH	hours
10		overheating discomfort (sum of T_{op} higher than 26 °C)	HS	Kelvin
11		potential for cold stress (heating hours)	CSH	hours
11		freshness discomfort (sum of T_{op} lower than 26 °C)	CS	Kelvin
12	Useful Total	TOT I = 1 + 2 + 3 (ventilation assumed natural)	$Q_{TOT\ I}$	kWh m^{-2} a^{-1}
13		TOT II = 1 + 2 + 3 + 4 + 5 (ventilation assumed mechanical)	$Q_{TOT\ II}$	kWh m^{-2} a^{-1}
Nota: For space reasons, only the outputs 1, 2, 3, 4, 7, 8, and 12 are shown and discussed in this report.				

1.6. Climate Boundary Conditions

1.6.1. The Temperate Mid-Latitude Climate of Mannheim

The German Weather Services provide the building professionals with climate information for Germany in form of one-year representative data named Test Reference Years TRY (Christoffer et al., 2004). The country is divided in 15 climate regions (i.e. 15 TRY) mostly influenced by the local topography and distance to see. A test reference year is an hourly-based data set, which primarily relies on long-term standard meteorological measurements at a specific site, subsequently made representative for one climate region by means of further statistical corrections. The climate data used in this research is the TRY12. It has Mannheim as reference station and covers the area of the upper Rhine and lower Neckar valley. The updated release of 2010 is being used (Christoffer et al., 2004, DWD 2011). Interestingly, these current data offer the possibility to include the urban climate effects by providing a static adjustment option based on rough assumptions about urban heat island formation as depending on urban occupation density and number of population. It confirms thereby the currency of the issue even though based on hypothetical theory. The present work, by contrast, seeks to demonstrate the necessity of a dynamic adjustment of the climate data for more reliability.

Figure 21 shows the main climate features of Mannheim (TRY12), which can be summarized as follows: The reference station is located in a low-density environment with few vegetation. The winter is temperate and the summer warm. The rather protected valley location experiences few wind ventilation and precipitation, yet pronounced warming (Christoffer et al. 2004). Monthly mean temperatures vary between 20.2 °C and 2.4 °C.

Yet, the air temperature can occasionally reach a minimum up to -9.3 °C in the winter and a maximum of 36.3 °C in the summer. The air humidity is moderate and ranges between 3.8 and 9.6 g kg^{-1} dry air, which corresponds to a relative humidity between 64 to 84%. The yearly total solar radiation potential amounts 1089 kWh m^{-2} a^{-1}, with the diffuse component being almost equal or higher than the direct part because of frequent cloud cover. The highest potential for solar radiation occurs in June with up to a monthly value of 177 kWh m^{-2}, whereas the less sunny month is December with a total of 20 kWh m^{-2}. The highest sun position in Mannheim is 17.0 ° in the winter and 63.9° in the summer. The monthly precipitation is moderate throughout the year and ranges between 42 and 67 mm. The wind is mostly constant throughout the year around 2.5 m s^{-1}.

The psychometric chart of Givoni (1976) is usually used to assess approximate potential of comfort and necessary design strategies. The psychometric chart as shown in Figure 22, uses

as background the Mollier diagram, which shows graphically the dependences between air dry bulb temperature, air humidity (absolute and relative) and enables the calculation of the dew point temperature. Based on air temperature and humidity, the psychometric chart illustrates i) the comfort zone where no corrective measure through design is necessary and ii) various other zones where passive and active design strategies are required to cope with possible heat or cold stress. The comfort zone ranges between 20 °C and 27 °C with an air humidity of 20 to 80%. Beyond this zone, either heating or cooling, with humidification or dehumidification and probably additional daytime and/or nighttime ventilation, etc. is necessary to ensure thermal comfort. Up-to-date thermal comfort analyses rely on more parameters, in particular the mean radiant temperature, wind speed and personal data like clothing and activity (see section I - 2.5, p 49, and Ali-Toudert 2005).

The Climate Consultant 5.3 freeware developed by the UCLA energy design tools group (UCLA 2013) is a computer-based application which enables the calculation of the psychometric chart using different comfort models (e.g. California energy code, ASHRAE based on standards or adaptive models). It provides as output the number of hours of year for which one or more design strategies are required. Such an approach is useful as first interpretation of a climate type in order to define general climate adaptive design rule of thumbs. Figure 22 and Table 19 show the results for Mannheim based on the ASHRAE 55-2004 using the predicted mean vote PMV as thermal index (ASHRAE 2004). This model assumes for example that a person would adjust its clothing to match the season and feel more comfortable in higher air velocities, more likely in naturally ventilated buildings than centrally air-conditioned. The comfort period amounts 8.9% (778 hours). If no climatically worthwhile measures are planned, the heating demand would apply to 87.5% of the year against 1.4% for cooling. Using appropriate passive design strategies like internal heat gains, passive solar gains combined with thermal mass (i.e. ID 3, 9, 11 in Table 19) bring the comfort period to 41% (3600 hours). To ensure comfort the whole year, additional heating during 54% of the time is necessary. Table 18 roughly expresses the need for heating or cooling by means of heating and cooling degree days.

1.6.2. The Mediterranean Warm-Humid Climate of Algiers

In this research, the main work deals with mid-European locations but a comparison with a subtropical climate adds to the understanding of the whole issue. Therefore, the Mediterranean location of Algiers (36.75°N, 3.00°E) is investigated as well.

The software Meteonorm 6.1 (Meteonorm 2011) provided the climate data of Algiers because no test reference year is available for this location. Figure 21 shows an overview of its main climatic characteristics. Figure 23 plots the data on a psychrometric chart for a first assessment listed in Table 19. Algiers experiences warm summers with a mean monthly air temperature up to 26 °C and mild winters around 10 °C. However, the air temperature is for about 14% of the year higher and can occasionally reach 39 °C and for about 19% of the year lower with a possible minimum of 1 °C. High daily amplitude of about 10 K is also usual. The air humidity is high ranging between 65% and 78% as mean monthly values. The air is nearly saturated (RH > 90%) for about one fifth of the year and corresponds to a specific humidity of about 14.5 g kg^{-1}. The global solar radiation potential expressed as a surface-related monthly average ranges between 65 and 227 kWh/m^2m. In summer, the direct component of solar radiation can be up to 68%, whereas the diffuse component occurs more often in the winter and can reach up to 57% of the global radiation. At yearly basis, the potential for global solar radiation G amounts 1650 kWh/m^2a, from which 922 kWh $m^{-2}a$ as direct part S and 728 kWh m^{-2} a as diffuse part D. This corresponds to a proportion of 56% and 44%, for S and D respectively. The mean wind is about 2 to 3 m s^{-1} but wind forces up to 14.5 m s^{-1} are possible. The sun course in Algiers is such that the highest sun position is 29.8° in the winter and 76.7° in the summer.

Figure 23 and Table 19 show graphically and quantitatively the design strategies for the climate of Algiers by means of the psychometric chart. The comfort period amounts 14.2% (1243 hours). In case no appropriate passive design strategies are adopted, the heating would be necessary in 5344 hours of the year (61%) and cooling almost in 1123 hours (13%). Table 18 expresses the need for heating or cooling roughly as degree days. By means of passive design measures, including internal heat gain, passive solar gains combined with high thermal mass the comfort period may reach 5149 hours (59%). For this location, a full year comfort requires additional heating for about 1833 hours (21%) and cooling for 790 hours (9%) including dehumidification in 12% of the year.

More about the climate of Algiers and its incidence on the energy performance of buildings based on dynamic building silumations is available in Ali-Toudert and Weidhaus (2017).

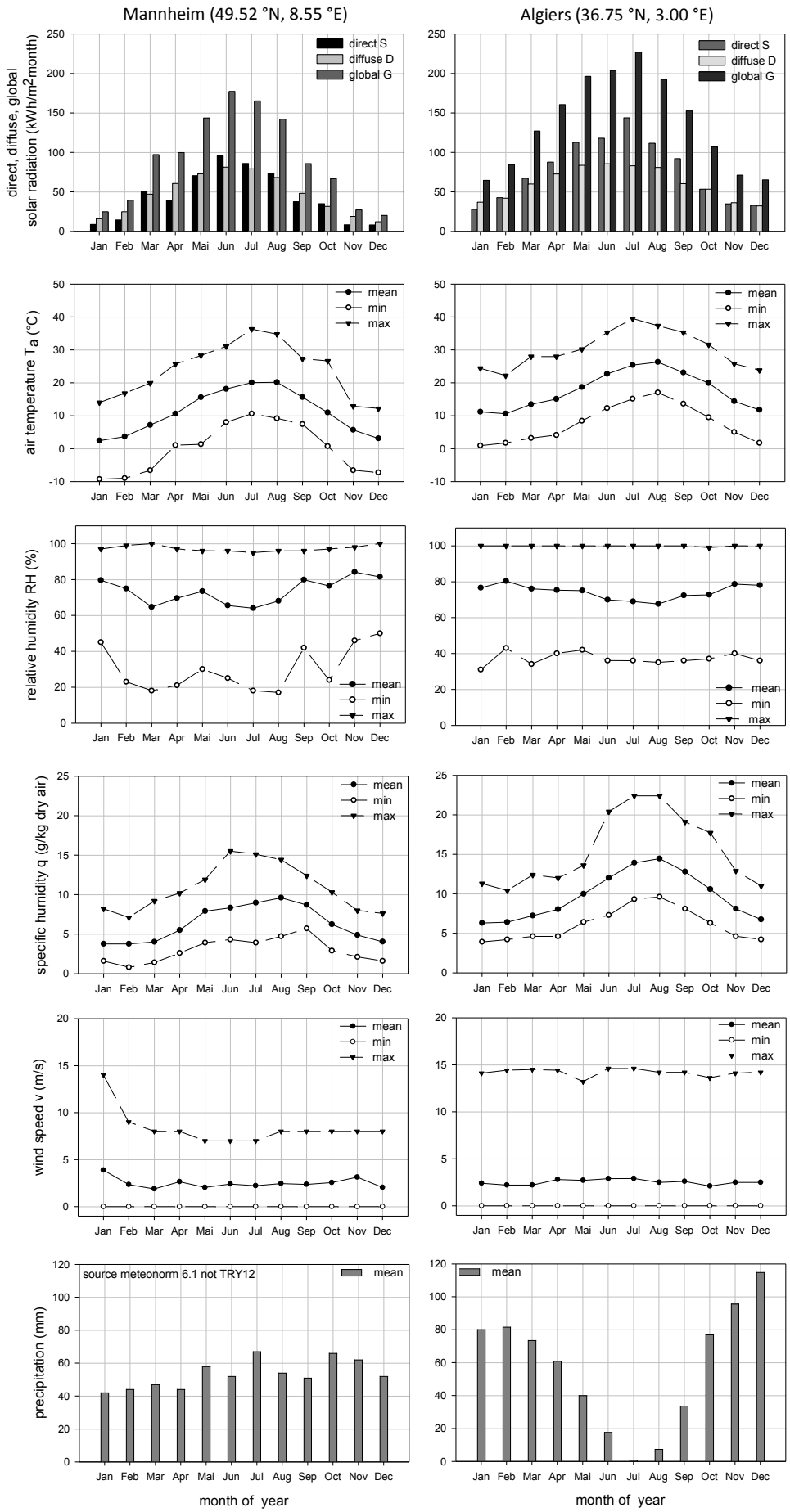

Figure 21: Overview on the mean climate conditions for Mannheim (TRY12) and Algiers (Meteonorm 6.1)

Table 18: Hypothetical frequency and intensity of heating and cooling degree days (with 18 °C and 24 °C base temperature, respectively) for Mannheim and Algiers

item	unit	MAN	ALG	MAN	ALG
HDD frequency	hours	6971	4587	3499	2023
CDD frequency	hours	474	1844	406	1425
HDD	Degree day	2825	1123	1374	449
CDD	Degree day	61	292	54	249

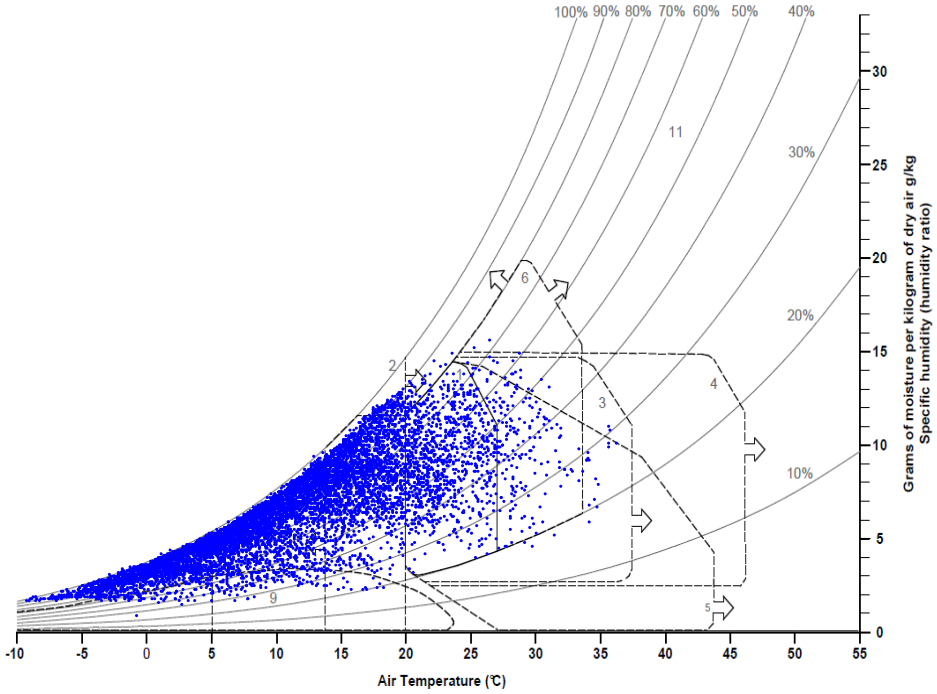

Figure 22: Climate analysis of Mannheim using the psychrometric chart (re-drawn from Lechner 2014)

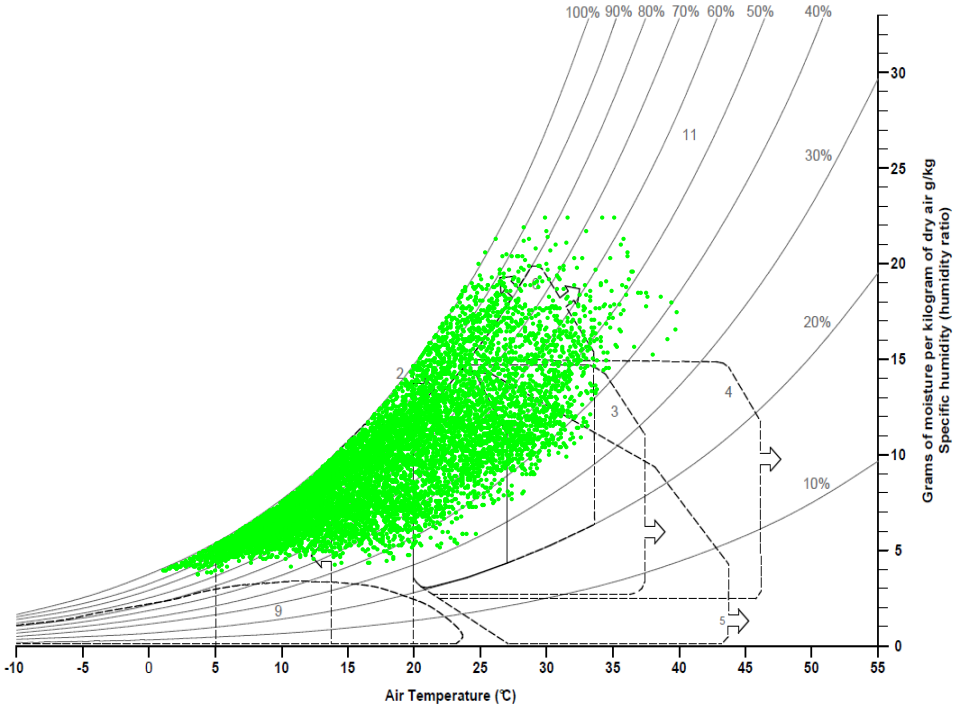

Figure 23: Climate analysis of Algiers using the psychrometric chart (re-drawn from Lechner 2014)

Table 19: Estimation of the climate adaptive design strategies for Mannheim using the psychrometric chart analysis of the Climate Consultant 5.3 (software © regents of UCLA)

ID	Design strategies	Mannheim MAN		Algiers ALG	
		%	hours	%	hours
1	Comfort	8.9	778	14.2	1243
2	Sun shading of windows	6.3	552	18.4	1615
3	High thermal mass [1]	1.1	93	3.8	333
4	High thermal mass with night flushed	1.1	93	3.8	333
5	Direct evaporative cooling [1]	0.8	68	2.4	209
6	Two-stage evaporative cooling	0.8	70	2.7	238
7	Natural ventilation cooling	0.7	58	2.5	219
8	Fan-forced ventilation cooling	0.7	61	2.7	236
9	Internal heat gain	25.5	2232	33.8	2962
10	Passive solar direct gain [1]	9.0	791	9.4	827
11	Passive solar direct gain with thermal mass	10.9	956	18.0	1577
12	Wind protection of outdoor spaces	1.1	93	0.1	8
13	humidification	0.0	0	0.0	0
14	dehumidification	2.2	189	12.0	1049
15	Cooling, add dehumidification if needed	0.3	29	9.0	790
16	Heating, add humidification if needed	54.2	4751	20.3	1782
Design Scenarios		comfort total			
I	only passive strategies [2]	41	3600	59	5149
II	including active measures [3]	100	8760	100	8760

[1] ID 4, ID 6, ID 10 are modifications of ID 3, ID 5 and ID 9 respectively and do not occur simultaneously.
[2] Strategies I: MAN [ID 1, 3, 9, 11] - ALG [ID 1, 3, 9, 11]
[3] Strategies II are additional measures to I, i.e. MAN [strategies I + ID 14, 15, 16] - ALG IDs [strategies I + ID 14, 15, 16]

1.6.3. Forcing Climate Data for TEB Simulations

For modelling the microclimate within the canyon using TEB in offline mode, the inputs of air temperature T_a, air humidity q and wind speed V are needed at a certain height above roof level. However, these are usually available at 2 m (T_a, q) or 10 m (V) above ground level from standard weather stations or from weather predicting software. Therefore, all reference climate data used in this project in both PART I and PART II have to be first numerically "shifted" to the desired height as illustrated in Figure 24 and following the procedure described in Météo France (2011). This is done using TEB for a free surface with several iterations (about 3 iterations). The resulting data are named Forcing data T_{frc}. The original data at 2 m and 10 m height are called reference or standard data and are used for comparison with the TEB calculated urban air temperature $T_{urb} - T_{stn}$. This deviation $\Delta T_{u\text{-}s}$ expresses the heating (heat island) or cooling (cool island) of the canyon due to urban influence. The outputs of TEB are calculated for mid-canyon but are differentiated in Figure 24 for better clarity of the principle.

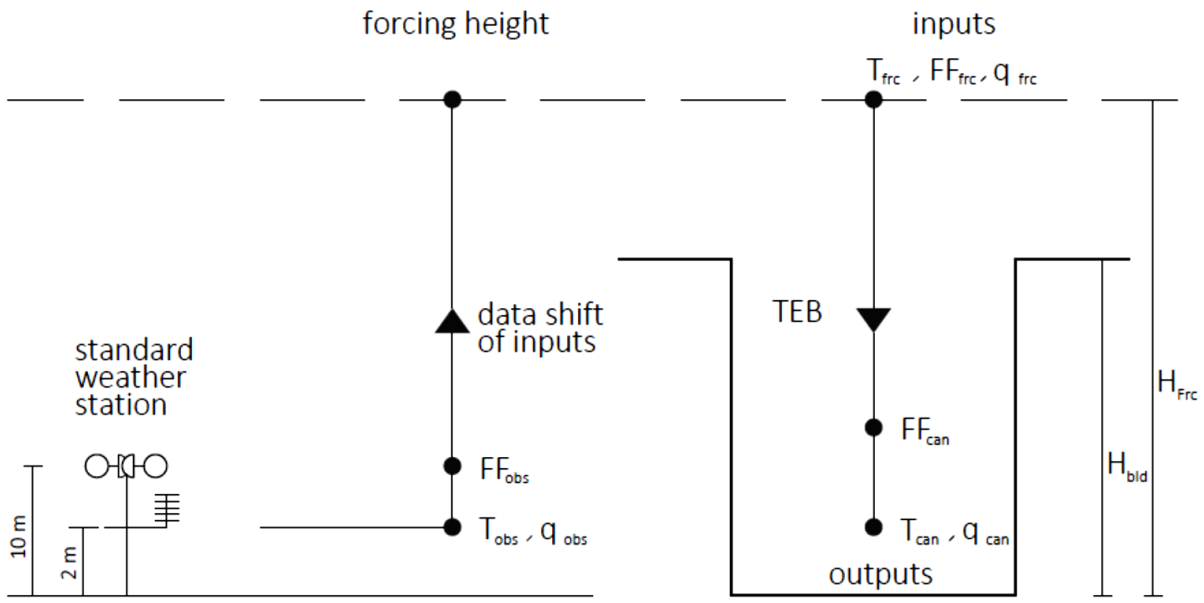

T_{obs} , q_{obs}	standard observed data (obs = stn)
T_{frc} , FF_{frc} , q_{frc}	climate data at forcing height (air temperature, wind speed, air humidity)
T_{can} , FF_{can}, q_{can}	climate data in-canyon at 2.00 m height

Figure 24: Schematic of the shifting procedure of reference climate data to a desired height above roof level for TEB calculations

2. THE RESULTS ABOUT THE URBAN CANYON MICROCLIMATE

The mechanisms underlying the development of urban microclimates in-canyon as calculated with TEB are presented based on two complementary sets of simulations:

1. A sensitivity analysis of TEB consisting of 729 runs which explore the part of responsibility of decisive thermo-physical urban and building variables as given in section II - 1.4 (p 85) and is named [SET I].
2. An excerpt set of 81 runs by assuming fixed values for some parameters, i.e. shortwave albedo F = 0.1 for road and 0.2 for wall and roof), longwave emissivity (G = 0.94), anthropogenic heat (H = [10 | 20], all of which are in a realistic range) in comparison to the sensitivity analysis. This set is the one used at next step for the building simulations (see Table 12 in section II - 1.3, p 77) and is named [SET II].

The results are discussed referring to the following metrics (see Table 16):

1. The urban canyon warming (heat island effect) or cooling (cool island effect) given by the difference between the TEB canyon air temperature and the reference input air temperature, expressed as yearly sums and hourly values (UHI, UCI, HS, CS).
2. The changes in the heating and cooling degree days (ΔHDD, ΔCDD) provided as a rough estimation of the impact of the urban microclimate on indoor conditions. Section II - 3 (p 125) gives more accurate calculations of such effects using extensive dynamic energy building simulations.
3. A DOE statistical analysis, which reveals the hierarchical importance of the investigated variables for the above target key metrics, including a quantification of their main effects and double interactions.
4. All terms of the energy balance of the canyon, taken as a whole system (town) and as single facets (road, wall and roof). Analysing the energy balance enables a better understanding of the thermal behaviour of the canyon in terms of caption of solar radiation, sensible heat transfer to the air, charge and discharge of heat in their dependence upon the numerous variables under consideration.

For more details on the investigation plan, description of outputs and their post-processing, see section I - 1 (p 67). The TRY12 (Mannheim) and Meteonorm data (Algiers) serve as standard climate for the inputs, which air temperature is named T_{stn} , whereas the T_{urb} states for the air temperature in-canyon as output by TEB. Regarding the forcing air temperature $T_{frc,}$ required as input in TEB simulations, refer to the previous section and Figure 24.

2.1. Annual Warming and Cooling of Canyon Air

Table 20 lists, for the sensitivity analysis [SET I], the combinations of parameters, which lead to maximal and minimal, warming or cooling of the canyon air when compared to the standard climate, expressed as annual heat sum HS and cool sum CS, respectively. All 729 outputs are ranked decreasingly and the first and last 18 cases are exemplarily reported in Table 20.

A warming of the canyon air (coded (I) in Table 20), is favoured at most by a combination of a high urban density given by deep canyons (A = 1) and high plan density (P = 1), a high level of anthropogenic heat (H = 1) and a weak thermal insulation (D = -1). High emissivity values and low albedo are additional favourable conditions. The thermal inertia, in contrast, is irrelevant in this case (ranks 1 to 18). Looking at the end of the list, the canyon becomes the less warm in the absence of anthropogenic heat (H = -1), better thermal insulation (D = 1 or 0) and weak thermal mass (E = -1). The role of the urban geometry (A, P) and radiative properties is less evident as depending on particular combinations (ranks 712 to 729).

As shown in list (II) of Table 20, the canyon cools at most in case of deep canyons (A = 1) together with low emissivity (G = -1), no or low anthropogenic heat (H = -1 or 0), better thermal insulation (D = 1 or 0) and low thermal mass (E = -1 or 0). The plan density and albedo have no clear impact (ranks 712 to 729). The canyons with the less cool sum are shallow canyons (A = -1) with low thermal insulation (D = -1), the lowest albedo (F = -1), high anthropogenic heat (H = 1 or 0) and rather high plan density (P = 1 or 0), whereas the thermal inertia E has no clear effect (ranks 1 to 18).

Table 20 gives a good overview on the most critical combinations of the investigated variables (A, P, D, E, F, G, H) leading to extreme warming and cooling of canyon air. However, some interactions between these variables make the interpretation in other cases rather difficult. Therefore, a DOE statistical regression analysis was undertaken, which quantitatively ranks the importance of all individual variables and their double interactions. Table 21 and Table 22 list the results of the regression analysis for the heat sum and cool sum of the series [SET I] respectively.

The adjusted coefficients of determination (adj. R^2) of 0.973 for the heat sum in Table 21 reveals the high hit rate of the predicted models. The anthropogenic heat H and the vertical profile A are responsible for 29.1% and 24.4% of the result, respectively, so that H and A both explain the warming of the canyon air (model 2) to up to 53.1%. The thermal insulation D with 10.2% is the third most influential parameter, bringing the total with the variables H, A and D to 63.5% (model 3). The surface emissivity G is the fourth decisive variable with 5.4% as main effect and 7.5% in interaction with the canyon shape A. The interaction AD logically

plays an additional role. The thermal inertia E, the plan density P and the albedo F are comparatively of less relevance and are both responsible for up to 7.9% of the total result, bringing the adjusted R^2 of the model 14 to 95.9%. All other terms and interactions improve the polynomial mathematical up to 1.4% (model 21). The quadratic terms in Table 21 (D^2, H^2, A^2, E^2) show slight non-linear effects of these variables, especially the thermal insulation D. Moreover, the positive or negative sign of the predictor coefficients in Table 21 tells whether an increase or a decrease in the variable's value according to the coding (-1, 0, +1) leads to more or less warming, respectively. So, increasing H and A, for instance from -1 to +1 lead to more canyon warming, whereas an opposite effect is reached for such change of D.

As far as the annual cool sum is concerned (Table 22), the adjusted coefficient of determination R^2 amounts 0.739, which is a good hit rate even though it is lower than that of the warming case. The vertical profile of the canyon A and the surface emissivity G together with their interaction AG are the most decisive parameters with a total of 53.4% of influence (model 3). These two variables also have non-linear effect. The thermal insulation D and the anthropogenic heat H follow with 7.0% and 6.3% respectively. The variables E and F have limited effect, whereas P proves to be irrelevant in this case. All surface-related variables show double interactions as expected.

Summing up the analysis above, the investigated variables (A, P, D, E, F, G, H) have the following thermal impacts. Increasing the vertical profile A induces both maximal warming and maximal cooling at different times and is thereby the only variable with such contrasting effects. A high aspect ratio increases the wall surfaces thereby providing more heat discharged to the street either from the stored solar radiation, supported by enough thermal mass E or as heat transferred from indoors, especially in case of low thermal insulation D. The roof plan density P has limited effect because it is not directly oriented towards the canyon volume. Increasing the anthropogenic heat source H logically has a substantial effect on the warming of the canyon air. Inversely, a lack of anthropogenic heat leads to more cooling. Increasing the thermal insulation D leads to less heat transfer from indoor spaces and therefore less additional heat in the canyon volume and this prevents additional warming; instead, it supports more cooling of the canyon air. Increasing the thermal mass E leads to more heat storage by solar exposure and thus more heat release at night, so that it helps keep the canyon cool in the daytime against more nocturnal warming, inversely lightweight construction leads to more canyon cooling due to the lack of stored heat. Moreover, the thermal storage is favoured by a low albedo F and the heat discharge by a high emissivity G.

Table 20: The maximal and minimal values of in-canyon warming and cooling expressed as annual heat sum and cool sum for the sensitivity analysis [SET I], Mannheim (49.52°N, 8.55°E)

(I) ranking warming of canyon									
rank ↓	A	P	H	D	E	F	G	ID	heat sum K a^{-1}
1	1	1	1	-1	1	0	1	481	2956.9
2	1	1	1	-1	0	0	1	724	2818.6
3	1	1	1	-1	-1	0	1	400	2739.4
4	1	0	1	-1	1	-1	1	478	2652.9
5	1	1	1	-1	1	0	0	319	2590.4
6	1	0	1	-1	0	-1	1	721	2499.3
7	1	1	1	-1	0	0	0	643	2433.2
8	1	0	1	-1	-1	-1	1	397	2421.9
9	1	1	1	0	1	-1	1	479	2360.8
10	1	1	1	-1	-1	0	0	238	2356.3
11	1	0	1	-1	1	-1	0	316	2286.8
12	1	1	1	0	0	-1	1	722	2193.5
13	1	1	0	-1	1	1	1	475	2188.9
14	1	-1	1	-1	1	1	1	484	2149.3
15	1	0	1	-1	0	-1	0	640	2107.9
16	1	1	1	0	-1	-1	1	398	2098.2
17	1	0	0	-1	1	0	1	472	2098.1
18	1	1	1	1	1	1	1	486	2060.1
(. . .)									
712	-1	1	-1	0	-1	0	1	329	29.0
713	-1	0	-1	1	-1	1	-1	9	26.1
714	-1	-1	-1	1	-1	0	1	330	25.0
715	0	1	-1	1	-1	1	0	198	23.3
716	-1	-1	-1	0	0	1	1	656	20.4
717	1	-1	-1	0	-1	-1	-1	56	19.9
718	1	0	-1	1	-1	-1	-1	57	17.0
719	-1	0	-1	1	0	1	1	657	15.6
720	-1	-1	-1	0	-1	1	0	170	14.0
721	0	0	-1	0	-1	1	-1	35	10.9
722	-1	0	-1	1	-1	1	0	171	10.1
723	1	0	-1	0	-1	0	-1	59	9.5
724	-1	-1	-1	0	-1	1	1	332	9.3
725	1	1	-1	1	-1	0	-1	60	8.3
726	0	1	-1	1	-1	1	-1	36	7.3
727	-1	0	-1	1	-1	1	1	333	6.9
728	1	1	-1	0	-1	1	-1	62	3.2
729	1	-1	-1	1	-1	1	-1	63	2.6

(II) ranking cooling of canyon									
rank ↓	A	P	H	D	E	F	G	ID	cool sum K a^{-1}
1	-1	1	1	-1	1	-1	-1	100	-0.75
2	-1	1	1	-1	-1	-1	-1	19	-0.89
3	-1	1	1	-1	0	-1	-1	505	-0.95
4	-1	1	1	-1	1	-1	0	262	-1.19
5	-1	0	0	-1	-1	-1	-1	10	-1.33
6	-1	1	1	-1	0	-1	0	586	-1.45
7	-1	0	0	-1	0	-1	-1	496	-1.51
8	-1	0	0	-1	1	-1	-1	91	-1.73
9	-1	1	1	-1	1	-1	1	424	-1.86
10	-1	1	1	-1	-1	-1	0	181	-1.89
11	-1	1	1	-1	0	-1	1	667	-2.15
12	-1	0	0	-1	0	-1	0	577	-2.49
13	-1	0	0	-1	-1	-1	0	172	-2.59
14	-1	-1	-1	-1	-1	-1	-1	1	-2.79
15	-1	-1	1	-1	-1	0	-1	22	-2.87
16	-1	0	0	-1	1	-1	0	253	-3.00
17	-1	-1	1	-1	0	0	-1	508	-3.53
18	-1	0	0	-1	0	-1	1	658	-3.90
(. . .)									
712	1	0	1	1	-1	0	-1	78	-4972.5
713	1	1	1	1	-1	1	-1	81	-4979.0
714	1	-1	1	1	-1	-1	-1	75	-5185.0
715	1	1	0	1	-1	-1	-1	66	-5209.8
716	1	0	-1	1	1	-1	-1	138	-5279.2
717	1	-1	-1	0	-1	-1	-1	56	-5558.1
718	1	1	-1	1	1	0	-1	141	-5621.6
719	1	0	-1	0	-1	0	-1	59	-5795.8
720	1	0	-1	1	0	-1	-1	543	-5871.0
721	1	0	0	1	-1	1	-1	72	-5921.6
722	1	-1	-1	1	1	1	-1	144	-6236.4
723	1	1	-1	1	0	0	-1	546	-6237.3
724	1	-1	0	1	-1	0	-1	69	-6256.0
725	1	1	-1	0	-1	1	-1	62	-6316.4
726	1	-1	-1	1	0	1	-1	549	-6932.8
727	1	0	-1	1	-1	-1	-1	57	-9404.9
728	1	1	-1	1	-1	0	-1	60	-9804.3
729	1	-1	-1	1	-1	1	-1	63	-10613.1

A	urban canyon H/W	**H**	anthropogenic heat	**D**	thermal insulation	**F**	Albedo
P	plan density (roof surf./total)			**E**	thermal inertia	**G**	emissivity

Table 21: A DOE based statistical regression analysis of the annual heat sum for [SET I], Mannheim (49.52°N, 8.55°E)

heat sum difference (canyon vs. Standard, in K a^{-1})						Full Model (N° 21)		
model summary						predictor	coef.	sig.
Model	R	R square	adjusted R square	R square change	sig. F change	(Constant)	595.000	.000
1	,539[a]	.291	.290	.291	.000	H	354.117	.000
2	,731P	.535	.533	.244	.000	A	323.976	.000
3	,798[c]	.636	.635	.102	.000	D	-209.341	.000
4	,843[d]	.711	.709	.075	.000	AG	219.652	.000
5	,875[e]	.765	.763	.054	.000	G	152.442	.000
6	,898[f]	.806	.805	.042	.000	AD	-163.925	.000
7	,915[g]	.837	.835	.030	.000	E	114.474	.000
8	,928[h]	.862	.861	.025	.000	P	104.312	.000
9	,941[i]	.886	.884	.024	.000	F	-101.072	.000
10	,952[j]	.905	.904	.020	.000	D^2	159.601	.000
11	,960[k]	.922	.920	.016	.000	PH	102.291	.000
12	,968[l]	.938	.936	.016	.000	AH	101.293	.000
13	,975[m]	.950	.949	.012	.000	AE	88.876	.000
14	,979[n]	.959	.959	.010	.000	AP	78.869	.000
15	,981[o]	.963	.962	.004	.000	HE	-49.303	.000
16	,983[p]	.966	.965	.003	.000	AF	42.220	.000
17	,984[q]	.968	.967	.002	.000	E^2	50.501	.000
18	,985[r]	.969	.969	.002	.000	HG	32.250	.000
19	,985[s]	.971	.970	.002	.000	H^2	45.411	.000
20	,986[t]	.972	.972	.001	.000	HF	-30.406	.000
21	,987[u]	.974	.973	.001	.000	A^2	-37.926	.000
All Predictors: (constant), H, A, D, AG, G, AD, E, P, F, D^2, PH, AH, AE, AP, HE, AF, E^2, HG, H^2, HF, A^2								

Table 22: A DOE based statistical regression analysis of the annual cool sum for [SET I], Mannheim (49.52°N, 8.55°E)

cool sum difference (canyon vs. Standard, in K a^{-1})						Full Model (N° 21)		
model summary						predictor	coef.	sig.
Model	R	R square	adjusted R square	R square change	sig. F change	(Constant)	34.375	.609
1	,377[a]	.142	.141	.142	.000	A	-545.493	.000
2	,500[b]	.250	.248	.108	.000	AG	582.983	.000
3	,597[c]	.357	.354	.107	.000	G	474.073	.000
4	,653[d]	.427	.424	.070	.000	D	-383.252	.000
5	,700[e]	.490	.486	.063	.000	H	363.706	.000
6	,733[f]	.538	.534	.048	.000	AD	-388.854	.000
7	,761[g]	.579	.575	.041	.000	DG	360.521	.000
8	,786[h]	.617	.613	.038	.000	AH	346.295	.000
9	,800[i]	.640	.636	.023	.000	EG	-267.893	.000
10	,812[j]	.660	.655	.020	.000	HG	-248.477	.000
11	,822[k]	.675	.670	.016	.000	HD	221.839	.000
12	,831[l]	.690	.685	.015	.000	G^2	-307.593	.000
13	,838[m]	.702	.697	.012	.000	DE	190.889	.000
14	,844[n]	.712	.706	.010	.000	H^2	-250.616	.000
15	,848[o]	.719	.713	.007	.000	E	121.664	.000
16	,852[p]	.725	.719	.006	.000	AE	139.810	.000
17	,855[q]	.731	.724	.005	.000	E^2	-182.717	.000
18	,858[r]	.735	.729	.005	.000	A^2	-175.715	.000
19	,860[s]	.740	.733	.005	.000	F	-99.066	.000
20	,863[t]	.744	.737	.004	.001	HE	115.528	.001
21	,864[u]	.746	.739	.002	.018	HF	79.469	.018
All Predictors: (constant), A, AG, G, D, H, AD, DG, AH, EG, HG, HD, G^2, DE, H^2, E, AE, E^2, A^2, F, HE, HF								

2.2. Heating and Cooling Degree Days

Table 23 shows the cases where the highest and lowest of HDD and CDD are expressed as difference from the standard climate (ΔHDD, ΔCDD) at the base temperature of 18 °C and 24 °C, respectively. The reference values for the standard climate data are 2823 for HDD_{stn} and 60 for CDD_{stn}. Table 23 gives the results as absolute values and in percentage of increase or decrease. The heating degree days increase when the canyon becomes cooler than the threshold of 18 °C and the increase in the cooling degree days states for a warming of the canyon above 24 °C. Hence, the combinations of parameters are similar but not identical to those in Table 20. A maximum additional heating of the buildings ΔHDD up to 14.9% (ranks 1 – 18, (I)) is expected to occur in case of deep canyons (A = +1), no anthropogenic heat (H = -1), low emissive surfaces (G = -1) combined to a low heat storage given by a medium to low thermal inertia (E = -1 or 0) and high thermal insulation (D = +1). Looking at the end of the ΔHDD list (ranks 712 – 729, (I)), the expected need for indoor heating can be lower up to -3.8% in comparison to standard climate for opposite conditions of H, D, G and to a less extent for E. The effects of A and P are basically the same as for ranks 1 to 18, which means that high urban density always leads to extreme deviations.

Most needs for additional cooling of the buildings (ranks 1 – 18, (II)) up to 15.6% is attributable to excessive anthropogenic heat (H = +1), low albedo (F = -1) and high thermal emissivity (G = +1), medium to weak thermal inertia (E = 0 or +1) and medium to high thermal insulation (D = 0 or +1). A high density given by deep canyons (A= +1) and high roof density (P = +1) also cause an increase in ΔCDD. Looking at the end of the ΔCDD list (ranks 712 – 729, (II)), the expected need for indoor cooling can be as low as -24.3% in comparison to standard climate for opposite conditions of P, H, E, F and G and to a less extent for D. The effects of A are mostly the same as for ranks 1 to 18. However, owing to the low absolute values of CDD in general and ΔCDD in particular, the significance of these combinations is relative. Moreover, the interpretive value of ΔHDD and ΔCDD is only indicative because the thermal behaviour indoors is more complex to assess. For example, a high thermal insulation would cool the canyon further and imply more need for building heating if expressed with HDD, but at the same time it will reduce the impact of the outdoor boundary condition on the indoors and lead to better heat conservation and less heating need by reducing the heat losses.

The deviation values ΔHDD and ΔCDD are relatively small because of the temperate climate type and the assumed base temperatures. Table 24 and Table 25 give the DOE statistical for ΔHDD and ΔCDD, respectively.

Table 23: Deviation in the heating and cooling degree days from standard climate (ΔHDD 18 °C base, ΔCDD 24 °C base) for the sensitivity analysis [SET I], Mannheim (49.52°N, 8.55°E)

(I) ranking heating degree days

rank ↓	A	P	H	D	E	F	G	ID	ΔHDD Kd a^{-1}	%
1	1	-1	-1	1	-1	1	-1	63	422	14.9
2	1	1	-1	1	-1	0	-1	60	392	13.9
3	1	0	-1	1	-1	-1	-1	57	378	13.4
4	1	-1	-1	1	0	1	-1	549	256	9.1
5	1	-1	0	1	-1	0	-1	69	249	8.8
6	1	1	-1	0	-1	1	-1	62	243	8.6
7	1	0	0	1	-1	1	-1	72	233	8.2
8	1	1	-1	1	0	0	-1	546	232	8.2
9	1	0	-1	0	-1	0	-1	59	226	8.0
10	1	0	-1	1	0	-1	-1	543	220	7.8
11	1	-1	-1	0	-1	-1	-1	56	218	7.7
12	1	-1	-1	1	1	1	-1	144	205	7.3
13	1	1	0	1	-1	-1	-1	66	197	7.0
14	1	-1	1	1	-1	-1	-1	75	196	6.9
15	1	1	-1	1	1	0	-1	141	185	6.6
16	1	0	1	1	-1	0	-1	78	177	6.3
17	1	0	-1	1	1	-1	-1	138	174	6.2
18	1	1	1	1	-1	1	-1	81	167	5.9
(. . .)										
712	1	-1	1	-1	0	1	1	727	-72	-2.6
713	1	1	0	-1	0	1	1	718	-75	-2.6
714	1	0	1	-1	0	-1	0	640	-77	-2.7
715	1	1	1	-1	1	0	-1	157	-77	-2.7
716	1	0	0	-1	1	0	1	472	-78	-2.8
717	1	1	1	0	1	-1	1	479	-79	-2.8
718	1	-1	1	-1	1	1	1	484	-80	-2.8
719	1	1	1	-1	-1	0	0	238	-81	-2.9
720	1	1	0	-1	1	1	1	475	-82	-2.9
721	1	0	1	-1	-1	-1	1	397	-84	-3.0
722	1	0	1	-1	1	-1	0	316	-85	-3.0
723	1	1	1	-1	0	0	0	643	-88	-3.1
724	1	0	1	-1	0	-1	1	721	-90	-3.2
725	1	1	1	-1	-1	0	1	400	-94	-3.3
726	1	1	1	-1	1	0	0	319	-96	-3.4
727	1	0	1	-1	1	-1	1	478	-98	-3.5
728	1	1	1	-1	0	0	1	724	-100	-3.6
729	1	1	1	-1	1	0	1	481	-109	-3.8

nota: HDD (standard climate) = 2981 Kd a^{-1}

(II) ranking cooling degree days

rank ↓	A	P	H	D	E	F	G	ID	ΔCDD Kd a^{-1}	%
1	1	1	1	0	-1	-1	1	398	9	15.6
2	1	1	1	0	-1	-1	0	236	8	13.2
3	1	1	1	1	-1	1	1	405	8	12.8
4	1	1	1	0	0	-1	1	722	7	12.2
5	0	1	1	1	-1	-1	1	372	7	12.1
6	1	0	1	1	-1	0	1	402	7	12.0
7	0	1	1	1	-1	-1	0	210	7	11.3
8	1	1	1	-1	-1	0	1	400	7	10.9
9	1	-1	1	1	-1	-1	1	399	6	10.4
10	1	1	1	1	-1	1	0	243	6	10.4
11	0	1	1	1	0	-1	1	696	6	10.3
12	1	1	0	1	-1	-1	1	390	6	10.3
13	0	0	1	0	-1	-1	1	371	6	10.1
14	0	1	1	0	-1	0	1	374	6	9.9
15	1	1	1	0	0	-1	0	641	6	9.9
16	0	1	1	1	-1	-1	-1	48	6	9.9
17	1	0	1	1	-1	0	0	240	6	9.6
18	1	0	1	-1	-1	-1	1	397	6	9.5
(. . .)										
712	1	-1	-1	1	0	1	-1	549	-8	-12.5
713	1	0	-1	-1	1	1	1	466	-8	-12.5
714	1	-1	-1	-1	1	0	0	301	-8	-12.7
715	1	1	-1	0	0	1	-1	548	-8	-12.8
716	1	-1	-1	1	1	1	0	306	-8	-13.7
717	1	1	-1	0	1	1	0	305	-8	-14.1
718	1	-1	0	0	1	1	-1	152	-9	-14.4
719	1	0	-1	1	1	-1	-1	138	-9	-15.3
720	1	0	-1	-1	0	1	-1	547	-9	-15.5
721	1	-1	-1	0	1	-1	-1	137	-9	-15.5
722	1	0	-1	-1	1	1	0	304	-10	-16.3
723	1	1	-1	1	1	0	-1	141	-11	-17.5
724	1	1	-1	-1	1	-1	-1	136	-11	-17.6
725	1	0	-1	0	1	0	-1	140	-11	-17.7
726	1	-1	-1	-1	1	0	-1	139	-12	-19.4
727	1	-1	-1	1	1	1	-1	144	-13	-21.7
728	1	1	-1	0	1	1	-1	143	-13	-21.9
729	1	0	-1	-1	1	1	-1	142	-15	-24.3

nota: CDD (standard climate) = 59 Kd a^{-1}

A urban canyon H/W **H** anthropogenic heat **D** thermal insulation **F** Albedo

P plan density (roof surf./total) **E** thermal inertia **G** emissivity

Table 24: A DOE based statistical regression analysis of the deviation in the heating degree days ΔHDD18 °C base for [SET I], Mannheim (49.52°N, 8.55°E)

Heating Degree Days difference ΔHDD (canyon vs. Standard, in Kd a^{-1})						Full Model (N° 23)		
model summary						predictor	coef.	sig.
Model	R	R Square	Adjusted R Square	R Square Change	Sig. F Change	(Constant)	-21.799	.000
1	,381[a]	.145	.144	.145	.000	D	25.157	.000
2	,521P	.272	.270	.127	.000	H	-23.519	.000
3	,631[c]	.398	.396	.126	.000	AG	-28.741	.000
4	,720[d]	.518	.516	.120	.000	G	-22.877	.000
5	,775[e]	.600	.598	.082	.000	AD	23.193	.000
6	,797[f]	.636	.633	.035	.000	AH	-15.206	.000
7	,818[g]	.670	.666	.034	.000	E	-12.156	.000
8	,837[h]	.700	.697	.030	.000	DG	-14.057	.000
9	,849[i]	.720	.716	.020	.000	AE	-11.476	.000
10	,859[j]	.737	.734	.017	.000	EG	10.626	.000
11	,866[k]	.749	.745	.012	.000	A	7.255	.000
12	,872[l]	.761	.757	.012	.000	G^2	12.308	.000
13	,879[m]	.772	.768	.011	.000	HD	-8.499	.000
14	,884[n]	.782	.778	.010	.000	HG	8.214	.000
15	,890[o]	.792	.787	.010	.000	DE	-7.921	.000
16	,893[p]	.797	.793	.005	.000	D^2	-8.261	.000
17	,895[q]	.802	.797	.005	.000	F	4.586	.000
18	,898[r]	.806	.801	.005	.000	H^2	7.682	.000
19	,900[s]	.811	.806	.004	.000	P	-4.349	.000
20	,902[t]	.814	.809	.004	.000	A^2	6.906	.000
21	,904[u]	.817	.811	.002	.003	AP	-3.852	.003
22	,905[v]	.819	.813	.002	.004	PH	-3.709	.004
23	,906[w]	.821	.815	.002	.005	E^2	5.128	.005
All Predictors: (constant), D, H, AG, G, AD, AH, E, DG, AE, EG, A, G^2, HD, HG, DE, D^2, F, H^2, P, A2, AP, PH, E^2								

Table 25: A DOE based statistical regression analysis of the deviation in the cooling degree days ΔCDD 24°C base for [SET I], Mannheim (49.52°N, 8.55°E)

Cooling Degree Days difference ΔHDD ((canyon vs. Standard, in Kd a^{-1})						Full Model (N° 24)		
model summary						predictor	coef.	sig.
Model	R	R Square	Adjusted R Square	R Square Change	Sig. F Change	(Constant)	1.538	.000
1	,554[a]	.306	.306	.306	.000	H	2.153	0.000
2	,679[b]	.462	.460	.155	.000	F	-1.532	0.000
3	,784[c]	.615	.613	.153	.000	E	-1.524	0.000
4	,830[d]	.690	.688	.075	.000	AG	1.302	.000
5	,872[e]	.761	.759	.071	.000	AE	-1.271	.000
6	,900[f]	.809	.808	.049	.000	AH	1.050	.000
7	,923[g]	.853	.851	.043	.000	G	.809	.000
8	,943[h]	.889	.887	.036	.000	A	-.736	.000
9	,953[i]	.907	.906	.019	.000	D	.533	.000
10	,960[j]	.922	.921	.015	.000	P	.474	.000
11	,966[k]	.934	.933	.012	.000	A2	-.734	.000
12	,972[l]	.945	.944	.011	.000	AF	.490	.000
13	,977[m]	.955	.954	.011	.000	PH	.490	.000
14	,981[n]	.962	.961	.007	.000	AP	.391	.000
15	,984[o]	.968	.967	.006	.000	AD	.359	.000
16	,985[p]	.971	.970	.003	.000	D2	-.379	.000
17	,987[q]	.973	.973	.002	.000	E2	-.334	.000
18	,988[r]	.976	.975	.002	.000	HE	.231	.000
19	,989[s]	.977	.977	.002	.000	G2	-.272	.000
20	,989[t]	.978	.978	.001	.000	F2	-.225	.000
21	,990[u]	.979	.979	.001	.000	HG	-.150	.000
22	,990[v]	.980	.979	.001	.000	H2	-.160	.000
23	,990[w]	.980	.980	.000	.000	EG	.089	.000
24	,990[x]	.981	.980	.000	.001	HF	.087	.001
All Predictors: (constant), H, F, E, AG, AE, AH, G, A, D, P, A2, AF, PH, AP, AD, D2, E2, HE, G2, F2, HG, H2, EG, HF								

2.3. Isotherm Patterns of Urban Canyon Air Temperature Change

The hourly deviation of the canyon air temperature from the reference air temperature differs depending on the canyon's characteristics given by the variables A to G, as discussed so far. Of the 729 cases investigated in [SET I], a number of representative isotherm patterns with most contrasting combinations of variables are listed in Table 26 and drawn in Figure 25 and Figure 26. These cases include all (-1) and (+1) combinations, except the albedo (G) selected for the step equal to zero because its influence was found to be limited in the assumed range (0 to 0.5). The values of variable (P) have no systematic evidence because they follow the part-factorial DOE plan intended to limit the simulation set to one third (729 instead of 2187, see Figure 9). Complementarily to the findings of the section above, further observations can be made on the patterns shown in Figure 25 and Figure 26 as follows:

- The canyon air temperature experiences the lowest deviation in case of shallow canyons (A = -1) and no anthropogenic heat (H = -1), e.g. IDs 04, 06 because they behave like a free horizontal surface with the distant walls having low impact on the canyon air.
- A pronounced distinction of the daytime hours from 7:00 to 19:00 is visible in case of substantial anthropogenic heat C because of the assumed day-night profile of C in the ratio of 3:1. This contrast is more visible if the thermal inertia is low (E = -1), e.g. IDs 22, 24, 76, 78, 400 and 402 as no nocturnal heat island takes place.
- By contrast, the night hours appear to be warmer in case of high thermal inertia (E = +1) because the heat stored during the daytime hours is released at night provoking a nocturnal heat island, e.g. IDs 85, 87, 139, 157, 159, etc. This is accentuated by a low thermal insulation (D = -1) because of more heat in-canyon transferred from indoors.
- A typical cool island in the daytime hours occurs in deep canyons (A = +1) and is further stressed in case of no anthropogenic heat (C = -1), e.g. IDs 139 and 463 and high thermal insulation e.g. IDs 141 and 465. The dependence upon the solar radiation availability on the canyon facets is evident at the fitting with the sun path course given by the hour of day (daylight hours) and day of year (season).
- The canyon appears to cool considerably in case of good thermal insulation (D = +1) combined with a very low emissivity (G = -1), on one hand because almost no heat is transferred from the heated spaces indoors towards the outside and on the other hand because the low emissivity limits the radiative heat discharge.
- The cases in Figure 26 are more realistic than those in Figure 25 are, because the longwave emissivity of most common building materials is higher than 0.80.

Table 26: Selected combinations of variables representing particular patterns of warming and cooling of canyon (for I and II see Figure 25 and for III and IV see Figure 26)

	ID	A	P	H	D	E	F	G
I	4	-1	0	-1	-1	-1	0	-1
	6	-1	-1	-1	1	-1	0	-1
	22	-1	-1	1	-1	-1	0	-1
	24	-1	1	1	1	-1	0	-1
	58	1	-1	-1	-1	-1	0	-1
	60	1	1	-1	1	-1	0	-1
	76	1	1	1	-1	-1	0	-1
	78	1	0	1	1	-1	0	-1

	ID	A	P	H	D	E	F	G
II	85	-1	0	-1	-1	1	0	-1
	87	-1	-1	-1	1	1	0	-1
	103	-1	-1	1	-1	1	0	-1
	105	-1	1	1	1	1	0	-1
	139	1	-1	-1	-1	1	0	-1
	141	1	1	-1	1	1	0	-1
	157	1	1	1	-1	1	0	-1
	159	1	0	1	1	1	0	-1

A	urban canyon H/W
P	plan density (roof surf./total)
H	anthropogenic heat (W)
D	thermal insulation (U-value)
E	thermal inertia
F	Albedo
G	emissivity

	ID	A	P	H	D	E	F	G
III	328	-1	0	-1	-1	-1	0	1
	330	-1	-1	-1	1	-1	0	1
	346	-1	-1	1	-1	-1	0	1
	348	-1	1	1	1	-1	0	1
	382	1	-1	-1	-1	-1	0	1
	384	1	1	-1	1	-1	0	1
	400	1	1	1	-1	-1	0	1
	402	1	0	1	1	-1	0	1

	ID	A	P	H	D	E	F	G
IV	409	-1	0	-1	-1	1	0	1
	411	-1	-1	-1	1	1	0	1
	427	-1	-1	1	-1	1	0	1
	429	-1	1	1	1	1	0	1
	463	1	-1	-1	-1	1	0	1
	465	1	1	-1	1	1	0	1
	481	1	1	1	-1	1	0	1
	483	1	0	1	1	1	0	1

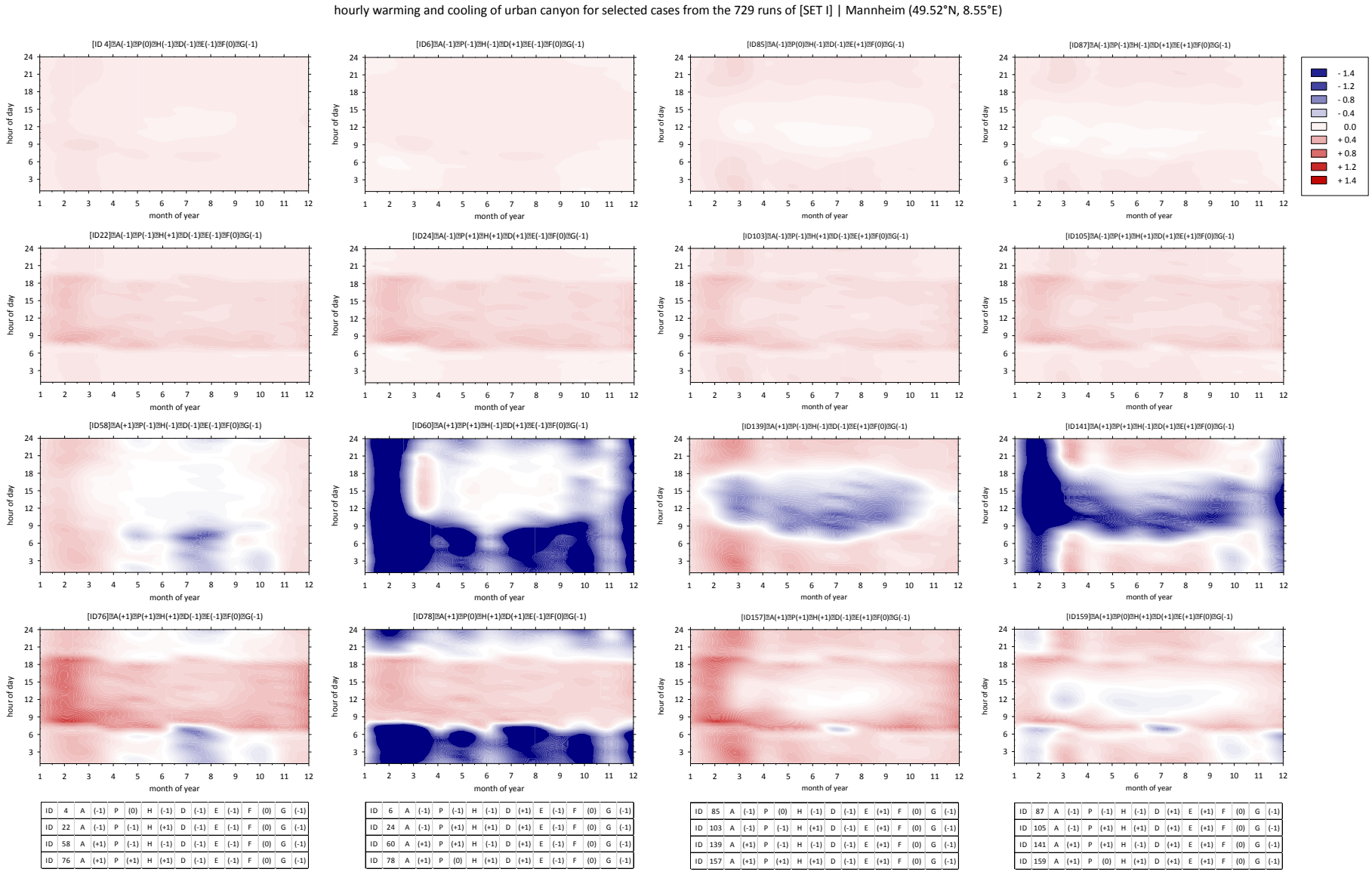

Figure 25: Hourly and monthly isotherm patterns of warming and cooling of canyon air for selected cases from the 729 runs of [SET I] (continued on Figure 26)

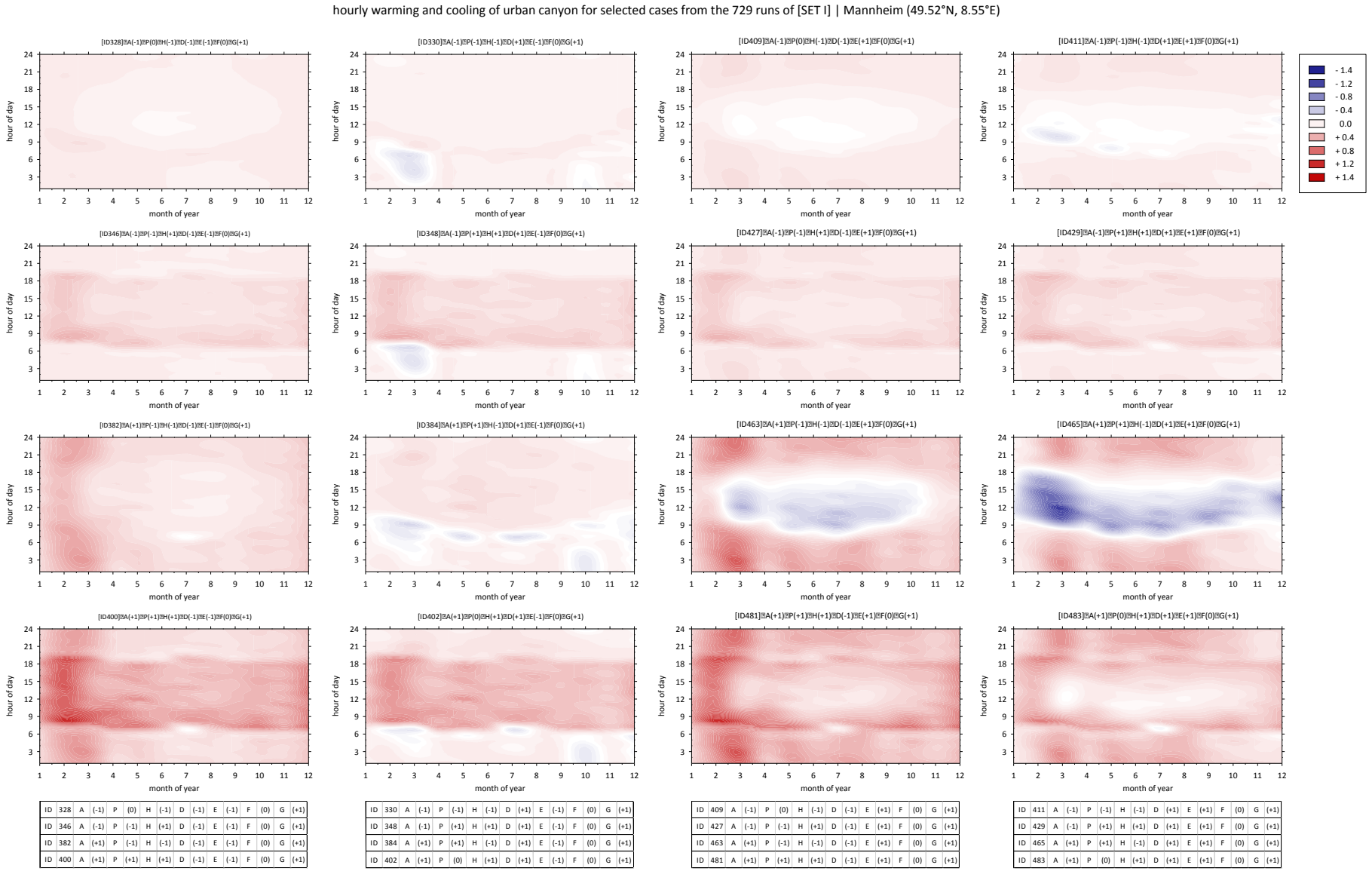

ID	328	A	(-1)	P	(0)	H	(-1)	D	(-1)	E	(-1)	F	(0)	G	(+1)
ID	346	A	(-1)	P	(-1)	H	(+1)	D	(-1)	E	(-1)	F	(0)	G	(+1)
ID	382	A	(+1)	P	(-1)	H	(-1)	D	(-1)	E	(-1)	F	(0)	G	(+1)
ID	400	A	(+1)	P	(+1)	H	(+1)	D	(-1)	E	(-1)	F	(0)	G	(+1)

ID	330	A	(-1)	P	(-1)	H	(-1)	D	(+1)	E	(-1)	F	(0)	G	(+1)
ID	348	A	(-1)	P	(+1)	H	(+1)	D	(+1)	E	(-1)	F	(0)	G	(+1)
ID	384	A	(+1)	P	(+1)	H	(-1)	D	(+1)	E	(-1)	F	(0)	G	(+1)
ID	402	A	(+1)	P	(0)	H	(+1)	D	(+1)	E	(-1)	F	(0)	G	(+1)

ID	409	A	(-1)	P	(0)	H	(-1)	D	(-1)	E	(+1)	F	(0)	G	(+1)
ID	427	A	(-1)	P	(-1)	H	(+1)	D	(-1)	E	(+1)	F	(0)	G	(+1)
ID	463	A	(+1)	P	(-1)	H	(-1)	D	(-1)	E	(+1)	F	(0)	G	(+1)
ID	481	A	(+1)	P	(+1)	H	(+1)	D	(-1)	E	(+1)	F	(0)	G	(+1)

ID	411	A	(-1)	P	(-1)	H	(-1)	D	(+1)	E	(+1)	F	(0)	G	(+1)
ID	429	A	(-1)	P	(+1)	H	(+1)	D	(+1)	E	(+1)	F	(0)	G	(+1)
ID	465	A	(+1)	P	(+1)	H	(-1)	D	(+1)	E	(+1)	F	(0)	G	(+1)
ID	483	A	(+1)	P	(0)	H	(+1)	D	(+1)	E	(+1)	F	(0)	G	(+1)

Figure 26: Hourly and monthly isotherm patterns of warming and cooling of canyon air for selected cases from the 729 runs of [SET I] (continued on Figure 25)

2.4. Daily Cycle of Urban Canyon Air Temperature Change

So far, the results using [SET I] were about a systematic understanding of the formation of an urban microclimate in-canyon. In the following, [SET II] as an excerpt of 81 runs, is assessed on in order to better visualise the hourly values and daily cycle of the air temperature deviation. Using [SET II], the part of influence of the window ratio C, thermal insulation D and thermal inertia E are highlighted because the albedo, emissivity and anthropogenic heat are kept identical for all runs.

Figure 27 shows the deviation of the canyon air temperature from the standard climate data ($T_{urb} - T_{stn}$) at 1 Kelvin intervals and differentiated according to the three urban geometries under study (wide, unity-like and deep canyons). Positive values denote the warming of the canyon while negative values mean cooler canyon. Figure 27 reveals that the urban air temperatures are mostly higher than the standard rural climate for an average of 7209 hours for H/W = 0.2, 6994 hours for H/W = 1.0 and 6943 hours for H/W = 1.8 (≈ 82 to 83% of the year). Hence, cooling of canyon amounts, in average, 1532, 1561, 1451 hours, respectively. The intensity of the temperature deviation mostly ranges between 1 and 2 Kelvin, whereas only a few hours in the year may have clearly higher or lower values (Figure 27). These extreme increments particularly take place as the urban canyon's depth increases.

Figure 28 differentiates the sum of warmer or cooler hours within the canyon in dependence upon the investigated urban and building variables (aspect ratio A, window ratio C, thermal insulation D, thermal inertia E).

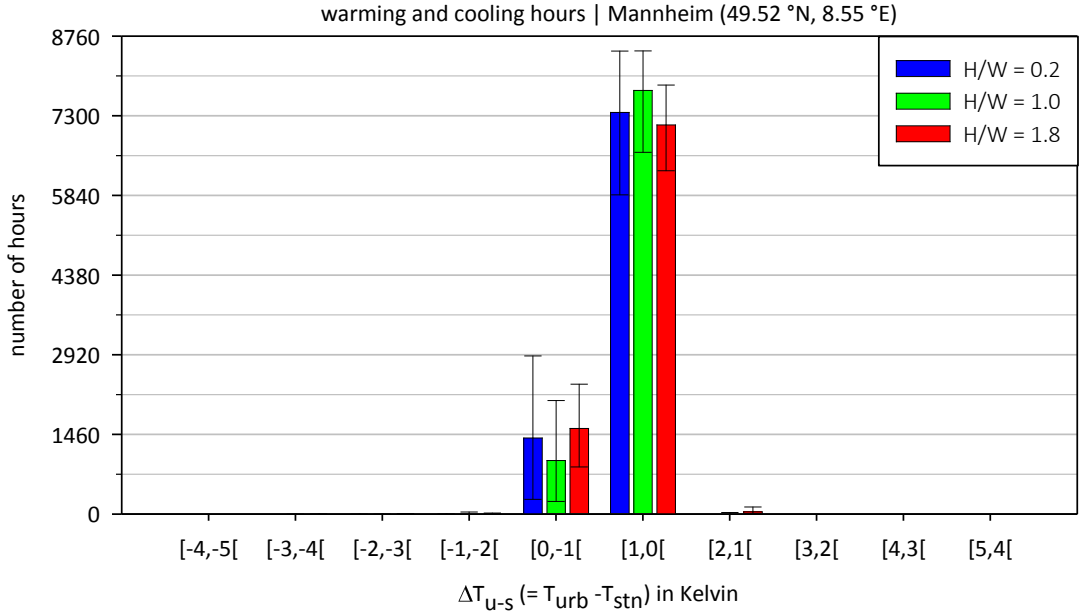

Figure 27: TEB-prognosis of the urban air temperature deviation from input standard climate TRY12

Table 27: TEB-prognosis of the deviation of urban air temperature from input standard climate TRY12 averaged for the [SET II] differentiated according to the canyon aspect ratio

Mannheim (49.52 °N, 8.55 °E)			H/W = 0.2				H/W = 1.0				H/W = 1.8			
			min	mean	max	range	min	mean	max	range	min	mean	max	range
cool island	[-6,-7[	hours	0	0	0	0	0	0	0	0	0	0	0	0
	[-5,-6[	hours	0	0	0	0	0	0	0	0	0	0	1	1
	[-4,-5[	hours	0	0	0	0	0	0	0	0	0	1	9	9
	[-3,-4[	hours	0	0	0	0	0	1	5	5	0	3	12	12
	[-2,-3[	hours	0	0	2	2	0	3	12	12	1	8	30	29
	[-1,-2[	hours	0	0	6	6	1	9	40	39	1	23	65	64
	[0,-1[	hours	271	1268	2900	2629	235	1365	2383	2148	237	1383	2541	2304
heat island	[1,0[	hours	5852	7491	8489	2637	6295	7352	8493	2198	5942	7185	8342	2400
	[2,1[	hours	0	0	0	0	0	30	131	131	19	152	359	340
	[3,2[	hours	0	0	0	0	0	0	0	0	0	5	45	45
	[4,3[	hours	0	0	0	0	0	0	0	0	0	0	0	0
	[5,4[	hours	0	0	0	0	0	0	0	0	0	0	0	0
	[6,5[	hours	0	0	0	0	0	0	0	0	0	0	0	0
	[7,6[	hours	0	0	0	0	0	0	0	0	0	0	0	0
min. deviation		C	-2.35	-0.71	-0.09	2.26	-3.85	-2.81	-1.08	2.77	-5.42	-3.62	-2.28	3.14
max deviation		C	0.43	0.51	0.62	0.19	0.97	1.25	1.61	0.64	1.29	1.83	2.42	1.13
cooler canyon		hours	271	1269	2908	2637	236	1378	2415	2179	240	1418	2657	2417
warmer canyon		hours	5852	7491	8489	2637	6345	7382	8524	2179	6103	7342	8520	2417
cooler canyon		%	3	14	33	30	3	16	28	25	3	16	30	28
warmer canyon		%	67	86	97	30	72	84	97	25	70	84	97	28

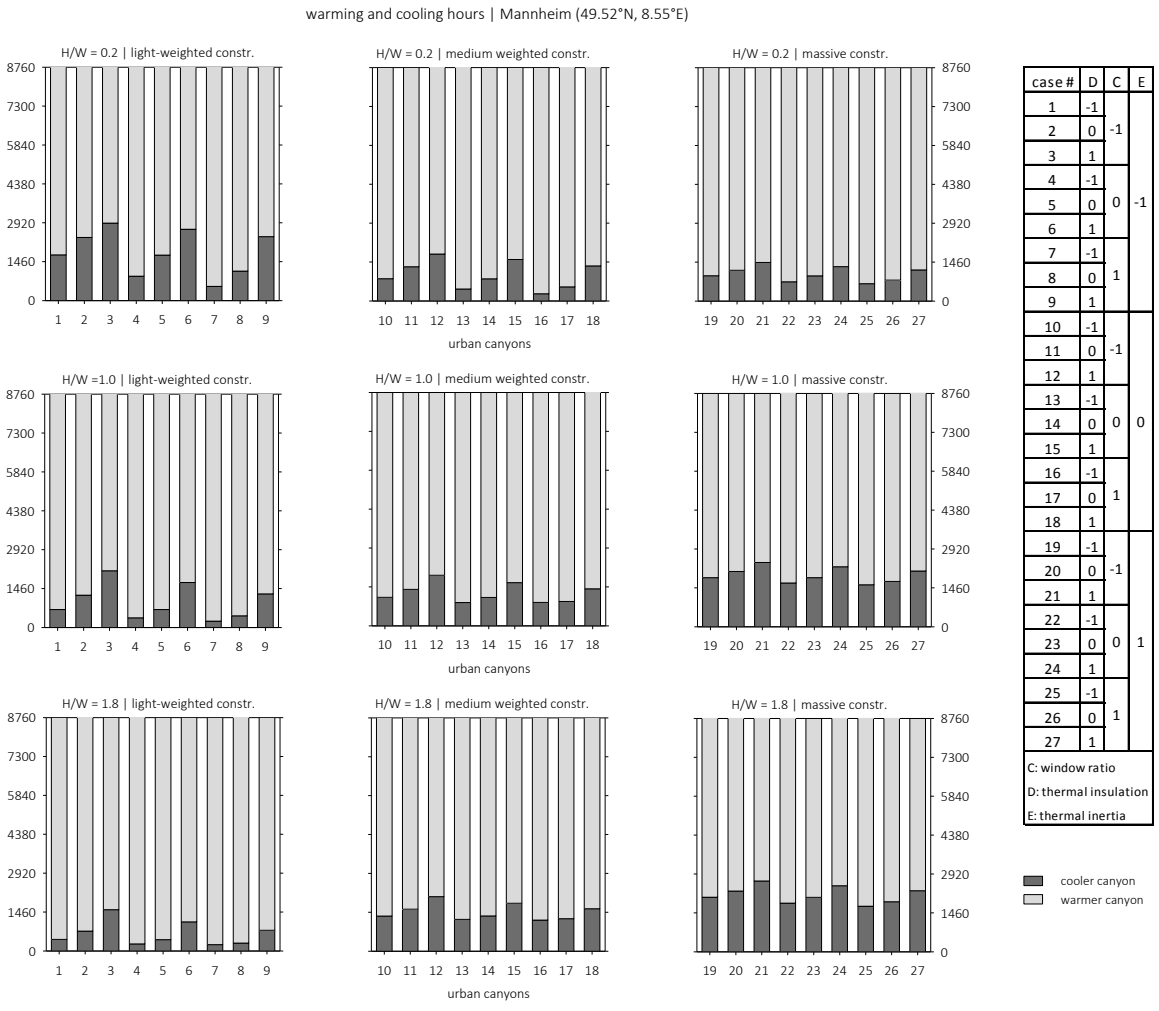

Figure 28: Warming and cooling hours of urban canyon depending on their vertical profile (H/W) and construction (C, D, E)

Figure 29 and Figure 30 represent the hourly thermal behaviour of the canyon air for a typical year expressed as (i) maximum and (ii) average deviation from the standard reference climate, respectively. The graphs are differentiated for each urban profile (A) and thermal mass (E) because these two variables show clearly different impact. The error bars show the range resulting from varying the thermal insulation (D), indirectly including the window ratio (C), i.e. nine combinations of CD (see Appendix 4). Moreover, the daytime and nighttime picture of this warming clearly depends on the thermal inertia (E). Lightweight construction leads to warmer canyon air in the daytime hours by contrast to massive construction in the nighttime and this reflects their differences in the heat storage and release cycles. Indeed, a lightweight construction does not offer the possibility for much heat storage in the hours with most solar radiation and so the transfer to the air as sensible heat occurs immediately. Massive construction, by contrast, stores much heat in the walls during the daytime and gives it back in the night thereby leading to a typical nocturnal heat island. The error bars are more visible as the canyon becomes deeper because the wall surfaces become more dominant in comparison to the ground surface. Therefore, the impact of the thermal insulation (D, CD) is more significant in this case.

Figure 30 shows a similar but not identical picture for average values. The trend in air temperature increase is indeed the same but the canyon also experiences cooling episodes (cool island). This particularly occurs for massive deep canyons in the daytime hours between 9:00 and 17:00. The intensities remain, however, low by ± 0.4 K. These results highlight the microclimate complexity and advocates for a systematic prognosis of the microclimate changes prior to building energy modelling.

Additionally, Figure 31 depicts the seasonal differences in canyon air temperatures, surface temperatures of road and walls for four representative seasons between lightweight and massive construction. The next section deals with the energy fluxes behind these thermal results. The effects of the urban fabric's heat storage capacity, given by the thermal inertia as well as the thermal insulating quality of the building envelope, are addressed as further critical building construction properties. All these results clearly underline the microclimate complexity and advocate for a systematic prognosis of the microclimate changes prior to building energy modelling.

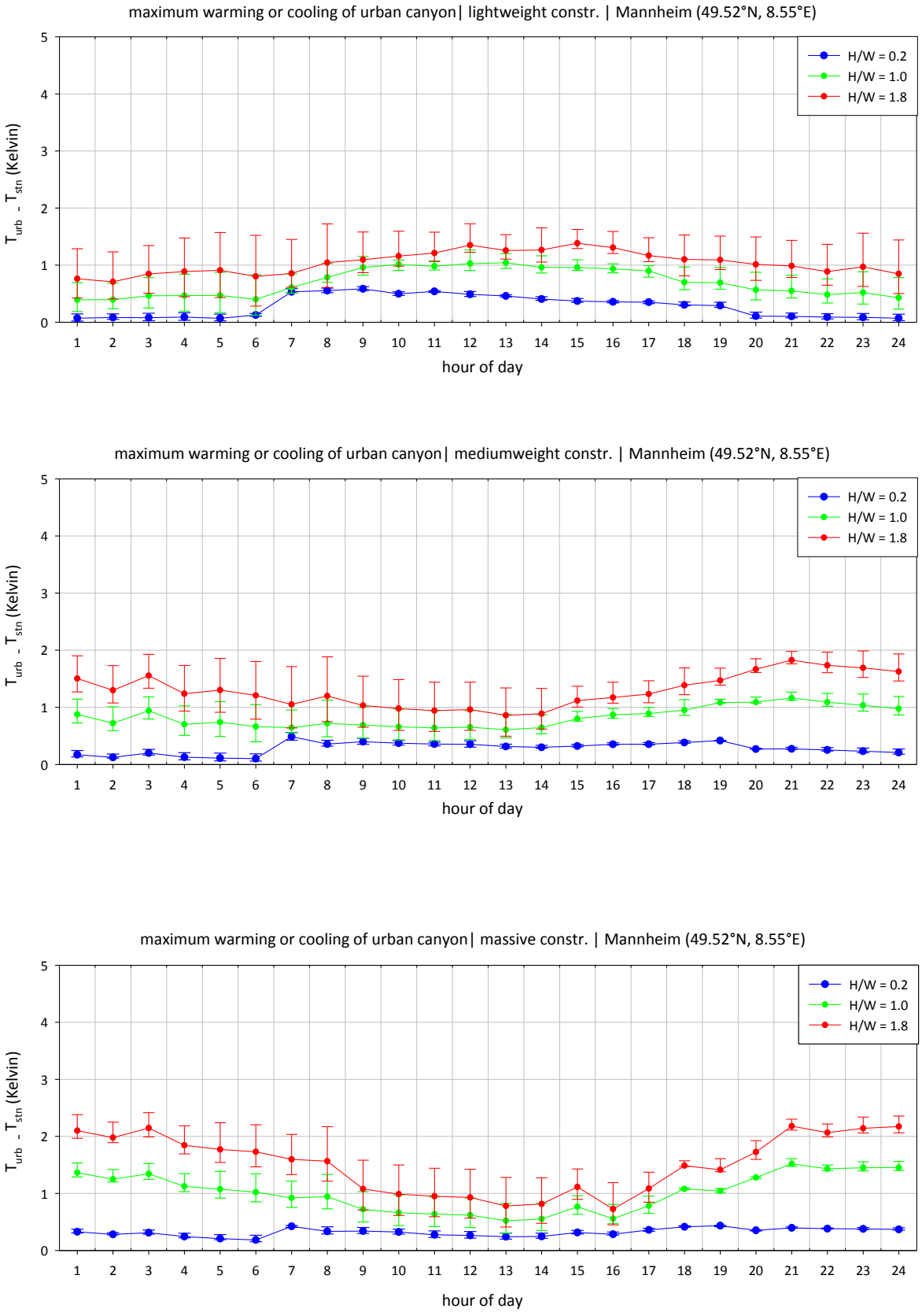

Figure 29: Hourly maximum deviation of urban air temperature from input standard climate differentiated according to the aspect ratio A and thermal mass E for a typical year TRY12 for Mannheim (49.52°N, 8.55°E)

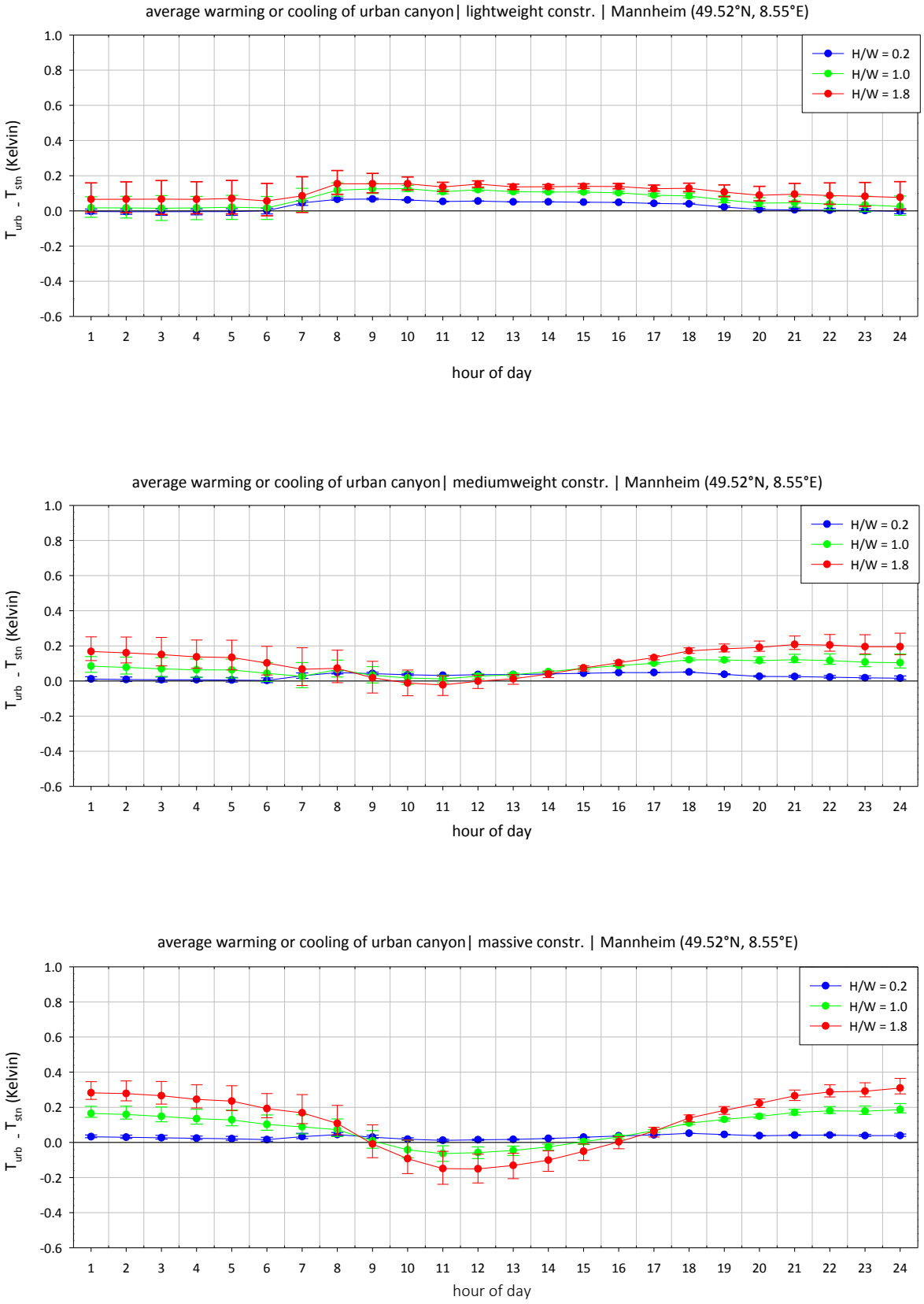

Figure 30: Hourly average deviation of urban air temperature from input standard climate differentiated according to the aspect ratio A and thermal mass E for a typical year TRY12 for Mannheim (49.52°N, 8.55°E)

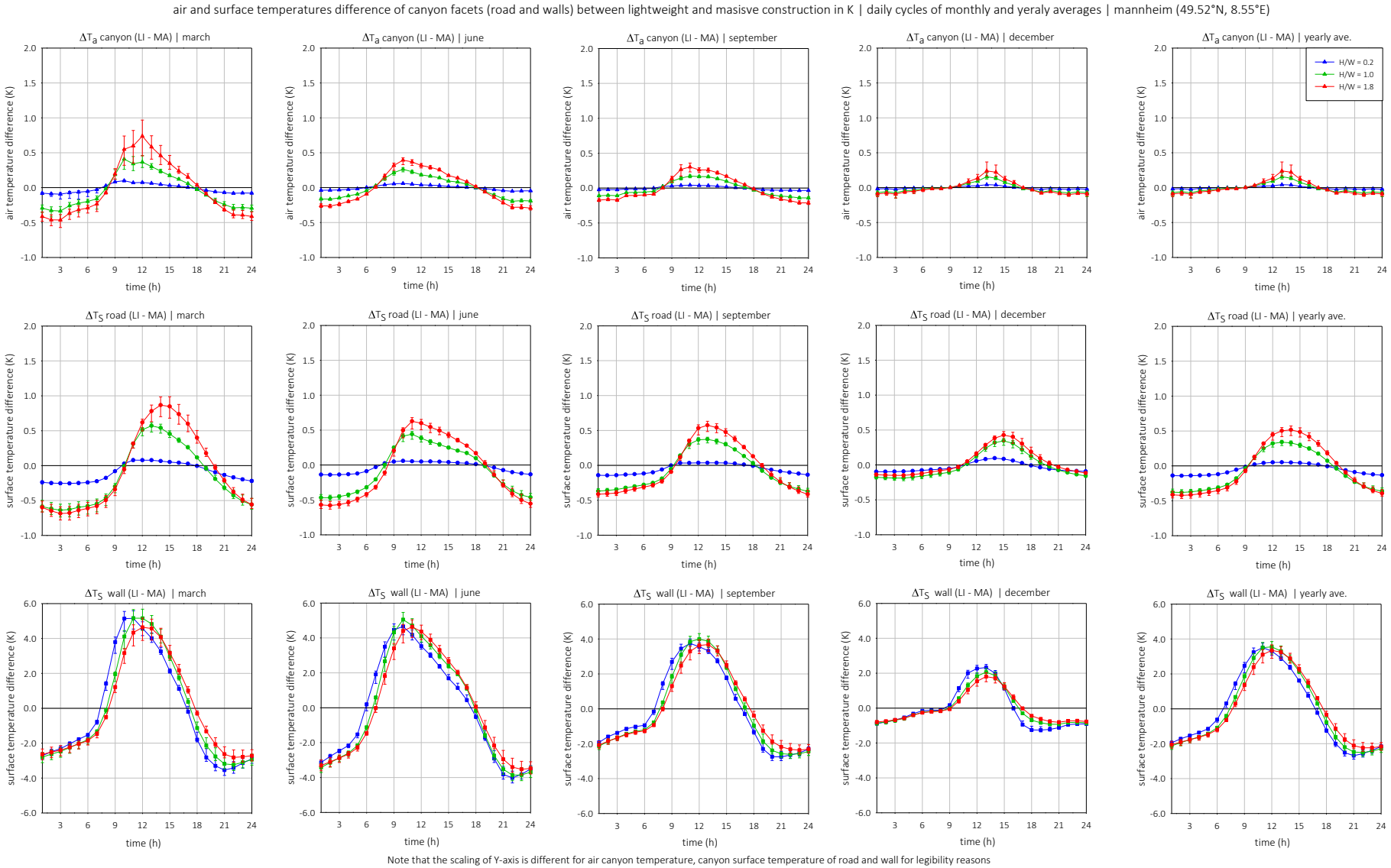

Figure 31: Differences in air and surface temperatures of road and walls between lightweight and massive construction for Mannheim (49.52°N, 8.55°E)

2.5. The Energy Balance Fluxes of the Canyon System

This section reports on the energy balance terms responsible in the warming or cooling of canyon air reported above. Appendix 1 provides the mathematical description of the canyon energy balance as calculated by TEB. The following terms as given in the equation of Appendix 1 are plotted for the town as whole system (road, walls and roof): (1) the total all-wave net radiation heat flux Q^*, the sensible heat flux Q_H and (3) the storage heat flux ΔQ_S. The latent heat flux Q_E is omitted because the values are very low (max range ± 37 Wm^{-2}) only attributable to cycles of due formation and evaporation of air humidity since the canyon is assumed to be dry i.e. no consideration of precipitation (not available in TRY12). This section reports on the results about the lightweight and massive constructions but not the mediumweight construction (MD) for space reasons, being an intermediate case between LI and MA.

Figure 32 and Figure 33 show the daily cycles of monthly average fluxes for representative seasons and as annual average for the canyon system (road, walls, roof), named here Town. Note that Appendix 7 provides an alternative representation in Figure 97 Figure 98, respectively. On Figure 32 and Figure 33, the three fluxes Q*, Q_H and ΔQ_S are plotted together in order to understand their share in the energy balance, whereas in Figure 97 and Figure 98 each heat flux is plotted separately for all canyon profiles for additional comparison with respect to urban density. Moreover, Table 62 in Appendix 7 lists the absolute minima, maxima and mean values of these fluxes.

The all-wave net radiation flux Q*, sensible heat flux Q_H and storage heat flux ΔQ_S are differentiated in lightweight construction LI (Figure 32) and massive construction MA (Figure 33), respectively. As already noticed, this distinction according to thermal mass is pertinent because of its impact on the storage amount ΔQ_S and thus on Q_H and so on the daily evolution and magnitude of the resulting urban air temperature. Indeed, according to the inputs (see Table 7), the simulated massive construction can charge up to 6 times more heat than the lightweight construction.

In the case of lightweight construction (Figure 32), the sensible heat flux Q_H is visibly higher than the storage heat flux ΔQ_S because the building materials with low heat capacity and low mass density enable only small amount of heat storage. In case of massive construction (Figure 33), the storage heat flux is clearly higher and even exceeds the sensible heat flux as the street canyons become deeper.

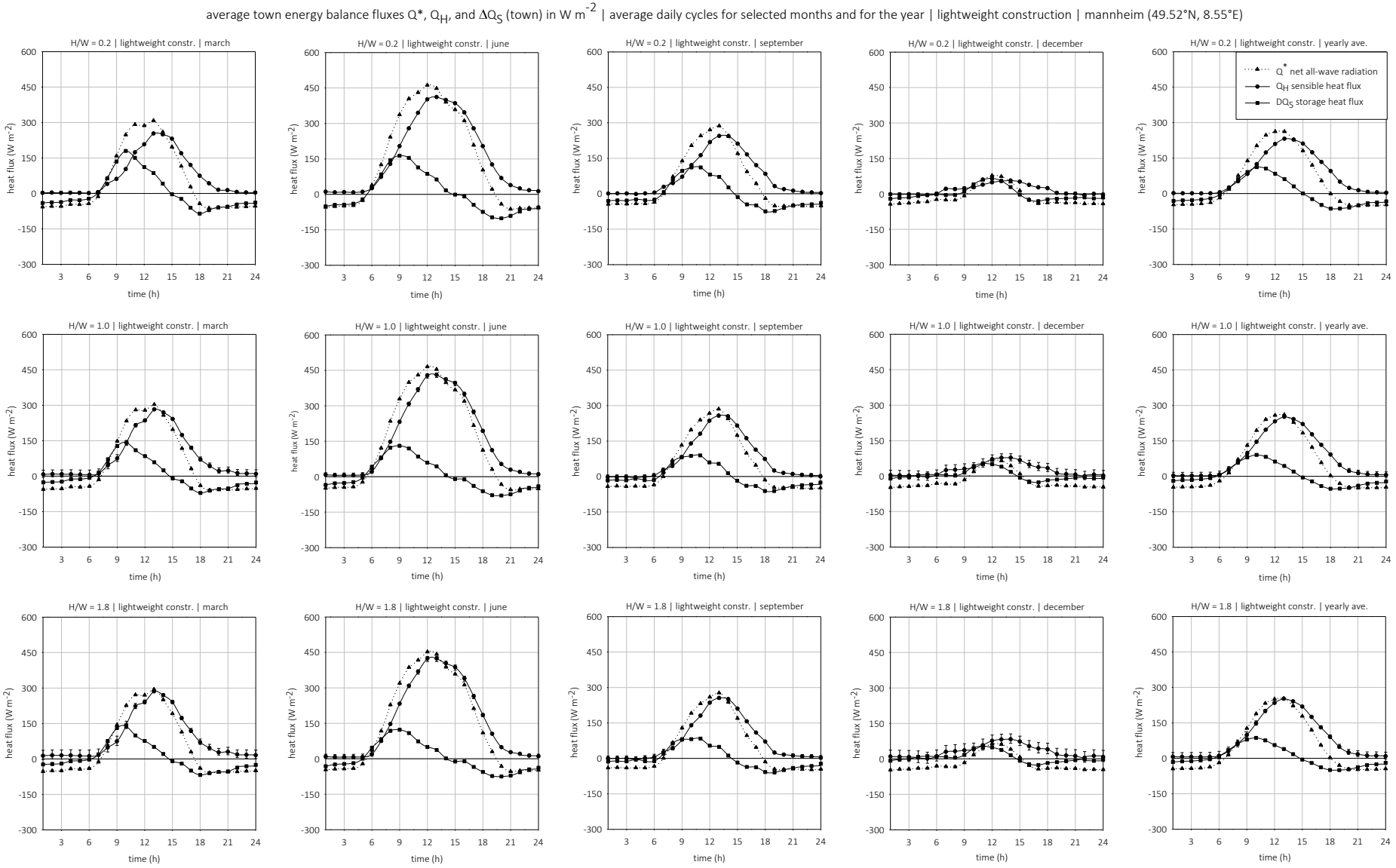

Figure 32: Seasonal and annual average town energy balance fluxes (Q*, Q_H, ΔQ_S) in W m-2 for lightweight construction for Mannheim (49.52°N, 8.55°E)

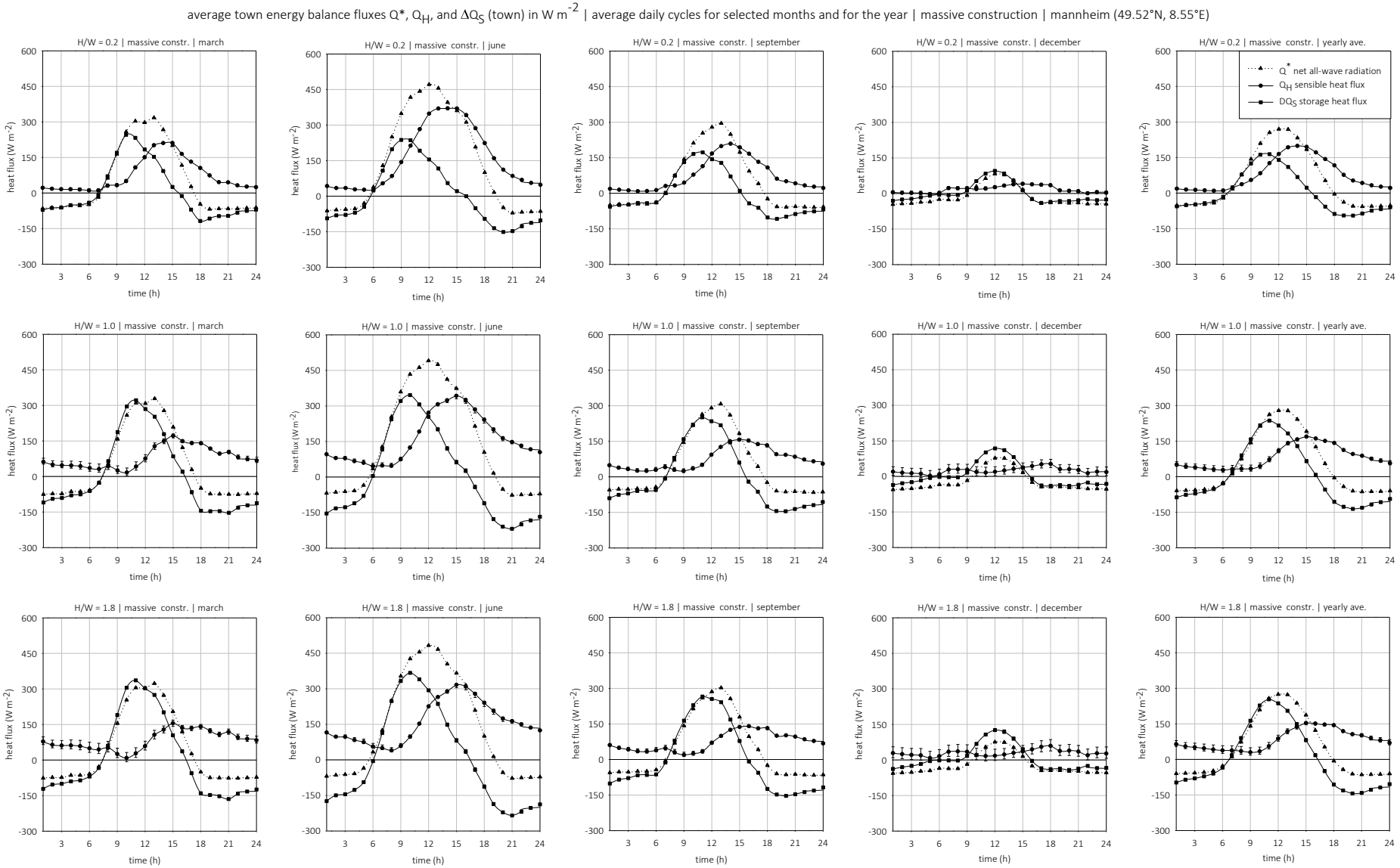

Figure 33: Seasonal and annual average town energy balance fluxes (Q*, Q_H, ΔQ_S) in W m-2 for massive construction for Mannheim (49.52°N, 8.55°E)

The dynamic share between Q_H and ΔQ_S is best understandable following the hourly cycle of day. The course of the storage heat flux ΔQ_S is strongly coupled with the total net radiation for massive constructions with a close fitting in the morning hours and a maximum reached around 10:00 – 11:00 LST, i.e. up to 2 hours before maximum Q*. In contrast, the sensible heat flux Q_H is strongly coupled with the total net radiation in case of lightweight construction with a time shift of up to 2 hours later (12:00 – 14:00 LST).

The sensible heat flux Q_H and the heat storage ΔQ_S take place immediately after sunrise and increase progressively until the canyon facets cannot charge more heat and the heat storage ΔQ_S starts to decrease in favour of more convective heat transfer to the air privileged by increasing surface temperatures. This reversal point occurs at some time before noon (span 9:00 – 11:00 LST) depending on the season and canyon geometry. The sensible heat flux rises forward to reach its maximum at sometime between midday and 14:00 LST depending on the season and canyon geometry. Between 15:00 and 16:30 LST, the canyon facets start to release their stored heat, rather early around 15:00 LST for wide canyons (H/W = 0.2) and increasingly later for deep canyons around 16:30 LST (H/W = 1.8). This makes the sensible heat although in decrease appear to be higher than the total net radiation. The sensible heat flux is near zero or slightly negative from 22:00 LST and remains as such till the next day at sunrise. During the night, the heat release reaches the level of the net radiation in deficit and remains almost constant until the next daily cycle after sunrise. These processes are similar in deeper canyons but with clearly lower magnitudes. The sensible heat flux in these cases mostly remains positive.

Figure 97 and Figure 98 (Appendix 7) provide some additional information by looking at the individual fluxes separately across the three canyon geometries. The all-wave net radiation Q* appear to vary very slightly between the different canyon profiles with a trend for an increase in the sunlight hours and a decrease at night for higher densities. More interesting is the different share between Q_H and ΔQ_S as function of the canyon geometry in case of massive construction, whereas lightweight construction clearly reveals smaller differences, yet with the same trend. With increasing street profile where the wall surfaces dominate over the road surface, the sensible heat flux shows lower magnitudes in the sunlight hours with a temporal shift of its maximum up to 2 hours. This is logically reversed for the heat storage ΔQ_S, which clearly experience higher magnitudes with a similar shift of its maximum up to 2 hours later. The nocturnal situation is correspondingly reversed with more heat release for deep canyons and higher amounts of sensible heat flux. The differences between the canyons with H/W = 1 and 1.8 show smaller differences than with the wide canyon of H/W = 0.2 which means that

the unity-like canyon already performs as relatively deep density. The error bars which inform about the effects of the thermal insulation of the building envelope are more pronounced in the cold season (March, December) and canyons with dominating walls due to the indoor heating. This is visible at the sensible heat flux, which reflects the conductive heat flux, rather than in the storage, term as this is the sum of the conductive heat flux Q_G and indoor heat restore Q_{FBLD} (see Appendix 1).

2.6. The Energy Balance Fluxes at the Canyon Walls

The impact of the building construction on the canyon microclimate is better understood by analysing the energy balance at the canyon walls, especially because the settings for the walls were varied and those of the road were kept unchanged in all cases.

Figure 34 and Figure 35 show the daily cycles of monthly averages for representative seasons and for the year for lightweight and massive construction respectively. The following energy balance terms are plotted: total net radiation Q*, sensible heat flux Q_H and storage heat flux ΔQ_S. The walls being of same height in all canyons, the energy balance values in these figures are weighted by the wall fraction in order to capture the effect of this part of the canyon system on the resulting microclimate changes. The wall fraction equals 0.25, 0.5 and 0.5625 for the canyons with H/W of 0.2, 1.0 and 1.8, respectively. Complementarily, the error bars visible in the previous figures due to the effects of the thermal insulating quality of the building envelopes are further addressed. Following the equations in Appendix 1, Figure 36 and Figure 37 show the share of the heat storage ΔQ_S between the conductive heat flux Q_G and the indoor heating flux Q_{FW} in dependence on the wall average thermal insulation D_{eq} for December as critical month in this respect (see Figure 101 and Figure 102 for June). Using the same legend, Figure 38 shows the corresponding surface temperatures for the coldest and warmest months.

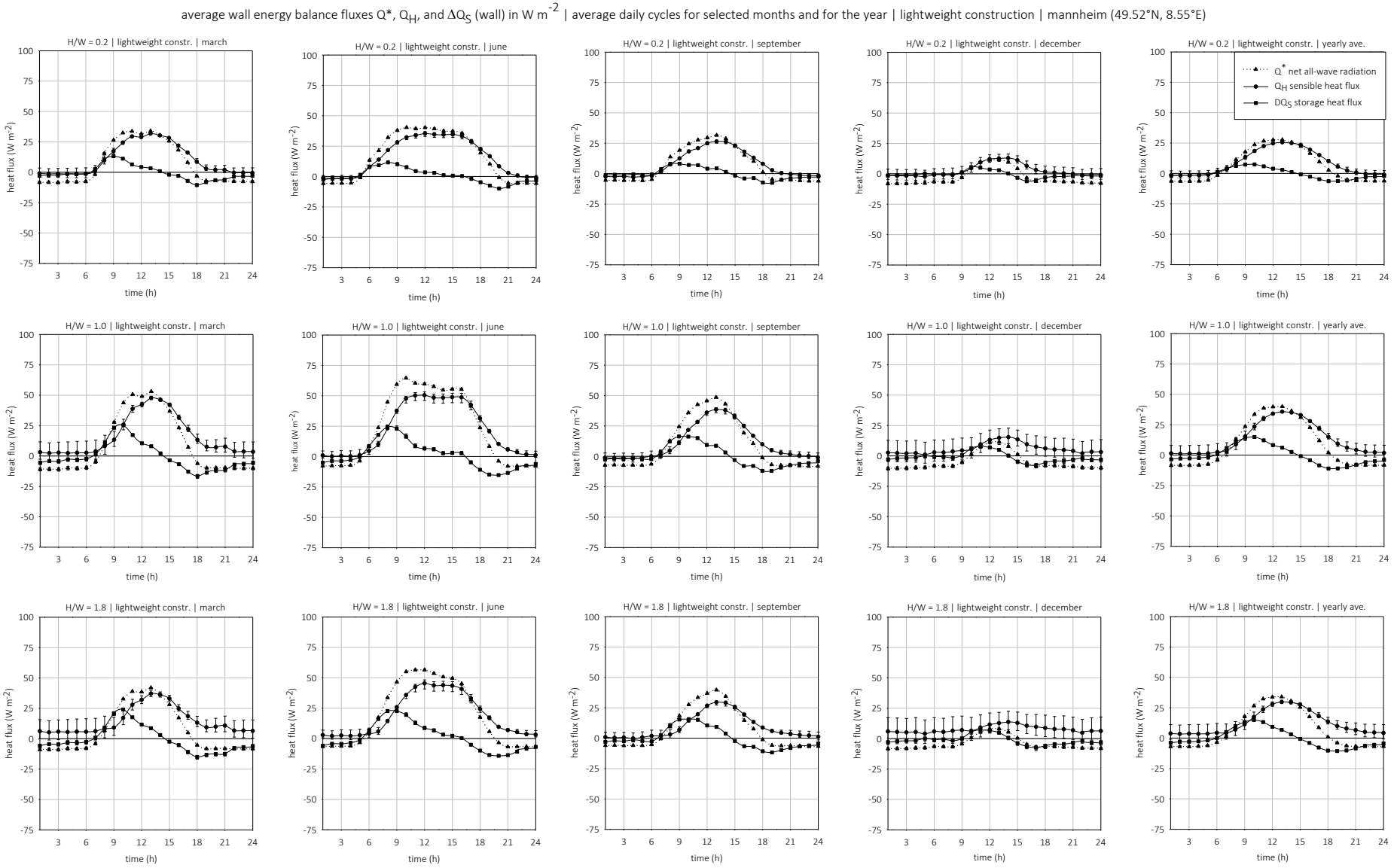

Figure 34: Seasonal and annual average energy balance fluxes (Q*, Q_H, ΔQ_S) at the walls in W m^{-2} for lightweight construction for Mannheim (49.52°N, 8.55°E)

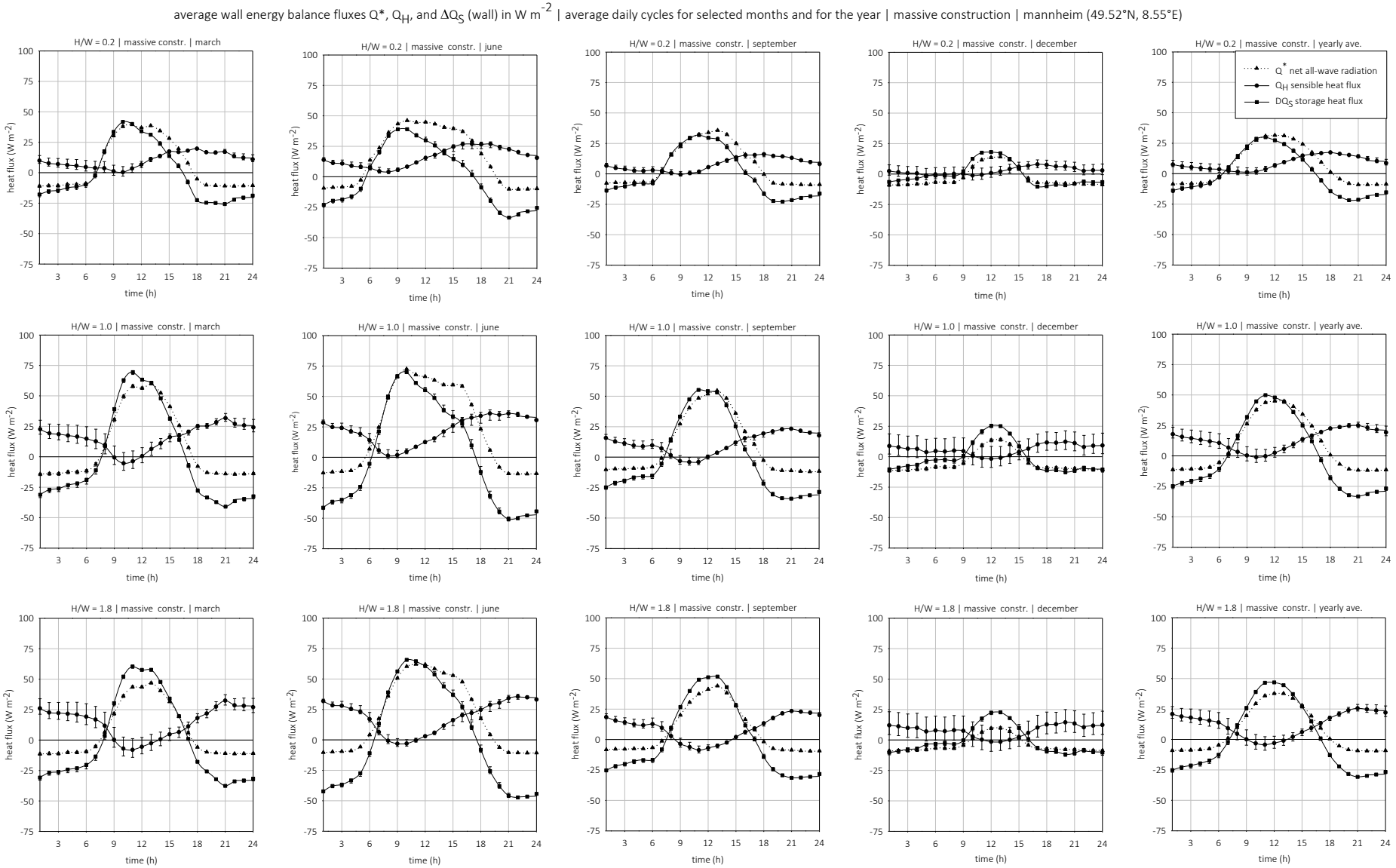

Figure 35: Seasonal and annual average energy balance fluxes (Q*, Q_H, ΔQ_S) at the walls in W m^{-2} for massive construction for Mannheim (49.52°N, 8.55°E)

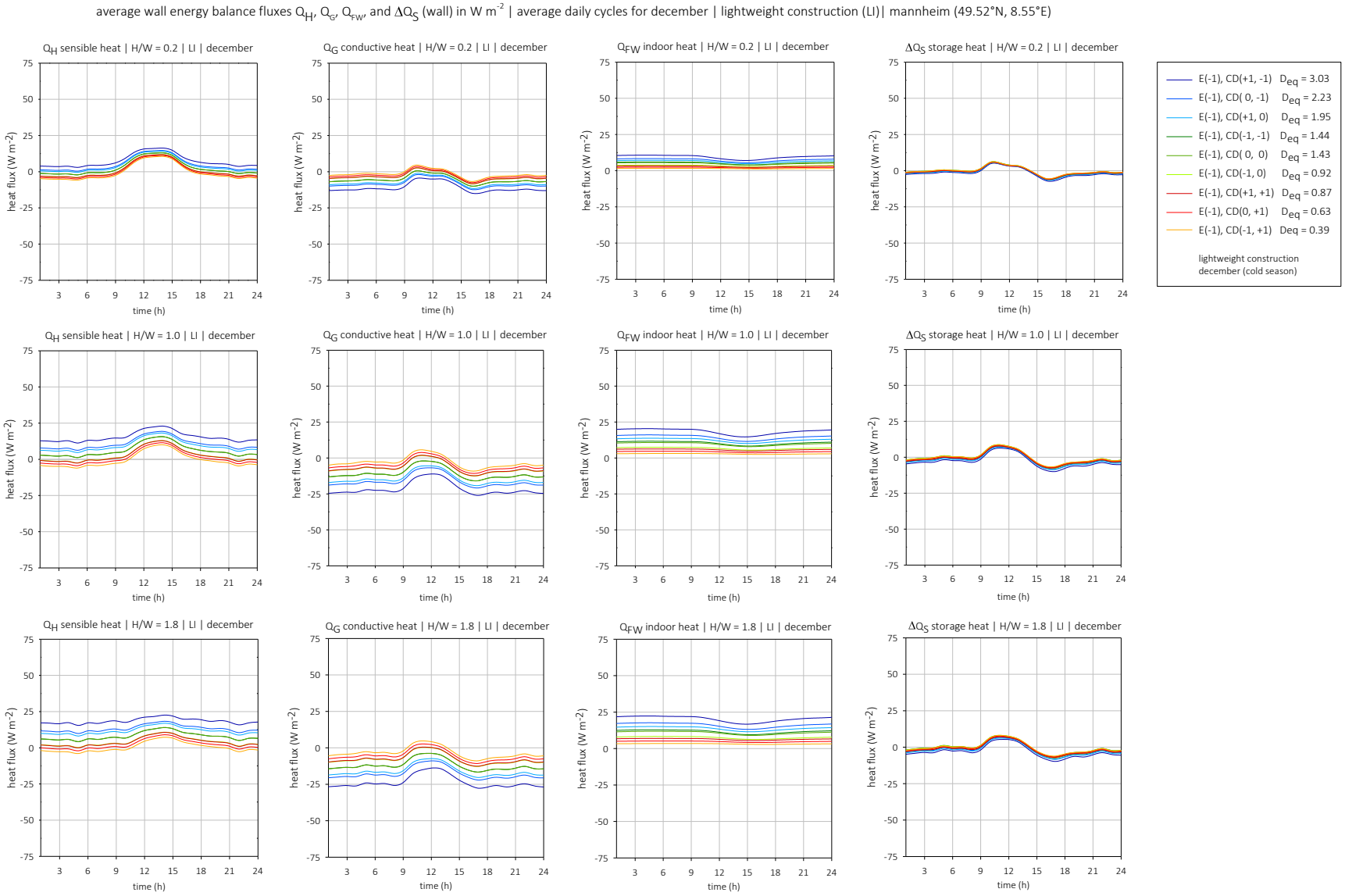

Figure 36: Average wall energy balance fluxes (Q_H, Q_G, Q_{FW} and ΔQ_S) in W m^{-2} for December and lightweight construction for Mannheim (49.52°N, 8.55°E)

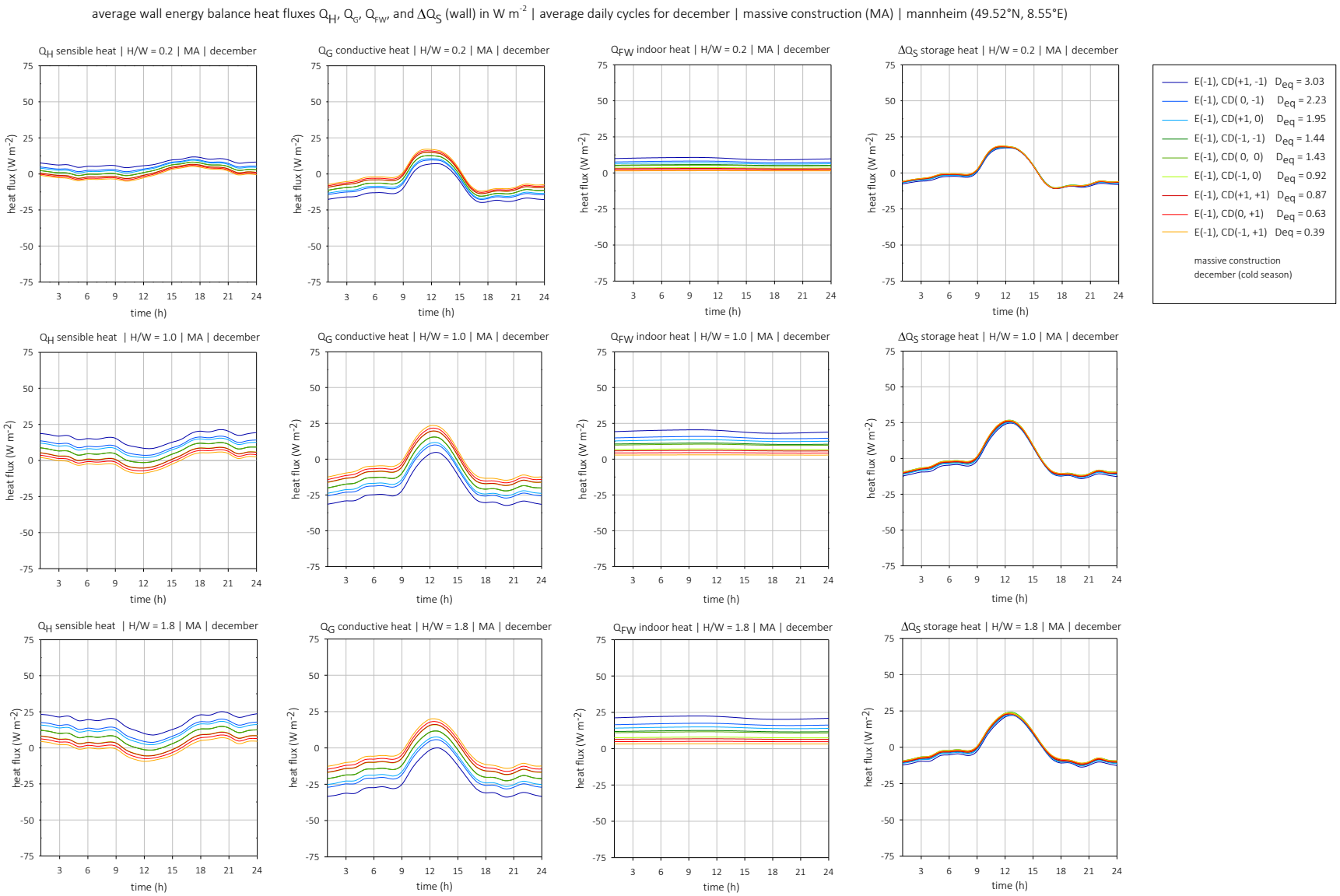

Figure 37: Average wall energy balance fluxes (Q_H, Q_G, Q_{FW} and ΔQ_S) in W m^{-2} for December and massive construction for Mannheim (49.52°N, 8.55°E)

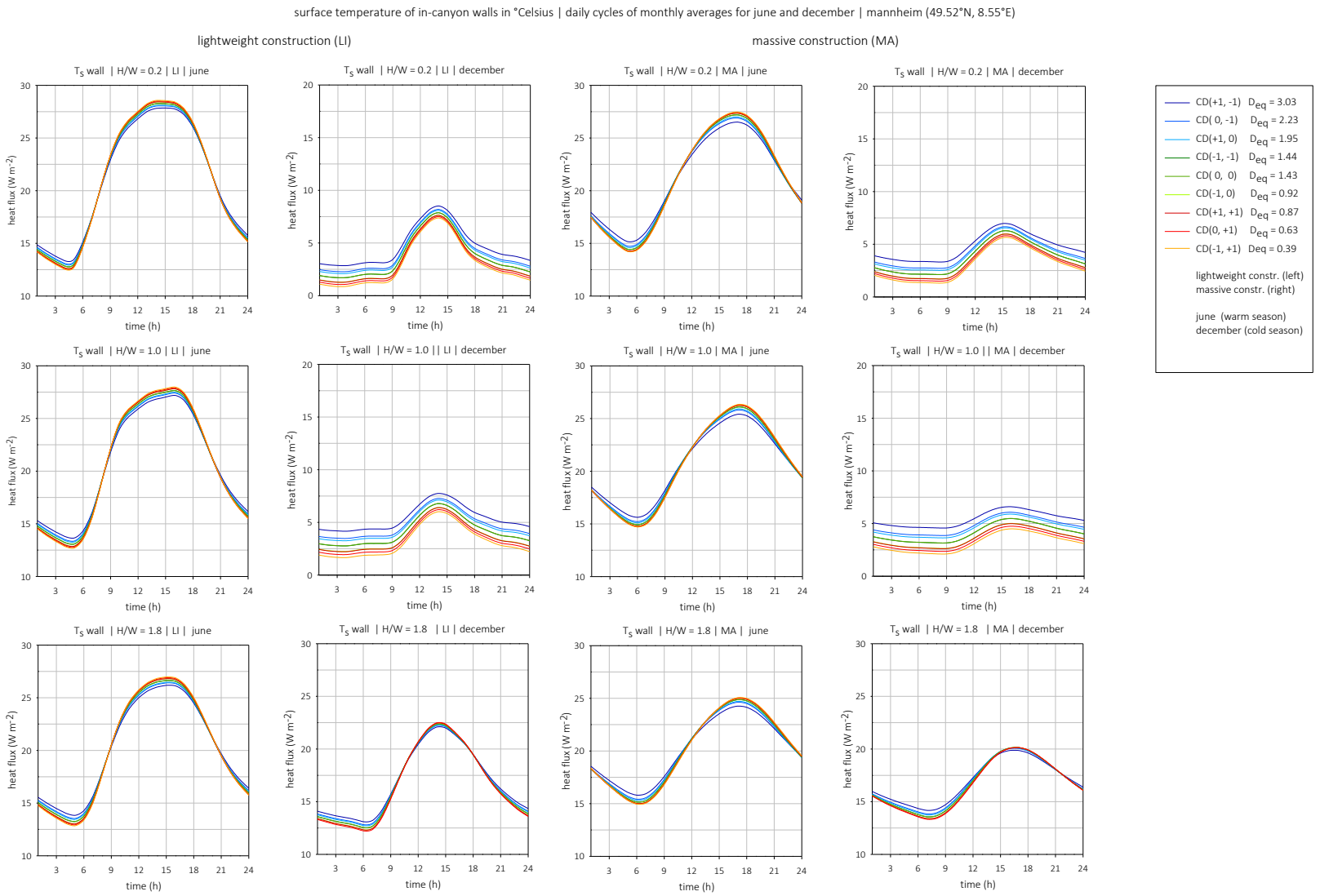

Figure 38: Average wall surface temperature T_{swall} in °C for June and December, lightweight and massive construction for Mannheim (49.52°N, 8.55°E)

3. THE RESULTS ABOUT THE BUILDING ENERGY DEMAND

This section discusses the findings about the useful energy demand for heating, cooling, lighting and ventilation (if mechanical) of the extensive parametric study applied on theoretical urban office buildings (see section II - 1.4, p 85). The results are presented i) for [SET IV] considering urban microclimate boundary conditions and ii) in comparison with the standard climate expressed as deviations [SET IV] – [SET III], see Table 14. The term whole building used in the following refers to the results averaged for the ten offices. The absolute values are surface-related (i.e. specific energy), calculated over one year and expressed in kWh m^{-2} a^{-1}. Firstly, the focus in analysing the SETs is put on: i) the useful energy demand range (max – min) for each single key metric, ii) on the best and worst combinations of the urban and building indicators (A to E, Table 12) in view of energy savings and iii) on a generalizable statistical analysis of the interactions between the variables A to E in a hierarchical order. Secondly, the energy demand is differentiated vertically by floor in order to evaluate the effects of the degree of openness to the sky, in other words accounting for the reduced sky view, which is typical in urban areas. Furthermore, the modifying effects on the energy demand of the building scenarios of use and operation as additional boundary conditions are checked.

3.1. The Useful Energy Demands for Heating, Cooling, Lighting and Ventilation

Figure 39 and Table 28 show the values range within the simulation series of 162 runs of [SET IV] for useful heating Q_{heat}, cooling C_{cool}, lighting Q_{light}, ventilation Q_{vent} (if mechanical) and their sum $Q_{TOT\ I}$ (without ventilation) and $Q_{TOT\ II}$ (incl. ventilation). Owing the small difference in magnitude and similarity in the information between $Q_{TOT\ I}$ and $Q_{TOT\ II}$, the totals in this report are given preferably for $Q_{TOT\ I}$ (i.e. without ventilation) because it is considered to be the more probable scenario.

The useful heating Q_{heat} varies between 3.6 and 60.6 kWh m^{-2} a^{-1} and the useful cooling C_{cool} ranges between 2.3 and 18.7 kWh m^{-2} a^{-1}. This proportion between heating and cooling is in good agreement with the temperate climate of Mannheim with cold winters. The lighting energy can reach a maximum of 37.2 kWh m^{-2} a^{-1} (from a maximum possible of 37.323 kWh m^{-2} a^{-1}, see Appendix 6) but can be as low as 8.0 kWh m^{-2} a^{-1}. The total ventilation if not ensured naturally would range between 7.2 and 10.0 kWh m^{-2} a^{-1}. The useful total energy demand reaches 86.19 or 94.01 kWh m^{-2} a^{-1} depending on whether the ventilation is natural ($Q_{TOT\ I}$) or mechanical ($Q_{TOT\ II}$), respectively. Figure 39 reveals that the variation range (min – max) is the highest for heating (57.0 kWh m^{-2} a^{-1}), followed by lighting (29.3 kWh m^{-2} a^{-1}) and then cooling (16.4 kWh m^{-2} a^{-1}). This underlines the impact of the choices made for the variables A

to E and the consequences of a proper design in this regard. The ventilation shows the smallest variation range due to the simulation settings limiting unnecessary air change (see section II - 1.3, p 77). Figure 40 shows for all investigated building models (18) a synopsis picture about the part of heating, cooling, lighting and ventilation energy demands. Figure 40 shows all variables at their 3-steps except for B restricted to the middle step (= 0) as average case because of its low modifying effect. In more detail, Figure 41 to Figure 44 show the values of all simulated cases, organised according to the 18 building models and differentiated for the urban variables (A, B) for each target key metric separately. Moreover, Table 63 in Appendix 8 provides the absolute values for all target key metrics in a decreasing ranking for the 162 cases including their corresponding A to E values, highlighting thereby the best and worst combinations of these variables. All these findings are commented hereafter.

3.1.1. Useful Heating Energy Demand

Table 63 in Appendix 8 shows that combining a low window ratio C (-1) with a high thermal insulation D (+1) yields the lowest heating energy demand, regardless of the thermal inertia (E), urban density (A) or solar orientation (B). The thermal inertia shows here no clear effect because of the moderate settings assumed for internal heat gains and ventilation, which if higher would most likely have exacerbate the positive effect of massive construction. The thermal insulation and window ratio are decisive here for their impact on heat conservation by reducing the transmission heat losses as expected for the cold winter of TRY12. The low percentage of glazing in this case helps keep an overall high thermal insulation of the building envelope since the opaque part is better insulating than the transparent one. The worst cases (see Appendix 8) with maximum heating energy demand occur in the opposite case of largely glazed façades (C = +1) combined with a low thermal insulation (D = -1) for the same reason, i.e. a resulting weak insulated envelope with important transmission heat losses.

Figure 41 shows an overview of all results. The differences are the largest between good and weak insulated buildings. Whereas, the heating for the best cases (D = +1) ranges between 3.6 and 11.8 kWh m^{-2} a^{-1}, it amounts 32.7 to 60.6 kWh m^{-2} a^{-1} for the worst cases (D = -1). The window ratio is the second most influencing variable with roughly 10 kWh m^{-2} a^{-1} difference between the various C steps. The urban canyon geometry (A) shows some visible impact for the cases with the highest heating energy demand (C = +1, D = -1) because of more outdoor – indoor exchange in these cases. Deep canyons lead to more energy demand than shallow ones. The thermal inertia E shows no clear impact. The solar orientation B shows minimal effects especially on the worst cases with the NS orientation being more favourable.

3.1.2. Useful Cooling Energy Demand

The best results for cooling are obtained with a weak thermal insulation (D = -1), massive construction (E = +1) and a low to moderate window ratio (C = -1 or 0), irrespective of the urban variables (Table 63). This is because the increased transmission heat losses via the building envelope, the reduced passive solar gains via the windows and the increased heat storage during the daytime hours all help prevent overheating. The highest demand for cooling occurs in case of a largely glazed façade (C = +1), lightweight construction (E = -1) and weak to medium thermal insulation (D = -1 or 0) in shallow to unity-like urban canyons (A = -1 or 0). In these cases, more conductive heat exchange with outdoors and little heat storage under high exposure to solar radiation increase the risk for overheating.

In contrast to heating, Figure 41 shows more relevance of the thermal inertia E on the cooling. For lightweight construction, the cooling ranges between 7.2 and 18.7 kWh m^{-2} a^{-1}, whereas for massive construction it varies between 2.3 and 13.8 kWh m^{-2} a^{-1}. Moreover, the thermal insulation D behaves differently in combination with the window ratio. The cooling energy demand increases with better thermal insulation in case of small openings, whereas it decreases in combination with largely glazed façades, even though the absolute values are higher in the latter case. The aspect ratio A has a certain effect on unfavourable cases characterised by large openings combined with low insulation quality. The solar orientation B also shows some small impact especially in case of high window ratio and large streets with the NS orientation being more advisable.

3.1.3. Useful Heating and Cooling Energy Demand

If heating and cooling are considered together (see Table 63), it appears that the window ratio C and thermal inertia E have no conflicting effect between the cold and warm seasons, so that a few to moderate glazing and massive construction are preferable to highly glazed façades combined with lightweight construction. In contrast, the thermal insulation has opposite effects between heating and cooling. Yet, keeping a high thermal insulation is the best choice because of the dominating heating period for this temperate climate. For the same reason, the worst cases for heating and cooling taken together mostly reflect the heating case.

3.1.4. Useful Lighting Energy Demand

The illuminance indoors is estimated from the solar irradiation reaching the offices (see Appendix 5). In Figure 43, the cases 1 to 9 are identical to cases 10 to 18 because the thermal inertia plays no role in respect to the lighting energy demand. With reference to Table 63 in

Appendix 8, the lowest energy demand for artificial lighting occurs for the buildings N°7 and N°16 with 8.0 to 12.9 kWh m^{-2} a^{-1} and the most energy demanding for lighting are buildings N°3 and N°12. The best cases correspond to shallow urban canyons (A = -1), largely glazed façades (C = +1), combined with high solar and light transmission factors of the glazing (g and τ) indirectly given by a weak thermal insulation (D = -1) as documented in Table 12. All these conditions indeed support high amounts of solar radiation entering the office rooms. In contrast, the worst cases for lighting are the opposite ones, i.e. those located in deeper urban canyons (A = +1 or 0) and combining low window ratio and high values of D with low g and τ values. The daylighting potential expressed in percentage is a reverse quantity to the lighting energy, so that the latter cases are better advisable than the former ones. Figure 43 also clearly illustrates the effects of the window ratio and glazing quality in terms of g and τ on the lighting as direct consequence of the solar gains and operation of shading devices. As expected, the canyon geometry A has a clear impact with the unity-like canyons requiring in most cases roughly estimated about 4 kWh m^{-2} a^{-1} and the deep canyons about 8 kWh m^{-2} a^{-1} more lighting energy than the shallow canyons.

3.1.5. Useful Ventilation Energy Demand

This research primarily foresees a natural ventilation via openings and the simulation settings have been chosen to be realistic for that (see section II - 1.3.2, p 81). In this case, ventilation energy would equal zero. The scenario of a mechanical ventilation is conceivable for instance for acoustical or pollution reasons. Referring to Figure 42, the absolute values of ventilation are relatively low with a maximum of 6.4 kWh m^{-2} a^{-1} during the usage time, 3.9 kWh m^{-2} a^{-1} outside the usage time and 10.0 kWh m^{-2} a^{-1} as total. The urban and building indicators A to E have less clear effects on the ventilation than on heating, cooling or lighting. Good thermal insulation D shows a slight effect in increasing the ventilation need and high aspect ratio A shows a small effect in decreasing it, whereas the other variables B, C and E have no evident effects. The lowest need during the usage time occurs in case of weak thermal insulation (D = -1) and deep canyons (A = +1). The risk for overheating, which explains additional ventilation, diminishes in these cases because of less solar gains due to shading from the surroundings and more heat losses via the heat transmissive building envelope. The highest need for ventilation during the usage time occurs in the opposite case of high thermal insulation (D = +1) and low thermal inertia (E = -1). The reason is that well-insulated building elements prevent the evacuation of the heat accumulated in the air resulting from lacking storage. Massive construction (E = +1) is preferable during the usage time i.e. daytime hours, whereas the

lightweight construction (E = -1) is better outside the usage time (mostly at night). Indeed, the advantage of the heat storage in the daytime hours turns out to be a disadvantage at night in case of massive construction when the stored heat is released back to the air. Lightweight construction just behaves in the opposite way. As no heat is stored during the day, no additional heat release occurs by night and this prevents any overheating risk.

3.1.6. Useful Total Energy Demand

Table 63 in Appendix 8 embodies the fact that finding an optimal urban and building energy efficient design solution is tasking. For example, the buildings N°12, N°3 are the best choice for heating, the buildings N°10 and 13 are better with respect to cooling and the buildings N°7 and N°16 require the less lighting, etc. The urban indicators A and B show no particular relevance for heating or cooling, whereas wide streets (cases I, IV and VII) are preferable for lighting and deep canyons (cases II, VI, IX) are preferable with respect to ventilation. The worst cases just provide the same picture of divergences. The comparison between the best and worst cases also clearly shows that the best choice for one key metric might be the worst for another one, e.g. the buildings (N°7 and 16) or (N°12 and N°3) for heating versus lighting or building N°12 for heating versus ventilation. This consequently explains that the best combinations of the variables A to E are less easy to interpret for the total energy demand than for the individual quantities. Yet, looking at Figure 44, the total energy demand ($Q_{TOT\ I}$) appears to follow the trend given by the heating due to the relatively high absolute values even though opposite to lighting, i.e. good thermal insulation, small windows and wide canyons being better advisable. In spite of these conflicting features, the ranking in Table 63 in Appendix 8 rather shows clear favourable and unfavourable combinations. The lowest total useful energy demand is calculated for the buildings N°18 and N°15, which correspond to high thermal insulation (D = +1), high thermal inertia (E = +1) and large to very large openings (C = +1 or 0). The urban structure is then preferably of low density (A = -1 or 0).

Worthy of note, however, is that the reported totals are useful energy values and the ranking is expected to be different if primary energy values are considered because of the different weighting primary factors e_p for the energy sources. The factor e_p would be about 1.265 for a condensing boiler for heating, 0.594 for an air conditioner with a COP of 3 and 1.8 for electrical lighting (DIN 4701-10, DIN V 18599-1, EnEV 2016). This issue is not handled in this report not only for space reasons but in fact because the focus is not put on the systems or on the kind of energy source used. The focus is put on the building as object and in this case the quantity useful energy is more informative.

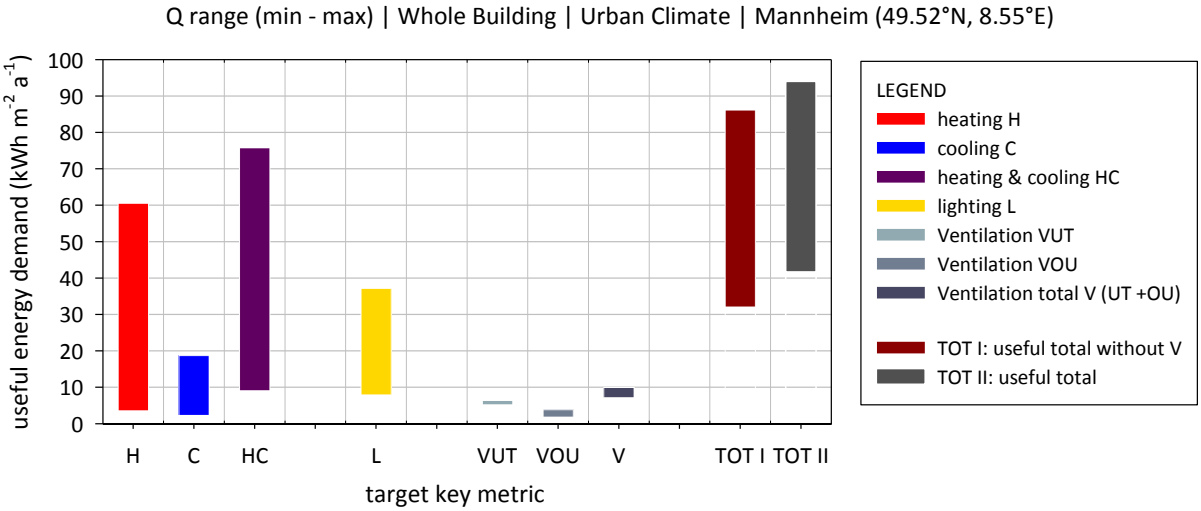

Figure 39: Range of useful energy demand for heating, cooling, lighting and ventilation for urban office buildings located in Mannheim (49.52°N, 8.55°E)

Table 28: Minimum and maximum values of useful energy demand (a) as absolute values and (b) as percentages to useful total energy demand for Mannheim (49.52°N, 8.55°E)

useful energy demand	heating H		cooling C		lighting L		ventilation during usage time V (UT)		ventilation outside usage time V (OU)		total ventilation V (UT + OU)		useful total (TOT I) H + C + L		useful total (TOT II) H + C + L + V	
	min.	max.	min.	max.	min.	max.	min.	max.	min.	max.	min.	max.	min.	max.	min.	max.
energy demand Q (kWh m^{-2} a^{-1})	3.58	60.57	2.30	18.73	7.95	37.21	5.25	6.43	1.83	3.89	7.19	9.98	32.07	86.19	41.69	94.01
(max - min) range Q (kWh m^{-2} a^{-1})	56.99		16.43		29.26		1.19		2.06		2.78		54.13		52.32	
percentage of useful total (TOT I) H + C + L (%)	7.82	77.63	3.59	33.85	9.50	80.33	0.00	0.00	0.00	0.00	0.00	0.00	Mannheim (49.52°N, 8.55°E) urban climate conditions average for whole building			
percentage of useful total (TOT II) H + C + L + V (%)	6.44	70.56	3.20	27.48	8.66	66.38	5.88	14.28	1.99	8.80	7.87	23.08				

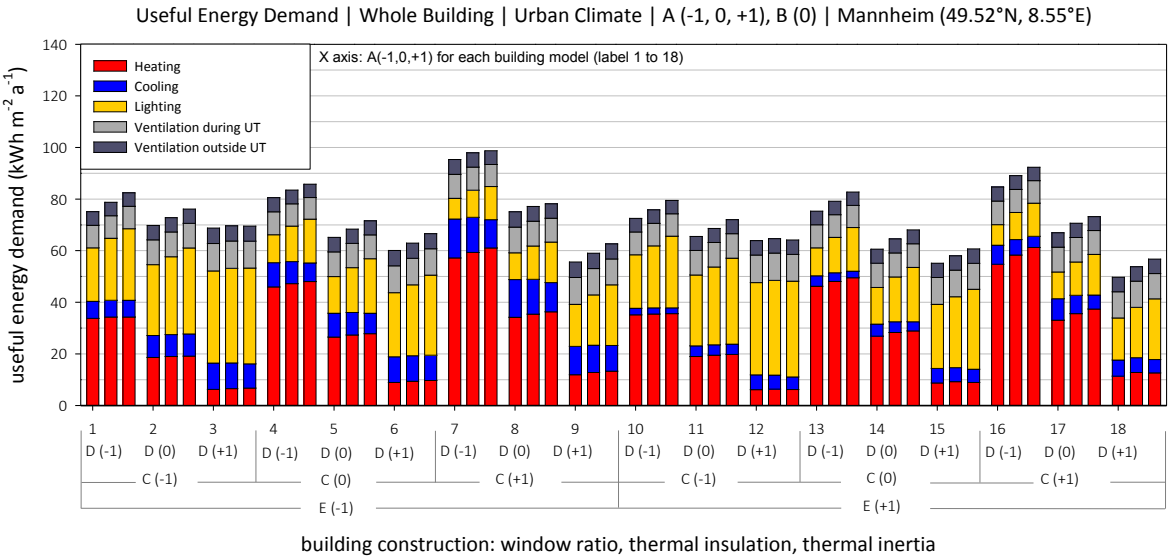

Figure 40: Useful energy demand in kWh m^{-2} a^{-1} for heating, cooling, lighting and ventilation during UT and OU for all 18 building types (C, D, E combinations), A (-1, 0, +1) and B = 0 for Mannheim (49.52°N, 8.55°E)

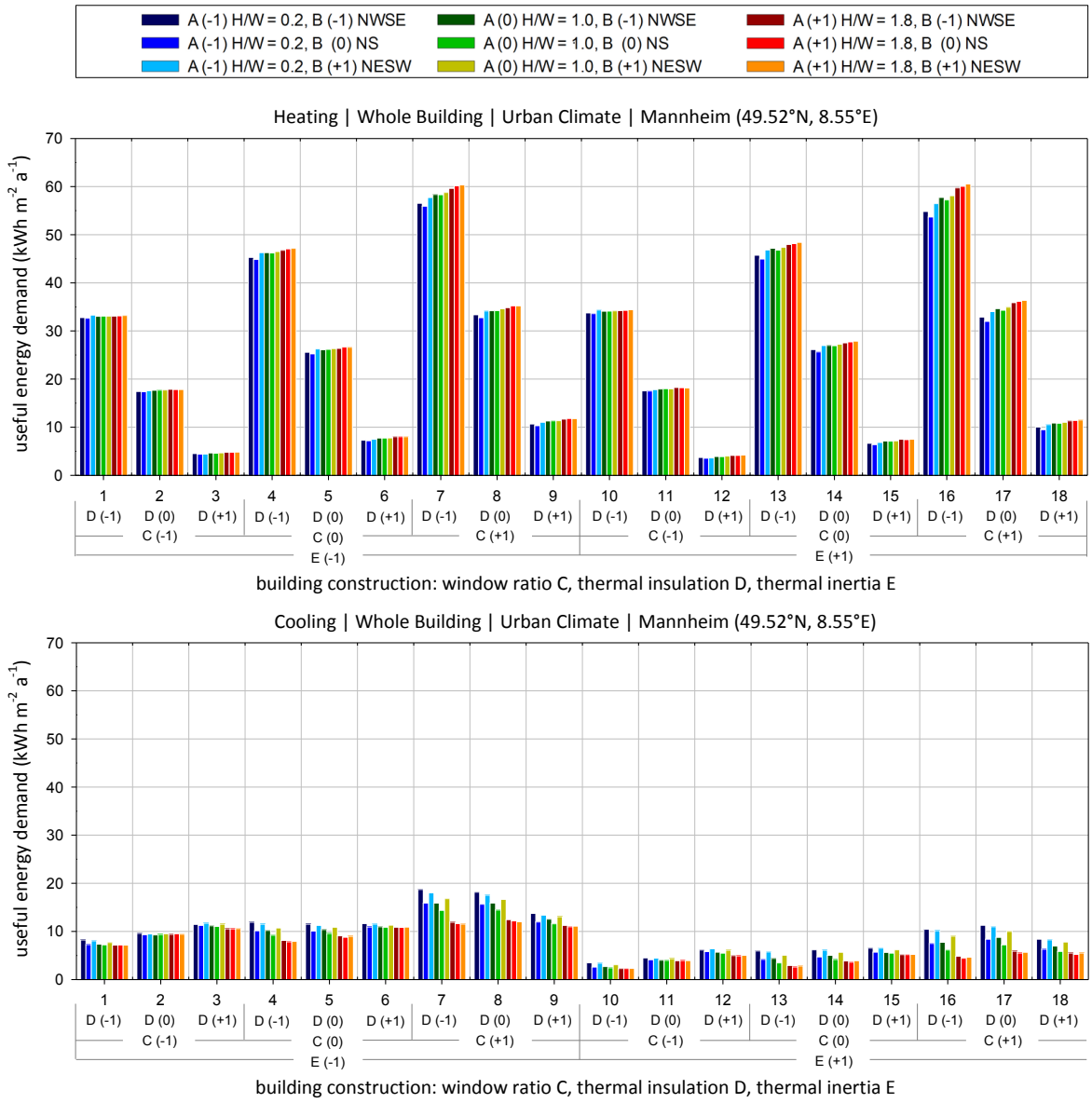

Figure 41: Annual average useful heating Q_{heat} and cooling Q_{cool} energy demands under urban climate boundary conditions for Mannheim (49.52°N, 8.55°E)

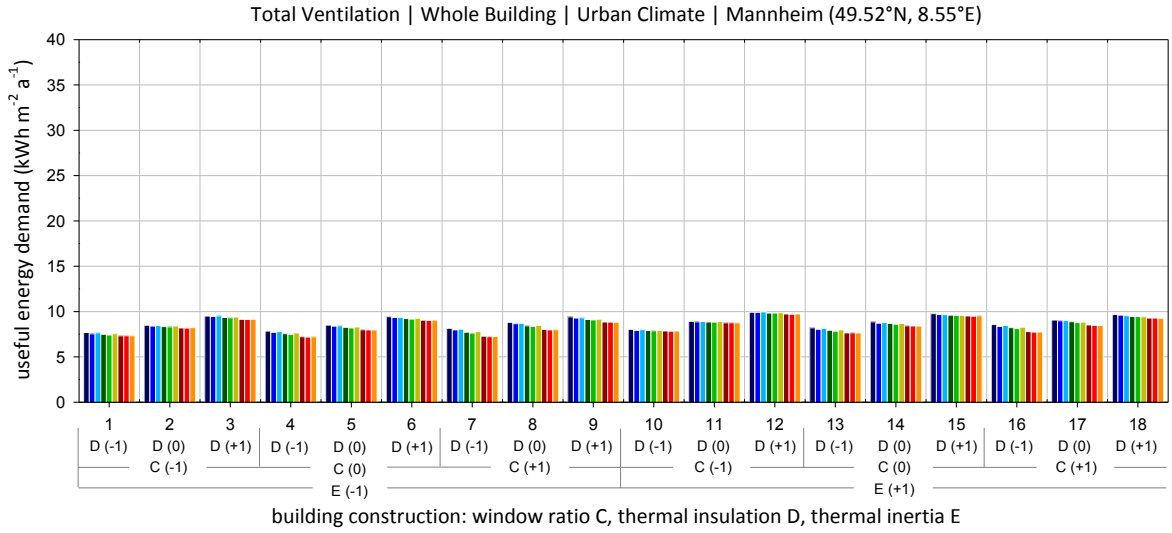

Figure 42: Annual average useful ventilation energy demand Q_{vent} under urban climate boundary conditions for Mannheim (49.52°N, 8.55°E)

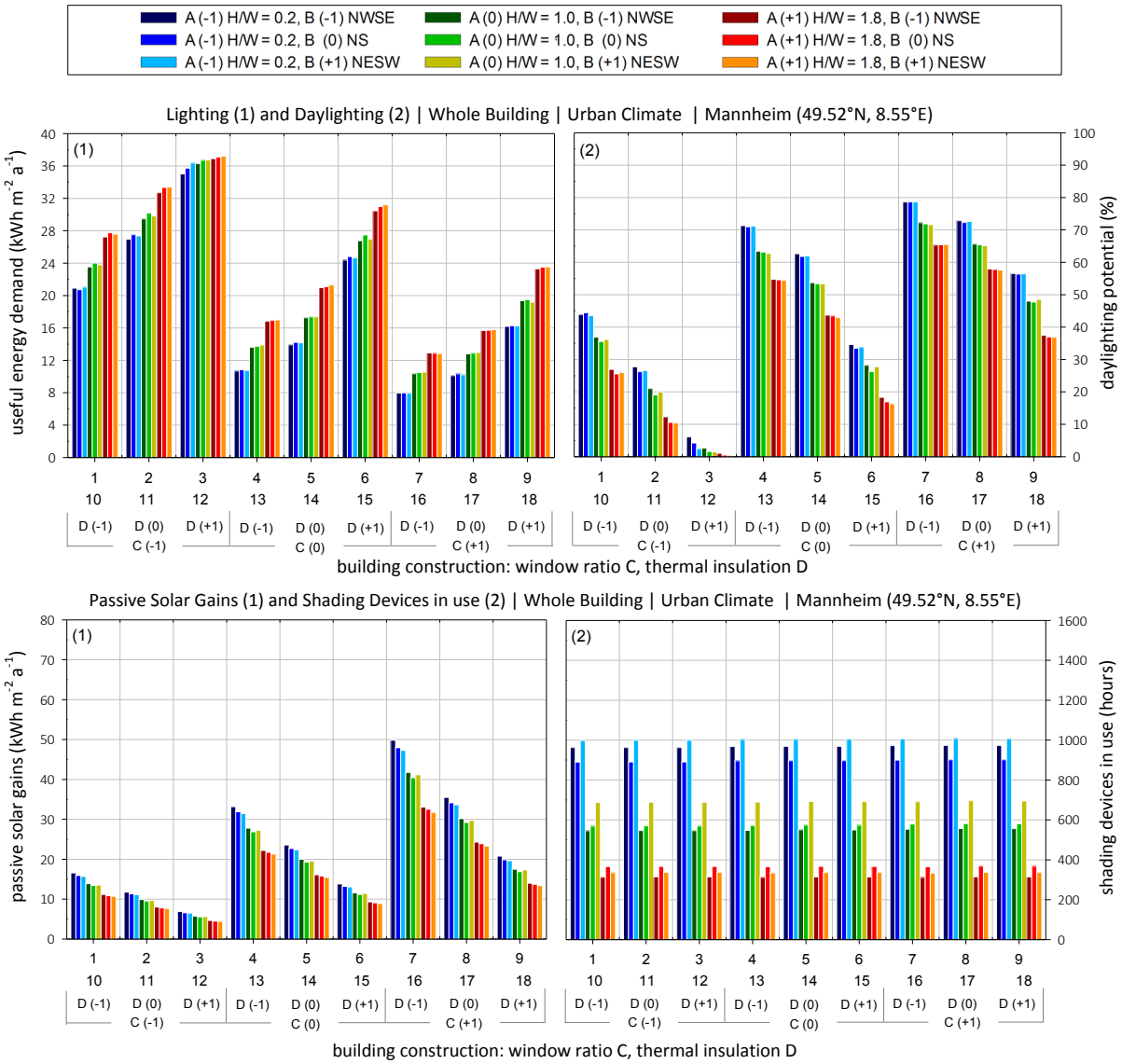

Figure 43: Annual average useful lighting energy demand Q_{light}, daylighting potential (%) and the related passive solar gains and shading devices operation under urban microclimate boundary conditions for Mannheim (49.52°N, 8.55°E)

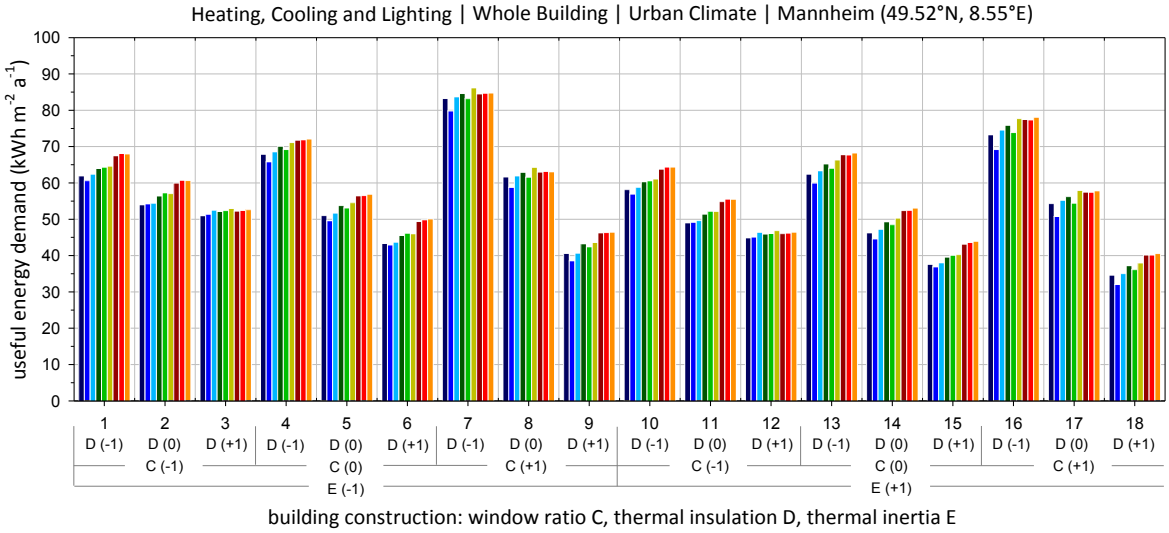

Figure 44: Annual average total useful energy demand $Q_{TOT\ I}$ including heating, cooling and lighting under urban climate boundary conditions for Mannheim (49.52°N, 8.55°E)

3.2. The DOE Statistical Analysis of the Useful Energy Demands

In order to support the qualitative observations made so far and to isolate the impact of each single variable (A to E) in [SET IV], a statistical regression analysis of the results is provided in Table 29 to

Table 33. The tables list for each target key metric a number of mathematical models with successively more predictors and increased accuracy. All predictors and their coefficients appear in a decreasing order of importance. Main effects, double interactions, as well as square terms may occur. Positive values of a predictor mean a proportional effect according to the coding (-1, 0, +1) whereas negative values mean inversely proportional effect. The effect of a variable, however, depends on the sum of all its weighted predictors.

Regarding the useful heating Q_{heat} (Table 29), the adjusted coefficients of determination adj. R^2 of 0.999 reveal the high hit rate of the predicted models. The thermal insulation D is responsible for 82.5% of the result and the window ratio (incl. interaction with D) brings this dependence to 96.7% in model 3, so that D and C could exclusively account for most of the building thermal behaviour in the cold season. All other parameters (main effects and double interactions) improve the polynomial mathematical model up to 3%, from which several interactions with C and D (AC, AD, DE). The coefficients also reveal that the effects of C and D are not linear.

With respect to useful cooling Q_{cool} (Table 30), the thermal inertia is the most decisive parameter with a coefficient of determination adj. R^2 of 58.8%. The window ratio C brings the adj. R^2 to 77.3% and the urban profile A improves the fitting to 82.9% in model 3. In addition to the thermal insulation D, the quadratic terms and double interactions of the variables already involved (AC, CD and C^2) bring the adj. R^2 to 93.3, which can be considered as sufficiently accurate. Further variables and interactions have an impact scope of less than 3% and lead to a final model with an adj. R^2 up to 96.1%.

Table 31 provides some quantification about the lighting energy. The variables involved are A, C, D and their interactions, which provide a high fit rate and an adjusted coefficient of determination adj. R^2 of 0.984 of the predicted model. The window ratio C is responsible for 56.23% of the useful lighting energy demand and the thermal insulation D (indirectly because of g and τ) brings this dependence to 85.4% in model 2. The urban profile increases the fitting rate further to 94.8% in model 3. The importance of C and D are emphasised with their quadratic terms C^2 and D^2, which also state for a non-linear relationship. The daylighting potential being calculated from the lighting data, its statistics are identical (Table 31), except the coefficients, which are different as these refer to the percentage of use of daylight.

The statistics for the ventilation during and outside usage time are very similar. Therefore, Table 32 presents only the statistics for their sum. From the total adj. R^2 of 99.3%, 82.8% are attributable to the thermal insulation D. Additionally, the thermal inertia E (with 8.2%) and the aspect ratio A (with 5.1%) bring the model 3 to 96.1%. The window ratio plays a role, also in interaction with D and A. Together with the quadratic terms and doubles interactions of the already named variables A, C, D and E, the model reaches 99.1%.

Including the ventilation term or not in the total energy demand leads to very similar models, therefore, only the sum of heating, cooling and lighting is given in

Table 33. As expected, the thermal insulation D plays the main roles with 73.6%, followed by the window ratio C, the thermal inertia E and aspect ratio A with additional 12.3%, 5.4% and 2.7% respectively and hence a total of 94.1% for model 4. The final model at 98.6% includes the quadratic terms C^2 and D^2 and the variable B to a small extent.

Table 29: Statistics of the useful heating energy demand Q_{heat} for [SET IV], Mannheim (49.52°N, 8.55°E)

Q_{heat} | whole building | urban climate | Mannheim (49.52°N, 8.55°E)

Model Summary					Full Model: Predictors and Coef.			
Model	R	R Square	Adjusted R Square	R Square Change	Model 13	predictor	B	Sig.
1	.909a	.826	.825	.826		const.	26.340	.000
2	.984b	.968	.967	.141		D	-19.265	.000
3	.998c	.997	.997	.029		C	7.970	.000
4	.999d	.998	.998	.001		CD	-4.420	.000
5	.999e	.998	.998	.000		A	.723	.000
6	.999f	.998	.998	.000		AC	.552	.000
7	.999g	.999	.999	.000		D^2	.545	.000
8	.999h	.999	.999	.000		AD	-.335	.000
9	.999i	.999	.999	.000		DE	-.239	.000
10	.999j	.999	.999	.000		C^2	-.353	.000
11	.999k	.999	.999	.000		B	.168	.002
12	.999l	.999	.999	.000		B^2	.277	.004
13	1.000m	.999	.999	.000		AE	.158	.004
						CE	-.136	.014
m. Predictors: (Constant), D, C, CD, A, AC, D^2, AD, DE, C^2, B, B^2, AE, CE								

Table 30: Statistics of the useful cooling energy demand Q_{cool} for [SET IV], Mannheim (49.52°N, 8.55°E)

Q_{cool} | whole building | urban climate | Mannheim (49.52°N, 8.55°E)

Model Summary					Full Model: Predictors and Coef.			
Model	R	R Square	Adjusted R Square	R Square Change	Model 13	predictor	B	Sig.
1	.769a	.591	.588	.591		const.	7.521	.000
2	.881b	.776	.773	.185		E	-2.881	.000
3	.912c	.833	.829	.057		C	1.975	.000
4	.939d	.881	.878	.048		A	-1.092	.000
5	.950e	.903	.900	.022		CD	-1.234	.000
6	.961f	.923	.920	.020		AC	-.838	.000
7	.967g	.935	.933	.012		C^2	1.131	.000
8	.973h	.946	.943	.011		D	.507	.000
9	.976i	.953	.951	.007		B^2	.826	.000
10	.979j	.959	.956	.006		CE	-.385	.000
11	.980k	.961	.958	.002		AD	.420	.000
12	.981l	.963	.960	.002		D^2	-.386	.002
13	.982m	.964	.961	.001		A^2	-.312	.013
						DE	.147	.042
i. Predictors: (Constant), E, C, A, CD, AC, C^2, D, B^2, CE								

Table 31: Statistics of the useful lighting energy demand Q_{light} and daylighting potential for [SET IV], Mannheim (49.52°N, 8.55°E)

Q_{light} | whole building | urban climate | Mannheim (49.52°N, 8.55°E)

Model Summary					Full Model: Predictors and Coef.			
Model	R	R Square	Adjusted R Square	R Square Change	Model 7	predictor const.	B 18.420	Sig. .000
1	.752a	.565	.562	.565		C	-7.926	.000
2	.937b	.877	.876	.312		D	5.891	.000
3	.974c	.949	.948	.072		A	2.832	.000
4	.985d	.971	.970	.021		C^2	2.660	.000
5	.990e	.980	.980	.010		D^2	1.812	.000
6	.992f	.984	.984	.004		CD	-.786	.000
7	.992g	.985	.984	.001		AC	.313	.016
g. Predictors: (Constant), C, D, A, C^2, D^2, CD, AC								

daylight potential

Full Model: Predictors and Coef.			
Model 7	predictor const.	B 50.648	Sig. .000
	C	21.236	.000
	D	-15.784	.000
	A	-7.588	.000
	C^2	-7.128	.000
	D^2	-4.854	.000
	CD	2.107	.000
	AC	-.839	.016
For the models see Q_{light}			

Table 32: Statistics of the total useful ventilation energy demand Q_{vent} (if mechanical) for [SET IV], Mannheim (49.52°N, 8.55°E)

Q_{vent} | whole building | urban climate | Mannheim (49.52°N, 8.55°E)

Model Summary					Full Model: Predictors and Coef.			
Model	R	R Square	Adjusted R Square	R Square Change	Model 13	predictor const.	B 8.463	Sig. .000
1	.910a	.829	.828	.829		D	.824	.000
2	.954b	.911	.910	.082		E	.212	.000
3	.981c	.962	.961	.051		A	-.205	.000
4	.988d	.976	.975	.014		CD	-.131	.000
5	.991e	.983	.982	.007		AC	-.091	.000
6	.993f	.986	.986	.003		C^2	.092	.000
7	.994g	.988	.988	.002		D^2	.066	.000
8	.995h	.990	.989	.002		AD	.045	.000
9	.996i	.991	.991	.001		AE	.034	.000
10	.996j	.993	.992	.001		B^2	.057	.000
11	.997k	.993	.993	.001		CE	-.020	.001
12	.997l	.993	.993	.000		A^2	-.034	.001
13	.997m	.994	.993	.000		C	-.019	.002
m. Predictors: (Constant), D, E, A, CD, AC, C^2, D^2, AD, AE, B^2, CE, A^2, C								

Table 33: Statistics of the useful total energy demand $Q_{TOT\ I}$ including heating, cooling and lighting for [SET IV], Mannheim (49.52°N, 8.55°E)

$Q_{TOT(H+C+L)}$ | whole building | urban climate | Mannheim (49.52°N, 8.55°E)

Model Summary					Full Model: Predictors and Coef.			
Model	R	R Square	Adjusted R Square	R Square Change	Model 10	predictor const.	B 52.165	Sig. .000
1	.859a	.738	.736	.738		D	-12.867	.000
2	.928b	.861	.859	.123		CD	-6.441	.000
3	.957c	.915	.913	.054		E	-2.845	.000
4	.971d	.942	.941	.027		A	2.464	.000
5	.980e	.960	.959	.018		C	2.020	.000
6	.989f	.978	.977	.018		C^2	3.438	.000
7	.992g	.984	.983	.006		D^2	1.971	.000
8	.992h	.985	.984	.001		B^2	.964	.000
9	.993i	.986	.985	.001		CE	-.520	.000
10	.993j	.987	.986	.001		B	.357	.012
j. Predictors: (Constant), D, CD, E, A, C, C^2, D^2, B^2, CE, B								

3.3. Urban Microclimate Effects on the Useful Energy Demands

The next level of analysis is to find out the extent urban microclimate influences the energy demand of the investigated buildings. The following graphics show the energy demand difference between the simulations series [SET IV] assuming urban microclimate conditions (presented above) and the series using standard climate [SET III], expressed as $\Delta Q_{u\text{-}s} = Q_{urb} - Q_{stn}$. The urban microclimate may influence the energy demand of buildings for two reasons: 1) because of the modified air temperatures and 2) because of the modified solar and heat radiation fluxes on the canyon facets due to in-canyon multiple reflections and longwave radiative heat. These effects are not easy to forecast without dynamic calculations because the various processes involved such as solar gains, operation of shading devices, internal heat gains in dependence on daylighting use versus artificial lighting, overheating prevention using additional ventilation, etc. are all interrelated and depend on these prevailing thermal and radiative conditions (see Figure 19).

Table 34 gives an overview about the range of deviation in the energy demands when urban microclimate conditions are included in comparison to standard conditions. It shows that the heating is always lower up to -3.67 kWh m^{-2} a^{-1} because of mostly higher air temperatures and more solar radiation and radiative heat from the warmer surrounding surfaces. The lighting decreases as well because of the additional solar gains due to the multiple reflections between the canyon facets and amounts up to -3.72 kWh m^{-2} a^{-1}. In contrast, the cooling and ventilation are always higher for the same reason with a surplus of up to 4.03 and 0.60 kWh m^{-2} a^{-1}, respectively. By summing the single key metrics, the total energy demand including urban microclimate effects can be up to -4.73 kWh m^{-2} a^{-1}.

These values, however, must be assessed by keeping in mind the simulation settings in TEB, which decide on the resulting magnitude, frequency and daily course of the canopy heat or cool islands. For example, the assumption of a moderate magnitude of anthropogenic heat (Table 12) as a simple daily profile explains the relatively moderate deviations in the energy demands indoors.

Table 34: Maximum, minimum and range of energy demand deviation between urban climate and standard climate boundary conditions $\Delta Q_{i(u\text{-}s)}$, Mannheim (49.52°N, 8.55°E)

Mannheim (49.52°N, 8.55°E)	heating H		cooling C		lighting L		ventilation during usage time V (UT)		ventilation outside usage time V (OU)		total ventilation V (UT + OU)		useful total (1) H +C +L		useful total (2) H +C +L+V	
	min.	max.	min.	max.	min.	max.	min.	max.	min.	max.	min.	max.	min.	max.	min.	max.
energy demand Q (kWh m^{-2} a^{-1})	-3.67	-0.10	0.21	4.03	-3.72	-0.02	0.54	0.67	0.02	0.28	0.60	0.92	-4.73	0.71	-3.87	1.47
(max - min) range Q (kWh m^{-2} a^{-1})	3.57		3.82		3.71		0.13		0.26		0.31		5.44		5.34	

The following graphs in Figure 45 to Figure 48 show for all 162 cases the deviation in heating, cooling, lighting and ventilation. For a better understanding of these differences, the solar gains and shading devices operation are also plotted.

These graphs show a clear picture of the urban microclimate effects on the energy demand of buildings and attest of the importance of accounting for the specificity of urban conditions. The heating and lighting are systematically lower, whereas the cooling and ventilation are higher under urban microclimate conditions. The level of deviation is in agreement with the absolute values (see e.g. building N°7 and N°16). For example, by comparing Figure 41 and Figure 45 the deviation in heating depends on the same building variables such as the thermal insulation D and window ratio C. The canyon vertical profile A appears to be important in the reduction of the heating energy demand because of more pronounced warming of air with high urban density as well as because of radiation trapping and reflections in-canyon. The deviation in cooling behaves similarly to heating in terms of magnitude depending on the variables under consideration, however in a reverse relationship, i.e. more instead of less energy demand. The low deviation in ventilation (Figure 46) for all cases is due to the simulation settings, which limit the air change to necessity. The lighting energy demand is lower when the radiation inter-reflections within the canyon are taken into account because of more solar gains and hence illuminance and this in spite of a few hours more operation of the shading devices. The reduction in the lighting energy demand (Figure 47) is clearly affected by the variables A to E under consideration as previously observed for the absolute values in Figure 43. The additional solar gains of up to 5.6 kWh m^{-2} a^{-1} and hence more daylighting potential of up to 10% is possible in rather largely glazed buildings, whereas this advantage is limited for façades with small openings. The deviation in the total energy demand shows a reduction for all cases except for the buildings N°3 and N°12 for which the absolute values for heating are already very low.

Table 64 in Appendix 9 shows a ranking of these deviations for each single target key metric. In contrast to the absolute values observed in Table 63, the deviations in the energy demand due to urban microclimate boundary conditions show less evident patterns. Yet, some statements can be made. The buildings N°7 and N°16, which correspond to the weak insulated largely glazed facades, show the largest the difference in heating, whereas the building N°12 and N°3 are the less influenced by the urban microclimate regarding heating and lighting. As far as cooling and ventilation are concerned, the building n°10 experiences the less change.

For the sake of completeness, Table 67 to Table 71 in Appendix 12 provide the corresponding statistics.

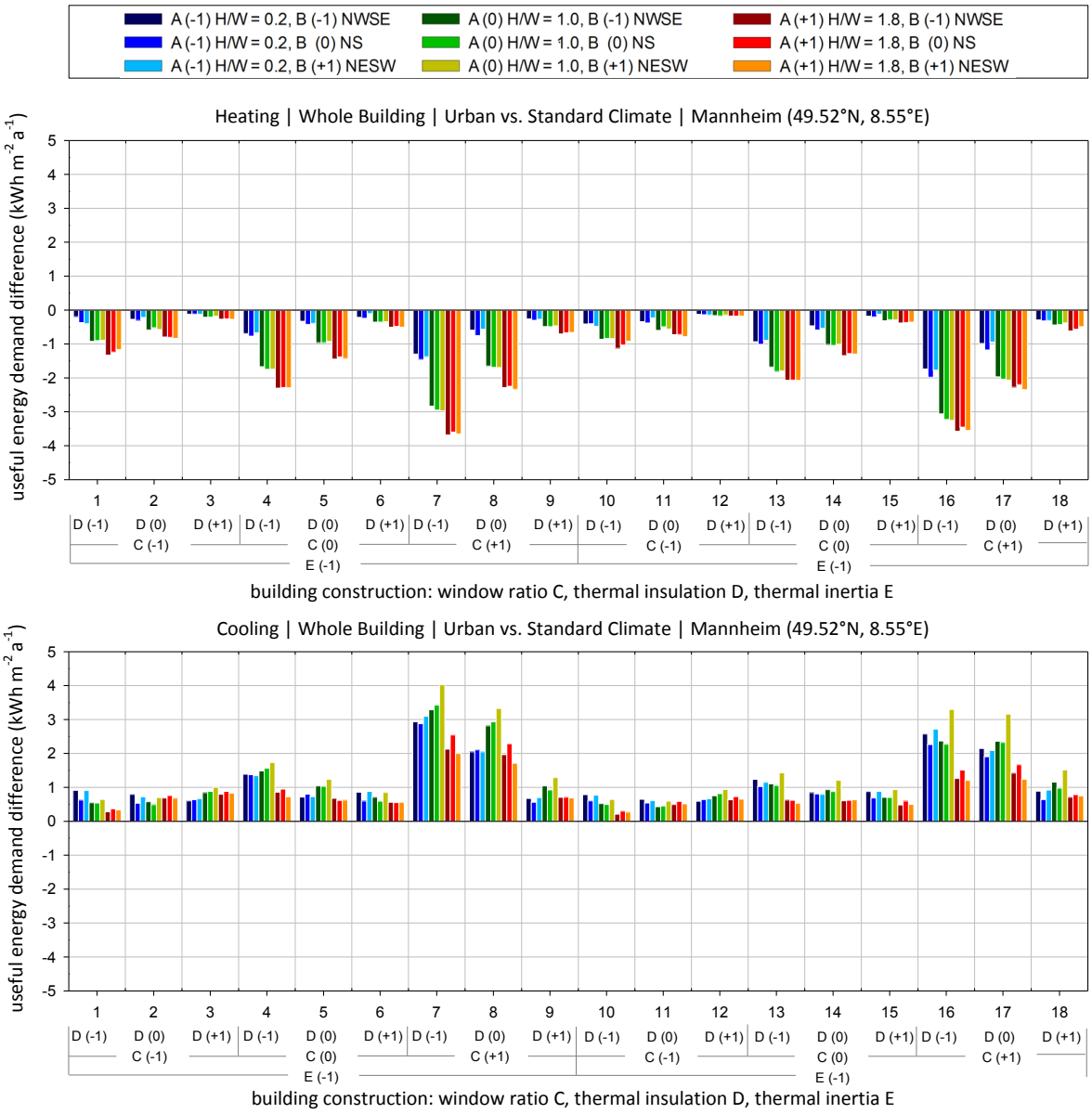

Figure 45: Annual average difference in the useful energy demand for heating ΔQheat(u-s) and cooling ΔQcool(u-s) between urban and standard climate boundary conditions for Mannheim (49.52°N, 8.55°E)

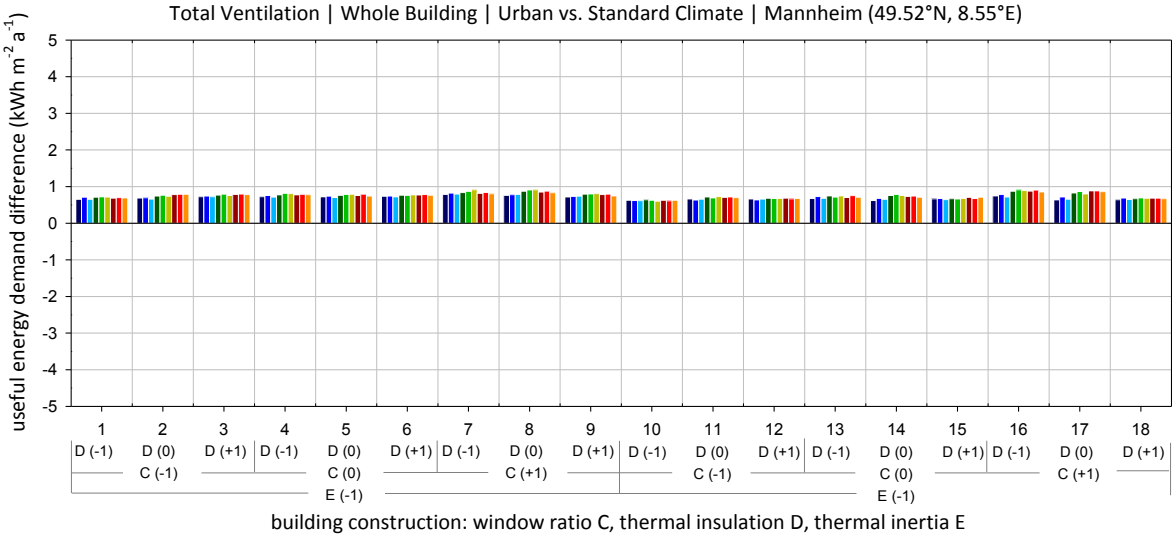

Figure 46: Annual average difference in the useful energy demand for ventilation ΔQvent(u-s) between urban and standard climate boundary conditions for Mannheim (49.52°N, 8.55°E)

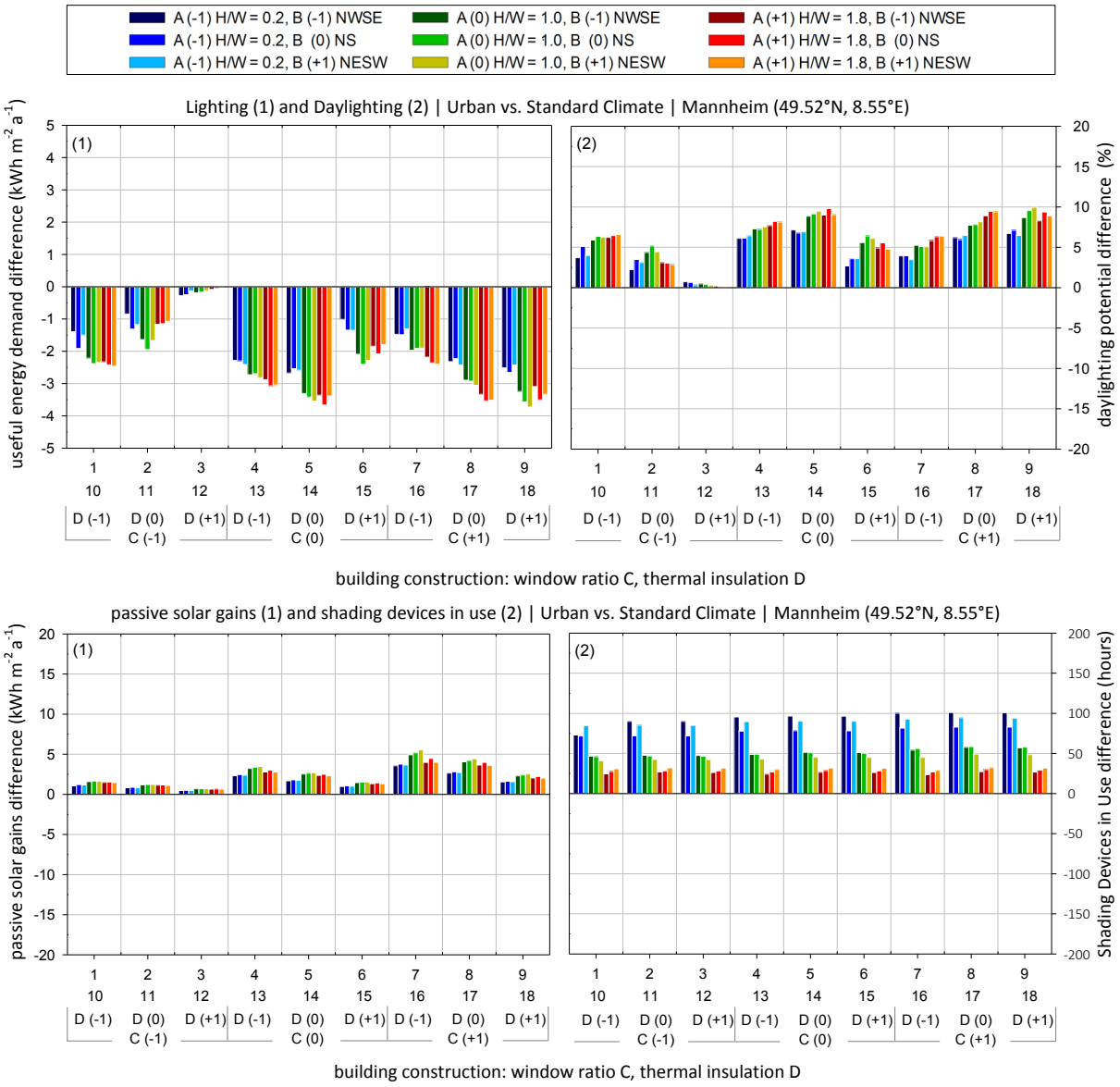

Figure 47: Annual average difference in useful energy demand for lighting $\Delta Q_{light(u\text{-}s)}$ and daylighting potential between urban and standard climate boundary conditions for Mannheim (49.52°N, 8.55°E)

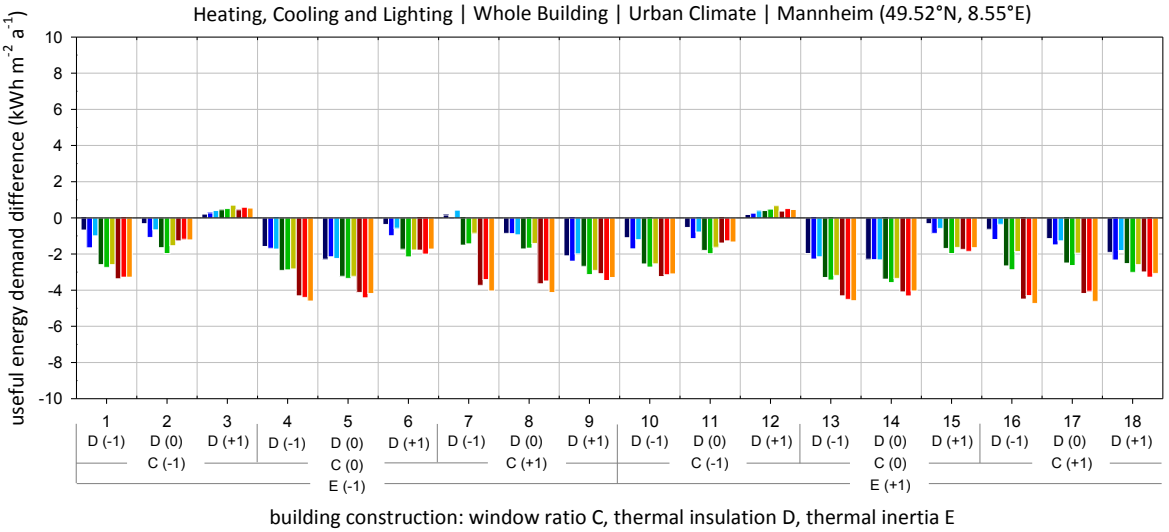

Figure 48: Annual average difference in total useful energy demand ΔQTOT I(u-s) (incl. heating, cooling and lighting) between urban and standard climate boundary conditions for Mannheim (49.52°N, 8.55°E)

3.4. The Energy Demand per Floor Level

This section addresses the effects of the canyon vertical geometry on the energy demand indoors and aims at showing the differences between the different offices of the same building in dependence on their floor, i.e. height position within the canyon. The comparison addresses the ground floor 1 at street level, the floor 3 at canyon mid-height and the upper floor 5. For each floor the average value for the two offices with opposite orientations are calculated. The following graphs show only the variation between floor 5 and floor 1. In order to isolate the role of the vertical profile, the effects of the roof as exterior building component at floor 5 are ignored in this comparison. This is possible by assuming the roof surface in TRNBuild as boundary surface instead of an external surface. In theory, the effects of the canyon geometry on the differences between the floors relate to the exposure of the floor's façade to the solar radiation and to the view factors of sky and canyon surfaces with respect to the diffuse and diffusely reflected solar radiation in-canyon as well as the radiative heat from the facing surfaces (see Appendix 5).

The energy demand for the lighting and heating are lower, whereas the need for cooling and ventilation is higher. The largest differences occur for the lighting, then for the cooling followed by the heating, with the maximum deviation as total reaching -10.3 kWh m^{-2} a^{-1} (Table 35). These effects are the most visible in deep canyons (A =+1) in case of largely glazed façades (C = +1) combined with high solar and light transmissive glazing (induced by D = -1). The differences are minimal in the opposite case (C = -1 and D = +1). This is attributable to the additional solar gains at canyon top floor in comparison to the ground floor, even though partly counteract by the more frequent operation of the shading devices (Figure 49).

Table 35: Minimum and maximum values of the useful energy demand difference between the upper floor 5 and the ground floor 1 for Mannheim (49.52°N, 8.55°E)

useful energy demand difference between the upper floor 5 and the ground floor 1	heating H		cooling C		lighting L		ventilation during usage time V (UT)		ventilation outside usage time V (OU)		total ventilation V (UT + OU)		useful total (TOT I) H +C +L		useful total (TOT II) H +C +L+V	
	min.	max.	min.	max.	min.	max.	min.	max.	min.	max.	min.	max.	min.	max.	min.	max.
energy demand Q (kWh m^{-2} a^{-1})	-6.27	0.13	-0.80	7.57	-9.25	-0.10	-0.03	0.45	-0.08	0.62	-0.08	0.93	-10.28	0.22	-10.04	0.70
(max - min) range Q (kWh m^{-2} a^{-1})	6.39		8.37		9.15		0.48		0.70		1.00		10.50		10.74	

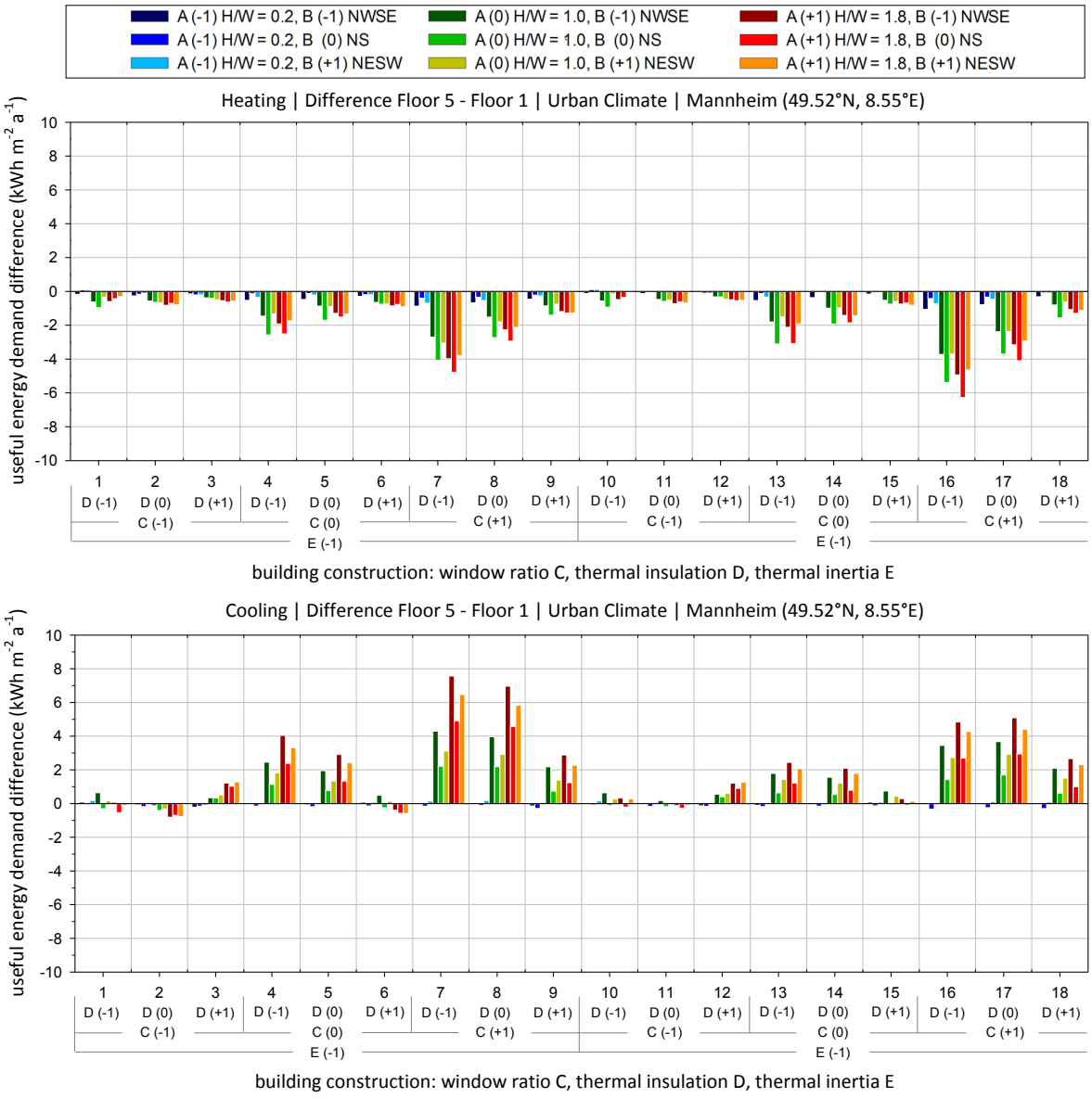

Figure 49: Annual useful heating and cooling energy demand difference between floor 5 and 1 ($\Delta Q_{heat(F5\text{-}F1)}$, $\Delta Q_{cool(F5\text{-}F1)}$) under urban climate boundary conditions for Mannheim (49.52°N, 8.55°E)

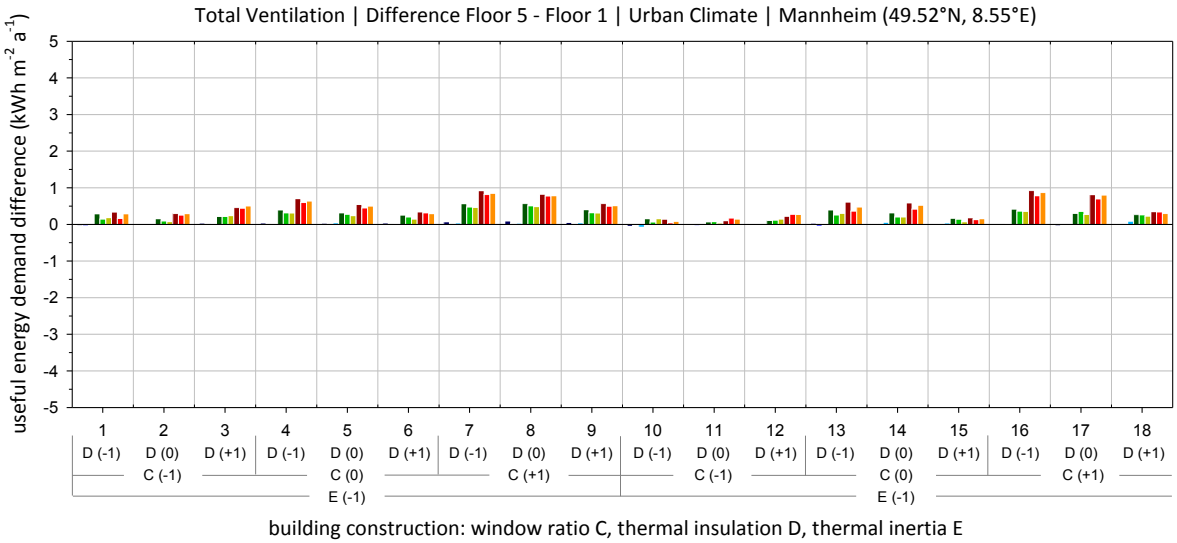

Figure 50: Annual useful ventilation energy demand difference between floor 5 and 1 $\Delta Q_{vent(F5\text{-}F1)}$) under urban climate boundary conditions for Mannheim (49.52°N, 8.55°E)

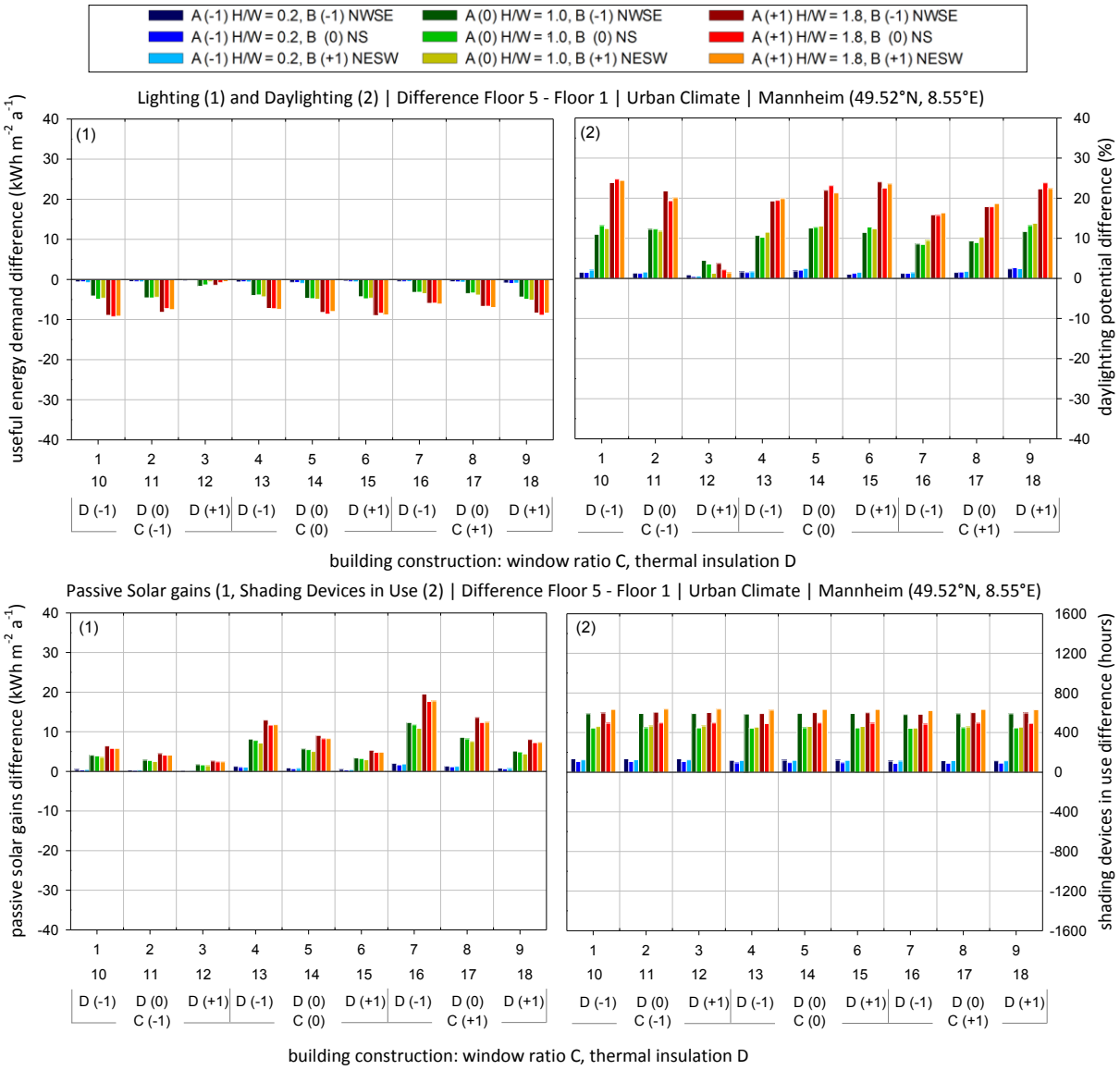

Figure 51: Annual useful lighting energy demand difference between floor 5 and 1 $\Delta Q_{light(F5\text{-}F1)}$ as well as the differences in the daylighting potential, passive solar gains and shading devices use under urban climate boundary conditions for Mannheim (49.52°N, 8.55°E)

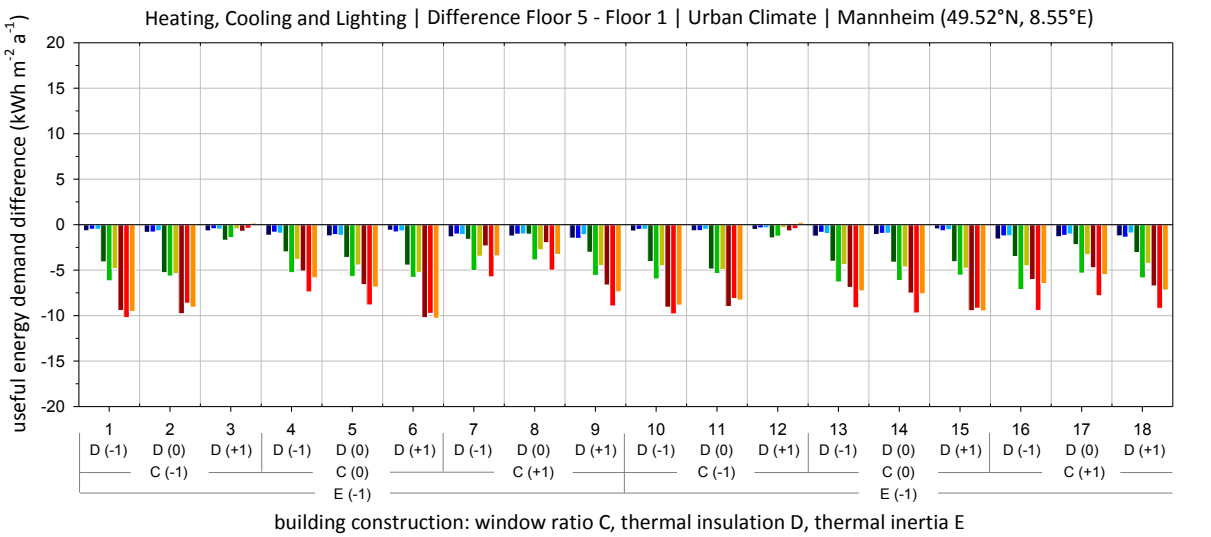

Figure 52: Annual total useful energy demand difference including heating, cooling and lighting between floor 5 and 1 $\Delta Q_{TOT\ l(F5\text{-}F1)}$ under urban climate boundary conditions for Mannheim (49.52°N, 8.55°E)

3.5. Effects of the Building Use and Operation Scenarios

In this section and on the basis of the office buildings investigated so far, further scenarios of use and operation, expected to be decisive, are varied in order to figure out, how these boundary conditions may modify the results for heating and cooling energy demands further (see Ali-Toudert 2013). As listed in Table 15, the variables of [SET V] include the efficiency of the shading devices (S), additional ventilation rates during UT and OU as a mean for reducing overheating and hence cooling (V and N), as well as the internal heat gains due to artificial lighting (I).

Table 37 shows synoptically the range of the energy demands for all 1458 runs and all key metrics, whereas Figure 53 differentiates the results according to the 27 possible combinations of the variables (S, V, N, I). In Figure 53, one can see a qualitative picture on the combinations, which lead to the largest or smallest spread of the results. For a precise quantitative evaluation of these results, see Appendix 10, which gives a ranking list in Table 65 of minimum and maximum heating and cooling for all 54 cases of urban and building variables (A, B, C, D, E) in dependence on the further variables (S, V, N, I). Hence, it shows the cases, which are the most affected by these additional variables.

Table 66 in Appendix 10 gives the full statistics, which are summarized hereafter in Table 36.

For the heating, Table 36 shows that, in addition to the thermal insulation D and the window ratio C and their interactions CD, the ventilation during usage time V and the internal heat gain due to lighting I play an important role in the result. For the cooling, in addition to the thermal inertia, thermal insulation and window ratio (E, D, C), the ventilation during the usage time V, the internal heat due to lighting I and the shading devices S have also important effects. All together the setting (S, V, N, I) have an adjusted R^2 of 57.6% for heating and 49.6% for cooling. These values are higher than the corresponding ones for the urban and building variables (A to E), namely 38.8% for heating and 15.7% for cooling. This calls for attention in the scenarios assumed for such simulations. In this work, a special attention was dedicated to the proper choice of these variables, inter alia with reference to guidelines and standards and after a large number of preliminary sensitivity tests.

Table 36: Summary of the statistical analysis about the effects of the building use and operation variable son the heating and cooling energy demand for [SET V], Mannheim (49.52°N, 8.55°E)

key metric	Coeficient of determination (adj. R^2)			decisive variables	adj. R^2
	(1) ABCDE	(2) SVNI	interactions (1) and (2)		
heating	0.388	0.576	0.016	D, V, I, C, CD, VI	0.952
cooling	0.157	0.496	0.182	I, V, E, N, DI, VI, CI, S	0.601

Table 37: Energy demand minima and maxima for heating and cooling for the simulation ensemble [SET V], Mannheim (49.52°N, 8.55°E)

useful energy demand	heating H		cooling C		lighting L		ventilation during usage time V (UT)		ventilation outside usage time V (OU)		total ventilation V (UT + OU)		useful total (TOT I) H +C +L		useful total (TOT II) H +C +L+V	
	min.	max.	min.	max.	min.	max.	min.	max.	min.	max.	min.	max.	min.	max.	min.	max.
energy demand Q (kWh m^{-2} a^{-1})	0.0	117.6	0.1	108.1	1.6	141.6	4.8	24.6	0.0	19.4	4.8	32.4	20.1	246.1	33.2	256.6
(max - min) range Q (kWh m^{-2} a^{-1})	117.6		108.0		140.0		19.8		19.4		27.5		226.0		226.0	
percentage of useful total (TOT I) H +C +L (%)	0.0	96.2	0.4	73.6	1.3	91.3	2.0	28.9	0.00	43.8	2.0	65.7	Mannheim (49.52°N, 8.55°E) urban climate conditions building use and operation			
percentage of useful total (TOT II) H +C +L+V (%)	0.0	83.5	0.3	69.0	1.1	76.6	1.9	21.5	0.00	26.5	1.9	39.6				

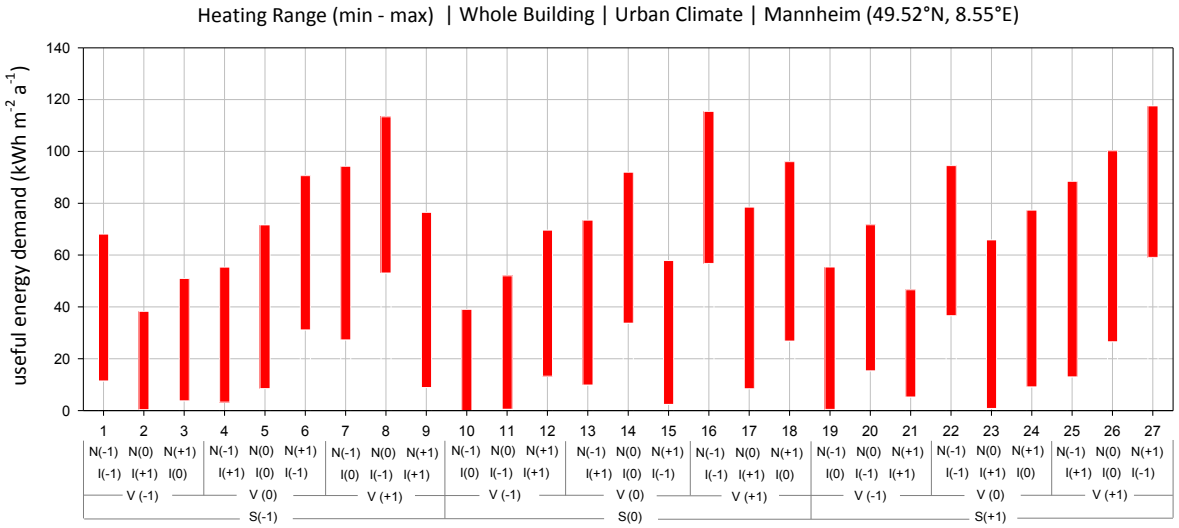

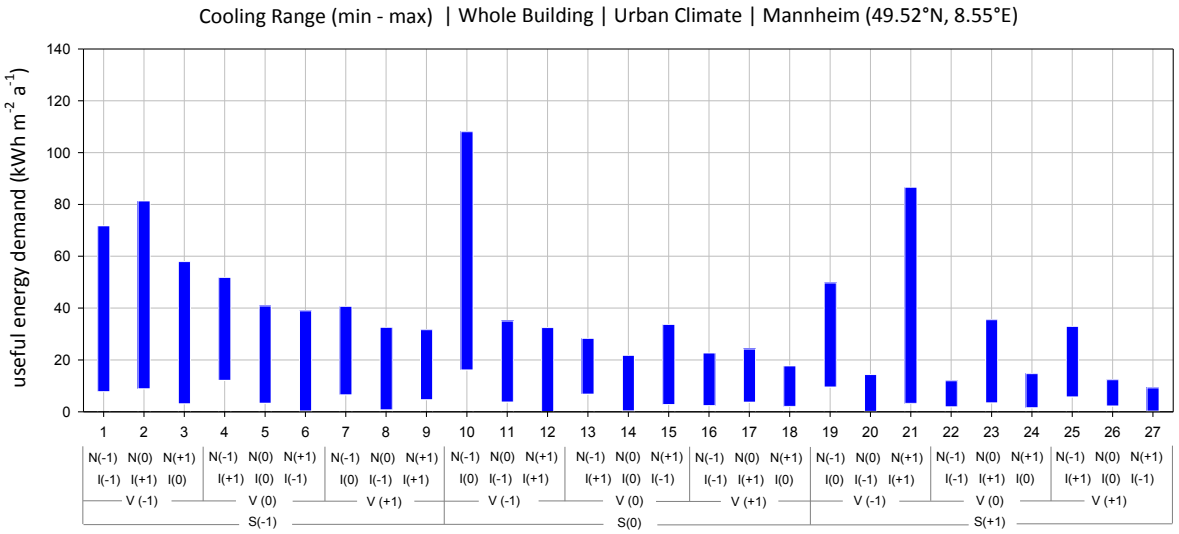

Figure 53: heating and cooling Energy demand in dependence with HVAC settings (PART II)

4. THE BUILDING ENERGY DEMAND FOR THE MEDITERRANEAN

This section aims at extending the discussion carried out so far by showing further results for a different climate type: The Mediterranean climate. The comparison is then between a temperate mid-latitude climate with cold winters (Mannheim, 49.52°N, 8.55°E) and a warm climate with typically hot summers (Algiers, 36.75°N, 3.00°E). The comparison is kept short and is focussed on the similarities and differences between the two locations regarding the urban microclimate changes as well as the resulting building energy demands. The background climate of both locations is available in section II - 1.6 (p 90).

4.1. The Urban Microclimate

Figure 54 und Figure 55 show the maximum and average deviations of air temperature within the canyon for [SET II]. The patterns of warming or cooling of the canyon air are very similar between Algiers and Mannheim (cf. Figure 29 and Figure 30). The similarities include the same contrasts in the thermal situation between lightweight and massive construction, the existence of daytime and nighttime periods with specific warming or cooling rates, the increase of warming air as the canyons become deeper and the fact that the building construction properties are more visible in deeper canyons (see error bars). About the differences, the maximum heat island is slightly more pronounced in Mannheim but the average deviation of canyon air temperature is larger in Algiers, either as increase or decrease. For example, the cool island around noon and the day-night amplitude are more pronounced in the warm climate, certainly because of higher impact of shading since the solar radiation is more intense. However, because of the different background climate sources, i.e. TRY versus Meteonorm, it is difficult to know with certitude whether some differences are due to the climate type or to the quality of the basis data. More investigation is necessary in this respect. In this work, this information is given for the sake of completeness in order to understand the following energy demand results.

4.2. The Useful Energy Demand in Buildings

Figure 56 to Figure 61 and Table 38 show the annual useful energy demand for heating, cooling, ventilation, lighting (incl. daylighting) and their sum for Algiers. These graphs correspond to Figure 39 to Figure 44 and Table 28 for Mannheim.

The comparison of Figure 56 with Figure 39 and Table 38 with Table 28 shows, as expected, that the energy demands for heating and cooling are roughly reversed between Mannheim and Algiers, yet, with the amounts being somewhat lower for Algiers. Indeed, the warm climate of

Algiers is more concerned with cooling to avoid overheating, whereas the temperate climate of Mannheim requires more heating to cope with the colder winter. The minimal need for lighting energy is smaller in Algiers due to more potential for daylighting given the higher amounts of solar radiation. The ventilation, if mechanical, is slightly higher in Algiers due to more overheating risk compensated by additional air renewal.

The overviews in Figure 57 and Figure 40 show different amounts of total energy demands between the two locations and hence different worst and best cases in dependence on the building construction variables, mostly due to contrasting shares of heating and cooling energy demands. However, the comparison of the ranking of the 162 cases in

Table 72 (Appendix 13) for Algiers with Table 63 (Appendix 8) for Mannheim show similar best and worst combinations when considering the target key metrics individually. Evidence of similar trends is indeed observable between Figure 58 to Figure 61 compared with Figure 41 to Figure 44, respectively, even though the absolute values show clear differences. A weak thermal insulation (D = -1) leads to the highest heating values in Algiers even though small in all cases and if combined with large windows, the heating energy demand increases further. The effects of the thermal inertia E is less visible for the heating than the cooling, as observed for Mannheim as well. The ventilation shows the most uniformity among the building types and is similar to Mannheim as well. The differences between the two locations are evident regarding the share between lighting and daylighting, between the passive solar gains and the use of the shading devices. This is not surprising owing the different sun paths and more decisively the more solar radiation received by the surfaces in the subtropics. The following statistical analysis better quantifies the differences and is commented in the next section.

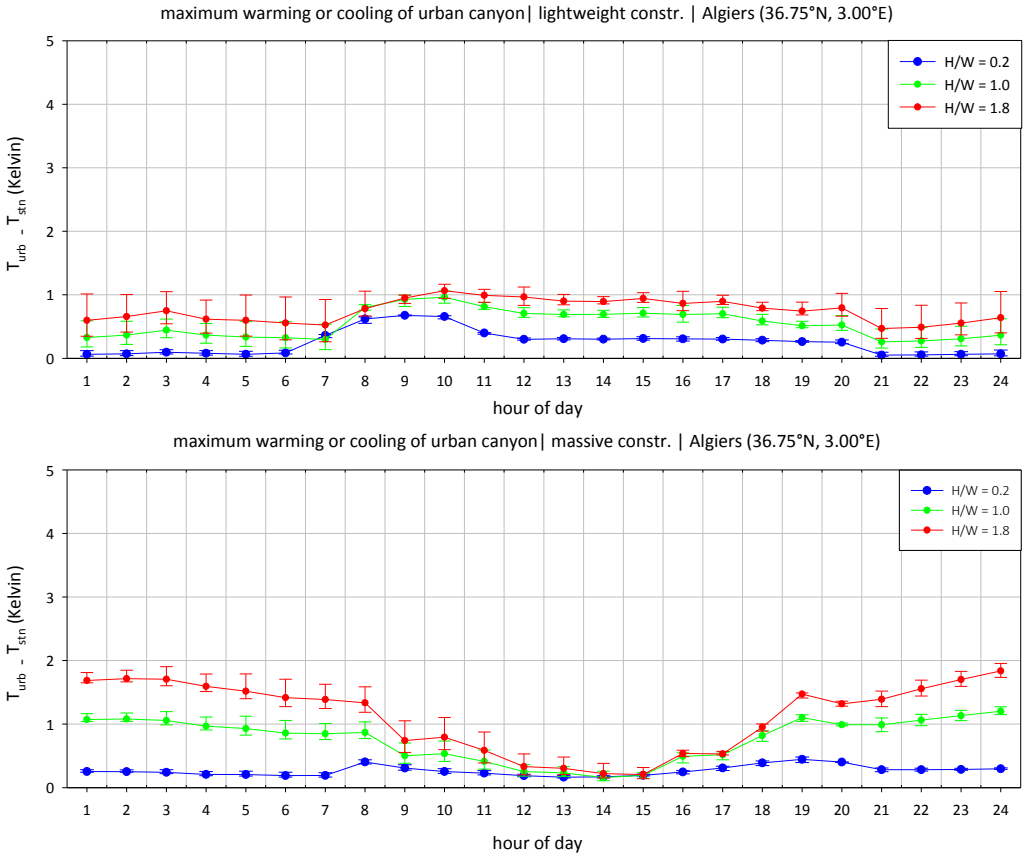

Figure 54: Hourly maximum deviation of urban air temperature from input standard climate differentiated according to the aspect ratio A and thermal mass E for a typical year for Algiers (36.75°N, 3.00°E)

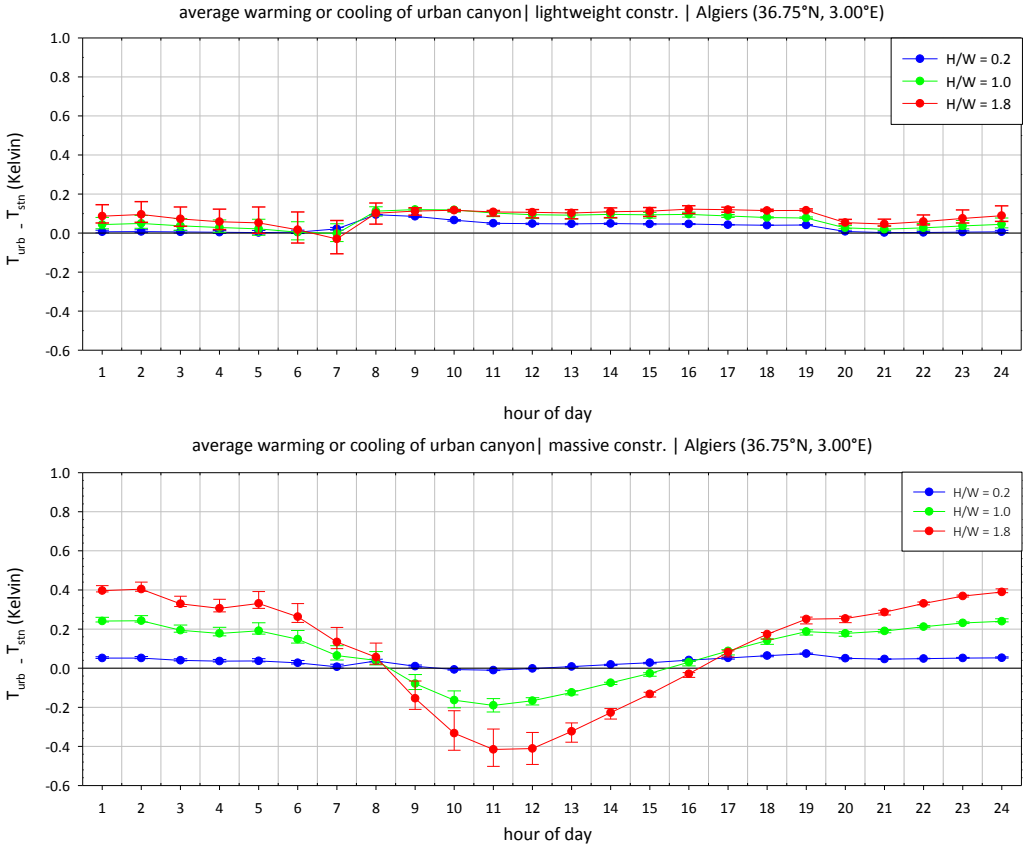

Figure 55: Hourly average deviation of urban air temperature from input standard climate differentiated according to the aspect ratio A and thermal mass E for a typical year for Algiers (36.75°N, 3.00°E)

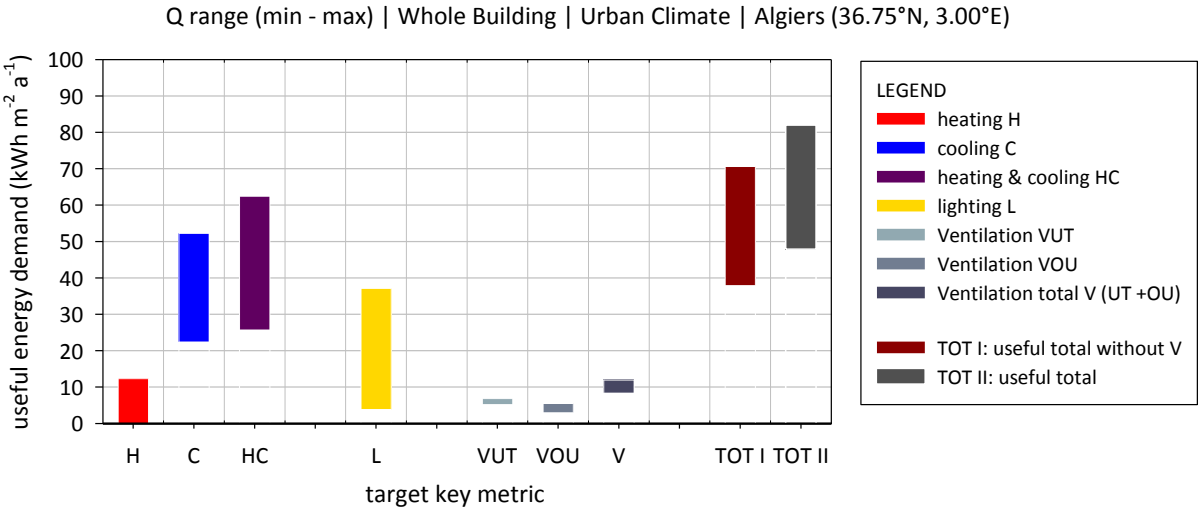

Figure 56: Range of useful energy demand for heating, cooling, lighting and ventilation for urban office buildings located in Algiers (36.75°N, 3.00°E)

Table 38: Minimum and maximum values of useful energy demand (a) as absolute values and (b) as percentages to useful total energy demands for Algiers (36.75°N, 3.00°E)

Algiers (36.75°N, 3.00°E)	heating H		cooling C		lighting L		ventilation during usage time V (UT)		ventilation outside usage time V (OU)		total ventilation V (UT + OU)		useful total (1) H +C +L		useful total (2) H +C +L+V	
	min.	max.	min.	max.	min.	max.	min.	max.	min.	max.	min.	max.	min.	max.	min.	max.
energy demand Q (kWh m^{-2} a^{-1})	0.05	12.34	22.42	52.26	3.89	37.16	5.22	6.89	2.98	5.54	8.36	11.96	37.91	70.62	47.89	81.98
(max - min) range Q (kWh m^{-2} a^{-1})	12.29		29.83		33.27		1.67		2.56		3.59		32.71		34.09	
percentage of useful total (1) H +C +L (%)	0.07	22.26	41.51	88.27	5.88	58.40	0.00	0.00	0.00	0.00	0.00	0.00	urban climate conditions			
percentage of useful total (2) H +C +L+V (%)	0.06	19.25	35.13	72.78	5.14	49.42	7.93	12.03	4.47	9.61	12.40	21.32	average for whole building			

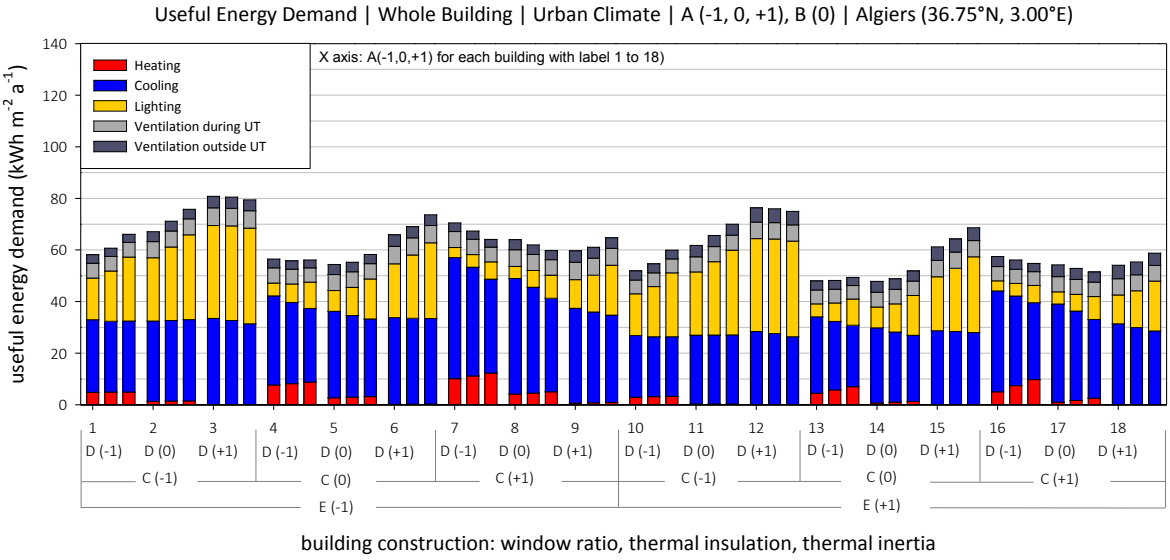

Figure 57: Useful energy demand in for heating, cooling, lighting and ventilation during and outside UT for all 18 building types (C, D, E combinations) and for all A (-1, 0, +1) and B = 0, Algiers (36.75°N, 3.00°E)

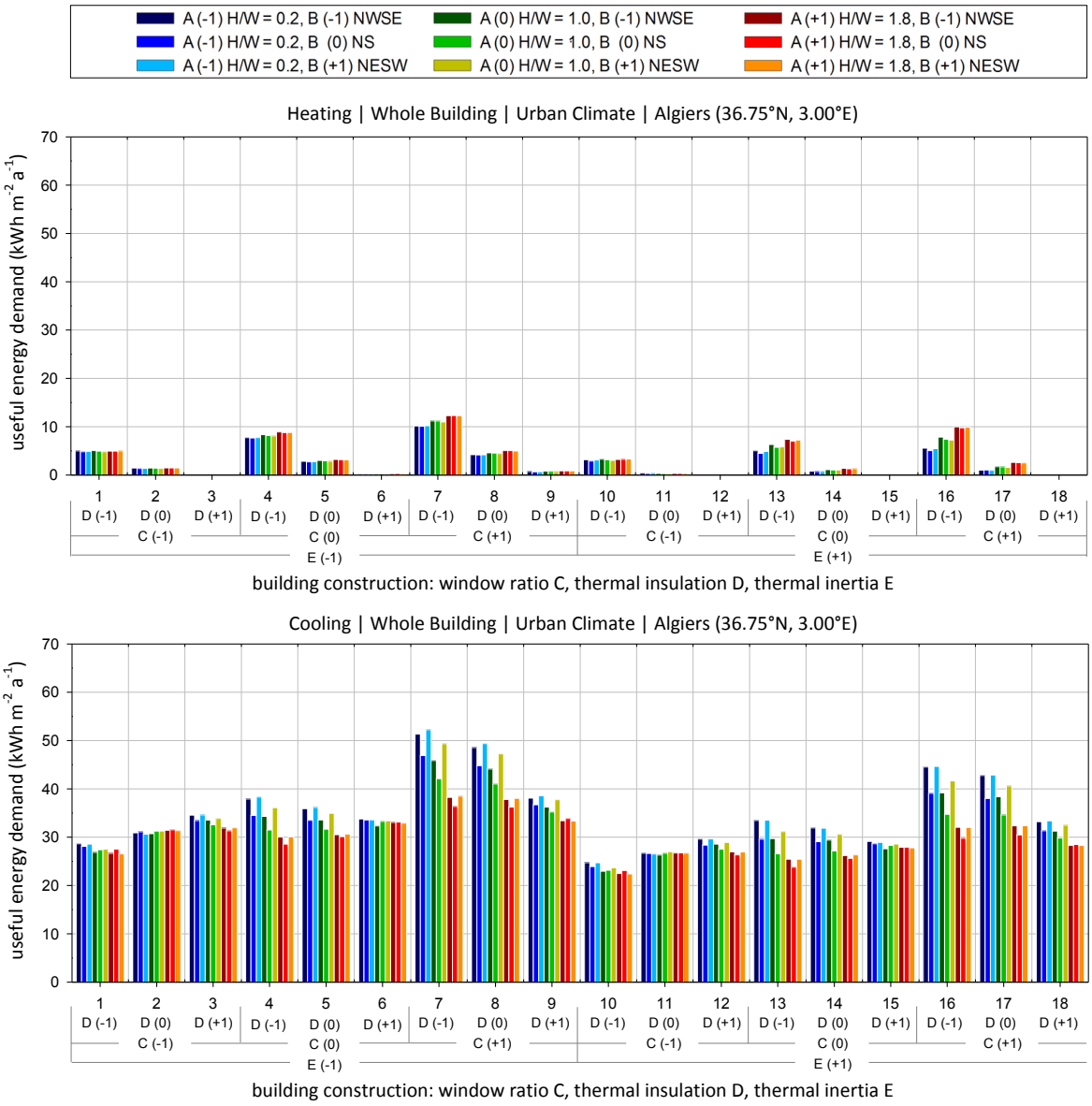

Figure 58: Annual average useful heating and cooling energy demand under urban climate boundary conditions for the Mediterranean Algiers (36.75°N, 3.00°E)

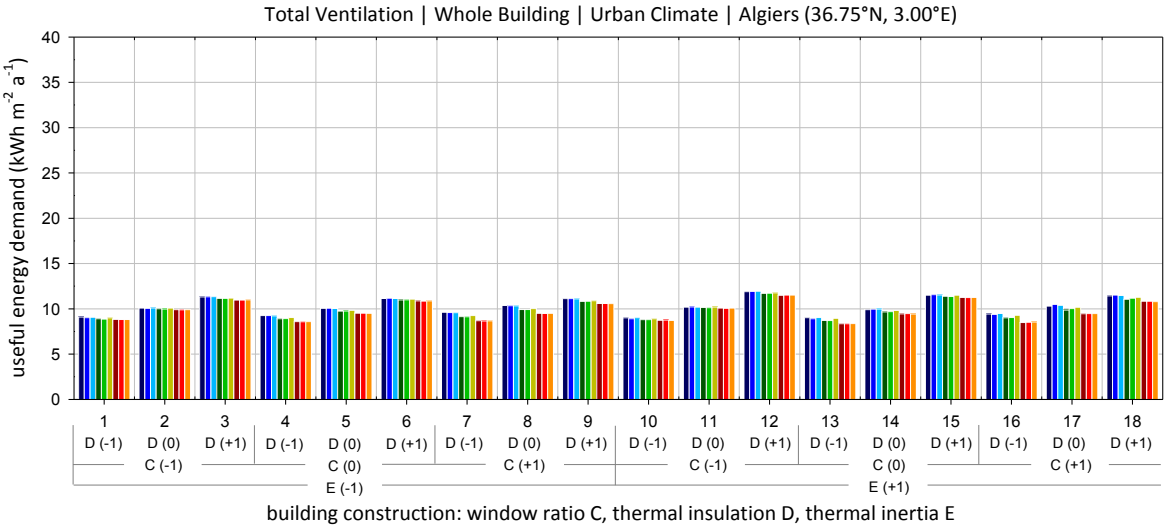

Figure 59: Annual average useful ventilation energy demand under urban climate boundary conditions for the Mediterranean Algiers (36.75°N, 3.00°E)

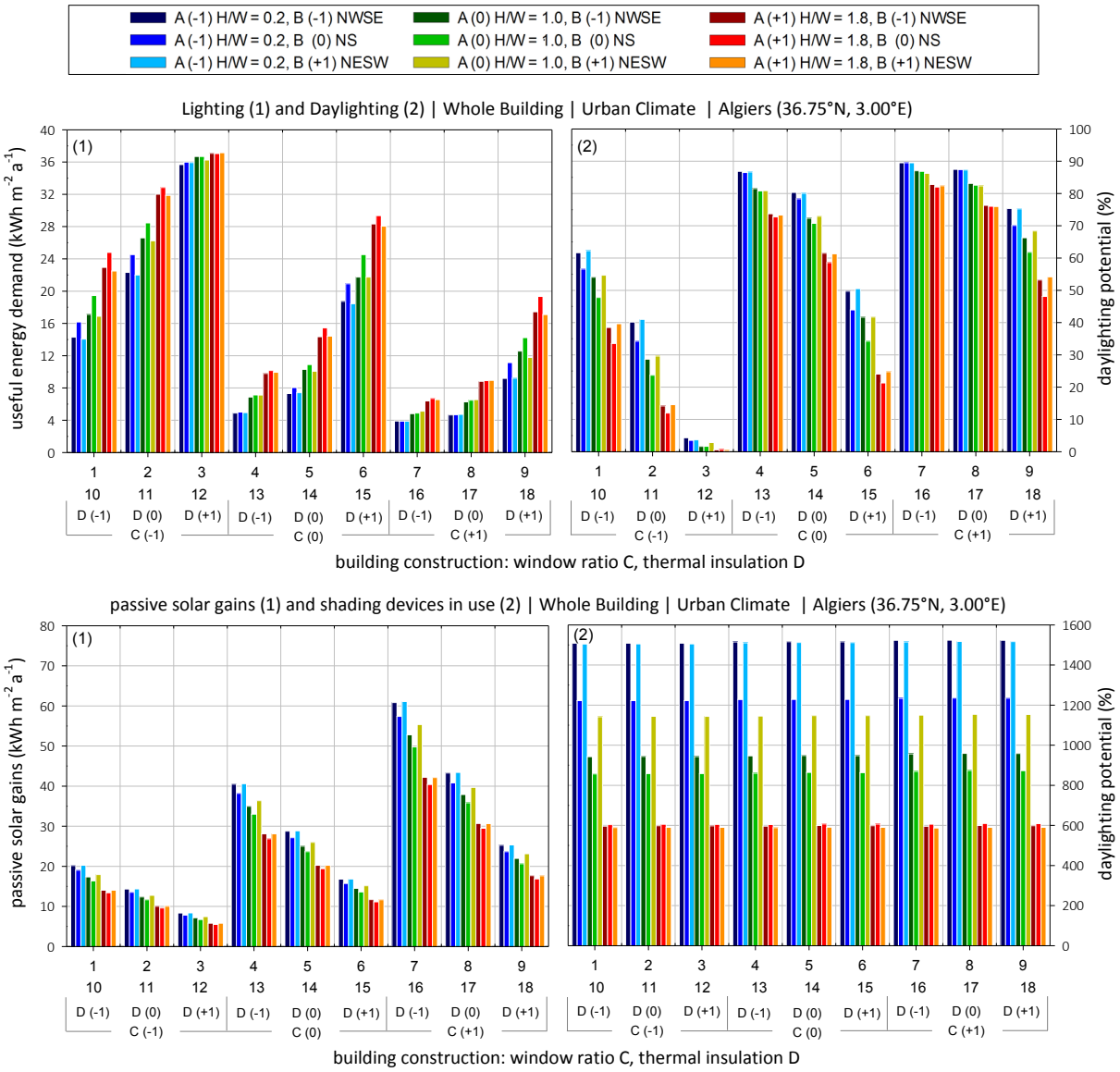

Figure 60: Annual average useful lighting energy demand as well as passive solar gains and shading devices operation under urban climate boundary conditions for the Mediterranean Algiers (36.75°N, 3.00°E)

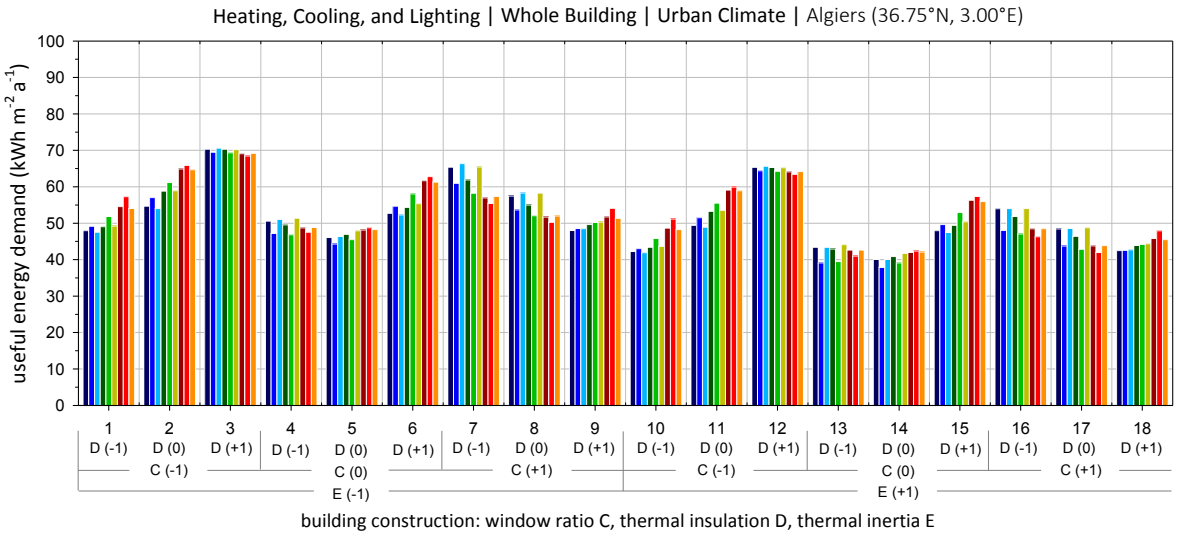

Figure 61: Annual average total useful energy demand under urban climate boundary conditions for the Mediterranean Algiers (36.75°N, 3.00°E)

4.3. The DOE Statistical Analysis of the Useful Energy Demands

For the heating, Table 39 shows the same ranking of the most influencing variables as in Mannheim, namely the thermal insulation D and window ratio C, including D^2 and the CD interaction. However, these variables with an adj. R^2 of 87.7 (83.1 + 4.6%) are less dominating in Algiers than in Mannheim with 99.7%. In Algiers, the thermal inertia E is then more influencing with a part of responsibility of 5.8% and to a smaller extent the aspect ratio A up to 2.3% including its further interactions (AD, AC, AE).

The most influencing variables (C, E, CD and A) for the cooling in Algiers are similar to Mannheim but not in the same ranking order. The window ratio is more important in Algiers (adj. R^2 of 42.4% and 12.25 as CD interaction) because of more solar radiation and hence more solar gains in spite of the more frequent operation of the shading devices. For the same reason, the aspect ratio A is more decisive in Algiers (10.3% as main effect of A and A^2; 5.4% as interactions of AC and AD) as it affects the façades exposure and solar access indoors. Internal heat gains originating from the lighting are lower in Algiers than in Mannheim because of more daylighting potential for the same reason. Once, the rooms experience surplus of heat, the thermal inertia E with 17,4% is the second variable of importance because eit helps damp the overheating risk.

As far as the lighting is concerned, the decisive variables C and D are almost the same with comparable level of influence. The window ratio C has a slightly higher importance with a non-linear effect as already noticed for the cooling. The aspect ratio is the third variable of importance with comparable influence.

The most decisive variable regarding the ventilation is the thermal insulation D in the two climates with a part of influence of 89.4% for Algiers and 82.8% for Mannheim. The aspect ratio A is equally important but the thermal inertia E as a passive thermal regulating measure appears less effective in Algiers, as already observed for the cooling, where the overheating levels and hence the need for air conditioning are higher.

Considering the total useful energy for heating, cooling and lighting together, the thermal insulation D and window ratio C are clearly the most important variables in both locations. This is visible in their main effects including quadratic terms (C^2, D^2) as well as their interaction CD. However, the window ratio C appears more influencing in the Mediterranean Algiers, whereas the thermal insulation D is more critical in the temperate Mannheim. The aspect ratio A and the thermal inertia E are more decisive in Algiers because of their particular influence on the summer conditions prevailing there.

Table 39: Statistics of the useful heating energy demand Q_{heat} for [SET IV], Algiers (36.75°N, 3.00°E)

Q_{heat} | whole building | urban climate | Algiers (36.75°N, 3.00°E)

Model Summary					Full Model: Predictors and Coef.			
Model	R	R Square	Adjusted R Square	R Square Change	Model 11	predictor	B	Sig.
1	.816a	0.665	0.663	0.665		const.	2.032	.000
2	.879b	0.772	0.769	0.107		D	-3.325	.000
3	.913c	0.834	0.831	0.062		C	1.333	.000
4	.944d	0.892	0.889	0.058		CD	-1.240	.000
5	.968e	0.937	0.935	0.046		E	-.799	.000
6	.978f	0.957	0.955	0.019		D^2	1.512	.000
7	.983g	0.966	0.964	0.009		DE	.564	.000
8	.987h	0.974	0.972	0.008		A	.395	.000
9	.990i	0.981	0.980	0.007		CE	-.356	.000
10	.993j	0.986	0.986	0.006		AD	-.425	.000
11	.994k	0.987	0.986	0.001		AC	.372	.000
						AE	.122	.001
k. Predictors: (Constant), D, C, CD, E, D^2, DE, A, CE, AD, AC, AE								

Table 40: Statistics of the useful cooling energy demand Q_{cool} for [SET IV], Algiers (36.75°N, 3.00°E)

Q_{cool} | whole building | urban climate | Algiers (36.75°N, 3.00°E)

Model Summary					Full Model: Predictors and Coef.			
Model	R	R Square	Adjusted R Square	R Square Change	Model 12	predictor	B	Sig.
1	.654a	.428	.424	.428		const.	30.980	.000
2	.776b	.601	.596	.174		C	4.891	.000
3	.851c	.724	.718	.122		E	-2.544	.000
4	.908d	.825	.820	.101		CD	-3.200	.000
5	.931e	.866	.862	.041		A	-2.380	.000
6	.948f	.898	.894	.032		AC	-1.857	.000
7	.956g	.914	.910	.016		C^2	2.311	.000
8	.964h	.929	.925	.015		B^2	1.650	.000
9	.968i	.937	.934	.008		AD	1.117	.000
10	.970j	.942	.938	.004		D^2	-1.189	.000
11	.972k	.945	.940	.003		D	-.492	.001
12	.973l	.946	.942	.002		CE	-.397	.006
						A^2	-.538	.030
j. Predictors: (Constant), C, E, CD, A, AC, C^2, B^2, AD, D^2, D								

Table 41: Statistics of the useful lighting energy demand Q_{light} and daylighting potential for [SET IV], Algiers (36.75°N, 3.00°E)

Q_{light} | whole building | urban climate | Algiers (36.75°N, 3.00°E)

Model Summary					Full Model: Predictors and Coef.			
Model	R	R Square	Adjusted R Square	R Square Change	Model 8	predictor	B	Sig.
1	.740a	.548	.545	.548		const.	12.553	.000
2	.921b	.849	.847	.301		C	-9.545	.000
3	.952c	.906	.904	.057		D	7.075	.000
4	.969d	.939	.937	.033		A	3.079	.000
5	.980e	.961	.960	.022		C^2	4.073	.000
6	.986f	.973	.972	.012		CD	-2.345	.000
7	.988g	.975	.974	.002		D^2	2.449	.000
8	.988h	.976	.975	.001		B^2	-1.028	.000
						A^2	.652	.021
h. Predictors: (Constant), C, D, A, C^2, CD, D^2, B^2, A^2								

daylight potential

Full Model: Predictors and Coef.			
Model	predictor	B	Sig.
8	const.	66.3678	5E-111
	C	25.5735	2E-107
	D	-18.957	1.4E-88
	A	-8.2495	2.5E-42
	C^2	-10.914	9.4E-31
	CD	6.28236	1.9E-23
	D^2	-6.5612	3.3E-15
	B^2	2.75359	0.00032
	A^2	-1.7476	0.02083
For the models see Q_{light}			

Table 42: Statistics of the useful ventilation energy demand Q_{vent} for [SET IV], Algiers (36.75°N, 3.00°E)

Q_{vent} | whole building | urban climate | Algiers (36.75°N, 3.00°E)

Model Summary					Full Model: Predictors and Coef.			
Model	R	R Square	Adjusted R Square	R Square Change	Model 13	predictor	B	Sig.
1	.946a	.895	.894	.895		D	1.143	.000
2	.970b	.940	.939	.045		A	-.257	.000
3	.976c	.953	.953	.013		DE	.140	.000
4	.982d	.965	.964	.011		CD	-.157	.000
5	.987e	.973	.972	.009		AC	-.137	.000
6	.989f	.979	.978	.005		D^2	.153	.000
7	.992g	.984	.983	.005		C^2	.149	.000
8	.993h	.986	.986	.003		E	.052	.000
9	.995i	.989	.988	.003		C	-.062	.000
10	.995j	.990	.989	.001		AD	.045	.000
11	.995k	.991	.990	.001		CE	-.036	.000
12	.996l	.991	.991	.000		B	.023	.012
13	.996m	.991	.991	.000		A^2	-.032	.048
m. Predictors: (Constant), D, A, DE, CD, AC, D^2, C^2, E, C, AD, CE, B, A^2								

Table 43: Statistics of the total useful energy demand Q_{TOT1} (heating, cooling and lighting) for [SET IV], Algiers (36.75°N, 3.00°E)

$Q_{TOT(H+C+L)}$ | whole building | urban climate | Algiers (36.75°N, 3.00°E)

Model Summary					Full Model: Predictors and Coef.			
Model	R	R Square	Adjusted R Square	R Square Change	Model 10	predictor	B	Sig.
1	.615a	.378	.374	.378		const.	47.202	.000
2	.728b	.530	.524	.152		CD	-7.364	.000
3	.819c	.670	.664	.140		E	-3.114	.000
4	.867d	.752	.745	.082		C^2	6.329	.000
5	.912e	.831	.826	.080		C	-2.792	.000
6	.925f	.855	.850	.024		D	2.763	.000
7	.937g	.877	.871	.022		AC	-1.843	.000
8	.945h	.892	.887	.015		D^2	2.509	.000
9	.948i	.898	.892	.006		A	1.203	.000
10	.950j	.902	.895	.004		AD	.917	.003
						CE	-.579	.022
j. Predictors: (Constant), CD, E, C^2, C, D, AC, D^2, A, AD, CE								

4.4. Urban Microclimate Effects on the Useful Energy Demands

This section discusses for Algiers the energy demand differences between the simulation series assuming urban microclimate conditions (urb) presented above and the series using standard climate (stn), expressed as $\Delta Q_{u\text{-}s} = Q_{urb} - Q_{stn}$. Figure 62 to Figure 65 show the annual energy demand deviations for heating, cooling, ventilation, lighting and as sum. The following comparison with Mannheim refers to Figure 45 to Figure 48.

The influence of the urban microclimate on the energy demand in Algiers is similar in many respects to the situation occurring in Mannheim. The heating and lighting energy demand are alike lower and the cooling and ventilation are higher under urban microclimate conditions in Algiers for all combinations of the variables A to E. The magnitudes, however, are different and the energy savings in Algiers, being in line with the absolute values, are smaller for the heating and larger for the cooling (cf. Table 44 and Table 34). The ventilation deviation shows no visible difference neither with respect to the variable nor in magnitudes. The saving in the lighting energy demand under urban conditions is higher for Algiers than Mannheim due to the higher amounts of passive solar gains in the former case, which increase when in-canyon reflections are included even though the shading devices are oftener in operation.

As total energy demand, the difference between urban and standard conditions shows contrasting situations, which are more stressed for Algiers than Mannheim, depending on the combinations of variables involved. This is due to the different share of heating, cooling and lighting in the totals. In Algiers, the cases responsible of most cooling deviations are the ones with a highest increase as total. For the sake of completeness, the statistics are given in Table 74 to Table 78 in Appendix 15.

Table 44. Maximum, minimum and range of energy demand deviation between urban climate and standard climate boundary conditions for Algiers (36.75°N, 3.00°E)

Algiers (36.75°N, 3.00°E)	heating H		cooling C		lighting L		ventilation during usage time V (UT)		ventilation outside usage time V (OU)		total ventilation V (UT + OU)		useful total (1) H +C +L		useful total (2) H +C +L+V	
	min.	max.	min.	max.	min.	max.	min.	max.	min.	max.	min.	max.	min.	max.	min.	max.
energy demand Q (kWh m^{-2} a^{-1})	-2.11	0.00	-0.11	10.28	-6.31	-0.03	0.56	0.75	0.02	0.35	0.61	0.35	-5.88	7.06	-5.05	8.06
(max - min) range Q (kWh m^{-2} a^{-1})	2.11		10.39		6.28		0.19		0.33		-0.25		12.94		13.11	

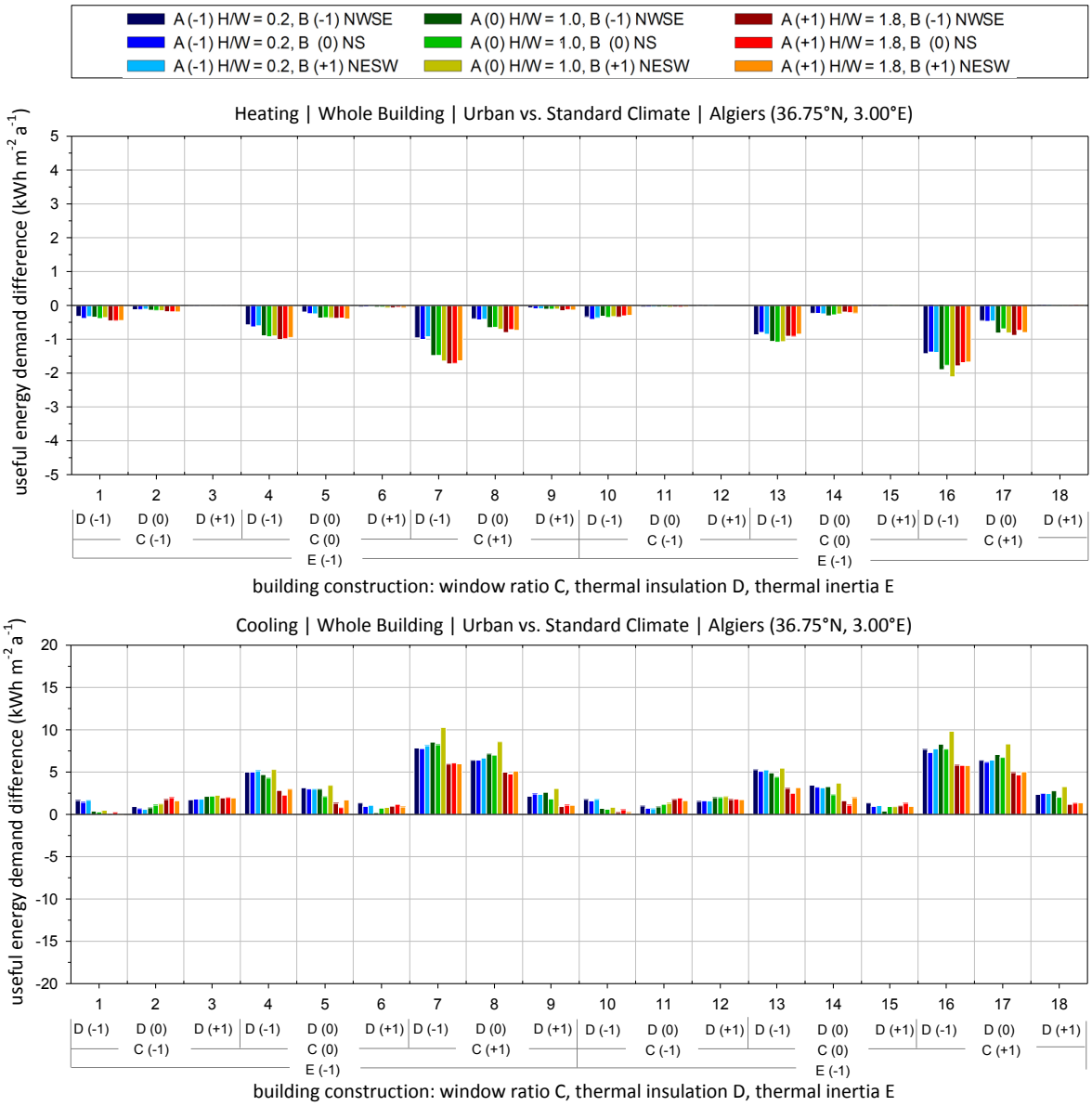

Figure 62: Annual average difference in the useful energy demand for heating and cooling between urban and standard climate boundary conditions for Algiers (36.75°N, 3.00°E)

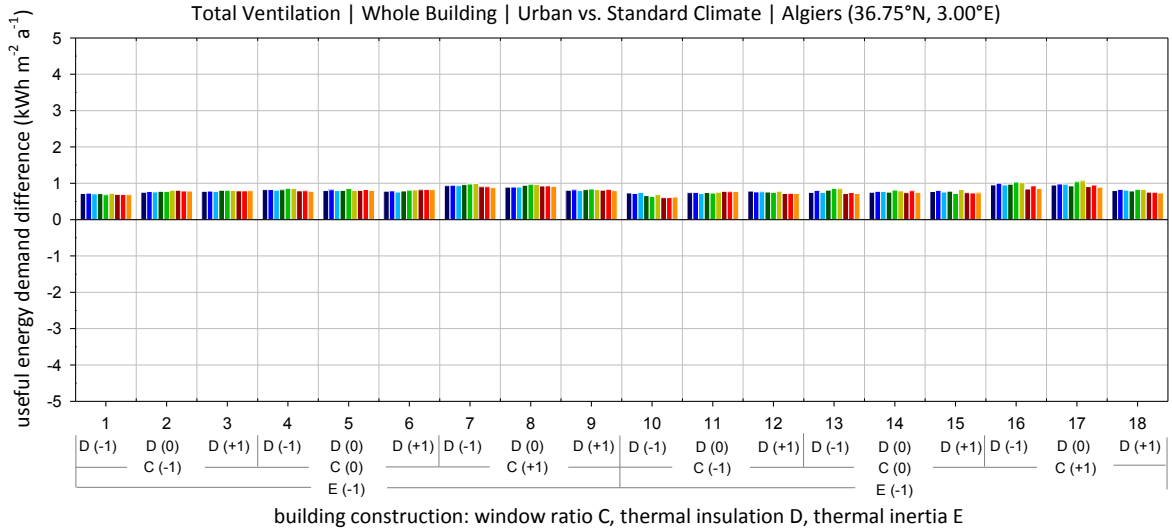

Figure 63: Annual average difference in the useful ventilation energy demand between urban and standard climate boundary conditions for Algiers (36.75°N, 3.00°E)

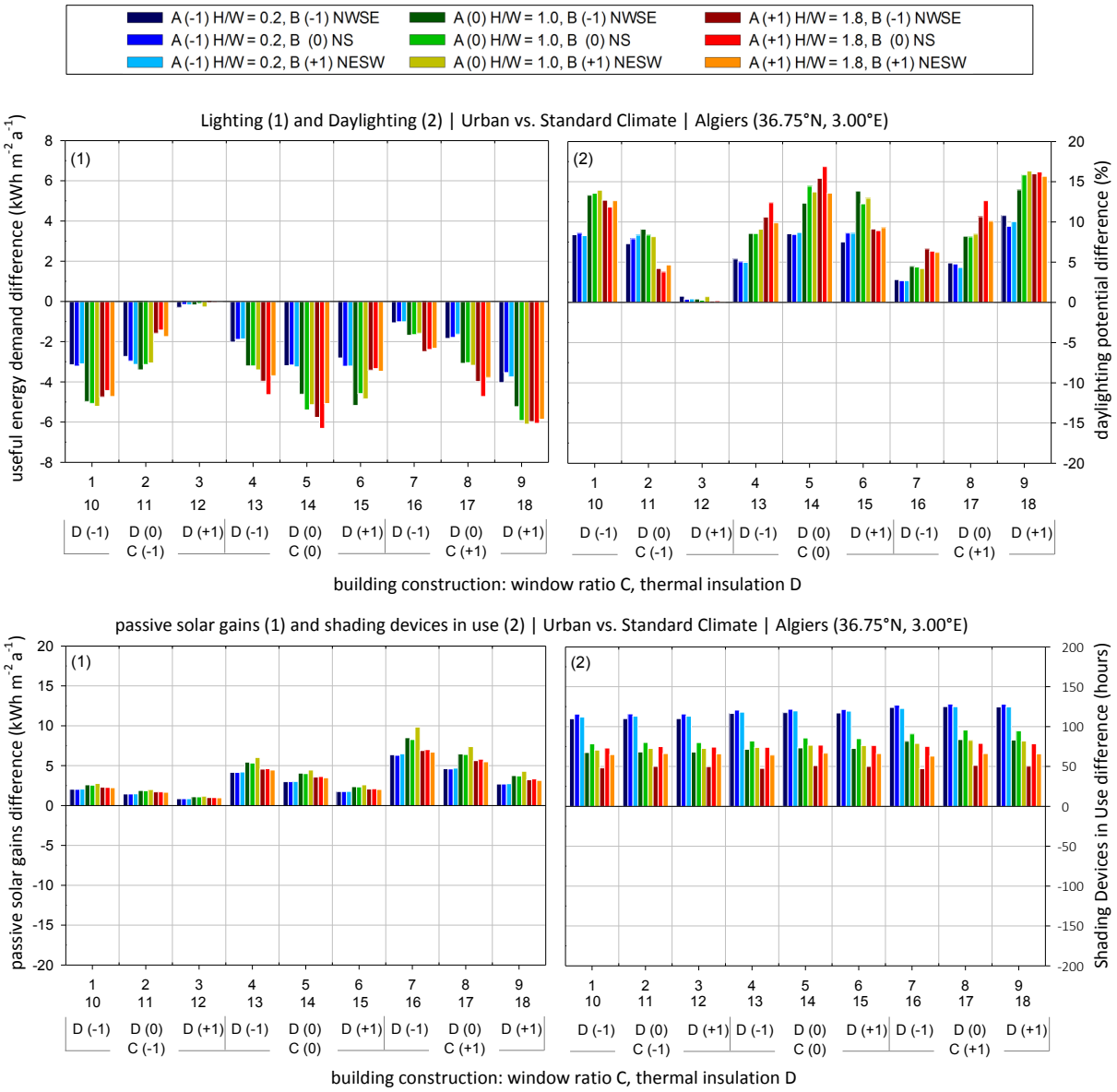

Figure 64: Annual average difference in the useful energy demand for lighting, passive solar gains and shading devices operation between urban and standard climate boundary conditions for Algiers (36.75°N, 3.00°E)

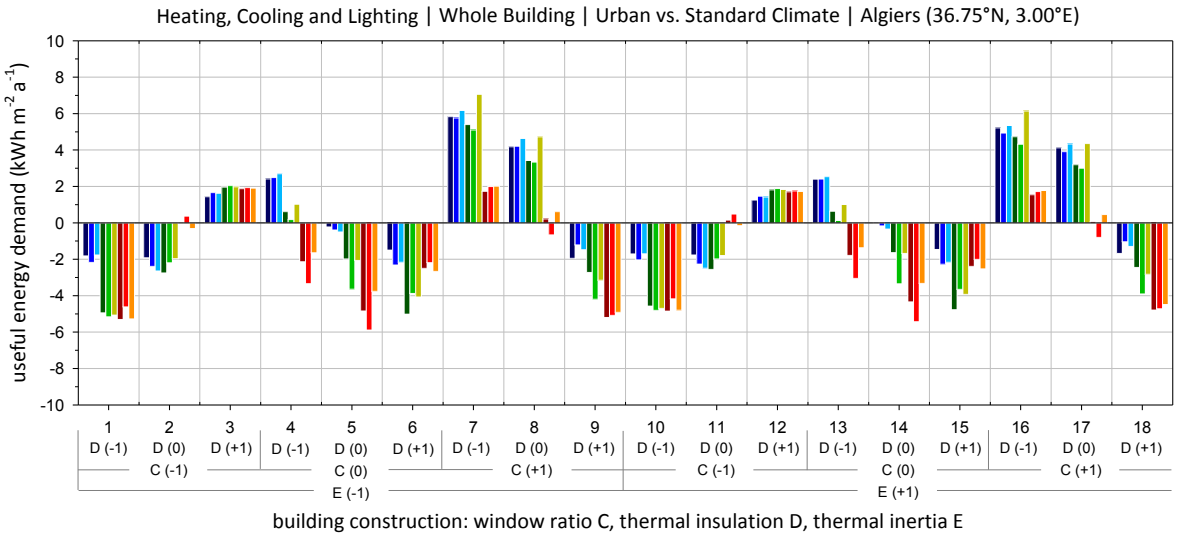

Figure 65: Annual average difference in the total useful energy demand between urban and standard climate boundary conditions for Algiers (36.75°N, 3.00°E)

5. COUPLING URBAN AND BUILDING ENERGY MODELLING

One of the main findings of PART I reported so far was to demonstrate the significant interdependence between the urban microclimate and the energy demand of urban buildings. In other words, rural climate data need to be adjusted to urban conditions prior to building energy modelling. The urban climate work reported in this research (PART I and II) was executed using the TEB model newly implemented as TRNSYS component, named Type 201 (Ali-Toudert and Böttcher 2011a, 2015, 2017). This chapter explains this new implementation and describes the technical content of Type 201.

5.1. Implementation of TEB Model in TRNSYS

5.1.1. Relevance of Embedding TEB in TRNSYS

The Town Energy Balance model (TEB) is part of the simulation package SURFEX, i.e. SURFace EXternalisée (Le Moigne 2009) which includes several modules addressing other land covers (vegetation, water). At the beginning of this research and during the first simulation attempts with SURFEX, several difficulties were encountered highlighting the major disadvantage of SURFEX, its user-unfriendly nature. This is understandable owing to the fact that SURFEX is not a commercial product; its development is attributed to various research efforts. Indeed, in spite of its numerical quality, the model (2010) had its weaknesses. Some of the model's weaknesses have been fixed lately, yet these motivated the implementation of TEB in TRNSYS in 2011 and are briefly recalled hereafter.

- Tedious installation process: SURFEX runs under the Linux operating system and needs to be compiled by the user. This requires the installation of several compilers such as C++ and FORTRAN. The compilation process was awkward and time consuming with several errors arising during compilation. To debug these errors, understanding the SURFEX source code was necessary and the SURFEX developers had to be contacted frequently. Thus, installing SURFEX is a hard task for users with little computer skills.
- Unfriendly graphical interface: SURFEX is a console application with no graphical user interface. This is a disadvantage for most end users who are increasingly familiar with graphical user interfaces. This may reduce the acceptance of such simulation programs among building engineers, with the risk to keep the urban climate issue unconsidered.
- *Time-consuming pre-processing and lack of consistency check:* For each SURFEX simulation run, user defined parameters have to be input and adapted in several configuration files according to the desired simulation setup. This makes SURFEX prone to setup

errors. For example, the user could overlook some parameters or input some others more than once without automatic check for consistency. This may happen in most cases because some parameters have to be adapted in a text based configuration file and other parameters have to be adapted in a FORTRAN file, which must be recompiled after every change of the corresponding parameters. Three additional (sub-) programmes have to be executed manually to apply a new simulation setup before the SURFEX simulation itself can be executed. This makes the simulation setup time-consuming and disadvantageous for large sets of investigations such as parameter studies or for geographically extended areas with different inputs.

- *Too large outputs:* SURFEX creates for every prognostic key metric a single output file in .nc or ascii format. Due to the large number of prognostic variables, numerous output files are created for each simulation instead of one output file containing all results. This could confuse the user, especially if a coupled simulation is performed, for which several output files must be prepared to act as input files, e.g. for a building simulation. Moreover, the output files become very large when stored as text (ascii). The outputs are rather foreseen to be stored as .nc files, which are indeed smaller, yet not readable, by commonly used tabular software.
- *Fragmented source code:* The original TEB code was fragmented in a large number of files, which hinder the comprehension of the processes behind the simulation or dependencies between the parameters.

These disadvantages together with the need in this research for a single urban - building modelling model motivated the implementation of the TEB part of the SURFEX package in the TRNSYS environment (Ali-Toudert and Böttcher 2011a).

As previously mentioned (see section I - 3.3, p 58), TEB has several properties which makes it favourable when combined with TRNSYS. These include input and time step compatibility, short simulation time and a detailed thermo-physical description of the urban canyon facets. Moreover, TRNSYS being modular-designed can easily be extended with self-developed modules, the so-called “Type”. TRNSYS provides a Graphical User Interface (TRNSYS Studio) which allows the user to create graphically complex simulation configurations consisting of different single Types connected to each other. Outputs of one Type may serve as inputs for other Types via user-defined connections. No text-based manipulations of configuration files are needed; instead, all required information of a Type and global simulation properties like the simulation time step are configured within the TRNSYS Studio. In addition, TRNSYS possesses a well-documented programming interface.

5.1.2. TEB as Type 201 for use in TRNSYS

Figure 66 shows the interface of a TRNSYS project using the newly implemented TEB called Type 201. The TEB-Type does not require tedious installation or compilation process. Now, a user can build TEB simulations on a graphical interface, write the desired simulation outputs into one (or more) *ascii* output file(s) using a printer (Type 25) along with displaying the simulation outputs in real time for check purposes with an online plotter Type 65 (Figure 67). Type 201 reads the inputs from a data reader named Type 204 (Ali-Toudert and Böttcher 2011b), especially configured for use with Type 201 (Figure 66). The plot in Figure 67 is a snapshot of a running simulation, which shows the input air temperature against the urban canyon air temperature as well as the surface temperatures of the 3 facets road, wall and roof instantaneously during the simulation run. This plot gives the possibility of real time control of outputs self-defined by the user. The new TEB-Type can be configured like every Type in TRNSYS by simple double clicking on the Type and manipulating the values in the corresponding tabs shown in Figure 68. Appendix 16 lists all parameters, inputs and outputs of Type 201, i.e. the tabs in Figure 68. All terms of the energy balance at each surface (street, roof and wall) can be designated as output, so that the physical processes prevailing in the formation of a specific urban microclimate can be analysed.

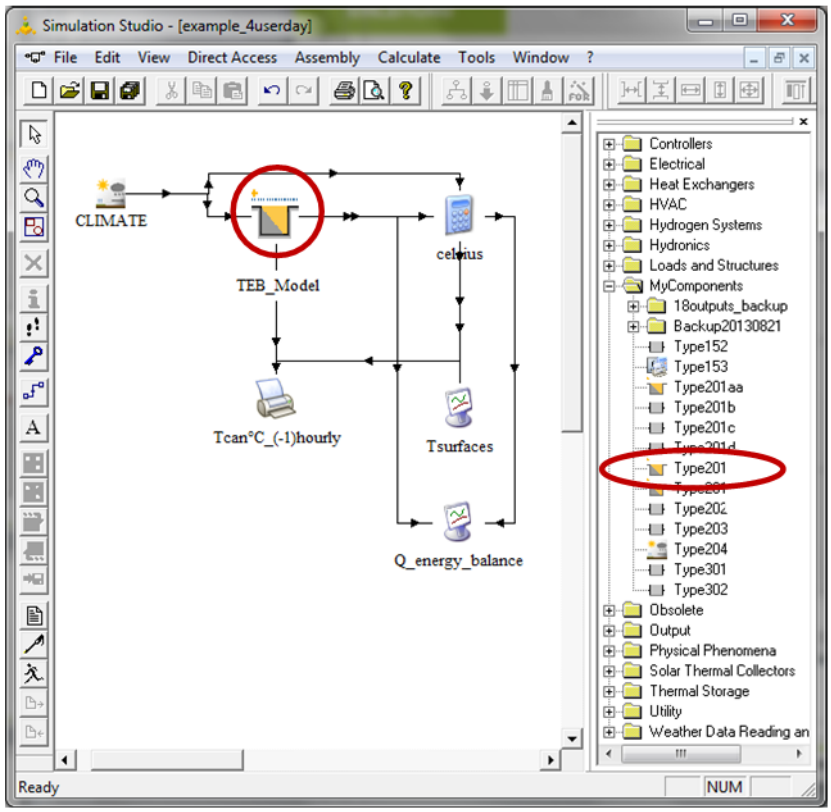

Figure 66: The TRNSYS-Studio interface showing TEB as new TRNSYS-Type 201

These outputs include the total received and absorbed direct and diffuse shortwave radiation, longwave radiation, total net radiation, the sensible and latent heat fluxes, the conductive heat, heat storage, the anthropogenic heat fluxes, as well as the single surface temperatures, canyon air temperature, humidity and wind speed. All terms of the energy balance can be designated as output for each surface separately (street, roof and wall) so that the physical processes prevailing in the formation of a specific urban microclimate can be analysed.

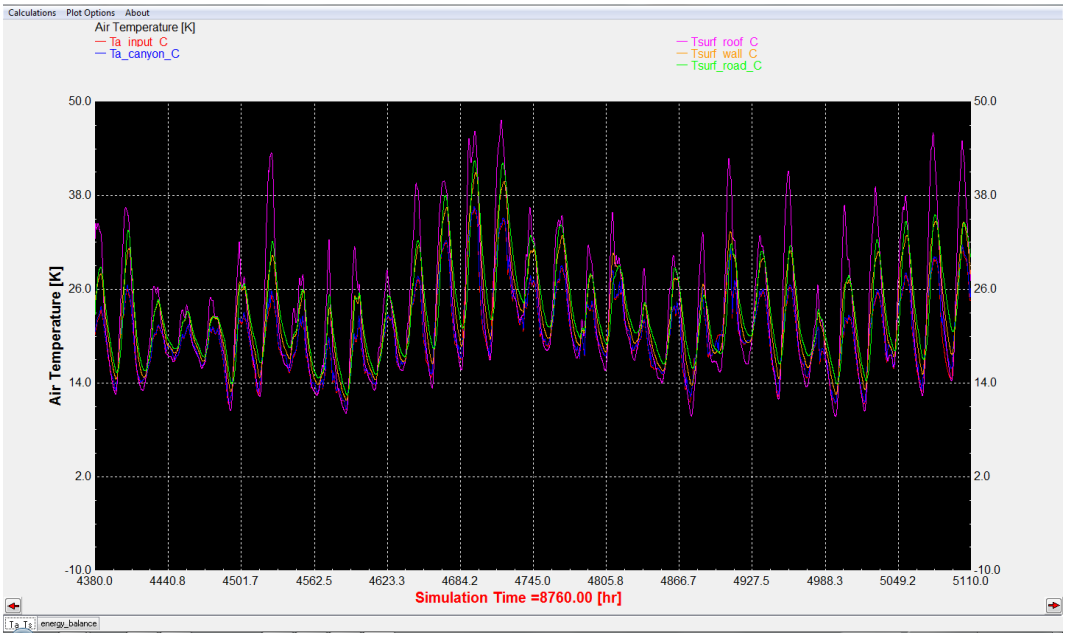

Figure 67: Output example of the new implemented TEB-Type. These outputs can be summed up for the canyon (wall + road) and for the "town" (road + walls + roof)

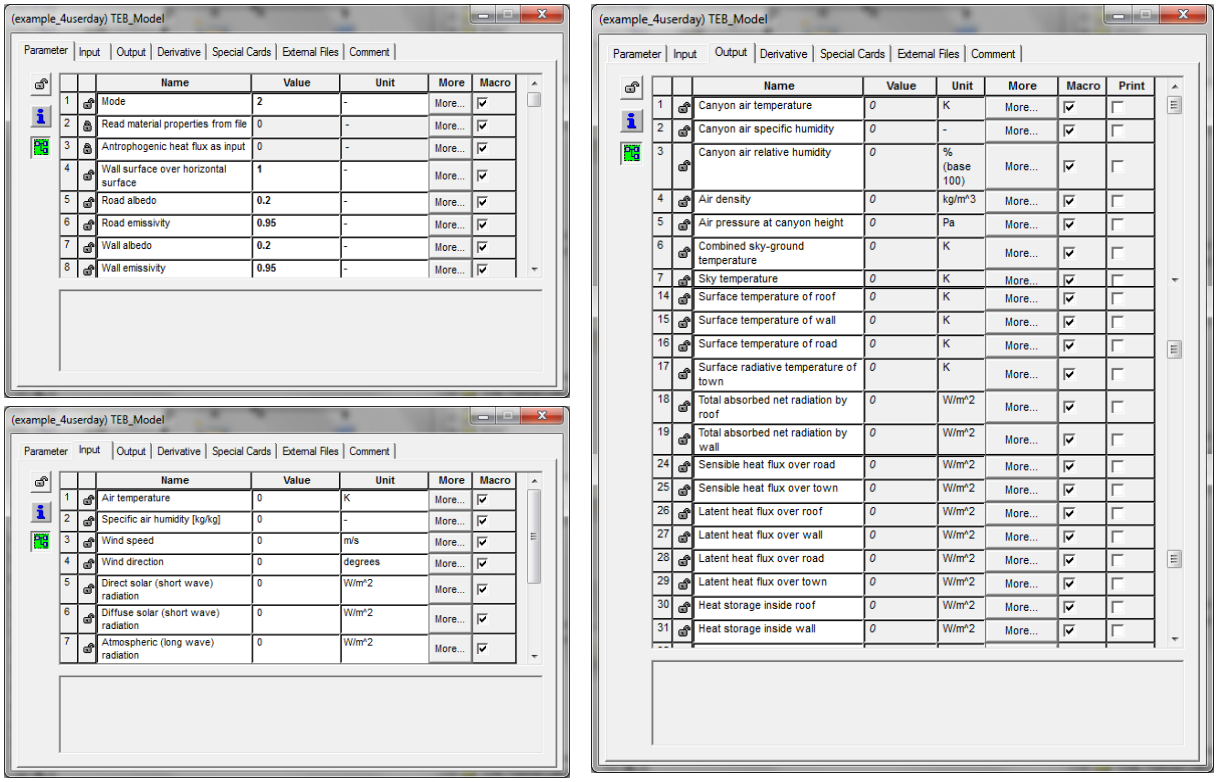

Figure 68: Tabs of Type 201 in TRNSYS Studio showing the inputs, parameters and selected outputs

5.1.3. Limits and Outlook of Type 201

The TEB - Type 201 partly solves the methodological problem of lacking connection between building climate and urban climate. Beside its user-friendliness, TEB-Type presents the major advantage of supporting systematic parametric studies, which are hardly possible with the original model. This feature enabled the extensive simulations reported in this research in both PART I and PART II which would not be possible otherwise. The next step is to overcome the current following simplifications of TEB –Type 201:

- Shortwave solar radiation is averaged for all possible canyon orientations. Due to this, no precise shading pattern per time step exists in TEB-Type 201. This is an arguable assumption for urban structure outdoors but improvable. Moreover, it is not accurate if dynamic calculations for indoor spaces are to be included. The refinement of the model in this respect by taking into account the solar orientation is necessary and possible as shown by Kusaka et al. (2001) and meanwhile added in TEB by Lemonsu et al. (2012).
- Currently, the urban canyon in TEB-Type 201 is a homogeneous and opaque two-dimensional structure with an infinitive length. For indoor simulation, a differentiation of opaque and transparent parts is decisive. So, the model must be extended in this regard by providing separate inputs for walls and windows including shading devices as introduced by the BEM model of Bueno et al. (2012). This would also improve the calculation indoors when incoming passive solar energy is more realistically accounted for.
- The anthropogenic heat from traffic or industry Q_{FTRF} (traffic) and Q_{FIND} (industry) fluxes are set as constant parameters in the original TEB. In Type 201, these fluxes are set as input, which can be read from a file for each simulation time step. This is important because the anthropogenic heat experiences in reality daily, weekly and seasonal variations (e.g. Sailor and Lu 2004, Fan and Sailor 2005, Ohashi et al. 2007). This issue is still widely ignored in numerical models because of lacking reliable experimental data (see Sailor 2011). This feature will become particularly relevant once the coupling with the TRNSYS is completed. Detailed information about the heat release of a building will then become available and can be utilized in the urban canopy model.

Some of these issues have been meanwhile added to TEB in the open source version distributed in 2013 (see TEB 2013) but not yet integrated in the TEB – Type 201. These are inter alia i) a differentiated orientation of the canyon after Lemonsu et al. (2012), ii) a simplified building energy model after Bueno et al. (2012c) and iii) the use of vegetation i.e. garden (Lemonsu et al. 2012) and green roof (De Munck et al. 2013). Nevertheless, these aspects may have only marginally affected the results reported here, as these details were not the fo-

cus of the work. Rather, a key issue, which needs real improvement and deserves more attention, is a synchronized urban – building energy modelling and for which Type 201 is the first milestone. The next section discusses this outlook.

5.2. Outlook on the Synchronized Urban - Building Energy Modelling

5.2.1. Description of the Problem

The chosen investigation method in this research revealed to be appropriate, yet time-consuming and perfectible in terms of accuracy. From this statement, the synchronized coupling of an urban canopy model with a building energy model has emerged as the next necessary research step. The literature review given in section I - 2.3 (p35) already addressed the state of the art on urban – building energy models and revealed this issue to be relatively new and currently in progress. This research is also a contribution in this sense and Type 201 can be seen as a first step towards the goal of developing a sophisticated urban canopy climate model, capable of reproducing that complexity. A new synchronized urban- building energy model will overcome the following disadvantages.

1. Lack of an integrative tool:

Using two different models separately (TEB, TRNSYS) is time consuming for preparing the object of study to be simulated. On the one hand, data must be input in TEB and in TRNSYS separately and using different formats (e.g. different key metrics and units). On the other hand, TRNSYS being not conceived for urban issues, extra calculations had to be added manually in the TRNSYS studio (see Appendix 5). Such adjustments require from the user more time and skills in urban climatology.

2. Lack of a simultaneous coupled simulation:

So far, TEB is initially executed and its output subsequently serves as inputs for TRNSYS. Even though acceptable as approximation, this does not reflect the reality because performing TEB and TRNSYS simulations successively means not including the feedback loop at every simulation time step between indoors and outdoors regarding heat and mass exchange, as a synchronized procedure would do when urban canopy and building models are coupled. This coupling also means eliminating the redundancy in solving the energy balance at urban facets, which are the shared surfaces between the two physical spaces and so the two models.

3. Simplified urban structure:

TEB-Type 201 models a simple repetitive urban canyon structure (symmetrical profile, opaque with no windows, no shading devices, etc.) which contrasts with the detailed capabili-

ties of TRNSYS in representing the building and its surroundings in detail. Simplified parameterizations of the turbulent heat fluxes are used, as well as a simple concept for in-canyon wind flow and averaged solar irradiations. Improvements on these issues are necessary.
The fact that TRNSYS is a commercial product might be perceived as disadvantage. Its choice in this work is motivated by the author's skills to use it. However, embedding TEB in another comparable model would be likewise possible.

5.2.2. Further Working Concepts

Existing urban climate models, which specifically address the issue of coupling urban and building scales or possess some potential of improvement for this purpose have been introduced in section I - 2.3 (p 35). These models use various interesting concepts, partly inspiring the following. General working concepts are sketeched hereafter for a possible new model development extending TEB under TRNSYS. One can imagine using another building energy model like EnergyPlus or a simplified version of ENVI-met. Figure 69 shows the structure of the coupled modelling system, including the information connections between (1) the urban canopy model and (2) the building model. Figure 70 expands on the physical domain to be simulated and shows the key metrics involved and their logical connections. These working concepts rely on the combination of the strengths of the two models, as outlined hereafter. The urban canopy model as extended TEB-Type under TRNSYS may include i) an atmospheric, ii) a vegetation and ii) a soil sub-model, as used in ENVI-met. In this respect, the latest updates made in TEB can be included. Using the modular principle of TRNSYS, these sub-models perform as stand-alone components.
An interface between the urban canopy model and the scale above as already existing in TEB is useful, either for an offline run or in connection with a regional atmospheric model or if climate change prognosis is included upstream. A climate data forcing routine must be included in order to generate the climate information required at some height above roof level from the data usually available at ground level as suggested by Bueno et al. (2012b).
TRNSYS17 uses the plugin TRNSYS3D under SketchUp® which enables the drawing and processing of complex geometries including neighbouring buildings, overhangs, etc. far beyond the simplified symmetrical scheme of TEB. By this means, TRNSYS also provides accurate calculation of the shading environment. The radiation processor (Type 16 or 15) calculates the incoming direct and diffuse solar radiation on any surface given by its slope and azimuth, which is better than the approximation assumed in TEB. However, the diffusely reflected solar radiation is better included in TEB as infinite multiple reflections. In the

longwave range as well, TRNSYS accounts only for the heat exchange of the simulated building with the sky via the sky temperature T_{sky} and with the physical surroundings via an averaged surface temperature (T_{sgrd}) usually set as equal to ambient air temperature, whereas the radiant surroundings are better calculated in TEB using surface temperatures.

Moreover, modelling the outdoor microclimate faces the difficulty of geometric precision in terms of 2D or 3D description as sketched in Figure 71. The 2D option schematizes roughly the principle used by Masson (2000), Kusaka et al. (2001) and Tanimoto et al. (2004) and the second concept follows 3D-wind flow models like ENVI-met (Bruse 1999) or the simple model proposed by Kanda et al. (2005a). In the 2D modelling concept, the spatial area corresponds to the immediate built surroundings of the building object of study, with the assumption that this pattern is repetitive. The atmosphere "contained" in this urban area is accounted for as one volume and calculations are made at mid-distance within this volume given by the dotted reference line. The surroundings are considered regardless of a specific orientation, i.e. integrated over 360° to account for all possible orientations as averages whereas the building to be simulated has explicit surface orientations. Different building heights are averaged, so that the final structure is an urban canyon structure where surfaces are weighted according to their view factors. This 2D-concept enables simplified parameterizations and presents the advantage of fast computations. By contrast, the 3D-modelling concept divides the atmosphere in a 3D-grid of cubical modules. All atmospheric key metrics like temperature, humidity, wind, etc. are calculated for each module and connected together. This 3D-concept faces the issue of computation time and will require numerical solution ssuch as parallel computing using GPU's, especially if several models are linked and run simultaneously.

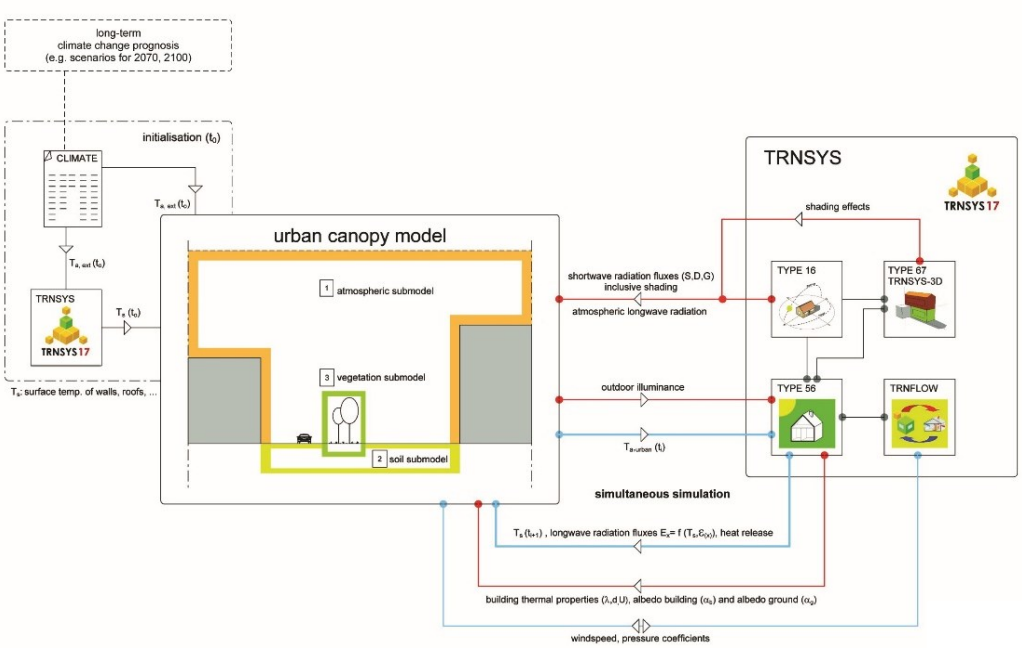

Figure 69: General coupling concept of the new urban canopy model in TRNSYS including exemplary information exchange fluxes

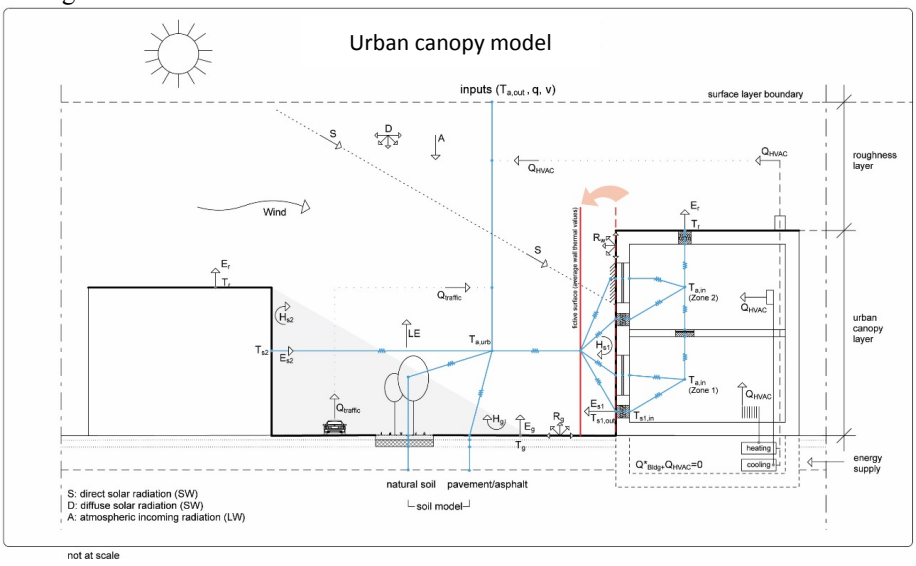

Figure 70: Representation of the main key metrics involved in the coupled urban-building modelling system

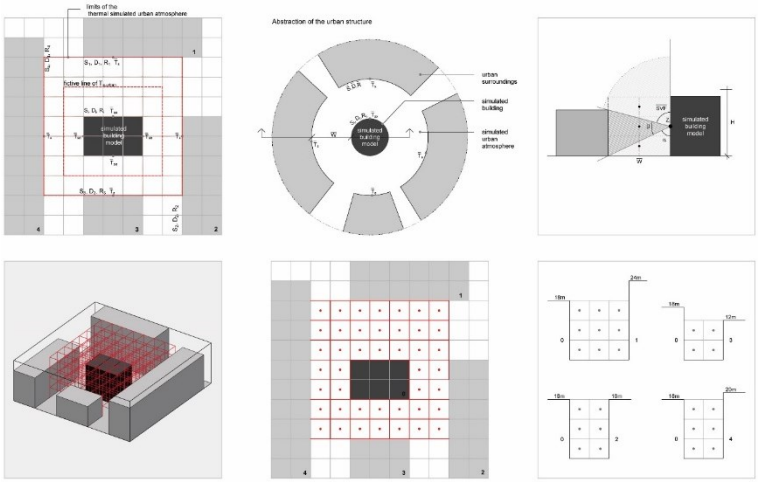

Figure 71: Two dimensional (top) and three dimensional (bottom) conceptualization of the urban canopy model as urban canyon structure

III

THE PRACTICAL PART II: THE CITY OF STUTTGART

1. INVESTIGATION PLAN OF PART II

PART II of this research reports on an investigation undertaken on a real case study, which applies the same methodology reported in PART I on theoretical urban office buildings. It extends the scope of assessing the effects of urban climate, urban geometry and building construction on the energy demand of buildings by highlighting more modifying elements directly linked to real conditions. Therefore, PART I and PART II are complementary in content and Table 45 gives an overview on their similarities and differences.

In PART I, a systematic theoretical DOE parameter study highlighted the expected effects of geometric, thermo-physical properties and HVAC settings of urban buildings, whereas PART II is based on real data describing individual buildings as they effectively exist. The ambition and peculiarity of this practical work is to proceed at the highest spatial and temporal resolutions while demonstrating the pertinence and feasibility of the investigation method introduced in PART I. In so doing, the challenge is to keep the pre-processing and post-processing times manageable while ensuring a precise physical modelling of the object of study on the one hand and a dynamic thermal simulation on an hourly basis for long periods on the other hand.

PART II was to a large extent conducted as KLISGEE[12] Project in the framework of the KLIMOPASS[13] program of the federal land Baden-Württemberg (BW). This was an argument for choosing the state capital Stuttgart as object of study. In addition, Stuttgart belongs to the same DWD climate region TRY12 addressed in PART I. More importantly, Stuttgart has been early at the forefront of German cities in urban climate studies with substantial achievements and background knowledge making it an ideal object for this research (see Stadtklima Stuttgart 2017). Stuttgart greater area is geographically located in the latitude range of 48.69 – 48.87°N and longitude range of 9.03 – 9.32°E. With 609 000 Inhabitants, it belongs to the largest German cities.

12 KLISGEE: Klimawandel, Stadtklima und Gebäudeenergieeffizienz: Wechselwirkungen und Handlungskonzepte für eine nachhaltige Stadt. (Ali-Toudert and Ji 2016)

13 KLIMOPASS: Klimawandel und modellhafte Anpassung in Baden-Württemberg, http://www4.lubw.baden-wuerttemberg.de/servlet/is/244199/

Table 45: List of the parameters and comparison of their modelling in the theoretical PART I and practical PART II of this research

Investigated parameter		Settings in PART I	Settings in PART II
general	object of study	Urban office buildings embedded in an urban canyon structure.	All buildings in the Stuttgart (inner) city.
	climate information	TRY12 (reference station Mannheim, region including Stuttgart) Mediterranean climate (Algiers).	Stuttgart using spatially interpolated recorded data using LARSIM model for the city area.
	climate resolution	not applicable	Grid cell of 1 km^2 for the inner city study area of 36 km^2.
urban	spatial scope	not applicable	Spatial distribution considered using GIS mapping.
	spatial resolution	not applicable	99 spatial units according to urban density within the study area of 36 km2 screened at 1 km^2 grids.
	anthropogenic heat (traffic | industry)	Set as variable in the sensitivity analysis. Otherwise, set to constant.	Based on actual CO_2 emission map.
	aspect ratio H/W	Set as variable in a 3-steps DOE plan.	Modelled as a variable in a 3-steps DOE plan but post-processed for actual values
	plan density (roof surf./total)	Set as variable in a 3-steps DOE plan for the sensitivity analysis. Otherwise, set constant.	99 spatial units according to urban density within the study area of 36 km2 screened at 1 km^2 grids.
	solar orientation	In TEB, all directions are assumed to occur equally. They are also accurately modelled in TRNSYS.	All direction are assumed to occur equally.
Urban and building	albedo (reflectance)	Variable is set in a 3-steps DOE plan for the sensitivity analysis. Otherwise, set constant to standard values.	Set constant to standard values
	emissivity		
	floor level	Buildings with five (5) floors are modelled. Post-processing is made for ground floor, mid-canyon floor and upper floor.	Building modelled as a whole but the outputs calculated per floor using an estimation of floor numbers for each building
building	building type of use	office use	Actual for each building: residential and non-residential modelled, weighting if mix-use calculated from outputs,
	window ratio	Set as variable in a 3-steps DOE plan. The window ratio is indirectly accounted for in TEB for the thermal insulation.	Set depending on building type and set according to IWU building catalogue.
	thermal insulation		
	thermal inertia	Set as variable in a 3-steps DOE plan in TEB.	Averaged
HVAC building operation	shading devices	Set as variable in the sensitivity analysis. Otherwise, set to one scenario as function of the incident solar radiation.	Set to one scenario as a function of the incident solar radiation.
	ventilation rate	Set as variable in the sensitivity analysis. Otherwise, one scenario is set with reference to German standards.	Set depending on the building type and plan with reference to German standards.

1.1. Investigation Concept and Stages

Figure 72 shows the investigation concept at the object Stuttgart city, including its successive working stages as explained hereafter.

I. Background data, which includes gathering of climate and necessary city data.

II. Data pre-processing, which includes the preparation of raw information in readily usable format for the numerical modelling with TEB and TRNSYS.

III. Urban climate simulations using TEB, including the statistical post-processing of TEB results to be used in next stage IV.

IV. Building Energy simulations using TRNSYS.

V. Statistical post-processing of TRNSYS results.

VI. Mapping of predicted results of urban climate changes and useful energy demand for heating and cooling at building and city block level.

Concerning stages (III) and (IV), it is important to note that the simulations in TEB and TRNSYS differ in one conceptual aspect. TEB simulations are run for actual values about the urban fabric (e.g. mean height of buildings, aspect ratio, anthropogenic heat release, etc.), differentiated in 99 spatial units depending on their built density as shown in Figure 74 and using the corresponding climate data file at a resolution of 1 km^2 within the study area of 36 km^2. TRNSYS simulations, in contrast, are based on a generic DOE experimental plan, which is based on a 3-steps matrix of thermally relevant urban and building parameters covering the whole range of possibilities occurring in Stuttgart (see section III - 3.1, p 182). Hence, the TEB outputs express the actual and location-specific adjustment of the microclimate situation for the screened study area, which are then forwarded to the building energy simulations. TRNSYS results, by contrast, have to be statistically post-processed (stage V) in order to derive the polynomial mathematical models required for translating those generic results to each individual building and city block on the basis of their relevant thermo-physical properties.

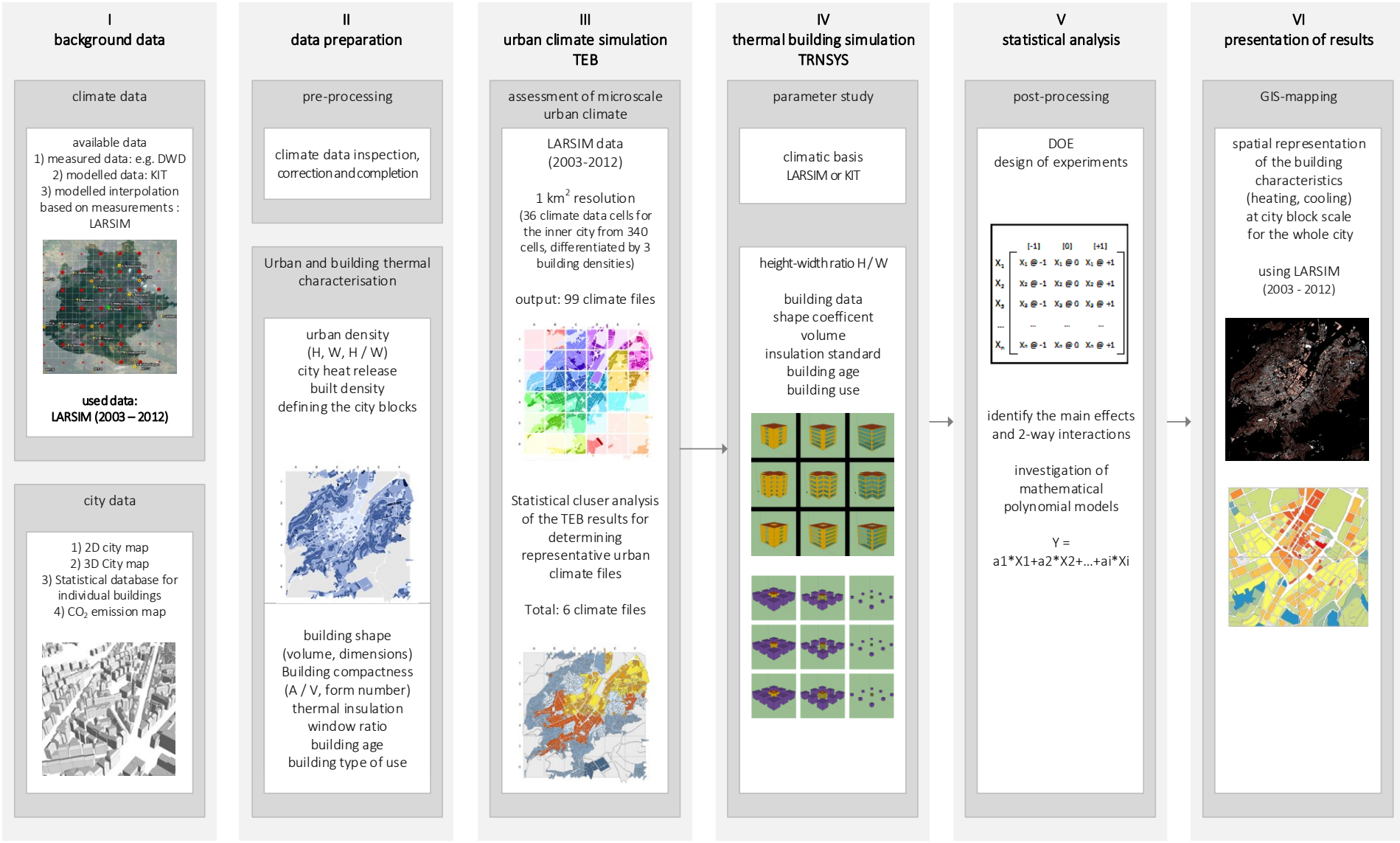

Figure 72: Investigation concept and stages of PART II dedicated to Stuttgart City

1.2. Spatial and Time Scope

The time processing required for TEB and TRNSYS simulations is substantial in spite of the speed of the models. This is due to the large size of the study area and to the necessary detailed physical description of the city at the scale of individual buildings. A systematic modelling of all cases, including 340 climate series for a normal period of 30 years and several hundreds of building models is therefore not reasonable. Instead and with no possible loss in accuracy and expressiveness of the investigation, the following choices were made for reducing the time costs:

- The study area has been limited to the inner city of Stuttgart, which corresponds to 36 km^2 from the total area of 340 km^2 as illustrated in Figure 73. The limitation to this area was motivated by its representativeness in terms of land use, urban density and building types. All graphs presented in PART II are focussed on this central area. The surrounding area is ignored mostly because either natural or of sparse urban development. The industrial area in the Neckartal and residential area at Feuerbach are dense but less relevant.
- For a better spatial precision, the 36 cells representing the 36 km^2 inner city have been partitioned to 99 sub-cells by taking into account further differences in urban density in 3 levels (dense, medium and sparse) for each 1 km^2 cell (Figure 74). Note that from the maximum of 108 (= 36 x 3), a few cells do not need a subdivision, bringing the total sub-cells to 99.
- The TEB and TRNSYS simulations were run for 10 years using the period of 2003 – 2012 (last decade at project's start) and not for the available normal period of 30 years since ten years are representative enough for describing the climate of a location.
- The results of TEB underlie a statistical cluster analysis and six (6) clusters were identified as representative urban climate patterns from the 99 cases investigated (see Figure 84). These six urban climate series were used for the building energy simulations with TRNSYS.

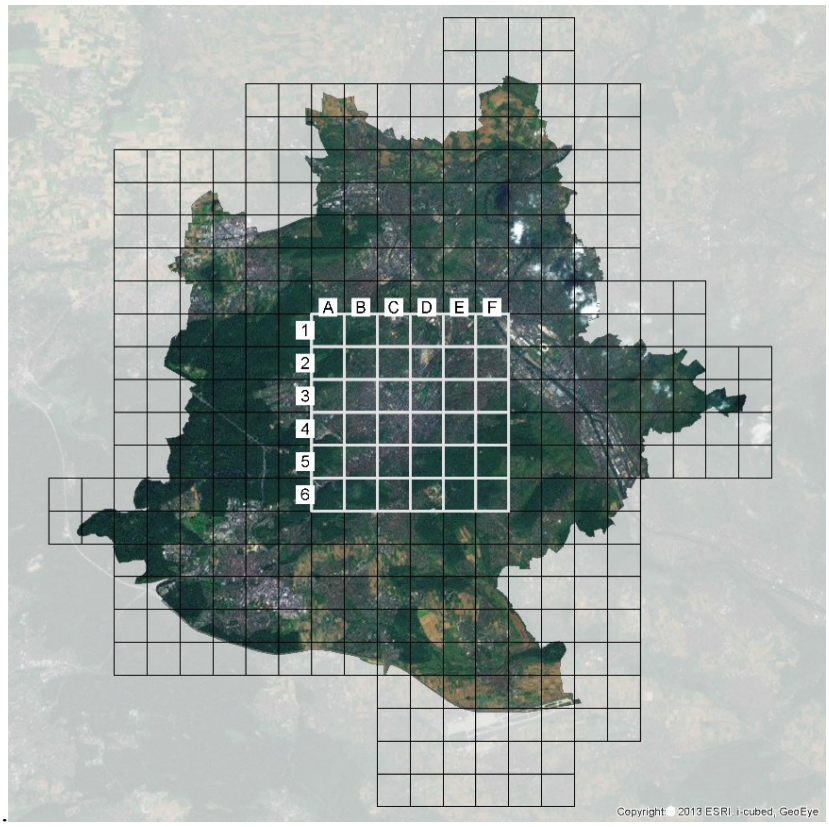

Figure 73: The selected study area of 36 km^2 [square A to F, 1 to 6] from the whole Stuttgart area and surroundings of 340 km^2

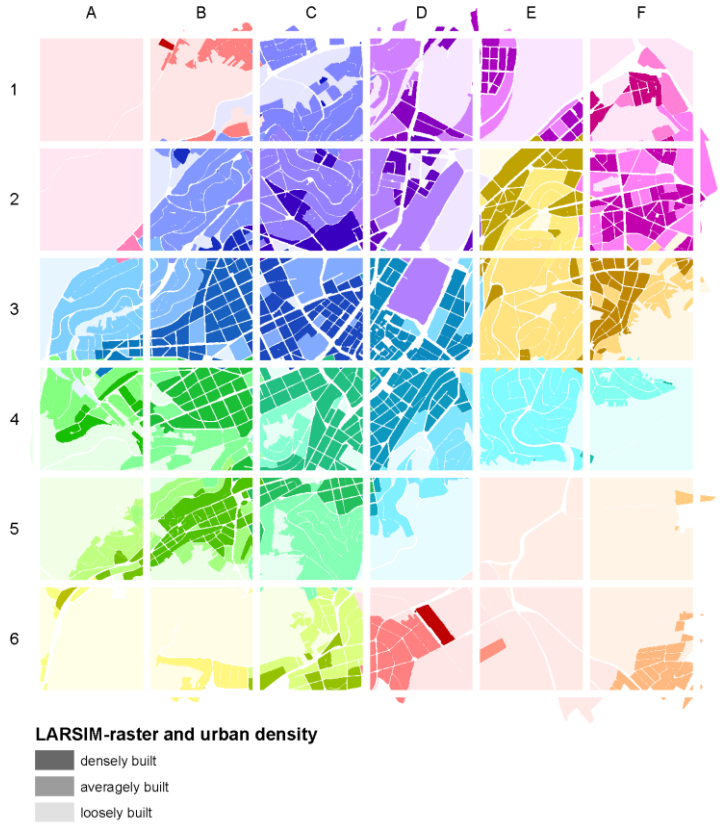

Figure 74: Differentiation of the different urban structures by density within each cell, with dark, medium and light colours stating for high, medium and low density

1.3. Simulation Sets in TEB and TRNSYS

Table 46 gives an overview about the simulation sets in terms of objects and number of simulation runs and are explained in the following:

- In TEB, one simulation set was run. It consists of 99 simulations, which provides the urban climate adjustments from the standard climate data.
- In TRNSYS, two simulation sets were run: (1) The one simulation set uses urban climate data and (2) the other runs with standard climate data as reference for comparison purposes, i.e. deviation in the energy demand due to urban climate effects.
- In TEB, 36 climate files are used for the study area of 36 km^2. In TRNSYS, the simulations run for six urban climate patterns determined as representative clusters.
- Based on a generic concept for a thermally relevant characterization of all buildings as explained thoroughly in section III - 3.2 (p 183), the buildings modelled in TRNSYS combine the following variables: shape coefficient (S), building volume (V), window ratio (W), thermal insulation (T) and aspect ratio (A). The combination of these variables leads to a total number of 243 building models following a systematic 3-steps DOE plan. The simulations for these buildings were then run for three different building types of use, i.e. residential, non-residential standard and non-residential special use, because they influence the HVAC settings (see Appendix 18). The full factorial plan of 729 building cases (i.e. 243 building models x 3 types of use) has been reduced to 1/3 using a part factorial plan, i.e. 243 cases, covering the main effects and double interactions.

Table 46: Overview on the simulation sets using TEB and TRNSYS

Item | number of	TEB (1)	TRNSYS (2)	comment
modelling concept	actual	generic	(1) real values for each 1 km^2 cell (2) theoretically relevant thermal characterization of buildings
input climate files	36	6	(1) reduced study area at 36 km^2 (2) Use of six climate files based on a cluster analysis.
buildings models	-	243	(2) five variables at 3 steps, i.e. 3^5
building type of use	-	3	(2) residential, non-residential standard (schools, offices, etc.) and non-residential non-standard (sport halls, industry, etc.)
simulation sets	1	2	(1) adjustment of standard to urban climate (2) simulation with both standard and urban climate background
total number of simulations	99	1458 (= 243 x 6) (x 2)	(1) The 36 climate "cells" partitioned into 99 by further differentiation depending on urban density and then reduced to 6 representative clusters. (2) part-factorial DOE plan (1/3 of the total factorial) of 1458 (243 buildings models x 6 clusters), simulated twice (2916 = 1458 x 2) including urban climate effects and as standard climate)

– In TRNSYS, one simulation set counts 1458 cases as 1/3 part factorial DOE plan instead of 4374 if full factorial. The DOE plan uses 6 representative boundary climate data for 243 building models and 3 building types of use

2. THE CLIMATE OF STUTTGART

2.1. Available Weather and Climate Data

At the beginning, climate information with the best possible spatial resolution was required for the whole area of Stuttgart because of the pronounced topography of the site. Different climate sources were collected, compared and analysed (see Ali-Toudert and Ji 2015a and 2015b). These are listed in Table 47 including recorded and modelled data, available at hourly basis for up to 30 years as well as an urban climate atlas. Figure 75 graphically illustrates their respective spatial raster and so the geographical locations of the single data series.

At early stages of the work, the lack of ready for use suitable climate information emerged as the most problematic issue in conducting this practical part of the research. Due to space limitations, the detailed climate analysis undertaken prior to decision will be made available in a separate publication. For the sake of conciseness, only the main arguments either favourable or unfavourable, which prevailed in the choice of the appropriate climate data for this study, are summarized below.

Table 47: Climate data sources for the whole study area of Stuttgart

data source		type of information	time period*
German Weather Services	DWD	13 stations available 3 stations initially selected	2003 – 2012
State Agency for the Environment, Measurements and Nature Conservation Baden-Württemberg	LARSIM (LUBW)	1.0 km^2 resolution: raster with 340 points	2003 -2012
Karlsruher Institut for Technology	KIT	7.0 km^2 resolution: raster with 5 points inside Stuttgart 2.8 km^2 resolution: raster with 31 points	1971 – 2000 2021 – 2050
Office for environmental Protection of Stuttgart City	AU	1 station at roof level (25 m a.g.l.)	From 1987 2003 - 2012
University of Hohenheim	UNI-H	1 station	From 1972 2003 - 2012
Climate atlas	CLM-ATLAS	maps of timely averaged meteorological key metrics	Version 2008
* Time period during which the data are either available and/or gathered for the project.			

1. DWD Data

The German Weather Services DWD holds 13 standard weather stations covering the greater area of Stuttgart. The spatial distribution of the stations offers the advantage of capturing the microscale differences due to geography and land use. However, differences were observed in the number of the meteorological factors and periods of recording, so that data compensation was partly necessary. Three (3) stations were initially identified to be appropriate, namely DWD-Echterdingen, DWD-Neckartal and DWD-Schnarrenberg (Figure 75), data of which were provided for the period of 2003 - 2012. However, these stations are mostly useful for verification purposes because they are not representative of the whole area and because of its pronounced topography, unless an appropriate interpolation model is used.

2. LARSIM Data

The LARSIM model provides the required interpolation of data within the whole study area. LARSIM is a hydrological balance model used in southern Germany and neighbouring countries (Bremicker et al. 2013), such as by the flood control centre of the state agency for environment, measurements and nature conservation Baden-Württemberg (LUBW). This agency provided this research with the necessary data at a resolution of 1 km^2 in the period of 2003 – 2012. The LARSIM data have been interpolated by means of geo-statistical methods accounting for topography and land use using measured data from available weather stations, following the procedure described in (Bremicker 2000). The data set consists of a total of 340 data series corresponding to as much cells covering the study area (Figure 75).

3. KIT Data

The data provided by the Karlsruher Institute of Technology KIT are atmospheric modelling data calculated using GCM (Global Climate Model) with the regional climate model COSMO-CLM. In this model, topography, slope inclination and land cover were set as initial data and boundary conditions (KIT 2014). The data were provided for two periods, 1971 – 2000 and 2021 – 2050 as past and future forecast normal periods (30 years), respectively. Two resolutions were available: 7 km (7 x 7 km^2) and 2.8 km (2.8 x 2.8 km^2), corresponding to 5 and 31 cells, respectively. However, the disadvantage of this data was to be bias corrected at daily average but not at hourly basis. Consequently, the air temperature is found to be systematically lower by several Kelvin (see Figure 76). Moreover, the daily course of the air temperature is smoother compared to available measured data. Moreover, the spatial resolution was insufficient for the purpose of this work.

4. City Station Data

The Office for Environmental Protection Stuttgart (AU, see AU Stuttgart 2015) has its own measuring station on the roof of its facility in the inner city at the corner of the streets Tor-strasse / Hauptstäterstrasse. The city station is at a height of 25 m above ground level and has being recording the most relevant meteorological factors since 1987. In addition, since the decommissioning of the DWD city measuring station in 1984, it has been the only measuring station in the city centre. The urban climate effects are thus recorded directly. The measuring data, however, have smaller time gaps with missing data. The site-specific character of the station and besides the data being gathered at roof top make them useless for the spatially widespread study area of this project.

5. Hohenheim Data

The weather station of the University of Stuttgart-Hohenheim has been collecting weather data since 1972. These, however, are restricted to air temperature, precipitation and sunshine duration and would be only useful for comparison purposes.

6. The Urban Climate Atlas

The urban climate atlas (Klimaatlas Stuttgart 2008) provides spatially differentiated climate data for the whole study area at specific times rather than long-term weather data series. The maps are mainly based on infrared thermal images. Therefore, this information is useful in giving an overview on the urban microclimates in the study area but not for the calculations strived for in this research.

2.2. Climate Data Selection

The meteorological data from these various sources were partly in space, time or due to the measurement scope not identical. Figure 76 illustrates exemplarily the monthly average daily cycle for air temperature and global radiation for these sources at one location and it reveals certain deviations.

In this study, the LARSIM data were used as they provide an appropriate resolution (1 km^2) that includes the spatial land use differences necessary for the microclimate investigation using TEB. These data also reveal to be in good agreement with the measured data from DWD stations. Six meteorological factors are given in the LARSIM weather data sets: wind speed, air temperature, air pressure, relative humidity, global radiation and rainfall. Figure 77 exemplarily shows their spatial distribution over the whole study area and clearly exhibits the local effects of topography and land use. The missing wind direction and cloud cover in LARSIM data were compensated using the DWD-Echterdingen and DWD-Schnarrenberg weather sta-

tions. Moreover, further missing data in LARSIM required as inputs in TEB needed to be determined. The solar radiation split in i.e. direct (S) and diffuse parts (D) and the sky temperature (T_{sky}) were calculated using the available global radiation, using the radiation generator Type 16 and psychrometric Type 69 in TRNSYS Studio. The simulation period in TEB and TRNSYS for the period of 2003-2012 corresponds to 87674 hours.

It is also noteworthy to mention that in spite of the weaknesses in the KIT data, they were useful in the KLISGEE project while investigating the climate change issue. In that case, both *past* and *future* climate series of KIT data were downscaled from a square grid resolution of 2.8 km to 1 km using the LARSIM data as reference. In so doing, TEB and TRNSYS results for both periods could be compared and the effects of global warming on the urban climate and building energy demand could be investigated (Ali-Toudert and Ji 2016). This part of the investigation is not reported here, but just briefly addressed in the outlook, because it exceeds the goals and scope of this research and for space limitations.

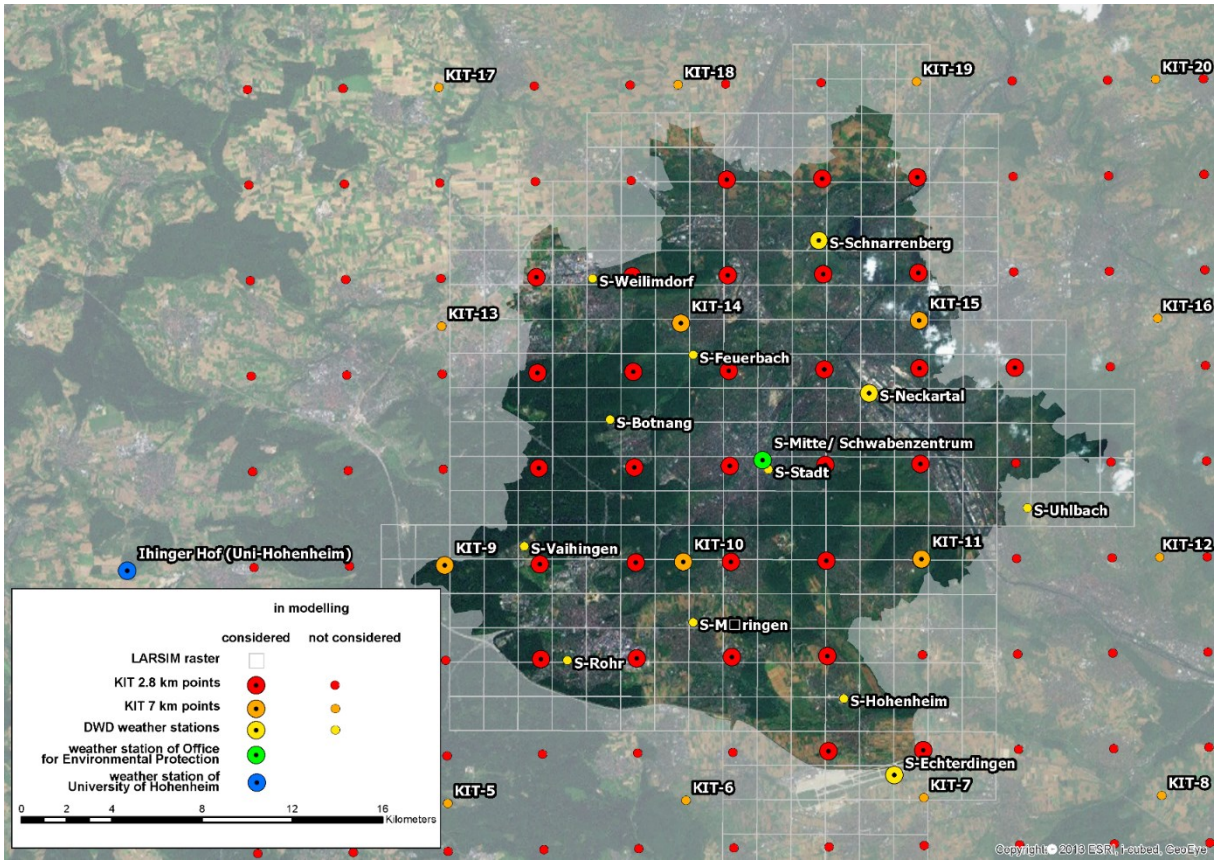

Figure 75: The climate data sources available for the area of Stuttgart city (data sources: DWD 2013, KIT 2014, AU Stuttgart 2015, LUBW 2013, University of Hohenheim, own representation)

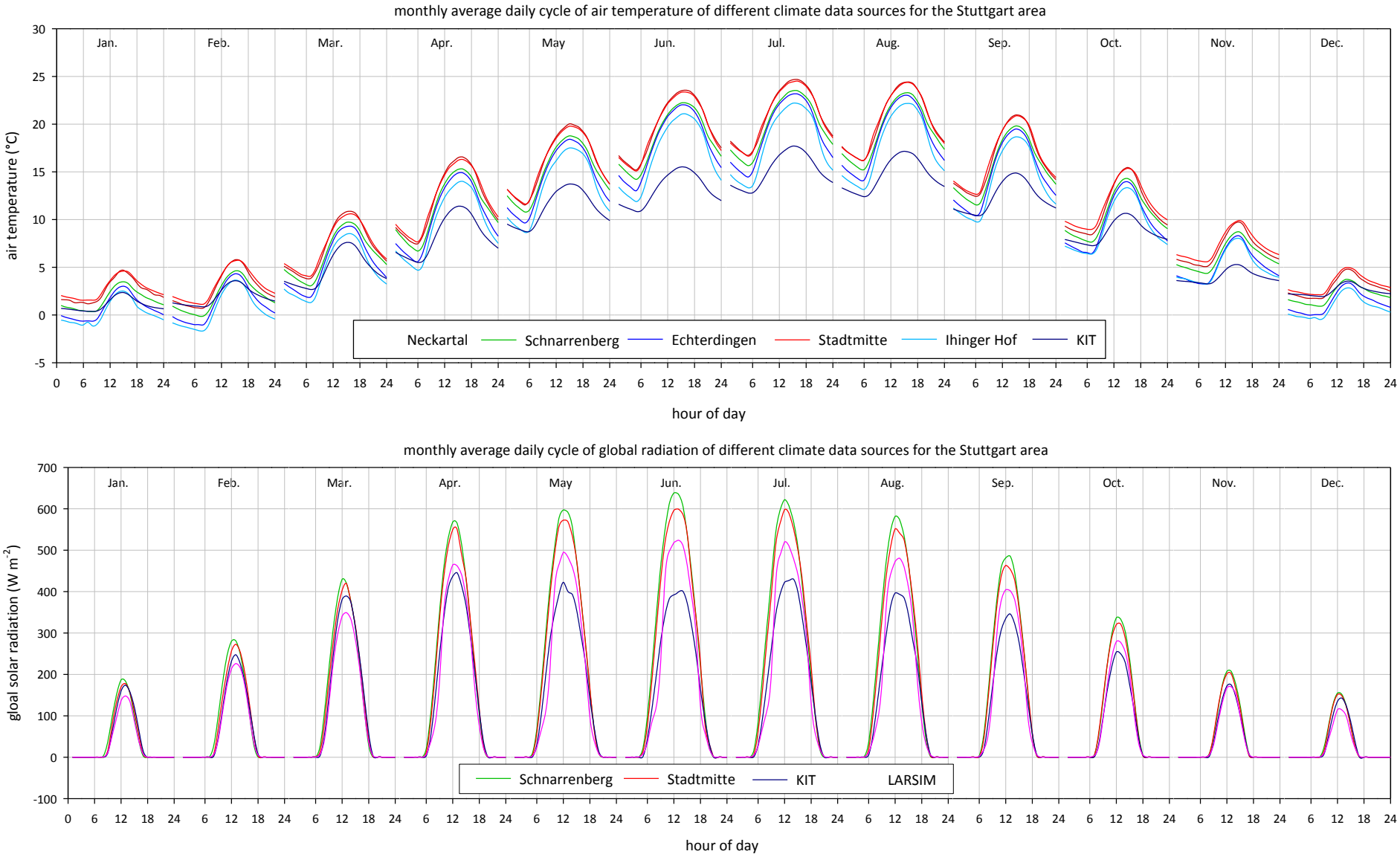

Figure 76: Average monthly daily cycles of air temperature and global radiation from the various climatic data sources for Stuttgart

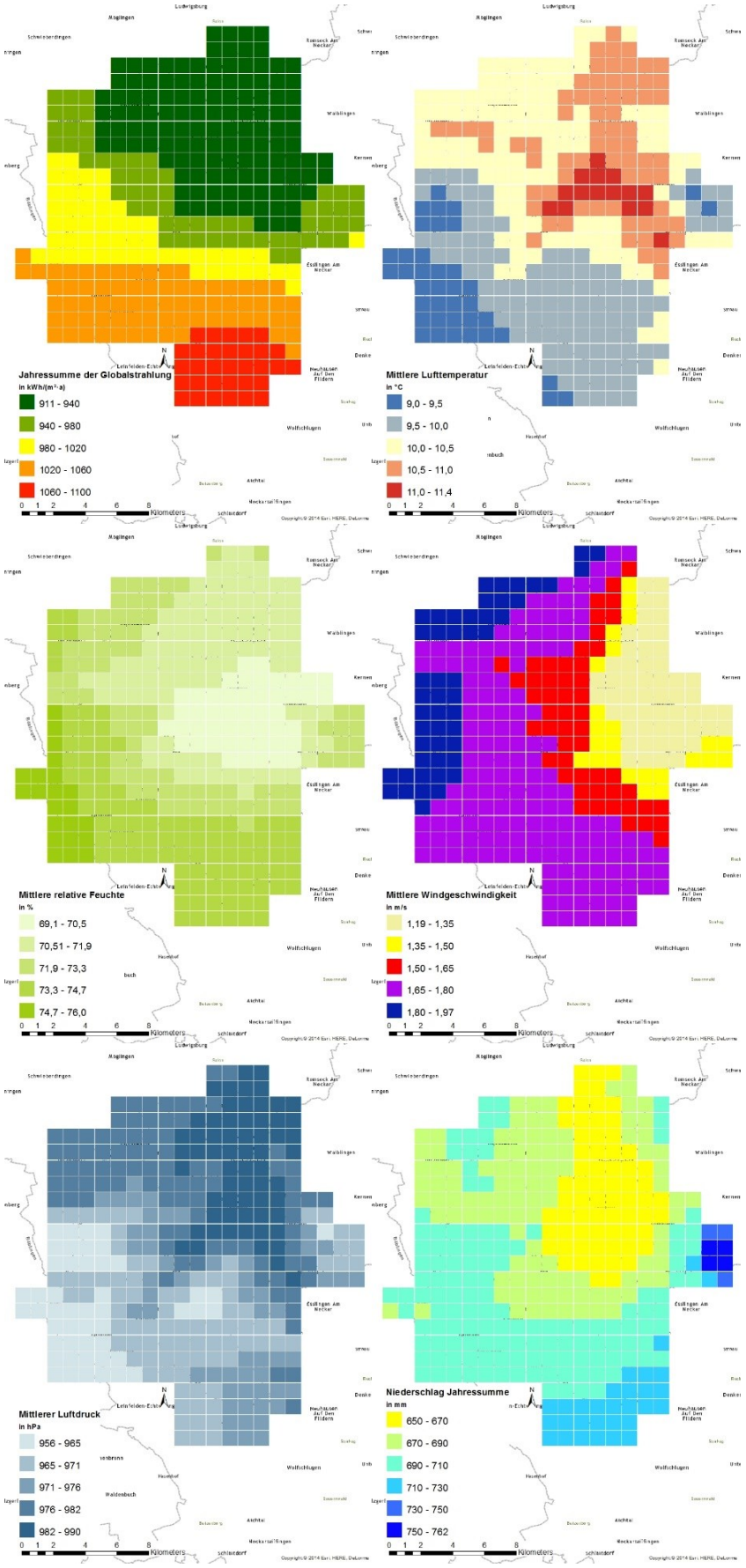

Figure 77: LARSIM-based spatial differentiation of average global radiation, air temperature, relative humidity, wind speed, air pressure and rainfall on average / yearly sum (data: LUBW 2013, own representation)

3. CITY DATA AND PRE-PROCESSING WORK

3.1. City Data Sources

For the purpose of this research, diverse sources of information about the city of Stuttgart were collected. The data used include a 2D city plan, a 3D city plan, a city block map (i.e. building plots and streets) as well as a digital map for gas emissions from transport (NO_2 immission and CO_2 emission) and a map of final heating energy consumption of 1995 from the energy atlas (AU Stuttgart 1997). Moreover, a tabular database associated to the 2D map provided further information on the individual buildings including their location, first construction year and subsequent renovation years, building volume, building type of use, etc.

More data were collected but were eventually not used directly, e.g. the topography map, the land use map, the statistical data about residential density and a traffic load map, either because the information was included in or used from other sources.

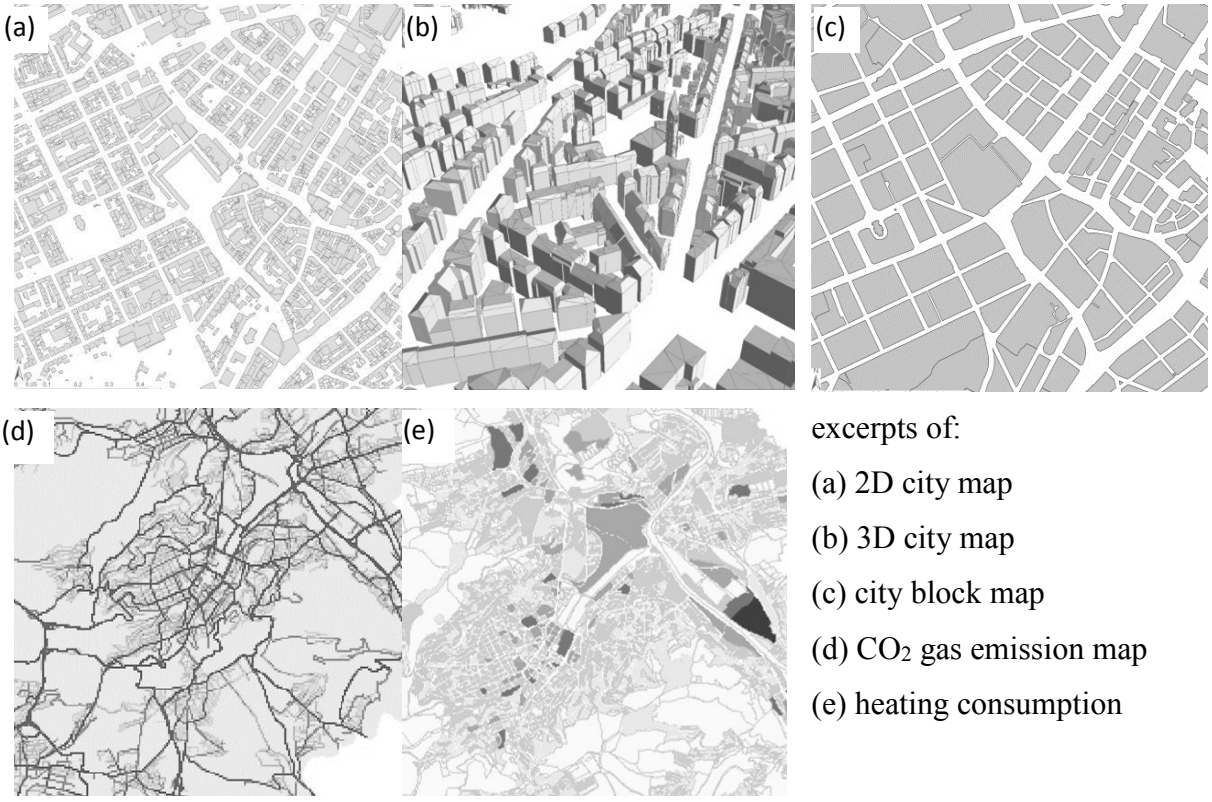

Figure 78: Data sources about the city of Stuttgart used in this research (sources: City of Stuttgart)

3.2. Thermally Relevant City Characterisation

The objective and peculiarity of this real case study is a systematic examination of all existing buildings in the city of Stuttgart with respect to urban climate effects and the resulting indoor energy demand for heating and cooling. Yet, dealing with the whole city as object of study poses the problem of time processing and so the question arises about a realistic characterization of the urban fabric for this purpose. In fact, modelling individual buildings with their actual geometrical and construction design properties is neither feasible nor effective. On the one hand, it is technically almost impossible due to time pre-processing and post-processing reasons because the statistical database of Stuttgart numbers about 75000 buildings. On the other hand, although feasible, the results would be case-specific with no transferability potential on further different cases, e.g. later changes in building and city clocks. Instead, a generic description of the urban structure and individual buildings is more efficient and timely fast in one, according to their relevant thermal properties being associated with a systematic 3-steps design of experiments DOE plan. Limiting the variables to the thermally relevant ones helps to reduce drastically the number of case studies to be investigated. The use of a DOE plan enables the transferability of the results to each single case study in the city by means of the mathematical polynomial models gained from the statistical regression analyses. This key methodological concept was adopted in this part (PART II) and lists these relevant thermal parameters used including their sources of information and spatial resolution for use in TEB and TRNSYS. The ID-marking refers to the coding used later in the experimental designs (different coding from that used in PART I). Most parameters were determined at building level and then summarized at city block level due to privacy reasons. All results reported here and graphically displayed in maps are at city block level despite their availability at building level for the same reason (see Figure 80 and next, cf. Figure 86). The single calculation procedures employed for quantifying those indicators relied on GIS techniques (ArcGIS) using city maps and further statistical data. Hence, the accuracy of these input data depends on the quality of the available raw information. This includes, but not limited to, the estimation of an average urban density by means of the height-to-width ratio and ground occupation density at city block level, the estimation of the anthropogenic heat from traffic CO2 emissions, or the calculation of the building volume and envelope surfaces needed for determining the shape coefficient. A detailed step-by-step description of all calculation procedures is omitted for its complexity and space reasons but will be reported later in other works specifically focusing on this issue. Instead, a brief explanation is given below as complement to Table 48.

Table 48: Generic urban and building indicators used for TEB and TRNSYS simulations

ID	indicators	source *	Comment	used in		available spatial resolution
				TEB	TRNSYS	
A	aspect ratio (H/W ratio) as density indicator	3D city map city block map	Building spaces and heights determined with GIS	√	√	city block
T	building type of use	2D digital city map	categorized in residential, not residential standard and not residential special use	-	√	building
U	thermal quality of building envelope with U-value	2D digital city map	estimated from the IWU building typology catalogue for Germany based on building age incl. renovation year using	√	√	building
S	shape coefficient for the compactness of building	3D digital city map	building volume and total surface of building envelope with GIS determined	-	√	building
W	window ratio	2D digital city map 3D digital city map	estimated from the IWU building typology catalogue for Germany based on building use	-	√	building
V	heated building volume	3D digital city map	building volume determined with GIS	-	√	building
H	average building height	3D digital city map City block map	Information required for H/W, building height determined with GIS	√	-	city block
OW	window orientation	none	N, S, E and W possible orientations assumed to be equally occurring	-	√	-
OS	street (or façade) orientation					
B	built to ground surface for built density	3D digital city map City block map	building ground surface and city block surface determined with GIS	√	-	city block
F	heat release from traffic	CO_2 traffic model of Stuttgart	Heat release calculated by converting CO2 emission values	√		50 m grid
O	Residential density	Statistical database	Not considered			city block

* In case an information not directly available, it was estimated from a relevant source as listed in the comment. The sign (-) means that the item is not applicable.

3.2.1. Urban Density - Aspect Ratio H/W

The street profile, which is also known as the aspect ratio or building height to street width ratio (H/W) appropriately simplifies the urban geometry in relation to climate and energy (see PART I). The concept of TEB is based on the aspect ratio and is therefore required. In TRNSYS, the surrounding buildings can also be modelled to account for possible obstructions leading to changes in the terms of energy balance. Therefore, the aspect ratio H/W is set here as the main urban density indicator. As an acceptable approximation, the variable H (height) is determined from the average height of all buildings of a city block and is determined by using the 3D city map. The average width of the street W is calculated from the digital city block map together with the building data using non-built-up-area sizes and the perimeter of building blocks and buildings are calculated as building block level.

3.2.2. Building Compactness - Shape Coefficient

The building envelope as the indoor-outdoor interface determines the amounts of heat transfer between the internal spaces and the outside environment in terms of heat gain or heat loss. Therefore, the building envelope can be expressed by its compactness, as a measure for its degree of heat conservation. A sphere is theoretically the most compact geometry whereas elongated geometries like slabs have low compactness. In addition, the building size given by its volume is also thermally relevant, since it affects the absolute quantity of heat available indoors. Both building compactness and building volume constitute the main components of the building shape, which is one parameter depicting the models to be simulated in TRNSYS. There are two ways for describing the compactness, either using the A/V ratio (total building external surfaces to building volume) or the shape coefficient. Although, the A/V ratio is most commonly used as an indicator of the building compactness, it has the disadvantage of depending on the building volume. In a 3-steps DOE plan, however, all parameters need to be equidistant and independent from each other. For this reason, instead of the A/V ratio, the building shape coefficient was used for describing the building compactness. The shape coefficient S correlates perfectly with A/V. Therefore, A/V is an equivalent metric with better suitability to a DOE plan and calculates as given in Figure 107. The building sum of surfaces A and volume V were calculated using the 3D city map in ArcGIS. The floor plate was halved, as it has no direct contact to the outside air. Thus, the building volume is assumed 5.5 instead of 6 surfaces. The buildings dimensions as required in the DOE plan in
Table 83 were reached by modelling three building geometries: cube, cross-like and block-like (Figure 108).

3.2.3. Thermal Insulation of Building Envelope – U-value

The thermal insulation quality of a building, given by an average thermal transmittance U-value of its components, is decisive on the indoor thermal behaviour and therefore on the energy demand possibly needed for restoring thermal comfort. However, this information is not directly available for the buildings in Stuttgart. Instead, with the age of the building being known, it allows for a rough estimation of the thermal insulation level of the building envelope by referring to the IWU building typology catalogue of Germany (IWU 2005, see Figure 110 and Table 84). The statistical database provides information on the year of construction and subsequent building renovations when applicable. In case of renovated buildings, it was assumed as an energetic retrofitting as well in accordance with the accepted standard back then. Obviously, this information is approximate but no better data source exists. Nevertheless, it is possible to correct retrospectively the results if new information about the thermal properties of a building becomes available, thanks to the investigation method applied here based on a generic experimental design.

3.2.4. Window Ratio

The window ratio is essential with respect to indoors solar gains. The 3D city maps provide no information about windows. Therefore, the ratio of window area to building envelope was estimated according to the classification of the IWU building typology catalogue of Germany. Here, the proportion of window area was defined for residential buildings (single-family, multi-family, or large multi-family house) and according to building age (updated by including subsequent renovations). The window area ratio varies in residential buildings, depending on the residential type between 11% and 19%. For non-residential buildings, 30% was assumed, since no information is available. See Table 84 in Appendix 18.

3.2.5. Building Type of Use

The building type of use is decisive in setting the operation schemes for HVAC space conditioning in TRNSYS. These include the set air temperatures for heating and cooling, the ventilation rates, internal heat gains originating from artificial lighting, persons and equipment and the daily schedules of use, etc. Three different types of use were selected: 1) residential, 2), non-residential "standard" as general rule for offices, schools or commercial buildings and 3) non-residential “non-standard” including a few special cases of industry and very large buildings like sports halls. This classification refers to the German thermal regulation (EnEV, DIN V 18599, see Appendix 18), which was used as basis for setting the HVAC inputs. The actual

types of use are available in the statistical database for each individual building. However, these types of use are very differentiated (see Appendix 18) and were not always easy to classify in the three predefined groups. A weighting was applied to buildings with mix use in the post-processing phase according to the occurrence of these three building types.

3.2.6. Average Building Height

The height of each individual building is not directly available but can be estimated based on other dimensions of the building contained in the statistical database, i.e. building volume, surface area, number of floors and floor area. The height of the building can be estimated based on the building volume divided by the base area, or floor area by the surface area multiplied by the floor height or number of floors multiplied by the floor height. The floor height is determined by correlation analysis according to the respective building type (building use). The correlation of the number of floors and height of the building is not significant for the other types of buildings, thus, the floor height cannot be calculated in these special cases. Through the application of the above three mentioned possibilities, the building height could be determined for about 90% of the buildings. For use in TRNSYS, the ceiling height and floor height were additionally needed. Using the IWU building type catalogue of Germany, the number of floors and hence the total useful floor area per building could be estimated. For residential and non-residential buildings, 3 m and 3.8 m were adopted, respectively. This was necessary to convert the absolute volumetric useful energy output by TRNSYS in kJ h^{-1} for the building as bulk into a specific useful energy demand in kWh m^{-2} a^{-1}, allowing thereby for a comparability in energy efficiency between the buildings.

3.2.7. Waste Heat from Traffic

The anthropogenic heat release is required in TEB and PART I, revealed its substantial importance in influencing the microclimate, therefore, it must be included. The waste heat was estimated using a traffic emissions map of the city of Stuttgart as follows. Gasoline and diesel have different calorific value, CO_2 emission factors and heat efficiency; therefore, they were dealt with separately. The proportion of cars, trucks and public transport vehicles mileage in Stuttgart (Görres 2010) determined the proportion of gasoline and diesel consumption. Percentage from the automobile stock according to different standards in Baden-Württemberg (Büringer and Schmidtmeier 2012) were used according to different emission standards in Baden-Württemberg to compensate for the lack of data specific to Stuttgart. For the conversion, the waste heat was estimated from the amount of gasoline or diesel consumption according to the emission limit values of European emissions standards.

3.2.8. Scale Reference Unit - City Block and Individual building

In order to represent graphically the thermally relevant individual parameters introduced above, a spatial scale issue must be clarified. The parameters could be and were calculated at building level, so that the energy demand results are also available at this scale. However, the results are grouped and displayed graphically at city block scale on the one hand for privacy reasons and for better legibility of the results on the other hand. Figure 79 shows an example of a scale-dependent information for the shape coefficient. The boundaries of the city blocks are available in the city block maps. A city block is one or a combination of some construction plots, usually defined by a physical boundary, ideally through streets. In some cases, these boundaries were corrected by combining small sized but structurally homogenous adjacent plots or splitting large and heterogeneous blocks.

The following graphs in Figure 80 show the spatial distribution of all indicators presented above for the study area: The inner city of Stuttgart (see section III - 1.2 on p. 173 for the choice of spatial scope).

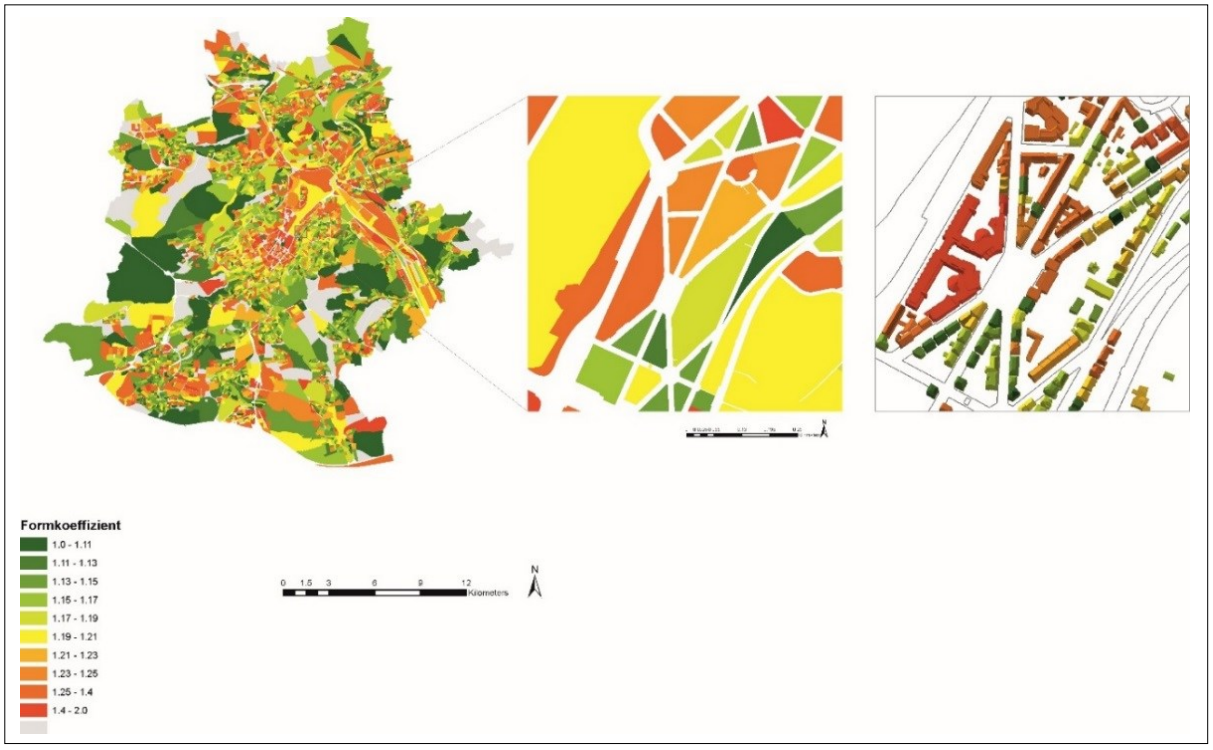

Figure 79: The successive scales considered in this study including the individual buildings (right), the corresponding city block (middle) and the overview on the whole city (left), shown exemplarily for the shape coefficient S

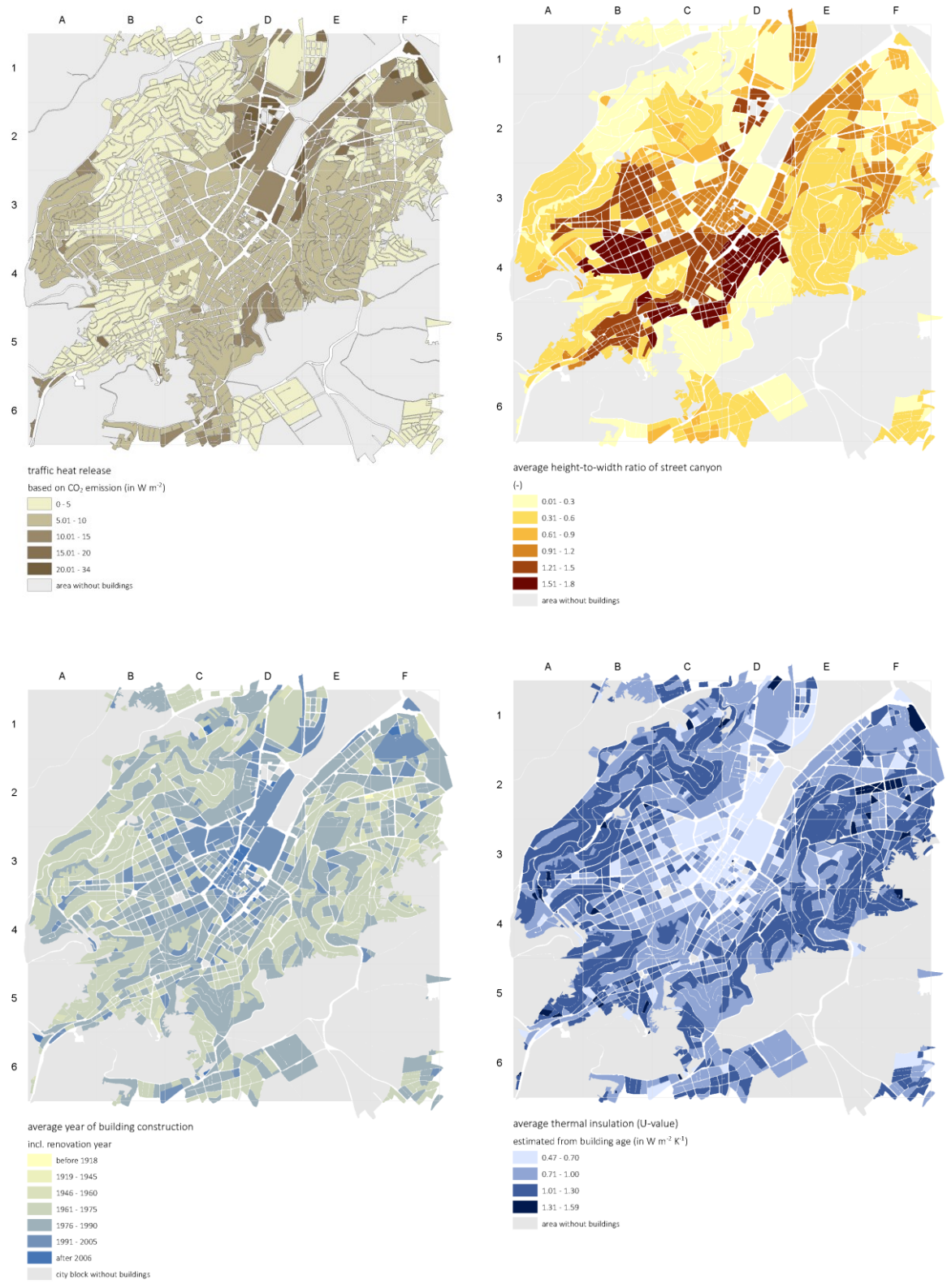

Figure 80: Spatial distribution of the thermally relevant urban and building parameters in Stuttgart inner city as used in TEB and TRNSYS modelling - (1) heat release from traffic, (2) aspect ratio, (3) building age and (4) thermal insulation (continued on next page)

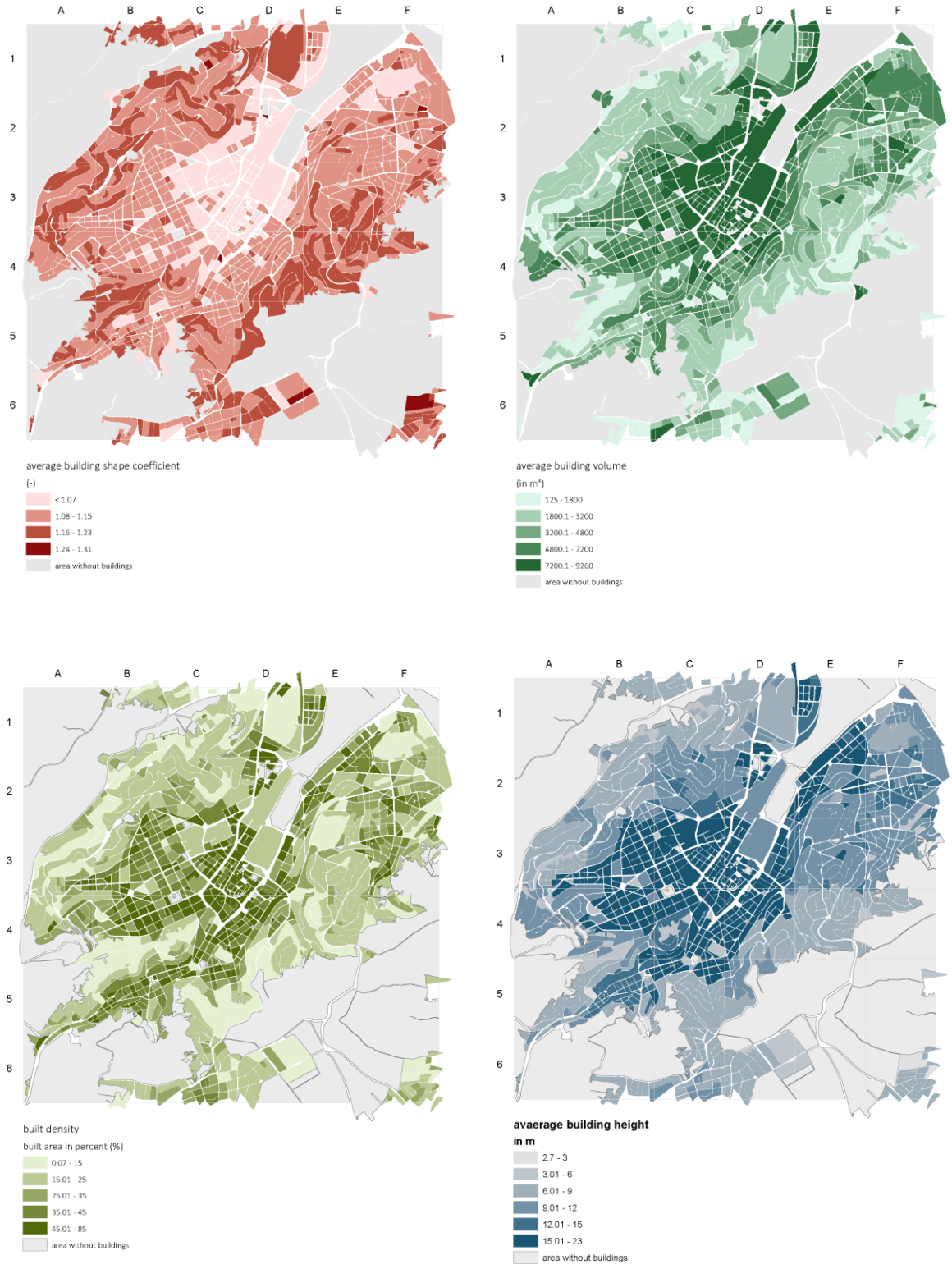

Figure 80 (continued): Spatial distribution of the thermally relevant urban and building parameters in Stuttgart inner city as used in TEB and TRNSYS modelling - (5) shape coefficient, (6) building volume (7) built density and (8) average building height (continued on next page)

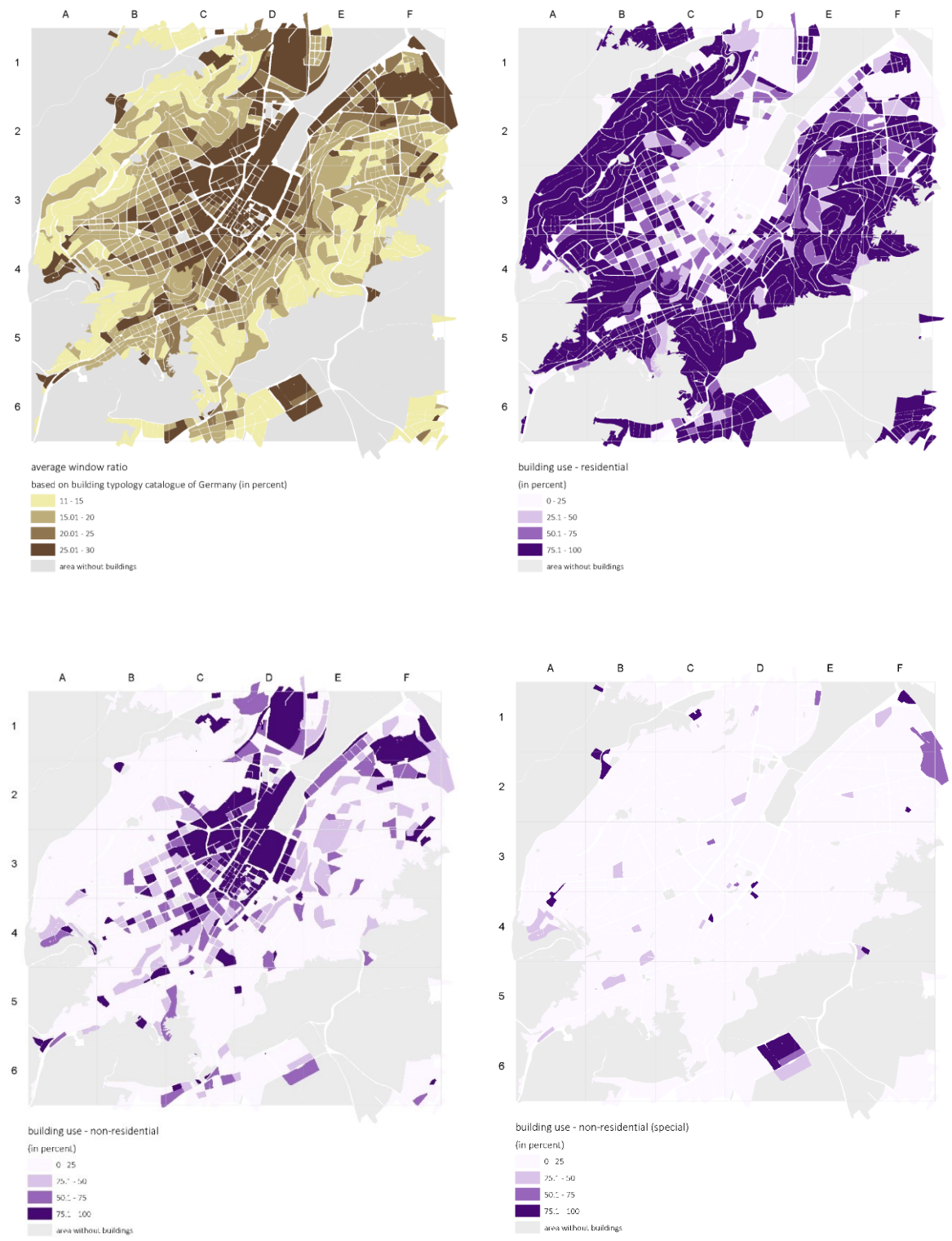

Figure 80 (continued): Spatial distribution of the thermally relevant urban and building parameters in Stuttgart inner city as used in TEB and TRNSYS modelling - (9) window ratio and (10) to (12) building types of use differentiated in residential, non-residential standard (e.g. offices, schools, retail) and non-residential special (e.g. industry and very large buildings)

4. THE RESULTS ABOUT THE URBAN CLIMATE

4.1. Warming and Cooling of the Air In-Canyon

In the following, the urban microclimate effects as calculated by the TEB model are presented and interpreted. The warming and cooling results refer to the air volume in-canyon i.e. outdoors, whereas the heating and cooling degree days refer to the indoors of the building, even though the graphs of this section show both streets and buildings in colours to aid understanding.

Appendix 19 shows the same results with isotherm representation, which might seem more appropriate, yet too rough to be properly interpretable.

Figure 81 and Figure 82 show the mean strength of the warming and cooling of the air in the urban canyons within the inner city of Stuttgart for the decade between 2003 – 2012, which is expressed as magnitude in Kelvin and as percentage, respectively. This corresponds to the air temperature difference between the calculated value using TEB and the reference rural standard air temperature ($\Delta T_{u\text{-}s} = T_{urb} - T_{stn}$). The canyon heats up to an average value of 0.83 K and cools to 1.07 K, whereas the maximal urban heat island amounts to 2.87 K as illustrated in Figure 84.

Both warming and cooling maps in Figure 81 and Figure 82 show spatial similarity, thereby suggesting similar causes. In fact, the spatial differentiation of warming or cooling depends strongly on the urban density. This is given by the street vertical profile H/W (cf. Figure 80). Another contributing factor is the waste heat from transport (cf. Figure 80). The higher the H/W ratio, the more pronounced the additional warming of the street air volume is due to more heat storage in the walls and later heat discharge in the nighttime, but also a certain cooling in the sunlight hours, when shading occurs. For example, urban areas in cells C5 but also in B3, B4, B5, C4 and D4 experienced extreme $\Delta T_{u\text{-}s}$ values where H/W ranges between 1.2 and 1.8. The same applies to cells C3, D3 and E2 even though they have slightly lower values with the H/W lying between 0.9 and 1.2. On the slopes surrounding the city centre, $\Delta Tu._{can}$ values are less than 0.5 K due to the relatively sparse construction. Cell C2 also indicates this relationship due to the slightly higher density, but with markedly less anthropogenic waste heat. The importance of the urban density and anthropogenic heat as well as further additional variables was previously discussed in the sensitivity analysis applied to theoretical objects in PART I (cf. section II - 2, p 97)

4.2. Heating and Cooling Degree Days

To better understand the significance of these urban microclimate changes on the buildings indoors, Figure 83 shows the corresponding change in the heating degree days ΔHDD (base 18 °C) and cooling degree days ΔCDD (base 24 °C) as compared to the reference rural climate. The decrease in annual heating degree days ΔHDD in the study area ranges from -241.6 to -18.8 because of higher urban air temperatures. For the sake of completeness and for comparison, see Figure 115 in
Appendix 19, which gives HDD and CDD absolute values.
The spatial distribution variance ΔHDD in Figure 83 is logically closely similar to the distribution of the average warming depicted in Figure 81 and this is mainly due to the high urban density expressed by narrow street profiles (cf. Figure 80). The urban climate effects are responsible for the deviation in the cooling degree days ΔCDD from -21.6 to +17.2. These are significantly lower than the heating degree days, induced by the background temperate climate of Stuttgart (cf. Figure 115). It is also worth noticing that both positive and negative values occur in the ΔCDD map. This either means that the base 24 °C can be cut across more often (positive, more cooling need) or undercut (negative, less cooling need). In the central city area (cells B, C, D across 3 and 4) the need for cooling is lower due to lower urban air temperatures provoked by shading during sunlit hours as compared to the reference climate (see Figure 84, right). Otherwise, more cooling is needed in the other urban areas, as urban air temperature is higher.

4.3. Clustering the Urban Climate Information

Based on these results, a cluster analysis was undertaken for two reasons. On the one hand, it was about looking for a simplified picture of the urban climate effects. However, more importantly, it was about determining a few representative climate files from the 99 series simulated in TEB for use in the following building energy simulations using TRNSYS in order to save processing time. Six representative clusters were identified as illustrated in Figure 84 (right) and described in
, which corroborates the findings in terms of air warming, air cooling, HDD and CDD is reported above. Mostly, the heat release from traffic combined with the urban density, given first by the aspect ratio H/W are the most decisive in their impact on the urban microclimate. The built density and building height as further expression of the urban density also play a role as well as the thermal insulation. The systematic sensitivity analysis reported in PART I provide more information on the impact of these variables (cf. section II - 2 on p 97).

Table 49: Main properties of clusters with relevance on urban microclimate

Clusters	variables					Description (min – max range values)
	(1)	(2)	(3)	(4)	(5)	
Cluster 1	-	-	o	o	-	traffic heat release (3.5 - 5.4 W m^{-2}), H/W (0 - 0.3), U-value (0.72- 1.05 W m^{-2} K^{-1}), built density (0 - 35%), building height (4.7 - 7.2 m)
Cluster 2	+	-	o	-	-	traffic heat release (0.1 – 21.4 W m^{-2}), H/W (0 – 0.7), U-value (0.65 - 1.24 W m^{-2} K^{-1}), built density (0 – 78%, building height (1.9 – 10.5 m)
Cluster 3	o	o	-	o	o	traffic heat release (1.1 – 29.6 W m^{-2}), H/W (0 - 0.7), U-value (0.47 - 1.21 W m^{-2} K^{-1}), built density (0 – 43%), building height (2.9 – 22.7 m)
Cluster 4	o	++	o	++	++	traffic heat release (4.7 – 14.3 W m^{-2}), H/W (0.8 - 1.8), U-value (0.94 - 1.15 W m^{-2} K^{-1}), built density (37 - 45%), building height (11 -17.8 m)
Cluster 5	+	+	+	++	++	traffic heat release (3.6 – 34.7 W m^{-2}), H/W (0.76 - 1.48), U-value (0.86 - 1.14 W m^{-2} K^{-1}), built density (35 - 56%), building height (11.9 -22.2 m)
Cluster 6	++	-	++	-	o	traffic heat release (6.3 - 51 W m^{-2}), H/W (0 – 0.42), U-value (0.71 - 1.13 W m^{-2} K^{-1}), built density (0 - 25%), building height (4 - 15.1 m)
legend: qualitative scale based on most cases (-) low, (o) medium, (+) high, (++) very high | (1) traffic heat release, (2) aspect ratio, (3) quality of thermal insulation U-value, (4) built density, (5) building height						

4.4. Daily, Monthly and Yearly Cycle of the Urban Air Temperature Change

The previous figures give average values for the decade with focus on the spatial distribution. Representing the daily, monthly, and yearly cycles enables a better understanding of the dynamic processes of heat storage and release at canyon facets, which result in an additional warming or cooling of the air. Figure 85 shows the six climate clusters determined as representative within the study area (cf. Figure 84, right).

In a densely built area (cluster 4 and 5), both warming and cooling of the canyon air occur. In general, the canyon is warmer for two-third of the entire observation period and cooler for one-third. The warming increases at night because of the stored heat being discharged. The strength is also highest in the summertime as expected for the urban heat island. However, cooling also occurs due to more shading of the canyon facets in case of high aspect ratio H/W. This happens somehow symmetrically around midday following the sun path with the total number of hours being in accordance with the season, e.g. larger periods in the summer due to longer days. The magnitude is lower in the afternoon around 16:00 when maximal air temperature is reached under rural conditions, making the difference $\Delta T_{u\text{-}s}$ smaller. In case of low density built areas (cluster 1, 2, 3, and 6), it is always warmer even if the values are small and less than 1 Kelvin. In these cases, the warming depends mostly on solar radiation, which in-

fluences the amount of sensible heat flux. Thus, the canyon becomes warmer shortly before noon and reaches its max at 14:00. This pattern is clearer in the summer months when the solar radiation is strongest. The presence of heavy traffic makes the warming of the canyon more visible in the period between 7:00 to 19:00, due to the assumption in TEB that traffic takes place during this period. Less warming is observed in case of good thermal insulation (e.g. cluster 6) because less additional heat is transferred from indoors to outdoors, making the day-night contrast smaller. More patterns are shown in section II2.3 (p 105) explaining the impact of the various variables and their interactions.

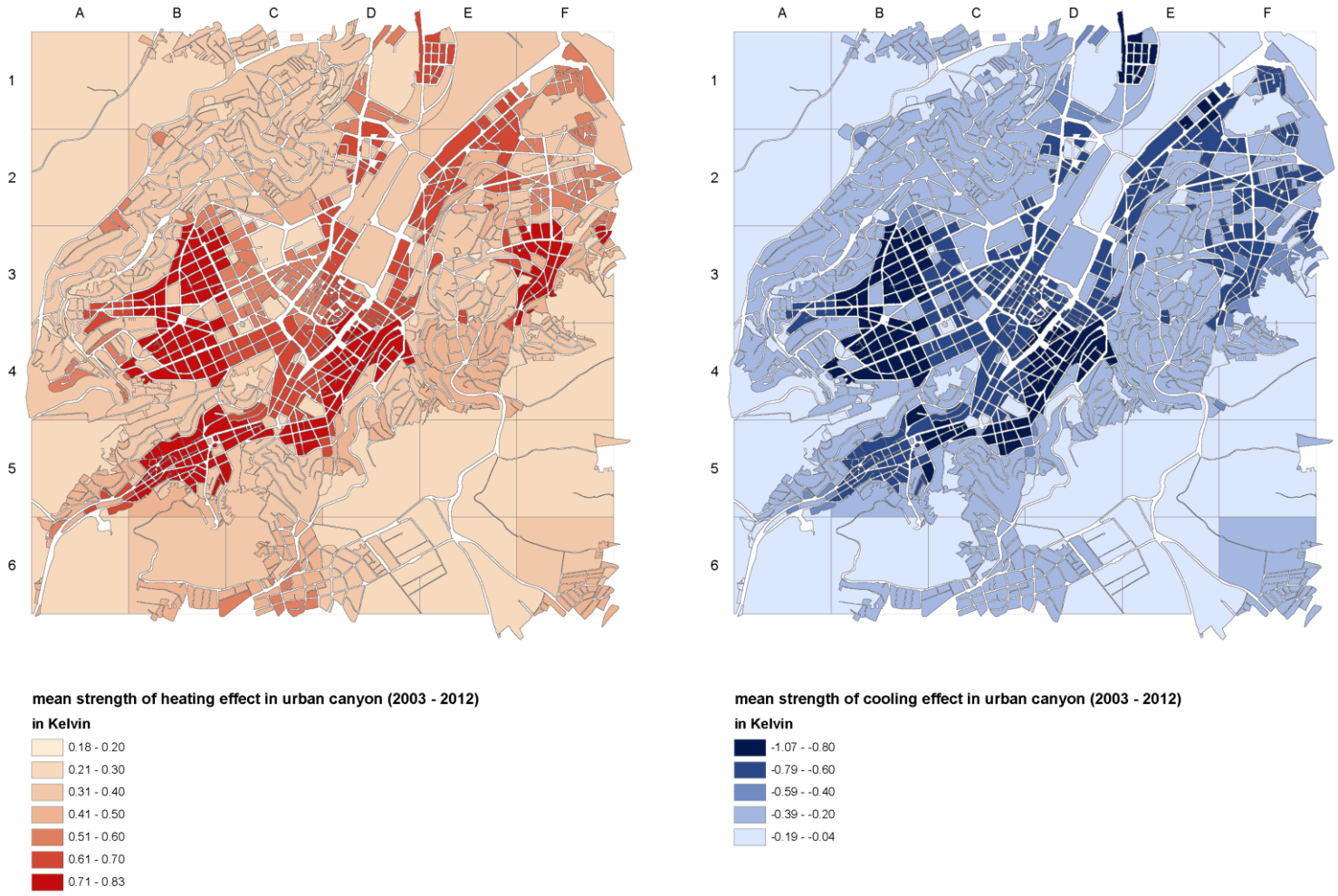

Figure 81: The average strength in Kelvin of the warming of the urban canyon for Stuttgart inner city for the period 2003 – 2012 (TEB calculation)

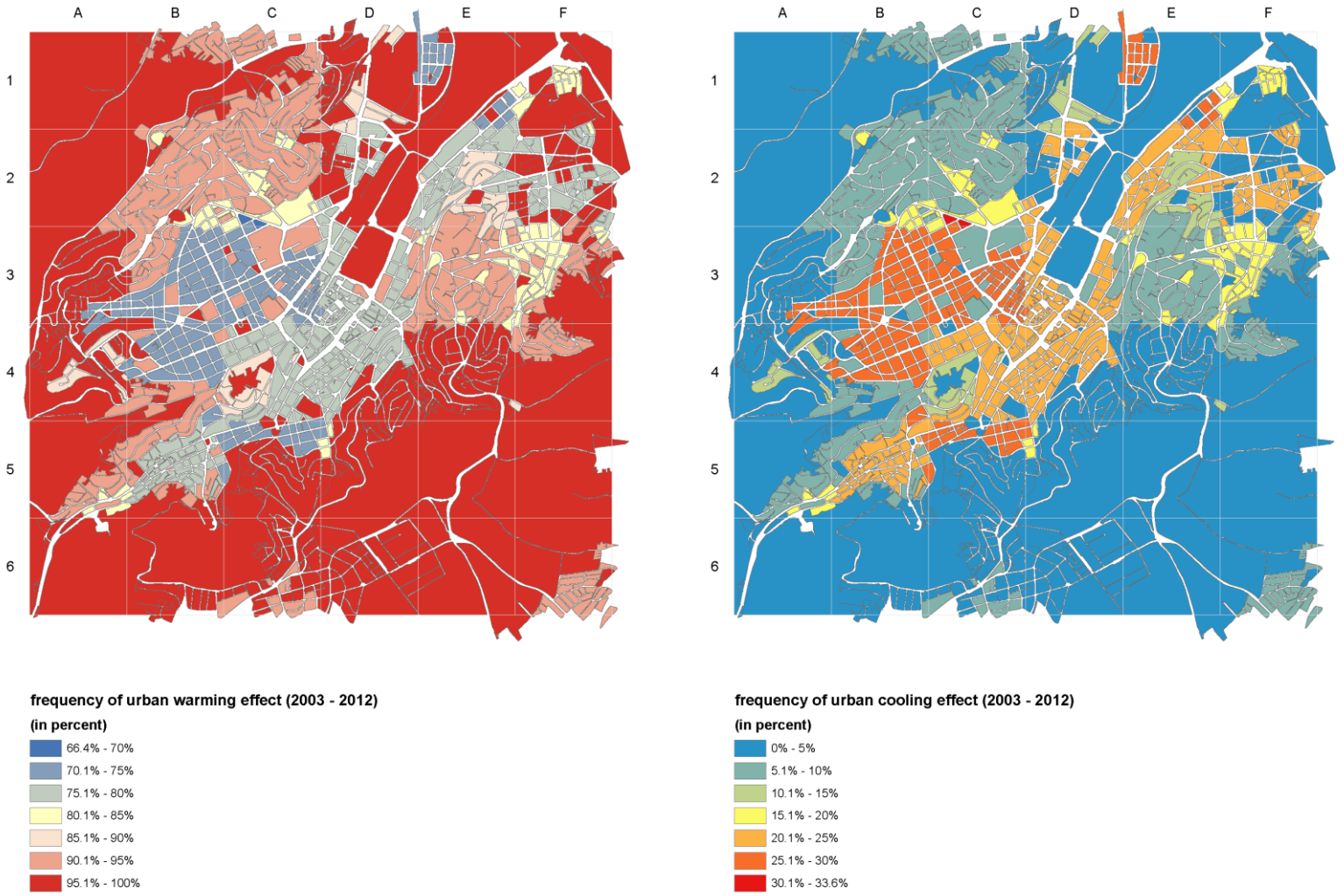

Figure 82: The frequency in hours of the warming of the urban canyon for Stuttgart inner city for the period 2003 – 2012 (TEB calculation)

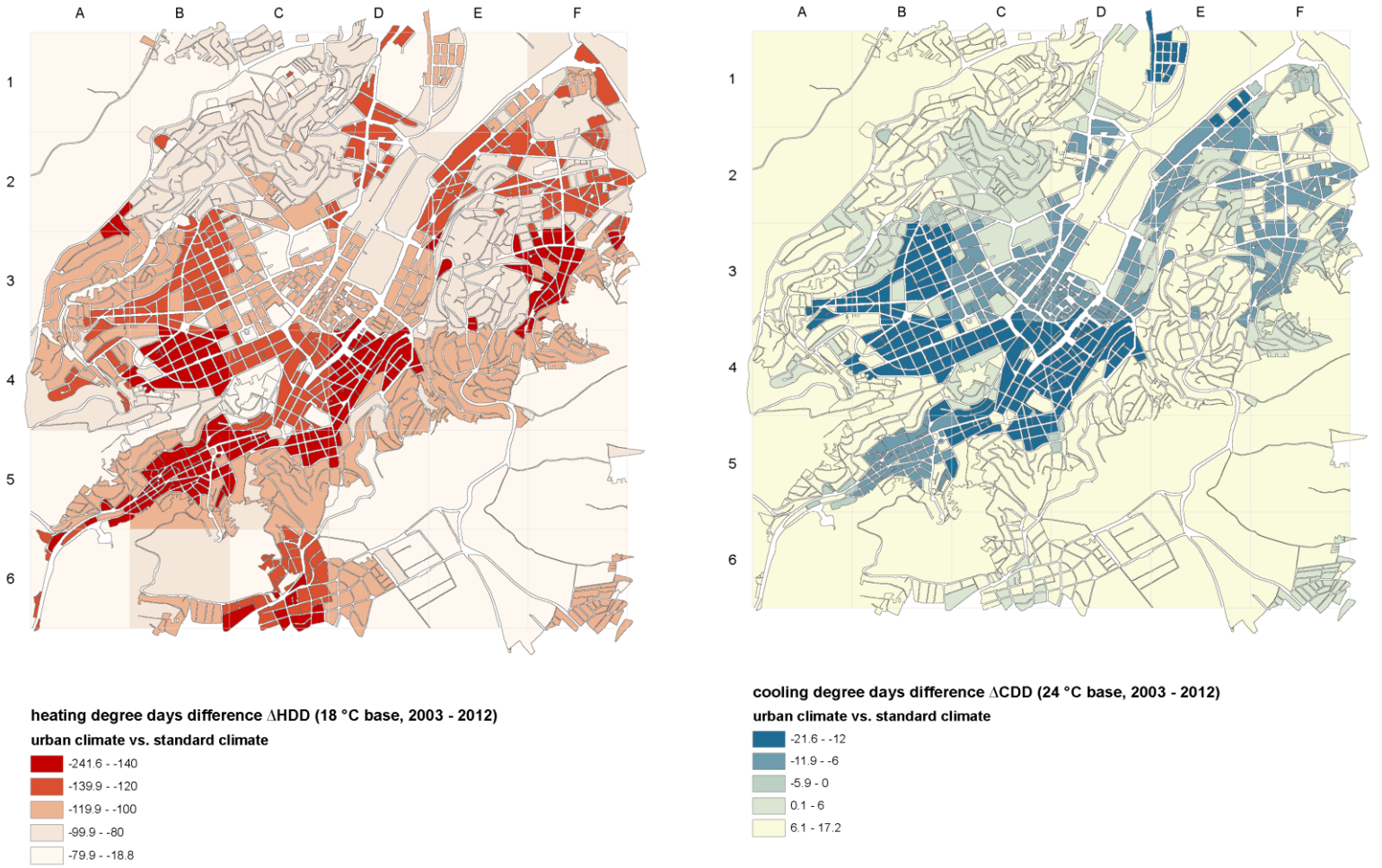

Figure 83: The difference in the heating and cooling degree days (ΔHDD, ΔCDD) between urban climate and standard climate boundary conditions in Stuttgart inner city for the period 2003 – 2012 with isotherm representation (TEB calculation)

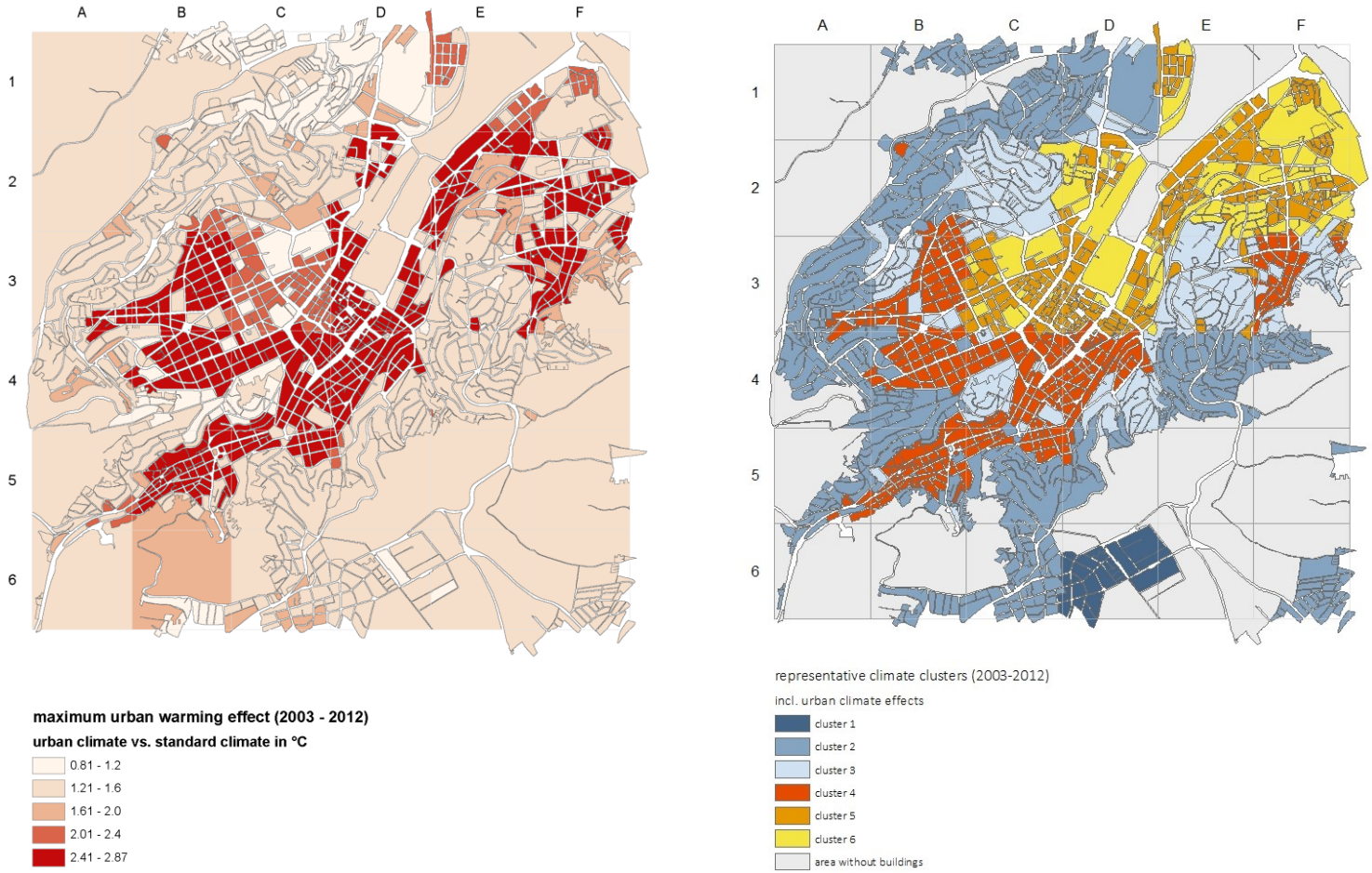

Figure 84: The maximal urban warming of the urban canyon (left) and representative climate clusters (right) in Stuttgart inner city for the period 2003 – 2012 (TEB calculation)

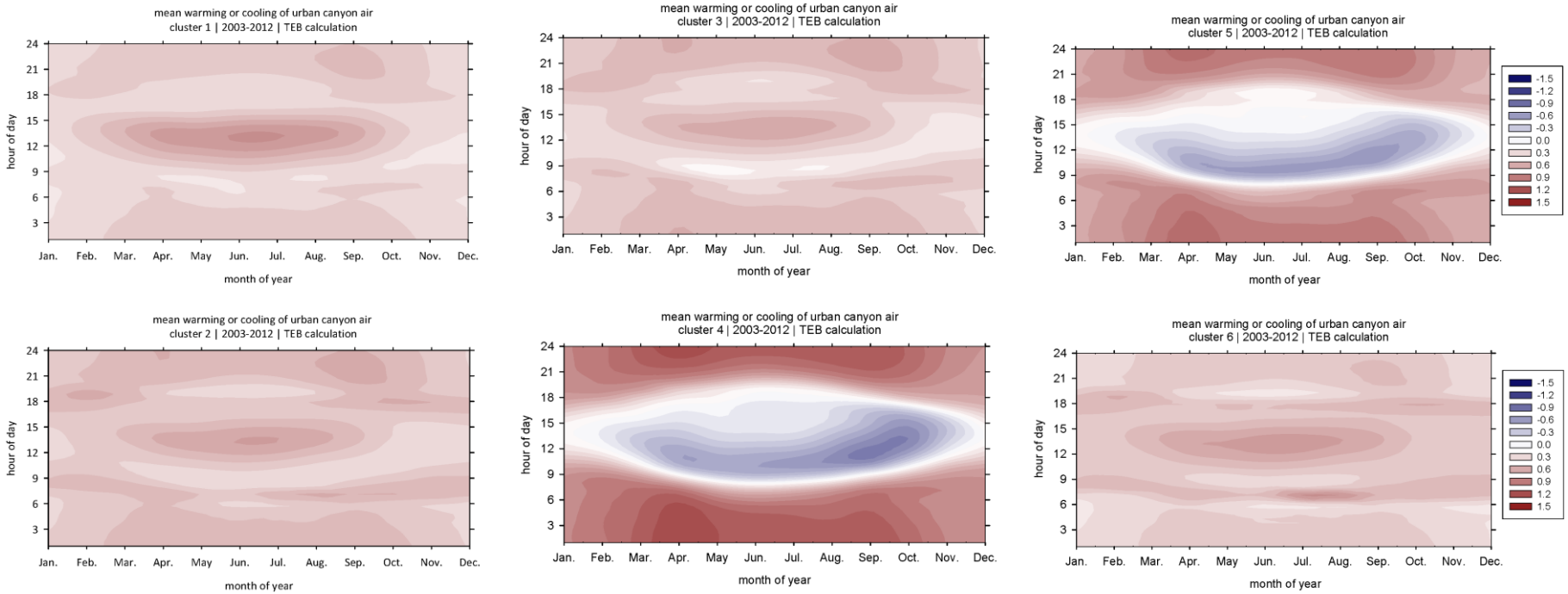

Figure 85: Average daily cycles throughout the year of the urban warming or cooling of the urban canyon air for representative climates gathered with the cluster analysis in Stuttgart inner city for the period 2003 - 2012 (TEB calculation)

5. THE RESULTS ABOUT THE BUILDING ENERGY DEMAND

Following the generic investigation concept presented in section III - 1.1 (p 171), the results about the useful heating and cooling energy demand could be calculated at building level as illustrated exemplarily in Figure 86[14]. Yet, for better legibility of these findings and better linking to the inputs in section 0III - 3.2, the next graphs depict the results at city block level.

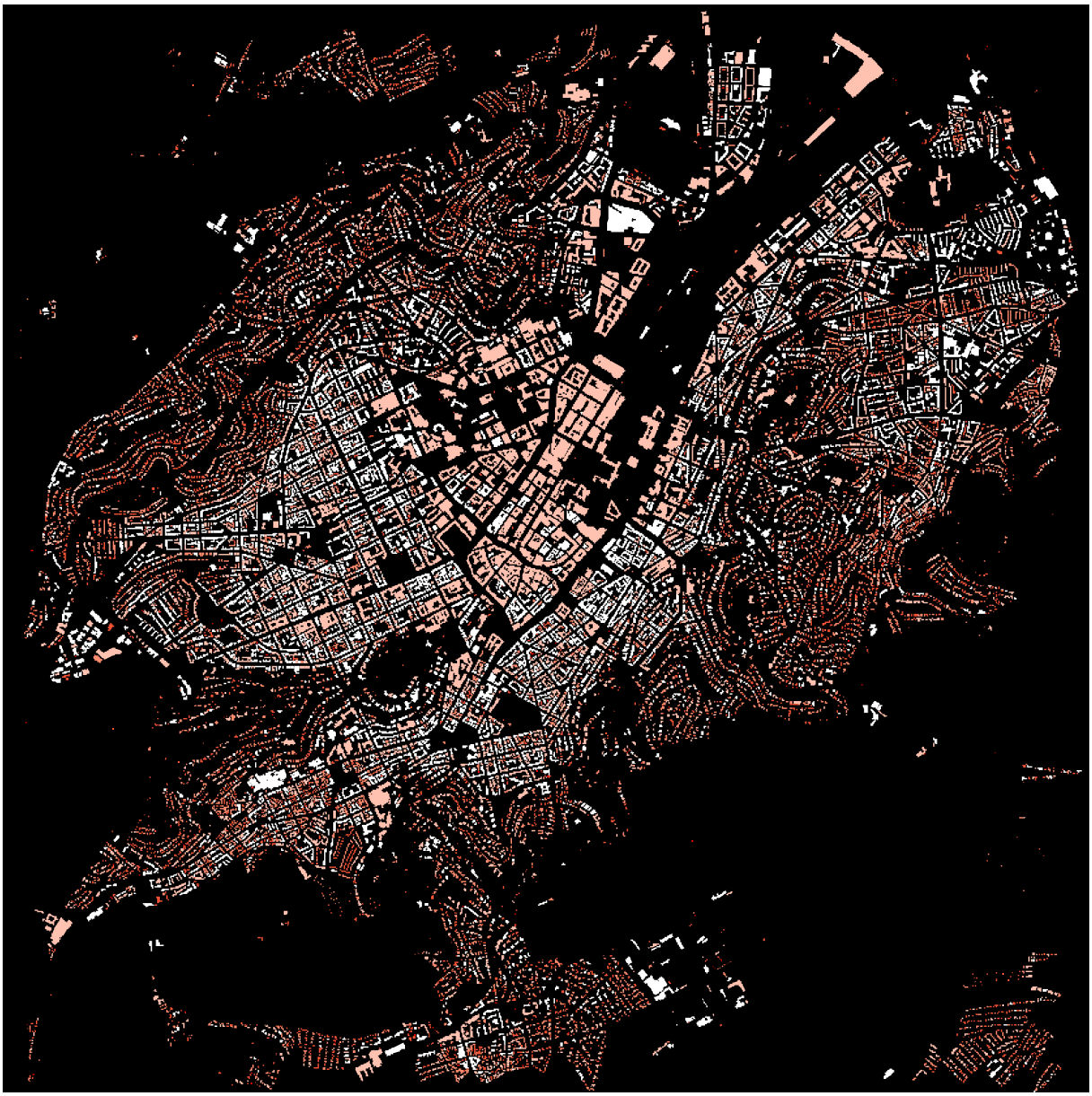

Figure 86: Overview on the useful heating energy demand of Stuttgart city at building level as calculated by TRNSYS and using climate data adjusted with TEB

[14] This Figure does not represent a violation in data protection because these calculations are based on numerous theoretical assumptions. In addition, the scale legend has been deliberately omitted.

5.1. The DOE Statistical Analysis of the Building Energy Demand

Table 50 shows an example of the statistical regression of the results obtained with TRNSYS computations for two contrasting clusters, 2 and 4 for residential and no-residential use. Linear regression technique was used in quantifying each dependent variable and inspecting their connection with heating or cooling. The so-called dependent variables, were defined in the experimental plan as 3-steps parameters (coded -1, 0, +1). This regression shows all the variables that have an impact on the heating or cooling energy requirements, and is sorted in a descending order according to the importance of their effect. These effects are twofold, either main effects (i.e. for one variable such as U, V or V^2) or a 2-way interaction between two variables (such as VU, SU, etc.). The coefficient of determination R^2 (or adj.-R^2 in its adjusted form) gives in percentage the amount of impact of each variable or 2-way interaction. Successive models with increasing dependency factors and accuracy are listed. The last models (N°10 for heating and N°8 for cooling) show the best possible score. For cluster 2 and residential use, an adj.-R^2 of 96.3% for heating, and 93.4% for cooling state for a very high fit rate and minimal unexplained variance. The adjusted R^2 is slightly lower for cooling, possibly due to the temperature-dependent air ventilation, which is activated in a certain range of indoor increase in air temperature. For the cluster 2 and residential use, the heating demand is ascribed the thermal quality of the building envelope, given by the U-value, with 46.0% responsibility in the final result, followed by the building volume V and their Interaction UV with 27% and 10.8% respectively. All other factors of influence are below 10% and thus have lesser impact. For cooling, the U-value is the most important with an adj.-R^2 of 81.8%, including the main effect as well as the square term U^2 at 19% stating for non-linear effect. No particular difference in the decisive variables and their hierarchical order is found between the clusters and the type of use. The proportion of the window area C, the building volume V and the street aspect ratio A play a minor role. The B-coefficients then quantify the respective variables and so provide the transposable polynomial formula. The positive or negative sign of the B-values gives information on whether the variable increases or decreases the energy demand depending on the coding adopted in the experimental design (-1, 0, +1). The actual energy needed for each building in the city is calculated using the corresponding polynomial formula generated by this statistical analysis by using the building's own real values for U, V, S, W and A, after conversion in their coded form (range between -1 and +1).

The DOE statistical analysis, as described above, best explains the next few figures for heating and cooling energy demand maps in their dependence upon the thermally characterising urban and building parameters listed in section III - 3.2 (p 183).

Table 50: Example of a statistical analysis for useful heating and cooling energy demand in case of residential and non-residential use in Stuttgart for the climate cluster N°2 (sloped edges with sparse construction) and cluster N°4 (dense city centre) for the period 2003 - 2012

urban climate cluster 2

heating | residential use

useful heating energy Qheat (2003 - 2012)

model #	Adjusted R^2	R^2 Change			Variable	B Coeff.
					(Constant)	117.266
1	0.460	0.467			U	141.234
2	0.730	0.270			V	-107.346
3	0.838	0.108			VU	-83.088
4	0.894	0.055		Model	V^2	83.851
5	0.920	0.026		10	W	33.039
6	0.939	0.019			S	28.603
7	0.949	0.010			SU	25.283
8	0.955	0.005			VW	-18.772
9	0.959	0.004			SV	-16.873
10	0.963	0.004			WU	15.965

heating | non-residential use (typical)

useful heating energy Qheat (2003 - 2012)

model #	Adjusted R^2	R^2 Change			Variable	B Coeff.
					(Constant)	127.84
1	0.426	0.433			U	179.08
2	0.713	0.287			V	-145.88
3	0.830	0.117			VU	-113.79
4	0.892	0.060		Model	V^2	115.87
5	0.916	0.024		10	W	42.43
6	0.932	0.016			S	34.44
7	0.942	0.010			SU	33.12
8	0.949	0.007			SV	-27.23
9	0.955	0.006			VW	-25.78
10	0.960	0.005			WU	24.40

heating | residential use

useful cooling energy Qcool (2003 - 2012)

model #	Adjusted R^2	R^2 Change			Variable	B Coeff.
					(Constant)	0.49
1	0.628	0.633			U	-1.77
2	0.818	0.190			U^2	1.68
3	0.854	0.037		Model	WU	0.52
4	0.890	0.036		8	VU	-0.51
5	0.923	0.033			V	0.40
6	0.929	0.006			W	-0.17
7	0.932	0.003			SV	-0.16
8	0.934	0.003			UA	0.16

heating | non-residential use (typical)

useful cooling energy Qcool (2003 - 2012)

model #	Adjusted R^2	R^2 Change			Variable	B Coeff.
					(Constant)	2.84
1	0.485	0.492			U	-9.33
2	0.623	0.140			U^2	8.63
3	0.708	0.087		Model	VU	-4.81
4	0.785	0.076		8	V	3.67
5	0.834	0.049			WU	3.60
6	0.866	0.032			W	-2.36
7	0.873	0.008			V^2	-2.12
8	0.880	0.008			SU	-1.46

climate cluster 4

heating | residential use

useful heating energy Qheat (2003 - 2012)

model #	Adjusted R^2	R^2 Change			Variable	B Coeff.
					(Constant)	111.876
1	0.460	0.467			U	135.381
2	0.730	0.269			V	-102.812
3	0.838	0.108			VU	-79.661
4	0.894	0.055		Model	V^2	80.279
5	0.920	0.026		10	W	31.776
6	0.939	0.019			S	27.341
7	0.949	0.010			SU	24.220
8	0.955	0.006			VW	-18.074
9	0.959	0.004			SV	-16.030
10	0.963	0.004			WU	15.402

heating | non-residential use (typical)

useful heating energy Qheat (2003 - 2012)

model #	Adjusted R^2	R^2 Change			Variable	B Coeff.
					(Constant)	121.81
1	0.425	0.432			U	171.65
2	0.712	0.287			V	-140.03
3	0.830	0.117			VU	-109.46
4	0.891	0.060		Model	V^2	111.26
5	0.916	0.024		10	W	40.89
6	0.932	0.016			S	32.90
7	0.942	0.010			SU	31.68
8	0.948	0.007			SV	-26.06
9	0.954	0.006			VW	-24.91
10	0.960	0.005			WU	23.66

cooling | residential use

useful cooling energy Qcool (2003 - 2012)

model #	Adjusted R^2	R^2 Change			Variable	B Coeff.
					(Constant)	0.47
1	0.639	0.643			U	-1.84
2	0.826	0.188			U^2	1.73
3	0.860	0.035		Model	WU	0.52
4	0.891	0.032		8	V	0.41
5	0.922	0.030			VU	-0.49
6	0.931	0.009			W	-0.22
7	0.933	0.003			SV	-0.16
8	0.936	0.003			UA	0.16

cooling | non-residential use (typical)

useful cooling energy Qcool (2003 - 2012)

model #	Adjusted R^2	R^2 Change			Variable	B Coeff.
					(Constant)	2.84
1	0.486	0.492			U	-9.47
2	0.622	0.139			U^2	8.71
3	0.705	0.084		Model	VU	-4.80
4	0.780	0.075		8	V	3.70
5	0.828	0.048			WU	3.60
6	0.861	0.033			W	-2.45
7	0.870	0.010			SU	-1.62
8	0.877	0.008			V^2	-2.14

5.2. The Useful Energy Demand for Heating and Cooling

The useful energy demand for each single building as reported below is calculated with one of the 72 statistically based polynomial formulae, depending on the corresponding case (standard or urban climate background, cluster 1 to 6, 3 types of use, target key metric heating or cooling). These data are then grouped accordingly in city blocks and displayed in maps.

Figure 87 (left) shows the specific useful energy demand for heating Q_{heat} for the decade 2003 - 2012. The useful heating energy Q_{heat} can reach 415 kWh m^{-2} a^{-1} for a few houses on the outskirt slopes of the study area due to the poor thermal insulation assumed from their old age, otherwise the heating demand lies mostly between 44 and 163 kWh m^{-2} a^{-1} for about 80% of the total city blocks. Heating demand is lowest for large buildings with very good thermally insulated building envelope, which predominantly occur in inner urban areas (cf. Figure 80).

Figure 87 (right) depicts a reverse situation, where the residential areas have low need for cooling by the fact that residential areas on the slopes undergo much transmission heat loss through their poorly insulated building envelopes. Whereas the inner city areas have more need for cooling, because they are better insulated. An amplifying reason for increased cooling energy requirements is the large proportion of window area.

In order to find out the extent to which the urban climate has played a role in the resulting indoors energy demand, a comparison with the results based on the reference rural climate is undertaken. Figure 88 illustrates this difference in the heating ΔQ_{heat} and cooling ΔQ_{cool} energy demand which is expressed as absolute values in kWh $m^{-2}a^{-1}$, whereas Figure 89 depicts the values in percentage %.

So, Figure 88 (left) reveals that by taking urban climate effects into account, it always lead to less demand on heating by up to -21 kWh $m^{-2}a^{-1}$. This is mostly visible where buildings are less properly insulated (mostly cluster 2, cf. Figure 84) and already experience high heating energy demand (cf. Figure 87). In most other areas the difference is clearly negligible lower than -6 kWh $m^{-2}a^{-1}$. Indeed, when thermal insulation is insufficient, the impact of the outdoor climate boundary condition is greater on the indoor spaces, because the outdoor - indoor thermal exchange is stronger through the building envelope. Yet, considering the relative change in the heating energy demand (expressed in percentage) (Figure 89, left) a very different picture is revealed, which points out the densest urban areas with most urban microclimate deviation as being the most affected (i.e. cluster 4, cf. Figure 84). This means that provided that the construction properties of the building are similar (e.g. thermal insulation level), urban climate microclimate effects are clearly visible in the energy demand for heating as pre-

viously discussed in the theoretical part.

Figure 88 (right) and Figure 89 (right) illustrate the effects of urban climate on the indoors energy demand for cooling (ΔQ_{cool}). These effects can be positive (less energy demand) or negative (more energy demand) ranging between -0.09 and 2.52 kWh $m^{-2}a^{-1}$ and this in accordance with the prevailing warming or cooling of air as reported in Figure 81. Yet, the negative values are little below 1 kWh $m^{-2}a^{-1}$ which mostly occur in dense urban areas (cluster 4). The highest values of ΔQ_{cool} occur for the cluster 6 because of the additional warming of air due to strong anthropogenic heat release from traffic.

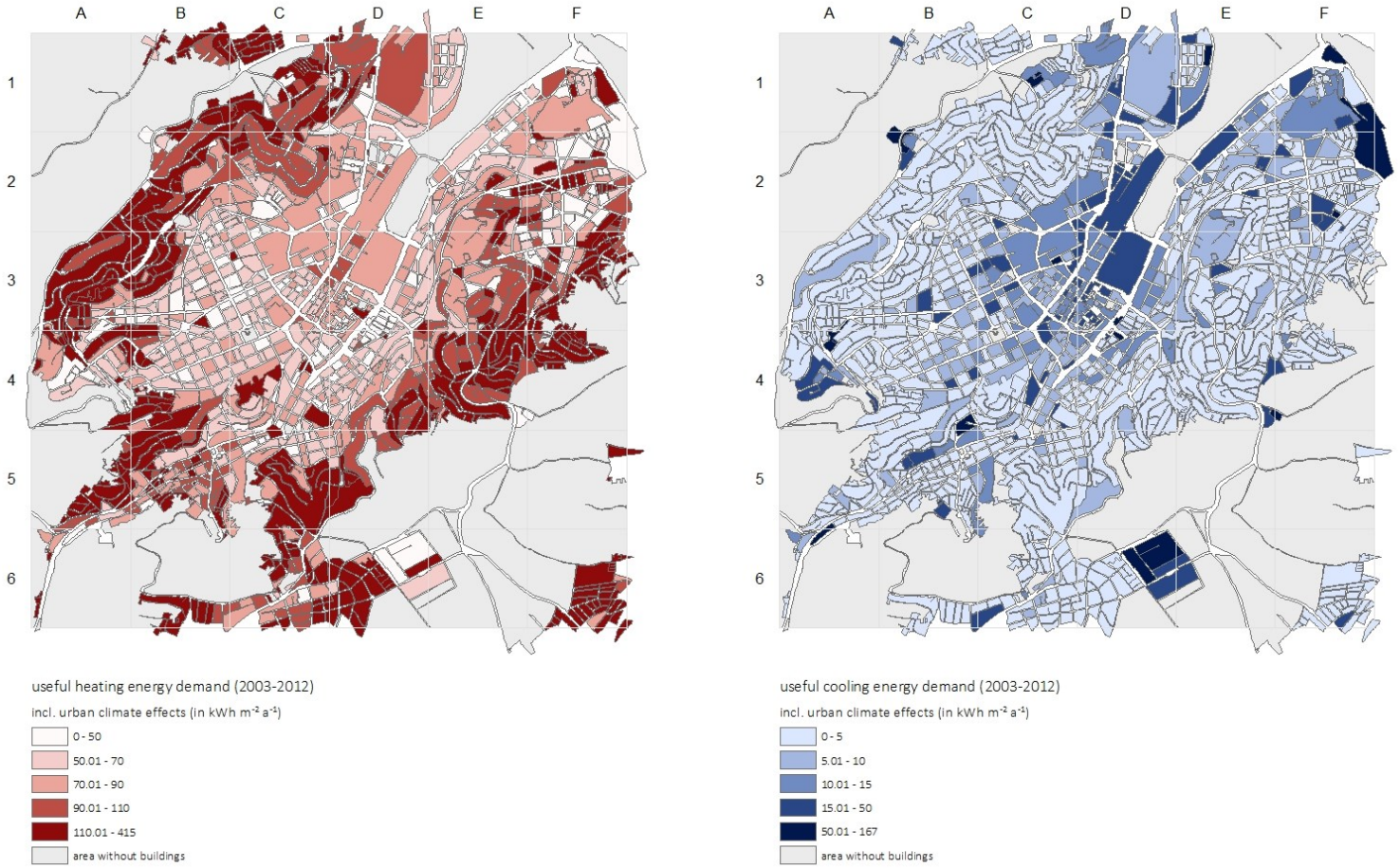

Figure 87: The useful heating energy demand Q_{heat} (left) and cooling energy demand Q_{cool} (right) in kWh m^{-2} a^{-1} for Stuttgart inner city for the period 2003 – 2012 (TRNSYS calculation)

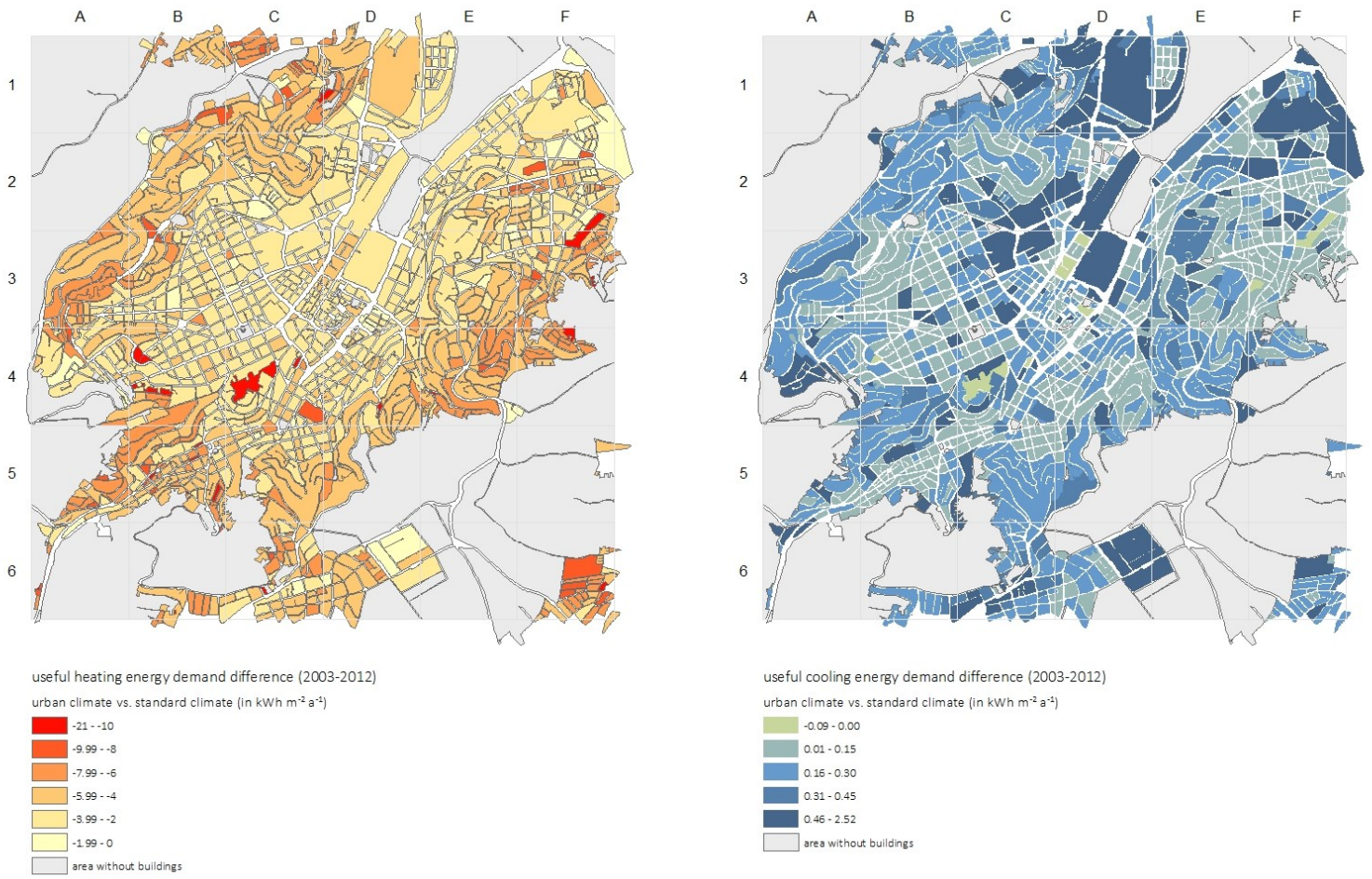

Figure 88: The useful heating energy demand difference ΔQ_{heat} (left) and cooling energy demand ΔQ_{cool} (right) in kWh m^{-2} a^{-1} for Stuttgart inner city for the period 2003 – 2012 (TRNSYS calculation)

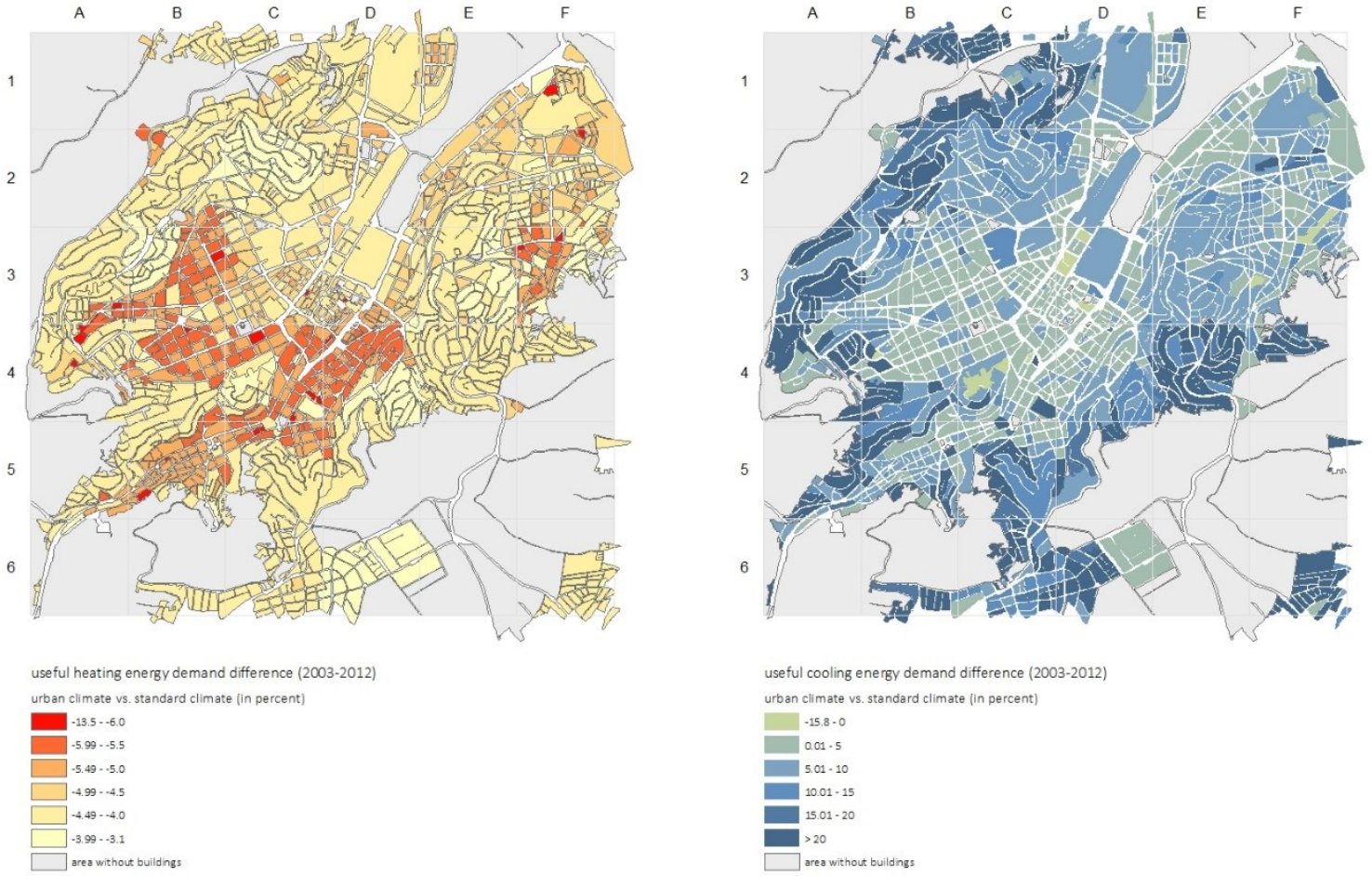

Figure 89: The useful heating energy demand difference ΔQ_{heat} (left) and cooling energy demand ΔQ_{cool} (right) in kWh m^{-2} a^{-1} for Stuttgart inner city for the period 2003 – 2012 in percentage % (TRNSYS calculation)

5.3. Validation of the Results

The investigation method developed in this research is applied on a vast real study area for the first time. In the absence of comparable studies from the literature, these results are new and at the same time not easy to compare. Nevertheless, an approach for attempting a first validation was identified and is presented hereafter.

One possibility for method validation is to juxtapose the calculated results with the energy atlas of the city of Stuttgart (Klimaatlas Stuttgart 2008), which provides actual energy consumption. However, this energy map is from 1995 and thus considered with care as an approximate picture of the reality. It is also only about heating energy. Figure 90 puts the calculated annual heating energy demand for the decade 2003 - 2012 and the energy map of 1995 for the study area of 36 km^2 side by side. Figure 91 shows the same comparison for the most central part of Stuttgart of 4 km^2 area. The energy map is available in terms of final heating energy density i.e. relating to the city block base area and so the calculated values were adapted accordingly, which includes a factor of 1.15 for converting useful energy into final energy. The calculated results give a similar picture and reflect the values in that energy map quite well. Given the high complexity of the task, including a heterogeneous city structure, the large number of parameters to account for, e.g. related to the buildings operation, as well as a certain limitation in the background source data, this finding clearly attests to the suitability of this generic investigation method and therefore constitutes a major outcome of this research work.

For the observed discrepancies, several possible causes can be named which are discussed below. One major difference detected in Figure 90 is that the residential areas on the outskirt slopes appear to be much warmer. This is probably due to i) the adoption of a systematic target indoor temperature of 20 °C, ii) systematic assumption of a daily usage period from 6:00 to 23:00 for the entire house, including the secondary rooms, iii) a constant ventilation rate of 0.79 h^{-1} for poorly insulated houses, which is mostly the case in this location according to the available information on the year of construction or renovation. These assumptions being kept identical for every day are possibly exaggerated when cumulated over the simulation period, considering the individual user behaviour (motivation for energy savings, periods of absence, thermal comfort preferences, irregular ventilation, etc.). For non-residential buildings, the HVAC settings are decisive as well. Even though simulating complex operation plans is feasible in TRNSYS thanks to its in-stationary dynamic calculation capabilities, however, information on real operation patterns is lacking. Instead, simple assumptions were made based on

stationary guidelines from the thermal regulation in force and this certainly explain part of the variance in the related areas.

The two results series (calculated and recorded) need to be represented on exactly the same city block map, i.e. with the same block boundaries to make them fully comparable. However this could not be ensured systematically. The map from the energy atlas of 1995 is not current whereas the city block map used in the course of this project is up-to-date, including a subsequent control and correction of the city block boundaries in order to make the map compliant with the 2D city plan; for example, when new buildings are modified or form a new city block. In this work, city blocks are defined by the streets as delimiter, whereas the energy atlas map sometimes split one city block in parts by following the buildings boundaries. The energy atlas map was reconstructed from tables, one list the energy values and the other list city block coding. This coding has changed once and might be inaccurate in a few cases.

Further reasons can be named, which may help understand the differences between the calculated results and the energy atlas map provided by the city of Stuttgart. The calculations were based on 2D and 3D city maps of 2012, whereas the energy atlas map refers to a city development state of 1995 which is not known to allow a retrospective comparison. The number of storeys were roughly determined assuming uniform constant values of floor height for residential (3.0 m) and non-residential (3.8 m) buildings, while more variety is expected to exist in reality. The thermal insulation of a building, which appeared to be a very sensitive variable, is set depending on its construction year and late renovations following the AWU German building typology catalogue in the absence of better references. The current state of the thermal quality of the buildings is not always documented with confidence depending on possible late renovations. No detailed information is available on how the data of the energy atlas map were gathered, making this source of information indicative.

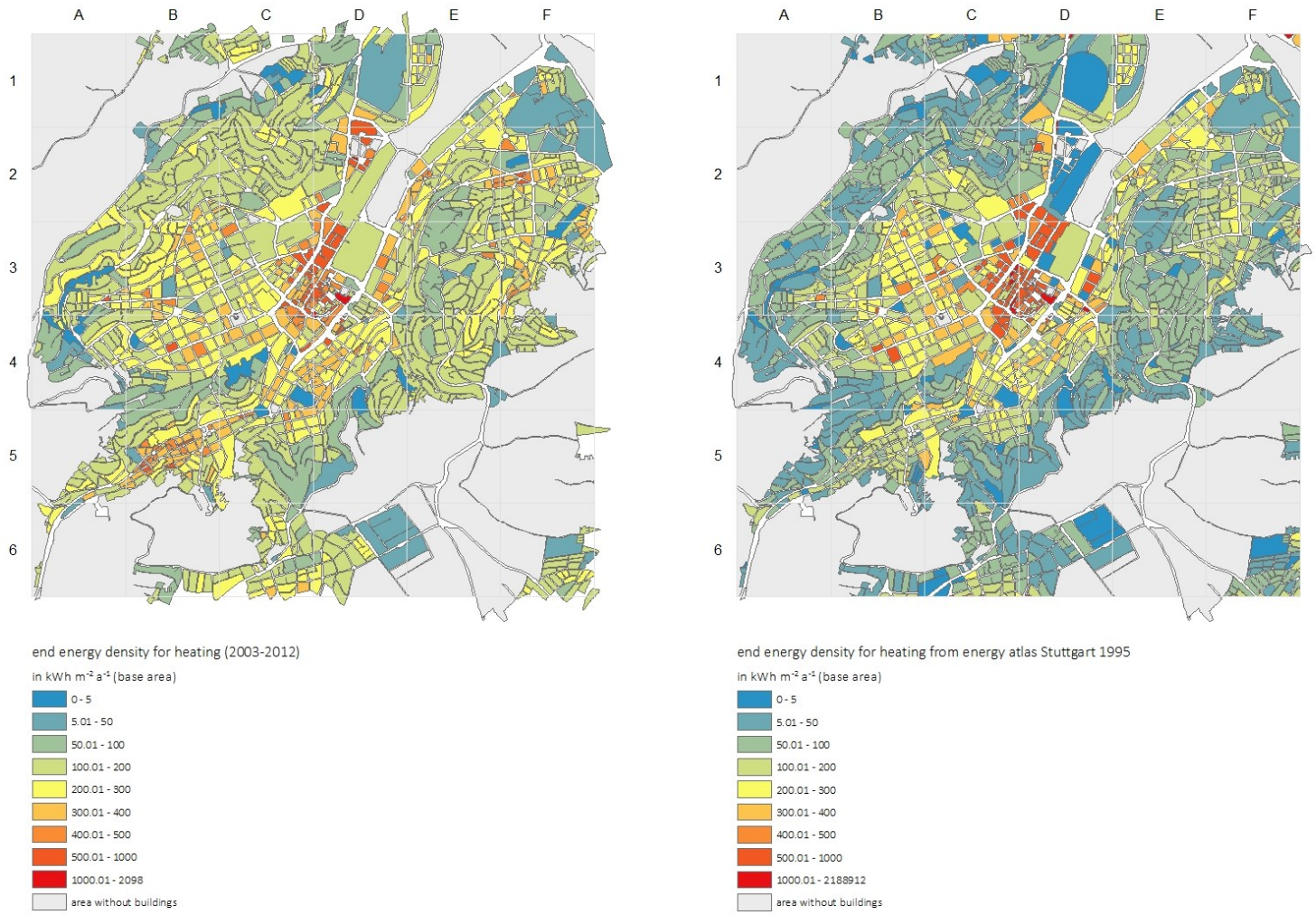

Figure 90: Comparison of the TRNSYS calculated energy demand for heating with the consumption values of the energy atlas (dated 1995) in Stuttgart inner city for the period 2003 – 2012

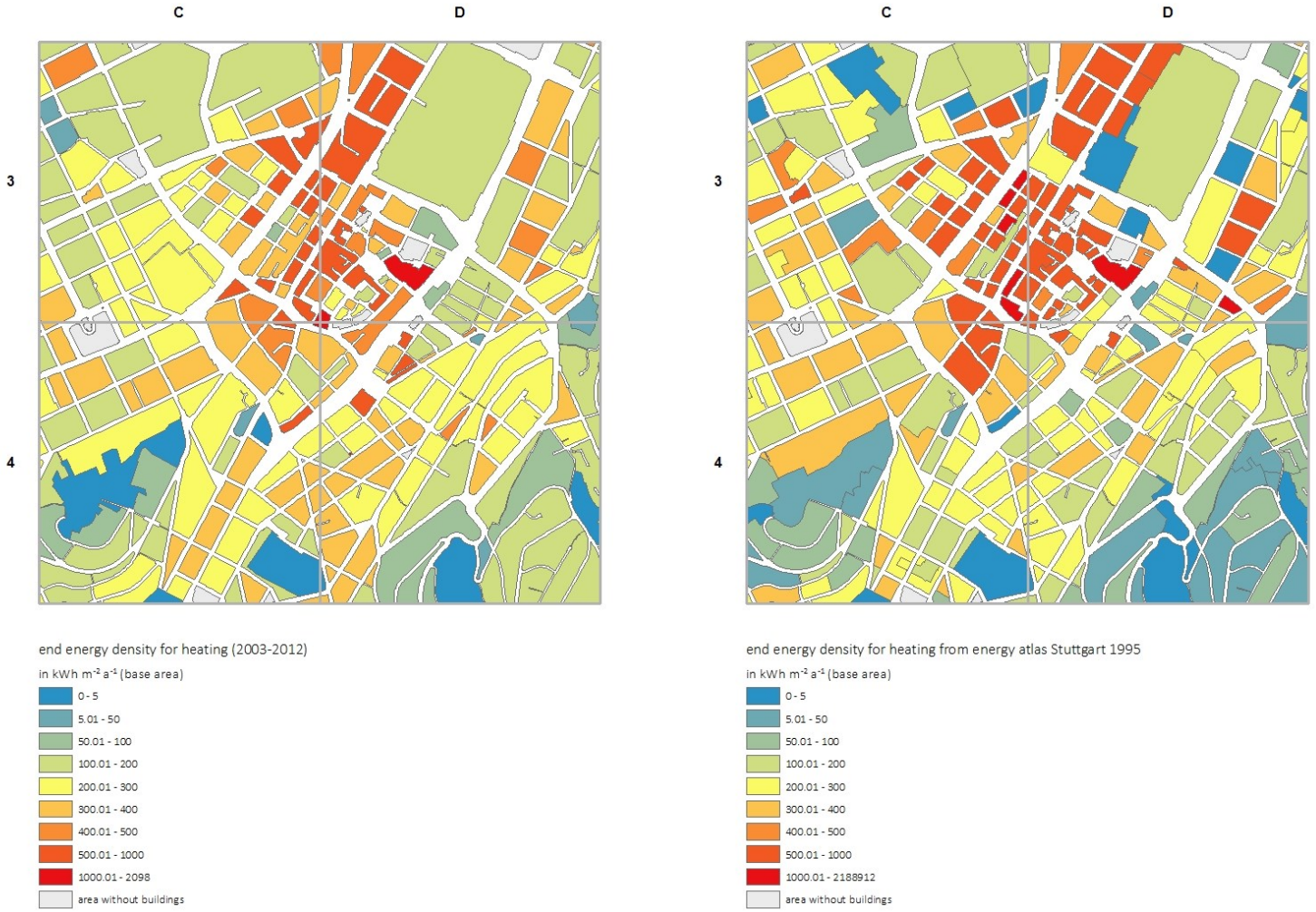

Figure 91: Excerpt of Figure 90 giving the comparison of the TRNSYS calculated energy demand for heating with the consumption values of the energy atlas (dated 1995) in Stuttgart inner city for the period 2003 – 2012 for the central area of 4 km^2

IV

SUMMARY, OUTLOOK AND CONCLUSION

1. SUMMARY OF THE FINDINGS

This executive summary recalls the guiding thread of the work and underlines its major findings. The reference made to particular sections in the main report better illustrates this synopsis.

1.1. Method Suitability: TEB, TRNSYS, DOE and GIS

This research addressed the question of gathering new knowledge about the prediction of the energy performance of buildings when these are explicitly located in urban areas. This means to account additionally to the building's construction and operation for the three-dimensional surrounding physical obstructions and locally developing urban microclimates as boundary conditions. Answering this question put methodological aspects in the foreground. It was about combining several computational models and techniques in order to master an interdisciplinary subject, involving both urban and building physics. The chosen method combined the urban canyon model TEB, the in-stationary building energy model TRNSYS, the statistical design of experiments DOE, and the geographic information system techniques GIS. See section I - 3 (p 55).

In PART I, the package TEB, TRNSYS and DOE was first applied on theoretical objects (i.e. urban structures and office buildings) with the aim of understanding the logic of formation of urban microclimates and the dependence of the energy demand indoors for keeping thermal comfort on those particular outdoor conditions. The focus thereby was put on investigating the modifying effects of selected thermo-physical properties of city structures and buildings by setting them as variables in systematic DOE experimental plans. A special attention was dedicated to an accurate modelling of the objects and their dynamic simulation, both outdoors (using TEB) and indoors (using TRNSYS) in order to make the results fully understandable and useful for some generalisation. This first stage of work provided quantitative results on complex interdependences. See section II - 2 (p 97) for the urban microclimate and section II - 3 (p 125) for the building energy demands.

Secondly, this investigation method was extended in PART II to the use of GIS techniques for an application on a real case study, i.e. the city of Stuttgart, in order to handle its widespread spatial scope. This practical part not only demonstrated the appropriateness of the method and confirmed the results of the theoretical part. In fact, it also provided answers related to the imperatives of real conditions including: 1) complex urban structures and buildings requiring appropriate thermally relevant characterisation and modelling, 2) a high spatial resolution dictated by the site-embossed topography and 3) a high temporal resolution applied to long-

term periods, necessary for dynamic building energy assessment. Refer to sections III - 2, p 176 and III - 3, p 182.

In PART I, the applied method proved suitable thank the compatible features of TEB and TRNSYS (required inputs, description of objects, processing times, etc.). The investigation method took advantage from the simplicity of TEB and the complexity of TRNSYS making the whole investigation timely manageable. In spite of its simple concept, TEB captures the most relevant energetic processes, which explain the formation of an urban microclimate as already confirmed in the published literature by several validation studies and by the inspiration role TEB played for other models (see section I - 2.3, p 35). By contrast, the complexity of TRNSYS allowed a precise modelling of the thermal behaviour of the building including a detailed physical description and operation. For instance, the building envelope modelling includes all thermally decisive features (e.g. thermal insulation, thermal inertia and window ratio). Moreover, the building was simulated at hourly basis for one year and was not analysed as one bulk volume but differentiated in offices at various floor levels. The HVAC operation scenarios strived to be realistic including the user behaviour. The use in TEB and TRNSYS of systematic DOE experimental design plans, which allow for sound statistical post-processing, facilitated greatly the quantitative interpretation of huge amounts of results and enabled some generalizations.

In PART II, the additional use of GIS techniques proved efficient in both pre-processing of urban and building data as well as in the post-processing of the results related to microclimate and building energy simulations. By this means, the multi-scale nature of this research stretching from individual buildings to an entire city could be mastered. The description of the 75 000 individual buildings by means of a generic thermally relevant characterisation solved the problem of their impracticable modelling using real geometric and constructive properties. This approach contrasts with the usual handling in terms of urban and building typologies, which results are specific and hardly transferable. In conjunction with partial factorial DOE plan matrices, this generic approach allowed manageable calculation times of all buildings in TEB and TRNSYS without loss in accuracy. A further motivation for using such a generic DOE modelling is the possibility to update the results in case building or city data change later. For example, provided better building information is subsequently available, e.g. about the thermal insulation or the window ratio, the indoor energy requirements from the previous encoded calculations can be calculated again using the corresponding statistical mathematical models with no need for new simulations.

Moreover, the work on the city of Stuttgart showed a way for handling the prediction of the

thermal and energy behaviour of a large area (36 km^2 were handled here) at high spatial resolution downscaled to individual buildings. The conclusive validation attempt using real values for heating energy consumption revealed a good agreement and hence demonstrated the pertinence of the applied procedure. This generic modelling method can be advised for use at other objects or the concept be embedded in more global models dedicated to city energy assessment including other sectors and fluxes (e.g. transportation and motor traffic, industrial activities, outdoor lighting, etc.) and offers an alternative to overcome the lack of extensive recordings about building energy consumption for large urban areas.

1.2. TEB Model as New TRNSYS Component

This research presented a new format of TEB usable under TRNSYS, without which this research would not have been possible to this extent. As a new TRNSYS component, named TEB-Type 201, the original TEB practicality was substantially improved, including: i) user friendliness, ii) short pre- and post-processing times, iii) consistent and checked inputs, iv) manageable outputs files, v) support of extensive parametric runs and vi) easy installation. Extensive microclimate parameter studies could be conducted using TEB-Type 201, which results were easily transferred to TRNSYS in a next step for dynamic building energy simulations. More about the outlook of this first implementation is available in the section IV- 2.1 below.

1.3. The Urban Canyon Energetics and Microclimate

The energetics and microclimate within the canyon were investigated by means of an extensive sensitivity analysis as well as by an excerpt of simulation runs selected for later use at building level. The analysis focussed on 1) the magnitude and frequency of warming or cooling of in-canyon air (canopy heat and cool islands) and 2) on the energetic and heat fluxes (net all-wave radiation, sensible heat, storage heat, anthropogenic heat, etc.) at the canyon boundaries either taken as a whole or addressed for an individual facet (e.g. walls). The dependence of the energetics and thermal situation in-canyon was investigated in its dependence on the following thermo-physically relevant urban and building parameters: canyon aspect ratio A, roof plan density P, anthropogenic heat (traffic, industry) H, , thermal insulation D (incl. window ratio C), thermal inertia E, shortwave albedo F and longwave emissivity G (see section II - 2, p 97).

A number of microclimate formation patterns could be identified. Increased anthropogenic heat appeared to have major effects in warming the outdoor air. Therefore, instead of using a simple hypothetic daily profile, precise information on real daily, weekly and seasonal cycles

of anthropogenic heat would improve the prediction of urban microclimate effects. The non-availability of such differentiated information from the literature in general and for Stuttgart city in particular impeded a more realistic modelling of this variable, even though it is technically possible using TEB-Type 201. This finding also stresses the importance of accounting for the dynamic heat release from buildings in a coupled urban-building modelling. Urban density, given by the height-to-width ratio H/W also influences greatly the air temperature deviation within the canyon. The vertical profile has the particularity to lead either to warming or to cooling of air depending on the time of day. This is due to the effects of shading from the solar radiation with respect to the sun course path in the daytime and to the reduced sky view factor with respect to nocturnal longwave emitted heat. The thermal inertia appeared to have substantial effects on outdoor microclimate especially in affecting the daily course of air temperature. This finding about the thermal mass effects outdoors corroborates the knowledge already established indoors but is demonstrated for the first time for outdoors. In other words, massive versus lightweight construction lead to different thermal conditions throughout the day within the canyon due to different patterns in the heat charge and discharge at the canyon facets. In fact, high thermal inertia supports more heat storage and limits thereby the increase in the air temperature during the sunlight hours, especially in case of dominant walls fraction given by a high aspect ratio. Low thermal inertia, by contrast, leads to little increase in the canyon air temperature in the daytime because of lacking heat charge in the walls. At night, the situation is correspondingly reversed: a typical nocturnal heat island is found in case of massive construction due to important heat release, whereas lightweight canyons experience little heat island because of less stored heat available for discharge. Nocturnal canopy heat island is therefore much visible in case of massive construction than lightweight construction. This situation will not only affect the thermal behaviour of buildings, it has also consequences on outdoor thermal comfort. The thermal insulation revealed to have an impact on the canyon air temperature, even though less pronounced. Weak thermal insulation leads to a greater outdoor – indoor heat exchange, so that the indoor heating affects more the outdoor climate in this case. Inversely, good thermal insulation reduces the quantity of additional heat into the canyon system originating from the buildings. The influence of the thermal insulation is greater in deep canyons because of the dominating wall surface fraction. The radiative properties of the canyon surfaces (albedo, emissivity) appear to affect clearly the urban air temperatures provided the investigated large scopes of 0 to 0.5 for the albedo and 0.5 to 1 for the emissivity. Lower albedos and higher emissivities lead to a warming of the canyon air. However, smaller variations of these quantities, e.g. lower or up to ± 0.1, are

expected to have limited impacts. See sections II - 2.1 (p 98) to II - 2.4 (p 109).
Furthermore, the causes underlying the evolution of the canyon air temperatures were identified by looking at the energy balance of the canyon system and walls as daily cycles for selected seasons and as year average. The aspect ratio shows differences in the magnitudes due to different road and wall fractions, whereas the thermal inertia and thermal inertia shows different shares of sensible versus storage heat throughout the day. Yet, the effects of the thermal insulation are more visible in the cold season due to indoor heating. See sections II - 2.5 (p 115) and II - 2.6 (p 119).

1.4. Effects of Urban Geometry and Building Construction on the Energy Demand

Next to the quantification of the urban microclimates, the energy demand for heating, cooling, lighting and ventilation (if mechanical) of office buildings was investigated in relation to the same urban geometry and building construction indicators under these new boundary conditions (see sections II - 3.1 and 3.2, p 125). The variables investigated in full combinations are the street aspect ratio A, the solar orientation B, the window ratio C, the thermal insulation D, the thermal inertia E and the floor level L. The results revealed large ranges among the set of 162 cases by location. In the temperate mid-latitude Mannheim, the heating is the dominating key metric (3.58 – 60.57 kWh m^{-2} a^{-1}), followed by the lighting (7.95 – 37.21 kWh m^{-2} a^{-1}), whereas the cooling is relatively moderate (2.3 – 18.73 kWh m^{-2} a^{-1}). The ventilation is assumed natural but if mechanical would be comparatively smaller with a maximum of 9.98 kWh m^{-2} a^{-1} and less affected by the variables investigated. The best cases with the minimal heating energy demand are those characterised by the best heat conservative envelope ensured by a high thermal insulation and small openings. These cases, however, are disadvantageous for the lighting because of less daylighting potential. The most demanding in terms of heating are the opposite combinations, i.e. weak insulated and largely glazed buildings. These are then less demanding for lighting because of more solar radiation entering the spaces favoured by larger window area and higher solar and light transmission coefficients (g and τ) induced by lower U-values of the simple glazing. The best combinations of variables are reversed between heating and cooling, e.g. the thermal insulation, but the consequences in terms of magnitude are less pronounced for the cooling. The thermal inertia is more decisive with respect to cooling, with the massive construction being more advisable, whereas its effect on the other key metrics is unclear. The results when expressed in ranking lists of each target key metric pointed out the necessity of finding a compromise with regard to the investigated variables in view of best energy savings because conflictual requirements between the various target key

metrics do occur. However, optimisation with regard to heating energy demand is the priority for the location under study characterised by a cold winter. The urban geometry given by the aspect ratio appeared most influential for the lighting because the reduced sky view clearly reduces the amounts of passive solar gains and hence indoor illuminance. Otherwise, the impact of the aspect ratio is the most visible for the most unfavourable cases with regard to heating or cooling as this increases the indoor-outdoor thermal exchange. The solar orientation has no significant impact as far as average values for the whole building are considered. However, the importance of the aspect ratio and to a less extent the solar orientation could be captured in the comparison by floor or by façade. With increasing H/W, ground floors experience more heating, more lighting, less cooling and less ventilation energy demand in comparison to the upper floors. The magnitudes vary substantially depending on the combinations with the building variables (C, D and E). The largest differences up to atotal of -10.28 kWh m^{-2} a^{-1} occur for the largely glazed buildings with weak thermal insulation (C = +1). The complexity of the matter lies inter alia in the balance between passive solar gains and operation of shading devices both affected by the openness to the sky of the offices.

Given the complexity due to the multidirectional interactions of the studied variables, the DOE statistical analysis proved to be a powerful medium for quantifying their part of responsibility in a hierarchical ranking by highlighting their main effects and double interactions, either linear or not (see section II - 3.2, p 133).

1.5. Effects of the Urban Microclimate on the Building Energy Demand

The deviation in the heating, cooling, lighting and ventilation energy demand was calculated in case of urban microclimate conditions in comparison to rural standard climate conditions. The results for Mannheim (TRY12) revealed that the heating and the lighting are lower under urban microclimate conditions for all building constructions and urban densities. This is attributable to higher urban air temperatures and more solar radiation received by the buildings because of more inter-reflections inside the canyon cavity. The maximum deviation of -3.67 kWh m^{-2} a^{-1} for heating and -3.72 kWh m^{-2} a^{-1} for lighting can be reached. For the same reason, the cooling and ventilation, in contrast, are systematically higher, up to 4.03 and 0.92 kWh m^{-2} a^{-1}, respectively. The magnitudes of deviation depend on the investigated urban and building variables which stress or not the effects of outdoor microclimate boundary conditions on the indoor spaces. The thermal insulation D and the window ratio C appear to be the most decisive with respect to heating deviation for the location investigated. This is mostly visible for the worst cases of highest heating demand for weak insulated buildings and largely glazed

façades. The effects of the urban canyon geometry are evident as well. With respect to lighting, the best energy savings are larger for the cases already benefiting from a high daylighting potential, which advantage is enhanced further under urban microclimate conditions. The best-to-worst energy demand ranking lists for each target key metric enabled the definition of the most critical combinations, either positive or negative. At the same time, they underlined the complexity of the issue and the difficulty of systematic generalisations. The sensitivity analysis about the importance of shading devices efficiency, ventilation rates and internal heat gains due to lighting further stressed the non-absoluteness of the results. A large range of energy demand by key metric is found depending on these settings, This stresses the decisiveness of an appropriate building design as a whole on the one hand and the necessity of careful numerical modelling and interpretation of the thermal behaviour of buildings on the other hand. Therefore, a special attention was put in this report on a detailed description of all assumptions made to ensure a proper analysis. Worth noticing as well, is the fact that the moderate deviation in the energy demands between urban and standard conditions, strongly depend on the assumptions made in TEB simulations for predicting these microclimate changes. For instance, higher levels of anthropogenic heat would have led to higher deviations in energy need indoors due to more pronounced canopy heat islands.

1.6. Mid-Latitude versus Mediterranean Climate Boundary Conditions

The additional investigation of a subtropical location for comparison with the mid-European Mannheim enabled a better understanding to which extent the climate type played a role in the obtained results. The temperate Mannheim and Mediterranean Algiers experience opposite energy requirements for maintaining thermal comfort. The former case is more concerned by heating in the cold season while the latter one must deal with the overheating risk in the warm season. The results confirmed this expectation with the amounts of energy required for heating and cooling being almost reversed between the two locations, yet to somewhat lower amounts for Algiers. The lighting need is lower in the subtropics as expected because of solar radiation is more available, whereas the ventilation showed comparable amounts due to the simulation settings in favour of just necessary air change. However, the best-to-worst energy demand ranking lists revealed similar favourable and unfavourable combinations of the variables A to E for each key metric. When comparing the deviations due to urban microclimate influence, the simulation sets for Mannheim and Algiers showed a number of similar features as well, namely lower heating, lower lighting, more cooling and more ventilation energy demands. However, the consequences as total are clearly different because of their different cli-

mate related design imperatives. Urban microclimate effects are negative in more cases in Algiers because the higher urban air temperatures and solar radiation stress the need for cooling further.

1.7. The Urban Climate in Stuttgart Inner City

The urban climate study in Stuttgart city showed that the urban density given by the street vertical profile and the ratio of built-up area primarily leads to the heating of the canyon air. This increase can reach 2.87 K, but is on average about 0.83 K. The heating tends to occur at night and states for a typical nocturnal canopy heat island. Concurrently, dense urban structures also experience episodes of cooling in-canyon due to additional shading. This occurs at noon and can be termed diurnal canopy cool island. In loose to medium building density areas, these phenomena are less pronounced in magnitude in comparison to high-density areas.
A number of microclimate clusters could be identified (see Figure 84) bringing the 99 processed climate files for the study area of 36 km^2 to six representative microclimatic areas. These clusters highlight in particular the importance of the urban density expressed by the street aspect ratio and the presence or not of additional anthropogenic heat.

1.8. The Energy Demand of the Buildings in Stuttgart City

The TRNSYS calculations, which are based on a systematic DOE experimental design, enabled the determination of the building energy demand for heating and cooling for each individual building by means of a generic modelling procedure. Subsequently, the results were reported for city blocks. The associated statistical analysis made it possible to identify the urban and building parameters with the greatest impact as well as the necessary mathematical models, which enabled the transferability of the generic outputs on the real buildings. The comparison of the calculated energy values with the existing consumption data confirmed the suitability of the employed procedure in the practice. The quality of the thermal insulation as well as the building volume is most important for the climate type of Stuttgart for both heating and cooling, even if the cooling requirements as absolute values are significantly lower. One highlight of this project was the handling of the object of study in a high spatial resolution with a fine representation of the energy data for heating and cooling at building scale but achieved for the entire city. The GIS techniques proved to be suitable for thermally characterising the investigated objects in the pre-processing phase and for a meaningful mapping the results.

2. LIMITS AND OUTLOOK OF THE WORK

2.1. Coupling Urban and Building Energy Modelling

This research addressed the necessity of considering the energy balance of urban outdoor and building indoor spaces as one system (section II - 5, p 157). Even though, the applied method based on the combination of several models and techniques succeeded largely in handling this complexity, it fails in two main respects: On the one hand, it does not account for the dynamic interactions of the energy fluxes between outdoors and indoors in a synchronised manner and on the other hand, it is time consuming. The work underlined the lack of an integral calculation model capable of dealing routinely with the building and its built-up surroundings as one system and such a model still needs to be developed. The literature review in section I - 2.3.20 (p 42) gave a synopsis about existing models or efforts of development. The present research provided a first milestone in this perspective as well, in the form of a TEB component for use in TRNSYS. However, substantial work is still required in order to extend its capabilities, either in terms of physics soundness or in terms of speed and user-friendliness. This is set as next research objective. Refer to section II - 5 (p 157) for further discussion.

2.2. Availability and Quality of Climate Data

The site of Stuttgart is certainly a privileged place in Germany to consider with respect to urban climate because of its decades of research background and expertise. Hence, numerous sources for climate information were available. However, the quality and appropriateness of the data in relation to the project's needs for high temporal and spatial resolution were variable and insufficient. This affected the course of the work and to some extent the achieved results. The time required for the acquisition and preparation of the climate data was substantial including comparison of all sources, bilinear interpolation, bias correction, compensation of missing data, etc. For the part of the KLIMOPASS project reported here, LARSIM data were finally used (see section III - 2, p 176). For the part of the project dealing with climate change (not reported here), KIT data were used. Due to the number and length of the climate data sets, the computational capacity required was very high and some decisions were necessary to shorten the calculation times. A period of ten years (2003 – 2012) was considered instead of a 30-years normal period and the investigation area was limited to 36 km^2 covering the inner city from the whole Stuttgart area of 340 km^2, reducing at the same time the required climate information. The 99 urban climate outputs obtained with TEB for the inner city could be further reduced to 6 representative climate files following a statistical cluster analysis, which

were subsequently used in TRNSYS (see section III - 4.3, p 193). Nevertheless, a special attention was paid to the representativeness of the selected information in order to ensure good quality of the results.

2.3. Availability and Quality of Building and City Data

All available information describing the city of Stuttgart and its buildings was used in this research. The 2D and 3D city maps and the statistical data allowed a satisfactory treatment of the challenging topic. Yet, a few important information was missing, for which simple assumptions had to be made, although an accurate modelling would have been technically possible. Thus, this shortage must be kept in mind while appreciating the results.

This applies inter alia to the quality of the thermal insulation of buildings, which was estimated only based on the age of the buildings including their subsequent renovations. Moreover, it is not clear whether all the energy renovations are documented in the provided database. The proportion of window area is not available, neither in the database nor in the 3D city map, so that rough estimates following the IWU building catalogue were made as well as equiprobable orientations towards the four cardinal directions.

Information about the residential density as well as an urban climate atlas and energy atlas were available. However, because there is no clear information in the literature about possible association between residential density and anthropogenic heat, the residential density could not be used for the determination of the waste heat. The anthropogenic heat was derived mainly from transportation maps as a mean value for the year for each of the 99 spatial units of the study area. No diurnal or weekly cycles could be considered. The waste heat from the buildings was set to one third of the traffic value to get a rough daily profile as reported in the literature because better information was missing. Owing the importance of the anthropogenic heat in the formation of urban microclimates as found in the theoretical part, these approximations probably have no negligible effects on the reliability of the results.

The building type of use as available from the statistical data is not uniformly differentiated in clear main groups. Instead, manifold types of use with no clear logic are listed. An effort for grouping the buildings in three main groups was done in view of setting the operation scenarios in the TRNSYS simulations. So, this assumption suffers some uncertainty. The results gathered at building scale were cumulated for city blocks following a principle of weighting between residential and non-residential buildings based on the description of the individual buildings composing the city block.

The terrain model is indeed available, but was not used because the building heights are in-

cluded in the 3D city map and the microclimate differences due the topography was already included in the LARSIM climate data. In addition, the land use map was used in the earlier phases of the project for sketching possible microclimates, however, this preliminary work was not used later. This material, however, could be useful for some later validation of the results provided it is combined with further useful information.

2.4. Validation of Method and Results

The calculated energy demands for heating could be validated against recorded data using an energy atlas of 1995. This validation effort is, however, limited to heating. The reservations in this comparison are explained in section III - 5.3 (p 209), in addition to all weaknesses introduced above in this section. All possible reasons for the discrepancy between the calculated energy demands and the recorded energy consumptions deserve to be further explored in a next step or in a follow-up project. Close cooperation with the city of Stuttgart would certainly be helpful. Details on the calculations could then be carefully checked and improvements proposed accordingly, An application on other cities or urban districts, which dispose of more reference data for validation, would be also advisable.

3. CONCLUSION

The present research was primarily motivated by the will to link between urban and building scales with respect to climate and energy in an interdisciplinary approach. It sought to contribute towards a deeper understanding of the dependence of the energy performance of buildings on the surrounding built-up environment, which is characterised by modified energetic and thermal conditions and hence microclimates.

The specific question addressed in the theoretical part was to understand the mechanisms underlying the formation of urban microclimates and the extent to which such specific boundary conditions, expressing alternatively canopy heat or cool islands, together with the obstruction effects of the 3D built surroundings influence the need for heating and cooling energy for maintaining thermal comfort indoors. The work succeeded in answering this question by means of a combination of several models and techniques (TEB, TRNSYS, DOE and GIS). In the theoretical PART I, the numerical simulations at both urban and building scales provided conclusive results at high level of detail. The highlight thereby was to provide a reliable quantification of the causal effects with respect to well-known thermo-physical properties of urban structures and buildings by means of statistically based experimental plans and post-processing. In spite of the informative value of the results, this part of the work underlined as well the complexity of the subject, which limits the generalisations and calls for a systematic use of supportive computational tools.

Moreover, the practical PART II dedicated to the city of Stuttgart demonstrated the applicability and usefulness of the proposed investigation method, in particular with focus on the widespread spatial scope and diversified climate background. The implemented generic modelling enabled the mapping of the urban microclimates as well as the energy demands at building scale and for city blocks for the study area. At the same time, however, it unveiled further difficulties related to real conditions.

In conclusion, the theoretical and practical parts of this research highlighted two typical hindrances regarding the subject and the use of numerical modelling: Either a model is capable of reproducing the physics of a phenomenon but the required input data is missing or the model suffers simplifications, which limits the accuracy in considering complex and well-documented real background situations. This argues for two research perspectives to be developed, namely the necessity of improving 1) the capabilities of related numerical models on the one hand and 2) the content, quality and scope of the building and city data in the practice in view of appropriate climate and energy studies on the other hand.

On the first shortage, integral urban - energy models with a comprehensive concept need to be developed. The TEB – Type 201 for use in TRNSYS introduced in this work is a first milestone in this perspective. The key task in a further work is to implement a synchronized processing, which includes the feedback loop between indoor and outdoor spaces. As an effective way to overcome the lack of interdisciplinary work, this will bring together all theoretical knowledge from urban climatology and building physics in an operational form in order to solve multifaceted problems. This will not only increase the reliability of the calculations, it will also help a cross-disciplinary dissemination of knowledge and give a sound understanding of interconnected matters. On the second deficiency, extensive additional validation work against real energy consumption data is necessary as well as more collaboration with cross-disciplinary professionals and various city authority actors.

V

APPENDICES

Appendix 1 | Calculation of the Canyon Energy Balance in TEB

The following equations describe the way TEB solves the canyon energy balance. The energetic and heat fluxes termed town are average values for the canyon system based on the weighting of each facet (street, wall, roof) according to their respective fractions ($frac_i$). The energy balance of a surface without anthropogenic heat ($Q_F = 0$) writes using eq. (6) after Oke (1988b):

$$Q^* = Q_H + Q_E + Q_G \quad (6)$$

Where Q_i^* is the total all-wave net radiation, Q_H the turbulent sensible heat flux, Q_E the turbulent latent heat flux and Q_G the conductive heat flux, the total net radiation Q^* of the canyon system named *town* writes:

$$Q^*_{town} = Q^{\downarrow}_{SW,town} + Q^{\uparrow}_{SW,town} + Q^{\downarrow}_{LW,town} + Q^{\uparrow}_{LW,town} \quad (7)$$

With Q_{SW} and Q_{LW} being the shortwave and longwave radiation fluxes respectively, either incoming from the atmosphere (↓) or outgoing from the terrestrial surface (↑). In case of available anthropogenic waste heat, the energy balance in eq. (6) writes:

$$Q^*_{town} + Q_{F,town} = Q_{H,town} + Q_{E,town} + \Delta Q_{S,town} \quad (8)$$

with

$$\Delta Q_{S,town} = Q_{GGRD} + Q_{FBLD} \quad (9)$$

and

$$Q_{FBLD} = Q_{FW} \times frac_{wall} + Q_{FR} \times frac_{roof} \quad (10)$$

With Q_{FBLD} is the storage heat flux in the wall Q_{FW} and in the roof Q_{FR}. In equation (11) the anthropogenic heat Q_F flux differentiates between sensible and latent heat (subscripts H, E) and may originate from traffic (TRF, daytime 7:00 to 19:00) and/or industry (IND, 24 hours).

$$Q_{F,town} = Q_{FBLD} + QF_{FHTRF} + QF_{FHIND} + QF_{FETRF} + QF_{FEIND} \quad (11)$$

The above equations for town write similarly for each facet, except Q_{FBLD} which is replaced by Q_{FW} Q_{FR} . The term Q_{FBLD} states for the sensible energy required inside the building to ensure the set indoor temperature and is transported through the components wall and roof. The fluxes Q_{FTRF} Q_{FIND} either sensible or latent are set as inputs, whereas the others are calculated. The latent heat flux Q_E is negligible because a dry canyon is investigated since no precipitation information is available in the TRY input data. The small values of latent heat flux are due to the condensation and evaporation of air humidity.

Appendix 2 | Comparison of TEB and ENVI-met Concepts and Physicals Basis

Table 51: Comparison of TEB and ENVI-met concepts and physical basis

TEB (early version and subsequent updates)	ENVI-met 4.0 (current version)
physical background	
+/- 2D urban canyon structure (roof, road, wall)	+ 3D Model (incl. buildings + vegetation) Atmosphere divided in a 3D grid of cubical modules (CFD)
simple-layer (extended to multi-layered)	multi-layer (equidistant or telescoping for important heights)
- Simple parameterization of atm. Turbulence (as resistance) of wind flow as logarithmic profile no account for wind direction sunlit/shaded situation (incl. solar orientation)	+ 3D atmospheric model including wind, temperature, humidity and turbulence prognosis fully based on the fundamental laws of fluid dynamics and thermo-dynamics.
- soil accounted for based on ISBA model	+ 3D soil model, multi-layered (ground thermal properties)
+ Green roofs possible Vegetation as separate tile via the sub-model ISBA in SURFEX package (i.e. no interaction with TEB)	+ integrated vegetation sub-model, multi-layered (incl. shading, evapotranspiration using LAD, LAI)
- Solar radiation depends on solar orientation. Gross differentiation between sunlit and shaded parts of canyon	+ Precise calculation of solar radiation (sunlit, shaded surfaces), spatially differentiated per grid module
Energy balance fluxes (radiation and heat fluxes)	
Sensible heat flux Q_H as resistance	Sensible heat flux from TKE-ε turbulence model (wall function)
Storage heat flux ΔQ_S diffusion method	Storage heat flux ΔQs in soil 3D model fully solved, in building system no storage term
No drag calculation	3D Navier-Stokes equations fully solved for drag calculation (CFD)
Latent heat flux Q_E as resistance, rain and snow included.	Evapotranspiration from soil and vegetation sub-models No rain, no snow.
Infinite shortwave reflection in-canyon	Multiple reflections using IVS method
No air pollution	- Air pollution as CO2 and PPM sources, NO, NO2 and Ozone or other gases including NO-NO_X-O_3 chemical reaction
Time issues (mode, step, duration, etc.)	
- stationary run mode	+ non-stationary run mode
Offline or coupled with an atmospheric model upstream (MESONH)	Stand-alone model (offline), simple or full climate forcing
- Simulation period unlimited according to input file.	- simulation period typically one day up to 48 hours
+ Time step 60 – 900 s, typically 300 s.	+ Time step typically 2 to 10 seconds.
+ Simulation run duration about 2 minutes for a simulation period of 1 year (= 8760 hours)	- Simulation run duration of several hours depending on the scope of the modelled area , the spatial resolution used and the computer capabilities

Parameters describing the urban structure and buildings			
+/-	Urban canyon: 1 roof, 1 street, 2 walls	+	high resolution of a modular grid. unity grid module from 10 m down to 0.5 m
-	Symmetrical profile with same height of buildings	+	Free choice for complex building plans and heights and various vegetation covers
+	Street, roof and wall in up to 9 material layers (thermal conductivity, thickness, density), emissivity, albedo	-	Transmittance U-value for roof and wall Walls and roofs can consist out of up to 3 layers of materials and heat transport/storage is solved using a non-stationary 7-node model. Individual physical properties can be assigned to all layers
	Building energy model updated incl. HVAC settings. Indoor building variably heated to a set temperature.		Building energy model integrated. Air temperature can be held constant or is calculated based on the energy fluxes of the building/zone
Inputs			
+/-	for each time step (read from file): air temperature, air humidity, wind speed, direct and diffuse solar radiation, incoming longwave radiation	+	initial (first time step) values for air, surface and soil temperatures, air and soil humidity, wind speed and direction
+	Precipitation included (rain, snow)	-	No precipitation included
+	Anthropogenic heat: domestic heat computed, traffic and industry input as constant	+	From heat transfer equations through walls
outputs (main)			
-	For canyon volume	+	For each grid module within the urban canopy and above.
-	wind speed assumed perpendicular to canyon	+	Wind field as 3 components x, y, z (speed and direction)
+	Air temperature in-canyon, surface temperature, air humidity, wind speed (average for canyon)	+	Air temperature in-canyon, surface temperature, air humidity
+	Shortwave radiation fluxes (direct, diffuse, diffusely reflected with infinite reflections)	+	Shortwave radiation fluxes (direct, diffuse, diffusely reflected using one reflection and SVF)
+	Longwave radiation fluxes (atm. und from built surroundings)	+	Longwave radiation fluxes (atm. und built surroundings)
+	Sensible and latent heat fluxes for canyon system (town) and for each facet (latent heat wall = 0)	+	Sensible and latent heat fluxes
+	Conductive and storage heat fluxes, incl. Heating energy in building		-
-	UTCI thermal comfort index for indoors and in-canyon (exposed to sun or in the shade)	+	Mean radiant temperature, thermal comfort indices (PMV, PET, UTCI, SET)
-	No pollution data	+	Pollution concentration depending on what run mode is used, up to 7 different pollutants
Output save and post-processing			
-	In Linux format or as text (ascii) possible	+	In binary format visualized with Leonardo. Save of single receptors possible. Possible extraction of partial results as text (ascii) format.
The (+) positive versus (-) negative sign means potential of feature in respect to possible coupling with building modelling.			

Appendix 3 | Input Settings for TEB Simulations in PART I

Table 52: Input file for TEB simulations in [SET I] and [SET II] in PART I

START	0
STOP	8760 hours
TIME STEP	300 seconds = 0.083333335 hour
WALLOHRZ	! 4 Wall surface over horizontal surface
VAR or 0.10	! 5 Road albedo
VAR or 0.94	! 6 Road emissivity
VAR or 0.20	! 7 Wall albedo
VAR or 0.94	! 8 Wall emissivity
VAR or 0.20	! 9 Roof albedo
VAR or 0.94	! 10 Roof emissivity
Td_road	! 11 Road deep temperature
Ts_road	! 12 Road surface temperature
Ta_bldg	! 13 Building inside air temperature
Ts_wall	! 14 Wall surface temperature
Ts_roof	! 15 Roof surface temperature
3	! 16 Number of road layer (i)
HC_road (i)	! 17 (Volumetric) Heat capacity of road layer (i)
TC_road (i)	! 18 Thermal conductivity of road layer (i)
D_road (i)	! 19 Thickness of road layer (i)
3	! 26 Number of wall layer (i)
HC_wall (i)	! 27 (Volumetric) heat capacity of wall layer (i)
TC_wall (i)	! 28 Thermal conductivity of wall layer (i)
D_wall (i)	! 29 Thickness of wall layer (i)
3	! 36 Number of roof layer (i)
HC_roof (i)	! 37 (Volumetric) Heat capacity of roof layer (i)
TC_roof (i)	! 38 Thermal conductivity of roof layer (i)
D_roof (i)	! 39 Thickness of roof layer (i)
BDLG_FRAC	! 46 Fraction of buildings
18	! 47 Building height
2	! 48 Height of air temperature and humidity measurement
2	! 49 Height of wind measurement
81200	! 50 Simulation start time in seconds at UTC ! start time set one hour before year's tart because this first time step is not output
31	! 51 Simulation start day
12	! 52 Simulation start month
2013	! 53 Simulation start year
49.52°	! 54 Latitude (Mannheim)
8.55°	! 55 Longitude (Mannheim)
116 m	! 56 Surface orography (altitude Mannheim)
116 m	! 57 Weather station orography (altitude Mannheim)
VAR or 20	! 58 Anthropogenic sensible heat flux due to traffic (7:00 – 19:00)
0	! 59 Anthropogenic latent heat flux due to traffic
VAR or 10	! 60 Anthropogenic sensible heat flux due to industry (day round)
0	! 61 Anthropogenic latent heat flux due to industry
1.0	! 62 Town roughness length z_0
0	! 63 Initial water on roof per m^2
0	! 64 Initial water on road per m^2

Table 53: Thickness d and thermal transmittance U-value of wall and roof of the investigated 18 building types including the combinations of window ratio, thermal insulation and thermal mass (C, D and E)

coded form		absolute values of C (%) and D (W m^{-2} K^{-1})				d wall layer (1)	d wall layer (2)	d wall layer (3)	total thickness d_{tot}	
						thickness d of walls and roof (m)				
C	D	window ratio	U_{wall}	U_{wdw}	U_{eq} (total)	wall layer	insula-tion	wall layer	LI	MA
-1	-1	0.3	0.65	3.3	1.442	0.04 or 0.12	0.020	0.04 or 0.12	0.100	0.260
-1	0	0.3	0.4	2.1	0.917		0.040		0.120	0.280
-1	1	0.3	0.15	1.0	0.391		0.110		0.190	0.350
0	-1	0.6	0.65	3.3	2.234		0.008		0.088	0.248
0	0	0.6	0.4	2.1	1.434		0.020		0.100	0.260
0	1	0.6	0.15	1.0	0.632		0.064		0.144	0.304
1	-1	0.9	0.65	3.3	3.026		0.002		0.082	0.242
1	0	0.9	0.4	2.1	1.952		0.011		0.091	0.251
1	1	0.9	0.15	1.0	0.872		0.042		0.122	0.282
roof (similar properties as walls but with no windows)										
-	-1	1	0.6		0.600	0.04	0.068	0.04	0.148	0.148
-	0	1	0.35		0.350		0.128		0.208	0.208
-	1	1	0.1		0.100		0.48		0.56	0.560
The window frame is assume dto be 10% in all cases for simplicity and ensuring equidistance										

Table 54: Buildings components (walls, roof)

wall and roof elements (1) (3)		thickness	density	thermal conductivity	heat capacity
		m	kg m^{-3}	W m^{-1} K^{-1} | kJ h^{-1} m^{-1} K^{-1}	kJ m^{-3} K^{-1}
massive [MA]	dense concrete	0.12	1	2.1 | 7.56	2400
mediumweight [MD] (4)	mid-dense concrete	0.08	1	1.3 | 4.68	1800
lightweight [LI]	light concrete	0.04	1	0.619 | 2.23	1200
thermal insula-tion [TI]	mineral insulation	variable (2)	0.9	0.05 | o.18	72
(1) The façade is assumed a double-skin concrete element with a thermal insulation layer in-between. (2) The thickness of the insulating layer is a function of the required total U-value of the building element					

Table 55: Urban and building geometry data

item	steps			comment
Coding	[-1]	[0]	[+1]	
H/W	0.2	1	1.8	Shallow, unity-like and deep canyons
BLD_FRAC	0.1667	0.5	0.6428	B / (B + W)
WALLOHORZ	0.3333	1.0	0.2858	2 (H / W) * (1 - BLD_FRAC)
TOT_O_HOR	1.33333	2.0	2.28571	(B + (2H + W) / (B + W)
ROOF_FRAC	0.125	0.25	0.28125	BLD_FRAC / TOT_O_HOR
WALL_FRAC	0.25	0.5	0.5625	WALL_O_HOR / TOT_O_HOR
ROAD_FRAC	0.62500	0.25	0.15625	(1- BLD_FRAC) / TOT_O_HOR
H = building height (18 m), W = road width (variable), B = building width (18 m or variable in [SET II])				

Table 56: Climate boundary conditions

item	Mannheim	Algiers	comments
ID	MAN	ALG	Study of two contrasting climate types for comparison purposes
climate type	temperate	warm-humid	
LAT	39.52°N	36.75°N	
LONG	8.55°E	3.00°E	
S_OROG	96 m	116 m	Altitude, same value in offline mode
WSTAT_OROG	96 m	116 m	
Ts_road (°C)	6.5 | 279.65	9.5 | 282.65	Air temperature at simulation start time
Ts_wall (°C)			
Ts_roof (°C)			
Ta_bldg (°C)	20 | 293.15	20 | 293.15	
Td_road (°C | K)	11.1 | 284.25	17.0 | 290.15	yearly mean air temperature
Ts_road (°C | K)	6.5 | 279.65	9.5 | 282.65	air temperature at simulation start time set equal to first hour in climate file
Ts_wall (°C | K)			
Ts_roof (°C | K)			
Ta_bldg (°C | K)	20 | 293.15	20 | 293.15	
Ta (°C)	Air temperature		All data at hourly basis from file. Rain and snow not available, set to zero and state for a dry canyon.
q [kg/kg]	Specific air humidity		
FF (m/s)	Wind speed		
DD (°)	Wind direction		
S (W m^{-2})	Direct solar (shortwave) radiation		
D (W m^{-2})	Diffuse solar (shortwave) radiation		
A (W m^{-2})	Atmospheric (long wave) radiation		
RR (mm)	Rain precipitation		
SN (mm)	Snow precipitation		
P (hPa)	Atmospheric surface pressure		

Table 57: Boundary conditions used in PART I based on DIN V 18599-10

cellular office for one person | (source DIN V 18599-10:2011-12. p 33)					
task	Control strategy		unit	from	to
usage times	daily use time		hour	07:00	18:00
	annual use days		d/a	250	
	annual use hours for daytime | at nighttime		h/a	2543	207
	daily operating time for Ventilation and cooling		hour	05:00	18:00
	annual operating days for ventilation. cooling and heating		d/a	250	
	daily operating time for Heating		hour	05:00	18:00
room conditions (provided conditioning foreseen)	set room temperature for heating		°C	21	
	set room temperature for cooling		°C	24	
	minimum set temperature interpretation for heating		°C	20	
	maximum set temperature interpretation for cooling		°C	26	
	room temperature drop for reduced operation		K	4	
	Humidification request		–	with tolerance	
minimum fresh air flow rate	by person		m3/(h . p)	40	
	by area		m3/(h · m2)	4	
	Minimum fresh air flow rate for buildings		m3/(h · m2)	2.5	
	relative Absence for ventilation system		-	0.3	
	Part service factor of buildings uptime		-	0.7	
mechanical fresh air flow rate or air exchange (practice)				from	to
	air change flow rate (general) h-1		h-1	2	3
	air change flow rate (full cooling function with inlet air)		h-1	4	8
lighting	maintained illuminance		lx	500	
	height of working plane		m	0.8	
	reduction factor		-	0.84	
	relative Absence		-	0.3	
	Room index		-	0.9	
	reduction factor of building operating time		-	0.7	
persons occupation	maximal occupation density m2 per person		low	mean	high
			18	14	10
internal heat gains (per person)		full use hours (h/d)	max. specific power W m-2		
			low	mean	high
	Persons (70 W per Person) equipment	6	4	5	7
	equipment (low/medium/high correspond to 50/100/150 W)	6	3	7	15
	supply of heat	Wh $m^{-2} \cdot d^{-1}$	42	72	132
Note: Items marked in grey are settings chosen in this research.					

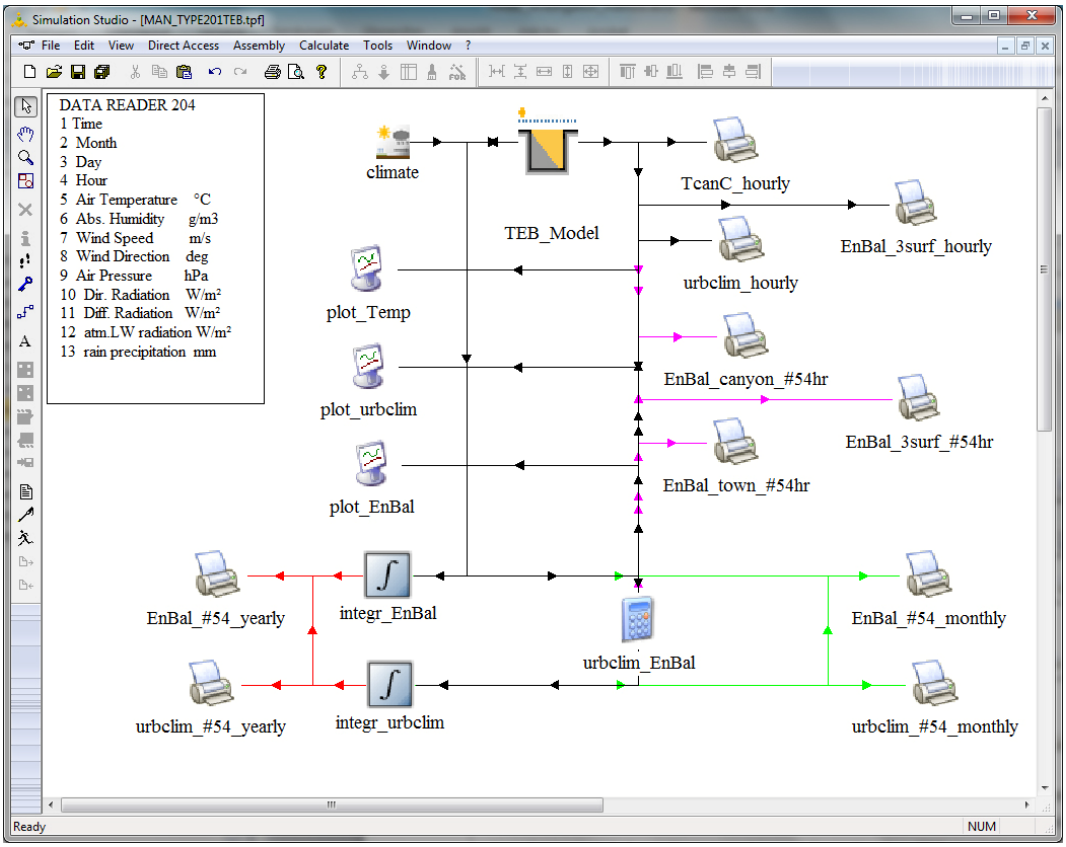

Figure 92: Interface the simulated project for urban microclimate adjustments using TEB as Type 201 in the TRNSYS-Studio environment

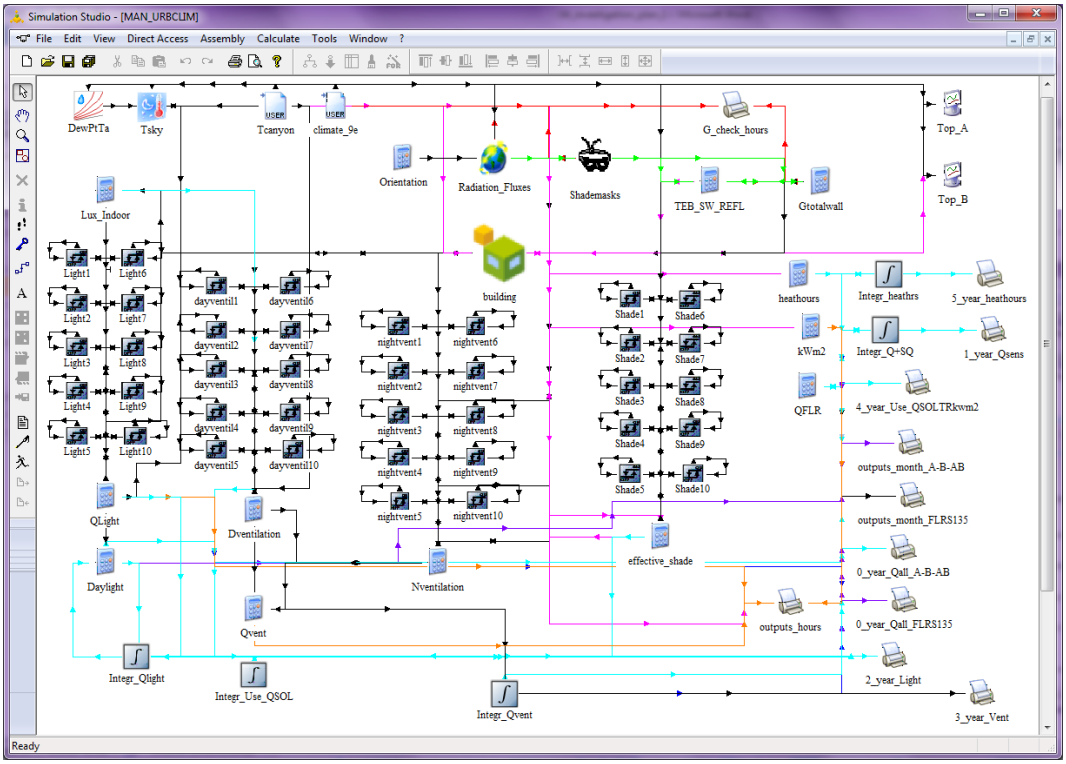

Figure 93: The interface of the simulated project in the TRNSYS-Studio Environment in PART I

Appendix 4 | Background on Building Thermal Behaviour

1. Thermal Insulation of the Building Envelope

In the simulation plan used in PART I, the thermal insulation of the opaque walls and transparent windows were varied concurrently as pairs based on the assumption that weak insulated walls include most likely weak insulated windows and inversely good insulated walls include good insulated windows (see Table 53). This means the window ratio and the thermal insulation (coded C and D), respectively are interacting in the resulting statistical analysis (effect on CD). This option was preferred to a systematic variation, which would have meant more case studies with no significant added-value if careful interpretation were ensured (i.e. CD interaction in the statistical analysis). This interaction is formulated as an equivalent thermal insulation including the window ratio U_{eq}.

2. Thermal Mass and Heat Storage

This Appendix recalls the basics on thermal mass and calculation procedures of the heat capacity as background to the choices made on this issue in PART I (section II - 1, p 67).

With respect to thermal behaviour, massive and lightweight constructions are fundamentally different. A massive construction is able to store heat during the day and release it at night and this helps attenuate the maxima and amplitudes of indoor air temperature in reaction to outdoor boundary conditions. As further consequence, a time lag occurs with peak air temperatures reached later in the afternoon (Figure 94). Under hot summer conditions, this thermal regulatory passive design measure can be very useful if properly planned in order to avoid overheating. This ability to charge and discharge thermal heat is very limited in lightweight constructions because of lacking thermal mass.

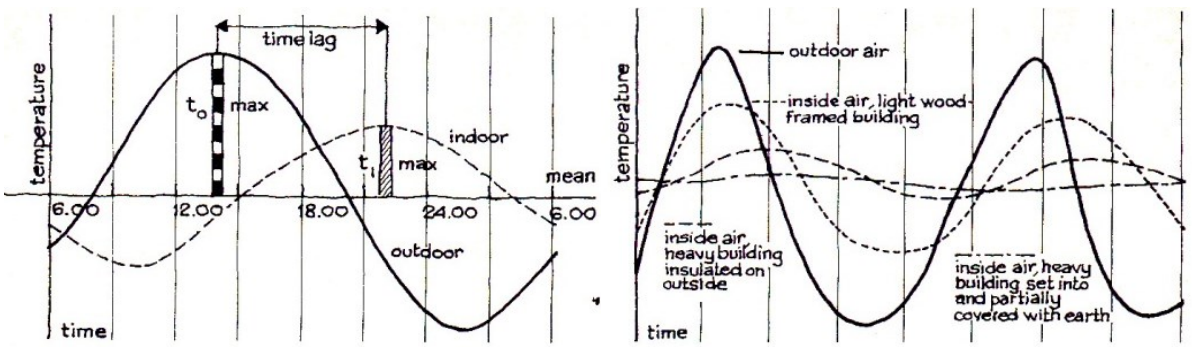

Figure 94: Thermal mass principle showing the charge and discharge of thermal heat and time lag (Konya 2011)

The heat capacity κ is the measurable physical quantity for describing thermal mass C or thermal inertia. It describes the ability of a body to store (and later release) thermal heat, mainly depending on the volumetric mass density (ρ) and specific heat capacity (c) and is expressed in J K^{-1}. A simple procedure for calculating the heat capacity of buildings is given in DIN 4108-2, whereas DIN EN 13786 provides a more detailed calculation procedure.

The issue is that the exposed surface (A) to the energy source and the thickness (d) of the element are further parameters responsible of the "effective" heat capacity, i.e. the part of building component active in this storage process. Generally, it is admitted that not the full thickness of a building element but one part of it from the exposed side up to a certain depth is active in this storage process. This so-called effective thickness dT can be either expressed as function of the thermal properties (λ, ρ, c) or as diffusivity (α) and the period of time (T) in which thermal fluctuations occur In a building, this period generally corresponds to a daily cycle governed by the availability of solar radiation.

According to DIN 4108-2, the heat capacity of a room is the sum of the heat capacities of its enclosing surfaces j as given by equation (12) with c is the specific heat capacity in J kg^{-1} K^{-1}, ρ the volumetric mass density in kg m^{-3}, d (or d_T) the effective thickness in metres and T the fluctuation period in seconds. With reference to the calculation procedures in DIN EN 13786, the effective thickness d_T is important: It is set as the smallest value from the following: i) half the total thickness of a single-layered element, ii) the thickness of the layers from the surface up to the first insulation layer or iii) the maximal thickness d_T as given by equation (13).

$$\kappa_{tot} = \sum_j c_j \,.\, \rho_j \,.\, d_j \, A_j \tag{12}$$

$$d_{T,max} = \sqrt{\frac{1}{2}} \cdot \sqrt{\frac{\lambda \, T}{\pi \, \rho \, c}} = \sqrt{\frac{\alpha \, T}{2\pi}} \tag{13}$$

The rule of 10 cm effective thickness assumed in the DIN 4108-2 relies on eq. (13) with the assumption of a daily cycle with T equals 1 day (in s) and an approximate thermal diffusivity applying for concrete, gypsum and mortar $\alpha = 0.7.10^{-6}$ m^2 s^{-1}. However, other materials would deviate from this rule. Therefore, it is difficult to set equidistant steps for thermal mass in a DOE experimental plan and this justifies the choice made for the TRNSYS simulations in this research for a 2-step plan including typically massive and typically lightweight construction with reference to VDI 2078. In this work a thickness of 12 cm was assumed.

3. Daytime and Nighttime Ventilation

This Appendix provides, in continuity to the section above, some elements about daytime and nighttime ventilation, as further possible passive and efficient strategies for preventing overheating and reducing the need for mechanical cooling. Using massive construction for a diurnal thermal regulation calls for a proper handling of its consequences in the nighttime. The thermal heat stored in the building fabric requires sufficient nighttime ventilation to avoid late overheating during the nocturnal heat discharge phase. In office buildings where the operating times exclude the night, late ventilation help cool the building elements in order to avoid an early overheating in the next working day. Lightweight construction, by contrast does not use the advantage of thermal storage, which leads to higher operative temperatures during the day, making the ventilation during the usage period crucial. Figure 95 shows the cumulative effects of this process (see Schild and Willems 2013).

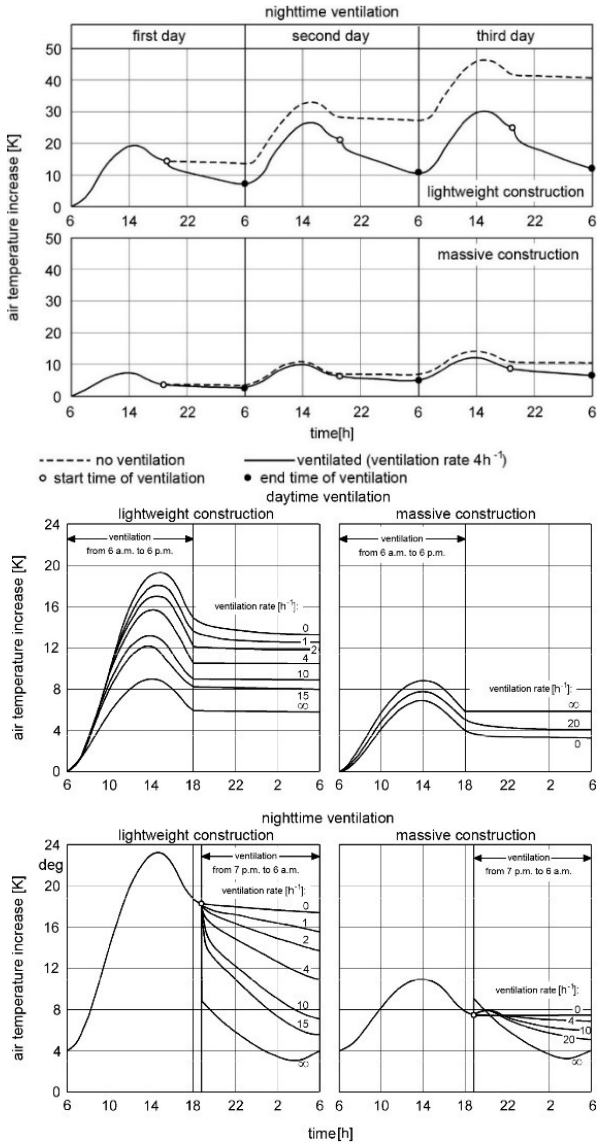

Figure 95: Indoor air temperature increase in dependence on thermal inertia combined with various nocturnal ventilation scenarios (Schild and Willems 2013)

Appendix 5 | Urban-related Additional Calculations in TRNSYS in PART I

In complement to section II - 1.2 (p 74), this appendix describes the self-defined equations added in the TRNSYS project to account for the effects of the surrounding urban structure on the amounts of shortwave and longwave radiation as well as daylight available for the building indoors. More specifically, it is about 1) the calculation of the diffusely reflected solar radiation in-canyon, the longwave radiation emitted by the surroundings and the indoor illuminance.

4. Shortwave radiation fluxes in the urban canyon

Procedure 1 – TEB-based calculation of in-canyon multiple reflections

This method is described in Masson (2000) and updated in Lemonsu et al. (2004). The solar (shortwave) radiation absorbed by each surface includes the diffusely reflected parts of direct and diffuse solar radiation. Infinite solar reflections between walls and road are considered, including a first reflection RF(0) and n further reflections. The equations are given hereafter, using the following key metrics, with the index "surf" used as generic term for road and wall for the sake of conciseness.

$B^{\downarrow}_{surf}$	Direct solar radiation received by the surface (road or wall) in W m^{-2}
$D^{\downarrow}_{surf}$	Diffuse solar radiation received by the surface (road or wall) in W m^{-2}
$G^{\downarrow}_{surf}$	Total global solar radiation received by the surface (road or wall) in W m^{-2}
G^{*}_{surf}	Net global solar radiation absorbed by the surface (road or wall) in W m^{-2}
$RF^{\uparrow}_{surf}(0)$	First solar reflection against the surface (road or wall) in W m^{-2}
$MR^{\uparrow}_{surf}$	Sum of all solar reflections against the surface (road or wall) in W m^{-2}
α_{surf}	Albedo of the surface (road or wall), dimensionless
σ_{surf}	Sky view factor of the surface (road or wall), dimensionless

The first solar reflection is calculated using eqs. (14) and (15)

$$RF^{\uparrow}_{road}(0) = \alpha_{road} B^{\downarrow}_{road} + \alpha_{road} D^{\downarrow}_{road} \quad (14)$$

$$RF_{wall}(0) = \alpha_{wall} B^{\downarrow}_{wall} + \alpha_{wall} D^{\downarrow}_{wall} \quad (15)$$

The sum of all solar reflections is then calculated using eqs. (16) and (17)

$$MR^{\uparrow}_{road} = RF^{\uparrow}_{road}(0) + \frac{(1 - \sigma_{road})\alpha_{road}\left(RF^{\uparrow}_{wall}(0) + \sigma_{wall}\,\alpha_{wall}\,RF^{\uparrow}_{road}(0)\right)}{1 - (1 - 2\sigma_{wall})\alpha_{wall} - (1 - \sigma_{road})\sigma_{wall}\,\alpha_{road}\,\sigma_{wall}} \quad (16)$$

$$MR^{\uparrow}_{wall} = \frac{RF^{\uparrow}_{wall}(0) + \sigma_{wall}\,\alpha_{wall}\,RF^{\uparrow}_{road}}{1 - (1 - 2\sigma_{wall})\alpha_{wall} - (1 - \sigma_{road})\sigma_{wall}\,\alpha_{road}\,\alpha_{wall}} \quad (17)$$

The total solar radiation received by road and wall is then calculated with eqs. (18) and (19):

$$G^{\downarrow}_{road} = B^{\downarrow}_{road} + D^{\downarrow}_{road} + (1 - \sigma_{road})MR^{\uparrow}_{wall} \quad (18)$$

$$G^{\downarrow}_{wall} = B^{\downarrow}_{wall} + D^{\downarrow}_{wall} + (1 - 2\,\sigma_{wall})MR^{\uparrow}_{wall} + \sigma_{wall}\,MR^{\uparrow}_{road} \quad (19)$$

And so, the net solar radiation absorbed can be calculated with eqs. (20) and (21):

$$G^{*}_{road} = (1 - \alpha_{road})\,G^{\downarrow}_{road} \quad (20)$$

$$G^{*}_{wall} = (1 - \alpha_{wall})\,G^{\downarrow}_{wall} \quad (21)$$

However, the diffusely reflected radiation from the wall in eq. (19) is calculated for the 2 walls of the canyon together as one receiving surface given the concept of TEB (according to Masson 2000 and Lemonsu et al. 2004). In this TRNSYS project, the diffusely reflected radiation is calculated for one receiving wall at a time, following the update of Lemonsu et al. (2012) in considering explicit differentiation of canyon walls. Therefore, the equation (19) is accordingly replaced by eq. (22) with (j) being either façade 1 or 2 of the canyon:

$$G^{\downarrow}_{wall\,(j)} = B^{\downarrow}_{wall(j)} + D^{\downarrow}_{wall(j)} + (0.5 - \sigma_{wall})MR^{\uparrow}_{wall} + \sigma_{wall}\,MR^{\uparrow}_{road} \quad (22)$$

The fraction of sky seen by the road and one wall, called here sky view factor of road and sky view factor of wall (needed above) are calculated as function of H/W, which is the canyon vertical profile (building height H to street width W) using eqs. (23) and (24) as follows:

$$\sigma_{road} = ((H/W)^2+1)^{0.5} - (H/W) \quad (23)$$

$$\sigma_{wall} = 0.5\left((H/W) + 1 - ((H/W)^2 + 1)^{0.5}\right)/(H/W) \quad (24)$$

As a street becomes shallower, the sky view factor of the road tends to 1 (i.e. an unobstructed horizontal surface) and the sky view factor of the wall tends to 0.5 because half of the sky can be seen by a vertical wall. For the investigated canyons, these factors correspond to Table 58.

Table 58: Sky view factors of road and wall for the simulated canyons according to (23) and (24)

H/W = 0.2		H/W = 1.0		H/W = 1.8	
σ_{road}	σ_{wall}	σ_{road}	σ_{wall}	σ_{road}	σ_{wall}
0.820	0.261	0.414	0.293	0.259	0.313

A number of further adjustments were necessary in order to implement the above calculations in the TRNSYS project. The solar radiation received by the road is not calculated in TRNSYS as done in TEB. This could be solved by using the average of the horizontal solar radiation received at the ground floor level as calculated by Type 67 for the two openings of floor 1 on the two opposite façades. This is a way to account for the case of partial solar exposure within the canyon. The direct and diffuse radiation parts are calculated using the outputs of Type 67 as averages of all ten floors. Moreover, unlike TEB, the walls in TRNSYS include windows

equipped with solar shading devices. Therefore, the average albedo of the walls was weighted according to opaque and transparent parts including the reflective effects of the shading devices when these are in operation as given by eqs. (25) and (26).

$$\alpha_{wall} = WR\ \alpha_{win,shd} + (1 - WR)\ \alpha_{op,wall} \quad (25)$$

$$\alpha_{win,shd} = \alpha_{win}\ (1 - ctrl_{shd}) + \overline{\alpha_{shd}}\ ctrl_{shd} \quad (26)$$

Where WR is the window ratio, α_{win} is the albedo of the window, $\alpha_{win,shd}$ is the albedo of the window including the shading devices, $\overline{\alpha_{shd}}$ is the average albedo of all shading devices in operation. The $ctrl_{shd}$ is the controller of the ten shading devices. If $ctrl_{shd} > 0$, at least one shading device for one office is in use, otherwise, it equals zero as all shading devices are off.

Procedure 2 - View Factors based calculation of simple reflections in-canyon

This procedure uses the view factors approach accounting for the exposure of the canyon surfaces and their impact on each office façade by considering the floor height for calculating a simple reflection (see e.g. Robinson and Stone 2004, Robinson 2010 for similar concept).

The global solar radiation $G^{\downarrow}_{wall(i)}$ received at the building's part of façade of floor (i) is the sum of the incident direct solar radiation $B^{\downarrow}_{wall(i)}$, the atmospheric diffuse radiation $D^{\downarrow}_{wall(i)}$ and the in-canyon diffusely reflected part $RF^{\downarrow}_{wall(i)}$ as given by eq. (27):

$$G^{\downarrow}_{wall(i)} = B^{\downarrow}_{wall(i)} + D^{\downarrow}_{wall(i)} + RF^{\downarrow}_{wall(i)} \quad \text{in W m}^{-2} \quad (27)$$

The diffuse irradiation $D^{\downarrow}_{wall(i)}$ corresponds to the part of the atmospheric scattered radiation the received by a surface from the visible part of the sky given by its view factor $\sigma_{surf(i)}$. Both direct and diffuse radiation parts are available as outputs from Type 67. By contrast, the diffusely reflected radiation $RF^{\downarrow}_{wall(i)}$ needs to be calculated. It corresponds in eq. (28) to the part of global radiation reflected as simple reflection by the built surroundings, i.e. from the facing wall A and the street ground B (see Figure 17).

$$RF^{\downarrow}_{wall(i)} = A_i\ RF^{\uparrow}_{surf(A)} + B_i\ RF^{\uparrow}_{surf(B)} \quad \text{in W m}^{-2} \quad (28)$$

With surface A states for the facing wall and B the

$$RF^{\uparrow}_{surf(A)} = \alpha_{surf(A)}\ G^{\downarrow}_{surf(A)} \text{ and } RF^{\uparrow}_{surf(B)} = \alpha_{surf(B)}\ G^{\downarrow}_{surf(B)} \quad \text{in W m}^{-2} \quad (29)$$

The parameters A_i and B_i are the view factors of the facing wall and the street ground surface respectively. Together with the sky view factor SVF_i , these factors summed equal 180 degrees. The factors SVF_i, A_i and B_i are differentiated for each floor's part of façade (i) and are calculated by eqs. (30), (31) and (32) respectively. Thereby, H is the building total height and H_i is the reference height of a floor (i) calculated from the ground level up to the mid-height of the floor (e.g. outside measure H_1 = 1.2 m for floor 1 and incrementing with 3.4 m for each

additional floor, see Figure 12). The Table 59 lists the SVF_i, A_i and B_i as used in this research in PART I for each office (i) calculated at the parapet height and expressed as quotients (with 1 corresponding to 180°).

$$SVF_i = \arctan\left(\frac{W}{H - H_i}\right) 180 \ / \pi \quad \text{in Degrees} \quad (30)$$

$$B_i = \arctan\left(\frac{W}{H_i}\right) \ / \pi \quad \text{in Degrees} \quad (31)$$

$$A_i = 1 - SVF_i - B_i \quad \text{in Degrees} \quad (32)$$

As described in the previous method, the windows and their shading devices are taken into account in determining the total albedo of wall as well. Moreover, the incident direct and diffuse radiation on the facing wall is estimated as an average of the five opposite floors.

Table 59 – Surface related view factors for shortwave radiation reflections in-canyon

Aspect ratio H/W	SVF (σ) as fraction				
	σ1	σ2	σ3	σ4	σ5
	σ6	σ7	σ8	σ9	σ10
0.2	0.444	0.455	0.467	0.479	0.492
1.0	0.268	0.304	0.348	0.399	0.460
1.8	0.177	0.212	0.262	0.330	0.428
Aspect ratio H/W	A View Factor of facing Wall				
	A1	A2	A3	A4	A5
	A6	A7	A8	A9	A10
0.2	0.063	0.063	0.063	0.063	0.063
1.0	0.266	0.287	0.295	0.289	0.269
1.8	0.383	0.443	0.466	0.450	0.391
Aspect ratio H/W	B View Factor of the Street				
	B1	B2	B3	B4	B5
	B6	B7	B8	B9	B10
0.2	0.493	0.481	0.469	0.457	0.445
1.0	0.467	0.409	0.357	0.312	0.272
1.8	0.440	0.345	0.272	0.220	0.181

Procedure 3 – TEB and view factors based calculation of multiple reflections in-canyon

The two procedures presented above can be combined for calculating more precisely the diffusely reflected solar radiation in-canyon. The aim is 1) to take advantage of the multiple reflections used in procedure 1 and 2) to add a specific calculation for each floor (i) using the surfaces view factors A_i and B_i. In doing so, the equations (16) and (17) are first calculated and then the weighting factors in equation (22) is replaced as given in eq. (33):

$$G^{\downarrow}_{wall(i)} = B^{\downarrow}_{wall(i)} + D^{\downarrow}_{wall(i)} + A_i MR^{\uparrow}_{wall} + B_i MR^{\uparrow}_{road} \quad (33)$$

In connection with Type 67, this third procedure is the one used in the theoretical part (PART I) of this research where the focus is put on the methodological discussion of the effects of the urban microclimate. In the practical part (PART II), however, the shading matrix generated by TRNSYS3D was more convenient owing the complex geometries and wide scope of the physical object of study, which make such additional calculations too time-consuming.

5. Longwave radiation fluxes in the urban canyon

For the longwave heat exchange between the building and its surroundings, an average surface temperature of the built surroundings T_{sgrd} is required by as input for the building in TRNBuild. In the absence of this quantity, the air temperature is usually used. In this work, using the TEB outputs, T_{sgrd} could be calculated as average of the facing wall and road surface temperatures weighted according to building height H and road width W as given by eq. (34):

$$T_{sgrd} = \left(H \,.\, T_{s,wall} + W \,.\, T_{s,road}\right)/(H + W) \quad \text{in °C} \quad (34)$$

6. Outdoor and indoor illuminance

Daylight is available when the sun is above horizon at some height. Illumination is less often available as measurement than solar irradiances and is therefore mostly calculated using its relationship to sunlight and sun path. The DIN 5034-2 expresses the horizontal illuminance under free horizon in dependence with the sun height γ_s. Under overcast sky conditions it is expressed with eq. (35) and under clear sky conditions with eq. (37) as um of the sun part E_S with eq. (38) and for the sky part E_H with eq. (39). These empirical formulations are considered to be good approximations for practical use in case of moderate turbidity (0.49). More complex mathematical expressions are given in DIN 5034-2 as well.

$$E_{G,overcast} = (300 + 21000\,\gamma_s) \quad \text{in Lux} \quad (35)$$

$$E_{G,clear} = E_S + E_H \quad \text{in Lux} \quad (36)$$

$$E_S = (85000\,.\sin^2\gamma_s + 6500\,\sin^2(2\,\gamma_s) \quad \text{in Lux} \quad (37)$$

$$E_H = 280 + \arctan\,(\gamma_s/18.9) \quad \text{in Lux} \quad (38)$$

Where γ_s is the sun height in degrees (°)

The calculation of the illuminance from the solar radiation and sky conditions data, covering all sky clearness ranges from completely overcast to clear is described in the TRY documentation (Christoffer et al. 2004), expressed as function of the direct and diffuse solar radiation, the zenith angle and the total water content in the atmosphere. More simply and according to Table 60, the following estimations are available.

Table 60: Examples showing the interdependence between irradiances and illumination levels (VDI 6011-1)

Time	sky conditions	horizontal irradiance	horizontal illumination	Radiation equivalent (*)
		W m^{-2}	kLux	lm W^{-1}
average	clear sky, sun high in the sky	600 – 1000	60 – 10	100
	completely overcast, sun high in the sky	170	20	118
Dec. 20th	direct horizontal irradiance, clear sky,	154	12	78
	diffuse horizontal, clear sky	75	9.4	125
	horizontal, fully overcast sky	65	7.5	115
Jun. 21th	direct horizontal irradiance, clear sky,	610	62	102
	diffuse horizontal, clear sky	196	24.5	125
	horizontal, fully overcast sky	170	19	112
For seasonal values latitude 50°N, 12:00. The DIN 5034-2 gives another estimate: 175 W m^{-2} ≈ 20 kLux at a latitude of 51°N. (*) radiation equivalent is the ratio of illumination to irradiation. Here, self-calculated and rounded from the two other columns.				

In average, 1 W m^{-2} equals 100 Lux under clear sky conditions and about 118 W m^{-2} under fully overcast sky according to VDI 6011-1. The illumination to irradiation ratio also called radiation equivalent km is set to 115 lm W^{-1} in DIN 5034-2 for completely overcast conditions. As the sky clearness levels are variable throughout a year, season and daytime, this leads to further differences (see

Table 60 for more values). In this research, the following assumption is therefore made: 1 W ≈ 110 lumen; 1 W m^{-2} ≈ 110 Lux, with (1 lux = 1 lm m^{-2}).

Office Illuminance based on indoor solar irradiance

The indoor illuminance $E_{z(i)}$ inside a thermal zone (i) of a certain floor can be calculated with good approximation from the global irradiation $G_{z(i)}$ received in the corresponding thermal zone by traversing the zone's windows. This corresponds in TRNSYS to the output solar radiation flux Q_{SOLTR} (in W) related to the zone area (in m^2).

$$E_{z(i)} = G_{z(i)}/110 \text{ (in Lux)} \quad (39)$$

The solar radiation received indoors $G_{z(i)}$ takes into account the direct, diffuse, diffusely reflected parts of the solar radiation prevailing outdoors as well as a possible reflections caused by shading devices in operation. This procedure is therefore advantageous and improves the one relying on daylight factor (see Tregenza an Wilson 2011), usually advised in related standards (VDI 6011, DIN 5034, DIN EN 12464-1 & -2) and used e.g. by Schlenger (2009) under free horizon conditions and by Ali-Toudert (2011) with consideration of additional urban obstructions.

Appendix 6 | Post-Processing of TEB and TRNSYS Outputs

The potential of microclimate change in-canyon expressed as the air temperature deviation from the input air temperature can be higher or lower, i.e. warming or heat island vs. cooling or cool island. The magnitude of these changes is calculated as yearly heat sum HS and yearly cool sum CS as given in equations (40) and (41). The same principle applies for HSH and CSH but expressed as sum of hours.

$$HS = \sum_1^{8760}(T_{urb} - T_{stn}) \text{ if } (T_{urb}) > T_{stn} \quad (40)$$

$$CS = \sum_1^{8760}(T_{urb} - T_{stn}) \text{ if } (T_{urb}) < T_{stn} \quad (41)$$

For an estimation of the impact of the outdoor microclimate changes on the thermal situation indoors, the change in heating and cooling degree days compared to the standard climate situation (ΔHDD, ΔCDD) are used as indicators. The annual HDD and CDD are calculated at hourly basis (i) for the whole year (i.e. 8760 hours for TRY12) with the assumption of a base of 18 °C and 24 °C, respectively.

$$HDD = \sum_1^{8760}(18 - T_i)/24 \text{ if } T_{urb} < 18\ °C \text{ and HDD} = 0 \text{ if } T_{urb} \geq 18\ °C \quad (42)$$

$$CDD = \sum_1^{8760}(T_i - 24)/24 \text{ if } T_{urb} > 24\ °C \text{ and CDD} = 0 \text{ if } T_{urb} \leq 24\ °C \quad (43)$$

$$\Delta HDD = HDD_{urb} - HDD_{stn} \quad (44)$$

$$\Delta CDD = CDD_{urb} - CDD_{stn} \quad (45)$$

In TRNSYS, Daylight is assumed for the period during which artificial lighting is not activated. It is deduced in relation to the maximum possible lighting $Q_{light(max)}$, which is determined as annual value by the settings for the power of the lighting appliance (13 W m^{-2}), the usage time in hours (11 hours) and the number of operation days of year DY (261 days):

$$DL = (1 - \Sigma\ Q_{light} / Q_{light(max)}) / 100 \quad \% \quad (46)$$

$$Q_{light(max)} = Q_{appl} \,.\, UT_h \,.\, DY_{use} = 13 \text{ x}11\ 261 = 37.323 \quad kWh\ m^{-2}\ a^{-1} \quad (47)$$

Two scenarios are assessed for the ventilation. First, it is assumed to be natural (i.e. openings) and so no energy demand is generated. Second, the ventilation is assumed to be mechanical. The ventilation energy demand was then determined from the total of air change per hour (ACH) which assumes that 0.56 W is needed for 1 h^{-1} (eq. (48), Schlenger 2009)

$$Q_{vent} = \left(\sum_{start}^{stop} n_i \,.\, V.\right).0.56 / A \quad kWh\ m^{-2}\ a^{-1} \quad (48)$$

Appendix 7 | More Results about the Urban Canyon Microclimate in PART I

Table 61: Deviation of urban air temperature from input standard climate TRY12 for the 18 case studies each canyon geometry (54 runs) as calculated by TEB

Mannheim (49.52 °N, 8.55 °E)

	case studies		1	2	3	4	5	6	7	8	9	10	11	12	13	14	15	16	17	18
H/W = 0.2	[-3,-4[	hours	0	0	15	0	0	4	0	15	0	0	0	0	0	0	0	0	0	0
	[-2,-3[	hours	1	11	24	0	1	21	0	24	13	0	0	0	0	0	0	0	0	0
	[-1,-2[	hours	12	15	37	1	11	30	0	39	14	3	4	7	1	3	4	0	7	4
	[0,-1[	hours	1706	2347	2842	911	1695	2625	532	2838	2380	943	1144	1437	720	941	1282	648	1438	1155
	[1,0[	hours	7040	6385	5841	7847	7052	6079	8225	5843	6351	7814	7612	7316	8039	7816	7474	8112	7315	7601
	[2,1[	hours	1	2	1	1	1	1	3	1	2	0	0	0	0	0	0	0	0	0
	[3,2[	hours	0	0	0	0	0	0	0	0	0	0	0	0	0	0	0	0	0	0
	[4,3[	hours	0	0	0	0	0	0	0	0	0	0	0	0	0	0	0	0	0	0
	[5,4[	hours	0	0	0	0	0	0	0	0	0	0	0	0	0	0	0	0	0	0
	minimal deviation	°C	-2.03	-2.79	-3.93	-1.03	-2.01	-3.51	-0.37	-3.94	-2.82	-1.47	-1.57	-1.60	-1.17	-1.48	-1.58	-0.73	-1.60	-1.58
	maximal deviation	°C	1.04	1.02	1.33	1.07	1.04	1.18	1.10	1.33	1.04	0.77	0.77	0.78	0.75	0.77	0.78	0.74	0.77	0.78
	cooler canyon	hours	1719	2373	2918	912	1707	2680	532	2916	2407	946	1148	1444	721	944	1286	648	1445	1159
	warmer canyon	hours	7041	6387	5842	7848	7053	6080	8228	5844	6353	7814	7612	7316	8039	7816	7474	8112	7315	7601
	-2 ≤ ΔTa < 0	hours	1718	2362	2879	912	1706	2655	532	2877	2394	946	1148	1444	721	944	1286	648	1445	1159
	0 < ΔTa ≤ 2	hours	7041	6387	5842	7848	7053	6080	8228	5844	6353	7814	7612	7316	8039	7816	7474	8112	7315	7601

	case studies		1	2	3	4	5	6	7	8	9	10	11	12	13	14	15	16	17	18
H/W = 1.0	[-3,-4[	hours	0	0	3	0	0	3	0	3	0	0	1	0	0	0	1	0	0	1
	[-2,-3[	hours	0	3	14	0	0	1	0	14	3	3	3	10	1	3	4	1	10	3
	[-1,-2[	hours	9	18	38	2	9	30	2	40	19	15	20	27	14	15	26	9	27	21
	[0,-1[	hours	674	1200	2078	363	673	1661	234	2079	1242	1822	2042	2377	1618	1819	2217	1559	2378	2056
	[1,0[	hours	7927	7435	6554	8219	7928	6985	8247	6551	7397	6685	6501	6184	6808	6686	6336	6782	6183	6487
	[2,1[	hours	150	104	73	176	150	80	277	73	99	217	174	141	297	219	157	363	140	173
	[3,2[	hours	0	0	0	0	0	0	0	0	0	18	19	21	22	18	19	46	22	19
	[4,3[	hours	0	0	0	0	0	0	0	0	0	0	0	0	0	0	0	0	0	0
	[5,4[	hours	0	0	0	0	0	0	0	0	0	0	0	0	0	0	0	0	0	0
	minimal deviation	°C	-1.86	-2.81	-3.92	-1.29	-1.82	-3.39	-1.13	-3.93	-2.86	-2.98	-3.03	-2.95	-2.72	-3.00	-3.00	-2.22	-2.95	-3.04
	maximal deviation	°C	1.66	1.59	1.49	1.80	1.67	1.53	1.99	1.49	1.59	2.31	2.30	2.41	2.37	2.31	2.36	2.47	2.41	2.31
	cooler canyon	hours	683	1221	2133	365	682	1695	236	2136	1264	1840	2066	2414	1633	1837	2248	1569	2415	2081
	warmer canyon	hours	8077	7539	6627	8395	8078	7065	8524	6624	7496	6920	6694	6346	7127	6923	6512	7191	6345	6679
	-2 ≤ ΔTa < 0	hours	683	1218	2116	365	682	1691	236	2119	1261	1837	2062	2404	1632	1834	2243	1568	2405	2077
	0 < ΔTa ≤ 2	hours	8077	7539	6627	8395	8078	7065	8524	6624	7496	6902	6675	6325	7105	6905	6493	7145	6323	6660

	case studies		1	2	3	4	5	6	7	8	9	10	11	12	13	14	15	16	17	18
H/W = 1.8	[-3,-4[	hours	0	0	4	0	0	2	0	4	0	2	12	12	1	2	13	0	12	12
	[-2,-3[	hours	2	5	3	2	2	6	2	3	5	15	17	34	4	15	29	3	34	18
	[-1,-2[	hours	9	9	23	4	9	12	1	25	10	54	64	70	40	55	66	34	70	64
	[0,-1[	hours	423	737	1521	257	421	1072	238	1524	764	1971	2175	2532	1774	1967	2354	1666	2532	2191
	[1,0[	hours	8043	7816	7083	8088	8042	7514	8055	7078	7791	6297	6148	5807	6461	6298	5979	6526	5807	6138
	[2,1[	hours	282	193	125	361	285	154	359	125	190	307	240	207	331	309	223	295	207	236
	[3,2[	hours	1	0	0	48	1	0	105	0	0	102	96	86	130	102	87	188	86	93
	[4,3[	hours	0	0	0	0	0	0	0	0	0	12	8	6	19	12	7	48	6	8
	[5,4[	hours	0	0	0	0	0	0	0	0	0	0	0	0	0	0	0	0	0	0
	minimal deviation	°C	-2.66	-2.86	-4.06	-2.42	-2.66	-3.48	-2.36	-4.07	-2.87	-3.21	-3.73	-5.21	-3.04	-3.23	-4.44	-2.78	-5.22	-3.77
	maximal deviation	°C	2.00	1.83	1.92	2.32	2.01	1.88	2.80	1.92	1.84	3.28	3.20	3.27	3.43	3.28	3.20	3.66	3.27	3.19
	cooler canyon	hours	434	751	1552	263	432	1092	241	1557	779	2042	2268	2654	1819	2039	2464	1703	2654	2285
	warmer canyon	hours	8326	8009	7208	8497	8328	7668	8519	7203	7981	6718	6492	6106	6941	6721	6296	7057	6106	6475
	-2 ≤ ΔTa < 0	hours	432	746	1544	261	430	1084	239	1549	774	2025	2239	2602	1814	2022	2420	1700	2602	2255
	0 < ΔTa ≤ 2	hours	8325	8009	7208	8449	8327	7668	8414	7203	7981	6604	6388	6014	6792	6607	6202	6821	6014	6374

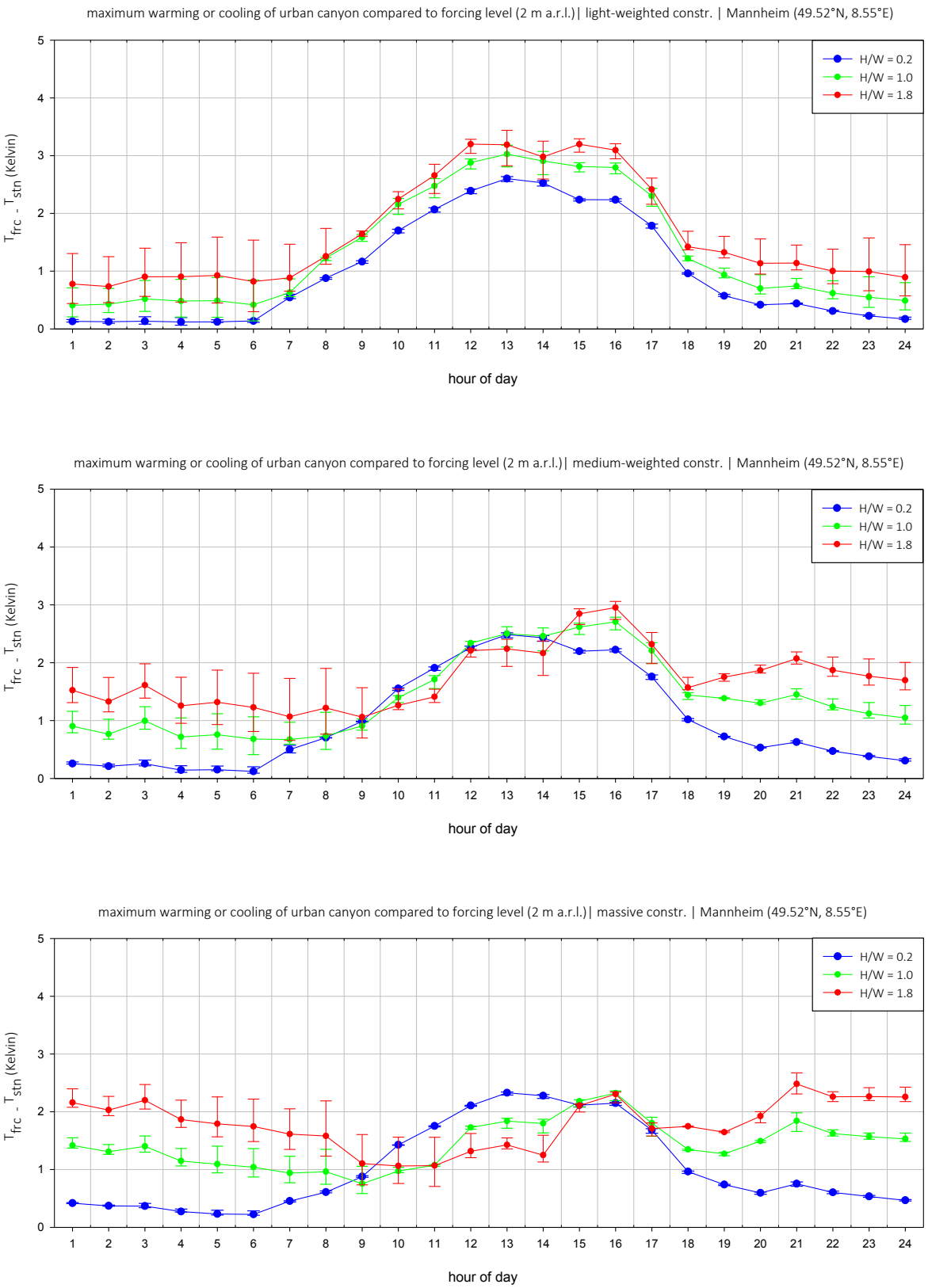

Figure 96: Hourly average deviation of urban air temperature from forcing height (2 m above roof level) differentiated according to the aspect ratio A and thermal mass E for a typical year TRY12 for Mannheim (49.52°N, 8.55°E)

Table 62: Minimum, mean and maximum yearly average heat fluxes at canyon top (W m^{-2}) for lightweight construction (left) and massive construction (right) for Mannheim (49.52°N, 8.55°E).

YEAR	(a) light-weighted construction											
MEAN	0.20				1.00				1.80			
RN	min	max	mean	range	min	max	mean	range	min	max	mean	range
1	-47.9	-46.3	-46.9	1.6	-48.0	-44.3	-45.9	3.7	-46.4	-42.6	-44.2	3.8
2	-46.7	-45.1	-45.7	1.7	-47.1	-43.3	-44.9	3.8	-45.4	-41.4	-43.2	4.0
3	-46.2	-44.5	-45.1	1.7	-46.8	-42.8	-44.5	4.0	-45.1	-41.0	-42.8	4.2
4	-44.1	-42.4	-43.0	1.8	-45.1	-41.0	-42.7	4.1	-43.4	-39.2	-41.0	4.3
5	-38.9	-37.1	-37.8	1.8	-40.3	-36.2	-37.9	4.2	-38.9	-34.5	-36.4	4.3
6	-19.3	-17.6	-18.3	1.8	-21.7	-17.6	-19.3	4.1	-20.8	-16.5	-18.4	4.3
7	17.0	18.7	18.0	1.6	12.8	16.7	15.1	3.9	12.5	16.6	14.8	4.1
8	75.6	77.0	76.4	1.4	69.1	72.4	71.0	3.4	66.8	70.4	68.9	3.6
9	138.0	139.0	138.6	1.0	129.9	132.4	131.3	2.5	125.5	128.2	127.1	2.7
10	202.0	202.7	202.4	0.7	193.6	195.3	194.6	1.6	187.3	189.1	188.3	1.8
11	246.8	247.2	247.0	0.4	240.1	241.0	240.6	0.9	232.4	233.5	233.1	1.0
12	262.2	262.4	262.3	0.2	258.2	258.8	258.5	0.5	250.4	251.1	250.8	0.6
13	262.1	262.2	262.2	0.1	260.4	260.7	260.6	0.3	253.0	253.4	253.2	0.4
14	228.1	228.1	228.1	0.0	228.5	228.7	228.5	0.2	222.0	222.3	222.2	0.3
15	181.1	181.2	181.2	0.1	183.1	183.3	183.2	0.2	178.1	178.4	178.2	0.3
16	120.2	120.3	120.3	0.2	123.0	123.4	123.3	0.4	119.6	120.1	119.9	0.5
17	54.0	54.3	54.2	0.3	57.5	58.2	57.9	0.7	55.7	56.5	56.2	0.8
18	-1.0	-0.5	-0.7	0.5	2.5	3.7	3.2	1.2	2.1	3.3	2.8	1.2
19	-34.0	-33.3	-33.6	0.7	-31.2	-29.5	-30.2	1.7	-30.7	-29.0	-29.7	1.7
20	-50.1	-49.1	-49.5	1.0	-48.1	-45.9	-46.8	2.2	-47.1	-44.9	-45.8	2.2
21	-51.5	-50.4	-50.8	1.2	-50.4	-47.7	-48.8	2.6	-49.2	-46.5	-47.6	2.7
22	-50.6	-49.3	-49.8	1.3	-50.0	-47.1	-48.3	2.9	-48.7	-45.7	-47.0	3.0
23	-50.0	-48.6	-49.1	1.4	-49.7	-46.4	-47.7	3.2	-48.2	-44.9	-46.3	3.3
24	-47.9	-46.4	-47.0	1.5	-47.7	-44.2	-45.7	3.5	-46.1	-42.5	-44.1	3.6

YEAR	(b) massive construction											
MEAN	0.20				1.00				1.80			
RN	min	max	mean	range	min	max	mean	range	min	max	mean	range
1	-53.0	-51.8	-52.2	1.1	-60.7	-58.6	-59.3	2.1	-61.1	-59.1	-59.8	2.0
2	-51.5	-50.2	-50.6	1.3	-59.1	-56.8	-57.6	2.4	-59.4	-57.2	-58.0	2.2
3	-50.7	-49.3	-49.7	1.4	-58.2	-55.6	-56.5	2.6	-58.5	-56.0	-56.9	2.4
4	-48.3	-46.9	-47.3	1.4	-55.7	-52.9	-53.8	2.8	-55.8	-53.2	-54.2	2.6
5	-42.6	-41.1	-41.6	1.5	-49.8	-46.9	-47.9	2.9	-50.0	-47.2	-48.2	2.8
6	-22.0	-20.5	-21.0	1.6	-28.9	-25.9	-26.9	3.1	-29.3	-26.4	-27.5	2.9
7	16.2	17.8	17.3	1.6	10.0	13.2	12.1	3.2	9.2	12.2	11.1	3.0
8	77.5	79.1	78.5	1.6	73.0	76.2	75.1	3.2	71.3	74.4	73.2	3.1
9	142.6	144.1	143.6	1.5	141.2	144.4	143.3	3.2	138.6	141.7	140.5	3.1
10	208.9	210.2	209.7	1.3	211.2	214.2	213.1	3.0	207.5	210.5	209.4	2.9
11	254.6	255.7	255.3	1.1	260.5	263.1	262.1	2.6	256.0	258.7	257.7	2.7
12	269.6	270.4	270.1	0.8	277.7	279.9	279.0	2.2	272.9	275.3	274.3	2.3
13	268.5	269.0	268.8	0.5	277.2	278.9	278.2	1.7	272.2	274.1	273.3	1.9
14	232.9	233.3	233.1	0.4	241.3	242.5	242.0	1.2	236.6	238.1	237.4	1.5
15	183.9	184.2	184.1	0.2	190.7	191.6	191.2	0.9	186.5	187.7	187.1	1.2
16	121.0	121.2	121.1	0.2	125.6	126.3	125.9	0.7	122.1	123.1	122.6	0.9
17	52.9	53.0	53.0	0.1	54.8	55.4	55.1	0.6	52.3	53.1	52.7	0.8
18	-4.0	-3.9	-4.0	0.1	-4.9	-4.4	-4.7	0.5	-6.6	-5.9	-6.3	0.7
19	-38.3	-38.2	-38.3	0.1	-41.9	-41.4	-41.6	0.5	-43.1	-42.3	-42.7	0.7
20	-55.3	-55.0	-55.1	0.3	-60.9	-60.2	-60.5	0.7	-61.8	-60.9	-61.3	0.9
21	-57.1	-56.6	-56.8	0.5	-64.0	-63.0	-63.4	1.0	-64.7	-63.6	-64.1	1.1
22	-56.1	-55.4	-55.6	0.6	-63.6	-62.3	-62.8	1.3	-64.3	-63.0	-63.5	1.3
23	-55.4	-54.6	-54.8	0.8	-63.2	-61.6	-62.1	1.6	-63.7	-62.2	-62.8	1.6
24	-53.2	-52.2	-52.5	1.0	-61.0	-59.1	-59.7	1.9	-61.4	-59.6	-60.3	1.8

YEAR	(a) light-weighted construction											
MEAN	0.2				1.0				1.8			
H	min	max	mean	range	min	max	mean	range	min	max	mean	range
1	-1.6	6.5	1.2	8.1	-6.2	17.3	1.7	23.5	-5.4	24.5	4.8	29.9
2	-2.5	5.6	0.3	8.1	-7.1	16.6	0.9	23.8	-6.3	24.0	4.1	30.3
3	-2.6	5.6	0.2	8.3	-7.3	17.0	1.0	24.2	-6.5	24.5	4.1	31.0
4	-3.0	5.5	-0.1	8.5	-7.9	17.1	0.6	25.0	-7.2	24.7	3.8	31.9
5	-2.7	5.9	0.2	8.6	-7.8	17.6	0.9	25.4	-7.3	25.2	3.9	32.4
6	1.9	10.2	4.8	8.3	-3.2	22.1	5.5	25.3	-3.2	29.4	8.2	32.6
7	22.5	29.9	25.1	7.4	17.9	41.6	26.3	23.7	16.7	47.5	27.5	30.7
8	49.1	55.4	51.4	6.3	50.7	72.1	58.5	21.4	48.8	77.6	59.2	28.8
9	80.5	85.4	82.4	4.8	89.2	106.3	95.6	17.2	87.7	111.8	96.6	24.1
10	122.9	126.2	124.2	3.3	140.4	152.7	145.2	12.3	139.8	158.4	146.9	18.6
11	172.5	174.5	173.4	2.0	193.2	201.2	196.6	8.0	193.9	207.0	199.1	13.1
12	208.9	210.1	209.5	1.2	229.8	235.0	232.2	5.2	230.0	239.2	233.9	9.2
13	231.4	232.1	231.8	0.7	249.7	253.2	251.4	3.5	248.4	255.1	251.3	6.7
14	227.6	228.2	227.9	0.5	240.6	243.3	241.8	2.7	238.1	243.6	240.4	5.5
15	210.7	211.4	210.9	0.6	219.7	222.5	220.7	2.8	216.3	221.8	218.3	5.5
16	173.9	175.1	174.3	1.3	176.0	180.4	177.5	4.3	172.0	179.2	174.5	7.2
17	132.7	135.1	133.5	2.4	130.2	137.6	132.6	7.3	126.6	137.0	130.1	10.5
18	93.7	97.4	94.9	3.7	87.7	98.5	91.2	10.8	85.1	99.3	89.8	14.2
19	48.2	53.0	49.7	4.8	42.3	56.2	46.8	13.9	41.5	59.1	47.3	17.6
20	21.4	27.3	23.3	5.9	16.4	33.3	21.9	16.9	16.8	37.9	23.8	21.1
21	11.1	17.8	13.3	6.8	6.9	26.2	13.2	19.3	7.8	31.9	15.8	24.1
22	4.2	11.4	6.6	7.2	0.2	20.9	7.1	20.6	1.2	27.1	9.8	25.9
23	2.1	9.5	4.5	7.4	-1.4	20.1	5.8	21.5	-0.2	27.0	9.0	27.1
24	0.0	7.7	2.6	7.7	-3.7	18.8	3.9	22.5	-2.5	26.0	7.1	28.5

YEAR	(b) massive construction											
MEAN	0.2				1.0				1.8			
H	min	max	mean	range	min	max	mean	range	min	max	mean	range
1	15.7	23.2	17.9	7.5	43.7	63.3	49.7	19.6	55.0	79.2	62.7	24.2
2	11.7	19.7	14.1	8.1	35.0	56.2	41.5	21.2	45.3	71.4	53.6	26.1
3	9.9	18.4	12.5	8.5	30.9	53.5	37.8	22.6	40.9	68.6	49.6	27.7
4	7.9	16.9	10.6	9.0	26.0	50.0	33.4	24.0	35.5	65.0	44.8	29.5
5	6.2	15.6	9.1	9.4	21.3	46.7	29.2	25.4	30.0	61.1	39.8	31.1
6	6.9	16.4	9.9	9.6	18.3	44.4	26.5	26.1	25.8	58.0	36.1	32.3
7	19.5	28.8	22.4	9.3	22.0	47.7	30.2	25.6	25.8	57.6	36.0	31.8
8	33.2	42.7	36.3	9.4	22.7	48.9	31.2	26.2	22.3	54.6	32.8	32.3
9	51.3	60.2	54.3	9.0	23.3	48.8	31.7	25.5	17.7	49.1	28.1	31.4
10	80.2	88.4	83.1	8.2	34.1	58.4	42.4	24.3	21.7	52.0	31.9	30.3
11	122.9	129.9	125.6	6.9	62.6	84.5	70.4	21.9	43.7	71.8	53.5	28.1
12	162.2	167.3	164.3	5.1	100.5	119.1	107.5	18.6	77.0	102.0	86.1	25.0
13	190.8	194.3	192.5	3.5	133.3	148.2	139.4	14.8	108.1	129.3	116.2	21.3
14	197.7	200.1	198.9	2.4	151.0	162.0	156.0	11.1	128.3	145.5	135.3	17.3
15	193.9	195.4	194.6	1.4	164.0	172.1	167.9	8.1	145.8	159.4	151.8	13.5
16	170.6	171.9	171.4	1.3	157.4	163.2	160.3	5.8	145.1	155.6	150.1	10.5
17	142.7	143.8	143.4	1.1	147.4	152.4	149.9	5.0	141.4	150.8	146.0	9.5
18	116.5	117.1	116.8	0.7	139.1	143.4	141.4	4.3	139.0	148.0	143.3	9.0
19	76.0	76.9	76.5	0.9	109.4	114.4	111.8	4.9	114.1	123.6	118.3	9.5
20	51.8	53.9	52.5	2.1	91.9	99.0	94.7	7.1	100.6	111.9	105.1	11.3
21	41.2	44.6	42.2	3.4	83.8	93.5	87.2	9.7	95.1	108.8	100.1	13.7
22	30.8	35.5	32.2	4.7	70.3	82.7	74.4	12.4	82.1	98.5	87.7	16.3
23	24.9	30.5	26.5	5.6	60.9	75.6	65.5	14.7	73.1	91.9	79.2	18.8
24	19.0	25.7	21.0	6.7	50.0	67.4	55.4	17.4	61.5	83.3	68.5	21.8

YEAR	(a) light-weighted construction											
MEAN	0.2				1.0				1.8			
G	min	max	mean	range	min	max	mean	range	min	max	mean	range
1	-43.8	-34.1	-37.5	9.8	-54.2	-26.7	-36.3	27.5	-59.4	-25.3	-37.3	34.0
2	-41.7	-31.8	-35.2	9.9	-52.5	-24.5	-34.3	27.9	-57.8	-23.1	-35.4	34.7
3	-41.1	-31.0	-34.5	10.1	-52.4	-23.9	-33.9	28.5	-57.9	-22.3	-34.9	35.5
4	-38.7	-28.4	-32.0	10.4	-50.6	-21.2	-31.6	29.4	-56.2	-19.6	-32.7	36.6
5	-34.0	-23.5	-27.2	10.5	-46.7	-16.8	-27.3	29.9	-52.4	-15.2	-28.5	37.2
6	-18.8	-8.6	-12.2	10.2	-32.9	-3.2	-13.8	29.8	-39.1	-1.9	-15.2	37.2
7	10.2	19.3	16.0	9.1	-6.4	21.3	11.3	27.7	-12.6	22.3	9.7	34.9
8	50.0	57.6	54.7	7.6	25.2	49.8	40.7	24.5	17.0	49.1	37.4	32.1
9	82.2	87.9	85.7	5.8	51.8	71.2	63.9	19.4	41.5	67.9	58.1	26.5
10	105.2	109.0	107.5	3.8	69.0	82.5	77.2	13.5	56.4	76.1	68.7	19.8
11	101.2	103.5	102.5	2.3	67.3	76.0	72.2	8.7	53.5	67.3	61.6	13.8
12	80.9	82.3	81.6	1.3	52.1	57.7	55.1	5.6	39.9	49.5	45.3	9.6
13	59.2	60.0	59.6	0.7	36.6	40.3	38.5	3.7	27.2	34.1	31.0	6.9
14	29.4	29.9	29.6	0.5	14.8	17.6	16.3	2.8	7.9	13.6	11.2	5.7
15	-0.7	0.0	-0.3	0.6	-9.6	-6.7	-7.8	2.9	-14.0	-8.3	-10.4	5.6
16	-25.2	-23.8	-24.2	1.4	-27.5	-22.8	-24.4	4.7	-29.7	-22.1	-24.7	7.6
17	-51.2	-48.5	-49.4	2.7	-50.2	-42.2	-44.8	8.0	-51.4	-40.2	-44.0	11.2
18	-68.5	-64.3	-65.6	4.2	-66.1	-54.1	-58.0	12.0	-67.2	-51.8	-57.0	15.4
19	-69.9	-64.3	-66.1	5.6	-70.2	-54.5	-59.7	15.7	-72.6	-53.2	-59.7	19.4
20	-67.3	-60.4	-62.7	6.9	-71.2	-52.0	-58.4	19.2	-74.7	-51.3	-59.3	23.5
21	-59.2	-51.2	-53.9	8.0	-66.1	-44.1	-51.5	22.1	-70.5	-43.5	-52.8	27.0
22	-51.7	-43.1	-46.0	8.6	-60.3	-36.6	-44.7	23.8	-65.1	-35.9	-46.0	29.2
23	-49.0	-40.1	-43.2	8.9	-58.9	-34.0	-42.6	24.9	-64.2	-33.4	-44.1	30.8
24	-45.0	-35.6	-38.8	9.4	-55.4	-29.1	-38.3	26.3	-60.7	-28.2	-39.6	32.5

YEAR	(b) massive construction											
MEAN	0.2				1.0				1.8			
G	min	max	mean	range	min	max	mean	range	min	max	mean	range
1	-66.0	-57.3	-59.9	8.7	-113.8	-92.1	-98.8	21.8	-130.1	-103.8	-112.3	26.3
2	-60.9	-51.5	-54.3	9.4	-105.1	-81.5	-88.9	23.6	-120.6	-92.2	-101.3	28.4
3	-58.8	-48.9	-51.9	10.0	-101.5	-76.3	-84.1	25.3	-116.9	-86.6	-96.3	30.2
4	-54.7	-44.2	-47.4	10.5	-95.3	-68.3	-76.8	27.0	-110.3	-78.0	-88.4	32.3
5	-47.7	-36.8	-40.2	11.0	-86.1	-57.7	-66.7	28.4	-100.6	-66.6	-77.5	34.0
6	-28.0	-16.7	-20.3	11.2	-63.0	-33.6	-43.0	29.4	-76.9	-41.5	-53.0	35.4
7	10.7	21.7	18.2	11.0	-14.5	14.5	5.2	29.0	-25.2	9.8	-1.6	35.0
8	65.2	76.3	72.6	11.1	54.3	84.0	74.3	29.6	47.0	82.6	70.9	35.7
9	112.7	123.2	119.7	10.5	122.9	151.7	142.1	28.8	120.0	154.6	143.0	34.6
10	150.5	160.1	156.7	9.6	182.9	210.3	200.8	27.4	185.7	219.0	207.6	33.3
11	154.2	162.2	159.1	7.9	205.7	230.2	221.4	24.5	213.9	244.6	233.8	30.7
12	131.5	137.2	134.8	5.7	188.2	208.8	201.0	20.6	200.4	227.5	217.6	27.1
13	103.5	107.4	105.6	3.9	158.7	175.1	168.3	16.3	172.5	195.5	186.6	23.0
14	62.2	65.0	63.6	2.7	109.0	121.1	115.6	12.1	120.7	139.3	131.7	18.6
15	18.1	19.7	18.9	1.6	48.3	57.1	52.8	8.8	56.7	71.2	64.8	14.5
16	-21.2	-19.7	-20.6	1.4	-7.9	-1.4	-4.6	6.4	-3.7	7.6	2.2	11.3
17	-61.1	-59.9	-60.6	1.2	-67.7	-62.3	-65.1	5.4	-68.7	-58.7	-63.6	10.1
18	-91.3	-90.5	-90.9	0.8	-118.5	-113.8	-116.3	4.7	-124.8	-115.3	-119.9	9.6
19	-98.1	-97.1	-97.7	1.0	-139.2	-133.8	-136.4	5.4	-149.6	-139.4	-143.9	10.2
20	-99.2	-96.8	-97.7	2.3	-150.0	-142.2	-145.3	7.8	-163.8	-151.6	-156.5	12.2
21	-91.7	-87.8	-89.0	3.9	-147.5	-136.8	-140.6	10.7	-163.6	-148.8	-154.3	14.8
22	-81.4	-76.0	-77.6	5.3	-136.2	-122.6	-127.1	13.7	-152.7	-135.0	-141.1	17.7
23	-75.8	-69.3	-71.2	6.5	-128.8	-112.5	-117.7	16.3	-145.7	-125.3	-132.0	20.4
24	-68.6	-60.9	-63.2	7.7	-118.3	-99.0	-105.0	19.3	-134.6	-111.0	-118.7	23.6

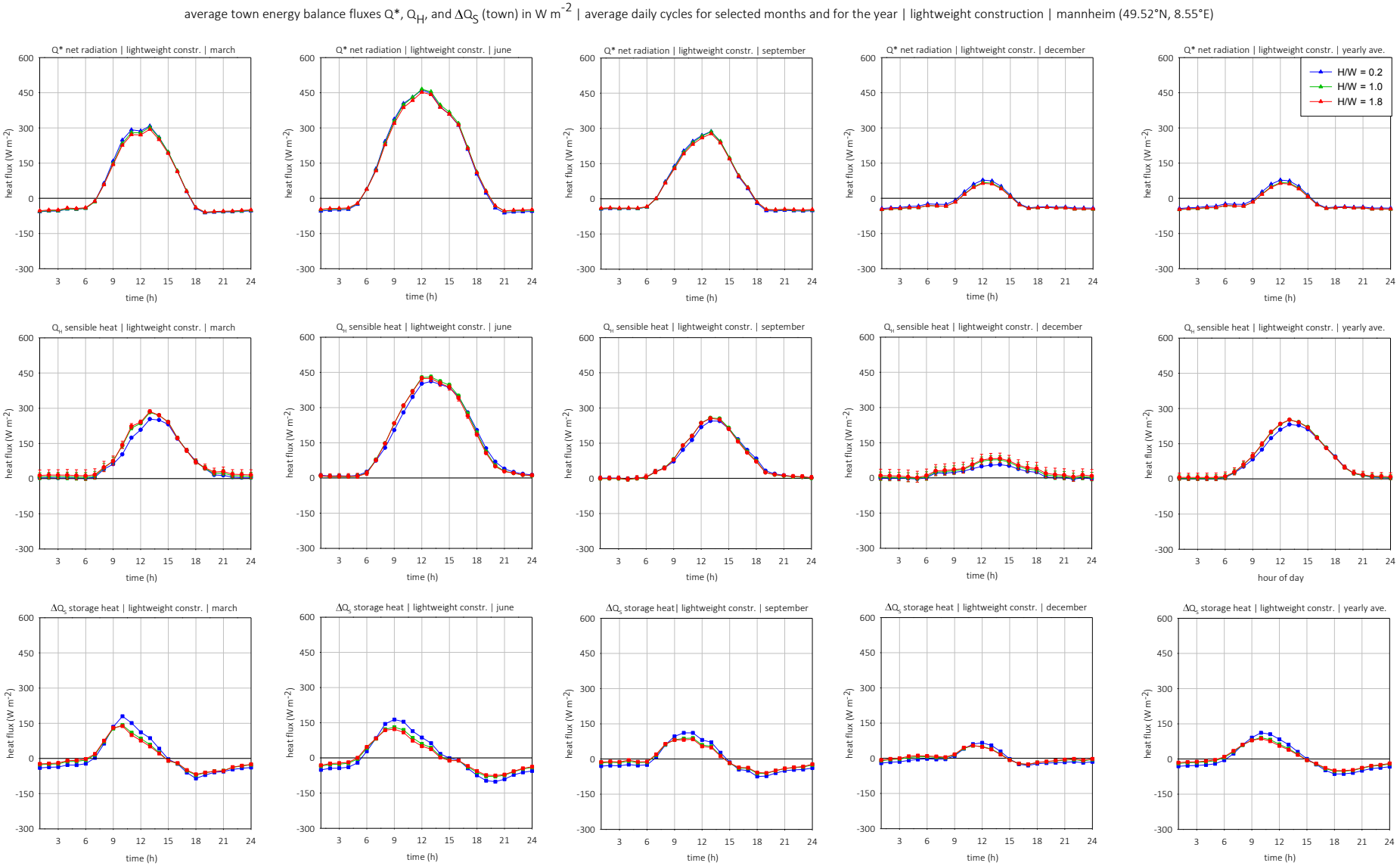

Figure 97: Seasonal and annual average town energy balance fluxes (Q*, Q_H, ΔQ_S) in W m^{-2} for lightweight construction for Mannheim (49.52°N, 8.55°E)

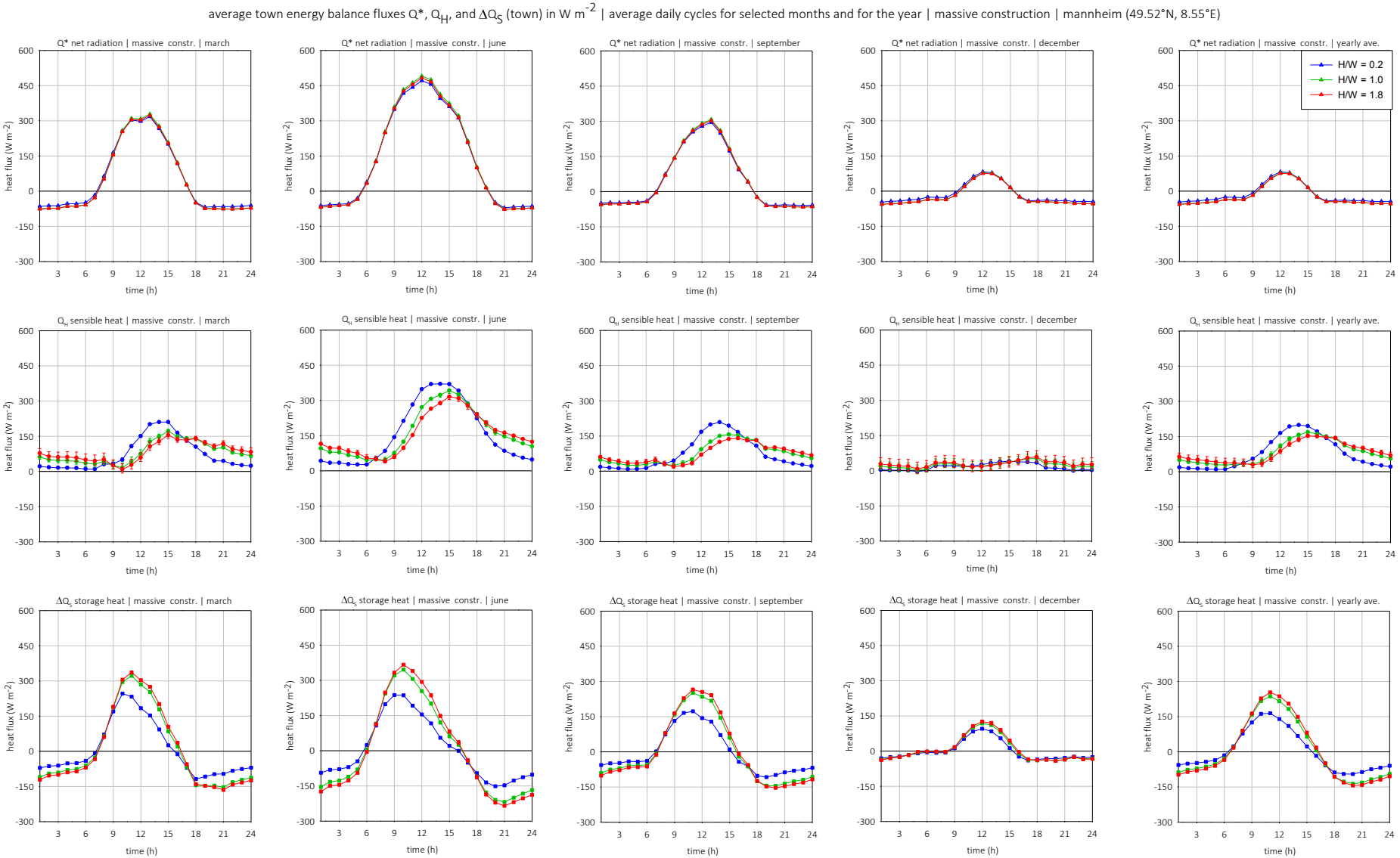

Figure 98: Seasonal and annual average town energy balance fluxes (Q*, Q_H, ΔQ_S) in W m^{-2} for massive construction for Mannheim (49.52°N, 8.55°E)

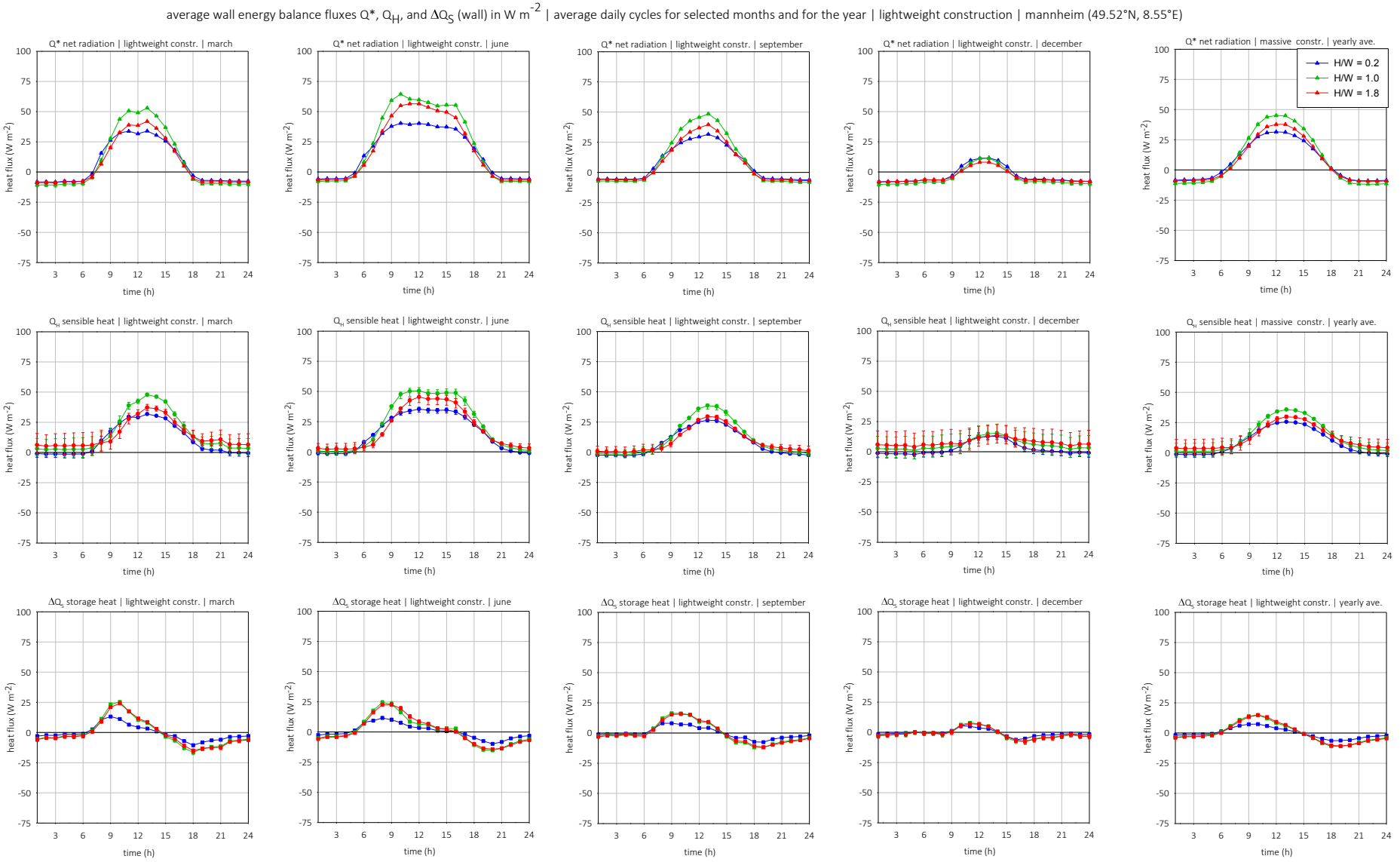

Figure 99: Seasonal and annual average energy balance fluxes (Q*, Q_H, ΔQ_S) at walls in W m^{-2} for lightweight construction for Mannheim (49.52°N, 8.55°E)

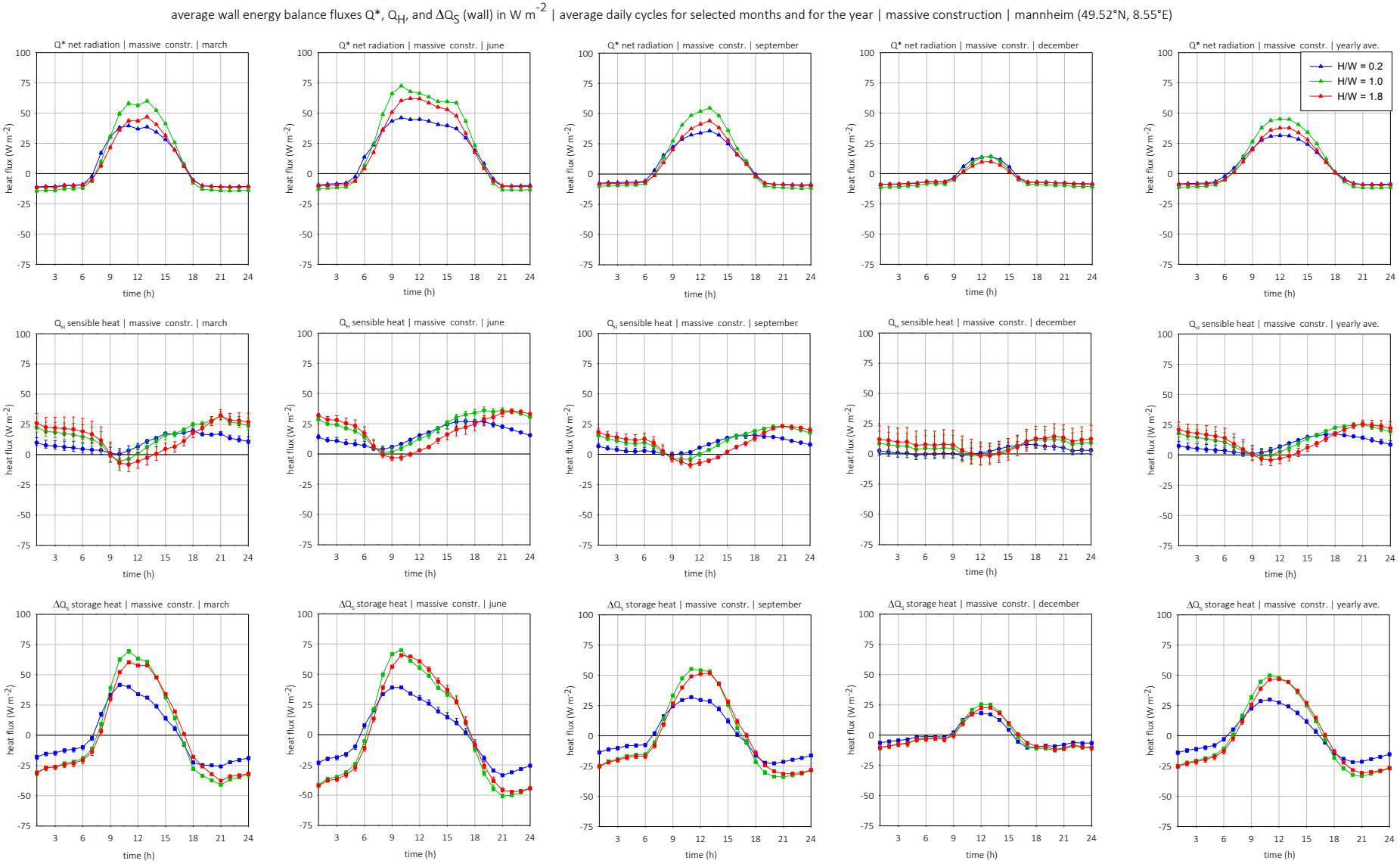

Figure 100: Seasonal and annual average energy balance fluxes (Q*, Q_H, ΔQ_S) at walls in W m^{-2} for massive construction for Mannheim (49.52°N, 8.55°E)

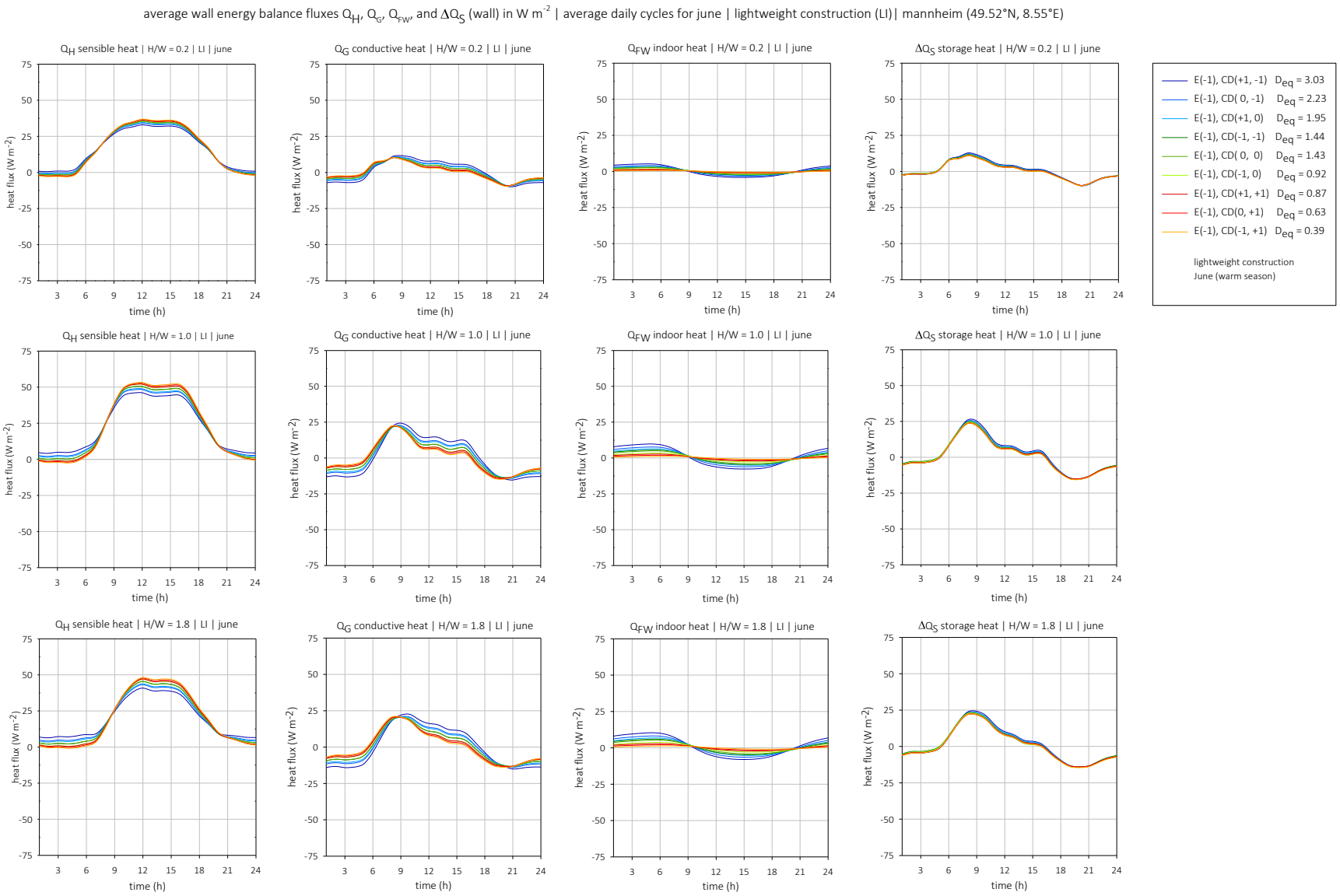

Figure 101: Average wall energy balance fluxes (Q_H, Q_G, Q_{FW} and ΔQ_S) in W m^{-2} for June and lightweight construction for Mannheim (49.52°N, 8.55°E)

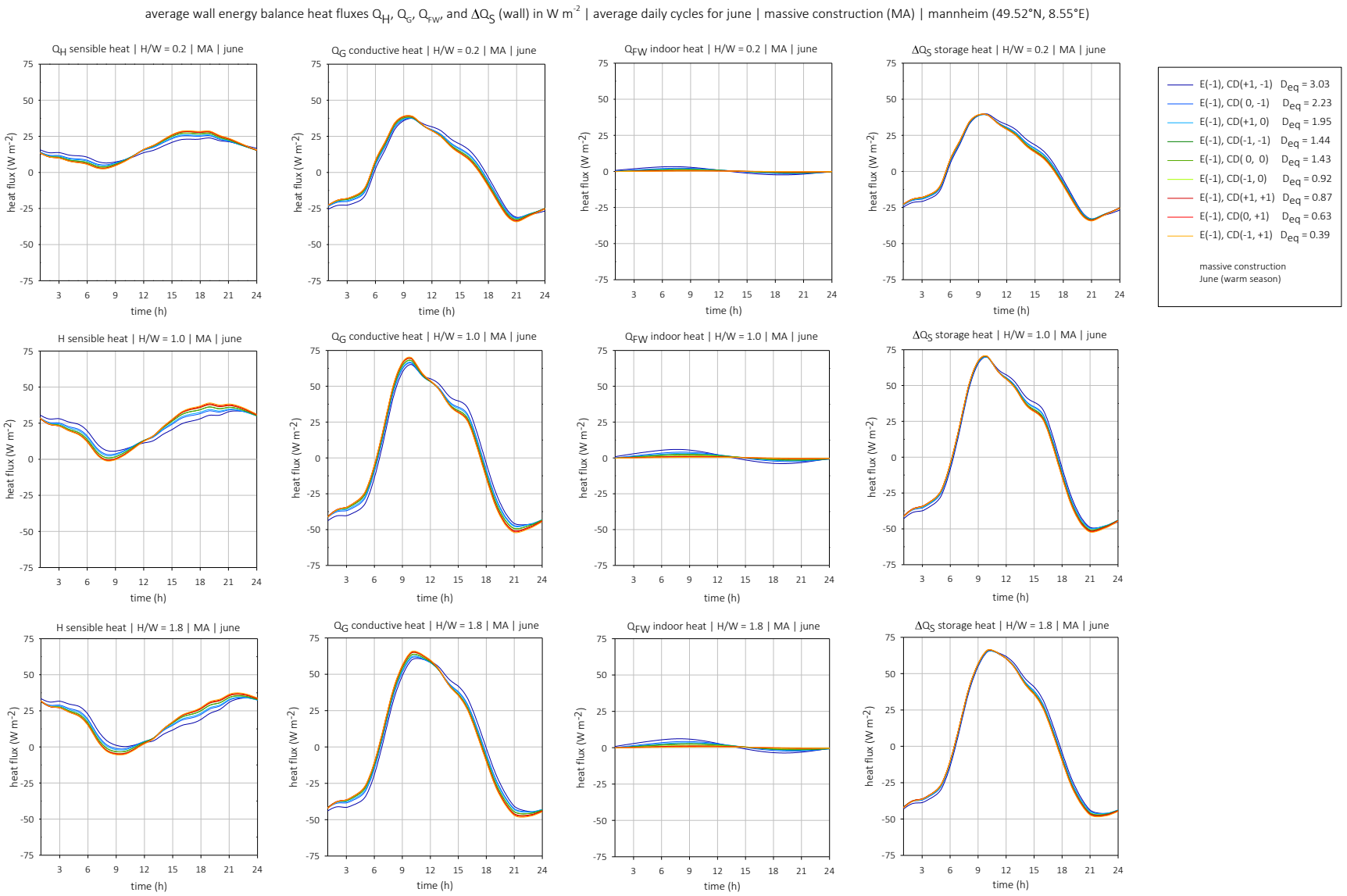

Figure 102: Average wall energy balance fluxes (Q_H, Q_G, Q_{FW} and ΔQ_S) in W m^{-2} for June and massive construction for Mannheim (49.52°N, 8.55°E)

Appendix 8 | Energy Demands of the Urban Office Buildings – Mannheim

Refer to section II - 3 (p 125) for explanation about these data. The following legend gives the colour coding used in Table 63 below.

Table 63: Useful energy demand average values for the whole building (10 zones) expressed as ranking for heating (Qheat), cooling (Qcool), artificial lighting (Qlight), ventilation (Q_{vent} during and outside usage time: UT, OU) and as sum (Q_{TOT}) for [SET IV], Mannheim (49.52°N, 8.55 °)

legend		
-1	PF	perforated façade (30%)
0	RF	row façade (60%)
+1	GF	glazed façade (90%)
-1	U -	weak insulation (0.65)
0	U o	medium insulation (0.40)
+1	U +	good insulation (0.15)
-1	LI	light-weighted
+1	MA	massive

A: urban vertical profile H/W
B: Facade's orientation
C: window ratio D: thermal insulation
E: thermal inertia

B			A
-1	0	1	
NWSE	NS	NESW	
I	IV	VII	0.2 (-1)
II	V	VIII	1.0 (0)
III	VI	IX	1.8 (+1)

C	D	E	ID
PF (-1)	U- (-1)	LI (-1)	1
PF (-1)	Uo (0)	LI (-1)	2
PF (-1)	U+ (+1)	LI (-1)	3
RF (0)	U- (-1)	LI (-1)	4
RF (0)	Uo (0)	LI (-1)	5
RF (0)	U+ (+1)	LI (-1)	6
GF (+1)	U- (-1)	LI (-1)	7
GF (+1)	Uo (0)	LI (-1)	8
GF (+1)	U+ (+1)	LI (-1)	9

C	D	E	ID
PF (-1)	U- (-1)	MA (+1)	10
PF (-1)	Uo (0)	MA (+1)	11
PF (-1)	U+ (+1)	MA (+1)	12
RF (0)	U- (-1)	MA (+1)	13
RF (0)	Uo (0)	MA (+1)	14
RF (0)	U+ (+1)	MA (+1)	15
GF (+1)	U- (-1)	MA (+1)	16
GF (+1)	Uo (0)	MA (+1)	17
GF (+1)	U+ (+1)	MA (+1)	18

rank	Heating			Cooling			Heating & Cooling			Lighting			Total Ventilation			Ventilation UT			Ventilation OU			Total (no Vent.)			Total (with Vent.)		
1	IV	12	3.58	III	10	2.30	VI	12	9.09	VII	16	7.95	VI	4	7.19	IX	13	5.25	VI	7	1.83	IV	18	32.07	IV	18	41.69
2	VII	12	3.63	VI	10	2.31	III	12	9.15	VII	7	7.95	IX	4	7.22	III	13	5.25	IX	7	1.85	I	18	34.65	I	18	44.33
3	I	12	3.71	IX	10	2.33	IX	12	9.27	I	16	7.97	III	4	7.24	VI	13	5.26	III	7	1.85	VII	18	35.07	VII	18	44.63
4	V	12	3.89	V	10	2.46	V	12	9.38	I	7	7.97	VI	7	7.24	IX	16	5.29	VI	4	1.87	V	18	36.16	V	18	45.62
5	II	12	3.93	IV	10	2.62	IV	12	9.40	IV	16	7.99	IX	7	7.26	VI	16	5.29	III	4	1.89	IV	15	36.93	IV	15	46.61
6	VIII	12	4.01	VI	13	2.62	II	12	9.64	IV	7	7.99	III	7	7.29	V	13	5.30	IX	4	1.89	II	18	37.24	II	18	46.70
7	VI	12	4.14	II	10	2.70	I	12	9.88	I	17	10.13	VI	1	7.33	III	16	5.31	VI	1	1.91	I	15	37.59	I	15	47.37
8	III	12	4.16	IX	13	2.84	VII	12	10.04	I	8	10.13	IX	1	7.33	VI	10	5.31	IX	1	1.92	VIII	18	38.02	VIII	18	47.46
9	IX	12	4.23	III	13	2.95	VIII	12	10.13	VII	17	10.22	III	1	7.34	II	10	5.32	III	1	1.92	VII	15	38.05	VII	15	47.72
10	IV	3	4.41	VIII	10	3.09	IV	15	12.10	VII	8	10.22	V	1	7.43	V	10	5.32	V	1	2.00	IV	9	38.58	IV	9	47.87
11	VII	3	4.42	VII	10	3.41	V	15	12.60	IV	17	10.34	V	4	7.48	III	10	5.32	V	7	2.03	II	15	39.59	II	15	49.20
12	I	3	4.52	V	13	3.47	VI	15	12.62	IV	8	10.34	II	1	7.50	IX	10	5.32	V	4	2.04	V	15	40.10	VI	18	49.47
13	V	3	4.62	I	10	3.49	III	15	12.70	II	16	10.36	IV	1	7.55	VIII	10	5.33	II	1	2.05	VI	18	40.18	III	18	49.49
14	II	3	4.65	VI	14	3.63	IX	15	12.73	II	7	10.36	II	4	7.57	VI	4	5.33	IV	1	2.09	III	18	40.19	V	15	49.68
15	VIII	3	4.69	III	14	3.88	II	15	12.80	V	16	10.49	VIII	1	7.57	IX	4	5.33	II	7	2.09	VIII	15	40.31	IX	18	49.86
16	III	3	4.78	III	11	3.92	I	15	13.21	V	7	10.49	V	7	7.64	IV	10	5.33	II	4	2.10	IX	18	40.59	VIII	15	49.91
17	VI	3	4.80	IX	14	3.93	VIII	15	13.36	VIII	16	10.56	VIII	4	7.65	II	13	5.34	VIII	1	2.11	I	9	40.63	VII	9	50.00
18	IX	3	4.84	IX	11	3.95	VII	15	13.38	VIII	7	10.56	IX	13	7.66	VII	10	5.35	IV	4	2.15	VII	9	40.68	I	9	50.05

Table 63 continued - Cases 19 to 54

rank	Heating			Cooling			Heating & Cooling			Lighting			Total Ventilation			Ventilation UT			Ventilation OU			Total (no Vent.)			Total (with Vent.)		
19	IV	15	6.39	VI	11	3.98	III	3	15.34	I	13	10.69	III	13	7.66	III	4	5.35	VIII	4	2.16	V	9	42.43	V	9	51.53
20	I	15	6.67	V	11	4.00	VI	3	15.34	I	4	10.69	VI	13	7.66	VIII	13	5.35	VIII	7	2.17	IV	6	42.96	IV	6	52.31
21	VII	15	6.84	II	11	4.03	IX	3	15.44	VII	13	10.78	VII	1	7.66	IV	13	5.37	IV	7	2.17	III	15	43.17	II	9	52.40
22	V	15	7.10	IV	11	4.13	IV	3	15.68	VII	4	10.78	I	1	7.71	I	10	5.37	VII	1	2.18	II	9	43.26	III	15	52.71
23	II	15	7.15	V	14	4.19	V	3	15.69	IV	13	10.83	IV	4	7.72	V	16	5.41	I	1	2.19	I	6	43.33	I	6	52.77
24	VIII	15	7.17	IV	13	4.20	IV	18	15.79	IV	4	10.83	II	7	7.73	VII	13	5.41	VII	4	2.23	VI	15	43.62	VIII	9	52.78
25	IV	6	7.20	VIII	11	4.37	II	3	15.84	II	17	12.81	VI	16	7.75	IX	7	5.41	I	4	2.24	VIII	9	43.62	VII	6	53.08
26	I	6	7.30	II	13	4.41	I	3	15.98	II	8	12.81	IX	16	7.76	VI	7	5.41	VII	7	2.26	VII	6	43.72	VI	15	53.12
27	VI	15	7.43	VI	16	4.44	VII	3	16.14	IX	16	12.86	III	16	7.80	IX	1	5.42	I	7	2.28	IX	15	43.94	IV	14	53.33
28	III	15	7.49	VII	11	4.47	VIII	3	16.22	IX	7	12.86	VII	4	7.80	VI	1	5.42	VI	8	2.28	IV	14	44.61	IX	15	53.48
29	IX	15	7.49	I	11	4.52	VI	18	16.66	VI	16	12.88	VIII	7	7.82	III	1	5.42	IX	8	2.29	I	12	44.91	II	6	54.77
30	VII	6	7.50	IX	16	4.67	V	18	16.67	VI	7	12.88	V	13	7.84	V	1	5.43	III	8	2.30	IV	12	45.13	I	12	54.85
31	V	6	7.76	IV	14	4.71	III	18	16.87	V	17	12.88	VI	10	7.85	I	13	5.43	VI	5	2.32	II	6	45.54	IV	12	55.05
32	II	6	7.77	III	16	4.84	IX	18	17.05	V	8	12.88	I	4	7.86	III	7	5.44	IX	5	2.33	II	12	45.97	I	14	55.14
33	VIII	6	7.79	VI	12	4.95	II	18	17.86	III	16	12.92	III	10	7.87	II	16	5.44	III	5	2.33	VIII	6	46.04	III	9	55.16
34	IX	6	8.03	III	12	4.99	IV	6	18.13	III	7	12.92	IX	10	7.87	VIII	16	5.45	VI	2	2.38	III	12	46.07	VI	9	55.19
35	VI	6	8.04	II	14	5.03	I	18	18.44	VIII	17	12.99	V	10	7.89	V	4	5.45	III	2	2.38	V	12	46.09	IX	9	55.28
36	III	6	8.04	IX	12	5.04	V	6	18.66	VIII	8	12.99	II	10	7.92	II	1	5.45	IX	2	2.40	V	6	46.16	VIII	6	55.30
37	IV	18	9.48	VIII	13	5.07	II	6	18.76	II	13	13.63	VIII	10	7.92	VIII	1	5.46	VI	13	2.41	VI	12	46.21	V	6	55.34
38	I	18	10.05	VI	15	5.19	VII	18	18.82	II	4	13.63	IV	10	7.94	IV	1	5.46	IX	13	2.41	I	14	46.27	II	12	55.82
39	IV	9	10.33	III	15	5.21	VIII	18	18.83	V	13	13.74	II	13	7.95	II	4	5.47	III	13	2.41	III	9	46.29	III	12	55.82
40	VII	18	10.56	IX	15	5.24	VI	6	18.89	V	4	13.74	IX	5	7.99	VII	1	5.48	VI	16	2.45	VI	9	46.35	VI	12	55.93
41	I	9	10.67	VI	18	5.24	III	6	18.92	VIII	13	13.90	IV	7	7.99	VIII	4	5.49	V	5	2.46	VII	12	46.42	V	12	55.94
42	V	18	10.82	V	12	5.49	IX	6	18.93	VIII	4	13.90	VIII	13	7.99	IV	16	5.49	IX	16	2.47	IX	9	46.45	VII	14	56.05
43	II	18	10.89	V	15	5.49	I	6	18.95	I	14	13.93	VI	5	7.99	I	1	5.51	V	8	2.49	IX	12	46.48	IX	12	56.22
44	VIII	18	11.03	III	18	5.52	VII	6	19.05	I	5	13.93	VI	8	8.00	IX	14	5.52	III	16	2.49	VIII	12	46.89	VII	12	56.40
45	VII	9	11.03	IX	18	5.52	VIII	6	19.09	VII	14	14.17	IX	8	8.01	VI	14	5.52	V	2	2.49	VII	14	47.25	VIII	12	56.76
46	II	9	11.32	VI	17	5.53	IV	11	21.67	VII	5	14.17	III	5	8.01	VII	16	5.52	II	5	2.50	V	14	48.52	V	14	57.14
47	III	18	11.35	II	15	5.66	II	11	21.97	IV	14	14.24	VII	10	8.02	III	14	5.53	II	2	2.52	I	11	49.05	I	11	57.98
48	V	9	11.35	VIII	14	5.68	V	11	22.03	IV	5	14.24	III	8	8.04	VI	17	5.54	II	8	2.53	IV	11	49.18	IV	5	57.99
50	VI	18	11.42	IV	15	5.71	IX	11	22.13	III	8	15.70	I	10	8.05	I	16	5.56	V	13	2.54	III	6	49.39	IV	11	58.06
51	IX	18	11.53	II	12	5.71	III	11	22.19	VI	17	15.73	VII	7	8.07	III	17	5.56	III	10	2.55	IV	5	49.60	III	6	58.45
52	III	9	11.70	VII	13	5.76	VI	11	22.21	VI	8	15.73	V	16	8.13	IV	4	5.57	IX	10	2.55	VII	11	49.66	VII	11	58.57
53	IX	9	11.80	IV	12	5.82	VII	11	22.27	IX	17	15.80	VII	13	8.15	VII	4	5.58	VIII	5	2.55	VI	6	49.89	VI	6	58.92
54	VI	9	11.83	V	18	5.85	IV	9	22.30	IX	8	15.80	I	7	8.17	V	14	5.58	IV	5	2.56	IX	6	50.14	VIII	14	59.03

Table 63 continued - Cases 55 to 90

rank	Heating			Cooling			Heating & Cooling			Lighting			Total Ventilation			Ventilation UT			Ventilation OU			Total (no Vent.)			Total (with Vent.)		
55	IV	2	17.38	III	17	5.90	VIII	11	22.36	I	18	16.21	VI	2	8.19	V	7	5.61	IV	2	2.56	VIII	14	50.33	IX	6	59.21
56	I	2	17.44	I	13	5.96	VI	9	22.83	I	9	16.21	III	2	8.21	VIII	14	5.61	V	10	2.57	IV	17	50.77	I	5	59.56
57	IV	11	17.54	VII	14	6.10	IX	9	22.90	VII	18	16.25	V	5	8.21	II	14	5.62	VIII	2	2.57	I	3	51.01	IV	17	59.77
58	I	11	17.58	VIII	12	6.12	V	9	22.94	VII	9	16.25	I	13	8.22	IV	14	5.62	VIII	8	2.59	I	5	51.04	VII	5	60.15
59	VII	2	17.58	V	16	6.15	III	9	22.97	IV	18	16.28	II	16	8.23	I	4	5.62	VIII	10	2.60	IV	3	51.41	II	11	60.29
60	II	2	17.70	I	12	6.17	II	9	23.88	IV	9	16.28	IX	2	8.23	VI	11	5.62	II	10	2.60	II	11	51.44	I	3	60.53
61	V	2	17.72	VIII	15	6.19	I	9	24.43	III	13	16.86	II	5	8.26	III	11	5.63	IV	10	2.61	VII	5	51.71	III	14	60.86
62	VIII	2	17.74	I	14	6.20	VIII	9	24.43	III	4	16.86	VIII	16	8.27	IX	11	5.63	II	13	2.61	II	3	52.17	IV	3	60.89
63	VII	11	17.81	IV	18	6.31	VII	9	24.43	VI	13	16.93	VIII	5	8.31	II	7	5.64	VII	5	2.61	VIII	11	52.19	VI	14	60.91
64	IX	2	17.84	VII	12	6.41	IV	2	26.73	VI	4	16.93	V	2	8.32	V	11	5.65	VII	2	2.62	V	11	52.23	V	11	61.07
65	VI	2	17.85	I	15	6.54	II	2	26.98	IX	13	17.01	II	2	8.35	VII	14	5.65	I	2	2.63	III	3	52.26	VIII	11	61.10
66	III	2	17.90	VII	15	6.54	I	2	27.06	IX	4	17.01	V	8	8.37	VIII	7	5.65	IV	8	2.63	V	3	52.40	V	5	61.37
67	II	11	17.94	II	18	6.97	VII	2	27.06	II	14	17.27	IV	16	8.37	II	11	5.65	VIII	13	2.64	III	14	52.41	III	3	61.41
68	VIII	11	17.99	III	1	7.17	V	2	27.09	II	5	17.27	IV	5	8.39	IV	11	5.66	I	5	2.64	VI	3	52.47	II	3	61.52
69	V	11	18.03	IX	1	7.17	VIII	2	27.26	V	14	17.38	IV	2	8.40	V	17	5.66	VII	10	2.67	VI	14	52.49	IX	14	61.52
70	IX	11	18.17	VI	1	7.20	IX	2	27.27	V	5	17.38	IX	14	8.41	IX	5	5.66	IV	13	2.68	VII	3	52.52	VI	3	61.60
71	VI	11	18.23	V	17	7.22	III	2	27.30	VIII	14	17.39	VIII	2	8.42	I	14	5.66	I	10	2.68	IX	3	52.65	V	3	61.73
72	III	11	18.27	V	1	7.24	VI	2	27.40	VIII	5	17.39	VI	14	8.42	VIII	17	5.67	VII	8	2.69	VIII	3	52.98	IX	3	61.82
73	IV	5	25.27	IV	1	7.27	IV	14	30.37	VIII	18	19.19	II	8	8.43	VIII	11	5.67	I	8	2.72	IX	14	53.12	II	5	62.06
74	I	5	25.59	II	1	7.38	V	14	31.15	VIII	9	19.19	III	14	8.44	VI	5	5.67	V	16	2.72	V	5	53.15	VII	3	62.07
75	IV	14	25.66	IV	16	7.50	VI	14	31.39	II	18	19.38	VII	5	8.44	VII	11	5.67	VI	9	2.72	II	5	53.80	VIII	3	62.39
76	II	5	26.12	VIII	1	7.71	III	14	31.42	II	9	19.38	VII	16	8.47	III	5	5.68	IX	9	2.73	I	2	54.01	I	2	62.51
77	I	14	26.14	II	16	7.76	IX	14	31.82	V	18	19.49	IX	17	8.47	I	11	5.68	III	9	2.74	IV	2	54.25	IV	2	62.65
78	V	5	26.20	VIII	18	7.80	II	14	32.06	V	9	19.49	VII	2	8.47	II	17	5.69	VII	13	2.74	I	17	54.34	VII	2	62.92
79	VII	5	26.27	VI	4	7.86	I	14	32.34	IV	10	20.73	VI	17	8.48	IX	8	5.71	I	13	2.79	V	17	54.43	VIII	5	62.92
80	VIII	5	26.34	IX	4	7.95	VIII	14	32.94	IV	1	20.73	VIII	8	8.49	VI	8	5.71	II	16	2.79	VII	2	54.45	V	17	63.22
81	III	5	26.39	VII	1	8.06	VII	14	33.08	I	10	20.92	I	2	8.50	IV	17	5.72	VI	6	2.82	VIII	5	54.61	I	17	63.41
82	IX	5	26.63	III	4	8.13	IV	5	35.36	I	1	20.92	I	5	8.51	VII	17	5.72	VIII	16	2.83	III	11	54.90	III	11	63.67
83	VI	5	26.65	I	1	8.23	VI	5	35.46	III	14	21.00	III	17	8.54	III	8	5.74	VI	3	2.84	VII	17	55.26	VII	17	64.27
84	V	14	26.95	VII	18	8.26	III	5	35.49	III	5	21.00	I	16	8.56	V	5	5.75	IX	6	2.84	IX	11	55.55	IX	11	64.33
85	VII	14	26.98	I	18	8.39	IX	5	35.63	VII	10	21.05	V	14	8.62	I	17	5.76	III	6	2.84	VI	11	55.57	VI	11	64.35
86	II	14	27.02	IV	17	8.40	V	5	35.78	VII	1	21.05	IV	8	8.67	II	5	5.76	III	3	2.85	II	17	56.25	III	5	64.50
87	VIII	14	27.26	II	17	8.77	IV	10	36.23	VI	14	21.10	VIII	14	8.69	VIII	5	5.77	IX	3	2.87	II	2	56.45	VI	5	64.55
88	III	14	27.54	VI	5	8.81	II	5	36.53	VI	5	21.10	II	14	8.70	VII	7	5.80	IV	16	2.88	III	5	56.49	II	2	64.80
89	VI	14	27.76	IX	5	9.00	III	10	36.56	IX	14	21.30	IV	14	8.72	VI	2	5.82	IX	14	2.89	VI	5	56.55	IV	10	64.89
90	IX	14	27.89	VIII	16	9.02	V	10	36.60	IX	5	21.30	VII	8	8.72	IV	7	5.82	V	9	2.90	IX	5	56.93	IX	5	64.92

Table 63 continued - Cases 91 to 126

rank	Heating			Cooling			Heating & Cooling			Lighting			Total Ventilation			Ventilation UT			Ventilation OU			Total (no Vent.)			Total (with Vent.)		
91	IV	17	32.03	III	5	9.10	VI	10	36.61	III	18	23.32	III	11	8.77	III	2	5.82	VI	14	2.90	IV	10	56.96	II	17	65.14
92	IV	1	32.66	V	4	9.24	IX	10	36.77	III	9	23.32	VI	11	8.78	V	2	5.82	III	14	2.92	VIII	2	57.10	VIII	2	65.52
93	IV	8	32.78	II	2	9.28	II	10	36.83	VI	18	23.52	IX	11	8.78	IX	2	5.83	IX	17	2.93	V	2	57.30	V	2	65.61
94	I	1	32.79	IV	2	9.34	I	5	37.11	VI	9	23.52	V	17	8.79	VII	5	5.83	II	9	2.94	VI	17	57.45	VI	17	65.94
95	I	17	32.91	V	2	9.37	VIII	5	37.22	IX	18	23.54	VII	14	8.80	II	2	5.83	V	6	2.94	III	17	57.50	III	17	66.03
96	II	1	33.06	III	2	9.40	I	10	37.25	IX	9	23.54	I	8	8.81	IV	5	5.83	VI	17	2.95	IX	17	57.86	I	10	66.22
97	III	1	33.10	IX	2	9.43	VIII	10	37.30	II	10	23.55	IX	9	8.83	VIII	2	5.84	VII	16	2.95	VIII	17	57.97	IX	17	66.33
98	V	1	33.10	VII	2	9.48	VII	5	37.54	II	1	23.55	VI	9	8.84	IV	2	5.84	V	3	2.97	I	10	58.17	VIII	17	66.82
99	VIII	1	33.11	VIII	2	9.53	VII	10	37.78	VIII	10	23.81	V	11	8.84	VII	2	5.85	II	6	2.97	IV	8	58.78	VII	10	66.85
100	VI	1	33.15	VI	2	9.55	IV	1	39.93	VIII	1	23.81	VIII	17	8.85	IX	18	5.85	III	17	2.97	VII	10	58.84	IV	8	67.45
101	IX	1	33.23	V	5	9.58	III	1	40.26	V	10	24.03	II	11	8.85	III	18	5.86	VIII	9	2.98	IV	13	59.99	IV	13	68.04
102	VII	1	33.31	I	2	9.62	V	1	40.34	V	1	24.03	III	9	8.87	VI	18	5.86	II	3	2.99	III	2	60.00	IV	1	68.21
103	I	8	33.38	VIII	17	10.01	VI	1	40.36	I	15	24.39	I	14	8.87	I	2	5.87	VIII	6	3.00	II	10	60.37	III	2	68.21
104	IV	10	33.61	IV	5	10.10	IX	1	40.40	I	6	24.39	IV	11	8.88	I	5	5.87	I	16	3.00	V	10	60.62	II	10	68.30
105	I	10	33.76	IV	4	10.14	IV	17	40.43	VII	15	24.66	II	17	8.89	V	8	5.88	IV	9	3.01	IV	1	60.66	V	10	68.51
106	VII	17	34.05	VII	16	10.17	II	1	40.44	VII	6	24.66	VIII	11	8.91	I	7	5.89	V	14	3.04	IX	2	60.69	IX	2	68.93
107	II	10	34.13	II	4	10.21	VIII	1	40.82	IV	15	24.83	VII	11	8.92	VIII	18	5.90	VIII	3	3.04	VI	2	60.76	VI	2	68.95
108	V	10	34.14	II	5	10.41	I	1	41.03	IV	6	24.83	I	11	8.93	VIII	8	5.90	IV	6	3.04	VIII	10	61.11	VIII	10	69.03
109	VII	8	34.18	I	16	10.46	VII	1	41.37	II	15	26.78	IV	17	8.99	II	18	5.90	VII	9	3.06	V	8	61.60	I	1	69.65
110	VIII	10	34.20	VI	3	10.54	V	17	41.55	II	6	26.78	VII	17	9.02	V	18	5.90	IV	3	3.07	I	8	61.68	V	8	69.97
111	II	8	34.24	III	3	10.55	VI	17	41.73	VIII	15	26.95	VI	6	9.04	II	8	5.91	II	14	3.08	I	1	61.95	VII	1	70.09
112	V	8	34.25	IX	3	10.60	III	17	41.80	VIII	6	26.95	III	6	9.06	VII	18	5.91	VII	6	3.08	VII	8	61.95	I	8	70.50
113	III	10	34.26	VIII	4	10.72	IX	17	42.06	I	11	26.96	IX	6	9.06	VI	15	5.92	VIII	14	3.08	I	13	62.41	I	13	70.63
114	VI	10	34.30	VI	6	10.86	II	17	43.44	I	2	26.96	I	17	9.07	IX	15	5.93	I	9	3.09	VII	1	62.42	VII	8	70.67
115	V	17	34.34	III	6	10.88	I	17	44.21	III	10	27.26	V	9	9.09	III	15	5.93	IV	14	3.10	II	8	62.95	III	8	71.06
116	VII	10	34.38	VIII	5	10.88	VIII	17	44.98	III	1	27.26	VI	3	9.13	V	15	5.94	I	6	3.11	III	8	63.02	IX	8	71.09
117	IX	10	34.44	V	6	10.90	VII	17	45.03	VII	11	27.38	II	9	9.14	VIII	15	5.95	I	3	3.11	IX	8	63.08	VI	8	71.17
118	VIII	8	34.62	IX	6	10.90	IX	8	47.28	VII	2	27.38	III	3	9.15	IV	18	5.95	VII	3	3.11	VI	8	63.17	II	8	71.38
119	II	17	34.67	IV	6	10.93	III	8	47.32	V	15	27.50	VIII	9	9.16	II	15	5.95	V	17	3.13	VII	13	63.38	II	1	71.49
120	III	8	34.86	VII	17	10.98	VI	8	47.45	V	6	27.50	IX	3	9.17	IV	15	5.97	III	11	3.14	III	10	63.81	VII	13	71.53
121	VIII	17	34.97	II	6	10.99	IV	8	48.44	IV	11	27.52	V	6	9.19	VII	15	5.97	IX	11	3.15	II	1	63.99	III	10	71.68
122	IX	8	35.25	VI	9	11.00	V	8	48.72	IV	2	27.52	II	6	9.23	I	18	5.98	VI	11	3.15	V	13	64.05	V	1	71.80
123	VI	8	35.25	V	3	11.07	IV	13	49.16	IX	10	27.60	VIII	6	9.26	IX	12	5.98	VII	14	3.15	VIII	8	64.30	V	13	71.89
124	III	17	35.90	IX	9	11.11	II	8	50.14	IX	1	27.60	IX	18	9.27	VI	12	5.98	VIII	17	3.18	V	1	64.37	VIII	1	72.21
125	VI	17	36.19	II	3	11.19	V	13	50.30	VI	10	27.76	IV	9	9.29	III	12	6.00	II	17	3.20	IX	10	64.37	VI	10	72.23
126	IX	17	36.38	IV	3	11.27	VI	13	50.80	VI	1	27.76	VI	18	9.29	I	15	6.02	V	11	3.20	VI	10	64.38	IX	10	72.24

Table 63 continued - Cases 127 to 162

rank	Heating			Cooling			Heating & Cooling			Lighting			Total Ventilation			Ventilation UT			Ventilation OU			Total (no Vent.)			Total (with Vent.)		
127	IV	4	44.86	III	9	11.27	III	13	50.93	II	11	29.47	III	18	9.30	VII	8	6.03	II	11	3.20	VIII	1	64.63	VIII	8	72.78
128	IV	13	44.97	VII	5	11.27	IX	13	51.28	II	2	29.47	VII	9	9.32	II	12	6.04	I	14	3.21	II	13	65.26	II	13	73.21
129	I	4	45.30	I	17	11.30	VIII	8	51.31	VIII	11	29.84	V	3	9.33	IV	8	6.04	IV	11	3.22	IV	4	65.84	IV	4	73.56
130	I	13	45.76	VIII	6	11.30	I	8	51.55	VIII	2	29.84	IV	6	9.35	V	12	6.05	VIII	11	3.23	VIII	13	66.34	VIII	13	74.33
131	V	4	46.22	I	3	11.46	II	13	51.62	V	11	30.20	II	3	9.36	VIII	12	6.05	VII	11	3.24	III	1	67.52	III	1	74.86
132	VII	4	46.28	I	5	11.52	I	13	51.72	V	2	30.20	VII	6	9.37	IV	12	6.08	I	11	3.25	VI	13	67.73	IX	1	75.33
133	II	4	46.29	VIII	3	11.53	VII	8	51.73	III	15	30.47	VIII	3	9.41	I	12	6.08	IV	17	3.27	III	13	67.79	VI	13	75.39
134	VIII	4	46.53	VII	4	11.53	VIII	13	52.44	III	6	30.47	I	9	9.42	VII	12	6.09	VII	17	3.29	I	4	67.92	VI	1	75.45
135	III	4	46.78	IX	7	11.55	VII	13	52.60	VI	15	31.00	VIII	18	9.44	IX	9	6.09	I	17	3.31	IX	1	68.00	III	13	75.46
136	V	13	46.83	VII	6	11.55	III	4	54.91	VI	6	31.00	I	6	9.44	I	8	6.10	IX	18	3.41	VI	1	68.12	I	4	75.79
137	VII	13	46.84	V	9	11.59	VI	4	54.95	IX	15	31.21	V	18	9.45	VI	9	6.12	VI	18	3.43	IX	13	68.28	IX	13	75.94
138	VI	4	47.09	I	6	11.65	IV	4	55.01	IX	6	31.21	II	18	9.46	III	9	6.13	III	18	3.44	VII	4	68.59	VII	4	76.39
139	IX	4	47.17	VI	7	11.65	IX	4	55.12	III	11	32.71	IV	3	9.47	VIII	9	6.18	VIII	18	3.54	IV	16	69.20	V	4	76.69
140	II	13	47.21	VII	3	11.71	V	4	55.46	III	2	32.71	VI	15	9.51	V	9	6.20	V	18	3.55	V	4	69.20	IV	16	77.58
141	VIII	13	47.37	III	7	11.93	II	4	56.50	VI	11	33.36	I	3	9.52	II	9	6.21	II	18	3.56	II	4	70.13	II	4	77.71
142	III	13	47.98	I	4	11.94	I	4	57.23	VI	2	33.36	III	15	9.53	VI	6	6.21	VI	15	3.59	VIII	4	71.15	VIII	4	78.80
143	VI	13	48.18	IV	9	11.97	VIII	4	57.25	IX	11	33.42	IX	15	9.54	III	6	6.21	III	15	3.61	III	4	71.77	III	4	79.01
144	IX	13	48.43	IX	8	12.04	VII	4	57.81	IX	2	33.42	VII	3	9.55	IX	6	6.22	IX	15	3.61	VI	4	71.88	VI	4	79.08
145	IV	16	53.72	VI	8	12.20	IV	16	61.21	I	12	35.03	VII	18	9.56	V	6	6.24	V	15	3.65	IX	4	72.13	IX	4	79.35
146	I	16	54.84	III	8	12.46	V	16	63.40	I	3	35.03	V	15	9.59	II	6	6.26	VII	18	3.65	I	16	73.28	I	16	81.84
147	IV	7	55.95	II	9	12.56	VI	16	64.51	IV	12	35.73	VIII	15	9.60	VII	9	6.26	VIII	15	3.66	V	16	73.89	V	16	82.02
148	VII	16	56.47	VIII	9	13.06	III	16	64.58	IV	3	35.73	II	15	9.62	VIII	6	6.26	II	15	3.66	VII	16	74.59	VII	16	83.06
149	I	7	56.54	VII	9	13.40	IX	16	65.23	II	12	36.33	IV	18	9.62	IV	9	6.28	IV	18	3.67	II	16	75.89	II	16	84.12
150	V	16	57.24	I	9	13.76	I	16	65.31	II	3	36.33	VII	15	9.67	VII	6	6.28	I	18	3.70	VI	16	77.39	VI	16	85.14
151	VII	7	57.74	V	7	14.39	II	16	65.54	VII	12	36.39	IV	15	9.68	VI	3	6.29	VII	15	3.70	III	16	77.50	III	16	85.30
152	II	16	57.77	V	8	14.47	VII	16	66.64	VII	3	36.39	I	18	9.68	IX	3	6.30	IV	15	3.71	VIII	16	77.72	IX	16	85.85
153	VIII	16	58.14	IV	8	15.66	VIII	16	67.16	V	12	36.71	VI	12	9.72	III	3	6.30	VI	12	3.73	IX	16	78.09	VIII	16	86.00
154	V	7	58.32	II	8	15.90	III	7	71.59	V	3	36.71	IX	12	9.74	IV	6	6.31	I	15	3.76	IV	7	79.85	IV	7	87.84
155	II	7	58.37	IV	7	15.91	VI	7	71.83	VIII	12	36.76	III	12	9.75	I	9	6.33	III	12	3.76	V	7	83.20	V	7	90.84
156	VIII	7	58.79	II	7	15.92	IV	7	71.86	VIII	3	36.76	I	15	9.77	I	6	6.33	IX	12	3.76	I	7	83.24	I	7	91.40
157	III	7	59.66	VIII	8	16.69	IX	7	71.92	III	12	36.92	II	12	9.85	V	3	6.36	V	12	3.81	VII	7	83.74	III	7	91.80
158	III	16	59.74	VIII	7	16.84	V	7	72.71	III	3	36.92	V	12	9.85	II	3	6.36	II	12	3.81	III	7	84.51	VII	7	91.81
159	VI	16	60.07	VII	8	17.55	II	7	74.29	VI	12	37.12	VIII	12	9.87	VIII	3	6.37	VIII	12	3.82	II	7	84.65	VI	7	91.96
160	VI	7	60.18	VII	7	18.05	I	7	75.27	VI	3	37.12	IV	12	9.92	I	3	6.41	IV	12	3.84	VI	7	84.72	IX	7	92.04
161	IX	7	60.37	I	8	18.17	VIII	7	75.63	IX	12	37.21	I	12	9.94	IV	3	6.41	I	12	3.86	IX	7	84.78	II	7	92.38
162	IX	16	60.57	I	7	18.73	VII	7	75.79	IX	3	37.21	VII	12	9.98	VII	3	6.43	VII	12	3.89	VIII	7	86.19	VIII	7	94.01

Appendix 9 | Energy Demand Deviation due to Urban Microclimate – Mannheim

Table 64: Useful energy demand deviation between urban climate and standard climate as annual average [SET IV] – [SET III] – 36 best and 36 worst cases

rank	Heating			Cooling			Heating & Cooling			Lighting			Total Ventilation			Ventilation UT			Ventilation OU			Total (no Vent.)			Total (with Vent.)		
1	III	7	-3.675	III	10	0.212	IX	16	-2.341	VIII	9	-3.725	VIII	10	0.602	IX	1	0.537	IV	12	0.022	IX	16	-4.731	IX	16	-3.873
2	IX	7	-3.648	IX	10	0.275	III	16	-2.306	VIII	18	-3.725	VI	10	0.617	IV	10	0.539	VII	15	0.040	IX	17	-4.613	IX	13	-3.861
3	VI	7	-3.594	III	1	0.285	VI	16	-1.933	VI	5	-3.658	VII	10	0.620	VIII	10	0.541	I	18	0.043	IX	4	-4.601	IX	4	-3.820
4	III	16	-3.570	VI	10	0.302	IX	7	-1.646	VI	14	-3.658	IV	10	0.622	II	10	0.542	VIII	12	0.048	IX	13	-4.572	VI	13	-3.749
5	IX	16	-3.547	IX	1	0.339	IX	4	-1.563	V	9	-3.566	I	14	0.624	VII	10	0.544	I	17	0.051	VI	13	-4.504	IX	17	-3.747
6	VI	16	-3.449	VI	1	0.371	III	7	-1.544	V	18	-3.566	III	10	0.629	III	1	0.545	II	12	0.051	III	16	-4.485	VI	5	-3.622
7	VIII	16	-3.250	II	11	0.435	IX	13	-1.534	VIII	14	-3.543	I	10	0.629	VI	1	0.546	VI	12	0.054	VI	5	-4.419	III	16	-3.607
8	V	16	-3.224	V	11	0.456	VI	13	-1.438	VIII	5	-3.543	IX	10	0.631	V	10	0.549	VI	18	0.055	VI	4	-4.394	III	13	-3.603
9	II	16	-3.057	III	15	0.484	III	4	-1.436	VI	17	-3.533	V	10	0.631	V	1	0.550	VII	12	0.056	VI	14	-4.318	VI	4	-3.600
10	VIII	7	-2.970	V	2	0.490	III	13	-1.435	VI	8	-3.533	IV	11	0.638	I	10	0.551	IX	18	0.057	III	4	-4.310	VI	14	-3.572
11	V	7	-2.946	III	11	0.495	VI	4	-1.327	IX	17	-3.510	IV	12	0.640	VI	10	0.554	II	15	0.058	III	13	-4.310	III	4	-3.531
12	II	7	-2.828	IX	15	0.497	IX	17	-1.103	IX	8	-3.510	I	17	0.640	II	1	0.556	V	12	0.059	VI	16	-4.292	IX	5	-3.431
13	IX	17	-2.343	V	10	0.499	VI	7	-1.047	VI	9	-3.500	I	18	0.645	I	14	0.559	I	15	0.059	IX	5	-4.178	VI	16	-3.384
14	IX	8	-2.329	IX	11	0.517	III	1	-1.038	VI	18	-3.500	II	10	0.646	IX	10	0.563	IX	12	0.060	III	17	-4.176	III	14	-3.358
15	III	4	-2.298	II	10	0.523	V	16	-0.950	V	14	-3.416	VII	15	0.647	VIII	1	0.563	V	15	0.061	IX	8	-4.125	III	5	-3.357
16	IX	4	-2.289	IX	13	0.535	III	10	-0.913	V	5	-3.416	VII	18	0.651	I	1	0.564	IV	11	0.061	III	5	-4.118	IX	14	-3.329
17	III	8	-2.281	IV	2	0.536	VI	1	-0.864	IX	5	-3.381	VII	14	0.654	VII	1	0.564	VIII	10	0.062	III	14	-4.093	IX	8	-3.289
18	VI	4	-2.280	V	1	0.542	III	17	-0.847	IX	14	-3.381	VII	1	0.655	V	13	0.565	VI	10	0.062	VI	17	-4.054	III	17	-3.288
19	III	17	-2.272	IV	11	0.543	IX	1	-0.823	III	5	-3.359	I	1	0.655	I	13	0.565	III	10	0.063	IX	14	-4.040	IX	7	-3.229
20	VI	8	-2.243	II	1	0.550	IX	5	-0.796	III	14	-3.359	VII	17	0.658	VI	4	0.565	I	14	0.065	IX	7	-4.035	VI	17	-3.167
21	VI	17	-2.193	VI	6	0.554	VI	5	-0.761	III	17	-3.329	VII	11	0.659	III	10	0.565	VIII	15	0.065	III	7	-3.723	III	7	-2.905
22	IX	13	-2.069	IX	6	0.563	III	5	-0.759	III	8	-3.329	VII	2	0.661	IV	1	0.567	VI	15	0.066	III	8	-3.643	V	14	-2.789
23	III	13	-2.065	III	6	0.564	V	13	-0.747	IX	9	-3.328	VII	12	0.662	IX	4	0.570	III	12	0.066	V	14	-3.576	III	8	-2.787
24	VIII	17	-2.064	IV	9	0.564	III	14	-0.734	IX	18	-3.328	I	12	0.665	III	4	0.574	IV	15	0.067	VI	8	-3.486	V	13	-2.723
25	VI	13	-2.058	II	2	0.577	VI	10	-0.726	II	14	-3.305	I	11	0.666	III	13	0.576	I	12	0.067	VI	9	-3.456	III	1	-2.676
26	V	17	-2.034	VI	11	0.591	II	16	-0.687	II	5	-3.305	V	15	0.666	IV	11	0.577	III	18	0.068	V	13	-3.440	VI	9	-2.659
27	IV	16	-1.975	I	12	0.595	VI	14	-0.659	II	9	-3.241	I	15	0.668	IX	5	0.577	IX	10	0.068	VI	7	-3.405	II	14	-2.624
28	II	17	-1.966	VIII	11	0.596	IX	14	-0.659	II	18	-3.241	VI	12	0.671	VII	13	0.577	I	11	0.069	II	14	-3.384	III	10	-2.608
29	V	13	-1.810	V	6	0.596	IX	10	-0.639	III	9	-3.089	II	15	0.672	III	5	0.578	VII	18	0.069	III	1	-3.362	VI	8	-2.605
30	VIII	13	-1.792	IV	6	0.601	IX	8	-0.615	III	18	-3.089	IX	18	0.673	V	2	0.578	VII	17	0.069	VIII	14	-3.340	VI	18	-2.586
31	VII	16	-1.769	VI	15	0.602	II	13	-0.564	VI	13	-3.067	II	18	0.674	IX	13	0.579	VII	11	0.070	V	5	-3.340	IX	1	-2.585
32	V	4	-1.744	IV	10	0.604	VI	17	-0.521	VI	4	-3.067	IV	15	0.676	VI	5	0.582	VII	14	0.072	IX	9	-3.294	VIII	14	-2.579
33	VIII	4	-1.740	I	3	0.605	II	1	-0.368	VIII	17	-3.050	I	13	0.676	VII	18	0.582	VII	2	0.075	II	13	-3.288	VI	1	-2.576
34	I	16	-1.731	III	14	0.606	VIII	13	-0.359	VIII	8	-3.050	VI	15	0.677	VII	14	0.582	VII	10	0.076	IX	1	-3.278	VI	7	-2.562
35	VIII	8	-1.692	VII	11	0.613	V	1	-0.356	IX	4	-3.038	V	12	0.678	IV	13	0.585	II	18	0.076	VI	1	-3.278	V	5	-2.550
36	V	8	-1.684	VI	5	0.620	V	10	-0.335	IX	13	-3.038	VIII	12	0.679	VII	2	0.586	VIII	18	0.077	VI	18	-3.273	IX	9	-2.545

Table 64 continued – Cases 127 10 162 (worst cases)

rank	Heating			Cooling			Heating & Cooling			Lighting			Total Ventilation			Ventilation UT			Ventilation OU			Total (no Vent.)			Total (with Vent.)		
127	VII	18	-0.308	II	4	1.491	I	18	0.605	IV	6	-1.342	VI	4	0.794	I	9	0.632	VIII	9	0.183	IV	8	-0.864	VII	8	-0.140
128	IV	2	-0.303	VI	16	1.515	IV	4	0.611	IV	15	-1.342	V	3	0.796	II	7	0.632	VI	9	0.183	I	8	-0.856	VII	11	-0.123
129	IV	9	-0.301	VIII	18	1.518	VII	18	0.615	IV	11	-1.309	VI	9	0.797	II	6	0.634	III	2	0.186	IV	15	-0.853	I	8	-0.093
130	VIII	15	-0.287	V	4	1.566	VI	3	0.627	IV	2	-1.309	VI	5	0.797	VI	3	0.635	II	4	0.187	VIII	7	-0.843	IV	8	-0.081
131	I	18	-0.287	VI	17	1.672	II	3	0.637	VII	16	-1.300	II	9	0.798	III	3	0.635	V	2	0.188	VII	11	-0.783	I	1	-0.014
132	V	15	-0.282	IX	8	1.714	V	12	0.646	VII	7	-1.300	VI	3	0.799	IX	6	0.637	VIII	4	0.189	I	1	-0.669	VII	2	0.004
133	VII	9	-0.271	VIII	4	1.736	I	6	0.652	VII	11	-1.170	VII	7	0.800	V	7	0.637	IX	2	0.191	VII	2	-0.657	VII	15	0.068
134	IX	3	-0.270	IV	17	1.908	VIII	15	0.652	VII	2	-1.170	V	9	0.803	IV	9	0.637	V	5	0.194	I	16	-0.630	VIII	7	0.073
135	I	2	-0.269	III	8	1.967	V	3	0.679	III	11	-1.162	VIII	17	0.804	VIII	17	0.638	IX	7	0.201	VII	15	-0.579	I	16	0.120
136	III	3	-0.266	IX	7	2.002	VII	4	0.682	III	2	-1.162	IX	7	0.806	I	3	0.638	VI	2	0.201	VII	6	-0.570	I	11	0.137
137	I	9	-0.260	I	8	2.052	I	15	0.698	VI	11	-1.141	VIII	4	0.811	VIII	6	0.638	III	4	0.204	I	11	-0.528	VII	6	0.156
138	VI	3	-0.256	VII	8	2.053	I	4	0.701	VI	2	-1.141	VIII	9	0.812	I	8	0.638	IX	8	0.206	I	6	-0.358	I	15	0.356
139	IV	6	-0.242	VII	17	2.092	I	1	0.722	IX	11	-1.067	V	4	0.818	V	3	0.639	II	7	0.209	VII	16	-0.351	VII	16	0.371
140	VII	11	-0.226	IV	8	2.109	II	18	0.723	IX	2	-1.067	III	7	0.818	VIII	16	0.639	IX	4	0.211	I	2	-0.313	I	2	0.378
141	VII	2	-0.214	III	7	2.130	IV	17	0.735	I	6	-1.010	IV	7	0.826	IX	3	0.640	VI	5	0.215	I	15	-0.312	I	6	0.379
142	I	6	-0.211	I	17	2.151	VII	15	0.769	I	15	-1.010	II	17	0.830	VII	9	0.641	V	17	0.216	IV	7	-0.056	IV	7	0.770
143	II	3	-0.209	IV	16	2.266	VII	6	0.778	I	11	-0.840	IX	8	0.837	I	7	0.642	III	7	0.218	I	7	0.166	I	12	0.858
144	V	3	-0.207	V	16	2.274	VIII	12	0.797	I	2	-0.840	II	7	0.842	I	6	0.643	IX	17	0.220	I	12	0.194	IV	12	0.904
145	IV	15	-0.198	VI	8	2.291	VIII	3	0.826	I	12	-0.274	VI	7	0.843	IV	3	0.643	II	8	0.221	I	3	0.212	I	3	0.941
146	I	1	-0.196	V	17	2.329	VIII	9	0.828	I	3	-0.274	III	8	0.856	VI	17	0.643	V	4	0.222	IV	12	0.264	I	7	0.956
147	I	15	-0.180	II	17	2.364	I	16	0.843	IV	12	-0.246	IX	16	0.858	II	3	0.644	III	8	0.224	IV	3	0.280	IV	3	1.025
148	VIII	3	-0.179	II	16	2.370	VII	16	0.949	IV	3	-0.246	IX	17	0.866	IV	8	0.645	III	17	0.228	III	12	0.383	VII	12	1.057
149	VI	12	-0.175	VI	7	2.547	VIII	7	1.058	II	12	-0.183	V	17	0.870	IX	17	0.646	VI	4	0.229	VII	12	0.395	III	12	1.072
150	III	12	-0.174	I	16	2.575	VIII	17	1.100	II	3	-0.183	V	7	0.871	VII	3	0.647	V	7	0.234	II	12	0.410	II	12	1.093
151	IX	12	-0.173	VII	16	2.718	VIII	18	1.144	V	12	-0.159	II	16	0.875	II	17	0.648	IX	16	0.241	VII	3	0.413	VII	3	1.142
152	V	12	-0.170	II	8	2.817	VII	17	1.153	V	3	-0.159	II	8	0.876	VIII	3	0.650	VI	7	0.243	VII	7	0.432	IX	12	1.145
153	II	12	-0.162	IV	7	2.880	I	17	1.171	VII	12	-0.134	III	16	0.878	IV	6	0.651	II	16	0.244	II	3	0.454	V	12	1.166
154	VII	12	-0.141	I	7	2.932	II	8	1.172	VII	3	-0.134	VI	8	0.881	V	17	0.654	VI	17	0.244	III	3	0.457	VI	12	1.192
155	VIII	12	-0.141	V	8	2.934	V	8	1.250	VIII	12	-0.120	VI	17	0.887	II	8	0.655	VIII	8	0.246	IX	12	0.465	II	3	1.227
156	IV	12	-0.135	VII	7	3.102	IV	8	1.359	VIII	3	-0.120	III	17	0.888	IV	7	0.658	VIII	7	0.247	V	12	0.488	VII	7	1.232
157	I	12	-0.127	VIII	17	3.164	IV	7	1.427	III	12	-0.079	VIII	16	0.893	VII	7	0.659	V	8	0.253	V	3	0.520	III	3	1.245
158	VII	3	-0.126	II	7	3.289	I	8	1.462	III	3	-0.079	VI	16	0.908	V	8	0.659	VIII	16	0.254	VI	12	0.521	V	3	1.316
159	VII	15	-0.120	VIII	16	3.299	VII	8	1.489	VI	12	-0.035	V	8	0.912	III	17	0.660	III	16	0.256	IX	3	0.547	IX	3	1.332
160	I	3	-0.118	VIII	8	3.329	VIII	8	1.637	VI	3	-0.035	VIII	7	0.915	VII	8	0.660	VI	8	0.260	VI	3	0.592	VIII	12	1.356
161	IV	3	-0.115	V	7	3.422	I	7	1.639	IX	12	-0.016	V	16	0.915	VIII	7	0.668	VI	16	0.283	VIII	12	0.677	VI	3	1.391
162	VII	6	-0.104	VIII	7	4.028	VII	7	1.732	IX	3	-0.016	VIII	8	0.917	VIII	8	0.670	V	16	0.284	VIII	3	0.707	VIII	3	1.467

Appendix 10 | Effects of the Building Use and Operation on the Energy Demand

Table 65: Ranking of the minimum and maximum heating and cooling energy demands for the 54 combinations of urban and building variables (54 cases) when submitted to various scenarios of building use and operation (S, V, N and I) for Mannheim (49.52°N, 8.55°E)

	HEATING						COOLING					
	minimum			maximum			minimum			maximum		
	A+B	C+D+E		A+B	C+D+E		A+B	C+D+E		A+B	C+D+E	
1	IX	12	0.03	IV	3	59.17	IX	12	0.11	III	13	16.83
2	II	12	0.03	IV	12	59.64	IV	12	0.18	IX	16	18.46
3	IV	12	0.04	II	3	59.68	II	12	0.21	V	13	20.43
4	II	3	0.05	II	12	60.58	III	11	0.32	I	10	24.51
5	IX	3	0.05	IX	3	60.61	VI	10	0.36	III	4	24.74
6	VIII	15	0.05	I	6	61.25	V	11	0.41	IX	7	25.84
7	IV	3	0.06	IX	12	62.00	VI	15	0.54	VI	17	26.00
8	VI	15	0.06	I	15	62.10	VII	11	0.57	V	4	28.24
9	I	15	0.11	VIII	6	62.47	VIII	10	0.64	VIII	10	28.58
10	III	18	0.23	VI	6	63.44	I	10	0.68	IX	14	31.14
11	VIII	6	0.28	VIII	15	63.67	VIII	15	0.79	II	14	31.24
12	V	18	0.29	VII	9	63.86	I	15	0.88	VI	10	32.79
13	I	6	0.31	V	9	64.85	IX	14	0.99	I	1	33.94
14	VI	6	0.31	VII	18	64.99	III	18	1.09	IV	14	34.22
15	VII	18	0.36	VI	15	65.21	III	13	1.10	II	16	35.71
16	III	11	0.73	III	9	66.12	IV	14	1.25	VI	8	35.84
17	VII	11	0.79	V	18	66.32	V	18	1.25	VIII	1	37.86
18	V	11	0.79	III	18	68.14	II	14	1.26	II	5	38.77
19	III	9	1.32	VII	2	75.87	V	13	1.31	VII	13	39.25
20	VII	9	1.35	V	2	76.28	VII	18	1.39	IX	5	40.26
21	V	9	1.36	III	2	76.86	VII	13	1.57	IV	5	41.23
22	III	2	2.82	VII	11	77.65	VI	17	1.77	II	7	42.77
23	V	2	2.85	V	11	78.35	IX	16	1.91	VII	4	43.19
24	VII	2	3.03	III	11	79.41	VIII	17	2.38	VI	1	43.47
25	IX	14	3.82	IV	5	81.71	I	17	2.46	VII	11	45.39
26	IV	14	4.32	II	5	82.37	II	16	2.63	IV	16	46.44
27	II	14	4.55	IV	14	83.80	IV	16	2.71	VIII	17	47.86
28	VI	10	5.63	IX	5	84.14	IX	3	3.52	VIII	8	51.31
29	VIII	10	5.75	II	14	84.67	IV	3	3.61	V	18	51.74
30	I	10	6.45	IX	14	86.84	II	3	3.74	V	11	53.16
31	IX	5	8.27	I	8	87.54	III	2	4.01	VII	18	53.67
32	IV	5	8.63	I	17	89.12	VI	1	4.05	VII	2	55.70
33	II	5	8.95	VIII	8	89.41	V	2	4.13	III	18	55.86
34	VI	1	10.58	VI	8	91.08	VII	2	4.28	V	9	58.55
35	VIII	1	10.90	VIII	17	91.38	VIII	1	4.53	VII	9	58.94
36	I	17	10.93	I	1	92.44	VI	6	4.63	IV	7	59.26
37	VIII	17	11.65	VIII	1	93.40	I	1	4.68	III	11	61.20
38	VI	17	11.71	VI	17	93.45	I	6	4.98	V	2	61.97
39	I	1	11.97	I	10	94.13	VIII	6	4.99	III	9	63.57
40	I	8	16.47	VI	1	94.15	IX	5	5.48	I	15	65.76
41	VI	8	16.61	VIII	10	95.33	III	4	5.82	I	17	67.85
42	VIII	8	16.78	VI	10	96.40	III	9	5.97	I	6	69.93
43	III	13	18.21	VII	4	103.12	IV	5	6.07	III	2	70.82
44	V	13	19.12	V	4	103.85	II	5	6.16	I	8	71.80
45	VII	13	19.50	VII	13	104.51	V	9	6.31	VIII	15	72.39
46	III	4	23.77	III	4	104.98	V	4	6.32	VIII	6	77.21
47	V	4	24.71	V	13	105.32	VII	9	6.37	VI	15	78.55
48	VII	4	24.85	III	13	106.74	VII	4	6.64	VI	6	84.15
49	IV	16	28.00	IV	7	112.69	VI	8	7.58	IV	12	100.61
50	II	16	32.74	IV	16	112.91	IX	7	7.82	II	12	102.95
51	IX	16	33.53	II	7	113.66	VIII	8	8.59	IV	3	103.86
52	IV	7	36.28	II	16	114.16	I	8	8.65	IX	12	104.01
53	II	7	38.12	IX	7	116.77	IV	7	9.02	II	3	106.57
54	IX	7	38.34	IX	16	117.63	II	7	9.25	IX	3	108.13

LEGEND

urban variables

B (facade's orientation)			profile)
NWSE	NS	NESW	
I	IV	VII	HW = 0.2
II	V	VIII	HW = 1
III	VI	IX	HW = 1.8

building describers

C	D	E	
PF	U -	LI	1
PF	U o	LI	2
PF	U +	LI	3
RF	U -	LI	4
RF	U o	LI	5
RF	U +	LI	6
GF	U -	LI	7
GF	U o	LI	8
GF	U +	LI	9
PF	U -	MA	10
PF	U o	MA	11
PF	U +	MA	12
RF	U -	MA	13
RF	U o	MA	14
RF	U +	MA	15
GF	U -	MA	16
GF	U o	MA	17
GF	U +	MA	18

C (windo ratio)		
-1	PF	perforated facade
0	RF	row facade
+1	GF	glazed facade
D (thermal insulation)		
-1	U -	weak insulation
0	U o	medium insulation
+1	U +	good insulation
E (thermal inertia)		
-1	LI	lightweight
+1	MA	massive

Table 66: Statistics about the effects of building use and operation variables S, V, N on the heating and cooling in addition to the urban and building variables A, B, C, D and E for [SET V], Mannheim (49.52°N, 8.55°E)

Heating						Coefficients			
Model Summary						Model 25	predictors and coef.		
Var.	Model	R	R Square	Adjusted R Square	R Square Change	rank	pred.	B	Sig.
							const.	34.993	.000
ABCE	1	,557[a]	.310	.309	.310	rank 1	D	-18.541	.000
	2	,609[b]	.371	.371	.062	rank 4	C	8.263	.000
0.388	3	,624[c]	.389	.388	.017	rank 5	CD	-5.381	.000
SVNI	4	,819[d]	.671	.670	.282	rank 2	V	17.696	.000
	5	,969[e]	.939	.939	.268	rank 3	I	-17.236	.000
	6	,976[f]	.953	.952	.014	rank 6	VI	-4.778	.000
	7	,979[g]	.958	.958	.005	rank 8	I^2	4.269	.000
	8	,981[h]	.962	.962	.004	rank 9	S	2.084	.000
	9	,981[i]	.963	.963	.001	rank 12	V^2	2.137	.000
	10	,982[j]	.964	.963	.000	rank 19	VN	-0.717	.000
	11	,982[k]	.964	.963	.000	rank 21	S^2	0.708	.001
	12	,982[l]	.964	.964	.000	rank 22	N	0.388	.002
	13	,982[m]	.964	.964	.000	rank 23	SI	-0.430	.006
0.576	14	,982[n]	.964	.964	.000	rank 24	NI	0.409	.007
interactions	15	,985[o]	.971	.970	.007	rank 7	DV	-3.337	.000
ABCDE	16	,987[p]	.973	.973	.002	rank 10	AI	-2.015	.000
with	17	,988[q]	.975	.975	.002	rank 11	CI	1.962	.000
SVNI	18	,988[r]	.977	.977	.001	rank 13	DI	1.502	.000
	19	,989[s]	.978	.978	.001	rank 14	CV	1.390	.000
	20	,989[t]	.979	.979	.001	rank 15	AS	-1.262	.000
	21	,990[u]	.979	.979	.000	rank 16	CS	0.860	.000
	22	,990[v]	.980	.980	.000	rank 17	DS	-0.843	.000
	23	,990[w]	.980	.980	.000	rank 18	EI	-0.576	.000
	24	,990[x]	.980	.980	.000	rank 20	ES	0.464	.000
0.0163	25	,990[y]	.980	.980	.000	rank 25	DN	0.312	.039

all Predictors: (Cont.), D, V, I, C, CD, VI, DV, I^2, S, AI, CI, V^2, DI, CV, AS, A, CS, DS, D^2, EI, AC, VN, ES, S^2, N, SI, NI, N^2, B2, DN, AE, DE, CE, AD

cooling						Coefficients			
Model Summary						Model 34	predictors and coef.		
Var.	Model	R	R Square	Adjusted R Square	R Square Change	rank	pred.	B	Sig.
							const.	6.325	.000
ABCDE	1	,307[a]	0.094	0.094	0.094	rank 3	E	-4.555	.000
	2	,352[b]	0.124	0.123	0.030	rank 9	D	3.127	.000
	3	,367[c]	0.135	0.133	0.011	rank 17	A	-1.883	.000
	4	,380[d]	0.145	0.142	0.010	rank 18	AC	-2.204	.000
	5	,391[e]	0.153	0.150	0.008	rank 20	CD	-2.050	.000
adj. R2	6	,398[f]	0.158	0.155	0.005	rank 25	C^2	2.288	.000
0.157	7	,401[g]	0.161	0.157	0.003	rank 29	C	0.915	.000
SVNI	8	,550[h]	0.303	0.299	0.142	rank 1	I	6.837	.000
	9	,662[i]	0.439	0.435	0.136	rank 2	V	-6.702	.000
	10	,717[j]	0.514	0.511	0.075	rank 4	N	-4.990	.000
	11	,744[k]	0.554	0.551	0.040	rank 6	VI	-4.440	.000
	12	,767[l]	0.588	0.585	0.034	rank 8	S	-3.362	.000
	13	,781[m]	0.609	0.606	0.021	rank 11	V^2	4.557	.000
	14	,791[n]	0.625	0.622	0.016	rank 13	N^2	3.987	.000
	15	,799[o]	0.638	0.634	0.013	rank 15	VN	3.001	.000
	16	,803[p]	0.646	0.642	0.008	rank 23	SI	2.021	.000
	17	,807[q]	0.651	0.647	0.006	rank 24	NI	-1.681	.000
adj. R2	18	,810[r]	0.656	0.652	0.005	rank 26	I^2	2.206	.000
0.496	19	,811[s]	0.657	0.653	0.001	rank 31	S^2	1.070	.001
interactions	20	,837[t]	0.701	0.697	0.044	rank 5	DI	4.648	.000
ABCDE	21	,858[u]	0.737	0.733	0.036	rank 7	CI	-4.210	.000
with	22	,872[v]	0.761	0.757	0.024	rank 10	CS	-3.460	.000
SVNI	23	,884[w]	0.782	0.778	0.021	rank 12	DV	-3.204	.000
adj. R2	24	,892[x]	0.796	0.793	0.014	rank 14	EN	-2.174	.000
0.182	25	,898[y]	0.807	0.804	0.011	rank 16	EV	1.922	.000

all Predictors: (Const.), E, D, A, AC, CD, C^2, C, I, V, N, VI, S, V^2, N^2, VN, SI, NI, I2, S^2, DI, CI, CS, DV, EN, EV, EI, AS, DN, DS, AI, CV, AN, ES, AV

Appendix 11 | Effects of the Orientation on the Energy Demand of Buildings

This Appendix adds to the main results in section II - 3 (p 125) by addressing the role of the solar orientation of the facades. Figure 103 to Figure 106 depict the difference between the two opposite facades of the buildings, namely the orientation towards south (SE, S and SE) and towards north (NW, N, NE).

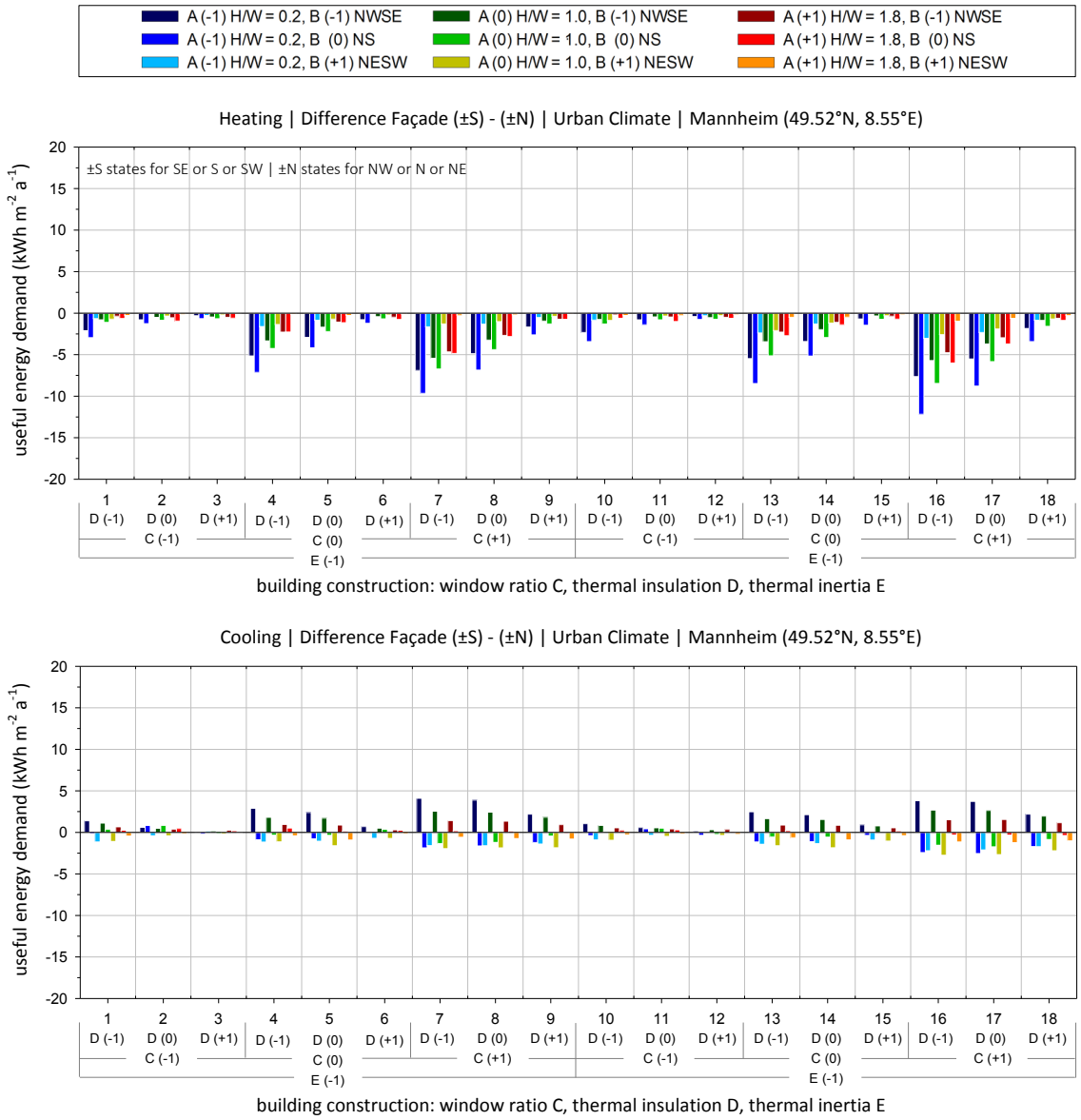

Figure 103: Annual average difference in the useful energy demand for heating and cooling between the orientations towards South (± 60°) and North (± 60°) under climate conditions for Mannheim (49.52°N, 8.55°E)

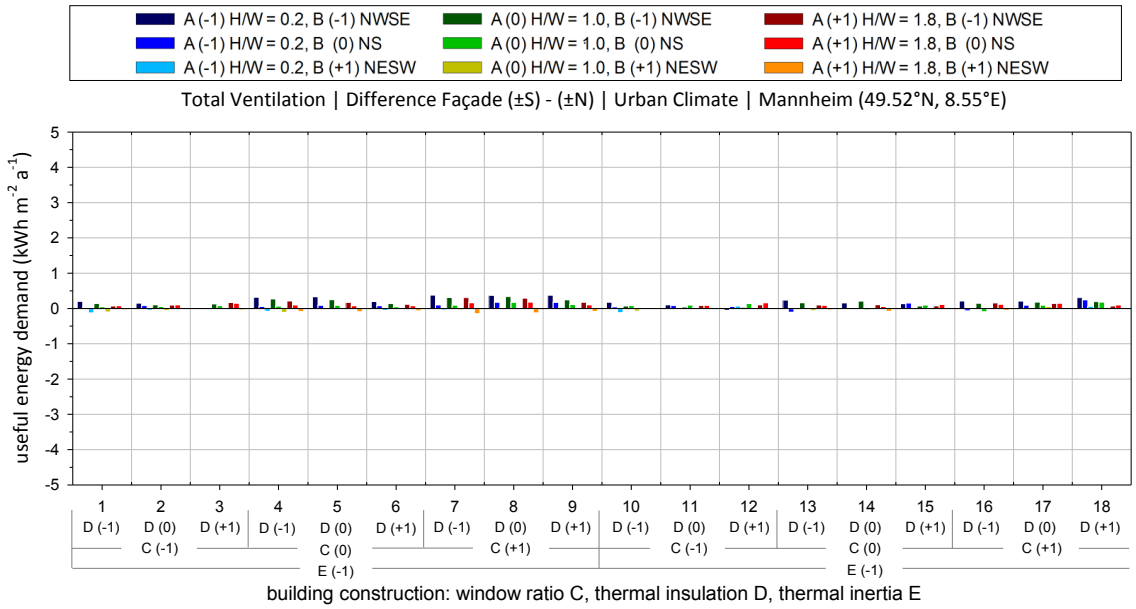

Figure 104: Annual average difference in the useful energy demand for ventilation between the orientations towards South (± 60°) and North (± 60°) under climate conditions for Mannheim (49.52°N, 8.55°E)

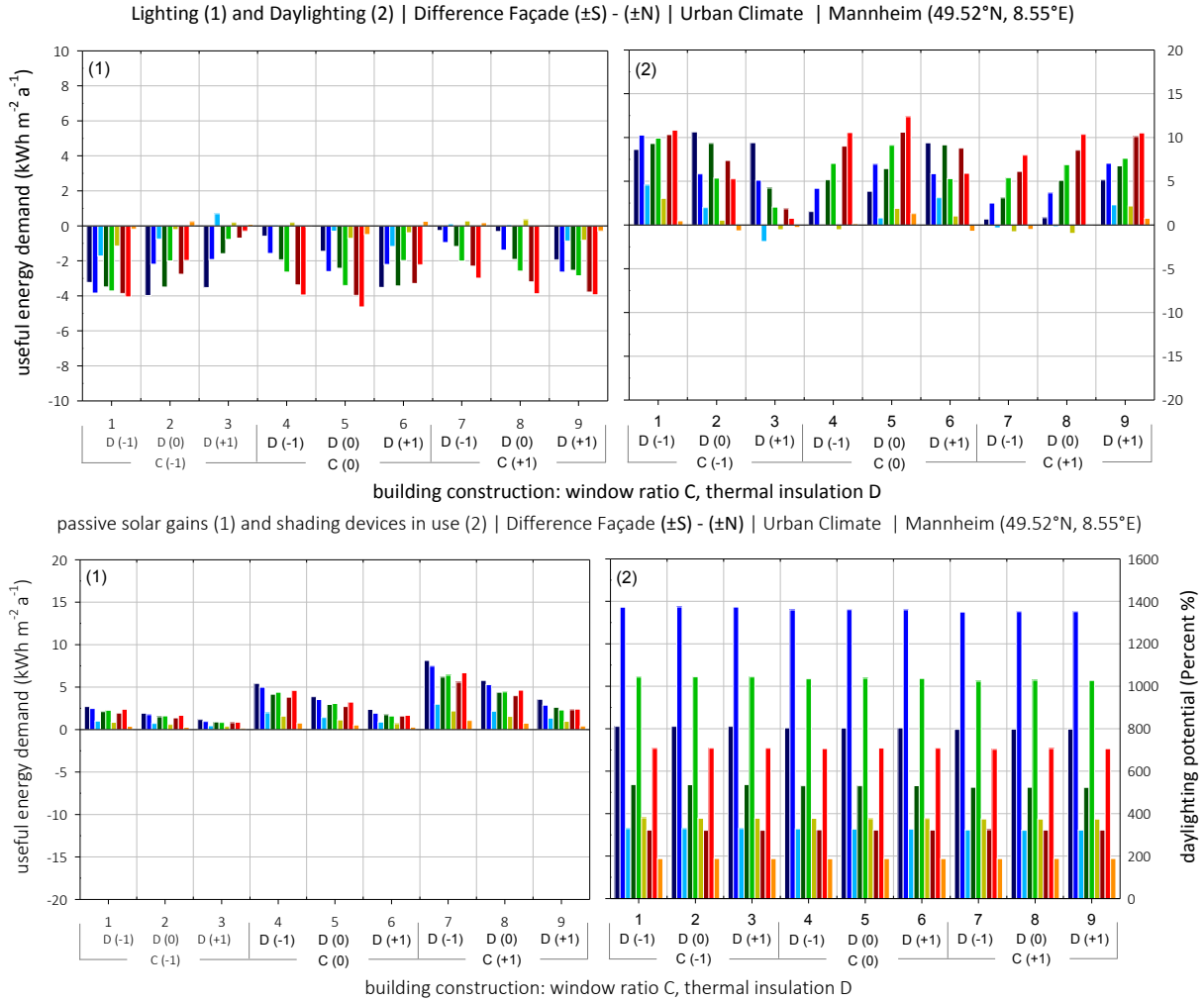

Figure 105: Annual average difference in the useful energy demand for lighting and daylighting potential, including passive solar gains and shading devices in use between the orientations towards South (± 60°) and North (± 60°) under climate conditions for Mannheim (49.52°N, 8.55°E)

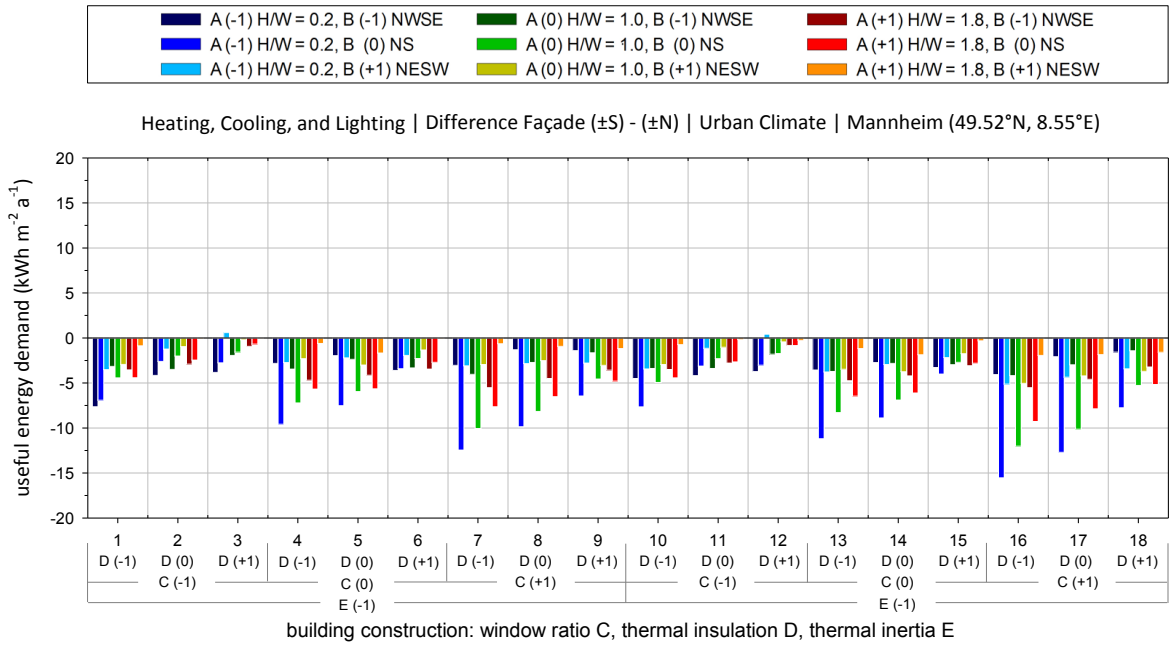

Figure 106: Annual average difference in the total useful energy demand including heating, cooling and lighting between the orientations towards South (± 60°) and North (± 60°) under climate conditions for Mannheim (49.52°N, 8.55°E)

Appendix 12 | Statistics of the Urban Microclimate Effects for Mannheim

Table 67: Statistics of the useful heating energy demand difference between urban and standard climate $\Delta Q_{heat\ (u\text{-}s)}$ for [SET IV] – [SET III], Mannheim (49.52°N, 8.55°E)

$\Delta Q_{heat(urb\text{-}stn)}$ | whole building | urban vs. standard clmate | Mannheim

Model Summary					Coefficients			
Model	R	R Square	Adjusted R Square	R Square Change	Model	predictor	B	Sig.
1	,632a	.399	.396	.399	11	Constant	-1.031	.000
2	,809b	.654	.650	.255		D	.697	.000
3	,895c	.801	.797	.147		C	-.556	.000
4	,947d	.897	.894	.096		A	-.422	.000
5	,970e	.941	.939	.045		CD	.418	.000
6	,982f	.963	.962	.022		AD	.285	.000
7	,984g	.969	.967	.005		AC	-.201	.000
8	,986h	.973	.971	.004		A^2	.135	.000
9	,988i	.976	.975	.004		AE	.070	.000
10	,989j	.978	.976	.001		C^2	-.118	.000
11	,989k	.978	.977	.001		CE	-.041	.002
						DE	.027	.045
k. Predictors: (Constant), D, C, A, CD, AD, AC, A^2, AE, C^2, CE, DE								

Table 68 Statistics of the useful cooling energy demand difference between urban and standard climate $\Delta Q_{cool\ (u\text{-}s)}$ for [SET IV] – [SET III], Mannheim (49.52°N, 8.55°E)

$\Delta Q_{cool(urb\text{-}stn)}$ | whole building | urban vs. standard clmate | Mannheim

Model Summary					Coefficients			
Model	R	R Square	Adjusted R Square	R Square Change	Model	predictor	B	Sig.
1	.652a	.425	.421	.425	12	Constant	1.197	.000
2	.768b	.589	.584	.164		C	.619	.000
3	.836c	.699	.694	.110		CD	-.471	.000
4	.866d	.750	.744	.051		D	-.315	.000
5	.892e	.796	.789	.046		C^2	.371	.000
6	.905f	.820	.813	.024		A^2	-.352	.000
7	.915g	.837	.830	.017		A	-.146	.000
8	.921h	.849	.841	.012		AD	.153	.000
9	.927i	.860	.851	.011		E	-.084	.000
10	.930j	.865	.856	.005		DE	.098	.001
11	.932k	.869	.860	.005		D^2	-.119	.014
12	.934l	.873	.863	.004		AC	-.078	.022
						CE	-.059	.035
j. Predictors: (Constant), C, CD, D, C^2, A^2, A, AD, E, DE, D^2								

Table 69: Statistics of the useful lighting energy demand difference between urban and standard climate $\Delta Q_{light\ (u\text{-}s)}$ and daylighting potential for [SET IV] – [SET III], Mannheim (49.52°N, 8.55°E)

$\Delta Q_{light(urb\text{-}stn)}$ | whole building | urban vs. standard clmate | Mannheim

Model Summary					Coefficients			
Model	R	R Square	Adjusted R Square	R Square Change	Model	predictor	B	Sig.
1	.590a	.348	.344	.348	10	Constant	-3.166	.000
2	.795b	.632	.627	.284		C	-.723	.000
3	.849c	.722	.716	.090		CD	-.800	.000
4	.887d	.787	.782	.065		C^2	.635	.000
5	.919e	.845	.840	.058		A	-.313	.000
6	.946f	.894	.890	.049		D^2	.511	.000
7	.957g	.916	.912	.022		D	.272	.000
8	.965h	.931	.927	.015		A^2	.316	.000
9	.967i	.934	.930	.004		AC	-.181	.000
10	.968j	.936	.932	.002		AD	.089	.004
						B^2	.099	.024
j. Predictors: (Constant), C, CD, C^2, A, D^2, D, A^2, AC, AD, B^2								

$\Delta_{Daylight(urb\text{-}stn)}$

Coefficients			
Model	predictor	B	Sig.
10	Constant	8.482	.000
	C	1.937	.000
	CD	2.142	.000
	C^2	-1.702	.000
	A	.840	.000
	D^2	-1.368	.000
	D	-.728	.000
	A^2	-.847	.000
	AC	.486	.000
	AD	-.239	.004
	B^2	-.265	.024
predictors as ΔQlight but different coef.			

Table 70: Statistics of the useful ventilation energy demand difference between urban and standard climate $\Delta Q_{vent(u-s)}$ for [SET IV] – [SET III], Mannheim (49.52°N, 8.55°E)

$\Delta Q_{vent(urb-stn)}$ | whole building | urban versus standard clmate

Model Summary					Coefficients			
Model	R	R Square	Adjusted R Square	R Square Change	Model 12	predictor Constant	B .785	Sig. .000
1	.530a	.281	.276	.281		C	.048	.000
2	.662b	.438	.431	.157		E	-.029	.000
3	.770c	.593	.586	.156		CD	-.044	.000
4	.834d	.696	.688	.102		A	.029	.000
5	.865e	.747	.739	.052		A^2	-.035	.000
6	.878f	.771	.762	.024		D^2	-.024	.000
7	.892g	.795	.786	.024		D	-.014	.000
8	.903h	.816	.806	.021		DE	-.013	.000
9	.909i	.826	.816	.011		B^2	-.016	.002
10	.913j	.834	.823	.008		AC	.010	.007
11	.917k	.840	.828	.006		C^2	.012	.019
12	.919l	.845	.832	.005		CE	.006	.031
l. Predictors: (Constant), C, E, CD, A, A^2, D^2, D, DE, B^2, AC, C^2, CE								

Table 71: Statistics of the total useful energy demand difference between urban and standard climate including heating, cooling and lighting $\Delta Q_{TOT\ I(u-s)}$ for [SET IV] – [SET III], Mannheim (49.52°N, 8.55°E)

$\Delta Q_{TOT(H+C+L)}$(urb-stn) | whole building | urban vs. standard climate | Mannheim

Model Summary					Coefficients			
Model	R	R Square	Adjusted R Square	R Square Change	Model 12	predictor Constant	B -3.010	Sig. .000
1	.505a	.255	.250	1.239		A	-.882	.000
2	.643b	.413	.406	1.103		CD	-.853	.000
3	.746c	.556	.548	.962		C	-.660	.000
4	.834d	.696	.688	.799		D	.653	.000
5	.884e	.782	.775	.678		C^2	.888	.000
6	.918f	.843	.837	.578		AD	.527	.000
7	.943g	.889	.884	.487		AC	-.461	.000
8	.953h	.909	.904	.443		D^2	.425	.000
9	.956i	.914	.909	.432		DE	.125	.002
10	.959j	.919	.914	.421		E	-.100	.002
11	.961k	.923	.917	.413		B^2	.181	.008
12	.962l	.926	.920	.405		CE	-.099	.012
l. Predictors: (Constant), A, CD, C, D, C^2, AD, AC, D^2, DE, E, B^2, CE								

Appendix 13 | Energy Demands of the Urban Office Buildings – Algiers

Refer to section II - 4 (p 145) for explanation about these data. The following legend gives the colour coding used in Table 72 below.

Table 72: Useful energy demand average values for the whole building (10 zones) expressed as ranking for heating (Q_{heat}), cooling (Q_{cool}), artificial lighting (Q_{light}), ventilation (Q_{vent} during and outside usage time: UT, OU) and as sum (Q_{TOT}) for [SET IV], Algiers (36.75°N, 3.00°E)

legend		
-1	PF	perforated façade (30%)
0	RF	row façade (60%)
+1	GF	glazed façade (90%)
-1	U -	weak insulation (0.65)
0	U o	medium insulation (0.40)
+1	U +	good insulation (0.15)
-1	LI	light-weighted
+1	MA	massive

A: urban vertical profile H/W
B: Facade's orientation
C: window ratio D: thermal insulation
E: thermal inertia

B			A
-1	0	1	
NWSE	NS	NESW	
I	IV	VII	0.2 (-1)
II	V	VIII	1.0 (0)
III	VI	IX	1.8 (+1)

C	D	E	ID
PF (-1)	U- (-1)	LI (-1)	1
PF (-1)	Uo (0)	LI (-1)	2
PF (-1)	U+ (+1)	LI (-1)	3
RF (0)	U- (-1)	LI (-1)	4
RF (0)	Uo (0)	LI (-1)	5
RF (0)	U+ (+1)	LI (-1)	6
GF (+1)	U- (-1)	LI (-1)	7
GF (+1)	Uo (0)	LI (-1)	8
GF (+1)	U+ (+1)	LI (-1)	9

C	D	E	ID
PF (-1)	U- (-1)	MA (+1)	10
PF (-1)	Uo (0)	MA (+1)	11
PF (-1)	U+ (+1)	MA (+1)	12
RF (0)	U- (-1)	MA (+1)	13
RF (0)	Uo (0)	MA (+1)	14
RF (0)	U+ (+1)	MA (+1)	15
GF (+1)	U- (-1)	MA (+1)	16
GF (+1)	Uo (0)	MA (+1)	17
GF (+1)	U+ (+1)	MA (+1)	18

rank	Heating			Cooling			Heating & Cooling			Lighting			Total Ventilation			Ventilation UT			Ventilation OU			Total (no Vent.)			Total (with Vent.)		
1	VII	3	0.05	IX	10	22.42	III	10	25.73	IV	16	3.89	VI	13	8.36	III	13	5.22	VI	7	2.98	IV	14	37.91	IV	14	47.89
2	IV	3	0.05	III	10	22.50	IX	10	25.77	IV	7	3.89	III	13	8.37	VI	13	5.22	III	7	3.00	IV	13	39.14	IV	13	48.05
3	I	3	0.05	II	10	22.98	II	10	26.28	VII	16	3.90	IX	13	8.39	IX	13	5.23	IX	7	3.01	V	14	39.14	V	13	48.22
4	VII	12	0.06	VI	10	23.13	V	10	26.37	VII	7	3.90	III	16	8.49	III	16	5.28	VI	4	3.03	V	13	39.51	V	14	48.85
5	II	12	0.06	V	10	23.18	VI	10	26.39	I	16	3.91	VI	16	8.52	VI	16	5.30	III	4	3.06	VII	14	40.08	VI	13	49.39
6	IV	12	0.06	VIII	10	23.69	VI	12	26.40	I	7	3.91	IX	16	8.55	IX	16	5.30	IX	4	3.07	I	14	40.09	I	14	50.01
7	VIII	12	0.06	VI	13	23.81	II	11	26.66	I	17	4.67	VI	4	8.59	V	13	5.30	VI	13	3.14	II	14	40.88	VII	14	50.07
8	I	12	0.06	IV	10	23.93	VIII	10	26.75	I	8	4.67	III	4	8.59	II	13	5.31	III	13	3.15	VI	13	41.03	II	14	50.56
9	V	12	0.06	VII	10	24.73	IV	10	26.84	IV	17	4.70	IX	4	8.60	II	10	5.32	IX	13	3.15	VIII	14	41.73	VII	10	50.95
10	IX	12	0.06	I	10	24.75	VII	11	26.90	IV	8	4.70	VI	7	8.67	IV	10	5.33	VI	1	3.18	VII	10	41.91	III	13	51.03
11	III	12	0.06	IX	13	25.46	VI	14	26.94	VII	17	4.74	IX	7	8.69	IX	10	5.33	IX	1	3.18	VI	17	41.99	IX	13	51.04
12	VI	12	0.06	III	13	25.46	IV	11	27.02	VII	8	4.74	III	7	8.70	III	10	5.34	III	1	3.18	III	14	42.00	I	10	51.28
13	VIII	3	0.06	VI	14	25.63	IX	12	27.03	II	16	4.83	V	13	8.71	V	10	5.34	II	7	3.21	IX	14	42.12	III	14	51.45
14	V	3	0.06	III	14	26.23	III	12	27.03	II	7	4.83	II	13	8.73	VIII	10	5.35	V	4	3.21	I	10	42.25	VI	17	51.48
15	II	3	0.06	II	11	26.32	V	11	27.05	I	13	4.90	IX	10	8.73	VI	10	5.36	V	7	3.21	VI	14	42.39	VIII	14	51.56
16	III	15	0.07	VI	12	26.34	IX	11	27.07	I	4	4.90	III	10	8.74	I	10	5.36	III	16	3.21	I	18	42.49	IX	14	51.56
17	IX	15	0.07	IX	14	26.36	III	11	27.10	V	16	4.90	VI	10	8.78	VII	10	5.37	VI	16	3.23	IV	18	42.58	II	13	51.67
18	VI	15	0.07	VII	11	26.53	I	11	27.10	V	7	4.90	II	10	8.82	IV	13	5.37	V	1	3.23	IX	13	42.66	VI	14	51.87

Table 72 continued – Cases 19 to 54

rank	Heating			Cooling			Heating & Cooling			Lighting			Total Ventilation			Ventilation UT			Ventilation OU			Total (no Vent.)			Total (with Vent.)		
19	VIII	15	0.07	IX	1	26.56	VI	11	27.12	VII	13	4.96	V	10	8.82	VIII	13	5.38	II	4	3.24	III	13	42.67	IV	10	51.96
20	II	15	0.07	V	13	26.59	VIII	11	27.34	VII	4	4.96	IX	1	8.83	I	13	5.40	IX	16	3.25	VII	18	42.71	II	10	52.23
21	V	15	0.07	IV	11	26.67	V	12	27.59	IV	13	5.03	VI	1	8.83	VII	13	5.41	II	1	3.27	V	17	42.85	VII	13	52.45
22	VII	15	0.07	III	1	26.68	III	14	27.63	IV	4	5.03	III	1	8.85	II	16	5.42	VIII	4	3.33	II	13	42.95	I	13	52.46
23	IV	15	0.07	I	11	26.71	II	15	27.68	VIII	16	5.13	V	1	8.87	V	16	5.44	IV	1	3.34	IV	10	43.04	VIII	10	52.57
24	I	15	0.07	V	11	26.72	IX	14	27.68	VIII	7	5.13	IV	13	8.91	VIII	16	5.50	VIII	1	3.34	VII	13	43.40	V	17	52.88
25	IX	3	0.08	IX	11	26.72	VII	10	27.85	II	17	6.29	VIII	10	8.91	IX	4	5.53	VIII	7	3.34	II	10	43.42	VIII	13	53.09
26	III	3	0.08	III	11	26.74	IX	15	27.90	II	8	6.29	II	1	8.91	III	4	5.54	IV	4	3.38	I	13	43.43	III	17	53.28
27	VI	3	0.08	VI	11	26.77	I	10	27.94	III	16	6.41	II	4	8.92	I	16	5.55	VII	1	3.38	VIII	10	43.65	IX	17	53.37
28	I	18	0.08	II	1	26.90	III	15	27.99	III	7	6.41	IV	10	8.92	IV	16	5.55	I	1	3.38	IV	17	43.79	I	18	53.94
29	VII	18	0.08	IX	12	26.97	VI	15	28.03	V	17	6.49	V	4	8.93	VI	4	5.56	I	4	3.39	III	17	43.81	IV	18	54.12
30	IV	18	0.08	III	12	26.98	V	14	28.24	V	8	6.49	VIII	13	8.96	VII	16	5.56	IV	7	3.40	IX	17	43.89	VII	18	54.21
31	II	18	0.09	VIII	11	27.02	III	18	28.40	IX	16	6.56	VIII	1	9.01	IX	14	5.58	IX	10	3.40	II	18	43.93	IV	17	54.29
32	VIII	18	0.09	V	14	27.18	IX	18	28.40	IX	7	6.56	II	16	9.02	III	14	5.59	III	10	3.40	VIII	13	44.13	IV	5	54.41
33	IX	18	0.09	V	1	27.42	V	15	28.40	VIII	17	6.57	I	10	9.03	III	17	5.59	I	7	3.40	V	18	44.21	V	10	54.67
34	V	18	0.09	VIII	1	27.51	IV	12	28.43	VIII	8	6.57	I	13	9.03	VI	14	5.60	VII	4	3.41	IV	5	44.33	VI	16	54.84
35	III	18	0.10	VI	1	27.52	VI	18	28.60	VI	16	6.72	IV	1	9.04	IX	17	5.60	V	13	3.41	VIII	18	44.39	II	18	55.00
36	VI	18	0.10	V	12	27.53	II	12	28.65	VI	7	6.72	VII	10	9.04	VI	17	5.60	II	13	3.42	IX	18	45.50	V	5	55.31
37	IV	6	0.21	II	15	27.61	VIII	15	28.69	II	13	6.88	VIII	4	9.05	V	1	5.64	VI	10	3.42	V	5	45.53	V	18	55.39
38	I	6	0.22	IX	15	27.83	IV	15	28.75	II	4	6.88	V	16	9.05	II	1	5.64	VII	7	3.44	V	10	45.84	VIII	18	55.67
39	VII	6	0.22	III	15	27.92	VIII	12	29.00	VIII	13	7.13	VII	13	9.05	II	14	5.65	V	10	3.48	III	18	45.85	V	4	55.79
40	VIII	6	0.23	VI	15	27.96	VII	15	29.01	VIII	4	7.13	VII	1	9.08	IX	1	5.65	VI	8	3.49	I	5	46.12	V	16	56.13
41	II	6	0.26	IV	1	28.13	I	15	29.23	V	13	7.15	I	1	9.10	VI	1	5.65	III	8	3.49	VI	16	46.32	VI	4	56.14
42	V	6	0.26	III	18	28.30	I	12	29.69	V	4	7.15	V	7	9.14	V	14	5.66	II	10	3.50	VII	5	46.38	I	5	56.18
43	III	6	0.29	IX	18	28.31	VII	12	29.72	I	14	7.33	II	7	9.15	III	1	5.67	IX	8	3.51	II	17	46.42	II	17	56.30
44	IX	6	0.30	V	15	28.34	IV	14	29.84	I	5	7.33	VII	4	9.24	VIII	1	5.68	IV	13	3.54	V	4	46.87	IX	18	56.31
45	VI	6	0.31	IV	12	28.37	V	18	29.96	VII	14	7.43	I	4	9.26	IX	7	5.68	VI	5	3.55	II	5	46.95	VII	5	56.44
46	VIII	11	0.32	VI	18	28.51	II	14	30.58	VII	5	7.43	IV	4	9.26	II	4	5.68	VIII	10	3.56	V	16	47.08	IV	4	56.50
47	V	11	0.33	VI	4	28.58	VI	13	30.86	IV	14	8.07	VIII	7	9.27	VI	7	5.69	IX	5	3.57	IV	4	47.24	VII	1	56.64
48	II	11	0.34	VII	1	28.58	II	18	31.36	IV	5	8.07	VIII	16	9.30	VII	1	5.69	III	5	3.57	VII	15	47.47	III	18	56.70
50	IV	11	0.35	VIII	15	28.62	VI	3	31.44	III	8	8.83	IX	14	9.44	IV	1	5.70	IV	10	3.60	VII	1	47.57	III	16	56.98
51	III	11	0.35	I	1	28.65	IX	1	31.57	VI	17	8.92	I	16	9.44	VIII	14	5.71	II	16	3.60	VIII	5	47.94	IX	10	57.01
52	IX	11	0.35	IV	15	28.68	III	1	31.64	VI	8	8.92	III	14	9.45	V	4	5.71	V	16	3.61	VI	18	47.96	I	1	57.07
53	VII	11	0.37	VII	15	28.94	VIII	14	31.65	IX	17	8.95	III	17	9.47	I	1	5.72	I	13	3.63	I	15	47.97	IX	16	57.08
54	I	11	0.39	VIII	12	28.94	II	1	31.95	IX	8	8.95	VI	14	9.48	VIII	4	5.72	VII	13	3.64	I	1	47.97	III	4	57.34

Table 72 continued – Cases 55 to 90

rank	Heating			Cooling			Heating & Cooling			Lighting			Total Ventilation			Ventilation UT			Ventilation OU			Total (no Vent.)			Total (with Vent.)		
55	IV	9	0.66	IV	14	29.10	III	3	31.99	I	18	9.19	IX	17	9.48	I	14	5.72	I	10	3.66	I	9	48.04	III	10	57.42
56	VII	9	0.70	I	15	29.15	VII	2	32.04	I	9	9.19	VI	17	9.48	II	17	5.72	VII	10	3.67	IV	16	48.06	IV	16	57.47
57	I	9	0.74	II	14	29.44	IX	3	32.04	VII	18	9.23	VI	8	9.49	VII	14	5.76	VI	2	3.69	III	5	48.15	IX	4	57.47
58	IV	14	0.74	IV	13	29.61	II	2	32.20	VII	9	9.23	VII	16	9.50	IV	14	5.76	II	8	3.69	IX	10	48.28	III	5	57.69
59	VIII	9	0.76	I	12	29.63	V	13	32.35	III	13	9.80	IX	8	9.52	V	17	5.77	II	5	3.71	IX	5	48.28	VIII	5	57.78
60	VII	14	0.76	VII	12	29.66	VIII	1	32.36	III	4	9.80	III	8	9.52	I	11	5.80	III	2	3.71	I	17	48.47	IX	5	57.80
61	V	9	0.77	II	13	29.73	I	2	32.37	IX	13	9.94	IX	5	9.52	VI	11	5.80	IX	2	3.71	III	16	48.48	II	1	58.00
62	II	9	0.81	VI	16	29.82	V	1	32.40	IX	4	9.94	VI	5	9.52	VII	11	5.81	V	8	3.72	VII	9	48.53	IV	1	58.21
63	I	14	0.82	V	18	29.87	VI	1	32.49	VIII	14	10.08	III	5	9.53	VIII	17	5.81	V	5	3.72	IX	16	48.53	VIII	1	58.27
64	III	9	0.86	III	4	30.02	IV	2	32.51	VIII	5	10.08	VII	7	9.59	IX	11	5.81	V	2	3.78	IV	9	48.56	VI	5	58.29
65	IX	9	0.87	IX	4	30.11	VIII	18	32.59	VI	13	10.16	IV	7	9.59	V	11	5.81	VIII	16	3.79	VII	17	48.60	II	4	58.49
66	VI	9	0.88	VI	5	30.13	II	6	32.61	VI	4	10.16	I	7	9.63	III	11	5.82	VIII	5	3.79	III	10	48.68	I	17	58.78
67	VII	17	0.97	VI	17	30.48	VII	14	32.65	II	14	10.31	II	14	9.67	II	11	5.82	II	2	3.80	III	4	48.75	VI	18	58.81
68	I	17	1.02	III	5	30.54	V	3	32.67	II	5	10.31	V	14	9.71	IV	11	5.83	VIII	8	3.82	VI	5	48.77	VIII	17	58.98
69	IV	17	1.05	VIII	14	30.59	VIII	2	32.69	V	14	10.91	II	5	9.75	VII	4	5.83	VIII	2	3.85	VIII	17	48.79	VII	17	58.99
70	V	14	1.05	VII	2	30.64	V	2	32.71	V	5	10.91	V	5	9.78	VIII	11	5.85	IV	16	3.85	IX	4	48.87	VII	15	59.02
71	VIII	14	1.06	IX	5	30.67	IX	13	32.72	IV	18	11.15	VIII	14	9.83	I	17	5.85	I	5	3.85	VII	11	48.91	VII	11	59.11
72	II	14	1.14	II	2	30.75	I	14	32.76	IV	9	11.15	VIII	5	9.84	I	4	5.87	IV	2	3.85	II	1	49.09	I	9	59.18
73	VI	14	1.31	I	2	30.92	IX	2	32.86	VIII	18	11.79	II	17	9.88	VII	17	5.88	IX	14	3.86	IV	1	49.17	I	15	59.49
74	IX	14	1.33	IV	2	31.14	III	13	32.87	VIII	9	11.79	VI	2	9.90	IV	4	5.89	III	14	3.86	VIII	1	49.26	I	11	59.62
75	IV	2	1.37	VIII	13	31.18	III	2	32.93	II	18	12.57	I	14	9.92	IV	17	5.92	III	17	3.87	I	11	49.43	VII	9	59.65
76	VIII	2	1.39	II	18	31.27	IV	1	32.97	II	9	12.57	III	2	9.93	V	7	5.93	IX	17	3.88	II	15	49.43	IV	9	59.70
77	VII	2	1.40	V	2	31.28	VI	2	33.05	VII	10	14.07	IX	2	9.93	VIII	7	5.93	IV	5	3.88	II	4	49.58	VI	8	59.75
78	III	14	1.40	VIII	2	31.30	VI	17	33.07	VII	1	14.07	II	8	9.93	II	7	5.95	VI	14	3.88	II	9	49.65	I	4	59.85
79	V	2	1.43	IV	18	31.35	IX	6	33.22	V	18	14.25	V	8	9.94	IX	5	5.95	VI	17	3.88	IV	15	49.67	VI	10	59.97
80	I	2	1.45	VI	3	31.36	I	18	33.30	V	9	14.25	IV	14	9.98	III	5	5.97	VII	5	3.88	V	9	50.25	VII	4	60.30
81	II	2	1.45	IX	2	31.38	VI	5	33.32	I	10	14.31	V	2	9.99	VI	5	5.97	I	2	3.89	VI	8	50.26	VIII	4	60.43
82	IX	2	1.48	III	2	31.45	III	6	33.37	I	1	14.31	VII	14	9.99	IX	8	6.00	VII	2	3.90	VIII	9	50.34	II	9	60.48
83	III	2	1.48	V	4	31.52	VI	6	33.45	III	14	14.36	II	2	10.03	VI	8	6.01	I	16	3.90	VIII	15	50.43	V	1	60.75
84	VI	2	1.49	VI	2	31.56	VII	18	33.48	III	5	14.36	V	17	10.03	III	8	6.03	I	8	3.91	I	4	50.59	II	15	60.84
85	VIII	17	1.60	V	5	31.68	VII	1	33.50	IX	14	14.43	VIII	8	10.03	II	5	6.04	IV	8	3.91	VII	4	51.06	II	16	60.90
86	V	17	1.72	VII	14	31.89	IV	3	33.51	IX	5	14.43	VII	5	10.06	VIII	5	6.05	VII	8	3.93	VI	10	51.20	V	9	61.10
87	II	17	1.73	III	3	31.92	V	6	33.54	VI	14	15.45	I	5	10.06	V	5	6.06	VII	16	3.94	IX	9	51.35	III	8	61.23
88	IX	17	2.53	I	14	31.94	II	3	33.62	VI	5	15.45	IV	2	10.07	IX	18	6.10	II	14	4.03	VIII	4	51.38	IV	15	61.25
89	VI	17	2.59	IX	3	31.96	VIII	6	33.64	IV	10	16.20	VI	11	10.07	III	18	6.12	V	14	4.05	IV	11	51.56	VIII	9	61.25
90	III	17	2.62	IX	16	32.04	I	1	33.66	IV	1	16.20	IV	5	10.09	VI	18	6.12	III	9	4.05	III	8	51.71	IX	8	61.52

Table 72 continued – Cases 91 to 126

rank	Heating			Cooling			Heating & Cooling			Lighting			Total Ventilation			Ventilation UT			Ventilation OU			Total (no Vent.)			Total (with Vent.)		
91	IV	5	2.74	III	16	32.07	III	5	33.79	VIII	10	16.90	VIII	2	10.09	VII	7	6.16	IX	9	4.05	III	9	51.76	IV	11	61.78
92	VII	5	2.78	II	6	32.35	IV	6	33.79	VIII	1	16.90	IX	11	10.09	II	18	6.17	VI	9	4.06	II	16	51.87	IX	9	61.94
93	I	5	2.85	III	17	32.36	IX	5	33.84	IX	18	17.10	I	2	10.09	VII	5	6.17	VIII	14	4.12	V	1	51.88	VIII	15	61.95
94	VIII	5	2.89	IX	17	32.40	VII	6	33.85	IX	9	17.10	III	11	10.10	IV	7	6.20	II	17	4.16	IX	8	52.00	V	8	62.01
95	IV	10	2.91	VIII	18	32.50	VIII	3	33.96	II	10	17.14	VII	2	10.10	IV	5	6.20	VI	6	4.19	V	8	52.08	III	9	62.37
96	V	5	2.95	V	3	32.60	I	6	34.01	II	1	17.14	V	11	10.14	VI	2	6.21	IX	6	4.20	VII	6	52.31	IX	1	62.91
97	II	5	3.05	IX	6	32.92	IV	13	34.11	III	18	17.46	II	11	10.17	I	2	6.21	I	14	4.20	I	6	52.75	VIII	16	63.34
98	VIII	10	3.06	III	6	33.07	IX	9	34.26	III	9	17.46	VIII	17	10.19	I	5	6.21	III	6	4.21	V	15	52.94	III	1	63.44
99	VII	10	3.12	VI	6	33.15	III	9	34.31	VII	15	18.46	I	11	10.19	VII	2	6.21	VI	3	4.21	II	11	53.28	II	11	63.45
100	IX	5	3.17	I	18	33.23	I	3	34.62	VII	6	18.46	VII	11	10.20	VIII	8	6.21	III	3	4.21	VIII	11	53.59	I	16	63.46
101	I	10	3.19	V	6	33.28	V	5	34.63	I	15	18.74	VIII	11	10.21	III	2	6.21	II	9	4.22	IV	8	53.67	VII	6	63.47
102	V	10	3.19	IX	9	33.39	VII	3	34.67	I	6	18.74	IV	11	10.23	IX	2	6.21	IV	14	4.22	I	16	54.01	VII	16	63.53
103	VI	5	3.19	VII	18	33.41	VI	9	34.76	VI	18	19.36	I	17	10.32	IV	2	6.21	IX	3	4.23	VII	16	54.03	VIII	11	63.79
104	III	10	3.23	VIII	6	33.41	IX	17	34.94	VI	9	19.36	VII	8	10.34	V	18	6.21	VII	14	4.24	VIII	16	54.04	I	6	63.90
105	III	5	3.24	III	9	33.44	III	17	34.99	V	10	19.48	IV	8	10.35	V	2	6.22	V	9	4.24	VII	2	54.05	IV	8	64.02
106	VI	10	3.25	IV	3	33.46	V	9	36.00	V	1	19.48	I	8	10.38	V	8	6.22	V	17	4.26	IX	1	54.08	VI	7	64.12
107	II	10	3.30	I	13	33.49	II	13	36.06	IV	15	20.92	VII	17	10.40	II	2	6.23	VI	11	4.27	VI	9	54.12	VII	2	64.15
108	IX	10	3.34	IV	5	33.52	IV	5	36.26	IV	6	20.92	IV	17	10.50	I	7	6.23	III	11	4.28	II	6	54.36	V	15	64.31
109	IV	8	4.17	VII	13	33.55	V	17	36.36	VIII	15	21.75	IX	9	10.59	II	8	6.24	IX	11	4.28	III	1	54.59	VI	9	64.72
110	VII	8	4.20	II	3	33.56	II	5	36.65	VIII	6	21.75	VI	9	10.60	VIII	2	6.24	VIII	9	4.30	I	2	54.70	I	2	64.79
111	I	8	4.24	IV	6	33.58	VIII	13	37.00	II	15	21.75	III	9	10.61	VIII	18	6.25	II	6	4.31	IV	6	54.71	II	8	64.96
112	VIII	8	4.46	II	5	33.60	II	9	37.07	II	6	21.75	IX	18	10.81	VI	15	6.28	V	6	4.32	II	8	55.03	II	6	65.36
113	IV	13	4.51	VII	6	33.63	VI	4	37.38	VII	11	22.01	II	9	10.83	IX	15	6.28	V	11	4.33	VIII	6	55.39	V	11	65.66
114	V	8	4.55	I	6	33.79	IV	9	37.41	VII	2	22.01	III	18	10.84	II	15	6.28	V	3	4.35	VI	7	55.45	III	7	65.68
115	II	8	4.60	VI	9	33.88	VIII	5	37.86	I	11	22.33	V	9	10.84	III	15	6.29	II	11	4.35	V	11	55.52	IV	6	65.89
116	IV	1	4.84	VIII	3	33.89	VII	13	38.44	I	2	22.33	VI	18	10.85	V	15	6.29	VIII	11	4.36	IX	15	55.96	IX	7	66.08
117	VIII	1	4.84	II	4	34.33	I	13	38.53	IX	10	22.51	VI	6	10.87	VI	12	6.30	II	3	4.36	III	15	56.32	VI	1	66.13
118	VII	13	4.89	IV	4	34.53	VIII	9	38.54	IX	1	22.51	IX	6	10.89	III	12	6.30	VIII	6	4.38	III	7	56.98	VIII	6	66.47
119	VII	1	4.92	I	3	34.57	I	5	38.79	III	10	22.95	III	6	10.89	I	18	6.30	VIII	17	4.38	IV	2	57.05	IV	2	67.11
120	VI	1	4.97	VII	3	34.62	I	9	38.85	III	1	22.95	VIII	9	10.91	VII	18	6.30	VII	11	4.39	VI	1	57.30	IX	15	67.23
121	III	1	4.97	V	17	34.64	IX	4	38.93	V	15	24.53	VI	3	10.97	IX	12	6.31	I	11	4.39	VI	15	57.39	V	7	67.38
122	V	1	4.98	V	16	34.76	III	4	38.95	V	6	24.53	III	3	10.98	I	15	6.31	VIII	3	4.39	IX	7	57.39	III	15	67.60
123	IX	8	4.99	VIII	5	34.97	VII	5	38.95	IV	11	24.54	II	6	11.00	VIII	15	6.32	I	9	4.40	I	8	57.49	I	8	67.87
124	IX	1	5.01	V	9	35.23	IV	17	39.09	IV	2	24.54	IX	3	11.00	VII	15	6.33	IV	11	4.40	V	6	58.07	VIII	8	68.32
125	I	1	5.01	I	5	35.94	VII	9	39.31	VI	10	24.81	V	6	11.01	IV	15	6.33	VII	9	4.42	V	7	58.24	VI	15	68.65
126	I	13	5.03	VIII	4	36.13	VI	16	39.60	VI	1	24.81	II	18	11.07	IV	18	6.33	IV	9	4.43	VIII	8	58.29	VII	8	68.67

Table 72 continued – Cases 127 to 162

rank	Heating			Cooling			Heating & Cooling			Lighting			Total Ventilation			Ventilation UT			Ventilation OU			Total (no Vent.)			Total (with Vent.)		
127	II	1	5.06	VII	5	36.17	V	4	39.71	VIII	11	26.25	VIII	6	11.09	II	12	6.35	I	6	4.44	VII	8	58.33	II	2	68.85
128	III	8	5.06	VI	8	36.26	II	17	40.13	VIII	2	26.25	VII	9	11.11	VIII	12	6.35	VII	6	4.45	II	2	58.82	VIII	2	69.03
129	IV	16	5.07	II	9	36.27	VI	8	41.33	II	11	26.62	IV	9	11.14	V	12	6.36	IV	3	4.46	VIII	2	58.94	IX	11	69.04
130	VI	8	5.07	VI	7	36.39	IX	16	41.97	II	2	26.62	I	9	11.15	I	12	6.39	I	17	4.46	IX	11	58.95	V	6	69.08
131	VII	16	5.47	IV	9	36.75	III	16	42.07	IX	15	28.07	I	6	11.15	IV	12	6.41	I	3	4.46	III	11	59.12	III	11	69.21
132	I	16	5.57	VIII	9	37.78	V	16	42.18	IX	6	28.07	VII	6	11.16	VII	8	6.41	IV	6	4.47	VI	11	59.97	VI	11	70.04
133	V	13	5.76	III	8	37.83	IV	4	42.21	III	15	28.34	V	3	11.17	VII	12	6.42	VII	3	4.47	IV	7	60.96	IV	7	70.56
134	VIII	13	5.82	I	4	37.93	VIII	17	42.22	III	6	28.34	II	3	11.18	IV	8	6.44	VII	17	4.52	V	2	61.18	II	7	71.08
135	II	13	6.33	IV	17	38.05	II	4	42.69	V	11	28.48	V	18	11.18	I	8	6.48	IV	17	4.58	IX	6	61.29	V	2	71.18
136	VI	13	7.05	IX	8	38.05	III	8	42.88	V	2	28.48	IV	6	11.18	IX	9	6.54	IX	18	4.70	III	6	61.70	IX	6	72.18
137	VIII	16	7.26	I	9	38.11	IX	8	43.05	VI	15	29.36	VIII	3	11.20	VI	9	6.54	III	18	4.72	II	7	61.92	III	6	72.60
138	IX	13	7.26	III	7	38.27	I	17	43.80	VI	6	29.36	VI	15	11.26	III	9	6.56	VI	18	4.73	VI	6	62.82	VI	6	73.69
139	III	13	7.41	VII	4	38.34	VII	17	43.86	IX	11	31.87	IX	15	11.27	V	9	6.60	II	18	4.90	VI	12	63.46	IX	2	74.66
140	V	16	7.42	II	17	38.40	IV	16	44.17	IX	2	31.87	III	15	11.27	VIII	9	6.61	V	18	4.96	III	12	64.13	VIII	7	74.77
141	IV	4	7.69	IX	7	38.51	VIII	4	44.26	III	11	32.02	VIII	18	11.28	II	9	6.61	VI	15	4.98	IX	12	64.19	III	2	74.87
142	I	4	7.76	VII	9	38.61	V	8	45.59	III	2	32.02	I	3	11.33	VI	6	6.68	III	15	4.99	V	12	64.28	VI	12	74.99
143	VII	4	7.76	IV	16	39.10	I	4	45.69	VI	11	32.85	IV	3	11.34	III	6	6.68	IX	15	4.99	IV	12	64.43	I	7	75.04
144	II	16	7.85	II	16	39.19	VII	4	46.10	VI	2	32.85	VII	3	11.36	IX	6	6.69	VIII	18	5.03	IX	2	64.73	III	12	75.64
145	VIII	4	8.13	VIII	17	40.63	II	16	47.04	I	12	35.70	V	15	11.37	V	6	6.69	V	15	5.08	III	2	64.95	IX	12	75.73
146	V	4	8.20	V	8	41.04	VI	7	48.74	I	3	35.70	II	15	11.41	II	6	6.69	II	15	5.12	VIII	12	65.26	VI	2	75.80
147	II	4	8.36	VIII	16	41.66	II	8	48.74	VII	12	35.95	I	18	11.45	VII	9	6.69	I	18	5.15	II	12	65.35	VII	7	75.96
148	VI	4	8.81	V	7	42.13	VIII	16	48.91	VII	3	35.95	VII	18	11.49	VII	6	6.71	VII	18	5.19	I	12	65.38	V	12	76.02
149	IX	4	8.82	I	17	42.78	IV	8	48.97	IV	12	36.00	III	12	11.51	I	6	6.71	VIII	15	5.20	I	7	65.41	IV	12	76.37
150	III	4	8.92	VII	17	42.89	I	16	50.10	IV	3	36.00	VIII	15	11.52	VIII	6	6.71	IV	18	5.20	VIII	7	65.49	VIII	12	77.03
151	VI	16	9.78	II	8	44.14	VII	16	50.13	VIII	12	36.26	I	15	11.52	IV	9	6.71	I	15	5.21	VII	12	65.66	II	12	77.07
152	IX	16	9.93	I	16	44.53	III	7	50.57	VIII	3	36.26	VI	12	11.53	IV	6	6.71	III	12	5.21	VI	2	65.90	I	12	77.30
153	III	16	10.01	VII	16	44.65	IX	7	50.83	V	12	36.70	IX	12	11.53	I	9	6.74	VII	15	5.23	VII	7	66.37	VII	12	77.62
154	IV	7	10.13	IV	8	44.80	VIII	8	51.72	V	3	36.70	IV	18	11.53	VI	3	6.76	IX	12	5.23	VI	3	68.49	VI	3	79.47
155	I	7	10.16	II	7	45.88	I	8	52.82	II	12	36.70	VII	15	11.55	IX	3	6.77	VI	12	5.24	III	3	69.09	III	3	80.07
156	VII	7	10.21	IV	7	46.94	V	7	53.34	II	3	36.70	IV	15	11.58	III	3	6.77	IV	15	5.25	IX	3	69.20	IX	3	80.21
157	VIII	7	11.01	VIII	8	47.26	VII	8	53.59	VI	12	37.06	II	12	11.72	VIII	3	6.81	II	12	5.37	V	3	69.36	V	3	80.53
158	V	7	11.21	I	8	48.58	IV	7	57.07	VI	3	37.06	V	12	11.74	II	3	6.82	V	12	5.38	IV	3	69.51	IV	3	80.85
159	II	7	11.21	VIII	7	49.36	II	7	57.09	III	12	37.09	VIII	12	11.77	V	3	6.82	VIII	12	5.42	VIII	3	70.21	VIII	3	81.42
160	III	7	12.30	VII	8	49.39	VIII	7	60.37	III	3	37.09	I	12	11.91	I	3	6.86	I	12	5.52	I	3	70.32	II	3	81.50
161	IX	7	12.32	I	7	51.34	I	7	61.50	IX	12	37.16	IV	12	11.94	IV	3	6.88	IV	12	5.54	II	3	70.32	I	3	81.65
162	VI	7	12.34	VII	7	52.26	VII	7	62.47	IX	3	37.16	VII	12	11.96	VII	3	6.89	VII	12	5.54	VII	3	70.62	VII	3	81.98

Appendix 14 | Energy Demand Deviation due to Urban Microclimate – Algiers

Table 73: Useful energy demand deviation between urban climate and standard climate as annual average [SET IV] – [SET III] – 36 best and 36 worst cases

rank	Heating			Cooling			Heating & Cooling			Lighting			Total Ventilation			Ventilation UT			Ventilation OU			Total (no Vent.)			Total (with Vent.)		
1	VIII	16	-2.11	III	1	-0.11	III	1	-0.56	VI	5	-6.31	III	10	0.61	V	1	0.56	VI	10	0.02	VI	5	-5.88	VI	5	-5.05
2	II	16	-1.90	IX	1	-0.10	IX	1	-0.55	VI	14	-6.31	VI	10	0.61	II	10	0.56	III	10	0.03	VI	14	-5.43	VI	14	-4.63
3	III	16	-1.78	II	6	0.21	VI	1	-0.19	VIII	9	-6.10	IX	10	0.63	IV	10	0.57	IX	15	0.04	III	1	-5.30	III	1	-4.61
4	V	16	-1.77	IX	10	0.22	III	10	-0.11	VIII	18	-6.10	V	10	0.64	II	1	0.57	IX	10	0.05	IX	1	-5.27	IX	1	-4.58
5	III	7	-1.73	III	10	0.24	V	1	-0.09	VI	9	-6.06	II	10	0.67	VI	1	0.57	IX	12	0.05	III	9	-5.19	V	1	-4.47
6	VI	7	-1.71	VI	1	0.26	IX	10	-0.07	VI	18	-6.06	V	1	0.69	VIII	10	0.57	III	15	0.05	V	1	-5.15	III	9	-4.38
7	VI	16	-1.69	V	1	0.30	II	1	0.04	III	9	-5.97	VIII	10	0.69	IX	1	0.58	VI	15	0.05	VI	9	-5.08	VIII	1	-4.33
8	IX	16	-1.67	II	1	0.38	VIII	1	0.15	III	18	-5.97	IX	1	0.69	VIII	1	0.58	III	12	0.06	VIII	1	-5.06	III	10	-4.24
9	VIII	7	-1.64	II	15	0.41	II	6	0.16	V	9	-5.92	VI	1	0.70	IX	10	0.58	V	15	0.06	II	6	-5.01	VI	9	-4.24
10	IX	7	-1.63	VIII	1	0.50	VI	10	0.26	V	18	-5.92	III	1	0.70	V	10	0.58	V	10	0.06	II	1	-4.94	II	1	-4.22
11	II	7	-1.48	VI	10	0.56	V	10	0.26	IX	9	-5.86	VII	1	0.71	III	1	0.58	VI	12	0.06	IX	9	-4.91	II	6	-4.22
12	V	7	-1.48	VII	2	0.60	II	15	0.41	IX	18	-5.86	II	1	0.72	III	10	0.58	IX	18	0.07	III	10	-4.85	IX	10	-4.17
13	I	16	-1.43	V	10	0.62	II	10	0.41	III	5	-5.76	VII	11	0.72	I	10	0.58	III	18	0.07	III	5	-4.83	V	10	-4.16
14	VII	16	-1.39	VII	11	0.68	VI	5	0.43	III	14	-5.76	III	13	0.72	VII	10	0.59	VI	18	0.07	V	10	-4.80	IX	9	-4.11
15	IV	16	-1.38	IV	2	0.69	VII	2	0.49	V	5	-5.39	V	15	0.72	VII	1	0.59	III	14	0.08	IX	10	-4.80	III	5	-4.03
16	V	13	-1.08	II	10	0.72	VIII	10	0.52	V	14	-5.39	IX	13	0.72	VI	10	0.59	V	12	0.08	III	18	-4.78	III	18	-4.02
17	VIII	13	-1.07	IV	11	0.74	IV	2	0.57	II	9	-5.23	IV	10	0.72	IX	4	0.59	VII	3	0.09	II	15	-4.76	VIII	10	-4.00
18	II	13	-1.06	V	6	0.75	VII	11	0.64	II	18	-5.23	I	1	0.72	I	1	0.59	III	11	0.09	VI	18	-4.72	II	15	-3.98
19	III	4	-1.01	II	2	0.79	II	2	0.65	VIII	1	-5.21	IX	12	0.73	III	4	0.59	II	12	0.09	VIII	10	-4.69	VI	18	-3.96
20	IV	7	-1.00	VI	5	0.80	IV	11	0.69	VIII	10	-5.21	III	12	0.73	IV	1	0.59	V	11	0.09	VI	1	-4.62	VI	1	-3.92
21	VI	4	-0.99	VIII	6	0.83	V	6	0.70	II	6	-5.17	VI	12	0.73	III	13	0.60	IX	14	0.09	II	10	-4.57	II	10	-3.90
22	I	7	-0.96	VIII	10	0.85	VIII	6	0.77	II	15	-5.17	VIII	1	0.73	I	13	0.60	VII	12	0.09	IX	18	-4.48	IX	18	-3.75
23	IX	4	-0.95	IX	6	0.87	III	9	0.78	VIII	5	-5.13	IV	1	0.73	III	5	0.60	II	11	0.10	III	14	-4.33	III	14	-3.59
24	VII	7	-0.92	II	11	0.90	IX	6	0.81	VIII	14	-5.13	V	11	0.74	IX	5	0.60	VIII	11	0.10	V	9	-4.19	VI	10	-3.56
25	V	4	-0.92	VIII	15	0.92	I	2	0.81	IX	5	-5.07	I	10	0.74	VI	4	0.60	IX	11	0.10	VI	10	-4.17	V	9	-3.34
26	VI	13	-0.91	V	15	0.93	II	11	0.85	IX	14	-5.07	IX	18	0.74	VII	13	0.60	I	3	0.10	VIII	6	-4.07	VIII	6	-3.25
27	III	13	-0.91	III	9	0.94	VI	14	0.88	V	1	-5.07	VI	15	0.74	IV	13	0.61	VII	11	0.10	VIII	15	-3.92	VIII	15	-3.09
28	VIII	4	-0.90	I	2	0.94	IV	6	0.91	V	10	-5.07	IX	15	0.74	IX	13	0.61	VII	15	0.10	V	18	-3.90	V	18	-3.06
29	II	4	-0.89	IV	15	0.95	III	6	0.92	II	1	-4.98	III	14	0.75	I	11	0.61	II	10	0.10	V	6	-3.87	V	6	-3.06
30	III	17	-0.88	IX	15	0.95	VIII	15	0.92	II	10	-4.98	I	11	0.75	V	13	0.61	VII	6	0.10	IX	5	-3.75	IX	5	-2.95
31	I	13	-0.87	IV	6	0.95	III	5	0.93	VIII	6	-4.84	III	15	0.75	VI	13	0.61	VI	11	0.10	V	15	-3.65	V	15	-2.92
32	VII	13	-0.85	III	6	0.98	V	15	0.93	VIII	15	-4.84	II	11	0.75	VIII	5	0.61	IV	11	0.11	V	5	-3.64	V	5	-2.78
33	IX	13	-0.85	I	11	1.01	V	2	0.94	III	1	-4.74	VI	13	0.75	VI	5	0.61	IV	3	0.11	V	14	-3.34	IX	14	-2.57
34	II	17	-0.82	III	15	1.03	IX	9	0.95	III	10	-4.74	V	12	0.75	I	14	0.62	II	18	0.11	VI	4	-3.33	VI	4	-2.53
35	VIII	17	-0.81	VII	15	1.05	IX	15	0.95	IX	1	-4.72	I	13	0.75	VII	11	0.62	II	14	0.11	IX	14	-3.32	V	14	-2.52
36	III	8	-0.80	VII	6	1.08	IV	15	0.95	IX	10	-4.72	IX	14	0.75	II	13	0.62	I	12	0.11	VIII	9	-3.15	VIII	9	-2.31

Table 73 continued – Cases 127 to 162

rank	Heating			Cooling			Heating & Cooling			Lighting			Total Ventilation			Ventilation UT			Ventilation OU			Total (no Vent.)			Total (with Vent.)		
127	III	3	-0.02	IX	8	5.13	IX	17	4.24	II	16	-1.67	V	13	0.86	V	16	0.68	IX	5	0.21	VI	3	1.94	VI	3	2.74
128	IX	3	-0.02	VII	4	5.16	IV	13	4.30	II	7	-1.67	V	4	0.86	I	9	0.68	IX	16	0.21	II	3	1.97	II	3	2.78
129	VI	3	-0.02	VII	13	5.26	IX	7	4.35	V	16	-1.65	IX	7	0.88	II	18	0.68	III	17	0.21	VIII	3	1.98	VIII	3	2.78
130	II	3	-0.01	I	13	5.29	IV	4	4.38	V	7	-1.65	I	8	0.90	III	8	0.69	VI	5	0.22	VI	7	2.00	V	3	2.87
131	VIII	3	-0.01	VIII	4	5.33	VI	7	4.38	VII	17	-1.62	IX	17	0.90	VI	18	0.69	IV	7	0.22	IX	7	2.02	IX	7	2.91
132	V	3	-0.01	VIII	13	5.48	IX	8	4.39	VII	8	-1.62	IV	8	0.90	I	17	0.69	V	4	0.22	V	3	2.05	VI	7	2.91
133	VII	3	-0.01	IX	16	5.78	VII	13	4.41	VIII	16	-1.58	VII	8	0.90	VI	15	0.69	V	5	0.22	I	13	2.41	I	13	3.16
134	II	18	-0.01	VI	16	5.80	VIII	13	4.41	VIII	7	-1.58	III	7	0.91	VII	17	0.69	VIII	4	0.23	IV	13	2.41	IV	13	3.22
135	V	18	-0.01	III	16	5.82	I	13	4.43	III	2	-1.58	VI	7	0.91	III	18	0.69	VIII	13	0.23	I	4	2.42	I	4	3.25
136	I	3	-0.01	III	7	5.96	VIII	4	4.43	III	11	-1.58	III	17	0.91	VII	3	0.69	II	8	0.23	IV	4	2.49	VII	13	3.30
137	IV	3	-0.01	IX	7	5.98	I	4	4.44	VI	2	-1.42	IX	8	0.92	VIII	18	0.69	IX	7	0.24	VII	13	2.55	IV	4	3.32
138	VIII	18	-0.01	VI	7	6.09	VII	4	4.56	VI	11	-1.42	III	8	0.93	VII	18	0.69	II	17	0.24	VII	4	2.70	VII	4	3.51
139	III	18	-0.01	IV	17	6.18	IV	17	5.70	I	16	-1.06	II	17	0.93	V	18	0.69	II	7	0.24	V	17	3.01	V	17	4.05
140	VII	18	-0.01	I	17	6.41	IV	16	5.95	I	7	-1.06	VI	16	0.93	III	11	0.69	III	8	0.24	II	17	3.20	II	17	4.13
141	IX	18	-0.01	I	8	6.41	VII	17	5.96	VII	16	-1.01	VI	8	0.94	II	17	0.69	III	7	0.24	V	8	3.34	V	8	4.32
142	I	18	-0.01	VII	17	6.42	I	17	5.96	VII	7	-1.01	I	7	0.94	IV	18	0.70	VI	17	0.25	II	8	3.43	II	8	4.38
143	VI	18	-0.01	IV	8	6.42	V	16	5.97	IV	16	-1.01	VII	7	0.94	IV	17	0.70	V	13	0.25	IV	17	3.92	IV	17	4.90
144	IV	18	0.00	VII	8	6.67	IV	8	6.00	IV	7	-1.01	IV	7	0.95	III	15	0.70	IX	8	0.25	I	17	4.13	I	8	5.08
145	VII	15	0.00	V	17	6.74	I	8	6.02	I	12	-0.29	II	8	0.95	IX	15	0.70	VI	7	0.25	I	8	4.18	I	17	5.08
146	IV	12	0.00	V	8	7.02	V	17	6.05	I	3	-0.29	I	17	0.96	V	7	0.70	VIII	8	0.26	IV	8	4.21	IV	8	5.12
147	I	15	0.00	II	17	7.08	VII	8	6.26	VIII	12	-0.27	VI	17	0.96	IX	17	0.70	VI	8	0.26	V	16	4.32	VII	17	5.31
148	III	15	0.00	II	8	7.16	II	17	6.27	VIII	3	-0.27	I	16	0.96	III	17	0.70	I	17	0.27	VII	17	4.34	V	16	5.36
149	IX	12	0.00	IV	16	7.33	I	16	6.28	VII	12	-0.17	VII	16	0.96	VI	17	0.71	V	8	0.27	VIII	17	4.36	VIII	17	5.43
150	VIII	12	0.00	I	16	7.71	VII	16	6.37	VII	3	-0.17	II	7	0.97	VIII	7	0.71	VI	16	0.27	VII	8	4.64	VII	8	5.54
151	IX	15	0.00	V	16	7.73	V	8	6.38	II	12	-0.16	VIII	8	0.97	V	8	0.71	V	7	0.29	VIII	8	4.73	VIII	8	5.70
152	II	12	0.00	VII	16	7.75	II	16	6.41	II	3	-0.16	VII	17	0.98	I	8	0.71	IV	17	0.29	II	16	4.73	II	16	5.71
153	III	12	0.00	IV	7	7.78	II	8	6.50	IV	12	-0.15	V	8	0.98	VIII	8	0.71	VII	17	0.29	IV	16	4.94	IV	16	5.95
154	VI	15	0.00	I	7	7.85	V	7	6.75	IV	3	-0.15	II	16	0.98	IV	8	0.71	VIII	7	0.29	V	7	5.11	V	7	6.09
155	VI	12	0.00	VII	7	8.11	IV	7	6.78	V	12	-0.10	IV	17	0.98	II	8	0.72	VII	16	0.30	I	16	5.22	I	16	6.18
156	V	12	0.00	V	7	8.23	I	7	6.90	V	3	-0.10	V	7	0.99	II	7	0.72	V	17	0.30	VII	16	5.36	VII	16	6.31
157	II	15	0.00	II	16	8.31	II	7	7.08	III	12	-0.06	VIII	7	1.00	VII	8	0.73	I	16	0.30	II	7	5.40	II	7	6.37
158	VIII	15	0.00	VIII	17	8.33	VII	7	7.19	III	3	-0.06	IV	16	1.01	IV	7	0.73	II	16	0.31	IV	7	5.77	IV	7	6.72
159	IV	15	0.00	II	7	8.56	VIII	17	7.53	VI	12	-0.05	VIII	16	1.02	I	7	0.74	VIII	17	0.33	I	7	5.84	I	7	6.77
160	VII	12	0.00	VIII	8	8.60	VIII	16	7.72	VI	3	-0.05	V	16	1.04	VIII	17	0.74	IV	16	0.33	VIII	16	6.15	VII	7	7.12
161	V	15	0.00	VIII	16	9.83	VIII	8	7.90	IX	12	-0.03	V	17	1.05	V	17	0.75	VIII	16	0.34	VII	7	6.18	VIII	16	7.17
162	I	12	0.00	VIII	7	10.28	VIII	7	8.64	IX	3	-0.03	VIII	17	1.07	VII	7	0.75	V	16	0.35	VIII	7	7.06	VIII	7	8.06

Appendix 15 | Statistics of the Urban Microclimate Effects for Algiers

Table 74: Statistics of the useful heating energy demand difference between urban and standard climate $\Delta Q_{heat(u-s)}$ for [SET IV] – [SET III], Algiers (36.75°N, 3.00°E)

$\Delta Q_{heat(urb-stn)}$ | whole building | urban vs. standard climate | Algiers

Model Summary					Coefficients			
Model	R	R Square	Adjusted R Square	R Square Change	Model	predictor	B	Sig.
1	.732a	.536	.533	.536	12	(Consta	-0.350	.000
2	.877b	.769	.766	.233		D	.448	.000
3	.953c	.908	.907	.140		C	-.295	.000
4	.962d	.925	.923	.017		CD	.280	.000
5	.968e	.938	.936	.013		D^2	-.137	.000
6	.973f	.946	.944	.008		A	-.069	.000
7	.976g	.953	.951	.006		AC	-.069	.000
8	.979h	.958	.955	.005		AD	.060	.000
9	.981i	.962	.959	.004		DE	.042	.000
10	.982j	.965	.962	.003		A^2	.067	.000
11	.984k	.968	.965	.003		CE	-.035	.000
12	.985l	.970	.968	.090		AE	.034	.000
						C^2	-.054	.000

l. Predictors: (Constant), D, C, CD, D^2, A, AC, AD, DE, A^2, CE, AE, C^2

Table 75 Statistics of the useful cooling energy demand difference between urban and standard climate $\Delta Q_{cool\ (u-s)}$ for [SET IV] – [SET III], Algiers (36.75°N, 3.00°E)

$\Delta Q_{cool(urb-stn)}$ | whole building | urban vs. standard climate | Algiers

Model Summary					Coefficients			
Model	R	R Square	Adjusted R Square	R Square Change	Model	predictor	B	Sig.
1	.666a	.444	.440	.444	10	(Consta	3.119	0.000
2	.802b	.644	.639	.200		C	1.987	0.000
3	.910c	.827	.824	.183		CD	-1.633	0.000
4	.925d	.855	.852	.028		D	-1.277	0.000
5	.935e	.874	.870	.019		A	-0.498	0.000
6	.943f	.888	.884	.014		C^2	0.707	0.000
7	.948g	.899	.895	.011		A^2	-0.619	0.000
8	.953h	.909	.904	.010		AD	0.380	0.000
9	.957i	.916	.911	.007		AC	-0.357	0.000
10	.958j	.918	.912	.002		D^2	-0.430	0.000
						B^2	0.242	0.046

j. Predictors: (Constant), C, CD, D, A, C^2, A^2, AD, AC, D^2, B^2

Table 76: Statistics of the useful lighting energy demand difference between urban and standard climate $\Delta Q_{light(u-s)}$ and daylighting potential for [SET IV] – [SET III], Algiers (36.75°N, 3.00°E)

$\Delta Q_{light(urb-stn)}$ | whole building | urban vs. standard climate | Algiers $\Delta_{Daylight(urb-stn)}$

Model Summary					Coefficients				Coefficients			
Model	R	R Square	Adjusted R Square	R Square Change	Model	predictor	B	Sig.	Model	predictor	B	Sig.
1	.749a	.561	.558	.561	8	(Consta	-4.511	.000	8	(Constan	12.0863	.000
2	.804b	.647	.642	.086		CD	-1.906	.000		CD	5.106	.000
3	.854c	.729	.724	.083		A	-.608	.000		A	1.629	.000
4	.884d	.781	.776	.052		C^2	1.035	.000		C^2	-2.773	.000
5	.906e	.820	.814	.039		C	-.475	.000		C	1.271	.000
6	.922f	.850	.844	.030		AC	-.501	.000		AC	1.342	.000
7	.928g	.861	.855	.011		A^2	.621	.000		A^2	-1.665	.000
8	.932h	.869	.862	.008		D^2	.382	.000		D^2	-1.022	.000
						AD	.222	.003		AD	-.595	.003

h. Predictors: (Constant), CD, A, C^2, C, AC, A^2, D^2, AD

For the coef. see Qlight

Table 77: Statistics of the useful ventilation energy demand difference between urban and standard climate $\Delta Q_{vent(u-s)}$ for [SET IV] – [SET III], Algiers (36.75°N, 3.00°E)

$\Delta Q_{vent(urb-stn)}$ | whole building | urban vs. standard climate | Algiers

Model Summary					Coefficients			
Model	R	R Square	Adjusted R Square	R Square Change	Model	predictor	B	Sig.
					12	(Consta	0.848	.000
1	.730a	.533	.530	.533		C	.079	.000
2	.845b	.714	.710	.181		CD	-.056	.000
3	.867c	.752	.747	.038		D^2	-.036	.000
4	.882d	.777	.772	.026		A^2	-.030	.000
5	.895e	.801	.795	.024		C^2	.029	.000
6	.904f	.817	.810	.016		E	-.011	.000
7	.912g	.832	.824	.014		AE	-.013	.000
8	.918h	.843	.835	.011		D	-.011	.000
9	.924i	.854	.845	.011		CE	.011	.000
10	.930j	.865	.856	.011		A	-.011	.000
11	.934k	.872	.863	.007		AD	.011	.003
12	.936l	.877	.867	.004		B^2	-.012	.022
l. Predictors: (Constant), C, CD, D^2, A^2, C^2, E, AE, D, CE, A, AD, B^2								

Table 78: Statistics of the useful total energy demand difference between urban and standard climate including heating, cooling and lighting $\Delta Q_{TOT1(u-s)}$ for [SET IV] – [SET III], Algiers (36.75°N, 3.00°E)

$\Delta Q_{TOT(H+C+L)}$(urb-stn) | whole building | urban vs. standard climate | Algiers

Model Summary					Coefficients			
Model	R	R Square	Adjusted R Square	R Square Change	Model	predictor	B	Sig.
					7	(Consta	-1.657	.000
1	.694a	.482	.479	2.266		CD	-3.259	.000
2	.764b	.583	.578	2.040		C	1.217	.000
3	.823c	.677	.671	1.801		A	-1.175	.000
4	.861d	.742	.735	1.616		C^2	1.687	.000
5	.888e	.789	.782	1.466		D	-.832	.000
6	.910f	.828	.821	1.328		AC	-.927	.000
7	.921g	.848	.841	1.253		AD	.662	.000
g. Predictors: (Constant), CD, C, A, C^2, D, AC, AD								

Appendix 16 | TEB-Type 201 for TRNSYS: Parameters, Inputs and Outputs Tabs

Table 79: List of parameters of Type 201

Parameter	Unit	Additional description
mode	-	For time synchronisation with TRNSYS
read material properties from file	-	either input material properties (0) or read them from file (1)
anthropogenic heat source as input	-	This parameter is 0 when heat flux is constant and 2 when anthropogenic heat lux is read from file
wall surface over horizontal surface	-	proportion of wall area to horizontal area
road albedo	-	solar reflectance of the wall surface
road emissivity	-	emissivity of the road surface
wall albedo	-	solar reflectance of the wall surface
wall emissivity	-	emissivity of the wall surface
roof albedo	-	solar reflectance of the roof surface
roof emissivity	-	emissivity of the roof surface
road deep temperature	K	deep soil temperature of road at simulation start
road surface temperature	K	initial surface temperature of road at simulation start
building inside air temperature	K	initial indoor air temperature at simulation start
wall surface temperature	K	initial wall surface temperature at simulation start
roof surface temperature	K	initial roof surface temperature at simulation start
number of road layers	-	Up to nine (09) material layers
volumetric heat capacity of road layer (i)	$J\ m^{-3}\ K^{-1}$	
thermal conductivity of road layer (i)	$W\ m^{-1}\ K^{-1}$	
thickness of road layer (i)	m	
number of wall layers	-	
volumetric heat capacity of wall layer (i)	$J\ m^{-3}\ K^{-1}$	
thermal conductivity of wall layer (i)	$W\ m^{-1}\ K^{-1}$	
thickness of wall layer (i)	m	
fraction of buildings		proportion of building area to total area
building height	m	
height of air temperature and humidity measurement	m	
height of wind measurement	m	height of wind measurement above the ground
simulation start time	s	must be a value between 0 and 86400
simulation start day	-	must be a value between 1 and 31
simulation start month	-	must be a value between 1 and 12
simulation start year	-	The calculation accounts for leap years
latitude	degree	
longitude	degree	
surface orography	m	height of relief
weather station orography	m	height of weather station
anthropogenic sensible heat flux due to traffic	$W\ m^{-2}$	The sensible heat flux is a constant value. Traffic begins every day at 21600s and stops at 64800s
anthropogenic latent heat flux due to traffic	$W\ m^{-2}$	The latent heat flux is a constant value. Traffic begins every day at 21600s and stops at 64800s
anthropogenic sensible heat flux	$W\ m^{-2}$	Industry is continuous over simulation time

due to industry		
anthropogenic latent heat flux due to industry	W m^{-2}	Industry is continuous over simulation time
town roughness length z_0	m	z_0 is a function of the urban density
initial water on roof	mm	
initial water on road	mm	

Table 80: List of inputs (climate data) of Type 201

Input	Unit	Additional description
air temperature	K	air temperature forcing at some height a.r.l.
specific air humidity	kg kg^{-1}	air humidity forcing at some height a.r.l.
wind speed	m s^{-1}	wind speed forcing at some height a.r.l.
wind direction	degree	wind direction clockwise from North
direct shortwave solar radiation	W m^{-2}	on a horizontal surface
diffuse shortwave solar radiation	W m^{-2}	scattered on a horizontal surface
longwave atmospheric radiation	W m^{-2}	on a horizontal surface
rain precipitation	kg s^{-1} m^{-2}	rain precipitation forcing
snow precipitation	kg s^{-1} m^{-2}	snow precipitation forcing
atmospheric surface pressure	Pa	atmospheric surface pressure forcing

Table 81: List of outputs (energy balance and temperatures) of Type 201

Output	Unit	Additional description
facet (i) states for roof, wall or road		
canyon air temperature	K	at canyon mid-height
canyon air specific humidity	kg kg_{-1}	at canyon mid-height
canyon air relative humidity	%	at canyon mid-height
canyon wind speed	m s^{-2}	at canyon mid-height
air pressure	Pa	at canyon mid-height
combined sky ground temperature	K	
sky temperature	K	Computed from atmospheric longwave radiation
absorbed shortwave radiation by roof	W m^{-2}	
absorbed shortwave radiation by walls	W m^{-2}	including inter-reflections between walls and road
absorbed shortwave radiation by roads	W m^{-2}	
longwave absorbed radiation by roof	W m^{-2}	
longwave absorbed radiation by roof	W m^{-2}	Incl. one re-emission and reflection at walls and road
longwave absorbed radiation by road	W m^{-2}	
surface temperature of facet (i)	K	
total absorbed net radiation by facet (i)	W m^{-2}	
total absorbed net radiation by town	W m^{-2}	Ttown means canyon system (road, walls, roof)
sensible heat flux over facet (i)	W m^{-2}	
sensible heat flux over town	W m^{-2}	
latent heat flux over facet (i)	W m^{-2}	
latent heat flux over town	W m^{-2}	
conductive heat flux through facet (i)	W m^{-2}	
conductive heat flux through the town	W m^{-2}	
heat storage flux through facet (i)	W m^{-2}	
heat storage flux through the town	W m^{-2}	
anthropogenic heat flux from roof	W m^{-2}	
anthropogenic heat flux from wall	W m^{-2}	
anthropogenic heat flux of domestic heating without force restore	W m^{-2}	

Appendix 17 | TEB Inputs for Stuttgart City in PART II

The variables in Table 82 are read from an external batch file using TRNEdit.

Table 82: Coded TEB input file for the Stuttgart simulations

START	! 0
STOP	! 87672 hours, corresponds to 10 years (2003 – 2012)
TIME STEP	! 300 seconds = 0.083333335 hour
wall_o_hor	! 4 Wall surface over horizontal surface
0.10	! 5 Road albedo
0.94	! 6 Road emissivity
0.20	! 7 Wall albedo
0.94	! 8 Wall emissivity
0.20	! 9 Roof albedo
0.94	! 10 Roof emissivity
Troad_deep	! 11 Road deep temperature
Tstart_surf	! 12 Road surface temperature
297.15	! 13 Building inside air temperature
Tstart_surf	! 14 Wall surface temperature
Tstart_surf	! 15 Roof surface temperature
3	! 16 Number of road layer (i)
HC_road (i)	! 17 (Volumetric) Heat capacity of road layer (i)
TC_road (i)	! 18 Thermal conductivity of road layer (i)
D_road (i)	! 19 Thickness of road layer (i)
3	! 26 Number of wall layer (i)
HC_wall (i)	! 27 (Volumetric) heat capacity of wall layer (i)
TC_wall (i)	! 28 Thermal conductivity of wall layer (i)
D_wall (i)	! 29 Thickness of wall layer (i)
3	! 36 Number of roof layer (i)
HC_roof (i)	! 37 (Volumetric) Heat capacity of roof layer (i)
TC_roof (i)	! 38 Thermal conductivity of roof layer (i)
D_roof (i)	! 39 Thickness of roof layer (i)
bld_frac	! 46 Fraction of buildings
bld_height	! 47 Building height
forcing_abv_roof	! 48 Height of air temperature and humidity measurement
forcing_abv_roof	! 49 Height of wind measurement
81200	! 50 Simulation start time in seconds at UTC ! start time set one hour before year's tart because this first time step is not output
31	! 51 Simulation start day
12	! 52 Simulation start month
2002	! 53 Simulation start year
latitude	! 54 Latitude (Mannheim)
longitude	! 55 Longitude (Mannheim)
altitude	! 56 Surface orography (altitude Mannheim)
altitude	! 57 Weather station orography (altitude Mannheim)
QF_H_traffic	! 58 Anthropogenic sensible heat flux due to traffic (7:00 – 19:00)
0	! 59 Anthropogenic latent heat flux due to traffic
0	! 60 Anthropogenic sensible heat flux due to industry (day round)
0	! 61 Anthropogenic latent heat flux due to industry
1.0	! 62 Town roughness length z_0
0	! 63 Initial water on roof per m^2
0	! 64 Initial water on road per m^2

Appendix 18 | TRNSYS Inputs for Stuttgart City in PART II

A prerequisite for a DOE plan is the definition of representative values ranges and levels for the city of Stuttgart, i.e. including all cases that occur. A matrix of the shape coefficient and building volume values, which cover the whole range of cases occurring in Stuttgart in three equidistant stages was defined (see Figure 107). On this, basis, three basic forms were determined, i.e. a cube, cross-like and block-shaped buildings. Figure 108 shows these generic building forms drawn with TRNSYS3D in sketch-up®, including their built-up environment. With regard to urban items, the distances to the neighbouring buildings were set using a height-to-width ratio H/W of 0.2, 1.0 and 1.8, which state for low, medium and high density.

The thermal transmittance U-value was determined according to IWU building typology catalogue for Germany, which provides average values depending on the age and typology of residential buildings (see Table 84). Figure 110 shows the resulting values set, which cover the whole range of thermal insulation quality for all buildings. For non-residential buildings, the same procedure was used, also based on the age of the building. Subsequent renovations of buildings were included by updating them to the corresponding thermal regulation standards.

The external components of the building envelope (exterior walls, roofs, base plate) were modelled in TEB and TRNSYS as 3-layered components according to Table 86 with the thermal insulation thickness depending on the target total U-value of the component. Table 87 lists the HVAC controls for heating, cooling, ventilation, lighting as well as the internal heat sources specified in TRNSYS. In the absence of more and differentiated information on real scenarios of use, these settings are very simple assumptions, which refer to the EnEV and DIN V 18599.

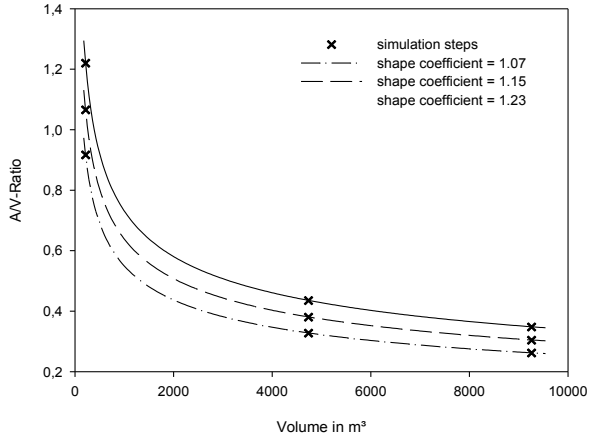

$$S = \frac{\sqrt{a}}{\sqrt[6]{4\pi\sqrt[3]{3v}}}$$

with
a: sum of the building surfaces
v: building volume
S shape coefficient

Figure 107: The building compactness and building volume step values in Stuttgart and used in the DOE simulation plan

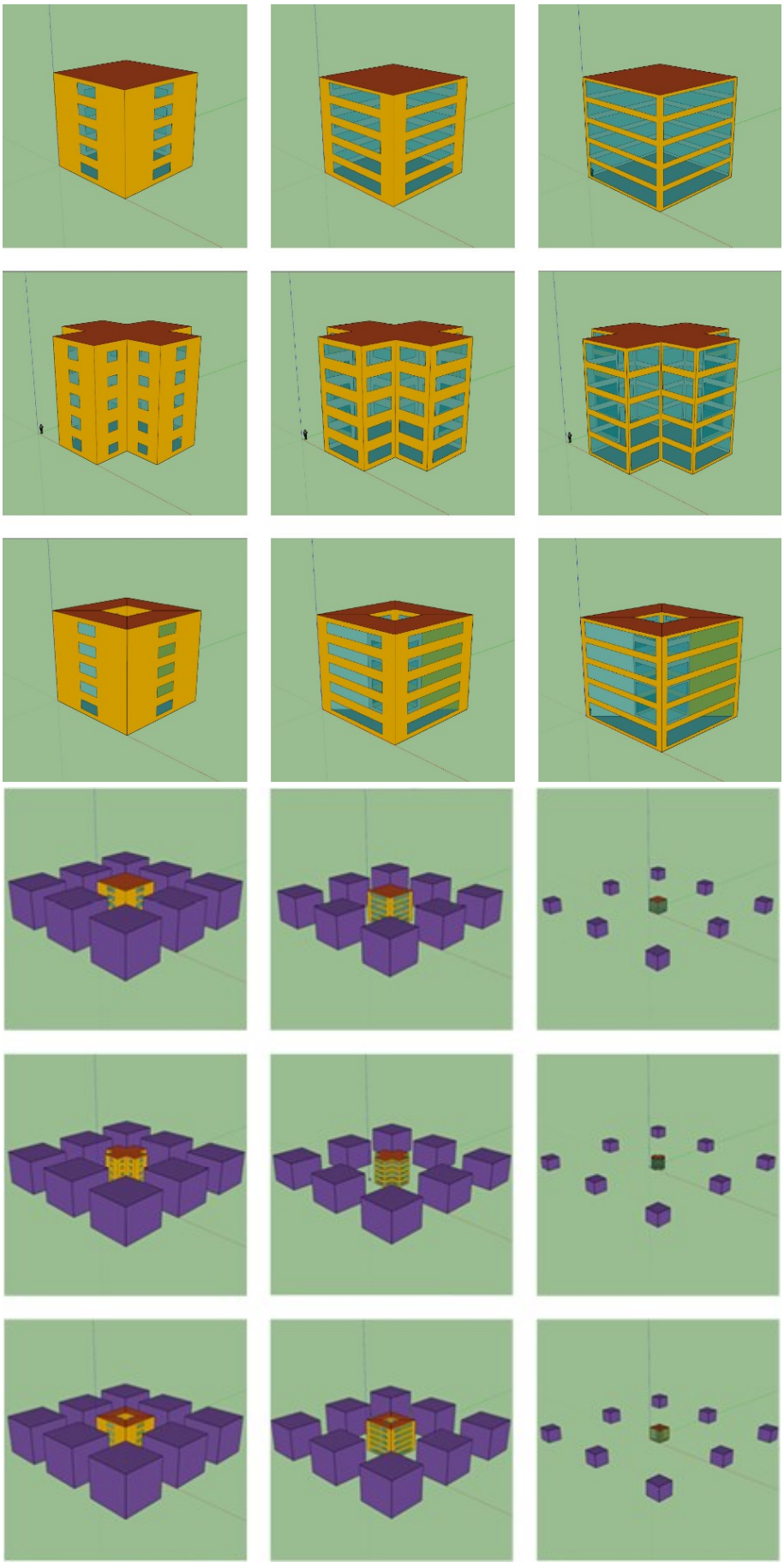

Figure 108: Examples of the building types and their urban surroundings as simulated in TRNSYS

Table 83: TRNSYS simulation settings for the generic building geometries in terms of compactness (shape coefficient S) and size (volume V)

	Key metric	unit	small	medium	large
CUBE	height	m	6.0	16.8	21.0
	width	m	6.0	16.8	21.0
	length	m	6.0	16.8	21.0
	volume	m^3	216.0	4738.5	9261.0
	total surfaces at 5.5 sides	m^2	198.0	1551.6	2425.5
	total surface / volume	m^{-1}	0.9	0.3	0.3
	shape coefficient	-	1.1	1.1	1.1
CROSS	Key metric		small	medium	large
	height	m	3.8	16.8	21.0
	width	m	3.7	8.7	10.9
	length	m	2.9	5.9	7.4
	volume	m^3	216.0	4738.5	9261.0
	total surfaces at 5.5 sides	m^2	230.1	1801.6	2816.3
	total surface / volume	m^{-1}	1.1	0.4	0.3
	shape coefficient	-	1.1	1.1	1.1
BLOCK	Key metric		small	medium	large
	height	m	3.2	16.8	21.0
	width	m	9.0	18.0	22.5
	length	m	3.7	6.4	8.0
	volume	m^3	216.0	4738.5	9261.0
	total surfaces at 5.5 sides	m^2	263.5	2060.2	3220.5
	total surface / volume	m^{-1}	1.2	0.4	0.3
	shape coefficient	-	1.2	1.2	1.2

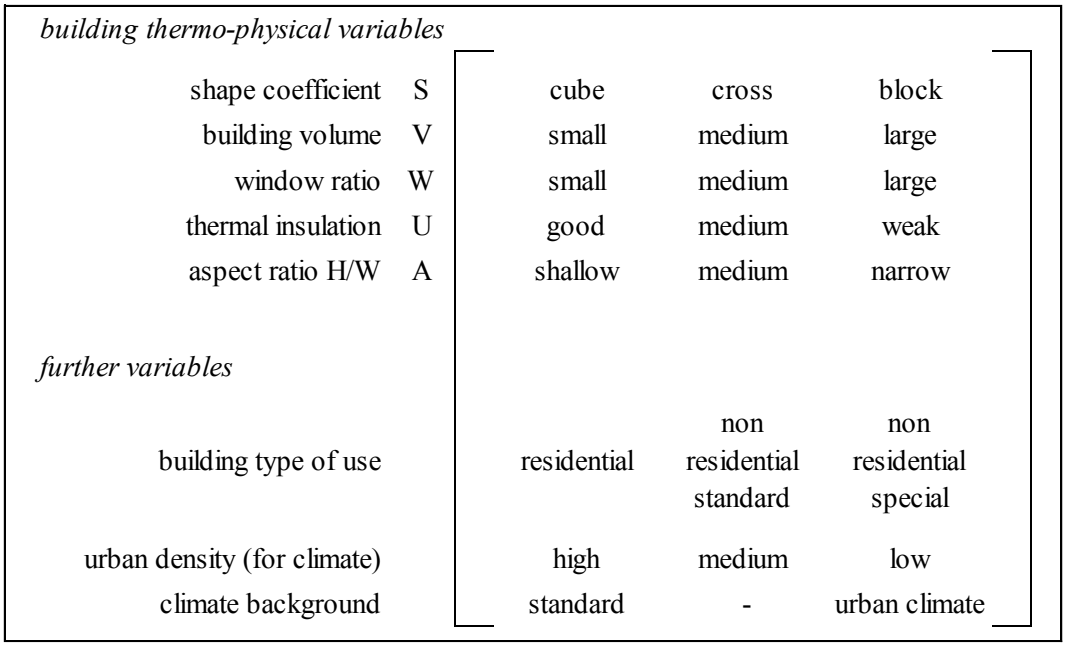

Figure 109: Building variables included in the design of experiments plan used in TRNSYS simulations

Table 84: An excerpt of the average thermal transmittance U-value and window ratio WR after the IWU building typology catalogue for Germany

building type	*Time period*	*ID*	*U-value*	*WR*	*Time period*	*ID*	*U-value*	*WR*
single-family detached house	from 1918 A	EFH_A	1.928	0.08	1969-1978	EFH_F	0.928	0.09
	from 1918 B	EFH_B	1.727	0.07	1979-1983	EFH_G	0.746	0.08
	1919-1948	EFH_C	1.727	0.10	1984-1994	EFH_H	0.564	0.11
	1949-1957	EFH_D	1.535	0.07	ab 1995	EFH-l	0.473	0.09
	1958-1968	EFH_E	1.49	0.09				
single-family row house	from 1918 B	RH_B	1.727	0.11	1969-1978	RH_F	0.928	0.16
	1919-1948	RH_C	1.727	0.15	1979-1983	RH_G	0.746	0.11
	1949-1957	RH_D	1.535	0.16	1984-1994	RH_H	0.564	0.13
	1958-1968	RH_E	1.49	0.12	ab 1995	RH_I	0.473	0.15
multi-family house / non-residential	from 1918 A	MFH_A	1.73	0.11	1969-1978	MFH_F	0.928	0.12
	from 1918 B	MFH_B	1.727	0.18	1979-1983	MFH_G	0.746	0.12
	1919-1948	MFH_C	1.727	0.12	1984-1994	MFH_H	0.564	0.14
	1949-1957	MFH_D	1.535	0.10	ab 1995	MFH_I	0.473	0.14
	1958-1968	MFH_E	1.49	0.15				
large multi-family house	from 1918 B	GMH_B	1.65	0.22	1969-1978	GMH_F	1.301	0.19
	1919-1948	GMH_C	1.30	0.15	1958-1968	HH_E	1.02	0.31
	1949-1957	GMH_D	1.397	0.15	1969-1978	HH_F	0.726	0.21
	1958-1968	GMH_E	1.173	0.17				
other buildings	1946-1960	N_MFH_D[1]	1.431	0.16	1970-1980	N_HH_F[1]	1.169	0.19
	1961-1969	N_GMH_F[1]	0.978	0.18	1981-1985	N_GMH_G[1]	1.091	0.15
	1961-1969	N_MFH_E[1]	1.354	0.20	1981-1985	N_HH_G[1]	0.803	0.28
	1969-1978	EFH_F_F[2]	0.473	0.11	1986-1990	N_GMH_H[1]	1.568	0.15
([1]) industrial residential building, ([2]) prefabricated house								

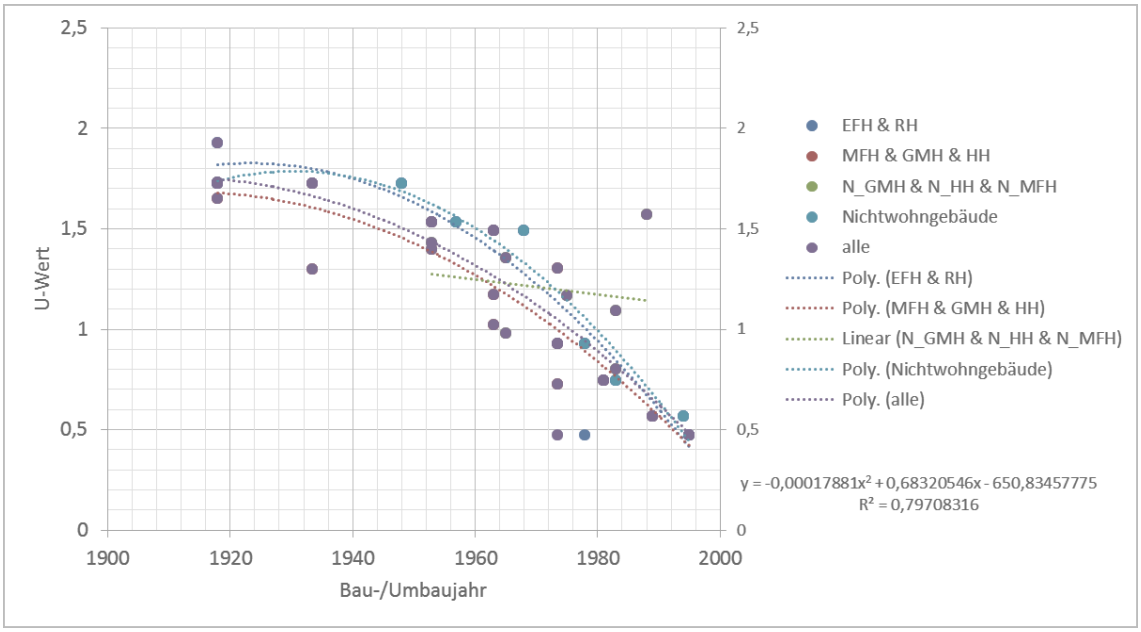

Figure 110: Average thermal transmittance U-value according to the IWU building typology catalogue for Germany (see Table 84 for details)

Table 85: TEB and TRNSYS simulation settings for the thermal insulation quality, window ratio and urban density

Var.	explanation variable		coded DOE simulation steps			comments
			-1	0	1	
U	Thermal transmittance U-value	opaque components (exterior walls)	0.1	1.2	2.3	U-value estimated for each building after IWU Building typology catalogue (IWU 2005); average values depending on building age incl. subsequent renovations.
		window	0.4	3.1	5.8	
W	window ratio	window	10%	30%	50%	Mean value after the IWU building typology catalogue for residential buildings. Used for all building types.
A	aspect ratio H/W	urban built-up surroundings	0.2	1	1.8	low, medium and high built density covering the range of cases occurring in Stuttgart.

Table 86: Simplified modelling of the thermal properties of the building envelope components in TEB and TRNSYS

building component layer	material thermal properties				
	thermal conductivity λ	specific heat capacity c	volumetric density (ρ)	thermal conductivity λ	Thickness d
	kJ h^{-1} m^{-1} K^{-1}	kJ kg^{-1} K^{-1} or Wh kg^{-1} K^{-1}	kg m^{-3}	W m^{-1} K^{-1}	m
concrete	5.76	1	2000	1.6	0.15
thermal insulation	0.18	0.9	80	0.050	Variable (*)
concrete	5.76	1	2000	1.6	0.15
(*) Thermal insulation thickness is set as function of the total U-value required for the building element					

Table 87: TRNSYS simulation settings for HVAC systems, lighting and shading devices (mostly according to EnEV and DIN V 18599)

issue	residential building	non-residential
period of use	from 6:00 to 23:00	from 07:00 to 18:00 from 05:00 to 18:00 for heating including pre-heating time
ventilation rate	0.70 h^{-1} bis 0.79 h^{-1}	ventilation rate depending on person occupation rate
Heating set temperature	20 °C during usage time 16 °C outside usage time	21 °C during usage time 17 °C outside usage time
Cooling set temperature	26 °C during usage time	26 °C during usage time
internal heat gains	2.815 W m^{-2}	depending on type of internal heat and person occupation rate
lighting	depending on the incoming solar radiation on the façade: ON if 120 W m^{-2} or less; OFF (i.e. daylight) if above 200 W m^{-2}	
shading devices	depending on the incoming solar radiation on the façade ON if 120 W m^{-2} or less; OFF if above 140 W m^{-2}	

Appendix 19 | Urban Climate Results for Stuttgart City using Isotherm Maps

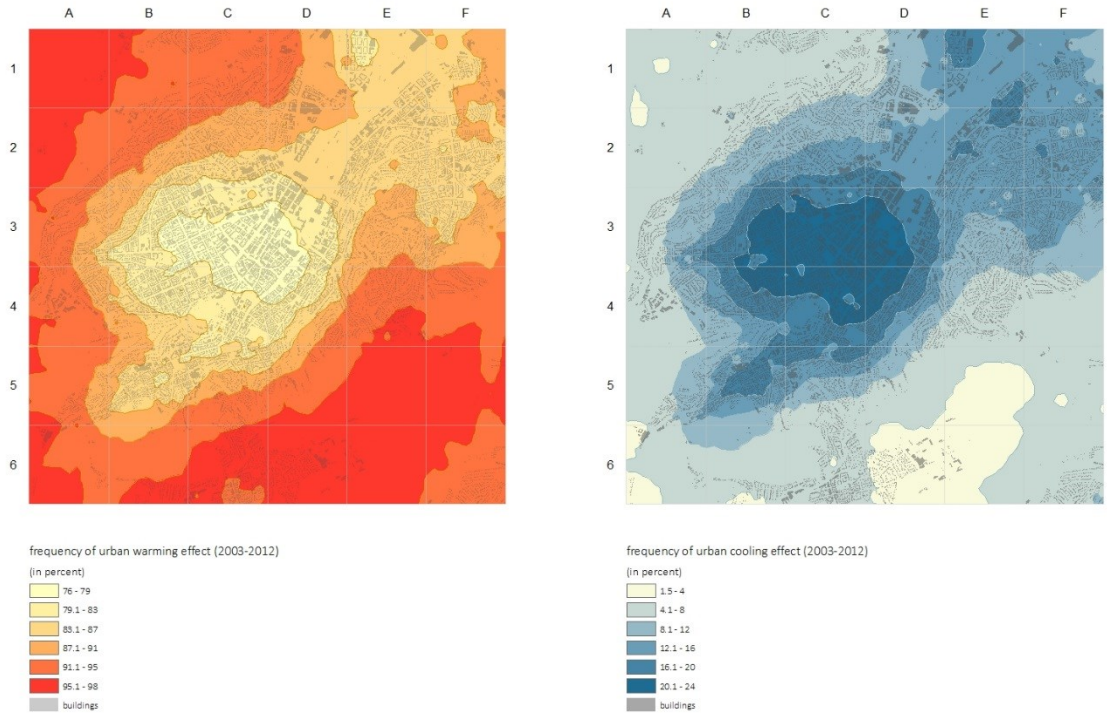

Figure 111: The strength of the warming of the urban canyon for Stuttgart inner city for the period 2013 – 2012 with isotherm representation (TEB calculation)

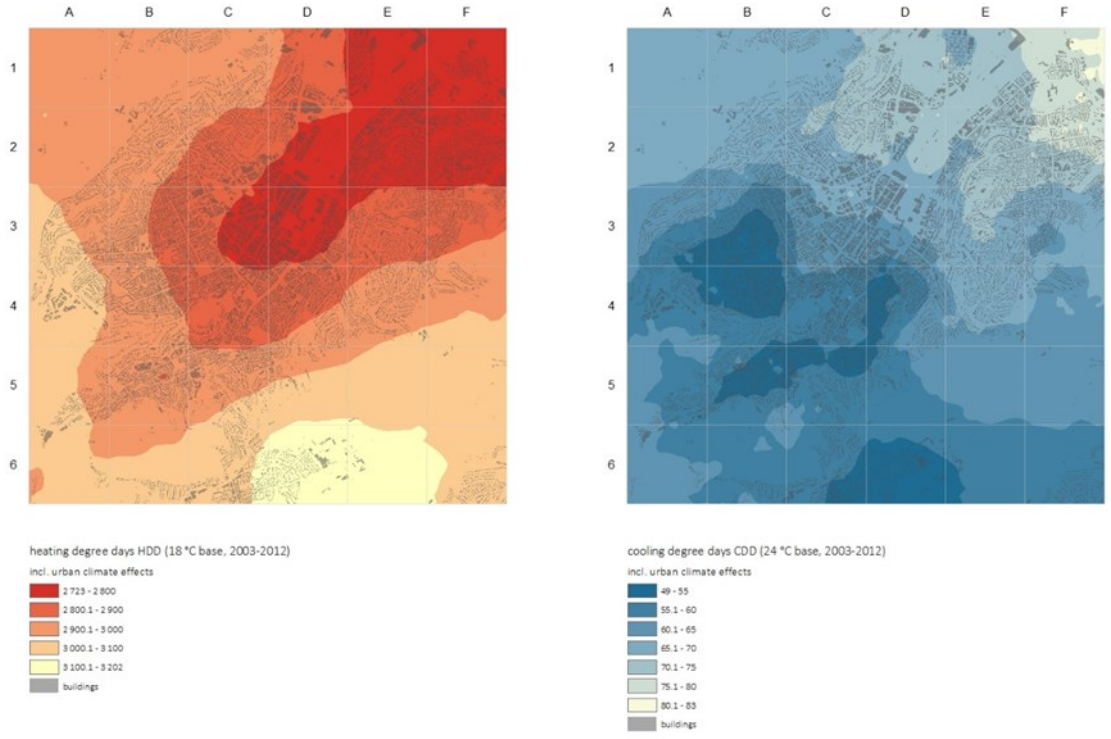

Figure 112: The heating and cooling degree days (HDD, CDD) due to urban climate effects in Stuttgart inner city for the period 2013 – 2012 with isotherm representation (TEB calculation)

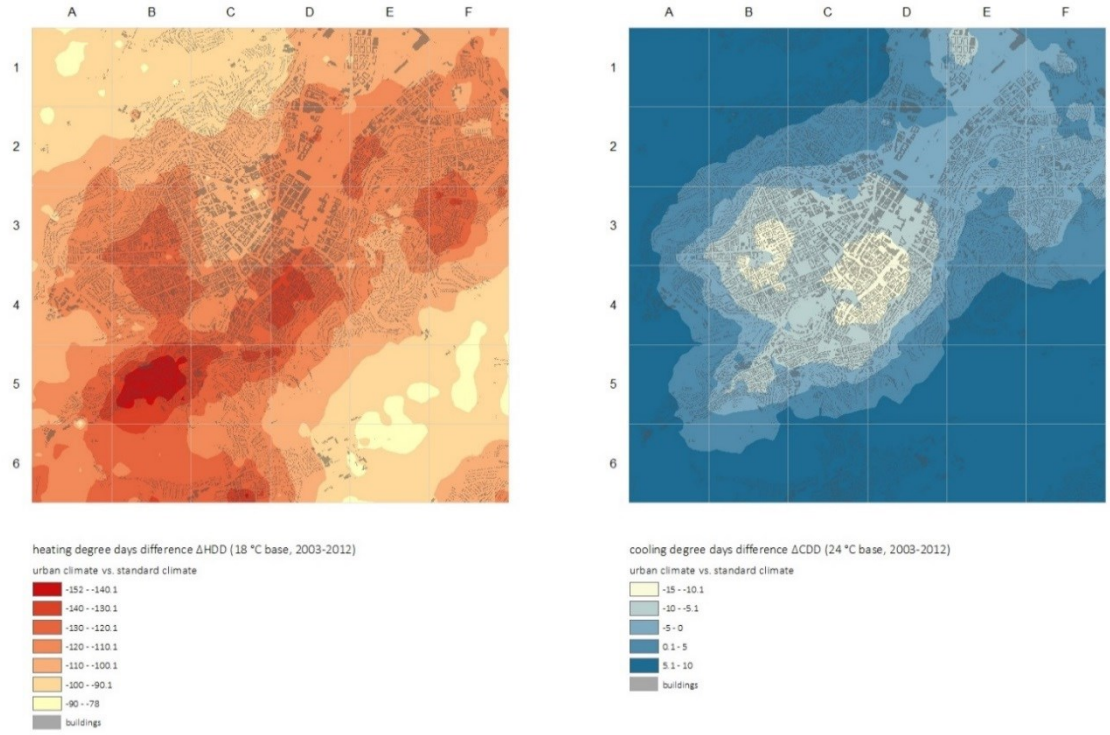

Figure 113: The difference in the heating and cooling degree days (HDD, CDD) between urban climate and standard climate boundary conditions in Stuttgart inner city for the period 2013 – 2012 with isotherm representation (TEB calculation)

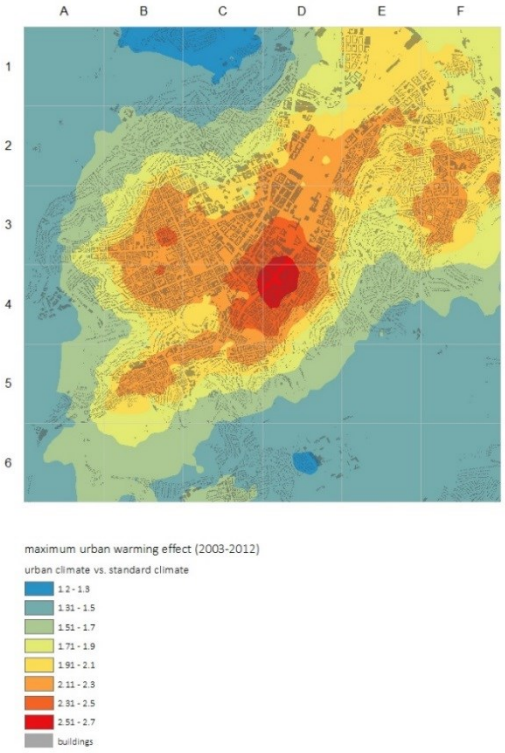

Figure 114: The maximal urban warming of the urban canyon UHI (left) and representative climate clusters (right) in Stuttgart inner city for the period 2003 – 2012 with isotherm representation (TEB calculation)

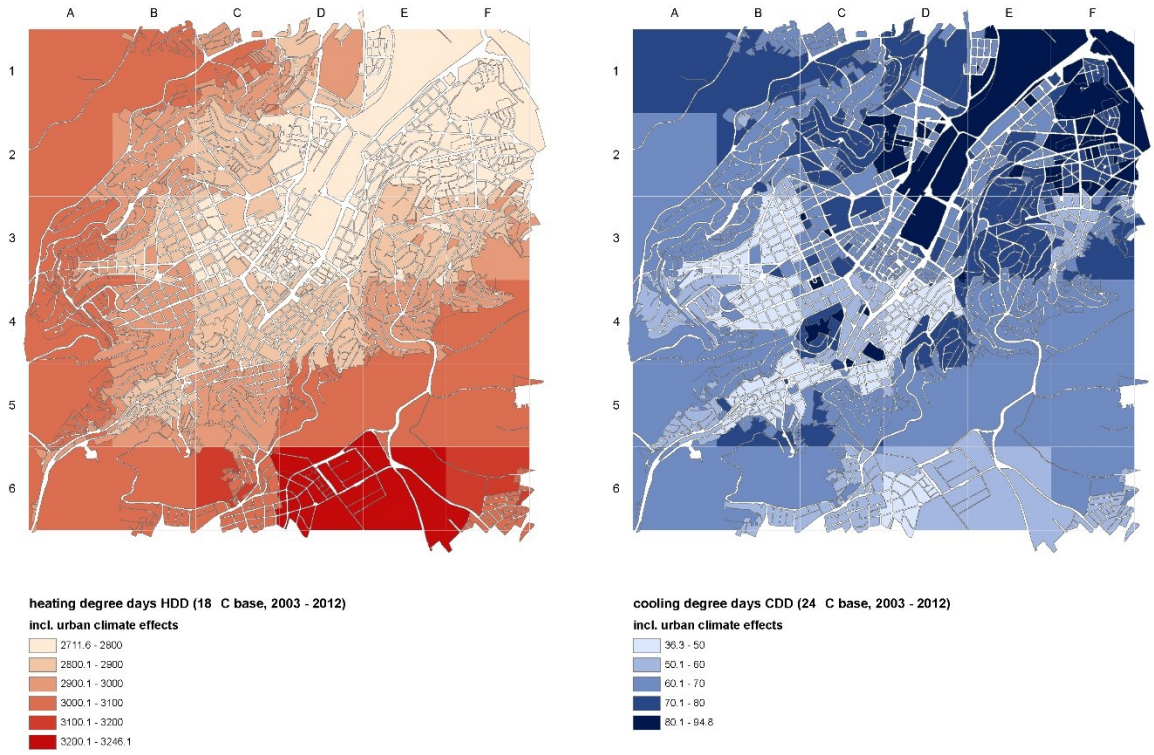

Figure 115: The heating and cooling degree days (HDD, CDD) due to urban climate effects in Stuttgart inner city for the period 2013 – 2012 (TEB calculation)

REFERENCES

Akbari H, Konopacki S (2004) Energy effects of heat-island reduction strategies in Toronto, Canada. Energy 29(2):191-210. doi: 10.1016/j.energy.2003.09.004

Akbari H, Taha H (1992) The impact of trees and white surfaces on residential heating and cooling energy use in four Canadian cities. Energy 17(2):141-149. doi: 10.1016/0360-5442(92)90063-6

Alameddine Z (2011) A computational assessment of the performance improvement potential of office buildings in Lebanon. Dissertation, Vienna University of Technology

Ali-Toudert F, Böttcher S (2018) Urban Microclimate Prediction prior to Building Energy Modelling using the TEB Model as embedded component in TRNSYS. Submitted to Urban Climate Journal (Elsevier). Under review.

Ali-Toudert F, Ji L (2017) Modeling and Measuring Urban Sustainability in Multi-Criteria-Based Systems - A Challenging Issue, Ecological Indicators 73:597-611. doi: 10.1016/j.ecolind.2016.09.046

Ali-Toudert F, Weidhaus J (2017) Numerical assessment and optimization of a low-energy residential building for Mediterranean and Saharan climates using a pilot project in Algeria. Renewable Energy 101:327-346. doi: 10.1016/j.renene.2016.08.043

Ali-Toudert F, Ji L (2016) Klimawandel, Stadtklima und Gebäudeenergieeffizienz: Wechselwirkungen und Handlungskonzepte für eine nachhaltige Stadt - KLISGEE. Final Report, KLIMOPASS-Teil 1 Programme. January 2016.

Ali-Toudert F, Böttcher S (2015) Implementation of the TEB model as a new TRNSYS-TYPE for the Assessment of Urban Microclimate prior to Building Thermal Simulation. Ninth International Conference on Urban Climate (ICUC9), Toulouse, France, July 20 - 24 2015

Ali-Toudert F, Ji L (2015a) Building Energy Demand under Urban Climate and Climate Change conditions with consideration of Urban Morphology and Building Typology - GIS Mapping of the City of Stuttgart. Ninth International Conference on Urban Climate (ICUC9), Toulouse, France, July 20 - 24 2015

Ali-Toudert F, Ji L (2015b) GIS-Mapping the Building Heating and Cooling Energy Demand for the City of Stuttgart, Germany. 17èmes Journées Internationales de Thermique (JITH 2015), Marseille, France, November 4 - 6 2015

Ali-Toudert F (2013) Impact of shading devices, ventilation and lighting operation on the energy efficiency of an office building under urban conditions. CLIMA 2013 Congress. 11th REHVA World Congress and 8th Int. Conference on Indoor Air Quality, Ventilation and Energy Conservation in Buildings, Prague, Czech Republic, 16.-19.06.2013.

Ali-Toudert F (2011) Openness to the Sky as Indicator for Daylighting Potential of Urban Office Buildings in a European Mid-Latitude Location. International Conference on Climate and Constructions, Karlsruhe, Germany, October 24 - 25 2011

Ali-Toudert F, Böttcher S (2011a) Type 201 "urban canyon climate", Town Energy balance (TEB) Model implementation for TRNSYS. User Guide. Version 1.0.27. Internal document for DFG final report

Ali-Toudert F, Böttcher S (2011b) Type 204 - Data Reader for the Town Energy Balance (TEB) Model implementation for TRNSYS. User Guide. Internal document for DFG final report

Ali-Toudert F (2010) Kombinierte Stadtklima- und Gebäudeenergiemodellierung zur Bestimmung des Energiebedarfs von urbanen Gebäuden. International building performance simulation association, IBPSA-Conference, Vienna, Austria, September 22-24 2010

Ali-Toudert F (2009) Energy Efficiency of urban buildings: Significance of urban geometry, building construction and climate. International Conference on Urban Climate, Yokohama, Japan, Jun. 29 - Jul.3 2009

Ali-Toudert F, Mayer H (2007a) Thermal comfort in an east-west oriented street canyon in Freiburg (Germany) under hot summer conditions. Theoretical and Applied Climatology 87(1):223-237. doi: 10.1007/s00704-005-0194-4

Ali-Toudert F, Mayer H (2007b) Effects of asymmetry, galleries, overhanging façades and vegetation on thermal comfort in urban street canyons. Solar Energy 81(6):742-754. doi: 10.1016/j.solener.2006.10.007

Ali-Toudert F (2007c) Sustainability and Human Comfort at urban level: Evaluation and Design Guidelines. Proceedings of the International Conference on Sustainable Building SB07. Lisbon 12-14.09.2007. Part 2:702 – 709.

Ali-Toudert F, Mayer H (2006) Numerical study on the effects of aspect ratio and orientation of an urban street canyon on outdoor thermal comfort in hot and dry climate. Building and Environment 41(2):94-108. doi: 10.1016/j.buildenv.2005.01.013

Ali-Toudert F (2005) Dependence of outdoor thermal comfort on street design in hot and dry climate. Dissertation, University of Freiburg. Report N°15. 224 pp. download: http://www.freidok.uni-freiburg.de/volltexte/2078

Ali-Toudert F, Djenane M, Bensalem R, Mayer H (2005) Outdoor thermal comfort in the old desert city of Beni-Isguen, Algeria. Climate Research 28(3):243-256. doi: 10.3354/cr028243

Allegrini J, Dorer V, Carmeliet J (2016) Impact of radiation exchange between buildings in urban street canyons on space cooling demands of buildings. Energy and Buildings 127:1074-1084. doi: 10.1016/j.enbuild.2016.06.073

Allegrini J, Dorer V, Carmeliet J (2015) Coupled CFD, radiation and building energy model for studying heat fluxes in an urban environment with generic building configura-

tions. Sustainable Cities and Society 19:385-394. doi: 10.1016/j.scs.2015.07.009

Allegrini (2012) Urban Climate and Energy Demand in Buildings. PhD Thesis. ETH Zürich. 188 pp. https://www.research-collection.ethz.ch/handle/20.500.11850/65361

Arnfield AJ (2006) Micro- and mesoclimatology. Progress in Physical Geography 30(5):677-689. doi: 10.1177/0309133306071150

Arnfield AJ (2005) Micro- and mesoclimatology. prog phys geogr 29(3):426-437. doi: 10.1191/0309133305pp458pr

Arnfield AJ (2003) Two decades of urban climate research: A review of turbulence, exchanges of energy and water, and the urban heat island. International Journal of Climatology 23(1):1-26. doi: 10.1002/joc.859

Arnfield AJ (1990) Street design and urban canyon solar access. Energy and Buildings 14(2):117-131

Asimakopoulos DN, Asimakopoulos VD, Chrisomallidou N, Klitsikas N, Mangold D, Michel P, Santamouris M, Tsangrassoulis A (2001) Energy and climate in the urban built environment. Earthscan / James & James, London

AU Stuttgart (1997) Amt für Umweltschutz Stadt Stuttgart (ed.) Energieatlas. http://www.stadtklima-stuttgart.de/index.php?klima_kliks_karten-energieatlas. Accessed 05.2017

AU Stuttgart (2015) Amt für Umweltschutz Stadt Stuttgart (ed.) Weather data in Stuttgart from the weather station on the roof of its facility in the inner city at the corner of the streets Torstrasse / Hauptstäterstrasse

Belcher S, Hacker J, Powell D (2005) Constructing design weather data for future climates. Building Services Engineering Research and Technology 26(1):49-61. doi: 10.1191/0143624405bt112oa

BMWi Energiewende (2017) Energy Transition topic on the website of the federal ministry for economic affairs and energy. http://www.bmwi.de/Redaktion/EN/Dossier/energy-transition.html. Accessed 04.2017

BMWi Energiewende (2016) The Energy of the Future Fifth "Energy Transition" Monitoring Report, 2015 Reporting Year - Summary. https://www.bmwi.de/Redaktion/EN/Publikationen/monitoring-report-2016-summary.html (in English)

Bouyer J, Inard C, Musy M (2011) Microclimatic coupling as a solution to improve building energy simulation in an urban context. Energy and Buildings 43(7):1549-1559. doi: 10.1016/j.enbuild.2011.02.010

Bouyer J (2009) Modélisation et simulation des microclimats urbains - Étude de l'impact de l'aménagement urbain sur les consommations énergétiques des bâtiments, PhD Thesis. University of Nantes, 324 pp.

Box GEP, Hunter JS, Hunter WG (2005) Statistics for experimenters: Design, innovation, and

discovery, 2nd Edition. Wiley-Interscience, Hoboken, New Jersey

Bozonnet E, Belarbi R, Allard F (2005) Modelling solar effects on the heat and mass transfer in a street canyon, a simplified approach. Sol. Energy 79(1):10-24. doi: 10.1016/j.solener.2004.10.007

Bremicker M, Brahmer G, Demuth N, Holle FK, Haag I (2013) Räumlich hoch aufgelöste LARSIM Wasserhaushaltsmodelle für die Hochwasservorhersage und weitere Anwendungen. KW Korrespondenz Wasserwirtschaft 9:509-514. doi: 10.3243/kwe2013.09.004

Bremicker M (2000) Das Wasserhaushaltsmodell LARSIM - Modellgrundlagen und Anwendungsbeispiele. Freiburger Schriften zur Hydrologie, Band 11. Institut für Hydrologie der Universität Freiburg. http://www.hydrology.uni-freiburg.de/publika/FSH-Bd11-Bremicker.pdf

Bruse M (1999) The influences of local environmental design on microclimate- development of a prognostic numerical Model ENVI-met for the simulation of Wind, temperature and humidity distribution in urban structures (in German). Dissertation, University of Bochum

Bruse M, Fleer H (1998) Simulating surface-plant-air interactions inside urban environments with a three dimensional numerical model. Environ. Model. Softw. 13(3-4):373-384. doi: 10.1016/S1364-8152(98)00042-5

Bueno B (2012) Study and prediction of the energy interactions between buildings and the urban climate. Dissertation, Massachusetts Institute of Technology

Bueno B, Norford L, Pigeon G, Britter R (2012a) A resistance-capacitance network model for the analysis of the interactions between the energy performance of buildings and the urban climate. Building and Environment 54(0):116-125. doi: 10.1016/j.buildenv.2012.01.023

Bueno B, Norford L, Hidalgo J, Pigeon G (2012b) The urban weather generator. Journal of Building Performance Simulation 6(4):269-281. doi: 10.1080/19401493.2012.718797

Bueno B, Pigeon G, Norford LK, Zibouche K, Marchadier C (2012c) Development and evaluation of a building energy model integrated in the TEB scheme. Geoscientific Model Development 5(2):433-448. doi: 10.5194/gmd-5-433-2012

Bueno B, Norford L, Pigeon G, Britter R (2011) Combining a Detailed Building Energy Model with a Physically-Based Urban Canopy Model. Boundary-Layer Meteorol 140(3):471-489. doi: 10.1007/s10546-011-9620-6

Bueno B (2010) An urban weather generator coupling a building simulation program with an urban canopy model. Master thesis, Massachusetts Institute of Technology

Büringer H, Schmidtmeier D (2012) Aktuelle Entwicklung des Straßenverkehrs in Baden-Württemberg. Statistisches Landesamt Baden-Württemberg (ed.) Statistisches Monatsheft Baden-Württemberg. http://www.statistik.baden-

wuerttemberg.de/veroeffentl/Monatshefte/PDF/Beitrag12_03_07.pdf. Accessed 05.2015

Cartalis C, Synodinou A, Proedrou M, Tsangrassoulis A, Santamouris M (2001) Modifications in energy demand in urban areas as a result of climate changes: an assessment for the southeast Mediterranean region. Energy Conversion and Management 42(14):1647-1656. doi: 10.1016/S0196-8904(00)00156-4

Chandler TJ (1965) The climate of London. Dissertation, Hutchinson of London

Chimklai P, Tanimoto J, Hagishima A (2003) Development of intelligent computer software (AUSSSM Tool) to estimate the urban heat island effects. Engineering sciences reports, Kyushu University. 24(4):343-350. doi: 10.15017/16679

Christenson M, Manz H, Gyalistras D (2006) Climate warming impact on degree days and building energy demand in Switzerland. Energy Conversion and Management 47(6):671-686. doi: 10.1016/j.enconman.2005.06.009

Christoffer J, Deutschländer T, Webs M (2004) Testreferenzjahre von Deutschland für mittlere und extreme Witterungsverhältnisse TRY. Dt. Wetterdienst, Offenbach a. Main

Colombert M (2008) Contribution à l'analyse de la prise en compte du climat urbain dans les différents moyens d'intervention sur la ville, Université Paris-Est. https://tel.archives-ouvertes.fr/tel-00470536

Cóstola D, Blocken B, Hensen J (2009) Overview of pressure coefficient data in building energy simulation and airflow network programs. Building and Environment 44(10):2027-2036. doi: 10.1016/j.buildenv.2009.02.006

Crawley DB, Hand JW, Kummert M, Griffith BT (2008) Contrasting the capabilities of building energy performance simulation programs: Part Special: Building Performance Simulation. Building and Environment 43(4):661-673. doi: 10.1016/j.buildenv.2006.10.027

Crawley DB, Hand JW, Kummert M, Griffith BT (2005) Contrasting the capabilities of building energy performance simulation programs. Report version 1. https://simulationresearch.lbl.gov/dirpubs/2005/05_compare.pdf. Accessed 05.2017

De Dear RJ, Brager GS (2002) Thermal comfort in naturally ventilated buildings: Revisions to ASHRAE Standard 55. Energy and Buildings 34(6):549-561. doi: 10.1016/S0378-7788(02)00005-1

De Dear R, Brager GS (2001) The adaptive model of thermal comfort and energy conservation in the built environment. International Journal of Biometeorology 45(2):100-108. doi: 10.1007/s004840100093

De Munck C (2013) Modélisation de la végétation urbaine et stratégies d'adaptation pour l'amélioration du confort climatique et de la demande énergétique en ville. Modelling of urban vegetation and adaptation strategies for improved comfort and energy demand in the city. Dissertation, Université de Toulouse

De Munck C, Pigeon G, Masson V, Meunier F, Bousquet P, Tréméac B, Merchat M, Poeuf P,

Marchadier C (2013) How much can air conditioning increase air temperatures for a city like Paris, France? Int. J. Climatol 33(1):210-227. doi: 10.1002/joc.3415

Dean A, Voss D (1999) Design and analysis of experiments. Springer, New York

Dickinson RE, Oleson KW, Bonan G, Hoffman F, Thornton P, Vertenstein M, Yang Z-L, Zeng X (2006) The Community Land Model and Its Climate Statistics as a Component of the Community Climate System Model. J. Climate 19(11):2302-2324. doi: 10.1175/JCLI3742.1

DWD (2013) Weather data of "Schnarrenberg", "Echterdingen" and "Neckartal" from the German weather services (DWD)

DWD (2011) Updated and extended Test Reference Years of the German weather Services, Deutscher Wetterdienst DWD, Release 2010. http://www.dwd.de/DE/klimaumwelt/klimaforschung/spez_themen/try/try_node.html. Accessed 05.2017

Edenhofer O, Pichs-Madruga R, Sokona Y, Kadner S, Minx JC, Brunner S, Agrawala S, Baiocchi G, Bashmakov IA, Blanco G, Broome J, Bruckner T, Bustamante M, Clarke L, Conte Grand M, Creutzig F, Cruz-Núñez X, Dhakal S, Dubash NK, Eickemeier P, Farahani E, Fischedick M, Fleurbaey M, Gerlagh R, Gómez-Echeverri L, Gupta S, Harnisch J, Jiang K, Jotzo F, Kartha S, Klasen S, Kolstad C, Krey V, Kunreuther H, Lucon O, Masera O, Mulugetta Y, Norgaard RB, Patt A, Ravindranath NH, Riahi K, Roy J, Sagar A, Schaeffer R, Schlömer S, Seto KC, Seyboth K, Sims R, Smith P, Somanathan E, Stavins R, von Stechow C, Sterner T, Sugiyama T, Suh S, Ürge-Vorsatz D, Urama K, Venables A, Victor DG, Weber E, Zhou D, Zou J, Zwickel T (2014) Technical Summary. In: Edenhofer O, Pichs-Madruga R, Sokona Y, Farahani E, Kadner S, Seyboth K, Adler A, Baum I, Brunner S, Eickemeier P,. Kriemann B, Savolainen J, Schlömer S, von Stechow C, Zwickel T, Minx JC (eds.) Climate Change 2014: Mitigation of Climate Change. Contribution of Working Group III to the Fifth Assessment Report of the Intergovernmental Panel on Climate Change. Cambridge University Press, Cambridge, United Kingdom and New York, NY, USA

EEA (2016) Trends and projections in Europe 2016 - Tracking progress towards Europe's climate and energy targets. http://www.eea.europa.eu/publications/trends-and-projections-in-europe. Accessed 05.2017

EEG (2014) Renewable Energy Sources Act (Erneuerbare-Energien-Gesetz). https://www.gesetze-im-internet.de/eeg_2014/index.html. Accessed 05.2017

Eisele J, Staniek B (2005) Bürobau Atlas: Grundlagen, Planung, Technologie, Arbeitsplatzqualitäten. Callwey, München

Emembolu (2004) Vergleichende Untersuchung zum Aufbau von innovativen Fassaden in Hinblick auf eine optimierte Tageslichtnutzung in Büroräumen: Degree Thesis, TU Dortmund

ENEV (2016) Website of the Energieeinsparverordnung, the German Energy Savings Act, http://www.enev-online.com/index.html

ENVI-met (2017) Website of the 3D-microscale climate model ENVI-met. http://www.envi-met.com/. Accessed 05.2017

ESRI (2012) Software ArcGIS versions 10.1

Fan H, Sailor DJ (2005) Modeling the impacts of anthropogenic heating on the urban climate of Philadelphia: a comparison of implementations in two PBL schemes. Atmospheric Environment 39(1):73-84. doi: 10.1016/j.atmosenv.2004.09.031

Frank T (2005) Climate change impacts on building heating and cooling energy demand in Switzerland: Research That Inspires 125 Years of EMPA. Energy and Buildings 37(11):1175-1185. doi: 10.1016/j.enbuild.2005.06.019

Fraunhofer (2017) Website of the Fraunhofer Institut https://www.ibp.fraunhofer.de/de/produktentwicklungen/software-fuer-die-praxis.html

Georgatou C, Kolokotsa D (2016) Urban climate models, in Urban Climate Mitigation Techniques. Santamouris and Kolokotsa (ed.): 175 – 194. Routledge

Givoni B (1997) Climate considerations in building and urban design. Van Nostrand Reinhold, New York

Givoni B (1976) Man, climate and architecture, 2. edition. Applied Science Publ., London (First edition 1969)

Golany G (1996) Urban design morphology and thermal performance. Atmospheric Environment 30(3):455-465. doi: 10.1016/1352-2310(95)00266-9

Görres J. (2010) Forschungsvorhaben Stadt mit Energie-Effizienz SEE Stuttgart. Landeshauptstadt Stuttgart, Amt für Umweltschutz. http://www.kommunale-stadtwerke.de/fileadmin/user_upload/pdfs/Stuttgart/Termine/2010/2010-06-26_SEE/Gesamtvortrag.pdf. Accessed 05.2015

Grimmond CSB, Blackett M, Best MJ, Baik J-J, Belcher SE, Beringer J, Bohnenstengel SI, Calmet I, Chen F, Coutts A, Dandou A, Fortuniak K, Gouvea ML, Hamdi R, Hendry M, Kanda M, Kawai T, Kawamoto Y, Kondo H, Krayenhoff ES, Lee, Loridan T, Martilli A, Masson V, Miao S, Oleson K, Ooka R, Pigeon G, Porson A, Ryu Y-H, Salamanca F, Steeneveld GJ, Tombrou M, Voogt JA, Young DT, Zhang N (2011) Initial results from Phase 2 of the international urban energy balance model comparison. Int. J. Climatol 31(2):244-272. doi: 10.1002/joc.2227

Grimmond CSB, Roth M, Oke TR, Au YC, Best M, Betts R, Carmichael G, Cleugh H, Dabberdt W, Emmanuel R, Freitas E, Fortuniak K, Hanna S, Klein P, Kalkstein LS, Liu CH, Nickson A, Pearlmutter D, Sailor D, Voogt J (2010a) Climate and More Sustainable Cities: Climate Information for Improved Planning and Management of Cities (Producers/Capabilities Perspective): World Climate Conference - 3. Procedia Environmental Sciences 1:247-274. doi: 10.1016/j.proenv.2010.09.016

Grimmond CSB, Blackett M, Best MJ, Barlow J, Baik J-J, Belcher SE, Bohnenstengel SI, Calmet I, Chen F, Dandou A, Fortuniak K, Gouvea ML, Hamdi R, Hendry M, Kawai

T, Kawamoto Y, Kondo H, Krayenhoff ES, Lee S-H, Loridan T, Martilli A, Masson V, Miao S, Oleson K, Pigeon G, Porson A, Ryu Y-H, Salamanca F, Shashua-Bar L, Steeneveld G-J, Tombrou M, Voogt J, Young D, Zhang N (2010b) The international urban energy balance models comparison project: First results from phase 1. J. Appl. Meteorol. Climatol 49(6):1268-1292. doi: 10.1175/2010JAMC2354.1

Grimmond C, Best M, Barlow J, Arnfield AJ, Baik J-J, Baklanov A, Belcher S, Bruse M, Calmet I, Chen F, Clark P, Dandou A, Erell E, Fortuniak K, Hamdi R, Kanda M, Kawai T, Kondo H, Krayenhoff S, Lee SH, Limor S-B, Martilli A, Masson V, Miao S, Mills G, Moriwaki R, Oleson K, Porson A, Sievers U, Tombrou M, Voogt J, Williamson T (2009) Urban Surface Energy Balance Models: Model Characteristics and Methodology for a Comparison Study. In: Baklanov A et al. (eds.) Meteorological and Air Quality Models for Urban Areas, pp 97-123. Springer. doi: 10.1007/978-3-642-00298-4_11

Halawa E, van Hoof J (2012) The adaptive approach to thermal comfort: A critical overview. Energy and Buildings 51:101-110. doi: 10.1016/j.enbuild.2012.04.011

Hamdi R, Deckmyn A, Degrauwe D, Delcloo A, Termonia P (2014) Coupling the Town Energy Balance Scheme to the High Resolution LAM ALADIN for Belgium. In: Steyn GD, Builtjes JP, Timmermans MR (eds.) Air Pollution Modeling and its Application XXII. Springer Netherlands, Dordrecht, pp 661-664

Hamdi R, Degrauwe D, Termonia P (2012) Coupling the Town Energy Balance (TEB) Scheme to an Operational Limited-Area NWP Model: Evaluation for a Highly Urbanized Area in Belgium. Wea. Forecasting 27(2):323-344. doi: 10.1175/WAF-D-11-00064.1

Hamdi R, Masson V (2008) Inclusion of a Drag Approach in the Town Energy Balance (TEB) Scheme: Offline 1D Evaluation in a Street Canyon. J. Appl. Meteor. Climatol. 47(10):2627-2644. doi: 10.1175/2008JAMC1865.1

Hassid S, Santamouris M, Papanikolaou N, Linardi A, Klitsikas N, Georgakis C, Assimakopoulos DN (2000) Effect of the Athens heat island on air conditioning load. Energy and Buildings 32(2):131-141. doi: 10.1016/S0378-7788(99)00045-6

Hauser G, Kempkes C, Schlitzberger S (2006) Vergleichende Untersuchungen von Standard-Klimadatensätzen (Testreferenzjahren) mit gemessenen Langzeit-Klimadatensätzen für den Standort Kassel. Bauphysik 28(4):221-232. doi: 10.1002/bapi.200610022

Hirano Y, Fujita T (2012) Evaluation of the impact of the urban heat island on residential and commercial energy consumption in Tokyo. 7th Biennial International Workshop "Advances in Energy Studies" 37(1):371-383. doi: 10.1016/j.energy.2011.11.018

Hottgenroth (2017) Website of Hottgenroth software. https://www.hottgenroth.de/index.html. Accessed 05.2017

Howard, L (1833) The climate of London: Deduced from meteorological observations made in the metropolis and at various places around it. W. Phillips, London

Huttner S (2012) Further development and application of the 3D microclimate simulation

ENVI-met. Dissertation, Johannes Gutenberg University of Mainz

IBM SPSS (2017) Website of IBM SPSS software in Germany. https://www-01.ibm.com/software/de/analytics/spss/. Accessed 05.2017

Ichinose T, Shimodozono K, Hanaki K (1999) Impact of anthropogenic heat on urban climate in Tokyo. Atmospheric Environment 33(24-25):3897-3909. doi: 10.1016/S1352-2310(99)00132-6

Ihara T, Kikegawa Y, Asahi K, Genchi Y, Kondo H (2008) Changes in year-round air temperature and annual energy consumption in office building areas by urban heat-island countermeasures and energy-saving measures. Applied Energy 85(1):12-25. doi: 10.1016/j.apenergy.2007.06.012

IPCC (2014) Climate Change 2014: Synthesis Report. Contribution of Working Groups I, II and III to the Fifth Assessment Report of the Intergovernmental Panel on Climate Change [Core Writing Team, Pachauri RK, Meyer LA (eds.)]. IPCC, Geneva, Switzerland

IWU (2005) Building Typology Catalogue of Germay. Institut Wohnen und Umwelt. http://www.iwu.de/downloads/fachinfos/altbausanierung/

Jentsch MF, Eames ME, Levermore GJ (2015) Generating near-extreme Summer Reference Years for building performance simulation. Building Services Engineering Research and Technology 36(6):701-727. doi: 10.1177/0143624415587476

Jentsch MF, Bahaj AS, James PAB (2008) Climate change future proofing of buildings - Generation and assessment of building simulation weather files. Energy and Buildings 40(12):2148-2168. doi: 10.1016/j.enbuild.2008.06.005

Kanda M (2006) Progress in the scale modeling of urban climate: Review. Theoretical and Applied Climatology 84(1):23-33. doi: 10.1007/s00704-005-0141-4

Kanda M, Kawai T, Kanega M, Moriwaki R, Narita K, Hagishima A (2005a) A Simple Energy Balance Model for Regular Building Arrays. Boundary-Layer Meteorol 116(3):423-443. doi: 10.1007/s10546-004-7956-x

Kanda M, Kawai T, Nakagawa K (2005b) A Simple Theoretical Radiation Scheme for Regular Building Arrays. Boundary-Layer Meteorol 114(1):71-90. doi: 10.1007/s10546-004-8662-4

Kavanaugh (2017) Website of http://kavanaugh.ca/design-of-experiments/

Kikegawa Y, Genchi Y, Kondo H, Hanaki K (2006) Impacts of city-block-scale countermeasures against urban heat-island phenomena upon a building's energy-consumption for air-conditioning. Applied Energy 83(6):649-668. doi: 10.1016/j.apenergy.2005.06.001

Kikegawa Y, Genchi Y, Yoshikado H, Kondo H (2003) Development of a numerical simulation system toward comprehensive assessments of urban warming countermeasures including their impacts upon the urban buildings' energy-demands. Applied Energy 76(4):449-466. doi: 10.1016/S0306-2619(03)00009-6

KIT (2014) Wetterdaten aus der atmosphärischen Modellierung im Zeitraum 1971-2000 und Prognose im Zeitraum 2021-2050. Karlsruher Institut für Technologie KIT.

Klein SA, Beckman WA, Mitchell JW, Duffie JA, Duffie NA, Freeman T, Mitchell JC, Braun JE, Evans BL, Kummer JP, Urban RE, Fiksel A, Thornton JW, Blair NJ, Williams PM, Bradley DE, Mc Dowell TP, Kummert M (2004) TRNSYS 16: A Transient System Simulation program, user manual. Solar energy Laboratory. University of Wisconsin-Madison, Madison

Klimaatlas Stuttgart (2008) Website of the climate atlas of Stuttgart, VRS, https://www.region-stuttgart.org/information-und-download/veroeffentlichungen/klimaatlas/. Accessed 05.2017

Knowles RL (1981) Sun, Rhythm and Form. MIT Press

Kolokotroni M, Ren X, Davies M, Mavrogianni A (2012) London's urban heat island: Impact on current and future energy consumption in office buildings. Energy and Buildings 47:302-311. doi: 10.1016/j.enbuild.2011.12.019

Kolokotroni M, Giannitsaris I, Watkins R (2006) The effect of the London urban heat island on building summer cooling demand and night ventilation strategies: Urban Ventilation. Solar Energy 80(4):383-392. doi: 10.1016/j.solener.2005.03.010

Kondo H, Genchi Y, Kikegawa Y, Ohashi Y, Yoshikado H, Komiyama H (2005) Development of a Multi-Layer Urban Canopy Model for the Analysis of Energy Consumption in a Big City: Structure of the Urban Canopy Model and its Basic Performance. Boundary-Layer Meteorol 116(3):395-421. doi: 10.1007/s10546-005-0905-5

Kondo H, Liu FH (1998) A Study on the Urban Thermal Environment Obtained Through a One-dimensional Urban Canopy Model. J. Jpn. Soc. Atmos. Environ. 33, 179-192 (in Japanese). doi: 10.11298/taiki1995.33.3_179

Kondo H (1995) The Thermally Induced Local Wind and Surface Inversion over the Kanto plain On Calm Winter Nights. J. Appl. Meteorol. 34:1439-1448. doi: 10.1175/1520-0450(1995)034<1439:TTILWA>2.0.CO;2

Konya A (2011) Design Primer for Hot Climates. London: Architectural Press Limited

Kusaka H, Kondo H, Kikegawa Y, Kimura F (2001) A Simple Single-Layer Urban Canopy Model For Atmospheric Models: Comparison With Multi-Layer And Slab Models. Boundary-Layer Meteorology 101(3):329–358. doi: 10.1023/A%3A1019207923078

Kuttler W, Miethke A, Dütemeyer D, Barlag A-B (2015) Das Klima von Essen: The climate of Essen. Westarp Wiss, Hohenwarsleben

Kuttler (2010) Urbanes Klima Teil 1. Gefahrstoffe – Reinhaltung der Luft. (70) 7/8, 329 -340

Landsberg HE (1981) The urban climate. International Geophysics Series, vol. 28. Academic Press, New York

Le Moigne P (2009) SURFEX-Scientific Documentation

Lechner N (2014) Heating, cooling, lighting: Sustainable design methods for architects, 4. ed.

Wiley, Hoboken NJ

Lemonsu A, Masson V, Shashua-Bar L, Erell E, Pearlmutter D (2012) Inclusion of vegetation in the Town Energy Balance model for modelling urban green areas. Geosci. Model Dev. 5(6):1377-1393. doi: 10.5194/gmd-5-1377-2012

Lemonsu A, Bélair S, Mailhot J, Leroyer S (2010) Evaluation of the Town Energy Balance Model in Cold and Snowy Conditions during the Montreal Urban Snow Experiment 2005. J. Appl. Meteor. Climatol. 49(3):346-362. doi: 10.1175/2009JAMC2131.1

Lemonsu A, Bastin S, Masson V, Drobinski P (2006) Vertical Structure of the Urban Boundary Layer over Marseille Under Sea-Breeze Conditions. Boundary-Layer Meteorol 118(3):477-501. doi: 10.1007/s10546-005-7772-y

Lemonsu A, Grimmond C, Masson V (2004) Modeling the Surface Energy Balance of the Core of an Old Mediterranean City: Marseille. Journal of Applied Meteorology (43):312-327. doi: 10.1175/1520-0450(2004)043<0312:MTSEBO>2.0.CO;2

Li DHW, Wong SL (2007) Daylighting and energy implications due to shading effects from nearby buildings. Applied Energy 84(12):1199-1209. doi: 10.1016/j.apenergy.2007.04.005

Li DHW, Wong SL, Tsang CL, Cheung GHW (2006) A study of the daylighting performance and energy use in heavily obstructed residential buildings via computer simulation techniques. Energy and Environment of Residential Buildings in China 38(11):1343-1348. doi: 10.1016/j.enbuild.2006.04.001

LUBW (2013) Hochwasserzentrale der Landesanstalt für Umwelt, Messungen und Naturschutz Baden-Württemberg. Herunterskalierte stündliche Wetterdaten in 1 km² Auflösung für den Zeitraum 2003-2012

Marciotto ER, Oliveira AP, Hanna SR (2010) Modeling study of the aspect ratio influence on urban canopy energy fluxes with a modified wall-canyon energy budget scheme. Building and Environment 45(11):2497-2505. doi: 10.1016/j.buildenv.2010.05.012

Martilli A (2014) An idealized study of city structure, urban climate, energy consumption, and air quality. ICUC8: The 8th International Conference on Urban Climate and the 10th Symposium on the Urban Environment 10, Part 2:430-446. doi: 10.1016/j.uclim.2014.03.003

Martilli A, Clappier A, Rotach MW (2002) An Urban Surface Exchange Parameterisation for Mesoscale Models. Boundary-Layer Meteorology 104(2):261-304. doi: 10.1023/A:1016099921195

Masson V, Seity Y (2009) Including Atmospheric Layers in Vegetation and Urban Offline Surface Schemes. J. Appl. Meteor. Climatol. 48(7):1377-1397. doi: 10.1175/2009JAMC1866.1

Masson V (2006) Urban surface modeling and the meso-scale impact of cities. Theoretical and Applied Climatology 84(1):35-45. doi: 10.1007/s00704-005-0142-3

Masson V, Grimmond CSB, Oke TR (2002) Evaluation of the Town Energy Balance (TEB)

Scheme with Direct Measurements from Dry Districts in Two Cities: Journal of Applied Meteorology. J. Appl. Meteor 41(10):1011-1026. doi: 10.1175/1520-0450%282002%29041<1011%3AEOTTEB>2.0.CO%3B2

Masson V (2000) A Physically-Based Scheme for the Urban Energy Budget in Atmospheric Models. Boundary-Layer Meteorology (94):357-397. doi: 10.1023/A:1002463829265

Météo France (2011) Evolution du climat urbain de Paris dans la perspective du changement climatique. Projet EPICEA - Volet 1. https://www.umr-cnrm.fr/IMG/pdf/epicea-rapport-volet1_def.pdf

Meteonorm (2011) Meteonorm 6.1. http://www.meteonorm.com/de/. Last accessed 05.2017

Mills G, Cleugh H, Emmanuel R, Endlicher W, Erell E, McGranahan G, Ng E, Nickson A, Rosenthal J, Steemer K (2010) Climate Information for Improved Planning and Management of Mega Cities (Needs Perspective): World Climate Conference - 3. Procedia Environmental Sciences 1:228-246. doi: 10.1016/j.proenv.2010.09.015

Mills GM (1993) Simulation of the Energy Budget of an Urban Canyon: I. Model Structure and Sensitivity Test. Atmospheric Environment 27B(2):157-170. doi: 10.1016/0957-1272(93)90002-N

Müller HFO, Emembolu A, Oetzel M, Schuster H, Soylu I (2005) Sonnenschutz und Tageslicht in Büroräumen. Bauphysik-Kalender, Abschnitt D2 Jahrgang 2005, Abschnitt D2: pp 397-439

Nakamura Y, Oke TR (1988) Wind, temperature and stability conditions in an east-west oriented urban canyon. Atmospheric Environment (1967) 22(12):2691-2700. doi: 10.1016/0004-6981(88)90437-4

Nunez M, Oke TR (1977) The Energy Balance of an Urban Canyon. J. Appl. Meteorol. (16):11-19. doi: 10.1175/1520-0450(1977)016<0011:TEBOAU>2.0.CO;2

Offerle B, Grimmond CSB, Oke TR (2003) Parameterization of Net All-Wave Radiation for Urban Areas. J. Appl. Meteor. 42(8):1157-1173. doi: 10.1175/1520-0450(2003)042<1157:PONARF>2.0.CO;2

Ohashi Y, Genchi Y, Kondo H, Kikegawa Y, Yoshikado H, Hirano Y (2007) Influence of Air-Conditioning Waste Heat on Air Temperature in Tokyo during Summer: Numerical Experiments Using an Urban Canopy Model Coupled with a Building Energy Model. J. Appl. Meteor. Climatol 46(1):66-81. doi: 10.1175/JAM2441.1

Oke TR (2006a) Towards better scientific communication in urban climate. Theoretical and Applied Climatology 84(1):179-190. doi: 10.1007/s00704-005-0153-0

Oke TR (2006b) Boundary layer climates, 2. ed., repr. Routledge, London (First edition 1978)

Oke TR (1988a) Street design and urban canopy layer climate. Energy and Buildings (11):103-113. doi: 10.1016/0378-7788(88)90026-6

Oke TR (1988b) The Urban Energy Balance. Prog. Phys. Geogr. (12):471-508. doi:

10.1177/030913338801200401

Oke TR (1982) The energetic basis of the urban heat island: Quarterly Journal of the Royal Meteorological Society. The energetic basis of the urban heat island 108(455):1-24. doi: 10.1002/qj.49710845502

Oleson KW, Bonan GB, Feddema J, Vertenstein M, Grimmond CSB (2008) An Urban Parameterization for a Global Climate Model. Part I: Formulation and Evaluation for Two Cities. J. Appl. Meteor. Climatol 47(4):1038-1060. doi: 10.1175/2007JAMC1597.1

Papadopoulos AM (2001) The influence of street canyons on the cooling loads of buildings and the performance of air conditioning systems. Energy and Buildings 33(6):601-607. doi: 10.1016/S0378-7788(00)00123-7

Papakostas K, Mavromatis T, Kyriakis N (2010) Impact of the ambient temperature rise on the energy consumption for heating and cooling in residential buildings of Greece. Special Section: IST National Conference 2009 35(7):1376-1379. doi: 10.1016/j.renene.2009.11.012

Passivhaus (2017): Website of Passivhaus Institut. http://www.passiv.de/. Accessed 05.2017

Pigeon G, Zibouche K, Bueno B, Le Bras J, Masson V (2014) Improving the capabilities of the Town Energy Balance model with up-to-date building energy simulation algorithms: an application to a set of representative buildings in Paris. Energy and Buildings 76:1-14. doi: 10.1016/j.enbuild.2013.10.038

Pültz G, Hoffmann S (2007) Zur Aussagekraft von Simulationsergebnissen auf Basis der Testreferenzjahre (TRY) über die Häufigkeit sommerlicher Überhitzung. Bauphysik 29(2):99-109. doi: 10.1002/bapi.200710016

Robinson D (2010) Computer modelling for sustainable urban design: Physical principles, methods, and applications. Earthscan, London

Robinson D, Stone A (2004) Solar radiation modelling in the urban context. Solar Energy 77(3):295-309. doi: 10.1016/j.solener.2004.05.010

Roth M (2007) Review of urban climate research in (sub)tropical regions. Int. J. Climatol 27(14):1859-1873. doi: 10.1002/joc.1591

Sailor DJ (2011) A review of methods for estimating anthropogenic heat and moisture emissions in the urban environment. Int. J. Climatol 31(2):189-199. doi: 10.1002/joc.2106

Sailor DJ, Lu L (2004) A top–down methodology for developing diurnal and seasonal anthropogenic heating profiles for urban areas. Atmospheric Environment 38(17):2737-2748. doi: 10.1016/j.atmosenv.2004.01.034

Salamanca F, Krpo A, Martilli A, Clappier A (2010) A new building energy model coupled with an urban canopy parameterization for urban climate simulations - part I. formulation, verification, and sensitivity analysis of the model: Theoretical and Applied Climatology 99(3-4):331-344. doi: 10.1007/s00704-009-0142-9

Santamouris M, Kolokotsa D (2016) Urban Climate Mitigation Techniques. Routledge

Santamouris M (2016) Urban warming and mitigation: Actual status, impacts and challenges, in Santamouris M, Kolokotsa D (eds.) Urban Climate Mitigation Techniques. Routledge

Santamouris M (2015) Regulating the damaged thermostat of the cities—Status, impacts and mitigation challenges. Energy and Buildings 91:43-56. doi: 10.1016/j.enbuild.2015.01.027

Santamouris M, Cartalis C, Synnefa A, Kolokotsa D (2015) On the impact of urban heat island and global warming on the power demand and electricity consumption of buildings - A review. Renewable Energy Sources and Healthy Buildings 98:119-124. doi: 10.1016/j.enbuild.2014.09.052

Santamouris M (2014a) Cooling the cities – A review of reflective and green roof mitigation technologies to fight heat island and improve comfort in urban environments. Solar Energy 103:682-703. doi: 10.1016/j.solener.2012.07.003

Santamouris M (2014b) On the energy impact of urban heat island and global warming on buildings. Energy and Buildings 82:100-113. doi: 10.1016/j.enbuild.2014.07.022

Santamouris M (2007) Heat island research in Europe: the state of the art. Advances in building energy research 1(1):123-150. doi: 10.1080/17512549.2007.9687272

Santamouris M, Papanikolaou N, Livada I, Koronakis I, Georgakis C, Argiriou A, Assimakopoulos DN (2001) On the impact of urban climate on the energy consumption of buildings: Urban Environment. Solar Energy 70(3):201-216. doi: 10.1016/S0038-092X(00)00095-5

Schild K, Willems WM (2013) Wärmeschutz: Grundlagen - Berechnung - Bewertung, 2. Auflage. Detailwissen Bauphysik. Springer Vieweg, Wiesbaden

Schlenger (2009) Climatic Influences on the Energy Demand of European Office Buildings, PhD Dissertation, TU Dortmund

Seto KC, Dhakal S, Bigio A, Blanco H, Delgado GC, Dewar D, Huang L, Inaba A, Kansal A, Lwasa S, McMahon JE, Müller DB, Murakami J, Nagendra H, Ramaswami A (2014) Human Settlements, Infrastructure and Spatial Planning. In: Edenhofer O, Pichs-Madruga R, Sokona Y, Farahani E, Kadner S, Seyboth K, Adler A, Baum I, Brunner S, Eickemeier P,. Kriemann B, Savolainen J, Schlömer S, von Stechow C, Zwickel T, Minx JC (eds.)Climate Change 2014: Mitigation of Climate Change. Contribution of Working Group III to the Fifth Assessment Report of the Intergovernmental Panel on Climate Change. Cambridge University Press, Cambridge, United Kingdom and New York, NY, USA.

Souch C, Grimmond S (2006) Applied climatology: urban climate. Progress in Physical Geography 30(2):270-279. doi: 10.1191/0309133306pp484pr

Stadtklima Stuttgart (2017) Website of the section of urban climatology of the city of Stuttgart, https://www.stadtklima-stuttgart.de/index.php?start_e. Accessed 05.2017

Staniek B, Staniek C (2011) A typology of organizational forms for offices. Detail Konzep 20011, 9, 1008 -1017

Strømann-Andersen J, Sattrup PA (2011) The urban canyon and building energy use: Urban density versus daylight and passive solar gains. Energy and Buildings 43(8):2011–2020. doi: 10.1016/j.enbuild.2011.04.007

Tanimoto J, Hagishima A, Chimklai P (2004) An approach for coupled simulation of building thermal effects and urban climatology. Energy and Buildings 36(8):781-793. doi: 10.1016/j.enbuild.2004.01.019

Tanimoto J, Hayashi T, Katayama T, Ohama J, Kasama M (1998) Quantitative analysis on factors of significant air temperature rising in urban areas by architecture-urban-soil simultaneous simulation model. Journal of Architecture Planning Environment Engineering (AIJ 504):87-93. doi: 10.3130/aija.63.87_1

TEB (2013) Open source website of TEB, https://opensource.umr-cnrm.fr/projects/teb/wiki

Tregenza P, Wilson M (2011) Daylighting: Architecture and lighting design. Routledge, 290 pp.

TRANSSOLAR (2017) Website of TRNSYS in Germany. http://www.transsolar.com/. Accessed 05.2017

UCLA (2013) Climate Consultant 5.3, 2012. www.energy-design-tools.aud.ucla.edu/climate-consultant/.

UN DESA PD (2014) World Urbanization Prospects: The 2014 Revision, Highlights (ST/ESA/SER.A/352). United Nations, Department of Economic and Social Affairs, Population Division. ISBN 978-92-1-151517-6. https://esa.un.org/unpd/wup/. Accessed 05.2017

UN SD (2016) Sustainable Development United Nations. https://sustainabledevelopment.un.org/sdgs. Accessed 05.2017

Vidrih B, Medved S (2008) The effects of changes in the climate on the energy demands of buildings and the efficiencies of building services: International Journal of Energy Research. The effects of changes in the climate on the energy demands of buildings 32(11):1016-1029. doi: 10.1002/er.1410

WISC (2017) official website of TRNSYS, http://sel.me.wisc.edu/trnsys/. Accessed 05.2017

Yoshida A, Tominaga K, Watatani S (1990) Field measurements on energy balance of an urban canyon in the summer season. Energy and Buildings 15(3-4):417-423. doi: 10.1016/0378-7788(90)90016-C

STANDARDS AND GUIDELINES

ANSI/ASHRAE Standard 140-2001 Standard Method of Test for the Evaluation of Building Energy Analysis Computer Programs: American Society of Heating, Refrigerating and Air-Conditioning Engineers ASHRAE, INC.

ANSI/ASHRAE Standard 55 (2013) Thermal Environmental Conditions for Human Occupancy. American Society of Heating, Refrigerating and Air-Conditioning Engineers ASHRAE, INC. Former versions 2010, 2004.

DIN 4108-2 (2013-02) Thermal protection and energy economy in buildings – Part 2: Minimum requirements to thermal insulation, German Institute for Normalisation DIN, Beuth, Berlin, 34 pp.

DIN 5034-2 (1985-02) Daylight in interiors; principles, German Institute for Normalisation DIN, Beuth, Berlin, 14 pp.

DIN EN 12464-1 (2011-08) Light and lighting – Lighting of work places – Part 1: Indoor work places; German Institute for Normalisation DIN, Beuth, Berlin, 59 pp.

DIN EN 12464-2 (2014-05) Light and lighting – Lighting of work places – Part 2: Outdoor work places; German Institute for Normalisation DIN, Beuth, Berlin, 34 pp.

DIN EN 12831 Bbl 1 (2008-07) Heating systems in buildings – Method for calculation of the design heat load – National Annex NA

DIN EN 12831 (2003-08) Heating systems in buildings – Method for calculation of the design heat load

DIN EN 13786 (2008-04) Thermal performance of building components - Dynamic thermal characteristics - Calculation methods (ISO 13786 (2007); German version EN ISO 13786 (2007)

DIN EN 15251 (2012-12) Indoor environmental input parameters for design and assessment of energy performance of buildings addressing indoor air quality, thermal environment, lighting and acoustics; German Institute for Normalisation DIN, Beuth, Berlin, 60 pp.

DIN EN ISO 7730 Ber 1 (2007-06) Ergonomics of the thermal environment – Analytical determination and interpretation of thermal comfort using calculation of the PMV and PPD indices and local thermal comfort criteria (ISO 7730:2005); Corrigenda to

	DIN EN ISO 7730:2006-05, German Institute for Normalisation DIN, Beuth, Berlin, 2 pp.
DIN EN ISO 7730 (2006-05)	Ergonomics of the thermal environment – Analytical determination and interpretation of thermal comfort using calculation of the PMV and PPD indices and local thermal comfort criteria (ISO 7730:2005); German Institute for Normalisation DIN, DIN, Beuth, Berlin, 59 pp.
DIN V 18599-1 (2011-12)	Energy efficiency of buildings – Calculation of the net, final and primary energy demand for heating, cooling, ventilation, domestic hot water and lighting – Part 1: General balancing procedures, terms and definitions, zoning and evaluation of energy sources, German Institute for Normalisation DIN, Beuth, Berlin, 79 pp.
DIN V 18599-10 (2011-12)	Energy efficiency of buildings – Calculation of the net, final and primary energy demand for heating, cooling, ventilation, domestic hot water and lighting – Part 10: Boundary conditions of use, climatic data, German Institute for Normalisation DIN, Beuth, Berlin, 102 pp.
DIN V 4108-6 (2003-06)	Thermal protection and energy economy in buildings - Part 6: Calculation of annual heat and annual energy use, German Institute for Normalisation DIN, Beuth, Berlin, 110 pp.
DIN V 4701-10 (2003-08)	Energy efficiency of heating and ventilation systems in buildings — Part 10: Heating, domestic hot water, ventilation, German Institute for Normalisation DIN, Beuth, Berlin, 156 pp.
VDI 2078 (2015 – 06)	Calculation of thermal loads and room temperatures, (design cooling load and annual simulation)", Verein deutscher Ingenieure VDI, Düsseldorf, 151 pp.
VDI 6007 - Part 3 (2015 – 06)	Calculation of transient thermal response of rooms and buildings Modelling of solar radiation", Verein deutscher Ingenieure VDI, Düsseldorf, 36 pp.
VDI 6011 - Part 1 (2016 – 07)	Optimisation of daylight use and artificial lighting, Fundamentals and basic requirements", Verein deutscher Ingenieure VDI, Düsseldorf, 80 pp.

LIST OF FIGURES

LIST OF TABLES